2008 Atomic, Molecular, Optical Sciences

Research Meeting

Airlie Conference Center
Warrenton, Virginia
September 14-17, 2008

Sponsored by:
U.S. Department of Energy
Office of Basic Energy Sciences
Chemical Sciences, Geosciences & Biosciences Division

Foreword

This volume summarizes the 2008 Research Meeting of the Atomic, Molecular and Optical Sciences (AMOS) Program sponsored by the U. S. Department of Energy (DOE), Office of Basic Energy Sciences (BES), and comprises descriptions of the current research sponsored by the AMOS program. The research meeting is held annually for the DOE laboratory and university principal investigators within the BES AMOS Program to facilitate scientific interchange among the PIs and to promote a sense of program identity.

The BES/AMOS program is vigorous and innovative, and enjoys strong support within the Department of Energy. This is due entirely to our scientists, the outstanding research they perform, and its relevance to DOE missions. While the FY2008 appropriation for DOE increased overall funding for science, planned new initiatives related to AMOS were not funded. Another flat budget in the program challenged our ability to meet established commitments to researchers. However, due to the relevance of AMOS research, BES continued to increase its strategic investments in the national laboratory ultrafast x-ray efforts.

We are deeply indebted to the members of the scientific community who have contributed valuable time toward the review of proposals and programs, either by mail review of grant applications, panel reviews, or on-site reviews of our multi-PI programs. These thorough and thoughtful reviews are central to the continued vitality the AMOS Program.

We owe special thanks to Elliot Kanter and Dick Hilderbrandt for their invaluable help in managing the AMOS program this year. Elliot has returned to Argonne National Laboratory, and Dick retired this past December. Jeff appreciates Michael's thoughtful advice in Michael's role as Team Leader of the Fundamental Interactions team. We are also pleased to welcome Mark Pederson to BES, as Program Manager in Computational and Theoretical Chemistry.

Thanks to the staff of the Oak Ridge Institute for Science and Education, in particular Margaret Lyday, Deneise Terry and Donna Thomas, and to the Airlie Conference Center for assisting with the meeting. We also thank Diane Marceau, Robin Felder, and Michaelena Kyler-King in the Chemical Sciences, Biosciences, and Geosciences Division for their indispensable behind-the-scenes efforts in support of the BES/AMOS program. Finally, thanks to Larry Rahn for his expert help in assembling this volume.

Jeffrey L. Krause
Michael P. Casassa
Chemical Sciences, Geosciences and Biosciences Division
Office of Basic Energy Sciences
Department of Energy

Cover Art Courtesy of Diane Marceau
Chemical Sciences, Geosciences and Biosciences
Division, Basic Energy Sciences, DOE

This document was produced under contract number DE-AC05-06OR23100 between the U.S. Department of Energy and Oak Ridge Associated Universities.

Agenda

2008 Meeting of the Atomic, Molecular and Optical Sciences Program

Office of Basic Energy Sciences
U. S. Department of Energy

Airlie Center, Warrenton, Virginia, September 14-17, 2008

Sunday, September 14

3:00-6:00 pm	**** Registration ****
6:00 pm	**** Reception (No Host) ****
7:00 pm	**** Dinner ****

Monday, September 15

7:30 am	**** Breakfast ****
8:45 am	*Welcome and Introductory Remarks* **Jeffrey Krause**, BES/DOE
Session I	Chair: **Henry Kapteyn**
9:00 am	*Laser Control of Molecular Alignment and Bond Strength* **Phil Bucksbaum,** Stanford/SLAC
9:30 am	*Theory and Simulations of Nonlinear X-Ray Spectroscopy of Molecules* **Shaul Mukamel**, University of California, Irvine
10:00 am	*High Brightness Table-top Sources of Coherent Soft X-Ray Light* **Jorge Rocca**, Colorado State University
10:30 am	**** Break ****
11:00 am	*Attosecond Science: Generation, Metrology and Application* **Lou DiMauro**, Ohio State University
11:30 am	*Atomic and Molecular Physics in Strong Fields* **Shih-I Chu**, University of Kansas
12:00 noon	*Controlling Attosecond Pulse Spectra with Carrier-Envelope Phase* **Zenghu Chang**, Kansas State University
12:30 pm	**** Lunch ****

Session II Chair: **Kelly Gaffney**

4:00 pm *Using Intense Short Laser Pulses to Manipulate and View Molecular Dynamics*
Bob Jones, University of Virginia

4:30 pm *Atomic Electrons in Strong Radiation Fields*
Joe Eberly, University of Rochester

5:00 pm *High Intensity Femtosecond XUV Pulse Interactions with Atomic Clusters*
Todd Ditmire, University of Texas at Austin

5:30 pm *Picosecond X-Rays at Argonne's Advanced Photon Source*
Bertold Krässig, Argonne National Laboratory

6:00 pm **** Reception (No Host) ****

6:30 pm **** Dinner ****

Session III Chair: **Itzik Ben-Itzhak**

7:30 pm *Towards the Complete Imaging of Molecular Dynamics with Ultra-Short Laser Pulses*
Uwe Thumm, Kansas State University

8:00 pm *Ultrafast EUV Photoelectron imaging from He Nanodroplets*
Oliver Gessner, Lawrence Berkeley National Laboratory

Tuesday, September 16

7:30 am **** Breakfast ****

Session IV Chair: **Dave Schultz**

8:30 am *Manipulation and Decoherence of Rydberg Wavepackets*
Carlos Reinhold, Oak Ridge National Laboratory

9:00 am *Coherent and Incoherent Evolution of Rydberg Atoms*
Francis Robicheaux, Auburn University

9:30 am *Carrier Multiplication and Auger Recombination in Semiconductor Nanocrystals*
Rich Schaller, Los Alamos National Laboratory

10:00 am *Exciton Fine Structure in CdSe Nanocrystals Revealed by Magnetic-Field and Single-Dot Spectroscopies*
Scott Crooker, Los Alamos National Laboratory

10:30 am **** Break ****

11:00 am *Inner-Shell Photoionization and Dissociative Electron Attachment of Small Molecules*
Ali Belkacem, Lawrence Berkeley National Laboratory

11:30 am *Electron Detachment in Ion-Atom Collisions*
Joe Macek, University of Tennessee and Oak Ridge National Laboratory

12:00 noon *Electron-Atom and Electron-Molecule Collision Processes*
Tom Rescigno, Lawrence Berkeley National Laboratory

12:30 pm **** Lunch ****

Session V Chair: **Ann Orel**

4:00 pm *Few-Body Fragmentation Interferometry*
Jim Feagin, California State University, Fullerton
4:30 pm *Resonant and Nonresonant Photoelectron-Vibrational Coupling*
Robert Lucchese, Texas A&M University
5:00 pm *Atomic Ion-Atom and Molecular Ion-Atom Electron Transfer*
Randy Vane, Oak Ridge National Laboratory
5:30 pm *The New Generation of Supermaterials*
Vladimir Tarnovsky, Stevens Institute of Technology

6:00 pm **** Reception (No Host) ****
6:30 pm **** Dinner ****

Wednesday, September 17

7:30 am **** Breakfast ****

Session VI Chair: **Dave DeMille**

8:30 am *Control of Molecular Dynamics: Algorithms for Design and Implementation*
Hersch Rabitz, Princeton University
9:00 am *Dual Quantum Gases of Bosons: Toward Ultracold Polar Molecules*
Chandra Raman, Georgia Tech
9:30 am *X-Ray Probes of Ultrafast Strong-Field Ionization*
Elliot Kanter, Argonne National Laboratory

10:00 am **** Break ****

10:30 am *Nonlinear Photoacoustic Spectroscopies Probed by Ultrafast EUV Light*
Keith Nelson, MIT
11:00 am *Low-energy 2D Electron Momentum Spectra of Atoms by Intense Laser Pulses*
Lew Cocke, Kansas State University
11:30 am *Closing Remarks*
Jeffrey Krause, BES/DOE

11:45 am **** Lunch ****

Table of Contents

Laboratory Research Summaries (by institution)

University Research Summaries (by PI)

Laboratory Research Summaries
(by institution)

AMO Physics at Argonne National Laboratory

R. W. Dunford, E. P. Kanter, B. Krässig, R. Santra, S. H. Southworth, L. Young
Argonne National Laboratory, Argonne, IL 60439

dunford@anl.gov, kanter@anl.gov, kraessig@anl.gov, rsantra@anl.gov,
southworth@anl.gov, young@anl.gov

Control of x-ray processes using intense optical lasers represents an emerging scientific frontier – one which combines x-ray physics with strong-field laser control. While the past decade has produced many examples where phase- and amplitude-controlled lasers at optical wavelengths are used to manipulate molecular motions, the extension to control of ultrafast intraatomic, inner-shell processes is quite new. Gas phase systems are particularly suitable for illustrating the basic principles underlying combined x-ray and laser interactions. Over the past year, we have investigated three scenarios by which strong electromagnetic fields can be used to modify x-ray absorption in a controlled manner: 1) ultrafast optical field ionization at laser intensities in the range of 10^{14}-10^{15} W/cm^2, 2) modification of the electronic structure of inner-shell excited systems by laser dressing at 10^{12}-10^{13} W/cm^2, 3) control of resonant x-ray absorption by molecules through laser-induced spatial alignment at 10^{11}-10^{12} W/cm^2. This work is described in a review article [4].

Our research represents a merging of two scientific areas - optical strong-field and x-ray physics. The advent of the world's first x-ray free electron laser, the Linac Coherent Light Source (LCLS) at Stanford in 2009 pushes this merger to an extreme as the exploration of nonlinear and strong-field phenomena in the x-ray regime becomes accessible for the first time. In preparation, we are investigating phenomena such as sequential multiphoton ionization, hollow atom production and Rabi cycling on resonant x-ray transitions, interatomic Coulombic decay following hard x-ray interaction, as well as assisting in the design of first experiments. Finally, we are strongly engaged in the Short Pulse X-ray Project to produce tunable, polarized 1-ps hard x-ray pulses at high average flux, 10^{13} x rays/s, at Argonne's Advanced Photon Source. Recent progress and future plans are described below.

X-ray absorption and scattering from laser-aligned molecules

E.R. Peterson, C. Buth, D.A. Arms[1], R.W. Dunford, C. Höhr, P. Ho, E. P. Kanter, B. Krässig, E.C. Landahl[1], S.T. Pratt, R. Santra, S.H. Southworth, L. Young

In the presence of a strong nonresonant linearly polarized laser field, molecules align due to interaction of the laser electric field vector with the molecular anisotropic polarizability. The alignment process is of intrinsic interest and of interest in applications to spectroscopy and photophysics, quantum control, high-harmonic generation, chemical reactivity, liquids and solvation, and x-ray structural determination. Molecular alignment is normally probed by additional laser pulses that dissociatively ionize the molecule within an ion spectrometer that projects the fragments onto a position-sensitive detector and displays asymmetric fragmentation patterns. Our approach is different; we employ an x-ray microprobe of an ensemble of aligned molecules, as shown in Fig 1.

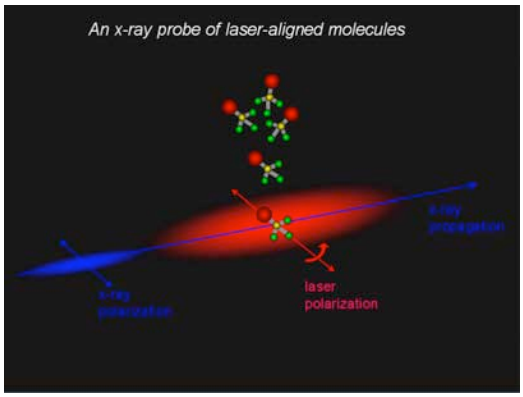

Fig. 1. Schematic of x-ray probe of laser-aligned molecules. Pulsed non-resonant laser fields are required to produce the field strength necessary to align small molecules quasiadiabatically. Microfocused x-ray pulses probe a region of a high degree of alignment. Control over the molecular axis is provided by the laser polarization.

X-ray probing of quasiadiabatically aligned bromotrifluoromethane molecules was demonstrated both experimentally and theoretically in Ref. [2]. After developing in Ref. [3] the theory of resonant x-ray absorption by laser-aligned symmetric-top molecules and applying it to quasiadiabatically aligned bromine molecules, we performed in Ref. [5] a detailed computational study of the rotational molecular dynamics of bromotrifluoromethane (CF_3Br) molecules in the gas phase. We examined resonant x-ray absorption as an accurate tool to study laser manipulation of molecular rotation. For our computations, we determined the dynamic polarizability tensor of CF_3Br using ab initio molecular linear-response theory in conjunction with wave-function models of increasing sophistication: coupled-cluster singles (CCS), second-order approximate coupled-cluster singles and doubles (CC2), and coupled-cluster singles and doubles (CCSD). The rotation was assumed to be manipulated with an offresonant, 800 nm laser. The molecules were treated as rigid rotors. For computational efficiency, we typically used a linear rotor model for CF_3Br, which we compared with selected results for full symmetric-rotor computations. The transition from impulsive to adiabatic alignment, the temperature dependence of the maximally achievable alignment and its intensity dependence were investigated. We examined the impact of the x-ray pulse duration on the signal (particularly its temporal resolution), and studied the temperature dependence of the achievable absorption. Most importantly, we demonstrated that using 1-ps x-ray pulses, one can accurately measure the expectation value of $\cos^2\theta(t)$ for impulsively aligned CF_3Br molecules. This is not possible with the 100-ps x-ray pulses currently available at most third-generation synchrotron radiation sources and is an opportunity for the 1-ps x-ray source to be developed at Argonne's Advanced Photon Source.

The next natural step is to consider elastic x-ray scattering. In Ref. [10], we present the theory of x-ray diffraction from an ensemble of symmetric-top molecules aligned by a short, intense optical laser pulse at finite rotational temperature. Employing quantum electrodynamics, we describe the x-ray/molecule interaction as an electronically elastic one-photon scattering process. We treat the short x-ray pulse as a multi-mode radiation field and examine the effect of its coherence properties. In the practically important case that the x-ray pulse is quasi-monochromatic and its coherence time is much shorter than the time scale of molecular rotational dynamics in the laser field, there is a simple connection between the rotational wave-packet dynamics and the diffraction pattern obtained. Our theory thus opens up a new perspective for quantum molecular imaging using x-ray radiation. An illustrative application to Br_2 is included in Ref. [10]. We have started collaborating with Abbas Ourmazd and Dilano Saldin from the

University of Wisconsin at Milwaukee to retrieve the molecular structure from x-ray diffraction patterns of laser-aligned molecules. Experimentally, we initially used the high-cross section process of x-ray absorption to probe molecular alignment [2]. From those studies, we estimate that by simply increasing the incident x-ray flux 100-fold, as is possible with higher repetition rate alignment lasers, will enable x-ray diffraction imaging. Work toward this goal is proceeding in collaboration with Jun Ye from JILA.

LCLS science: Strong-field AMO physics with x rays

N. Rohringer, R. Santra,
B. Krässig, E. P. Kanter, S. H. Southworth, L. Young

The LCLS construction timeline indicates first light from the FEL into the front experimental hall in May, 2009 with AMO experiments to begin in July, 2009. The first beams will be in the soft x-ray region, 800 - 2000 eV, with estimated pulse parameters ~10^{13} photons/pulse, ~100 fs, 120 Hz. The AMO endstation includes Kirkpatrick-Baez mirrors that will focus the x rays to a ~1 μm spot and produce power densities ~7×10^{18} W/cm^2. In comparison with storage-ring x rays, LCLS pulses will be orders-of-magnitude faster and more intense. The high peak intensity will enable studies of non-linear x-ray processes or of tenuous targets with high signal:background. The short pulse duration will enable ultrafast x-ray probes of systems excited by optical lasers, e.g. impulsively aligned molecules and laser-dressed atoms. A versatile AMO instrument is being designed that will include gas jets, ion, electron, fluorescence spectrometers, and pulse diagnostics [http://wwwssrl.slac.stanford.edu/lcls/AMO.]. Our group has largely focused on initial experiments to observe non-linear x-ray processes as evidenced by absorption of two or more photons from a single x-ray pulse by a single atom or molecule. These processes are of fundamental interest and are relevant to LCLS experiments on macromolecules and materials.

In stark contrast to the long-wavelength regime, x-ray nonlinear optical processes are characterized in general by sequential single-photon single-electron interactions. This dominant interaction process can be characterized by measurement of ion yield as a function of the incident x-ray energy and intensity. Since theoretical calculations are in substantial disagreement, these first measurements will be extremely valuable benchmarks. These multiphoton processes are most easily characterized in helium and neon (a simple target for both experimental and theoretical studies). Our calculations [12] will serve to guide the experiments. A variation in the mechanism of multiphoton ionization is expected as a function of the photon energy due to the opening of new ionization channels. As an example, one can contrast two six-photon absorption processes: at energies below the Ne K threshold, six-photon valence ionization is expected, whereas at energies above the Ne^{9+} ionization threshold another six-photon process (successive photoionization-Auger events) is predicted to produce fully stripped Ne. Intermediate photon energies will cause multiple ionization by different mechanisms. Investigating the photon energy dependence of the ion yield will be important to distinguish sequential versus simultaneous multiphoton absorption. We plan to investigate these phenomena in collaboration with John Bozek, Lou DiMauro, Nora Berrah and other members of the LCLS AMO instrument team.

Hollow atoms, where the inner K-shell is empty and the outer shells are occupied, are formed following x-ray-induced excitation of two K-shell electrons. At low x-ray intensity, hollow atoms are formed purely through electron correlation (between the photoejected electron and its K-shell partner) and the [KK]/[K] yield is ~0.3% [Southworth et al, Phys. Rev. A67, 062712 (2003)]. However, at high x-ray intensities, hollow atom formation can proceed directly through the absorption of two photons – the direct photoionization rate can exceed that of Auger decay which refills the initial K-hole. At x-ray intensities of ~10^{18} W/cm^2 the yield of [KK] can approach unity [12]. Whereas a given ion charge state can be formed through a number of different pathways, a definitive signature of hollow atom formation is the appearance of hypersatellites in the Auger electron emission spectrum. These hypersatellites are shifted significantly upward in energy from the standard "diagram" lines originating from single hole states. Hypersatellites also appear in the x-ray emission spectrum, and this is an alternative method to monitor hollow atom formation. The electron ejection mechanism leading to hollow atoms will leave imprints on the recoil ion momentum which can be monitored via velocity map imaging. These non-linear x-ray processes are affected by the limited longitudinal coherence of the SASE LCLS pulses. We plan to investigate the contrasting expectations in the x-ray regime [12] with those in the optical regime where the chaotic enhancement for N-photon transitions was shown to scale as N-factorial.

After studying non-resonant phenomena as described above as first steps, it is natural to proceed to the study of resonant phenomena. Here one has the potential to use coherent x-ray radiation to control inner-shell electron dynamics. In Ref. [1], we discuss the resonant Auger effect of atomic neon exposed to high-intensity x-ray radiation in resonance with the 1s-3p transition. High intensity here means that the x-ray peak intensity is sufficient (~ 10^{18} W/cm^2) to induce Rabi oscillations between the neon ground state and the $1s^{-1}3p$ (^{1}P) state within the relaxation lifetime of the inner-shell vacancy. For the numerical analysis presented, an effective two-level model, including a description of the resonant Auger decay process, was employed. Both coherent and chaotic x-ray pulses were treated. The latter are used to simulate radiation from x-ray free-electron lasers based on the principle of self-amplified spontaneous emission. Observing x-ray-driven atomic population dynamics in the time domain is challenging for chaotic pulse ensembles. A more practical option for experiments using x-ray free-electron lasers is to measure the line profiles in the kinetic energy distribution of the resonant Auger electron. This provides information on both atomic population dynamics and x-ray pulse properties.

X-ray absorption by laser-dressed atoms

C. Buth, H. R. Varma, L. Pan, D. Beck, R. Santra
A. Belkacem[3], R.W. Dunford, D.L. Ederer[2], T.E. Glover[3], M. Hertlein, E.P. Kanter,
B. Krässig, R.W. Schoenlein[3], S. H. Southworth, L. Young

A longstanding interest of our group has been the modification and control of x-ray processes using strong optical fields. The laser-induced modification of the x-ray photoabsorption cross section is the most basic of processes. In pursuit of this, we have developed an *ab initio* theory for the x-ray photoabsorption cross section of atoms in the field of an intense optical laser (up to 10^{13} W/cm^2) [13]. The laser dresses the core-

excited atomic states, which introduces a dependence of the cross section on the angle between the polarization vectors of the two linearly polarized radiation sources. Calculations of this effect in neon have predicted the phenomenon of electromagnetically induced transparency (EIT) for x-rays on the 1s→3p resonance in neon at 867 eV [14]. Experiments are underway to demonstrate EIT for x rays at Berkeley's Advanced Light Source using the femtosecond laser slicing beamline to produce 200 fs soft x-ray pulses resonant with the 1s→3p transition. Overlap with an 800 nm dressing beam at an intensity of 10^{13} W/cm^2 is predicted to produce a 13x change in the 1s→3p absorption cross section. Beamtimes at the ALS to date have demonstrated the feasibility of the experiment, and identified technical issues that must be resolved, e.g. long term laser/x-ray spatial overlap and a higher precision laser/x-ray timing method.

In pursuit of improved timing methodology for these experiments, at Argonne we have recently measured the intrinsic time response of GaAs MSM photodiodes to x rays and to 800 nm radiation using our x-ray microprobe methodology [26] to overlap focused x-rays and laser pulses to a precision of a few microns. The fast time response of these photodiodes will improve the timing 10-fold over the previous avalanche photodiodes currently used as the beamline standard. At Argonne, improved spatial overlap tools are also being developed. At Berkeley, improved laser power transmission and stability to the experimental endstation and post-target diagnostics are being developed.

In support of the ongoing experiment in Berkeley, we have revisited an uncertainty in the theoretical model we had employed to predict EIT for x rays at the 1s-3p resonance of Ne [14]. Specifically, the magnitude of the laser-induced suppression of the x-ray absorption cross section at the 1s-3p resonance position depends on the energy splitting between the $1s^{-1}3s$ (^1S) and $1s^{-1}3p$ (^1P) states. This energy splitting must not differ from the dressing laser photon energy (1.55 eV) by much more than the 1s Auger width (0.27 eV). The Hartree-Slater model underlying our laser-dressing calculations predicted an energy splitting between the $1s^{-1}3s$ and $1s^{-1}3p$ states of 1.69 eV. There was a concern that if the true splitting were much greater than this, the EIT effect predicted in Ref. [14] would not be observable. In collaboration with us, Lin Pan and Donald Beck (Michigan Technical University) have calculated an accurate value for this energy splitting by doing separate relativistic configuration interaction calculations for the initial and final states. The result is 1.875 eV, which is not quite within one Auger width with respect to the photon energy. Nevertheless, laser-dressing calculations we have performed using this value (by adjusting the energy of the 3s orbital and leaving all other orbital energies unchanged) show that the slightly increased energy separation between the $1s^{-1}3s$ and $1s^{-1}3p$ states has almost no effect on the efficiency of EIT in Ne. One reason for this is that at the necessary laser intensities of 10^{12} W/cm^2 or higher, the core-excited states are not only broadened by Auger decay but also by laser-induced ionization. This effectively increases the resonance window for laser dressing. At 10^{13} W/cm^2, the resonance window is more than 0.5 eV wide.

There were two more issues that Refs. [13,14] had not yet addressed. First, we still had to explain how we had calculated in Ref. [14] the dynamic x-ray polarizability of laser-dressed Ne. Second, it was an open question whether EIT can be extended to harder x rays. We therefore investigated the complex index of refraction in the x-ray regime for laser-dressed atoms [11]. The laser (intensity up to 10^{13} W/cm^2, wavelength 800 nm) modifies the atomic states reached via x-ray absorption, but, by assumption,

does not excite or ionize the atoms in their ground state. Using quantum electrodynamics, we devised an ab initio theory to calculate the dynamic dipole polarizability and the photoabsorption cross section, which were subsequently used to determine the real and imaginary part, respectively, of the refractive index. The interaction with the laser was treated nonperturbatively; the x-ray interaction was described in terms of a one-photon process. We numerically solved the resolvents involved using a single-vector Lanczos algorithm. Finally, we formulated rate equations to copropagate a laser pulse and an x-ray pulse through a gas cell. Our theory was applied to argon. We studied the x-ray polarizability and absorption near the argon K edge (3.2 keV) over a large range of dressing-laser intensities. We found EIT for x rays on the Ar 1s-4p pre-edge resonance. We demonstrated that EIT in Ar allows one to imprint the shape of an ultrafast laser pulse on a 100-ps, 3.2-keV x-ray pulse. Our work thus opens new opportunities for research with hard x-ray sources.

X-ray probes of ultrafast strong-field ionization

E. P. Kanter, R. W. Dunford, D. L. Ederer[2], C. Höhr, B. Krässig, E. C. Landahl[1], E. R. Peterson, N. Rohringer, J. Rudati[1], R. Santra, S. H. Southworth, L. Young

When strong optical lasers are focused on gas-phase atoms and molecules, one necessarily produces a transient plasma when the target atoms are ionized by the laser. This is a common feature of many of our experiments and this has required us to investigate the ensuing ion and electron dynamics following the production of such plasmas.

We recently completed a comprehensive set of measurements investigating the spatial- and time-dependence of the ion distributions for various densities [6]. This work was carried out with both circular and linearly polarized light. This allowed us to explore the dependence of the expansion on the electron velocity distribution resulting from the initial strong-field ionization. We characterized the time evolution of ion spatial distributions in a laser-produced plasma. Krypton ions are produced in strong, linearly- and circularly-polarized optical laser fields (10^{14} - 10^{15} W/cm^2). The Kr^+ ions are preferentially detected by resonant x-ray absorption. Using micro-focused, tunable x rays from the Advanced Photon Source, we measured ion densities as a function of time with 10 μm spatial resolution for times <50 ns. For plasma densities of the order of 10^{14} cm^{-3}, we observe a systematic expansion of the ions outward from the laser focus. We find the expansion timescale to be independent of the plasma density though strongly dependent upon the plasma shape and electron temperature. The former is defined by the laser focus,

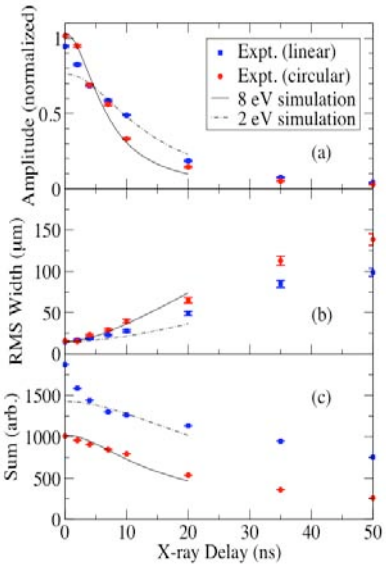

Fig. 2. Central amplitude, RMS width and integral sum of the Kr^+ ion spatial distributions as a function of time following ultrafast field ionization.

while the latter is controlled by the laser polarization state. We have developed a fluid description, assuming a collisionless quasineutral plasma, which is modelled using a particle-in-cell approach. This simulation provides a quantitative description of the observed behavior and demonstrates the role of the very different electron temperatures produced by circularly- and linearly-polarized light. These results demonstrate the utility of this method as an in situ probe of the time and spatial evolution of laser-produced plasmas. Fig. 2 shows various properties of the spatial distributions of the Kr^+ ions for different delays of the x-ray probe from the ionizing laser pulse. The simulated results are shown as lines. With the hotter electron distribution created by the circularly-polarized laser, one observes a faster rate of expansion of the ion cloud which is reproduced by the simulation.

We also performed an extensive set of measurements of the laser-produced alignment in the presence of an external magnetic field as a function of the angle between the laser polarization and the magnetic field. These results clarified our previous findings which had suggested a substantially slower depolarization time with parallel magnetic field than without. Although full analysis is not yet complete, these data have shown that the depolarization is not affected by field orientation. It was found that the presence of transverse field components can give rise to Larmor precession on a timescale which can be confused with depolarization.

With a higher time-resolution probe we may be able to detect coherences formed in ultrafast field ionization. In Refs. [16, 29], we have demonstrated that, at least in the case of Kr and Xe, the laser electric field even at saturation is not sufficiently strong to break spin-orbit coupling. However, our treatment was unsuitable to predict coherences in the density matrix of the residual cation that may be caused by the finite photon energy or the finite duration of the laser pulse. In addition, the ion quantum-state populations extracted from experimental data show good qualitative, but not quantitative agreement with the prediction of the adiabatic (tunneling) approximation [15,16]. This makes a full time-dependent quantum treatment necessary. All shortcomings of the adiabatic approximation can be avoided in this way. Therefore, we have extended the d-SAE method developed in Refs. [25, 33] by including spin-orbit interaction. We have derived the relevant multichannel equations of motion and implemented them in a computer program. This code will be used to investigate whether in the process of optical strong-field ionization, coherences remain in the ion density matrix. For certain reasons, we expect that this will be the case for the light noble gases, but probably not for the heavier ones. If this turns out to be correct, then strong-field-ionized Ne (and maybe Ar) would be an excellent system for studying ultrafast electronic wave-packet dynamics in a time-resolved manner. This work provides theoretical support for a planned experiment of Argonne's AMOP group in collaboration with Lou DiMauro and Pierre Agostini from Ohio State University.

There we plan to study strong-field ionization in an ion with lower Z, Ne^+, where the spin-orbit period (43 fs) is longer than in Kr^+ and the field strength necessary for ionization is higher. Such a measurement will require shorter pump and probe pulses. We intend to use few-cycle infrared pump pulses and few-fs high-harmonic probe pulses produced in the Attosecond Laboratory at Ohio State University. We will measure the $2s \rightarrow 2p$ cycling transition in Ne^+ as a function of the pump probe delay for both parallel and perpendicular polarization directions to search for the characteristic oscillations of

coherently excited quantum states.

Search for Interatomic Coulombic Decay (ICD) Following Hard-X-ray Interactions

S.H. Southworth, R. W. Dunford, D.A. Arms[1], E. M. Dufresne[1], E. P. Kanter, B. Krässig, R. Santra, D. A. Walko[1], L. Young

In general, the absorption of an x-ray by an atom leads to the ejection or excitation of an inner-shell electron, thus creating a vacancy state which sets off a cascade of x-ray and Auger transitions as the atom relaxes. The different possible decay paths lead to a range of possible final charge states. If the cascade occurs in an atom that is part of a molecule or cluster, it can lead to the removal of valence electrons not localized on the central atom and produce two or more charge centers. This is then followed by a Coulomb explosion of the system. The process, termed Interatomic Coulombic Decay (ICD), was recently observed by Morishita, et al. [Phys. Rev. Lett. 96, 243402 (2006)] in experiments on argon dimers. In that work, a 2p hole in one of the Ar atoms decayed via the Auger process into a state with holes in the 3s and 3p subshells of the same atom. This Auger final state sometimes decayed by ICD where another 3p electron fills the 3s vacancy while at the same time one of the 3p electrons of the other atom of the dimer is ejected. This processs was predicted by Cederbaum et al. [Phys. Rev. Lett. 79, 4778 (1987), Phys. Rev. Lett. 90, 153401 (2003)]. Also, Buth, Santra and Cederbaum [J. Chem. Phys. 119, 10575 (2003)] have described interatomic decay processes in xenon fluoride molecules. The main point is that ICD leads to the production of more positive charges per absorbed x-ray photon and boosts damage in materials when they are exposed to x rays. Understanding such fundamental processes therefore has important practical implications. To explore this process, we compared the charge states produced following inner-shell photoionization of Xe and XeF_2. This was the first experiment to explore ICD in the case of deep inner-shell vacancies of a heavy atom of a molecule.

The apparatus used in the experiment is similar to that we used to study vacancy cascades following K-shell photoionization in Kr and Xe atoms [G.B. Armen et al., Phys. Rev. A 69, 062710 (2004)]. Beams of Xe and XeF_2 are crossed at right angles to the incident 35 keV x-ray beam provided by Argonne's Advanced Photon Source (APS). The x-rays photoionize the K-shell of Xe. Photons from the interaction region are observed by a Ge x-ray spectrometer. This detector measures the fluorescence as the inner-shell vacancy decays. The photon also provides the start signal for determining the ion time-of-flight TOF. We get improved timing over what is normally possible with a Ge detector because we can resolve the bunch structure of the APS, identify the particular bunch associated with the event and correct the start time. This allows us to obtain sharp TOF peaks. The photon energy also tags the first step in the cascade decay. A multi-hit position sensitive detector located on the opposite side of the interaction region is used to detect ions. The mass and charge states of the ions are determined by measuring the ion TOF. Using the x-ray energy measured by the Ge detector to tag the initial state, we determine the changes in the ion charge state distributions as a function of the initial hole state.

The data analysis for this experiment is still in progress but some preliminary data are presented in Fig. 3. The figure shows a comparison of the Xe charge state distribution with the distribution of total charge for a subset of XeF_2 events. The subset includes all events in which a triple coincidence was observed involving a F^{2+} ion, a F^{3+} ion, and a

Xe^{q+} ion of charge q. One can see that for this particular subset of events, the center of the XeF_2 total charge distribution is higher than that for the atomic Xe target by more than two charge states. To determine if this shift is due to ICD will require further data analysis and theoretical modeling, but it is an interesting observation.

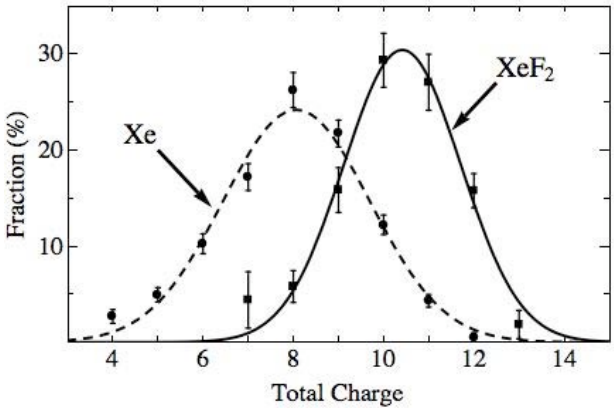

Fig. 3. Total Ionic charge for events in which a Xe Ka x-ray was detected. Solid circles are results obtained with an atomic Xe target and solid squares were obtained using a XeF_2 target. The dashed and solid lines are Gaussian Fits to the data. The XeF_2 data correspond to the total charge measured for triple coincidences in which both a F^{2+} ion and a F^{3+} ion were detected. Data were corrected for pressure effects and ion detection efficiency. These data were obtained with the energy of the x-ray beam set at the center of the K absorption edge of Xe.

Picosecond x rays at Argonne's Advanced Photon Source

B. Krässig, R.W. Dunford, E.P. Kanter, S.H. Southworth, L. Young,
Photosynthesis Group, FOCUS, APS staff

Efforts are underway to shorten the duration of the x-ray pulses produced at Argonne's Advanced Photon Source by a factor of 100 down to about 1 picosecond. This complex project has been named the Short Pulse X ray project (SPX). This will enable researchers from a variety of different fields to study the time evolution of their x-ray irradiated samples on an atomic scale. The bunch shortening will be achieved by rotating the electron bunch in its phase space using a set of deflecting RF cavities, a scheme developed by Zholents et al. [Nucl. Instrum. Meth. A 425, 385 (1999)]. In this scheme the bunch rotation induced by the first cavity is reversed by the second, leaving the beam characteristics outside the section between the two deflecting cavities unaffected. This rf-deflection scheme works well only on high energy storage rings of large diameter.

Work on the realization of short pulse x rays at the APS was begun soon after the workshop "Time Domain Science Using X-ray Techniques" held in 2004. This meeting was part of a series of similar workshops on the Future Scientific Directions for the APS and highlighted the scientific merits of providing such a capability at the APS. Initially, it was envisioned to build a "fast track" system that could be implemented within 2-3 years and with existing funds. This would have been a water-cooled system, pulsed at low repetition rate (<1 kHz), to be operating only during the hybrid-singlet mode of operation of the storage ring (6 weeks/year) and on one beam line. This approach was abandoned because of the prohibitive cost associated with the complex final engineering design produced after three years of R&D, considering also its limited scope and availability. Instead, the APS is now pursuing as part of the APS Renewal a cryogenically cooled system that would be compatible with any of the operational modes (year-round availability) and at the high repetition rate (6.5 MHz) of the storage ring, possibly encompassing more than one beam line. This exciting possibility will create a tunable,

picosecond hard/soft x-ray source with ~10^{13} photons/s in a bandwidth of 1% enabling many applications in x-ray science ranging from AMO science, photochemistry, condensed matter physics and nanoscale materials science.

[1]Advanced Photon Source, Argonne National Laboratory, Argonne, IL 60439
[2]Tulane University
[3]Lawrence Berkeley National Laboratory, Berkeley, CA 94720

Publications 2006 – 2008

[1] Resonant Auger effect at high x-ray intensity
N. Rohringer and R. Santra, Physical Review A **77**, 053404 (2008).
[2] An x-ray probe of laser-aligned molecules
E. R. Peterson, C. Buth, D. A. Arms, R. W. Dunford, E. P. Kanter, B. Krässig, E. C. Landahl, S. T. Pratt, R. Santra, S. H. Southworth, and L. Young, Applied Physics Letters **92**, 094106 (2008).
[3] Theory of x-ray absorption by laser-aligned symmetric-top molecules,
C. Buth and R. Santra, Physical Review A **77**, 013413 (2008).
[4] Strong-field control of x-ray processes
R. Santra, R. W. Dunford, E. P. Kanter, B. Krässig, S. H. Southworth, and L. Young, *Advances in Atomic, Molecular and Optical Physics*, accepted (2008).
[5] Rotational molecular dynamics of laser-manipulated bromotrifluoromethane studied by x-ray absorption
C. Buth and R. Santra, Journal of Chemical Physics, submitted (2008).
[6] Characterization of the Spatiotemporal Evolution of Laser-generated Plasmas
E.P. Kanter, J. Rudati, D.A. Arms, E.M. Dufresne, R.W. Dunford, D.L. Ederer, C. Höhr, B. Krässig, E.C. Landahl, E.R. Peterson, R. Santra, S.H. Southworth, L. Young, Journal of Applied Physics, submitted (2008).
[7] Using strong electromagnetic fields to control x-ray processes
L. Young, C. Buth, R.W. Dunford, P. Ho, E.P. Kanter, B. Krässig, E.R. Peterson, N. Rohringer, R. Santra, and S.H. Southworth, Proceedings of the Pan-American Advanced Studies Institute, Buzios, Brazil, 2008.
[8] Refraction and absorption of x rays by laser-dressed atoms
C. Buth, R. Santra, and L. Young, Proceedings of the Pan-American Advanced Studies Institute, Buzios, Brazil, 2008.
[9] Theory of x-ray diffraction by laser-aligned molecules
P. Ho and R. Santra, Proceedings of the Pan-American Advanced Studies Institute, Buzios, Brazil, 2008.
[10] Theory of x-ray diffraction by laser-aligned molecules
P. Ho and R. Santra, Physical Review A, submitted (2008).
[11] X-ray refractive index of laser-dressed atoms
C. Buth and R. Santra, Physical Review A, submitted (2008).
[12] X-ray nonlinear optical processes using a self-amplified spontaneous emission free-electron laser
N. Rohringer and R. Santra, Physical Review A **76**, 033416 (2007).

[13] Theory of x-ray absorption by laser-dressed atoms
C. Buth and R. Santra, Physical Review A **75**, 033412 (2007).
[14] Electromagnetically induced transparency for x rays
C. Buth, R. Santra, and L. Young, Physical Review Letters **98**, 253001 (2007).
[15] *K*-edge x-ray absorption spectroscopy of laser-generated Kr^{+} and Kr^{2+}
S. H. Southworth, D. A. Arms, E. M. Dufresne, R. W. Dunford, D. L. Ederer, C. Höhr, E. P. Kanter, B. Krässig, E. C. Landahl, E. R. Peterson, J. Rudati, R. Santra, D. A. Walko, and L. Young, Physical Review A **76**, 043421 (2007).
[16] Quantum state-resolved probing of strong-field-ionized xenon atoms using femtosecond high-order harmonic transient absorption spectroscopy,
Z.-H. Loh, M. Khalil, R. E. Correa, R. Santra, C. Buth, and S. R. Leone, Physical Review Letters **98**, 143601 (2007).
[17] Strong-field control of x-ray absorption,
R. Santra, C. Buth, E. R. Peterson, R. W. Dunford, E. P. Kanter, B. Krässig, S. H. Southworth, and L. Young, Journal of Physics: Conference Series **88**, 012052 (2007).
[18] Measurement of the x-ray mass attenuation coefficient and determination of the imaginary component of the atomic form factor of tin of the energy range of 29-60 keV, M. de Jonge, C. Tran, C.T. Chantler, Z. Barnea, B.B. Dhal, D. Paterson, E.P. Kanter, S.H. Southworth, L. Young, M.A. Beno, J. A. Linton and G. Jennings, Physical Review A **75**, 032702 (2007).
[19] A simple short-range point-focusing spatial filter for time-resolved x-ray fluorescence
C. Höhr, E.R. Peterson, E.C. Landahl, D. A. Walko, R.W. Dunford, E.P. Kanter, and L. Young, SYNCHROTRON RADIATION INSTRUMENTATION: Ninth International Conference on Synchrotron Radiation Instrumentation, AIP Conference Proceedings 879, 1226-1229 (2007).
[20] Alignment dynamics in a laser-produced plasma
C. Höhr, E.R. Peterson, J. Rudati, D.A. Arms, E.M. Dufresne, R.W.Dunford, D.L. Ederer, E.P. Kanter, B. Krässig, E.C. Landahl, R.Santra, S.H. Southworth, and L. Young, Phys. Rev. A 75, 011403R (2007).
[21] Double *K*-shell photoionization of silver
E. P. Kanter, I. Ahmad, R. W. Dunford, D. S. Gemmell, B. Krässig, S. H. Southworth and L. Young, Phys. Rev. A **73**, 022708, 1-11 (2006).
[22] Photo double detachment of CN^{-}: electronic decay of an inner-valence hole in molecular anions
R. C. Bilodeau, C. W. Walter, I. Dumitriu, N. D. Gibson, G. D. Ackerman, J. D. Bozek, B. S. Rude, R. Santra, L. S. Cederbaum and N. Berrah, Chem. Phys. Lett. **426**, 237-241 (2006).
[23] Two-photon decay in gold atoms
R. W. Dunford, E. P. Kanter, B. Krässig, S. H. Southworth, L. Young, P. H. Mokler, T. Stöhlker and S. Cheng, Phys. Rev. A **74**, 012504, 1-11 (2006).
[24] Three-step model for high harmonic generation in many-electron systems
R. Santra and A. Gordon, Phys. Rev. Lett. **96**, 073906 (2006).
[25] Role of many-electron dynamics in high harmonic generation
A. Gordon, F. X. Kärtner, N. Rohringer and R. Santra, Phys. Rev. Lett. **96**, 223902

(2006).
[26] X-ray microprobe of orbital alignment in strong-field ionized atoms
L. Young, D. A. Arms, E. M. Dufresne, R. W. Dunford, D. L. Ederer, C. Höhr, E. P. Kanter, B. Krässig, E. C. Landahl, E. R. Peterson, J. Rudati, R. Santra and S. H. Southworth, Phys. Rev. Lett. **97**, 083601 (2006).
[27] Low-energy nondipole effects in molecular nitrogen valence-shell photoionization,
O. Hemmers, R. Guillemin, D. Rolles, A. Wolska, D. W. Lindle, E. P. Kanter, B. Krässig, S. H. Southworth, R. Wehlitz, B. Zimmermann, V. McKoy and P. W. Langhoff, Phys. Rev. Lett. **97**, 103006 (2006).
[28] Why complex absorbing potentials work : a DVR perspective,
R. Santra, Phys. Rev. A **74**, 034701 (2006).
[29] Spin-orbit effect on strong-field ionization of krypton,
R. Santra, R. W. Dunford and L. Young, Phys. Rev A **74**, 043403 (2006).
[30] X-ray microprobe of optical strong-field processes,
L. Young, R. W. Dunford, C. Höhr, E. P. Kanter, B. Krässig, E. R. Peterson, S. H. Southworth, D. L. Ederer, J. Rudati, D. A. Arms, E. R. Dufresne and E. C. Landahl, Radiat. Phys. Chem. **75**, 1799 (2006).
[31] Double *K*-photoionization of heavy atoms,
E. P. Kanter, R. W. Dunford, B. Krässig, S. H. Southworth and L. Young, Radiat. Phys. Chem. **75**, 1529 (2006).
[32] Nondipole asymmetries of *K*-shell photoelectrons of Kr, Br_2, and $BrCF_3$,
S. H. Southworth, R. W. Dunford, E. P. Kanter, B. Krässig, L. Young, L. A. LaJohn and R. H. Pratt, Radiat. Phys. Chem. **75**, 1574 (2006).
[33] Configuration-interaction-based time-dependent orbital approach for ab initio treatment of electronic dynamics in a strong optical laser field
N. Rohringer, A. Gordon, and R. Santra, Phys. Rev. A **74**, 043420 (2006).
[34] Higher-order processes in x-ray photoionization of atoms,
E. P. Kanter, R. W. Dunford, B. Krässig, S. H. Southworth and L. Young, Radiat. Phys. Chem. **75**, 2174 (2006).
[35] Coster-Kronig transition probability f_{23} in gold atoms,
R. W. Dunford, E. P. Kanter, B. Krässig, S. H. Southworth, L. Young, P. H. Mokler, T. Stöhlker, S. Cheng, A. G. Kochur and I. D. Petrov, Phys. Rev. A **74**, 062502 (2006).
[36] Imaging molecular orbitals using photoionization,
R. Santra, Chem. Phys. **329**, 357 (2006).
[37] Interaction of intense vuv radiation with large xenon clusters,
Z. B. Walters, R. Santra and C. H. Greene, Phys. Rev. A **74**, 043204 (2006).

J.R. MACDONALD LABORATORY - OVERVIEW 2008

The J.R. Macdonald Laboratory focuses on the interaction of intense-laser pulses with matter. The targets include neutral single atoms and molecules in the gas phase, single ions in our accelerator beams, trapped atoms in our MOTRIMS systems, and nanostructures. In addition we pursue several outside collaborations at other facilities and with other groups (e.g., ALS, ALLS, Århus, Auburn University, University of Colorado, Columbia University, FLASH, LCLS, Max-Planck Institutes for Quantum Optics (MPQ) and Kernphysik (MPI-K), Sao Carlos, Tokyo, Weizmann Institute of Science). Most of the laser work is associated with one or more of the following themes[1]:

1) **Attosecond physics:** The ultimate goal of this work is to follow, in real time, electronic motion in atoms and molecules. We have developed a double optical gating method (polarization gating combined with second harmonics) which greatly increases the efficiency with which single attosecond pulses can be generated. EUV/infrared pump-probe experiments are being carried out. These measurements can also be used as diagnostics for the attosecond pulses. Theoretical analyses of EUV/EUV pump-probe experiments have shown that highly correlated electron motion in atoms can be probed with attosecond pulse pairs. The general role of electron extraction and rescattering, including harmonic generation and elastic scattering, has been investigated both theoretically and experimentally, leading to the recent observation of back rescattering ridges (BRR) in the above threshold ionization (ATI) spectra.

2) **Time-resolved dynamics of heavy-particle motion in neutral molecules:** We continue to develop methods for following the evolution of heavy particle motion in simple molecules in real time, following excitation by short laser pulses. On the theory side, this involves including nuclear vibration and rotation in addition to the electron excitation as part of the quest for a more complete theoretical description of atoms and molecules in strong fields. Methods to extract the ro-vibrational dynamics and the dressed potential energy surfaces have been explored. Experimentally, we have identified rotational wave packet revivals in molecular H_2 and D_2 and have investigated the time evolution of N_2. We have studied the wavelength dependence of dissociative ionization of H_2 and ionization of Ne and Ar.

3) **Control:** Methods for controlling the motion of heavy particles in small molecules continue to be developed. Theoretically, the ability to control the dissociation of molecules (e.g., H_2^+) into different final channels has been investigated by the application of pulse pairs or carrier-envelop phase (CEP) control. Experimentally, we have demonstrated the ability to control the final above threshold dissociation (ATD) state of H_2^+ and D_2^+ via the pulse duration and the final product of ND^+ dissociation via the peak intensity. Molecular alignment by laser pulses is being explored. The use of MOTRIMS to analyze in real time the evolution of population distributions in laser-pumped targets has been extended to associative ionization. Short, shaped (chirped) pulses from the Kansas light source (KLS), which present a broad range of frequencies whose relative phases are known, are being used to explore mechanisms for the latter process.

---

[1]Details of the projects are provided in the individual contributions of the PIs:
I. Ben-Itzhak, Z. Chang, C.L. Cocke, B.D. DePaola, B.D. Esry, V. Kumarappan, C.D. Lin, I.V. Litvinyuk and U. Thumm.

4) **Studies involving simultaneous use of laser and accelerators:** Ionization and dissociation of H_2^+, D_2^+, and N_2^+ has been investigated using the ion beams from our ECR source. New mechanisms for these processes have been identified using the momentum distributions from the products. Recently, we extended these studies to simple polyatomic molecules and conducted the first measurements of D_3^+ dissociation and ionization. Development of short ion (picosecond) pulses from our Tandem accelerator continues.

5) **Photons from the KLS interacting with solids and clusters:** Electron dynamics in photo-ionization and excitation of nanotubes continues mainly in collaboration with Professor T. Heinz from Columbia University. Theoretical investigation of neutralization of negative ions near surfaces has been carried out.

In addition to the laser related research, we are conducting some collision studies using our high and low energy accelerators. Some of this work is conducted in collaboration with visiting scientists (for example, S. Lundeen, J. Shinpaugh, E. Wells).

Finally, it is hard to summarize this year without mentioning the impact on our work of the tornado that hit Kansas State University in mid June (see http://jrm.phys.ksu.edu/). The physics department was not spared and, although we are up and running again, we are still feeling the impact of that storm – for example, the physics building has been closed recently for a few days due to an asbestos contamination. On the positive side no one was harmed, and in a short while everything will be back to normal.

Structure and Dynamics of Atoms, Ions, Molecules, and Surfaces:
Molecular Dynamics with Ion and Laser Beams

Itzik Ben-Itzhak, J. R. Macdonald Laboratory, Kansas State University
Manhattan, Ks 66506; ibi@phys.ksu.edu

The goal of this part of the JRML program is to study the different mechanisms for molecular dissociation initiated by ultrashort intense laser pulses or following fast or slow collisions. To that end we typically use molecular ion beams as the subject of our studies.[1]

A couple of examples are given below.

Dissociation and ionization of N_2^+ & ND^+ by intense few-cycle laser pulses, *J. McKenna, A.M. Sayler, B. Gaire, Nora G. Johnson, E. Parke, K.D. Carnes, B.D. Esry, and I. Ben-Itzhak*

The goal for this project was to expand the knowledge we have gained from a close collaboration between theory and experiment on H_2^+ studies to more complex molecules and identify their dissociation and ionization pathways, mechanisms and control parameters.

High kinetic energy release (KER) in N_2^+ breakup – Extensive laser-molecule interrogation of the hydrogen molecular ion and other small molecules [1] continues to unveil new surprises (see, e.g., [2] & Pub. #6,16), helping to generate a more complete view of molecular dynamics. Recently we observed a surprising high KER peak in the dissociation spectrum of an N_2^+ molecular ion beam exposed to an intense few cycle laser pulse, in addition to the previously observed low KER peak (e.g. [3]). This observation is made possible in our experimental technique as both the neutral and charged fragments are detected in coincidence, while in previous studies it would be obscured by N^+ fragments from N_2^{2+} dissociation that have similar energy. Another unexpected phenomenon is that the KER distribution of the $N^+ + N^+$ ionization channel extends well beyond the energy expected for direct ionization of N_2^+ as shown in Fig. 1. We suggest that the high KER in both cases is due to dissociation on steep repulsive potentials of N_2^+, also shown in Fig. 1. For the ionization, which most likely occurs when the N_2^+ has stretched by more than 1 a.u., that implies almost equal contributions to the KER gained by the dissociating molecule before its ionization at large *R* as well as after.

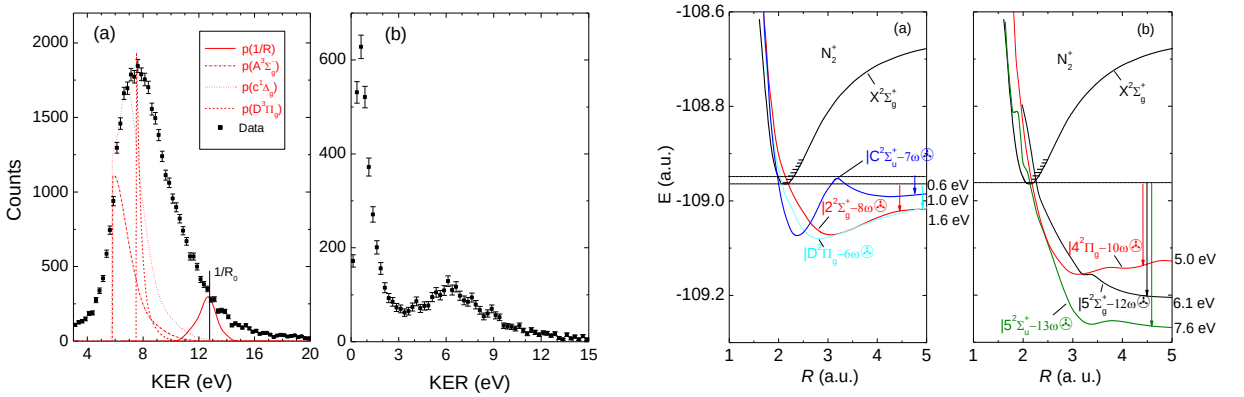

Figure 1 (adapted from Ref. [4]). *Left*: KER spectrum for (a) ionization and (b) dissociation of an N_2^+ beam by a 6×10^{15} W/cm^2, 7 fs laser pulse. A new high-KER peak appears in addition to the previously observed low KER dissociation [3]. Note also the high KER following ionization. *Right*: Dressed-states diabatic picture of N_2^+ (potential energy curves have been reproduced from Ref. [5,6]) illustrating dissociation pathways that lead to (a) low- and (b) high-KER dissociation.

[1]Some of our studies are done in collaboration with *Z. Chang's* group, *C.W. Fehrenbach*, and others.

Controlling the dissociation branching ratio of ND^+ – Laser-induced dissociation of ND^+ was measured as a function of peak intensity. This molecular ion has an interesting alternating sequence of dissociation limits to $N^+ + D$ and $N + D^+$ separated by less than the photon energy at 795 nm wavelength. By exposing the ND^+ beam to a 40 fs laser pulse and measuring the ion fragments in coincidence with the neutral fragments, we find that the branching ratio of the final dissociation channel depends strongly on intensity in the range 2×10^{13}–3×10^{15} W/cm^2 as shown in Fig. 2. Therefore, the peak intensity can serve as a control knob for ND^+ dissociation [Pub. #15].

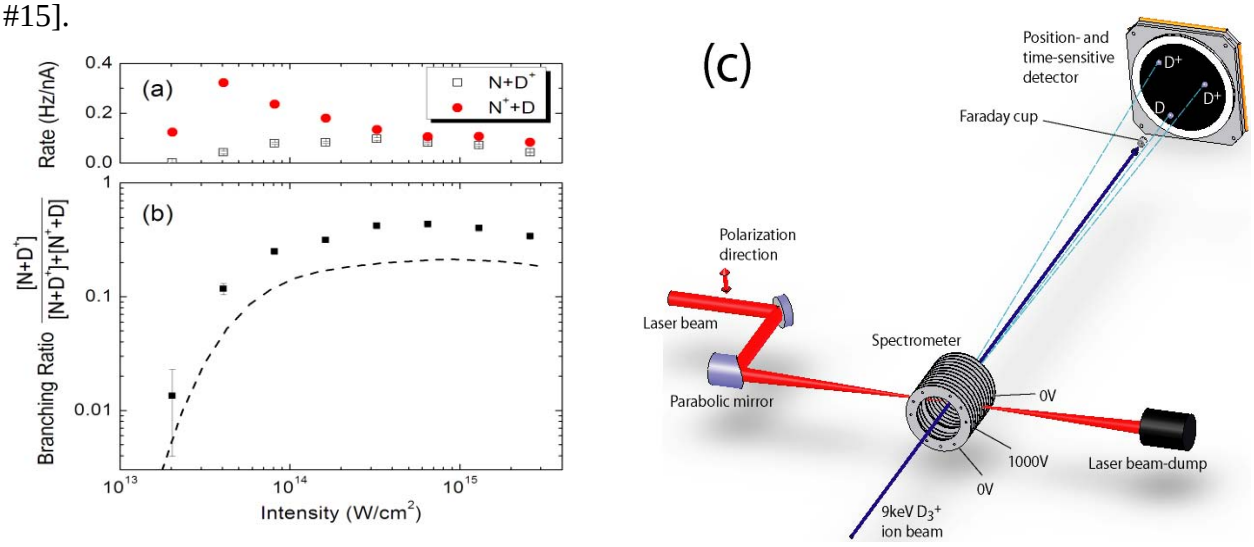

Figure 2. *Left*: (adapted from Pub. #15) (a) Rates for the $N + D^+$ **(**squares) and $N^+ + D$ (circles) dissociation channels as a function of intensity, normalized to the ion-beam current. (b) Branching ratio for dissociation of the $N + D^+$ channel. The dashed curve is a lower limit estimate of the absolute value of this ratio allowing for Faraday cup losses and detection efficiency. *Right*: (adapted from ICOMP-08 invited abstract) (c) Schematic view of the experimental setup used for 3-body molecular dissociation imaging.

Dissociation and ionization of H_3^+, the simplest polyatomic molecule, by intense ultrashort laser pulses – *J. McKenna, A.M. Sayler, B. Gaire, Nora G. Johnson, K.D. Carnes, B.D. Esry, and I. Ben-Itzhak*

The goal for this project was to expand the knowledge we have gained from H_2^+ *studies to more complex molecules and identify their dissociation pathways and mechanisms.*

The bench mark system on the road to better understanding of polyatomic molecules in intense ultrashort laser fields is the two-electron H_3^+ ion. This molecular ion is a challenge to theorists as it is just beyond their current capabilities. However, providing bench mark results to motivate such cutting edge calculations have eluded experimentalists probing molecules with intense few-cycle laser pulses.

Some of the interesting questions one may ask involve the competition between two-body dissociation, $H^+ + H_2$ or $H + H_2$, and complete three-body disintegration, $H^+ + H + H$. This question is also relevant for single ionization of H_3^+, specifically, which of the following outcomes are more likely, $H^+ + H_2^+$ or $H^+ + H^+ + H$? In addition, the unique geometry of this molecular ion, an equilateral triangle in its electronic ground state, introduces some interesting questions about the angular distribution of the dissociating fragments with respect to the laser polarization.

Recently, we conducted coincidence 3D momentum imaging measurements of the dissociation and ionization of a few keV D_3^+ beam target. This isotope was selected over the lighter H_3^+ to avoid overlapping contributions to the two-body breakup channels from the HD^+ contaminant beam. The molecular dissociation imaging technique used for these measurements is in most parts similar to the one used in our previous work on H_2^+ (Ref. [7] and Pub. #7,12,13, 16), except that up to three fragments were measured in coincidence. Briefly, a beam of D_3^+ is crossed with an intense laser beam and the dissociating fragments are imaged on a detector. From the position and time information the momenta of all dissociating fragments of each molecule is determined. The intensity of the 790 nm, 7-40 fs, 1 kHz (linearly polarized) laser pulses spanned the 10^{13}-10^{16} W/cm^2 range in our measurements.

The kinetic energy release (KER) upon dissociation and the angular distributions are determined from the measured momentum information. The three-body breakup in particular provides information about the likelihood of dissociation and ionization as a function of the angle between the molecular plane and the laser polarization. In addition, these processes depend on the angle between the laser field component within the molecular plane and the velocity of a single fragment.

The H_3^+ isotopes have the same electronic structure within the Born-Oppenheimer approximation, but different nuclear wave-packet propagation speeds. This may lead to some isotopic dependencies, which will be investigated next.

In addition to the projects described in some detail above, we have studied a few other molecular-ion beams with our short-pulse laser. Furthermore, we have conducted a few ion-molecule collision experiments [see, for example, Pub. #10,14]. A main effort along this line was the development of an experimental setup for the study of dissociative capture (DC) and collision induced dissociation (CID) in slow (a few keV) collisions. We are conducting our first kinematically complete measurements of H_2^+ + Ar/He at 3 and 4 keV collision energy at this time. Analysis of this incoming data is needed to shed light on the intriguing preliminary results.

Future plans: We are in the process of analyzing recent measurements of molecular-ion beams interrogated by intense few cycle pulses. We will continue interrogating H_2^+ beams with shorter pulses and will attempt to measure the predicted effects of the carrier envelop phase (CEP) on HD^+ laser induced dissociation [8], once we complete the upgrade of our experimental apparatus. Finally, we plan to pursue our most recent kinematically-complete studies of DC and CID in slow collisions between simple molecular ions and atomic targets.

References:

1.J.H. Posthumus, Rep. Prog. Phys. **67**, 623 (2004); and references therein.
2. A. Staudte *et al*., Phys. Rev. Lett. **98**, 073003 (2007).
3. J.P. Nibarger, S.V. Menon, and G.N. Gibson, Phys. Rev. A **63**, 053406 (2001).
4. B. Gaire *et al*., Phys. Rev. A (2008) - submitted.
5. H.T. Aoto *et al*., J. Chem. Phys. **124**, 234306 (2006).
6. A. Ehresmann *et al*., J. Phys. B **39**, 283 (2006).
7. I. Ben-Itzhak *et al*., Phys. Rev. Lett. **95**, 073002 (2005).
8. V. Roudnev, B.D. Esry, and I. Ben-Itzhak, Phys. Rev. Lett. **93**, 163601 (2004).

Publications of DOE sponsored research in the last 3 years:

17. "Molecular ion beams interrogated with ultrashort intense laser pulses", I. Ben-Itzhak, *Progress in Ultrafast Intense Laser Science* IV, edited by *Kaoru Yamanouchi* and *Andreas Becker* (Springer Book Series Chemical Physics 2007) – **accepted**.

16. "Enhancing high-order above-threshold dissociation of H_2^+ beams with few-cycle laser pulses", J. McKenna, A.M. Sayler, F. Anis, B. Gaire, Nora G. Johnson, E. Parke, J.J. Hua, H. Mashiko, C.M. Nakamura, E. Moon, Z. Chang, K.D. Carnes, B.D. Esry, and I. Ben-Itzhak, Phys. Rev. Lett. **100**, 133001 (2008); and *Virtual Journal of Ultrafast Science* **7** (May 2008), at http://www.vjultrafast.org.
15. "Measuring the dissociation branching ratio of heteronuclear ND^+", J. McKenna, A.M. Sayler, B. Gaire, Nora G. Johnson, E. Parke, K.D. Carnes, B.D. Esry, and I. Ben-Itzhak, Phys. Rev. A **77**, 063422 (2008).
14. "Soft fragmentation of carbon monoxide by slow highly charged ions", E. Wells, T. Nishide, H. Tawara, K.D. Carnes, and I. Ben-Itzhak, Phys. Rev. A **77**, 064701 (2008).
13. "Ionization and dissociation of molecular ion beams caused by ultrashort intense laser pulses", I. Ben-Itzhak, A.M. Sayler, P.Q. Wang, J. McKenna, B. Gaire, Nora G. Johnson, M. Leonard, E. Parke, K.D. Carnes, F. Anis, and B.D. Esry, Journal of Physics: Conference Series **88**, 012046 (2007).
12. "Determining intensity dependence of ultrashort laser processes through focus *z*-scanning intensity-difference spectra: application to laser-induced dissociation of H_2^+", A.M. Sayler, P.Q. Wang, K.D. Carnes, and I. Ben-Itzhak, J. Phys. B **40**, 4367 (2007).
11. "Picosecond Ion pulses from an EN tandem created by a femtosecond Ti:sapphire laser", K.D. Carnes, C.L. Cocke, Z. Chang, I. Ben-Itzhak, H.V. Needham, and A. Rankin, Nucl. Instrum. Methods B **261**, 106 (2007).
10. "Systematic study of charge state and energy dependence of TI to SC ratios for F^{q+} ions incident on He", R. Ünal, P. Richard, I. Ben-Itzhak, C.L. Cocke, M.J. Singh, H. Tawara, and N. Woody, Phys. Rev. A **76**, 012710 (2007).
9. "Determining laser-induced dissociation pathways of multi-electron diatomic molecules: application to the dissociation of O_2^+ by high intensity ultrashort pulses", A.M. Sayler, P.Q. Wang, K.D. Carnes, B.D. Esry, and I. Ben-Itzhak, Phys. Rev. A **75**, 063420 (2007); and *Virtual Journal of Ultrafast Science* 6 (July 2007), at http://www.vjultrafast.org.
8. "Determining the absolute efficiency of a delay line microchannel-plate detector using molecular dissociation", B. Gaire, A.M. Sayler, P.Q. Wang, Nora G. Johnson, M. Leonard, E. Parke, K.D. Carnes, and I. Ben-Itzhak, Rev. Sci. Instrum. **78**, 024503 (2007).
7. "Dissociation of H_2^+ in intense femtosecond laser fields studied by coincidence three-dimensional momentum imaging", P.Q. Wang, A.M. Sayler, K.D. Carnes, J.F. Xia, M.A. Smith, B.D. Esry, and I. Ben-Itzhak, Phys. Rev. A **74**, 043411 (2006); and *Virtual Journal of Ultrafast Science* **5** (November 2006), at http://www.vjultrafast.org.
6. "Above threshold Coulomb explosion of molecules in intense laser pulses", B.D. Esry, A.M. Sayler, P.Q. Wang, K.D. Carnes, and I. Ben-Itzhak, Phys. Rev. Lett. **97**, 013003 (2006); and *Virtual Journal of Ultrafast Science* **5** (August 2006), at http://www.vjultrafast.org..
5. "Preference for breaking the O-H bond over the O-D bond following HDO ionization by fast ions", A.M. Sayler, M. Leonard, K.D. Carnes, R. Cabrera-Trujillo, B.D. Esry, and I. Ben-Itzhak, J. Phys. B **39**, 1701 (2006).
4. "Measurement of alignment dependence in single ionization of hydrogen molecules by fast protons", Nora G. Johnson, R.N. Mello, Michael E. Lundy, J. Kapplinger, Eli Parke, K.D. Carnes, I. Ben-Itzhak, and E. Wells, Phys. Rev. A **72**, 052711 (2005).
3. "One- and two-electron processes in collisions between hydrogen molecules and slow highly charged ions", E. Wells, K.D. Carnes, H. Tawara R. Ali, E.Y. Sidky, C. Illescas, and I. Ben-Itzhak, Nucl. Instrum. and Methods B **241**, 101 (2005).
2. "Proton-carbon monoxide collisions from 10 keV to 14 MeV", I. Ben-Itzhak, E. Wells, Vidhya Krishnamurthi, K.D. Carnes, N.G. Johnson, H.D. Baxter, D. Moore, K.M. Bloom, B.M. Barnes, and H. Tawara, Phys. Rev. A **72**, 022726 (2005).
1. "Dissociation and ionization of H_2^+ by ultrashort intense laser pulses probed by coincidence 3D momentum imaging", I. Ben-Itzhak, P.Q. Wang, J.F. Xia, A.M. Sayler, M.A. Smith, K.D. Carnes, and B.D. Esry, Phys. Rev. Lett. **95**, 073002 (2005); and *Virtual Journal of Ultrafast Science* **4** (September 2005), at http://www.vjultrafast.org.

Double optical gating for attosecond pulse generation

Zenghu Chang
J. R. Macdonald Laboratory, Department of Physics,
Kansas State University, Manhattan, KS 66506, chang@phys.ksu.edu

The goals of this aspect of the JRML program are (1) to study a new gating method for generating single isolated attosecond pulses with multi-cycle lasers, (2) to develop carrier-envelope phase stabilization technologies.

1. Double optical gating, *Hiroki Mashiko, Steve Gilbertson, Chengquan Li, Eric Moon, and Zenghu Chang.* Single isolated attosecond pulses are powerful tools for studying electron dynamics in atoms and molecules. Such XUV pulses, as short as 80 as, have been generated by using 3.3 fs lasers. However, it is still a technical challenge to reproduce such laser pulses daily. We developed a double optical gating (DOG) technique for generating single isolated attosecond pulses with multi-cycle pump lasers [1-4].

The double optical gating is a combination of the two-color gating and the polarization gating (PG) and. When a weak second harmonic field is added to break the symmetry of the pump field, one attosecond pulse is produced every full fundamental light cycle, which is the two-color gating. The polarization gating is based on the fact that XUV attosecond pulses can only be efficiently generated with a linearly polarized laser field [5, 6]. The required laser field can be generated by superimposing a left-hand circularly polarized pulse to a time-delayed right-hand circularly polarized pulse. The field with a time-dependent ellipticity can be resolved into a driving field and a gating field, as shown in Fig. 1. The high harmonics are generated by the driving field but are suppressed by the gating field. During the time range where the time-dependent ellipticity is less than 0.2, the suppression power is so weak that high harmonics can be efficiently generated. This time range is called the polarization gate. Two requirements must be met to generate single isolated attosecond pulses with the double optical gating. First, the polarization gate width should be shorter than one optical cycle (2.5 fs for Ti:Sapphire laser). Second, the target atom should not be fully ionized by the laser field before the polarization gate. The DOG allows a wider gate than the polarization gating, which significantly reduces the depletion of the ground state population. The longest pulses one can use for generating single attosecond pulses with DOG are ~12 fs.

The DOG was demonstrated with a carrier-envelope (CE) phase stabilized chirped pulse amplifier followed by a hollow-core fiber compressor. The laser produces 25 fs, 2.5 mJ pulses centered at 790 nm at 1 kHz [7]. The slow drift from the amplifier was compensated by feedback control of the grating separation [8]. The output beam from the hollow-core fiber/chirped mirrors was incident onto a nonlinear crystal for the second harmonic generation. The double gating laser field was synthesized in a Mach-Zehnder interferometer. The second harmonic and fundamental beams were separated by a dichroic beam splitter. The fundamental arm was equipped with a PZT delay stage to stabilize the relative delay by using a CW laser beam propagating inside the interferometer as feedback. The PG pulse was produced by a birefringent quartz plate and an achromatic quarter-wave plate. These conditions yielded a calculated polarization gate width of ~2 fs. The SH and the PG field are combined by another beam splitter. After the interferometer, we measured the pulse duration of the fundamental to be 9.1 fs. The

laser field components under these conditions are as shown in Fig. 1.The DOG laser beams were focused by a spherical mirror to an argon gas filled interaction cell. The generated harmonics were measured with a grating spectrometer.

The dependence of the high harmonic spectrum and intensity on the CE phase of the DOG laser was investigated. The CE phase was varied by controlling the effective grating separation in the laser system [9-11]. The harmonic spectra are shown in fig. 2(a) and were measured simultaneously with the CE phase measurement. The intensity of the normalized spectrally integrated signal repeats with a period of 2π, as shown in fig. 2(b). This is consistent with the predictions from the numerical simulations [2], also shown for comparison. This 2π periodic dependence of the harmonic spectra on the CE phase provides strong evidence that the observed XUV supercontinuum is from DOG. We also observed harmonics from neon gas using a collinear setup for the DOG [3]. It was constructed by two birefringent quartz plates and a barium borate crystal. The first plate thickness sets the polarization gate width to 2.5 fs, i.e. one optical cycle. The second quartz plate and the BBO work together to serve as a quarter wave plate and convert the two pulses from the first quartz plate into a PG pulse. The main feature of the spectrum is the cutoff and plateau regions combine to form a smooth distribution covering more than 20 nm. The spectrum is capable of supporting a 130 as duration.

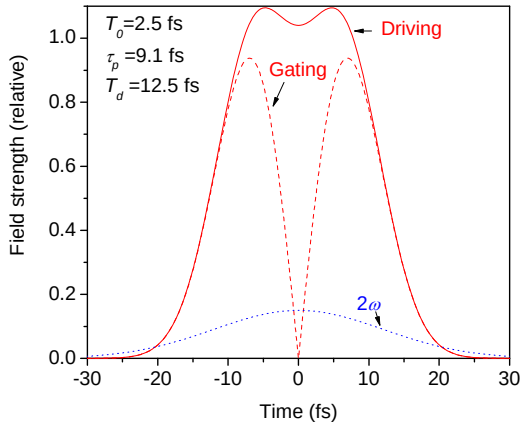

Fig.1. The laser field components for double optical gating. The driving and gating fields are orthogonally polarized. The *2ω* field is polarized along the driving field.

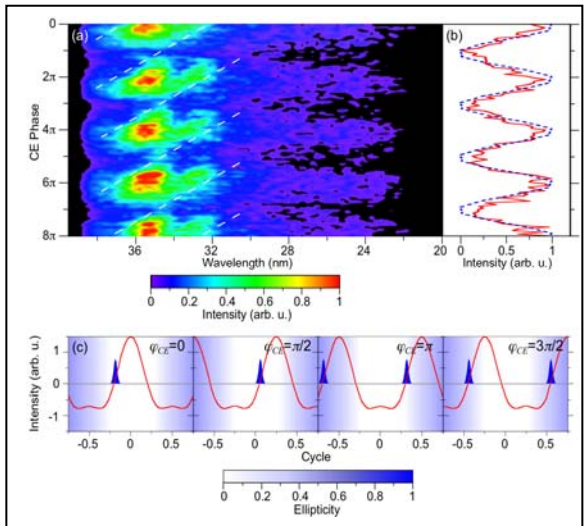

Fig.2. Dependence of the double optically gated high harmonic spectra on the carrier-envelope phase of the laser.

We searched the phase-matching conditions for high harmonic generation with the double optical gating [4]. We chose 8 fs to increase the field strength ratio between the driving field inside the polarization gate to that of the outside, in order to suppress the unwanted ionization of the atom by the leading edge of the DOG fields. At the optimized gas target location and pressure, the single XUV pulse energy is 6.5 nJ for argon and 170 pJ for neon, which are much higher than those generated with conventional polarization gating. In addition, the carrier-envelope phase effects with a 2π periodicity were attained when the highest extreme ultraviolet photon flux was produced, indicating the robustness of the double optical gating.

2. Carrier-envelope phase stabilization, *Chengquan Li, Eric Moon, He Wang, Hiroki Mashiko, Steve Gilbertson, and Zenghu Chang.* To generate single isolated attosecond pulses, the carrier-envelope (CE) phase φ_{CE} of the femtosecond pulse, which can be described by an electric field $E(t)=E_0(t)\cos(\omega_0 t+\varphi_{CE})$ must be stabilized and controlled. Previously, the CE phase stabilized laser pulses were generated from prism-based chirped pulse amplification (CPA) laser systems, where the pulse energy was limited by the prism material itself. On the other hand, grating-based CPA lasers can generate femtosecond pulses with much higher power than material-based laser systems. We have demonstrated that the CE phase of a grating-based CPA system could be stabilized by feedback controlling the effective grating separation in a *stretcher* [9, 11]. However, for some stretcher designs, implementation of this technique might be difficult if the size of the controllable optic in the stretcher is much larger and heavier than that in the compressor. Thus, it is beneficial to translate the smaller optics in the *compressor* to reduce the response time and to stabilize the CE phase.

The laser system, the Kansas Light Source (KLS), was used for demonstrating the CE phase locking with gratings in the compressor [11, 12]. It consists of two multi-pass amplifiers sharing one oscillator and one grating-based stretcher. The laser is designed for synthesizing two amplified pulses in the future, which will require locking the CE phase of the two amplifiers simultaneously and independently. It cannot be accomplished by controlling the dispersion in the shared stretcher because the phase error introduced by the two amplifiers is not the same. For this application, it is highly desirable to lock the CE phase through feedback control of the grating separation in the compressor. The CE phase offset frequency of the oscillator was stabilized by using a standard Mach-Zehnder *f*-to-2*f* interferometer [13]. Pulses from the oscillator with the same CE phase were selected by a Pockels cell for amplification at a repetition rate of 1 kHz and sent to the stretcher. The seed pulses had ~100 nm bandwidth centered at 800 nm and were stretched to ~80 ps. The stretched pulses were amplified to 5 mJ (named as KLS1). The output energy was stabilized to reduce the error of the CE phase measurements caused by the laser energy fluctuation [14, 15].

A small portion (3%) of the amplified beam was split in front of the grating compressor of KLS1. This beam was used as the seed for another liquid nitrogen cooled 7-pass Ti:Sapphire amplifier (named as KLS2), which yielded 2 mJ pulses after amplification. The amplified pulses were compressed by a grating-pair compressor to 38 fs with 1 mJ energy. In the compressor, one of the gratings was mounted on a piezoelectric transducer (PZT) stage for the KLS2 CE phase stabilization. In order to stabilize the CE phase of the laser pulses of KLS2, the output of the *f*-to-2*f* interferometer served as the error signal for feedback controlling the compressor grating separation. The phase was stabilized over 270 seconds with a 230 mrad RMS error. This residual error is at the same level as the one in KLS1 when the grating separation in the *stretcher* was used to compensate the phase drift [10]. The locking time is determined by the phase locking condition of the oscillator. We locked the CE phase of KLS2 over 30 minutes before the oscillator CE phase locking was lost. The phase stability is as good as that obtained by controlling the grating separation in the stretcher.

We have participated in studying dynamics in molecules (lead by Ben-Itzhak) [16], nanotubes (lead by Richard) [17, 18], and x-ray lasers (lead by Rocca at Colorado State University) [19]. We also worked on accelerating ultrashort ion pulses [20].

PUBLICATIONS (2006-2008) (Publications in 2005 are not included due to the limited space):

1. H. Mashiko, S. Gilbertson, C. Li, S. D. Khan, M. M. Shakya, E. Moon, and Zenghu Chang, "Double optical gating of high-order harmonic generation with carrier-envelope phase stabilized lasers," Phys Rev. Lett. **100**, 103906 (2008).
2. Z. Chang, "Controlling attosecond pulse generation with a double optical gating," Phys. Rev. A **76**, 051403(R) (2007).
3. S. Gilbertson, H. Mashiko, C. Li, S. D. Khan, M. M. Shakya, E. Moon, and Zenghu Chang, **"**A low-loss, robust setup for double optical gating of high harmonic generation," Appl. Phys. Lett. **92**, 071109 (2008).
4. H. Mashiko, S. Gilbertson, C. Li, E. Moon, and Zenghu Chang, "Optimizing the photon flux of double optical gated high-order harmonic spectra," Phys. Rev. A **77**, 063423 (2008).
5. M. M. Shakya, S. Gilbertson, H. Mashiko, C. Nakamura, C. Li, E. Moon, Z. Duan, J. Tackett, Zenghu Chang, "Carrier envelope phase effects on polarization gated attosecond spectra," Proc. SPIE Int. Soc. Opt. Eng. **6703**, 67030 (2007).
6. S. Ghimire, X. Feng, and Zenghu Chang, "Measurement of attosecond XUV pulses generated with polarization gating by two-dimensional photoelectron spectroscopy," Proc. SPIE Int. Soc. Opt. Eng. **6703**, 67030 (2007).
7. B. Shan, C. Wang and Zenghu Chang, "High peak-power kilohertz laser systems employing singe-stage multi-pass amplification", U. S. Patent No. 7,050,474, issued on May 23, 2006.
8. H. Mashiko, C. M. Nakamura, C. Li, E. Moon, H. Wang, J. Tackett, and Zenghu Chang, "Carrier-envelope phase stabilized 5.6 fs, 1.2 mJ pulses," Appl. Phys. Lett. **90**, 161114 (2007).
9. C. Li E. Moon, H. Mashiko, C. Nakamura, P. Ranitovic, C. L. Cocke, and Zenghu Chang, G. G. Paulus, "Precision control of carrier-envelope phase in grating based chirped pulse amplifiers," Optics Express **14**, 11468 **(**2006).
10. C. Li, E. Moon, and Zenghu Chang, "Carrier-envelope phase shift caused by variation of grating separation," Optics Letters **31**, 3113 (2006).
11. Zenghu Chang, "Carrier envelope phase shift caused by grating-based stretchers and compressors," Applied Optics **45**, 8350(2006).
12. C. Li, H. Mashiko, H. Wang, E. Moon, S. Gilbertson, and Zenghu Chang, **"**Carrier-envelope phase stabilization by controlling compressor grating separation," Appl. Phys. Lett. **92**, 191114 (2008).
13. E. Moon, Chengquan Li, Zuoliang Duan, J. Tackett, K. L. Corwin, B. R. Washburn, and Zenghu Chang,"Reduction of fast carrier-envelope phase jitter in femtosecond laser amplifiers," Optics Express **14,** 9758 (2006).
14. H. Wang, C. Li, J. Tackett, H. Mashiko, C. M. Nakamura, E. Moon and Zenghu Chang, "Power locking of high-repetition-rate chirped pulse amplifiers," Appl. Phys. B **89**, 275 (2007).
15. C. Li, E. Moon, H. Wang, H. Mashiko, C. M. Nakamura, J. Tackett, and Zenghu Chang, "Determining the Phase-Energy Coupling Coefficient in Carrier-envelope Phase Measurements," Optics Letters **32**, 796 (2007).
16. J. McKenna, A. M. Sayler, F. Anis, B. Gaire, Nora G. Johnson, E. Parke, J. J. Hua, H. Mashiko, C. M. Nakamura, E. Moon, Z. Chang, K. D. Carnes, B. D. Esry, and I. Ben-Itzhak, "Enhancing High-Order Above-Threshold Dissociation of H_2^+ Beams with Few-Cycle Laser Pulses," Phys. Rev. Lett. **100,** 133001 (2008).
17. M. Zamkov, A. S. Alnaser, B. Shan, Z. Chang, and P. Richard, "Exciton in bundles of single walled carbon nanotubes," Chemical Physics Letters **437**, 104 (2007).
18. M. Zamkov, A. S. Alnaser, N. Woody, B. Shan, Z. Chang, and P. Richard , "Probing the intrinsic conductivity of multiwalled carbon nanotubes," Appl. Phys. Lett. **89**, 093111 (2006).
19. M. A. Larotonda, Y. Wang, M. Berrill, B. M. Luther and J. J. Rocca, M. Man Shakya, S. Gilbertson and Zenghu Chang, "Pulse duration measurements of grazing incidence pumped table-top Ni-like Ag and Cd transient soft x-ray lasers," Optics Letters **31**, 3043-3045 (2006).
20. K.D. Carnes, C.L. Cocke, Z. Chang, I. Ben-Itzhak, H.V. Needham, A. Rankin, "Picosecond ion pulses from an EN tandem created by a femtosecond Ti:sapphire laser," Nucl. Instr. M. B **261**, 106 (2007).

Structure and Dynamics of Atoms, Ions, Molecules and Surfaces:
Atomic Physics with Ion Beams, Lasers and Synchrotron Radiation

C.L.Cocke, Physics Department, J.R. Macdonald Laboratory, Kansas State University, Manhattan, KS 66506, cocke@phys.ksu.edu

During the past year we have concentrated at KSU on two projects. We have measured momentum images of electrons ejected from rare gas atoms and rescattered by the parent ions in order to reveal the role played by free electron-ion scattering in determining the observed patterns. We have generated attosecond pulse trains by passing intense laser IR pulses through gas filled capillaries and have used these to do pump/probe experiments (EUV/IR) on the ionization of He. We have continued collaborations at the ALS and Univ. of Colorado.

Recent progress:

1) Momentum images of electrons released from rare-gas targets by intense laser pulses: *D.Ray, B.Ulrich, I.Bocharova, C.Mahaharjan, P.Ranitovic, B.Gramkow, M.Magrakvelidze, S.De, I.V.Litvinyuk, A.T.Le, T.Morishita, C.D.Lin, G.G.Paulus and C.L.Cocke.* It was predicted by Morishita et al. [1] that ATI electrons produced by the ionization of atomic targets should show "back rescattering ridges" (BRR) near the end of the ionization plateau (energy near 10 times the ponderomotive energy, U_p). In momentum space, these ridges form circles which are centered not about zero but about the vector potential of the laser at the time a returning electron is rescattered. It can be shown that this value of the vector potential is near its maximum value. The physical process giving rise to these ridges is the emission of an electron at a time for which it returns to the mother ion with maximum energy (3.17 U_p), followed by elastic scattering by the ion. Morishita *et al.* predicted that strong angular structure in the angular distribution along these ridges should be seen. This structure can be readily calculated from the scattering of electrons

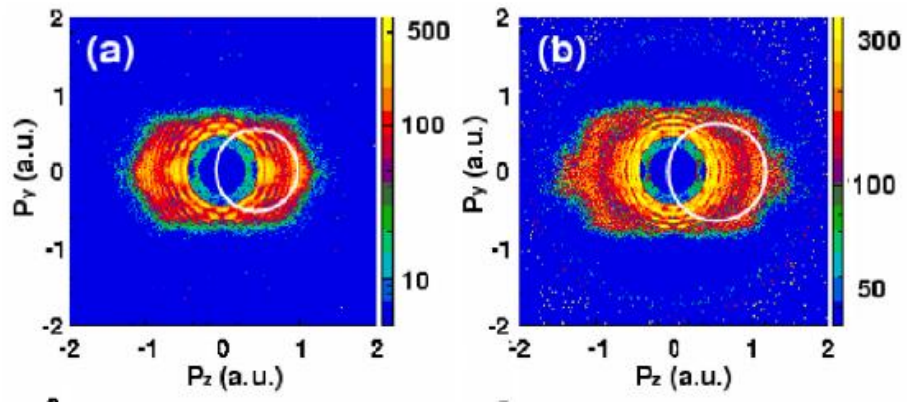

Figure 1. Momentum images of electrons ejected from Xe by intense 7 fs , 800 nm pulses at two different intensities. The angular structure in the diffraction scattering is seen on the outer edges of the spectrum.

from the appropriate ionic target. We have performed experiments to observe these BRRs in the laboratory. Since the yield of backscattering (plateau) ATI electrons is much weaker than that of directly ionized electrons, the usual COLTRIMS momentum imaging system proved inadequate to give sufficient statistics in the region of interest. We therefore adapted a stereo-phasemeter [2], which has a much larger target thickness, to the task. Time-of-flight spectra of the electrons were measured in two oppositely situated detectors, and the angular distribution was mapped out by rotating the polarization vector of the laser with respect to the time-of-flight axis. The spectra were then transformed to momentum spectra. A sample result is shown in figure 1.

For the case of Xe, strong angular structure is predicted and observed. Angular distributions deduced from these data are shown in figure 2, and compared to calculations of the differential cross sections for elastic scattering from Xe^+ ions. As discussed by Morishita *et al.* [3], this approach to the analysis of ATI spectra in the rescattering plateau can be exploited to greatly simply the calculation. The isolation of a component of the ATI spectrum attributable solely to the structure of the target system is a first step toward the ultimate goal of using rescattering electrons to image the parent ionic system in a time-dependent fashion.

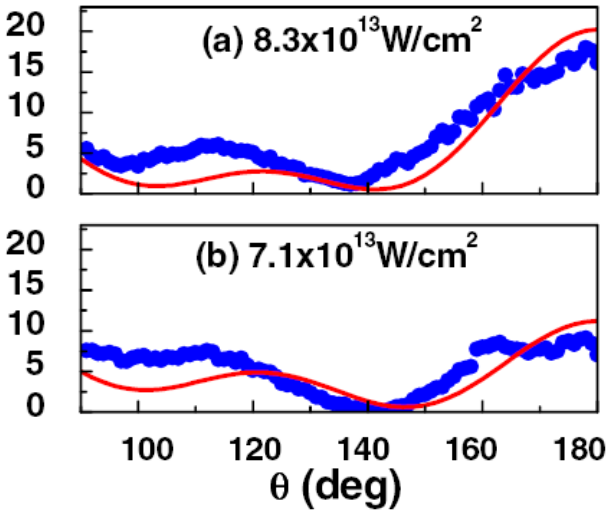

Figure 2. The data points show the angular distributions of electrons scattered from Xe^+, as deduced from the laser momentum images. The solid curves are calculated differential scattering cross sections for free electrons on Xe+. From publication 2.

2) EUV/IR Pump/probe experiments. *P.Ranitovic, B.Gramkow, D.Ray, I.Bocharova, H.Mashiko, M.Trachy, S.De, K. Singh, W.Cao, I.Litvinyuk, A.Sandhu, E.Gagnon, M.Murnane, H.Kapteyn, X-M.Tong, C.L.Cocke.* Pump probe experiments have been carried out using an attosecond pulse train (APT) in the EUV as a pump and a short infrared pulse (~1x10 ^{13} w/cm^2, 50 fs) as a probe. The reaction products are detected in a COLTRIMS geometry, which allows ion-electron coincidences to be measured. The development of the apparatus has taken several years. The first experiment has been the ionization of He by an APT formed from the 11th through the 17th harmonics (17-26 eV) of 800 nm radiation produced by focusing an intense laser pulse (50 fs) into a glass capillary filled with Xe gas. This approach was enabled through a collaboration with the Murnane/Kapteyn group at the University of Colorado, and a first publication from the collaborative work has been published in [4]. At the time we started this work, it had not previously been reported that a stable APT can be produced in a capillary. Our results clearly show that it can.

The overview of results (fig. 3) , and some conclusions, can be summarized as follows:

1) Since only the weak 17th harmonic has sufficient energy to ionize He, little He^+ is produced by EUV alone.
2) If the IR precedes the EUV, nothing changes. The IR pulse is too weak to significantly affect the tightly bound ground state of He.
3) If the IR comes after the EUV, a large enhancement of the He^+ yield occurs. This is attributed to the ionization by the IR of excited states of He populated by the 13th and 15th harmonics of the APT.
4) If the IR comes during the EUV, an even greater enhancement occurs, which is attributed to the cooperative ionization of the He by the simultaneous action of both fields.

Close examination of the dependence of the He^+ yield on the time delay between APT and laser field reveals that, in the overlap region, the yield oscillates (fig. 3) with a periodicity of half the optical cycle. The He^+ yield depends on the phase of the IR at which the APT strobes the dressed He. Further investigation has shown that the resonant structure of the He neutral plays an important role, and that, as a result, the results are sensitive to the wavelength of the IR laser used to generate the harmonics. It is believed that resonant excitation of the He through the 4p state dominates the production of He^+ when no IR is present, and that the presence of the IR during the APT brings the 2p (and perhaps other) np states of He into play through the broadening and shift which the IR produces on these states. Some evidence that this is the case is provided by the photoelectron spectra. Theoretical analysis of this system has been presented in ref. [5], and has also been carried out by X-M.Tong in collaboration with us. In addition, a simple model has been developed to try to dissect and isolate the different ionization processes which are occurring. The use of a second IR probe has also been used, producing a full-cycle oscillation period in the He^+ yield. The possible use of such a pump-probe-probe system to determine the absolute phase of the APT with respect to the driving IR field will be discussed.

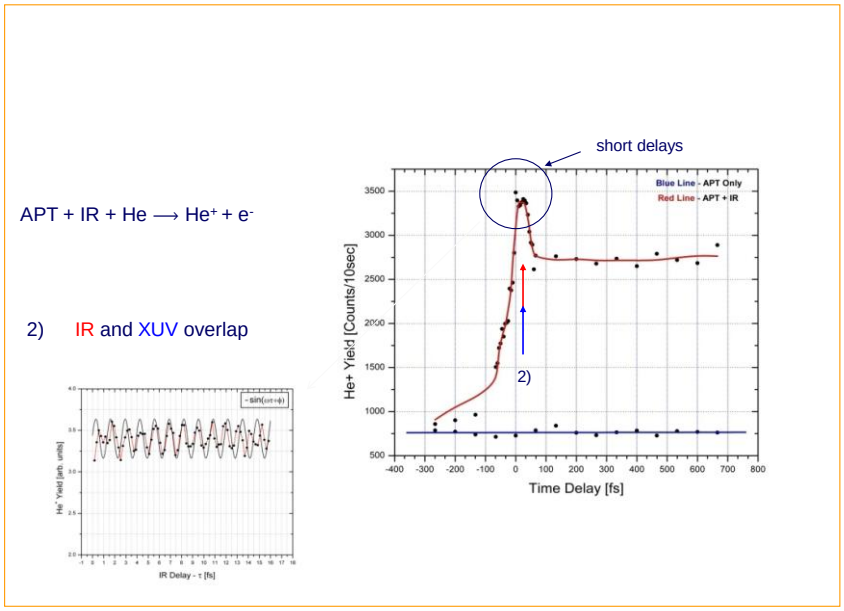

Figure 3. The yield of He^+ resulting from a EUV APT and IR (800 nm) pulse. The horizontal axis is the time delay of the IR relative to the APT. The long-time scan shows the overall structure of the process. The short-time scan shows that the yield oscillates with a period of one half the optical cycle of the IR.

3) Synchrotron radiation experiments, *T. Osipov, P.Ranitovic, C.Marhajan, B.Ulrich, C.L. Cocke (KSU), A. Landers (Auburn Univ.), R. Dörner, Th. Weber, L. Schmidt,A. Staudte, H. Schmidt-Böcking, et al. (U. Frankfurt), M.H. Prior (LBNL) and others.* We continue to participate in a multi-laboratory collaboration involving the University of Frankfurt, LLBL, Auburn Univ. and KSU at the ALS. Recent projects include studies of core-hole localization when a K electron is removed from N2, the dissociation and isomerizaiton pathways which acetylene follows when a carbon K electron is removed from it, and two-slit interference patterns in the continuum electron structure when H2 is (doubly) photoionized well above threshold.

Future plans:
The backscattering momentum project is being pursued in collaboration with the theoretical group of C.D.Lin to examine to what extent the full experimental momentum distributions can be described in terms of the angular and energy dependent electron-ion scattering interaction. The

EUV/IR project will be exploited to do both attosecond science and to follow the dynamics of light molecules excited by EUV and probed by short IR pulses. We continue to participate in the ALS collaboration in (3).

Publications 2007-2008 not previously listed:

1."Ultrafast Probing of Core Hole Localization in N_2", M.S.Schöffler, J.Titze, N.Petridis, T.Jahnke, K.Cole, L.Ph.H.Schmidt, A.Czacsh, D.Akoury, O.Jagutzki, J.B.Williams, N.A.Cherepkov, S.K.Semenov, C.W.McCurdy, T.N.Rescigno, C.L.Cocke, T.Osipov, S.Lee, M.H.Prior, A.Belkacem, A.L.Landers, H.Schmidt-Böcking, Th.Weber and R.Dörner, Science **320**, 920 (2008).

2."Large-Angle Electron Diffraction Structure in Laser-Induced Rescattering from Rare Gases", D.Ray, B.Ulrich, I.Bocharova, C.Mahaharjan, P.Ranitovic, B.Gramkow, M.Magrakvelidze, S.De, I.V.Litvinyuk, A.T.Le, T.Morishita, C.D.Lin, G.G.Paulus and C.L.Cocke, Phys.Rev.Letters **100**, 143002(2008).

3. "Fragmentation pathways for selected electronic states of the acetylene dication", T.Osipov, T.N.Rescigno, T.Weber, S.Miyabe, T.Jahnke, A.S.Alnaser, M.P.Hertlein, O.Jagutzki, L.Ph.H.Schmidt, M.Schöffler, L.Foucar, S.Schössler, T.Havermeire, M.Odenweller, S.Voss, B.Feinberg, A.L.Landers, M.H.Prior, R.Dörner, C.L.Cocke and A.Belkacem, J.Phys.B. **41**, 091001 (2008).

4."Interference in the Collective Electron Momentum in Double Photoionizaiton of H_2", K.KLreidi, D.Akoury, T.Jahnke, Th.Weber, A.staudte, M.Schoeffler, N.Neumann, J.Titze, L.Ph.H.Schmidt, A.Czach, O.Jagutzki, R.A.Costa Fraga, R.E.Grisenti, M.Smolarski, P.Ranitovic, C.L.Cocke, T.Osipov, H.Adaniya, J.C.Thompson, M.H.Priour, A.Belkacem, A.L.Landers, H.Schmidt-Böcking and R.Dörner, Phys.Rev.Lett **100**, 133005 (2008).

5."Direct time resolved observation of molecular dynamics induced by soft-x.ray photoionization", A.S.Sandhu, E.Gagnon, P.Ranitovic, X-M Tong, C.L.Cocke, M.M.Murnane and H.C.Kapteyn, J.Phys.:Conf. Series **88**, 012037 (2007).

6. "Direct Coulomb-explosion imaging of coherent nuclear dynamics induced by few-cycle laser pulses in light and heavy hydrogen", I.A.Bocharova, H.Mashiko, M.Magrakvelidze, D.Ray, P.Ranitovic, C.L.Cocke and I.V.Litvinyuk, Phys. Rev. A**77**, 053407 (2008).

References:

[1] T.Morishita, A.T.Le, Z.Chen and C.D.Lin, Phys.Rev.Lett.**100**, 013903 (2008).
[2] G.G.Paulus *et al.*, Phys.Rev.Lett. **91**, 253004 (2003).
[3] T.Morishita, A.T.Le, Z.Chen and C.D.Lin, New J.Phys. **10**, 025011 (2008).
[4] E.Gagnon *et al.*, Science **317**, 1374 (2007).
[5] P.Johnsson *et al.*, Phys.Rev.Lett. **99**, 233001 (2007).

Coherent Control of Photoassociation and Excitation of Cold Atoms Using Shaped Ultrafast Optical Pulses

B. D. DePaola
J. R. Macdonald Laboratory Department of Physics
Kansas State University
Manhattan, KS 66056
depaola@phys.ksu.edu

Program Scope

Photoassociation [#1] is the process by which colliding pairs of ultracold atoms are induced to form a molecule by means of a catalysis photon. In the specific case of Rb, the process can be represented by:

$$Rb(5s) + Rb(5s) + \hbar\omega \rightarrow Rb_2(5s, 5p) \rightarrow Rb_2(5s, 5s) + \hbar\omega' \quad (1)$$

(The asymptotic atomic designations are used to describe the molecular states throughout this abstract.) Here, ω is the optical frequency of the catalysis photon, and $\hbar\omega'$ is the energy of the photon that is emitted when the excited molecule relaxes to its electronic ground state. Photoassociation has received a great deal of attention recently because of the potential applications of ultracold molecules. Our interest is that this process provides a convenient and interesting subject for coherent control investigations. In our work we are particularly interested in a special form of photoassociation in which an additional photon brings the molecule to a doubly excited molecular state. [Pub. #1] Because this process consists of photoassociation followed by excitation, it is referred to as PAE. Note that relaxation to the electronic ground state is not considered part of the PAE process. In the work described here, the same ultrafast laser pulse that provides the catalysis photon, also excites the molecule to the $Rb_2(5p, 5p)$ manifold, the final step in the PAE process. The $Rb_2(5p, 5p)$ manifold is then probed with a narrow linewidth cw laser which excites to an autoionizing state in the $Rb_2(5p, 4d)$ manifold. [Pub. #2] *The goal of this project is to measure the extent to which shaping the spectral phase of the pulse can enhance the PAE process.* The spectral phase patterns that have been investigated to date include linear chirp, π-step function, $\pi/2$-pulse, and sinusoidal functions. In these experiments, it was often found to be advantageous to additionally measure the time between the initiation of the PAE process and the detection of Rb_2^+: The individual states in the $Rb_2(5p, 4d)$ manifold take different amounts of time to autoionize due to the variations in the curvatures of their molecular potentials. Thus, this "incubation time" helps to further distinguish PAE to different states.

The apparatus consists of a magneto-optical trap (MOT) containing ^{87}Rb atoms at a temperature of approximately 100μK, and having a density of approximately $10^{10} - 10^{11}$ atoms/cm^3. The atoms are trapped inside an electrostatic time-of-flight (TOF) mass spectrometer. Thus, any ions produced are extracted and directed onto a particle detector. The ultrafast laser is the Kansas Light Source, which operates at a 1 kHz repetition rate. Its pulses, attenuated to about 1μJ in a roughly 1 cm diameter spot, are shaped by an acousto-optic programmable dispersive filter (AOPDF). The

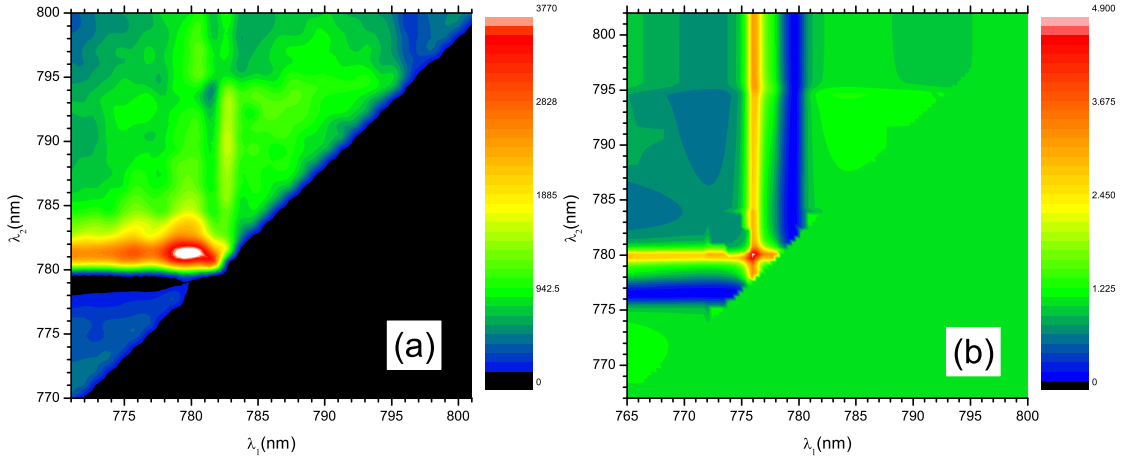

Figure 1: Experimental (a) and theoretical (b) results for the $\pi/2$ spectral phase pulse of Eq. 2. The Rb_2^+ counts are plotted *versus* the wavelengths at which the $\pi/2$ phase changes occur.

cw probe laser has a linewidth of less than 1 MHz, and is actively locked to a frequency 54 MHz to the blue of the $5p_{3/2}, F = 3 \rightarrow 4d_{5/2}$ atomic transition.

Recent Progress

Figure 1 shows some results from an experiment in which the $\pi/2$ phase pulse,

$$\phi(\lambda) = \begin{cases} 0 & \lambda \leq \lambda_1 \\ \pi/2 & \lambda_1 < \lambda < \lambda_2 \\ 0 & \lambda \geq \lambda_2, \end{cases} \tag{2}$$

was applied to the ultrafast laser pulse. Plotted in Fig. 1a is the measurement of Rb_2^+ counts *versus* λ_1 and λ_2, the wavelengths at which the left and right edges, respectively, of the $\pi/2$ phase pulse are located. Plotted in Fig. 1b is the corresponding second order perturbation theory calculation result. The theoretical model is fashioned along the ideas of Silberberg's group [#2]. While the qualitative agreement between theory and experiment is striking, some quantitative differences remain. It is very likely that these are due to the simplicity of the model, in which the bands of molecular energy levels are approximated by a few discrete levels. Furthermore, these levels are modeled as being independent of internuclear separation. The model greatly simplifies the calculations and allows for qualitative comparisons. However, more sophisticated modeling will have to be done before we can say with any confidence that we completely understand the process.

A disadvantage of the AOPDF-type pulse shapers is the resolution limit imposed by the transit time of the optical pulse through the modulator crystal. That is, the transit time of 3.5 ps means that the maximum temporal width of the shaped pulse is limited to 3.5 ps. Therefore, the degree of "sharpness" that one can impose on the spectral phase and/or spectral amplitude is limited, since the sharper the structure in the frequency domain, the broader the pulse in the time domain. For example, in the above results, we could not really use the idealized pulse of Eq. 2. Instead the infinite slope of an idealized pulse was replaced by the gradual edge of an error function. Another approach is to use phase functions that have no sharp features, and yet allow one to vary all orders

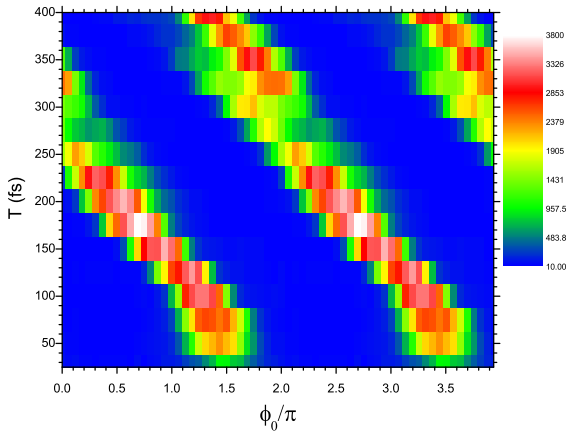

Figure 2: Experimental results for the sinusoidal spectral phase of Eq. 3. The Rb_2^+ counts are plotted *versus* the two parameters ϕ_0 and T. Here, $A = 1.2$.

of phase. An example of this is the sinusoidal phase,

$$\phi(\lambda) = A \sin\left[2\pi cT\left(\lambda^{-1} - \lambda_0^{-1}\right) + \phi_0\right], \tag{3}$$

where A, T, and ϕ_0 are parameters, and λ_0 is an arbitrary constant, usually chosen to be near a resonant frequency of the system. An example of some data taken with this phase is shown in Fig. 2. Here, A was chosen to be 1.2. The same information about the PAE process is contained in Fig. 2 as in Fig. 1. Here, the wavelengths at which PAE is enhanced is determined from the slopes of the structures in Fig. 2. For reasons not completely understood (but perhaps related to the resolution issue discussed above) the contrast between maximum and minimum PAE signals is much greater (> 250) for the sinusoidal phase than for the $\pi/2$-step phase.

Future Plans

In the future, we will continue our measurements of PAE, and effects of various spectral phases on it. We will also try to improve our modeling of the process by using more realistic potential curves. Thus far, we have used well-defined functions for the spectral phases. These were based on our intuitive understanding of the PAE process. However, it is very possible that even more control can be exerted on this process by using a spectral phase that we have not yet thought of. We have now started to implement a genetic algorithm (GA) [#3] approach to guide the laser's spectral phase such the PAE process is maximally efficient. We then plan to use the technique of *principal control analysis* [#4] to help us to identify any unanticipated phase functions that may be used to control the PAE process. If such functions are found, we will then experimentally test their suitability for control.

References

1. K. M. Jones, E. Tiesinga, P. D. Lett, and P. S. Julienne, Rev. Mod. Phys. **78**, 483 (2006).

2. N. Dudovich, B. Dayan, S. M. Gallagher-Faeder, and Y. Silberberg, Phys. Rev. Lett. **86**, 47 (2001).

3. J. H. Holland, Sci. Am. **267**, 66 (1992).

4. J. L. White, B. J. Pearson, and P. H. Bucksbaum, J. Phys. B: At. Mol. Opt. Phys. **37**, L399 (2004).

Recent Publications

1. "Photoassociation in Cold Atoms via Ladder Excitation", M. L. Trachy, G. Veshapidze, M. H. Shah, H. U. Jang, and B. D. DePaola, Phys. Rev. Lett. **99**, 043003 (2007).

2. "Pathway for Two-Color Photoassociative Ionization with Ultrafast Optical Pulses in a Rb Magneto-Optical Trap", G. Veshapidze, M. L. Trachy, H. U. Jang, C. W. Fehrenbach, and B. D. DePaola, Phys. Rev. A **76**, 051401(R) (2007).

3. "An Auto-Incrementing Nanosecond Delay Circuit", H. U. Jang, J. Blieck, G. Veshapidze, M. L. Trachy, and B. D. DePaola, Rev. Sci. Instrum. **78**, 094702 (2007).

4. "MOTRIMS: Magneto-Optical Trap Recoil Ion Momentum Spectroscopy", B. D. DePaola, R. Morgenstern, and N. Andersen, Adv. At. , Mol. , Opt. Phys. **55**, 139-189 (2007).

5. "Measurement of Population Dynamics in Stimulated Raman Adiabatic Passage", M. A. Gearba, H. A. Camp, M. L. Trachy, G. Veshapidze, M. H. Shah, H. U. Jang, and B. D. DePaola, Phys. Rev. A **76**, 013406 (2007).

6. "Model-Independent Measurement of the Excited Fraction in a Magneto-Optical Trap", M. H. Shah, H. A. Camp, M. L. Trachy, G. Veshapidze, M. A. Gearba, and B. D. DePaola, Phys. Rev. A **75**, 053418 (2007).

7. "A Novel Method for Laser Beam Size Measurement", G. Veshapidze, M. L. Trachy, M. H. Shah, and B. D. DePaola, Appl. Opt. **45**, 6197 (2006).

8. "Relative Charge Transfer Cross Section from Rb(4d)", M. H. Shah, H. A. Camp, M. L. Trachy, X. Fléchard, M. A. Gearba, H. Nguyen, R. Brédy, S. R. Lundeen, and B. D. DePaola, Phys. Rev. A **72** 024701 (2005).

9. "Entropy Lowering in Ion-Atom Collisions", H. Nguyen, R. Brédy, T. G. Lee, H. A. Camp, H. Awata, and B. D. DePaola, Phys. Rev. A **71** 062714 (2005).

10. "Numerical Exploration of Coherent Excitation in Three-Level Systems", H. A. Camp, M. H. Shah, M. L. Trachy, O. L. Weaver, and B. D. DePaola, Phys. Rev. A **71** 053401 (2005).

Time-dependent Treatment of Three-body Systems in Intense Laser Fields

B.D. Esry
J. R. Macdonald Laboratory, Kansas State University, Manhattan, KS 66506
esry@phys.ksu.edu
http://www.phys.ksu.edu/personal/esry

Program Scope

The primary goal of my program is to quantitatively understand the behavior of H_2^+ in an ultrashort, intense laser field. As we gain this understanding, we will work to transfer it to other more complicated molecules. In this effort, my group works closely with the experimental groups in the J.R. Macdonald Laboratory, including, in particular, the group of I. Ben-Itzhak.

Because even H_2^+ has more degrees of freedom than can currently be directly treated computationally when an intense field is present, past theoretical descriptions have artificially reduced the dimensionality of the problem or excluded one or more of the important physical processes: ionization, vibration, and rotation. Such simplifications were most often justified with intuitive arguments, but have been little tested. One component of this work is thus to systematically include these processes in three dimensions and gauge their importance based on actual calculations. Further, as laser pulses get shorter and more intense, approaches that have proven useful in the past may become less so. The application of kinematically complete measurement techniques is also revealing effects that are likely not captured correctly in these simplified models. A second component of my program is to develop novel analytical and numerical tools to more efficiently and more generally treat these systems. The ultimate goal is to understand the dynamics of these strongly coupled systems in quantum mechanical terms.

Recent progress

We now routinely solve the problem of H_2^+ in an intense laser including nuclear vibration and rotation as well as electronic excitation. The only physical process excluded is ionization. We can thus reliably perform full-dimensionality calculations for H_2^+ up to an intensity of roughly 10^{14} W/cm^2 for 800 nm Ti:sapphire laser pulses. For higher intensities, ionization plays a non-negligible role.

We have recently used this capability to demonstrate theoretically the contribution of the first excited manifold of states in H_2^+ to dissociation [12]. Our calculations accompanied experimental measurements by I. Ben-Itzhak's group, allowing for the interpretation of their data. We showed that not only did the states correlating to H(n=2)+p contribute to the dissociation, but also that they displayed above threshold dissociation. That is, dissociation via these states proceeded with absorption of more than the minimum number of photons necessary. This phenomenon would have been extremely difficult to identify based on the experiment alone as all of the features overlap in energy and in angle, so we relied on the ability to clearly separate their contributions theoretically. The analysis was completed by studying the isotopic, intensity, and pulse length dependence of these processes.

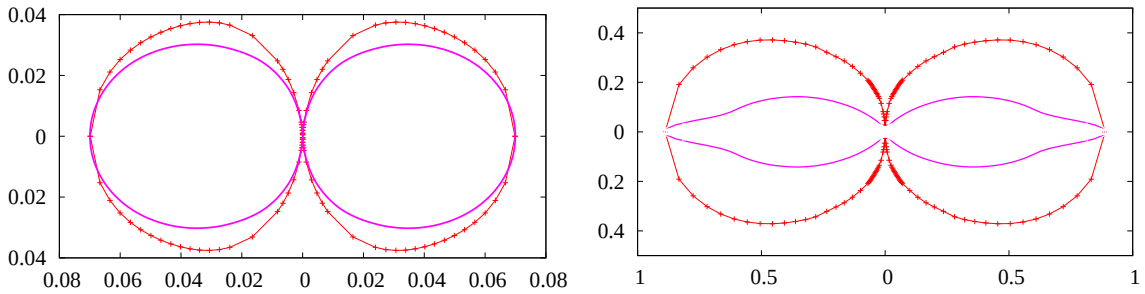

Figure 1: The angular distribution of p and H following dissociation of H_2^+ in an intense, 10 fs, 785 nm laser pulse. The red lines (+) indicate the results without nuclear rotation and the magenta line (no symbol) shows the results including rotation. The left panel is for $I = 10^{13}$ W/cm^2; and the right, for $I = 10^{14}$ W/cm^2. These angular distributions were evaluated at the end of the pulse, thus excluding any post-pulse evolution.

We have also compared the results for dissociation of H_2^+ calculated with and without nuclear rotation in pulses of 45 fs and 135 fs [11]. Both pulses are already much shorter than the free rotation period of H_2^+, ∼550 fs, so many have argued that rotation is not important and that modeling the system including only vibration is sufficient to understand the dynamics in an intense field. This notion persists even though it was shown many years ago (see Ref. [1], for instance) that inclusion of rotation virtually eliminates vibrational trapping. We confirmed that there is no substantial vibrational trapping when rotation is included and further showed that the "vibrational trapping" remaining is already present for one-photon absorption calculated in first order perturbation theory. Since the explanation of vibrational trapping relies on the many-photon dressing of the Born-Oppenheimer potential curves, a phenomenon reproduced in first order perturbation theory certainly does not qualify.

Possibly the most surprising result of including rotation so far comes from a recent sequence of calculations we have done for H_2^+ in very short pulses. This work has not yet been published, but will be submitted in the near future. These calculations show that it is crucial to include nuclear rotation in order to correctly predict what will be measured experimentally — even for pulses as short as 5 fs! Given that these pulses are two orders of magnitude shorter than the free rotation period of H_2^+, this result is quite surprising. A little more investigation shows that the angular distribution of the molecule does not, in fact, change very much during the pulse, as one would expect, but does continue to evolve substantially on the way to the detector (see Ref. [2] for a semiclassical discussion of this effect). Even this statement, however, only holds for intensities below roughly 10^{13} W/cm^2. Figure 1 shows the angular distribution calculated with and without nuclear rotation, showing clearly that rotation is important even during the laser pulse for high intensities. (The calculation without rotation was carried out with the internuclear axis held at a fixed angle with the laser polarization.) Figure 2 shows the post-pulse evolution for different pulse parameters, which necessarily includes nuclear rotation. In particular, the post-pulse evolution for the pulse shown in the right panel of Fig. 1 is shown in Fig. 2(b). It can be clearly seen that the angular distribution becomes substantially more aligned before it reaches the detector. The other cases shown in the figure also display clear effects of post-pulse rotation, including

Figs. 2(c)-(d) for 5 fs.

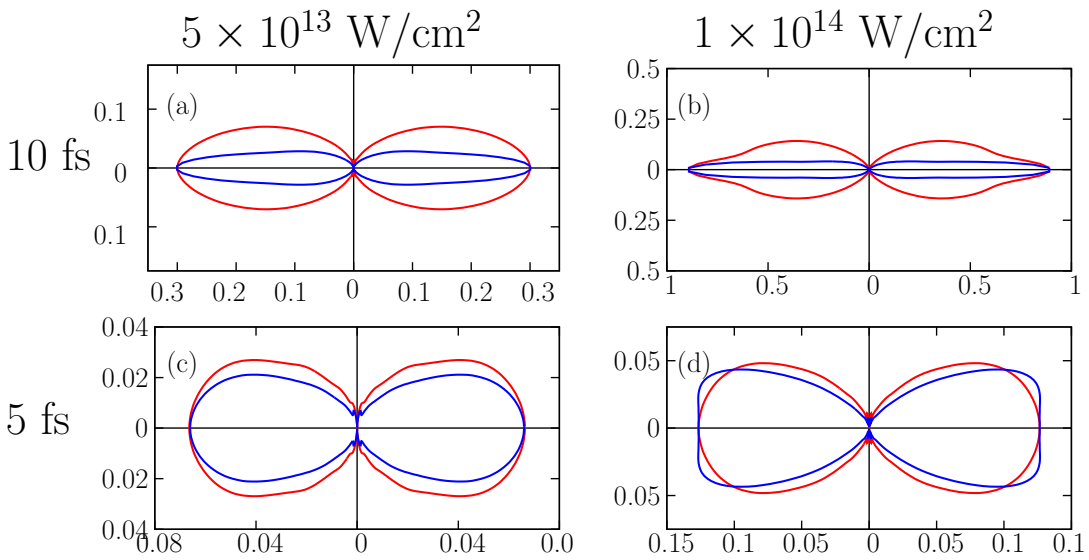

Figure 2: Post-pulse evolution of the angular distribution of dissociating fragments from H_2^+ in an intense laser. In all plots, the red curves show the angular distribution at the end of the pulse; and the blue curves, at the detector ($t \to \infty$). The red curve in (b) is the same as the magenta curve in the right panel of Fig. 1.

Future plans

We will continue to develop the theoretical methods and computer codes described above. In particular, we plan to work closely with I. Ben-Itzhak's group to refine the methods and resolve lingering differences between theory and experiment. We are in the process, for instance, of producing a quantitative comparison between experiment and theory for dissociation of H_2^+ in a 10 fs pulse. We are also working to generalize the code to work for any diatomic molecule since the only input required is the Born-Oppenheimer potential curves and dipole matrix elements. This improvement will allow us to treat some of the multielectron systems being studied in the J.R. Macdonald Laboratory. Finally, we continue to search for novel effects — such as the carrier-envelope phase dependence as revealed by the momentum distribution of dissociation fragments — in these systems.

References

1. E. E. Aubanel, A. Conjusteau, and A. D. Bandrauk, Phys. Rev. A **48**, R4011 (1993).

2. X. M. Tong, Z. X. Zhao, A. S. Alnaser, S. Voss, C. L. Cocke, and C. D. Lin, J. Phys. B **38**, 333 (2005).

Publications of DOE-sponsored research in the last 3 years

13. "Intensity dependence in the dissociation branching ratio of ND^+ using intense femtosecond laser pulses," J. McKenna, A.M. Sayler, B. Gaire, N.G. Johnson, E. Parke, K.D. Carnes, B.D. Esry, and I. Ben-Itzhak, Phys. Rev. A **77**, 063422 (2008).

12. "Enhancing high-order above-threshold dissociation of H_2^+ beams with few-cycle laser pulses," J. McKenna, A.M. Sayler, F. Anis, B. Gaire, N.G. Johnson, E. Parke, J.J. Hua, H. Mashiko, C.M. Nakamura, E. Moon, Z. Chang, K.D. Carnes, B.D. Esry, and I. Ben-Itzhak, Phys. Rev. Lett. **100**, 133001 (2008).

11. "Role of nuclear rotation in dissociation of H_2^+ in a short laser pulse," F. Anis and B.D. Esry, Phys. Rev. A **77**, 033416 (2008).

10. "Ionization and dissociation of molecular ion beams caused by ultrashort intense laser pulses," I. Ben-Itzhak, A.M. Sayler, P.Q. Wang, J. McKenna, B. Gaire, N.G. Johnson, M. Leonard, E. Parke, K.D. Carnes, F. Anis, and B.D. Esry, J. Phys.: Conf. Ser. **88**, 012046 (2007).

9. "General theory of carrier-envelope phase effects," V. Roudnev and B.D. Esry, Phys. Rev. Lett. **99**, 220406 (2007).

8. "HD^+ in a short strong laser pulse: Practical consideration of the observability of carrier-envelope phase effects," V. Roudnev and B.D. Esry, Phys. Rev. A **76**, 023403 (2007).

7. "Determining laser induced dissociation pathways of multi-electron diatomic molecules: application to the dissociation of O_2^+ by high intensity ultrashort pulses," A.M. Sayler, P.Q. Wang, K.D. Carnes, B.D. Esry, and I. Ben-Itzhak, Phys. Rev. A **75**, 063420 (2007).

6. "Dissociation of H_2^+ in intense femtosecond laser field studied by coincidence 3D momentum imaging," P.Q. Wang, A.M. Sayler, K.D. Carnes, J.F. Xia, M.A. Smith, B.D. Esry, and I. Ben-Itzhak, Phys. Rev. A **74**, 043411 (2006).

5. "Above threshold Coulomb explosion of molecules in intense laser pulses," B.D. Esry, A.M. Sayler, P.Q. Wang, K.D. Carnes, and I. Ben-Itzhak, Phys. Rev. Lett. **97**, 013003 (2006).

4. "Laser assisted charge transfer in He^{2+}+H collisions," F. Anis, V. Roudnev, R. Cabrera-Trujillo, and B.D. Esry, Phys. Rev. A **73**, 043414 (2006).

3. "Isotopic preference of O-H over O-D bond cleavage following HDO ionization by fast ions," A.M. Sayler, M. Leonard, K.D. Carnes, R. Cabrera-Trujillo, B.D. Esry, and I. Ben-Itzhak J. Phys. B **39**, 1701 (2006).

2. "Lattice approach for $\alpha + H_2^+$ collisions," S.C. Cheng and B.D. Esry, Phys. Rev. A **72**, 022704 (2005).

1. "Dissociation and ionization of H_2^+ by ultra-short intense laser pulses probed by coincidence 3D momentum imaging," I. Ben-Itzhak, P.Q. Wang, J.F. Xia, A.M. Sayler, M.A. Smith, K.D. Carnes, and B.D. Esry, Phys. Rev. Lett. **95**, 073002 (2005).

Controlling Rotations of Asymmetric Top Molecules: Methods and Applications

Vinod Kumarappan
James R. Macdonald Laboratory, Department of Physics
Kansas State University, Manhattan KS 66506
vinod@phys.ksu.edu

Program Scope:

This part of the JRML program aims to

(a) develop better methods of alignment and orientation of asymmetric top molecules, and

(b) use aligned molecules to make angle-resolved measurements of ultrafast processes.

This is a new endeavor, and at this point no experiments have been conducted. This abstract describes the progress made towards setting up a new lab within JRML.

Introduction:

Linear molecules have a simple rotational energy level structure, and it is relatively straightforward to use the interaction of a strong laser field with the induced dipole moment to set up a rotational wavepacket that aligns the molecules with the laser polarization vector. With a suitably chosen combination of laser pulse duration and intensity, the peak of the alignment occurs in field-free conditions and revives periodically. Alignment of linear molecules is now used in a large number of groups to study angle dependent processes, such as high harmonic generation (HHG) [1], in molecules.

Asymmetric tops are not so simple. First, the field-free motion of a classical asymmetric top rotor is not always stable. In the quantum domain, this shows up as an irregular energy level structure that cannot be described analytically. Second, the interaction Hamiltonian is more complex, involving two Euler angles (which can be used to define the orientation of a molecule-fixed coordinate system with respect to a lab-fixed one) even for the simplest case of a linearly polarized laser field. These two features imply that any motion induced a laser field will, in general, involve more than one axis of rotation in the molecule, and any alignment produced by such motion will not revive completely. Moreover, asymmetric tops must be 3D aligned for complete elimination of orientational averaging [2,3].

All these issues taken together make the problem of alignment significantly more difficult for asymmetric tops than for linear or symmetric top molecules. But most molecules are asymmetric tops, there is a strong impetus for developing methods of aligning them. The availability of molecules well-aligned in three dimensions will open up new experimental possibilities in, for example, HHG and the study of ultrafast processes using HHG and photoelectron spectroscopy.

Plans and current status:

Most of the planned experiments will use Coulomb explosion imaging to detect alignment. To this end, a velocity map imaging (VMI) spectrometer has been designed and is being constructed. The target molecules will be seeded in helium in a pulsed supersonic expansion at 1 kHz, using an Even-Lavie valve. This valve is capable of cooling molecules to rotational temperatures below 1 K, and the valve itself can be operated between 300 K and 550 K (a jacket to cool it down to 77 K will be designed and built later). The valve and the VMI spectrometer will be housed in two differentially-pumped chambers. The VMI spectrometer will be shielded from external magnetic fields so that it can be used to measure photoelectron distributions from aligned molecules.

The Kansas Light Source (KLS), the femtosecond laser system in JRML, will be used to non-adiabatically align the molecules and to measure the degree of alignment. KLS has two amplifiers feed by the same optical pulse from a Ti:Sapphire oscillator. One of these amplifier systems is equipped with a Dazzler electro-optic pulse shaper. Shaped pulses from this system will be used to optimize the degree of alignment. A genetic algorithm (GA), which includes mutation, crossover, elite selection and incest avoidance, will be used to control the pulse shapes generated by the Dazzler. The ability to control the nature of rotational wavepacket by simply changing the pulse duration of the pump laser has already been demonstrated [4,5]; we expect that shaped pulses will allow us to direct the motion of the molecules more effectively.

In order to enable rapid feedback to the GA, and to best utilize the limited beam-time available from KLS, the experiment has been designed to operate at 1 kHz, the repetition rate of the laser. This requires a high throughput vacuum system, fast camera and image acquisition system, and parallel processing of acquired images for rapid evaluation of the degree of alignment. The data acquisition program has been written and tested to the extent possible without an actual spectrometer. The GA program has also been written, but hasn't yet been interfaced with the Dazzler.

3D alignment of asymmetric top molecules has been demonstrated in adiabatic [6] and non-adiabatic [7] conditions, as well as a combination of the two [8]. But none of these is satisfactory, suffering either from poor 3D alignment, or the presence of the strong adiabatic field. The best 3D alignment measured to date was obtained by the "hold and spin" method [8] - an adiabatic (ns) pulse holds the most polarizable axis of the molecule tightly aligned, and a perpendicularly polarized non-adiabatic pulse (fs) spins the molecule about this axis. We will attempt to convert this 3D alignment into field-free alignment by rapidly truncating the adiabatic pulse.

Collaborators: This work is being done with Ren Xiaoming.

References:

1. See, for instance, Merkel, M. *et al.*, Science **320**, 1478 (2008) and references therein.

2. H. Stapelfeldt and T. Seideman, Rev. Mod. Phys. **75**, 543 (2003).

3. T. Seideman and E. Hamilton, Ad.At.Mol.Opt.Phys. **52**, 289 (2006).

4. Holmegaard L. *et al.* Phys. Rev. A **75**, 051403 (2007).

5. Rouzee A. *et al.*, Phys. Rev. A **73**, 033418 (2006).

6. Larsen J. J. *et al.*, Phys. Rev. Lett. **85**, 2470 (2000).

7. Lee K. F. *et al.*, Phys. Rev. Lett. **97,** 173001 (2006).

8. Viftrup S. S. *et al.*, Phys. Rev. Lett. **99**, 143206 (2007).

Interactions of intense lasers with atoms and molecules and dynamic chemical Imaging

C. D. Lin
J. R. Macdonald Laboratory, Kansas State University
Manhattan, KS 66506
e-mail: cdlin@phys.ksu.edu

Program Scope:

We investigate the interaction of intense laser pulses with atoms and molecules. In the last year we have developed a quantitative rescattering theory (QRS) which allows us to extract photoionization cross section and elastic electron-ion scattering cross sections, from laser-induced high-order harmonic generation and high-energy photoelectron momentum spectra, respectively. Since laser pulses of duration of a few femtoseconds are already available, this opens up the possibility of using ultrafast laser pulses for carrying out dynamic chemical imaging of transient molecules with femtosecond temporal resolution. Progress in extracting the structural information is also reported.

Introduction

When an atom or molecule is exposed to an intense infrared laser pulse, an electron which was released earlier may be driven back by the laser field to recollide with the parent ion. The collisions of electrons with the ion may result in photo-recombination (the inverse of photoionization), with the emission of high-energy photons (high-order harmonic generation--HHG), or with the emission of high-energy electrons, when the returning electrons are backscattered. Both electron scattering and photoionization are the conventional means for studying the structure of atoms and molecules. Thus HHG spectra and high-energy photoelectrons generated by lasers intrinsically contain information on the structure of the target. If such information can be extracted, then infrared lasers can be used for dynamic chemical imaging with temporal resolution down to a few femtoseconds.

In the last year, we have developed a quantitative rescattering theory (QRS) which shows that photo-recombination cross sections can be extracted from the HHG spectra, and elastic scattering cross sections between electrons and ions can be extracted from the high-energy photoelectron spectra, respectively. In the meanwhile, a parallel effort is taking place in extracting the structure of atoms and molecules from photon and electron data, toward the goal of dynamic chemicl imaging.

Quantitative rescattering theory (QRS) for HHG and high-energy photoelectrons induced by lasers

Recent progress

There are basically only two theoretical methods for studying the nonlinear interactions between intense lasers with atoms or molecules. One is the direct solution of the time-dependent Schrödinger equation (TDSE), the other is the strong field approximation (SFA). While SFA can be easily employed even for complex systems, it is not an accurate theory. On the other hand, TDSE, while accurate, can only be efficiently solved for a one-electron atomic system. Thus at present there is no reliable quantitative theory available for describing the nonlinear interactions between lasers with atoms or molecules. By examining the validity and the limitation of the SFA, in the last year, we have developed a quantitative rescattering theory (QRS) which has the accuracy comparable to TDSE but with computational ease comparable to the SFA.

In paper #A1 we established the validity of the QRS model using TDSE results from model one-electron atoms. We showed that the HHG spectra can be expressed as the product of a returning electron wave packet, multiplied by the photo-recombination cross sections. We also established the relation between the high-energy photoelectron momentum spectra and the elastic differential scattering cross sections in the backward directions. In #A1, this relation was shown for returning electrons with the maximum kinetic energies—i.e., the so-called backward rescattered ridge (BRR) electrons. We showed photoelectron angular distributions along the BRR can be used to extract electron-ion elastic differential cross sections. This prediction has since been confirmed by two experiments, see #A3 from the group of C. L. Cocke at Kansas State and #A4 from the group of Ueda in Japan.

In papers #A2, #A8 and preprint #B1, we further showed that the "returning electron wave packet" depends mostly on the lasers only. Thus the returning electron wave packet can be obtained from the SFA model or from an atomic target where TDSE calculations can be carried out. This forms the basis of the quantitative rescattering model (QRS). Unlike SFA, in the QRS theory, the electron-ion recombination or elastic scattering cross sections are not calculated in the Born approximation. Instead, the cross sections are calculated using scattering waves (SW), the same as employed in the study of photoionization and electron collisions with atoms or molecules. Using the QRS model, the theory of the interaction of lasers with atoms in the region where rescattering dominates becomes equivalent to the theory of the interaction of photons or electrons with atoms.

In paper #A5 we established that the QRS model also works well for the simplest molecular ions, H_2^+. This is the only molecular system where accurate HHG spectra can be calculated by solving the TDSE. This paper also shows that the alignment dependence of the HHG is correctly predicted by the QRS model.

In preprint #B1 we showed that the phase of the high-order harmonics extracted from the QRS model is also correct for atoms. The phase of the harmonics is needed in order to account for the macroscopic propagation effect of the HHG generated by single atoms.

In preprint #B2 we extended the QRS model to returning electrons with kinetic energies smaller than the cutoff energy of 3.17 U_p, where U_p is the ponderomotive energy. Thus the QRS model can be used to calculate photoelectron spectra for energies above about 4 U_p -- these electrons result from the backscattering of the returning electrons by the ion. Based on the QRS, we showed that the flatness of high-energy electrons in the plateau region can be attributed entirely to the elastic electron-ion differential cross sections.

In paper #A7 the QRS model has been applied to the detachment of negative ions by lasers.

Ongoing projects and future plan

So far the QRS model has been applied to model atomic systems except for the experimental results reported in papers #A3 and A4. At present, we are applying the QRS model to compare with experimental data where effect from focus volume in the interaction region has to be included. In particular, high-energy photoelectron spectra generated by carrier-phase stabilized few-cycle laser pulses from Garching, Germany, are being analyzed. The preliminary results indicated that, based on the QRS model, we have a consistent method for determining the pulse duration, peak laser intensity, and the carrier-envelope phase of the laser, as well as the elastic electron-ion scattering cross sections. Experimentally, high-energy electron spectra are being investigated at many different laboratories, including the JRM Laboratory at Kansas State University. The QRS model will offer an efficient method for providing quantitative results to compare with these experiments.

Our major effort in the coming year will be to extend the QRS model to molecular targets. The HHG spectra of partially aligned CO_2 and N_2 molecules have been reported at a number of laboratories, and with controversies. To use the QRS model we need to be able to obtain fixed-molecule photoionization cross sections and the phase of the dipole amplitudes. We are collaborating with Dr. M.-T. Lee from Brazil for this purpose. Dr. Lee has been studying photoionization of polyatomic molecules for more than a few decades. This informal collaboration is already underway.

To compare HHG spectra with experiments, the macroscopic propagation effect has to be considered. We are developing our own propagation code at this moment and it is expected to be fully tested in the next few weeks. In the coming year, the QRS model will also be tested for combined light pulses, such as two IR lasers or one XUV pulse and one IR laser.

Retrieving atomic and molecular structure from laser-induced HHG and photoelectrons – dynamic chemical imaging with infrared lasers

The QRS model has established the theoretical basis for identifying the role of target structure in laser-induced HHG and photoelectron spectra. The model shows that photoionization cross sections and electron-ion scattering cross sections can be extracted from laser generated data. Since laser pulses of a few femtoseconds are widely available, it is thus possible to use such lasers for probing the time-resolved structural change of a chemical reaction in a pump-probe setting. This idea was outlined in paper #A2 where we showed that electron scattering cross sections are very sensitive to the change of structure of a transient molecule, such as the interatomic separations. Thus we view the problem of chemical imaging is to extract the interatomic separations from the laser-induced data, or equivalently, the photoionization cross sections and elastic scattering cross sections.

In a widely cited paper by Itatani *et al*, **Nature** ,432, 867 (2004), it was suggested that one can retrieve the highest occupied molecular orbital (HOMO) by measuring the alignment dependence of laser-generated HHG. By analyzing their model, we concluded that a number of assumptions in their paper are not valid in general. In paper #A9 we addressed these problems, and proposed, instead, that one should try to retrieve the interatomic separations from the HHG spectra for the purpose of retrieving the structural change of a molecule. An iterative scheme was proposed. In paper #A6 we illustrated that such an iterative method indeed works well and only a small subset of HHG data is needed to retrieve the interatomic distances. Examples for O_2, N_2 and CO_2 molecules were shown, using HHG spectra calculated based on SFA in order to test the method.

Future plan

The next goal is to retrieve structure of a polyatomic molecule where the number of internuclear separations to be retrieved is much larger. The simple method used in paper #A11 was based on the least-square fitting which is difficult to extend to multi-parameter problems. Other methods should be used. We are using genetic algorithm for this propose. The method is being used to retrieve accurate model potential for atomic systems, starting with elastic scattering cross sections calculated from an input potential. The test results show that the method works well. We are in the process of extending the method to model polyatomic systems. We believe that this method can be applied to reactions involving complex molecules. For transient complex molecules, the number of atoms involved in the transformation is small in general, thus we expect that the number of atomic position parameters to be retrieved will not be too large. We perceive this as a big advantage compared to methods based on the Coulomb explosion of a large molecule.

Publications (16 papers published between January 2006- June 2007 are not listed)
Published papers

A1. Toru Morishita, A. T. Le, Z-J Chen, and C. D. Lin. "Accurate retrieval of structural information from laser-induced photoelectron and high-order harmonic spectra by few-cycle laser pulse", **Phys. Rev. Lett.** 100, 013902 (2008).

A2. Toru Morishita, A. T. Le, Z. J. Chen and C. D. Lin, "Potential for ultrafast dynamic chemical imaging with few-cycle infrared lasers", **New J. of Physics** 10, 025011 (2008).

A3. D. Ray, B. Ulrich, I. Bocharova, C. Maharajan, P. Ranitovic, B. Gramkow, M. Magrakvelidze, S. De, I. V. Litvinyuk, A. T. Le, T. Morishita, C. D. Lin, G. G. Paulus and C. L. Cocke, "Large-angle electron diffraction structure in laser-induced rescattering from rare gases", **Phys. Rev. Lett**. 100, 143002 (2008).

A4. M. Okunishi, T. Morishita, G. Prumper, K. Shimada, C. D. Lin, S. Watanabe and K. Ueda", "Experimental retrieval of target structure from laser induced rescattered photoelectron momentum distributions", **Phys. Rev. Lett.** 100, 143001 (2008).

A5. A. T. Le, R. Della Picca , P. D. Fainstein, D. A. Telnov, M. Lein and C. D. Lin, "Theory of high-order harmonic generation from molecules with intense laser pulses", **J. Phys. B**41**,** 081002 (2008) (Fast Track Comunications)

A6. V. H. Le, N. T. Ngugen, C. Jin, A. T. Le and C. D. Lin, "Retrieval of interatomic separations of molecules from laser-induced high-order harmonic spectra", **J. Phys. B** 41, 085603 (2008).

A7. XiaoXin Zhou, Z. J. Chen, T. Morishita, A. T. Le and C. D. Lin, " Retrieval of electron-atom scattering cross sections from laser-induced electron rescattering of atomic negative ions in intense laser fields", **Phys. Rev. A**77, 053410 (2008).

A8. Z-J Chen, T. Morishita, A. T. Le and C. D. Lin, "Analysis of two-dimensional high-energy photoelectron momentum distributions in single ionizaiton of atoms by intense laser pulses", **Phys. Rev. A**76, 043402 (2007).

A9. V. H. Le, A. T. Le, R. H. Xie and C. D. Lin, "Theoretical analysis of dynamic chemical imaging using high-order harmonic generation", **Phys. Rev. A**76, 013414 (2007)

A10. A. T. Le, X. M. Tong and C. D. Lin, "Alignment dependence of high-order harmonic generation from CO2", **J. Mod. Optics**, 54, 967 (2007).

B. Papers submitted for publication

B1. A. T. Le, T. Morishita and C. D. Lin, " Extraction of the species dependent dipole amplitude and phase from high-order harmonic spectra in rare gas atoms", submitted to Phys. Rev. A.

B2. Zhangjin Chen, A. T. Le, T. Morishita and C. D. Lin, "Origin of species dependence of laser-induced high-energy plateau photoelectron spectra", submitted to Phys. Rev. Lett.

Structure and Dynamics of Atoms, Ions, Molecules and Surfaces:
Atomic Physics with Ion Beams, Lasers and Synchrotron Radiation

I.V. Litvinyuk, J. R. Macdonald Laboratory, Physics Department, Kansas State University, Manhattan, KS 66506, ivl@phys.ksu.edu

COLTRIMS studies of strong-field laser-matter interactions

Program Scope: *We use coincident momentum imaging technique ("reaction microscope" or COLTRIMS) to study experimentally interactions of intense (10^{13}-10^{16} W/cm^2) ultrashort (6-60 fs) laser pulses with atoms and molecules in gas phase. In particular, we are interested in such aspects of laser-matter interactions as (i) mechanisms of strong-field double ionization of atoms and molecules; (ii) ultrafast coherent nuclear dynamics induced in molecules by few-cycle laser pulses; and (iii) imaging molecular structure using intense laser pulses. To explore these aspects we (i) measure wavelength dependence of various strong-field processes; (ii) conduct pump-probe studies with short intense pulses; (iii) employ rotational wavepacket technology to produce strongly anisotropic ensembles of molecules to interrogate; and (iv) perform electron-ion coincidence momentum imaging experiments at longer laser wavelength (1600 – 2000 nm).*

1. Mechanisms of strong-field double ionization of atoms and molecules studied by ion recoil momentum spectroscopy at Advanced Laser Light Source (ALLS)

This international collaboration is directed towards understanding dynamics and mechanisms of multiple ionization of atoms and molecules by intense laser pulses. To achieve that, we measure momentum spectra of resulting ion fragments for a series of different laser intensities, polarizations and wavelengths using high power OPA beamline at ALLS.

Recent progress:

1a. Strong-field non-sequential double ionization: wavelength dependence of ion momentum distributions for neon and argon, A.S. Alnaser, D. Comtois, A.T. Hasan, D.M. Villeneuve, J.-C. Kieffer and I.V. Litvinyuk.

Strong-field double ionization of atoms in non-sequential regime produces longitudinal ion momentum distributions with a characteristic double-peak structure. At 800 nm laser wavelength in Ne^{2+} the structure is very pronounced with a well resolved dip at zero momentum, while for Ar^{2+} the dip is very shallow, possibly indicating different mechanisms in the two atoms. We investigated the source of this difference by measuring longitudinal momentum distributions of Ne^{2+} and Ar^{2+} ions at different laser wavelengths (485, 800, 1313 and 2000 nm) and intensities. The shapes of the experimental momentum distributions for the two atoms exhibit strong dependence on laser wavelength: for both the dip becomes more pronounced at longer wavelengths. At 1300 nm longitudinal

momentum spectrum for Ar^{2+} is similar to that of Ne^{2+} at 800 nm. On the other hand, Ne^{2+} spectrum measured at 485 nm has the same shape as that of Ar^{2+} at 800 nm. This observation indicates that the difference between Ne and Ar observed at 800 nm should not be attributed *solely* to differences in relative electron impact ionization and excitation cross-sections of the two atoms. It is, to larger extent, due to interplay between the ponderomotive energy of electron and the ionization potentials of the target atom. We found that the momentum distribution for Ne^{2+} and Ar^{2+} ions exhibit similar wavelength dependence with universal scaling parameter $\alpha = (I_p^3/\omega^2)$, where I_p is the ionization potential and ω is the laser frequency. The results of this study were recently published (see Pub. 4).

1b. Wavelength-dependent study of strong-field Coulomb explosion of hydrogen, I.V. Litvinyuk, A.S. Alnaser, D. Comtois, D. Ray, A.T. Hasan, J.-C. Kieffer and D.M. Villeneuve.

We conducted the first systematic wavelength-dependent study of laser Coulomb explosion of deuterium molecules at various peak intensities and polarizations. We measured the kinetic energy spectra of D^+ for laser wavelengths in the range of 480 - 2000 nm. In addition to the well-known enhanced ionization channel present for all wavelengths, we observe a new high-energy band at short wavelengths. This new band exhibits wavelength dependence, with fragment's energy decreasing with increasing wavelengths until it merges with the enhanced ionization band for 800 nm and longer. We attribute the emergence of this band to a new pathway that involves resonant three-photon coupling to the first excited electronic state of the molecular ion during the Coulomb explosion process. This pathway should be accounted for in controlling molecular dynamics of hydrogen by intense laser pulses. The article presenting the results of this study will appear soon in New Journal of Physics (see Pub. 1).

Future plans: We are planning to continue studying non-sequential double ionization of atoms by measuring its ellipticity dependence at longer wavelengths (1300 – 2200 nm). We will also study wavelength dependence of dissociative ionization for larger molecules (N_2 and O_2).

2. Ultrafast nuclear dynamics induced in molecules by few-cycle laser pulses

Our goal is to study and understand the physics of ultrafast processes involving the motion of nuclei associated with the rotation, vibration, rearrangement and dissociation of molecules and molecular ions. We apply pump-probe techniques in combination with COLTRIMS detection to study the dynamics of nuclear motion as it takes place in real time with the ultimate goal of recovering the time-dependent molecular structure and orientation — making a "molecular movie".

Recent Progress:

2a. Direct Coulomb explosion imaging of coherent nuclear dynamics induced by few-cycle laser pulses in light and heavy hydrogen, I. Bocharova, H. Mashiko, M. Magrakvelidze, D. Ray, P. Ranitovic, C.L. Cocke and I.V. Litvinyuk

We followed fast evolution of coherent nuclear wavepackets in H_2 and D_2 molecules after their interaction with 8 fs 800 nm laser pulses. The molecules were probed by another few-cycle pulse time-delayed for up to 10 ps in respect to the pump. For neutral molecules we observed coherent rotational dynamics characterized by periodic revivals without noticeable decoherence within the 10 ps time-scale. For heavy hydrogen up to 4 rotational states were involved in the wavepackets for each of the two spin isomers. In light hydrogen the resulting dynamics was dominated by beating of just two rotational states. For neutral molecules the experimental results are in excellent agreement with our numerical simulations obtained by solving time-dependent Schrödinger equation. By measuring time-dependent yields for singly ionized rotating D_2 molecules we conclude that for an 8 fs 3×10^{14} W/cm^2 pulse ionization probability is nearly independent of the angle between molecular axis and electric field – we put an upper limit of 1.25 on the ratio of ionization probabilities for molecules aligned parallel and perpendicular to the electric field . For those molecules that were ionized by the pump pulse we observed both vibrational and rotational dynamics. In molecular ions coherent vibrational wavepackets evolving on the bound σ_g potential surface also exhibit revivals. Time-dependent angular distributions for the molecular ions exhibit transient alignment only soon after the pulse (18 fs for H_2^+ and 35 fs for D_2^+) with no consequent revivals within the next 10 ps due to broad distribution of active vibrational states with different rotational constants. The results of this study were recently published (see Pub. 2).

2b. Pump-probe studies of nuclear dynamics in N_2 excited and probed with few-cycle laser pulses, I. Bocharova, S. De, M. Magrakvelidze, D. Ray, P. Ranitovic, C.L. Cocke and I.V. Litvinyuk

We completed a series of pump-probe experiments on N_2 using a pair of few-cycle (8fs) laser pulses of linear and circular polarizations with variable time delay (up to 1000 fs). The pump produces a range of molecular ions (N_2^+, N_2^{2+}, N_2^{3+}) which exhibit fast vibrational, rotational and dissociative dynamics. The dynamics was observed in real time by further ionizing the molecules with the probe pulse to reach even higher charged very repulsive states (N_2^{4+}, N_2^{5+}, N_2^{6+}). The resulting fragments were detected in coincidence and their full 3D momenta were measured. In addition to time-dependent yields for each channel, the fragment momenta contain information on time dependent internuclear separation and orientation of molecular axes. The results of these experiments are currently being analyzed and prepared for publication.

Future plans: First, we are planning to conduct a series of pump probe experiments on O_2 and compare the results with those for N_2. Next, we will study the dynamics of linear tri-atomic molecules (CO_2, CS_2). As a triple coincidence COLTRIMS experiment requires higher laser repetition rates (multi-kHz) than those available at JRML, we have established collaboration with group of Prof. Francois Legare at INRS Quebec, with experiments to be conducted at ALLS.

Articles published and accepted in 2006-2008

1. I.V. Litvinyuk, A.S. Alnaser, D. Comtois, D. Ray, A.T. Hasan, J.-C. Kieffer and D.M. Villeneuve, *Wavelength-dependent study of strong-field Coulomb explosion of hydrogen*, New Journal of Physics accepted.

2. I. Bocharova, H. Mashiko, M. Magrakvelidze, D. Ray, P. Ranitovic, C.L. Cocke and I.V. Litvinyuk, *Direct Coulomb explosion imaging of coherent nuclear dynamics induced by few-cycle laser pulses in light and heavy hydrogen*, Phys. Rev. A **77**, 053407 (2008).

3. D. Ray, B. Ulrich, I. Bocharova, C. Maharjan, P. Ranitovic, B. Gramkow, M. Magrakvelidze, S. De, I.V. Litvinyuk, A.T. Le, T. Morishita, C.D. Lin, G.G. Paulus, and C. L. Cocke, *Large-Angle Electron Diffraction Structure in Laser-Induced Rescattering from Rare Gases*, Phys. Rev. Lett. **100**, 143002 (2008).

4. A.S. Alnaser, D. Comtois, A.T. Hasan, D.M. Villeneuve, J.-C. Kieffer and I.V. Litvinyuk, *Strong-field non-sequential double ionization: wavelength dependence of ion momentum distributions for neon and argon,* J. Phys. B: At. Mol. Opt. Phys. **41**, 031001 (2008).

5. A.S. Alnaser, C.M. Maharjan, P. Wang and I V Litvinyuk, *Multi-photon resonant effects in strong-field ionization: origin of the dip in experimental longitudinal momentum distributions*, J. Phys. B: At. Mol. Opt. Phys. **39**, L323 (2006).

6. A.S. Alnaser, I.V. Litvinyuk, T. Osipov, B. Ulrich, A. Landers, E. Wells, C.M. Maharjan, P. Ranitovic, I. Bocharova, D. Ray and C.L. Cocke, *Momentum-imaging investigations of the dissociation of D_2+ and the isomerization of acetylene to vinylidene by intense short laser pulses*, J. Phys. B: At. Mol. Opt. Phys. **39**, S485 (2006).

7. C.M. Maharjan, A.S. Alnaser, I.V. Litvinyuk, P. Ranitovic and C.L. Cocke, *Wavelength dependence of momentum-space images of low-energy electrons generated by short intense laser pulses at high intensities*, J. Phys. B: At. Mol. Opt. Phys. **39,** 1955 (2006).

Structure and Dynamics of Atoms, Ions, Molecules and Surfaces: Atomic Physics with Ion Beams, Lasers and Synchrotron Radiation

Uwe Thumm, J.R. Macdonald Laboratory, Kansas State University
Manhattan, KS 66506 thumm@phys.ksu.edu

1. Laser-molecule interactions*

Project scope: We seek to develop numerical and analytical tools to i) efficiently predict the effects of a strong laser field on the bound and free electronic and nuclear dynamics in small molecules and ii) to fully image the laser-controlled molecular dynamics.

Recent progress: We continued our investigations of the dissociation and ionization of $H_2^{(+)}$ and $D_2^{(+)}$ in short intense laser pulses by applying wave-packet propagation methods. We investigated the possibility of controlling the electronic motion in dissociating D_2^+ and studied the controlled manipulation of bound vibrational wave packets with a sequence of short control laser pulses at minimal dissociative loss. We introduced a harmonic imaging technique that allows vibrational and rotational beat frequencies, ro-vibrational couplings, molecular potential curves, and the nodal structure of nuclear wave functions to be derived from either measured kinetic-energy-release (KER) spectra or numerical probability densities.

Example 1: Strong-field modulated diffraction effects in the correlated electronic-nuclear motion in dissociating molecular ions (with Feng He and Andreas Becker). The electronic dynamics in a molecule driven by a strong laser field is complex and in part even counterintuitive. As a prototype example, we have studied the electronic motion inside dissociating H_2^+ molecules that are exposed to a fs IR laser pulse. The sensitive dependence of the correlated electronic-nuclear motion can be explained in terms of the diffractive electronic momentum distribution of the dissociating molecule. This distribution is dynamically modulated by the nuclear motion and periodically shifted in the oscillating IR electric field (Fig.1). Depending on the IR laser intensity, the direction of the electronic motion can follow or oppose the IR laser electric force.

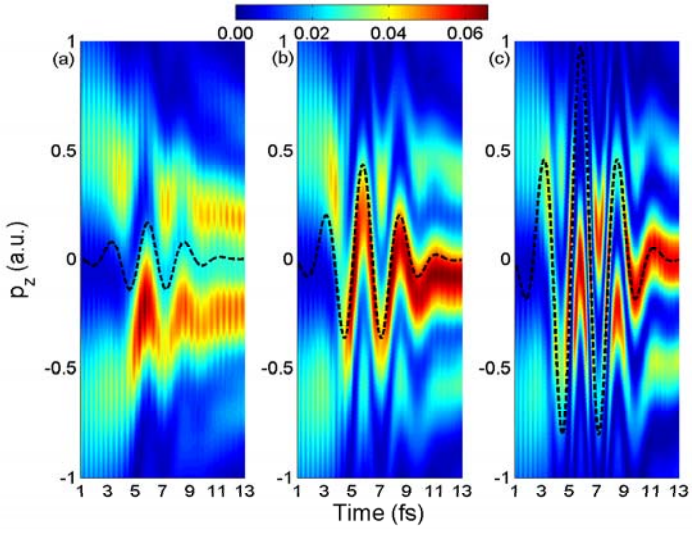

Fig.1. Electron momentum distribution along the laser polarization during the dissociation of H_2^+ in a 5.3 fs IR laser pulse with a time delay of 5.8 fs and intensities of $3x10^{12}$ (a), $2x10^{13}$ (b), and 10^{14} W/cm^2 (c). Dashed lines indicate the classical free-electron momentum in the IR field with zero initial momentum. The dissociating wave packet was launched from the initial $1s\sigma_g$ onto the $2p\sigma_u$ state of H_2^+ in a resonant single-photon transition, induced by a 2-cycle, 106 nm, 10^{13} W/cm^2 attosecond Gaussian pump pulse.

Our interpretation of this effect in terms of a Wigner phase-space distribution [1] is based on the passage of electronic flux through diffractive "momentum gates" of the two-center system that may or may not allow the electron to transfer to the other nucleus. It reveals that the oscillating vector potential of IR laser field periodically shifts these gates, directiong the electron through different gates at different laser intensities.

Future plans: We intend to further investigate the control - at a sub-fs time scale - of the internuclear electronic dynamics by tuning (IR) laser parameters.

Example 2: Imaging the ro-vibrational nuclear dynamics of small molecules in strong laser fields (with Maia Magrakvelidze, Thomas Niederhausen, Bernold Feuerstein, Martin Winter, and Rüdiger Schmidt). We investigated the extent to which measured time-dependent fragment kinetic energy release (KER) spectra and calculated nuclear probability densities can reveal 1) transition frequencies between stationary vibrational states [2,3], 2) stationary rotational states and ro-vibrational couplings [4], 3) the nodal structure of stationary rotational and vibrational states [2-4], 4) field-free and laser-field-dressed adiabatic electronic potential curves of the molecular ion [2-4], and 5) the progression of decoherence induced by random interactions with the environment [3].

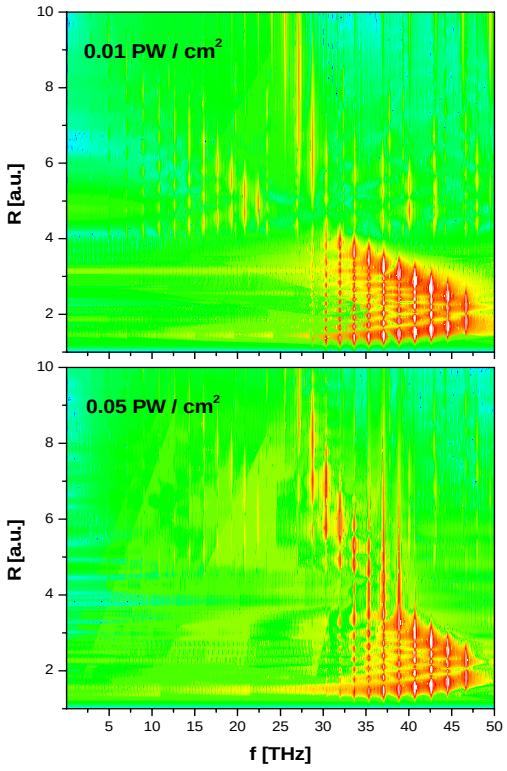

Fig. 2. Power spectra, $|w(R,\theta,f)|^2$, for D_2^+ as a function of the beat frequency f and the internuclear distance R, based on the propagation of an initial Franck-Condon vibrational wave packet for probe-pulse pedestals with peak intensities of 10^{13} W/cm^2 (top) and $5x10^{13}$ W/cm^2 (bottom) and pulse lengths (FWHM) of 50 fs. The wave packet is sampled at the center of the probe pedestal. The sampling time is 10 ps. Both graphs are plotted with the same logarithmic color scale.
Both graphs show i) bond hardening in the transient 1ω adiabatic Floquet potential well, ii) bond softening across the 1ω adiabatic Floquet barrier, iii) the R-dependent nodal structure of pairs of beating vibrational states of D_2^+, and iv) (weakly) "intruder lines" from quantum beats between more distant vibrational states with $\Delta v>1$. The bottom graph also shows the onset of bond softening across the 3ω Floquet barrier.

Our imaging method is based on the Fourier transformation, w(R, θ, f), over finite samplig times T, of the time-, internuclear distance (R)-, and molecular orientation (θ)- dependent probability density w(R, θ, t) of the D_2^+ nuclear wave packet. Applied to numerically propagated D_2^+ ro-vibrational wavepackets, it allows us to simulate novel experiments that record a time series of pump-probe-delay (τ)-dependent KER spectra by Coulomb-explosion mapping for $0 < \tau < T$.

We performed simulations for different initial nuclear wave packets in D_2^+, corresponding to different models for the rapid ionization of D_2 in a short and intense IR pump laser pulse [5]. Our numerical results for vibrational wave packets demonstrate that the obtained two-dimensional R-dependent power spectra enable the comprehensive characterization of the wave-packet dynamics and directly visualize the field-modified molecular potential curves in intense, ultra-short laser pulses, including `bond softening' and `bond hardening' processes (Fig. 2). Further, the harmonic time-series analysis leads to a general scheme for the full reconstruction, up to an overall phase factor, of the initial wave packet based on measured KER spectra [3]. This reconstruction enables the clear distinction between commonly assumed stationary (ro-) vibrational state distributions of the initial nuclear wave packet in the molecular ion.

Including rotation of the molecular ion, beat frequencies that correspond to a vibrational transition ν→ν' are split into multiple lines due to rotational-vibrational coupling [4]. These lines represent individual angular-momentum contributions to the ro-vibrational wave packet (Fig. 3).

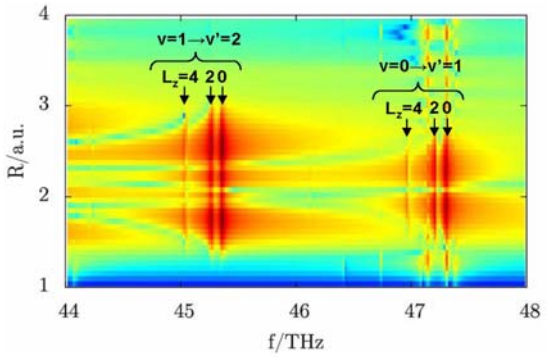

Fig. 3. Angle-integrated power spectra for D_2^+, $|\int d\theta\ w(R,\theta,f)|^2$, as a function of the beat frequency f and the internuclear distance R.

Due to ro-vibrational couplings, lines for the same vibrational transition and different angular momenta L_z do not coincide. Vibrational transitions at larger L_z appear at lower frequencies.

Future plans: We intend to simulate the extent to which the quantum-beat analysis of measured time-dependent fragment KER spectra can quantify the laser-modulated ro-vibrational structure of H_2^+ and other diatomic molecules. Extending this technique to more complicated polyatomic molecular systems and reaction complexes may enable the investigation of molecular dynamics across the (field-modified) potential barrier along a particular reaction coordinate, and, thus, provide a basis for novel multidimensional optical-control schemes for chemical reactions. We further envision to apply this method to quantify the progression of decoherence in the nuclear motion based on a time series of KER spectra [3].

Example 3: Controlling bound vibrational wave packets and the dissociation dynamics of D_2^+ with intense infrared laser pulses (with Thomas Niederhausen). Ionization of neutral D_2 molecules by a short and intense pump laser pulse may create a vibrational wave packet on the lowest ($1s\sigma_g^+$) adiabatic potential curve of the D_2^+ molecular ion. We showed numerically that ultra–short intense near-IR control pulses with appropriate time delays can strongly quench the vibrational-state distribution of the nuclear wave packet by increasing the contribution of selected stationary vibrational states of D_2^+ [5]. Quenching (that is "stopping") the wave packet into a stationary vibrational state offers the possibility to experimentally asses the quality of this Raman–control mechanism by Coulomb-explosion imaging, i.e., by fragmenting the molecular ion with a probe pulse and by identifying the nodal structure of the surviving (excited) vibrational state in the KER spectrum of the molecular fragments.

We continued to investigate the control of the vibrational motion and the dissociation and ionization dynamics of D_2^+ with strong infrared laser pulses in the multi-photon regime. Extending our previous Born-Oppenheimer calculations [3,5], we explicitly included all electronic degrees of freedom to account for non-Born-Oppenheimer effects and the detailed electronic interaction with the intense laser field. We assumed that the molecules remain aligned along the laser polarization and solved the 3D time-dependent Schrödinger equation on a numerical lattice, taking advantage of the cylindrical symmetry. After launching the vibrational wave packet from the neutral molecule, we are currently applying precisely timed control pulses in order to explore the feasibility of manipulating the bound nuclear motion, dissociation, and the nuclear vibrational state composition of D_2^+ nuclear wave packets.

Future plans: Coherent control schemes for quenching moving vibrational wave packets into stationary states using one or several standardized control pulses will be further examined. Based on our new 3D calculations, we intend to investigate the influence of control-laser parameters (intensity, pulse shape and duration, delay relative to the pump pulse, and wave length) on the

fragment KER spectra and the angular distribution of photoelectrons that are ejected during the Coulomb explosion of D_2^+.

2. Neutralization of negative hydrogen ions near flat and vicinal metal surfaces (with Boyan Obreshkov and Himadri Chakraborty)

Project scope: We attempt to understand the transfer of a single electron, initially bound to the projectile, during the reflection of a slow ion or atom at an arbitrarily shaped, nanostructured metal surface as a function of the collision parameters, the surface electronic structure, and crystal orientation of the surface.

Recent progress: We improved our density functional model of the ground-state electronic structure for arbitrarily shaped metallic surfaces [6,7] by including linear and quadratic electronic response terms and heuristic core potentials centered at the lattice points in order to provide realistic, self-consistent surface potentials. We imployed these potentials to model the charge-transfer dynamics during ion-surface collisions, based on a Newns-Anderson approach, including image-charge interactions and electron translation factors [8]. For flat surfaces, we compared the neutralization of H^- near Be, Li, Au, Cu, and Pd surfaces in order to uncover the dependence of the ion survival on the size and position of the surface band gap and on surface and image states [9].

Future plans: We plan to further investigate resonance formation and charge exchange near nano-structured surfaces, in particular, with regard to lateral confinement effects (evidence for which was found in photo-emission experiments). We plan to extend our comparative study of H^- neutralization near metal surfaces of different electronic and morphological structure.

** These research efforts have benefitted significantly from the continous exchange of ideas with my local AMO colleagues at KSU, in particar, with I. Ben-Izhak, K. Carnes, Z. Chang, C.L. Cocke, B. DePaola, B.Esry, C.D. Lin, and I. Litvinyuk.*

[1] *Strong-field modulated diffraction effects in the correlated electronic-nuclear motion in dissociating H_2^+*, F. He, A. Becker, and U. Thumm, submitted to Phys. Rev. Lett.

[2] *Towards a complete characterization of molecular dynamics in ultra-short laser fields*, B. Feuerstein, T. Ergler, A. Rudenko, K. Zrost, C.D. Schroeder, R. Moshammer, J.Ullrich, T. Niederhausen, and U. Thumm, Phys. Rev. Lett. **99**, 153002 (2007).

[3] *Time-series analysis of vibrational nuclear wave packet dynamics in D_2^+*, U. Thumm, T. Niederhausen, and B. Feuerstein, Phys. Rev. A **77**, 063401 (2008).

[4] *Quantum-beat analysis of the rotational-vibrational dynamics in D_2^+*, M. Winter, R. Schmidt, and U. Thumm, to be published.

[5] *Controlled vibrational quenching of nuclear wave packets in D_2^+*, T. Niederhausen and U. Thumm, Phys. Rev. A **77**, 013407 (2008).

[6] *Neutralization of H^- near vicinal metal surfaces*, B. Obreshkov and U. Thumm, Phys. Rev. A **74**, 012901 (2006).

[7] *Step-up vs. step-down scattering asymmetry in the neutralization of H^- on free-electron vivinal surfaces*, B. Obreshkov and U. Thumm, Surf. Sci. **601**, 622 (2007).

[8] *Non-resonant formation of H^- near unreconstructed Si(100) surfaces*, B. Obreshkov and U. Thumm, Phys. Rev. A **76**, 052902 (2007).

[9] *Neutralization of H^- near Be(0001)*, H.S. Chakraborty and U. Thumm, to be published.

Other DoE-sponsored publications (2005-2008):

H.S. Chakraborty, T. Niederhausen, and U. Thumm, Nucl. Instrum. Methods B **241**, 43 (2005).
T. Niederhausen and U. Thumm, Phys. Rev. A **73**, 041404(R) (2006).

Multiparticle Processes and Interfacial Interactions in Nanoscale Systems Built from Nanocrystal Quantum Dots

Victor I. Klimov
Chemistry Division, C-PCS, MS-J567, Los Alamos National Laboratory
Los Alamos, New Mexico 87545, klimov@lanl.gov, http://quantumdot.lanl.gov

1. Program Scope

Using semiconductor nanocrystals (NCs) (known also as nanocrystal quantum dots) one can produce extremely strong spatial confinement of electronic excitations not accessible with other types of nanostructures. Because of spatial constraints imposed on electron and hole wavefunctions, electronic energies in NCs are directly dependent upon their dimensions, which is known as the quantum-size effect. This effect has been a powerful tool for controlling spectral responses of NCs, enabling potential applications such as multicolor labeling, optical amplification, and low-cost lighting. In addition to spectral tunability, strong spatial confinement results in a significant enhancement of carrier-carrier interactions that lead to a number of novel physical phenomena including large splitting of electronic states induced by electron-hole (e-h) exchange coupling, ultrafast mutiexciton decay via Auger recombination, high-efficiency intraband relaxation via e-h energy transfer, and direct generation of multiple excitons by single absorbed photons via carrier multiplication (CM). Understanding the fundamental physics of electronic and magnetic interactions under conditions of extreme quantum confinement and the development of methods for controlling these interactions represents the major thrust of this project. Research topics studied here include single-exciton optical gain using engineered exciton-exciton interactions, tunable magnetic exchange interactions with paramagnetic ions in core/shell hetero-structures, and Auger recombination and CM in NCs of direct- and indirect-gap materials. In addition to their fundamental significance, these studies are relevant to a number of emerging applications of NCs in areas such as low-threshold lasing, magnetic imaging, electro- and magneto-optical switching, and solar-energy conversion.

2. Recent Progress

2.1 Progress summary. In FY2007, the work in this project has concentrated on experimental and theoretical studies of electronic and optical properties of semiconductor NCs with emphases on the spectral and dynamical properties of single and multiexciton states, multiexciton generation via CM, and the effect of quantum confinement on radiative decay rates of NCs of indirect-gap semiconductors. Specific research topics included:

- Engineered exciton-exciton interactions and single-exciton gain in core/shell hetero-NCs
- CM mechanism and competing relaxation processes
- CM activation thresholds
- Scaling of multiexciton lifetimes
- Fine structure of NC band-edge states probed by single-dot, magnetic-field spectroscopy
- Indirect- to direct-gap transformation in Si NCs

The results of this project were highlighted in several internal and external press releases. Specifically, the work on single-exciton lasing using giant exciton-exciton repulsion was reviewed in *Physics Today* (Engineering the energy levels in quantum dots leads to optical gain, July, 2007), *Scientific American* (Brighter prospects for cheap lasers in rainbow colors, May 25, 2007), *Nature* (Laser technology: Less excitement for more gain, May 23, 2007), *Technology Reviews* (Colorful lasers from Q-dots, May 29, 2007), etc.

Below we provide three representative examples that describe our work related to CM, single-exciton gain, and fine-structure splitting of the band-edge NC exciton states.

2.2 Photogeneration of multiple excitons by single photons. A usual assumption is that absorption of a single photon by a semiconductor produces a single e-h pair (exciton), while the photon energy in excess of the energy gap is dissipated as heat by exciting lattice vibrations. In 2004, we reported for the first time that NCs of PbSe could respond to absorption of a single photon by producing two or more e-h pairs with 100% efficiency via the CM process (*Phys. Rev. Lett.* **92**, 186601, 2004). During the past year, we have conducted experimental and

theoretical studies with a goal to elucidate the CM mechanism and establish parameters that control the spectral onset of this process.

In bulk materials, CM is typically explained by impact ionization, which is a process in which a high-energy conduction-band electron (or a valence-band hole) interacts with the valence-band electron promoting it across the energy gap. Our recent theoretical studies indicate that in NCs, CM may be dominated by a different effect. Specifically, we have analyzed the process in which the virtual biexciton is generated from NC vacuum by the Coulomb interaction between two valence-band electrons. This virtual state is then converted into a real, energy-conserving biexciton by photon absorption on an intraband optical transition. The proposed mechanism is not active in bulk semiconductors as momentum conservation suppresses intraband transitions. However, it becomes highly efficient in the case of zero-dimensional NCs, where quantum confinement results in relaxation of momentum conservation, which is accompanied by the development of strong intraband absorption.

We have also examined factors that control the spectral onset ($\hbar\omega_{CM}$) of the CM process. Based on the analysis of optical selection rules and energy conservation, we have derived a criterion, which relates $\hbar\omega_{CM}$ to the effective carrier masses (m_e and m_h, for electrons and holes, respectively). This criterion accurately predicts trends previously observed for CM onsets in semiconductor NCs and indicates that the CM threshold can be reduced to the energy-conservation-defined minimum of two energy gaps ($2E_g$) using materials with a significant difference between m_e and m_h. Using InAs NCs, for which $m_e << m_h$, we indeed observe CM thresholds that approach the fundamental $2E_g$ limit. We have further considered the possibility of obtaining the CM onset of less than $2E_g$ in the circumstance of strong Coulomb attraction, which would decrease the energy required to produce a biexciton compared to twice a single-exciton energy. The low threshold observed by us for CM in a III-V material indicates that these are promising candidates for application in CM-enhanced photovoltaics and photocatalytics.

2.2 Single-exciton gain via engineered exciton-exciton (X-X) repulsion. Optical gain in ultrasmall semiconductor nanocrystals requires that some of the nanoparticles in the ensemble are excited with multiple e-h pairs (multiexcitons). A significant complication arising from this multiexciton nature of optical amplification is ultrafast gain decay induced by nonradiative Auger recombination.

Potential approaches to reducing Auger rates include the use of elongated NCs (quantum rods) or core-shell hetero-NC, which enables a decreased X-X coupling without losing the benefits of strong quantum confinement. However, the most radical strategy to solving the Auger-decay problem is through the development of approaches that could allow realization of optical gain in the single-exciton regime, for which Auger recombination is simply inactive. In this project, we have demonstrated one such approach, which involves the use of type-II core/shell hetero-NCs. Spatial separation of electrons and holes in these nanostructures produces a significant imbalance between negative and positive charges, which results in a strong local electric field. This field displaces the absorbing transition in singly excited NCs with respect to the emission line via the carrier-induced Stark effect and allows optical amplification due to single excitons.

As part of these studies, we have developed a model for treating optical gain in NCs in the presence of X-X interactions for the arbitrary degeneracy (γ) of the emitting quantized states. This model shows that in the case when the X-X interaction is repulsive and its energy (Δ_{xx}) is greater than the ensemble linewidth of the emitting transition, the optical gain threshold reduces to $\langle N \rangle_{th} = \gamma/(\gamma + 1) < 1$. The latter expression indicates that lasing does *not* require multiexcitons and, hence, can be realized without complications associated with Auger recombination. Specifically, in the case of the two-fold degeneracy of the emitting states, the gain threshold requires that only two thirds of the NCs in the ensemble contain single excitons, while the rest remains unexcited. Further, we have demonstrated both theoretically and experimentally that giant X-X repulsion with energies of more than 100 meV by can be obtained using type-II hetero-NCs of compositions such as CdS(core)/ZnSe(shell) and ZnTe(core)/CdSe(shell). Finally, we have performed side-by-side comparison of transient-absorption spectra and dynamics for type-II CdS/ZnSe NCs and traditional type-I CdSe NCs. We observe a significant difference in optical-gain properties for these two types of the nanostructures, which points toward the single-exciton nature of light amplification in type-II NCs.

2.3 Exciton "fine structure" in CdSe NCs revealed by single-dot, magnetic-field spectroscopy. In *epitaxially-grown* quantum dots, in-plane anisotropy mixes the lowest optically allowed (spin ±1) bright excitons, giving a "fine structure" of two eigenstates, $|X\rangle = (|+1\rangle + |-1\rangle)$ and $|Y\rangle = (|+1\rangle - |-1\rangle)$, that are linearly and orthogonally polarized and typically split in energy by 0.01- 0.50 meV. Despite the broad and topical interest in $|X,Y\rangle$ exciton

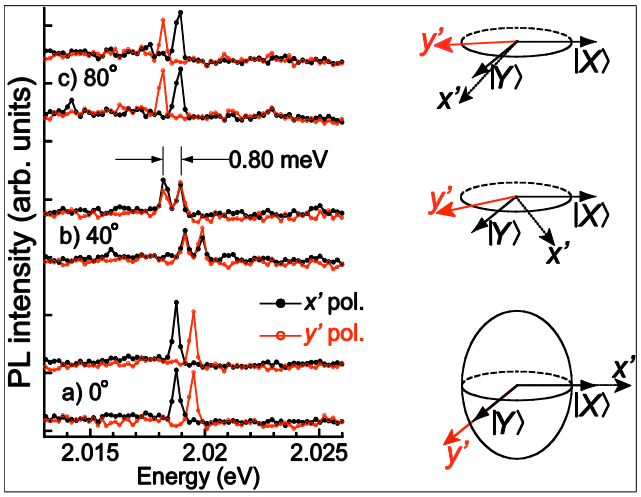

Figure 1. Polarization-resolved bright-exciton PL from a single CdSe NC at 4K. Two 20s exposures are shown for each orientation of the linear detection axes *x'* and *y'*: a) 0, b) 40, and c) 80 degrees with respect to the NC's intrinsic |X> and |Y> emission axes.

fine structure in epitaxially-grown dots, there were no reported studies of a corresponding |X,Y> fine structure in colloidal NCs.

In this project, we have conducted the first single-NC study of the |XY>-splitting of the emitting exciton state. Specifically, we have used high-resolution, polarization-resolved, low-temperature photoluminescence (PL) of *single* CdSe NCs to detect and quantify this splitting. To minimize the effects of spectral diffusion and blinking, we simultaneously detected both orthogonal, linearly-polarized PL components (labeled *x'* and *y'*) by using a polarizing beamsplitter in front of an imaging spectrometer. Using this scheme, we found that at 4 K, approximately 10% of the surveyed NCs exhibited narrow PL lines and a well-resolved splitting between orthogonal linearly polarized PL components. Figure 1 shows direct spectroscopic evidence for an |X,Y> fine structure of bright excitons in one such NC. With the x' and y' detection axes aligned with this NC's particular |X> and |Y> emission axes, two clear PL peaks are observed, orthogonally polarized and split by Δ_{XY} = 0.8 meV. By carefully analyzing the intensities of these two emitting states as a function of analyzer angle, we have also shown that it is possible to measure the absolute orientation of the NC with respect to the fixed laboratory axis.

3. Future Plans

3.1 The effect of NC charging on carrier recombination and photogeneration dynamics. Understanding properties of charged NCs is an important step toward NC-based photovoltaic and electro-optical applications. It is also of fundamental importance as it may provide useful insights into single-NC phenomena such as PL spectral wandering and blinking. Recently, it has been demonstrated that colloidal NCs can be charged in a controlled way either by chemical or electrochemical methods. It was also shown that charging has a distinct effect on optical properties of NCs including spectral shifts, bleaching of band-edge interband absorption, and the development of new IR absorption features due to intraband transitions. Despite a number of important insights gained in these earlier studies, the current understanding of the effect of charging on carrier recombination dynamics is still limited. Building on our expertise in studies of Auger processes and relaxation dynamics, we will extensively study carrier dynamics in charged NCs. We will focus on topics such as the "dark-to-bright" transformation of the lowest-energy emitting transition induced by injected electrons, charged-exciton (trion) versus biexcion recombination dynamics, and the effect of charging on the carrier multiplication threshold and efficiency.

3.2 Spectral and dynamical properties of single- and multiexciton states in NCs of indirect-gap semiconductors. Electronic and optical properties of NCs of indirect-gap materials remain understood significantly poorer than those of direct-gap semiconductors. Most of the previous research in this area has focused on Si nanostructures. Because of highly developed processing capabilities, there is great interest in the realization of Si-based optoelectronic devices such as light emitting diodes and lasers. However, bulk Si is an indirect-gap semiconductor, and thus, the radiative recombination in this case can only occur via low-efficiency, phonon-assisted processes. On the other hand, relaxation of momentum conservation in Si NCs can open an efficient channel for radiative recombination via pseudo-direct transitions. Because of large energy separation between direct- and indirect-gap minima in Si (~2 eV), the onset for pseudodirect recombination corresponds to very small NCs sizes (< 4 nm) that are difficult to obtain using existing fabrication techniques. As an alternative to Si, in this project, we will synthesize and study NCs of Ge. Electronic and optical properties of Ge offer several advantages over Si for photovoltaic and lasing applications. Ge possesses a narrower band gap and higher absorption cross-sections than Si, key for photovoltaic application, especially for carrier-multiplication-enhanced devices. Some of the proposed research topics are "direct-to-indirect" gap transformation induced by quantum

confinement, spectral and dynamical signatures of multiexciton states in photoluminescence and transient absorption, multiexciton recombination and photogeneration pathways including carrier multiplication.

4. Publications (2006 - 2008)

1. M. Sykora, L. Mangolini, R. D. Schaller, U. Kortshagen, D. Jurbergs, and V. I. Klimov, Size-dependent intrinsic radiative decay rates of silicon nanocrystals at large confinement energies, *Phys. Rev. Lett*. **100**, no. 6, 067401-1-4 (2008).
2. V. I. Klimov, J. A. McGuire, R. Schaller, and V. I. Rupasov, Scaling of multiexciton lifetimes in semiconductor nanocrystals, *Phys. Rev. B* **77**, 195324 –1- 12 (2008).
3. H. Htoon, M. Furis, S. A. Crooker, S. Jeong, V. I. Klimov, Linearly-polarized 'fine structure' of the bright exciton state in individual CdSe nanocrystal quantum dots, *Phys. Rev. B* **77**, no. 3, 035328-01-7 (2008)
4. R. D. Schaller, J. M. Pietryga, and V. I. Klimov, Carrier Multiplication in InAs Nanocrystal Quantum Dots with an Onset Defined by the Energy Conservation Limit, *Nano Lett.* **7**, no. 11, 3469 – 3476 (2007)
5. V. I. Rupasov and V. I. Klimov, Carrier multiplication in semiconductor nanocrystals via intraband optical transitions involving virtual biexciton states, *Phys. Rev. B* **76**, no. 12, 125321 (2007).
6. X. Jiang, R. D. Schaller, S. B. Lee, J. M. Pietryga, V. I. Klimov, and A. A. Zakhidov, PbSe nanocrystal/conducting polymer solar cells with an infrared response to 2 micron, *J. Mat. Res.* **22**, 8, 2204-2210 (2007)
7. V. I. Klimov, S. A. Ivanov, J. Nanda, M. Achermann, I. Bezel, J. A. McGuire, and A. Piryatinski, Single-exciton optical gain in semiconductor nanocrystals, *Nature* **447**, 441 (2007).
8. A. Piryatinski, S. A. Ivanov, S. Tretiak, and V. I. Klimov, Effect of quantum and dielectric confinement on the exciton-exciton interaction energy in type II core/shell semiconductor nanocrystals, *Nano Lett.* **7**, 108 (2007)
9. V. I. Klimov, Spectral and dynamical properties of multiexcitons in semiconductor nanocrystals, *Annu. Rev. Phys. Chem.* **58**, 635 (2007).
10. J. Nanda, S. A. Ivanov, J. Nanda, M. Achermann, I. Bezel, A. Piryatinski, V. I. Klimov Light Amplification in the single-exciton regime using exciton-exciton repulsion in type-II nanocrystal quantum dots, *J. Phys. Chem. B* (2007).
11. S. A. Ivanov, A. Piryatinski, J. Nanda, S. Tretiak, D. Werder, V. I. Klimov, Type-II core/shell CdS/ZnSe nanocrystals: Synthesis, electronic structures, and spectroscopic Properties, *J. Am. Chem. Soc.* **129**, no. 38, 11708-11719 (2007).
12. N. G. Liu, B. S. Prall, and V. I. Klimov, Hybrid gold/silica/nanocrystal quantum-dot superstructures: Synthesis and analysis of semiconductor-metal interactions, *J. Am. Chem Soc.* **128**, 15362-15363 (2006).
13. V, I. Klimov, Mechanisms for photogeneration and recombination of multiexcitons in semiconductor nanocrystals: Implications for lasing and solar energy conversion, *J. Phys. Chem. B, Feature Article* **110**, 16827 (2006).
14. R. D. Schaller, M. Sykora, S. Jeong, and V. I. Klimov, High-efficiency carrier multiplication and ultrafast charge separation in semiconductor nanocrystals studied via time-resolved photoluminescence, *J. Phys. Chem. B* **110**, 25332 (2006).
15. V. I. Klimov, Detailed-balance power-conversion limits of nanocrystal-quantum-dot solar cells in the presence of carrier multiplication, *Appl. Phys. Lett.* **89**, 123118 (2006).
16. M. Sykora, M. A. Petruska, J. Alstrum-Acevedo, I. Bezel, T. J. Meyer, and V. I. Klimov, Photoinduced charge transfer between CdSe nanocrystaline quantum dots and Ru-polypyridine complexes, *J. Am. Chem. Soc.* **128**, 9984 (2006).
17. M. Achermann, A. P. Bartko, J. A. Hollingsworth, and V. I. Klimov, The effect of Auger heating on intraband relaxation in semiconductor quantum rods **2**, 557 *Nature Physics* (2006).
18. M. Achermann, M. A. Petruska, D. D. Koleske, M. H. Crawford, and V. I. Klimov, Nanocrystal-based light emitting diodes utilizing high-efficiency nonradiative energy transfer for color conversion, *Nano Lett.* **6**, 1396 (2006).
19. R. D. Schaller and V. I. Klimov, Non-Poissonian exciton populations in semiconductor nanocrystals via carrier multiplication, *Phys. Rev. Lett.* **96,** 097402 (2006).
20. J. Nanda, S. A. Ivanov, H. Htoon, I. Bezel, A. Piryatinski, S. Tretiak, and V. I. Klimov, Absorption cross sections and Auger recombination lifetimes in inverted core/shell nanocrystals: Implications for lasing performance, *J. Appl. Phys.* **99**, 034309 (2006).
21. R. D. Schaller, M. Sykora, J. M. Pietryga, and V. I. Klimov, Seven excitons at a cost of one: Redefining the limits for conversion efficiency of photons into charge carriers, *Nano Lett.* **6**, 424 (2006).
22. G. R. Maskaly, M. A. Petruska, J. Nanda, I. V. Bezel, R. D. Schaller, H. Htoon, J. M. Pietryga, and V. I. Klimov, Enhancements to the stimulated light emission of semiconductor nanocrystals due to a photonic crystal pseudogap, *Advanced Materials* **18**, 343 (2006).
23. M. Furis, H. Htoon, M. A. Petruska, V. I. Klimov, T. Barrick, and S. A. Crooker. Bright-exciton fine structure and anisotropic exchange in CdSe nanocrystal quantum dots, *Phys. Rev. B* **73**, 241313 (R) (2006).

Atomic, Molecular and Optical Sciences at LBNL

A. Belkacem, C.W. McCurdy, T. Rescigno and T. Weber

Chemical Sciences Division, Lawrence Berkeley National Laboratory, Berkeley, CA 94720

Email: abelkacem@lbl.gov, cwmccurdy@lbl.gov, tnrescigno@lbl.gov, tweber@lbl.gov

Objective and Scope

The AMOS program at LBNL is aimed at understanding the structure and dynamics of atoms and molecules using photons and electrons as probes. The experimental and theoretical efforts are strongly linked and are designed to work together to break new ground and provide basic knowledge that is central to the programmatic goals of the Department of Energy. The current emphasis of the program is in three major areas with important connections and overlap: inner-shell photo-ionization and multiple-ionization of atoms and small molecules; low-energy electron impact and dissociative electron attachment of molecules; and time-resolved studies of atomic processes using a combination of femtosecond X-rays and femtosecond laser pulses. This latter part of the program is folded in the overall research program in the Ultrafast X-ray Science Laboratory (UXSL).

The experimental component at the Advanced Light Source makes use of the Cold Target Recoil Ion Momentum Spectrometer (COLTRIMS) to advance the description of the final states and mechanisms of the production of these final states in collisions among photons, electrons and molecules. Parallel to this experimental effort, the theory component of the program focuses on the development of new methods for solving multiple photo-ionization of atoms and molecules. This dual approach is key to break new ground and solve the problem of photo double-ionization of small molecules and unravel unambiguously electron correlation effects.

The relativistic collisions part of the program has been phased out in favor of branching into dissociative electron attachment measurements using COLTRIMS in support of the theoretical effort in the area of electron driven chemistry. These studies make use of the group's expertise at performing "complete" experiments using COLTRIMS. The theoretical project seeks to develop theoretical and computational methods for treating electron driven processes that are important in electron-driven chemistry and that are beyond the grasp of first principles methods.

Inner-Shell Photoionization and Dissociative Electron Attachment of Small Molecules

Ali Belkacem and Thorsten Weber

Chemical Sciences Division, Lawrence Berkeley National Laboratory, Berkeley, CA 94720

Email: abelkacem@lbl.gov, tweber@lbl.gov

Objective and Scope

This program is focused on studying photon and electron impact ionization, excitation and dissociation of small molecules and atoms. The first part of this project deals with the interaction of X-rays with atoms and simple molecules by seeking new insight into atomic and molecular dynamics and electron correlation effects. These studies are designed to test advanced theoretical treatments by achieving a new level of completeness in the distribution of the momenta and/or internal states of the products and their correlations. The second part of this project deals with the interaction of low-energy electrons with small molecules with particular emphasis on Dissociative Electron Attachment (DEA). Both studies are strongly linked to our AMO theoretical studies led by C. W. McCurdy and T. Rescigno and are designed to break new ground and provide basic knowledge that is central to the programmatic goals of BES in electron-driven chemistry. Both experimental studies (photon and electron impact) make use of the powerful COLd Target Ion Momentum Spectroscopy (COLTRIMS) method to achieve a high level of completeness in the measurements.

Ultrafast probing of core-hole localization in nitrogen molecule.

K-shell photo-ionization of a many-electron atom in a molecule yields a photo-electron followed by emission of at least one Auger electron and the fragmentation of the molecule. It has been generally believed that the photo-emission and Auger processes are independent so that, e.g. the Auger electron angular distribution in the molecular frame should not depend on the photon energy or the orientation of the photon's linear polarization with respect to the molecular axis. In this work we investigate the entanglement between the photo-electron and the Auger electron in the photo double ionization of N_2 molecules. Valence electrons in molecules owe their binding forces to delocalization over two or more sites. For inner-shell electrons in contrast the wave function is rather confined at the nuclei. The overlap of these wave functions from neighboring atoms is almost negligible. Still the electronic structure of molecules with equivalent sites is generally calculated by using symmetry adapted delocalized wave functions also for inner-shell electrons. For N_2, as a show case example, the innermost electrons are usually described by a $1\sigma_u$ and $1\sigma_g$ molecular orbital, which are delocalized over two atoms. This has led to very controversial questions about core-hole localization and numerous papers can be found in the literature arguing for or against the veracity of the core-hole localization concept: The question posed is “does the photo-ionization process create a localized hole, or does it create a delocalized hole that preserves the symmetry of the target molecule?”. A puzzling topic throughout this controversy is what kind of physical process could possibly break the symmetry of the system: For larger molecules with equivalent sites asymmetric vibrational modes can be excited and the vibrational excitation breaks the original symmetry of the molecule and allows

localization of the core hole. For diatomic molecules such as N_2 this is not possible. Does that mean that the symmetry has to be conserved? In this present work we used a completely new approach to address this question. A core ionized molecule is not stable and decays by Auger electron emission. The Auger electron carries information (energy and angle) about the hole which was filled and we seek this information in coincidence with the photoelectron emission angle. Thus in the break up process one needs to detect the momenta of four particles ($e_{photoelectron}$, e_{Auger}, $N^+ + N^+$). In reality it is sufficient to detect the momentum vector of only three particles since the fourth 3d-momentum vector (Auger electron in this case) can be calculated via momentum conservation. By measuring the photoelectron and deducing the 7 fsec delayed Auger electron, we find that whether the hole is better thought of as localized or delocalized depends on the emission angle of the photoelectron: The angular distribution of the Auger electrons show a strong symmetry breaking for certain directions of the emitted photoelectron. Thus the photoelectron and Auger electron are in an entangled Bell state, and their coincident measurement disentangles this state, demonstrating that in some cases the K-hole behaves like a localized state while in others it acts like a delocalized one. This work was published in Science.

Interference and decoherence in the photo-double ionization of molecular hydrogen.

At high photon energies electrons with de Broglie wavelengths λ_e close to the size (0.72 Å) of the H_2 (or D_2) molecule can be expected to show angular distributions similar to Young's double slit diffraction of light. The idea of using a homonuclear molecule as a slit-scattering center of a photoelectron goes back to a paper published by Cohen and Fano [H. Cohen, U. Fano, Phys. Rev. 150, 30 (1966)]. Due to the coherence in the initial molecular state, the absorption of one photon by the homonuclear molecule launches two coherent electron waves at each of the protons of the molecule. The interference pattern of these waves should be visible in the angular distribution of the electron with respect to the molecular axis. In this work we extended the idea of Cohen and Fano from single ionization to double ionization to study the two body interference of an electron pair. The two electrons are distinguishable by their energy, which allows us to study the interference pattern as a function of the interaction strength or momentum exchanged between the two particles. One of the fundamental problems we set to investigate in this experiment is to reveal why wave properties of particles are rarely seen in nature. One of the more fundamental causes is that particles couple to their surrounding environment that alter their phase, thus inducing decoherence. Decoherence is thought to be a main cause of the transition from quantum to classical behavior. In our experiment the slow electron acts as an inactive (0 to 5eV) or active (>5eV) observer of the interference process of the fast electron and thus represents a controllable environment, which is responsible for decoherence. Although the coherence of the fast electron gets lost, the correlated momenta of the entangled electron pair continue to exhibit quantum interference. We published the results of this work in Science.

Fragmentation pathways for selected electronic states of the acetylene dication.

Acetylene is an important prototypical small hydrocarbon for the study of photo initiated processes. Of particular interest are the yields into symmetric (CH^+/CH^+), deprotonation (HCC^+/H^+) and quasi-symmetric (HHC^+/C^+) channels, the latter involving isomerization from the neutral acetylene structure to the vinylidene configuration prior to break up. One expects that the products of dissociation, their Kinetic Energy Releases (KER) and the

isomerization times will depend on the particular initial electronics states. While the fragmentation and the isomerization of the acetylene dication have been studied for a number of years, the only experimental information previously available on the energetic pathways are the measurements of appearance energies. In this work we used the COLTRIMS set up modified with a detection technique based on the deceleration of the Auger electron to achieve high energy resolution. The dication is prepared by Auger decay following core-hole level x-ray photoionization at 310 eV. The energy and angular distribution of the Auger electron is measured in coincidence with the kinetic energy of the fragments. This experimental approach, in combination with ab initio quantum mechanical calculations by T.N. Rescigno, yield a comprehensive map of the two-body dissociation pathways including the transition through different electronic energy surfaces and transitions through barriers to direct dissociation and the associated rearrangement channels. This work was published in J. Phys. B.

Dissociative electron attachment of small molecules.

A COLTRIMS method is developed for measuring the angular distribution of fragment negative ions arising from dissociative electron attachment of molecules. A low energy pulsed electron gun is used in combination with pulsing the extraction plates of the COLTRIMS spectrometer. The emission pattern of the fragments is influenced by selection rules, which connect the states of the neutral molecule to the negative ion resonant states, and the orientation of the neutral molecule with respect to the momentum vector of the incoming electron. Thus the angular distribution contains information on the symmetry of the negative ion state and the angular momentum of the captured electron. Therefore the angular distribution measurements are of particular importantance for the understanding of dissociative electron attachment. The formation of the resonant dissociative negative molecular states typically peak at electron energies below 10 eV. A major technical problem is the production of a controlled and defined low energy electron beam that can strike the molecular jet within the uniform electric field of the COLTRIMS spectrometer. Our approach uses a uniform electric field and an orthogonal uniform magnetic field. This ExB field steers the electrons along the directions of the gas jet without (or minimally) affecting their energy. Earlier studies of DEA found in the literature measured angular distributions of negative ion products as well, however the COLTRIMS approach will result in higher sensitivity and simultaneous coverage of a wide range of negative ion final momenta. We applied this modified COLTRIMS technique to the the measurement of dissociative electron attachment of O_2. The formation of O^- from O_2 is known to appear as a broad peak centered at 6.5 eV in the kinetic energy spectrum and thus can be used as a calibration of our apparatus. The angular distribution of O^- changes as the energy of the electrons is swept across the broad resonance. At the maximum of cross section (6.5 eV) the distribution shows clear minima when the O_2 molecule is aligned parallel or perpendicular to the electron beam direction. The maximum yield is observed at 45^0 degree angles which is interpreted as astrong signature of a Π contribution.

Future Plans

We plan to continue the application of the COLTRIMS approach to achieve complete descriptions of the single photon double ionization of CO and its analogs. New measurements will be made close to the double ionization threshold and approaching the regime where the outgoing electrons and the ions have nearly the same velocities. Our earlier observations of the isomerization of acetylene to the vinylidene configuration

forms a basis for possible further studies of this phenomena perhaps using deuterated acetylene to alter the relative time scales of molecular rotation and the dissociation dynamics.

Recent Publications

D. Akoury, K. Kreidi, T. Jahnke, Th. Weber, A. Staudte, M. Schoeffler, N. Neumann, J. Titze, L. Ph. H. Schmidt, A. Czasch, O. Jagutzki, R.A. Costa Fraga, R.E. Grisenti, R. Diez Muino, N.A. Cherepkov, S.K. Semenov, P. Ranitovic, C.L. Cocke, T. Osipov, H. Adaniya, J.C. Thompson, M.H. Prior, A. Belkacem, A. L. Landers, H. Schmidt-Boecking, R. Doerner, "*The simplest double slit: Interference and Entanglement in double photoionization of H_2*", Science **318**, 949 (2007).

M.S. Schoeffler, J. Titze, N. Petridis, T. Jahnke, K. Cole, L.Ph.H. Schmidt, A. Czasch, D. Akoury, O. Jagutzki, J.B. Williams, N.A. Cherepkov, S.K. Semenov, C.W. McCurdy, T.N. Rescigno, C.L. Cocke, T. Osipov, S. Lee, M.H. Prior, A. Belkacem, A.L. Landers, H. Schmidt-Boecking, Th. Weber, R. Doerner, "*Utrafast probing of core hole localization in N_2*", Science, **320**, 920 – 923 (2008)

F. Martin, J. Fernandez, T. Havermeier, L. Foucar, Th. Weber, K. Kreidi, M. Schoeffler, L. Schmidt, T. Jahnke, O. Jagutzki, A. Czasch, E.P. Benis, T. Osipov, A. Landers, A. Belkacem, M.H. Prior, H. Schmidt-Boecking, C.L. Cocke, R. Doerner, "*Single photon-induced symmetry breaking of H_2 Dissociation*", Science **315**, 629 (2007).

K. Kreidi, D. Akoury, T. Jahnke, Th. Weber, A. Staudte, M. Schoffler, N. Neumann, J. Titze, L. Ph. H. Schmidt, A. Czasch, O. Jagutzki, R.A. Costa Fraga, R.E. Grisenti, M. Smolarski, P. Ranitovic, C.L. Cocke, T. Osipov, H. Adaniya, J.C. Thompson, M.H. Prior, A. Belkacem, A. Landers, H. Schmidt-Bocking, R. Doerner, "*Interference in the collective electron momentum in double photoionization of H_2*", Phys. Rev. Lett., **100**, 133005-1 to 4 (2008)

K. Hosaka, J. Adachi, A.V. Golovin, M. Takahashi, T. Teramoto, N. Watanabe, T. Jahnke, Th. Weber, M. Schoeffler, L. Schmidt, T. Osipov, O. Jagutzki, A. Landers, M.H. Prior, H. Schmidt-Boecking, R. Doerner, A. Yagishita, S. Semenov and N. Cherepkov, "*Nondipole effects in the angular distribution of photoelectrons from the C K-shell of the CO molecule*", Phys. Rev. A **73**, 022716 (2006).

A.Belkacem and A. Sorensen, "*The pair-production channel in atomic processes*", Rad. Phys. and Chem. **75**, 656 (2006).

T. Osipov, T.N. Rescigno, Th. Weber, S. Miyabe, T. Jahnke, A.S. Alnaser, M.P. Hertlein, O. Jagutzki, L. Ph. Schmidt, M. Schoffler, L. Foucar, S. Schossler, T. Havermeier, M. Odenweller, S. Voss, B. Feinberg, A.L. Landers, M.H. Prior, R. Doerner, C.L. Cocke, A. Belkacem, "*Fragmentation pathways for selected electronic states of the acetylene dication*", J. Phys. B: At. Mol. Opt. Phys., **41**, 091001 (2008)

M. Schoeffler, K. Kreidi, D. Akoury, T. Jahnke, Th. Weber, A. Staudte, N. Neumann, J. Titze, L. Ph. H. Schmidt, A. Czasch, O. Jagutzki, R.A. Costa Fraga, R.E. Grisenti, R. Diez Muino, N.A. Cherepkov, S.K. Semenov, P. Ranitovic, C.L. Cocke, T. Osipov, H. Adaniya, J.C. Thompson, M.H. Prior, A. Belkacem, A. L. Landers, H. Schmidt-Boecking, R. Doerner, "*Photo double ionization of H2: Two-center interference and its dependence on the internuclear distance*", accepted for publication in Phys. Rev. A

Electron-Atom and Electron-Molecule Collision Processes

T. N. Rescigno and C. W. McCurdy
Chemical Sciences, Lawrence Berkeley National Laboratory, Berkeley, CA 94720
tnrescigno@lbl.gov, cwmccurdy@lbl.gov

Program Scope: This project seeks to develop theoretical and computational methods for treating electron processes that are important in electron-driven chemistry and physics and that are currently beyond the grasp of first principles methods, either because of the complexity of the targets or the intrinsic complexity of the processes themselves. A major focus is the development of new methods for solving multiple photoionization and electron-impact ionization of atoms and molecules. New methods are also being developed and applied for treating low- energy electron collisions with polyatomic molecules and clusters. A state-of-the-art approach is used to treat multidimensional nuclear dynamics in polyatomic systems during resonant electron collisions and predict channeling of electronic energy into vibrational excitation and dissociation.

Recent Progress and Future Plans: We report progress in two areas covered under this project, namely photo-double ionization and electron-polyatomic molecule collisions.

1. Photo-Double Ionization

Our theoretical AMO program continues to focus on the study of strongly correlated atomic and molecular processes that involve several electrons in the continuum. Using the exterior complex scaling (ECS) approach, we have extended our earlier studies of double ionization in helium by single photon absorption to the more difficult case of two-photon double ionization. Our initial studies, published as a Rapid Communication in Phys. Rev. A (ref. 18) focused on total and singly differential cross sections and showed that even below the threshold for sequential ionization (54.4 eV), there is a striking change in the magnitude and shape of the cross section – a process we termed "virtual sequential ionization". We have since extended these studies to include the fully differential cross sections (TDCS) (refs. 24, 26) and have discovered that the signature of sequential ionization is also be visible in the nuclear recoil cross sections, even when integrated over all photoelectron energy sharings. The energy-integrated nuclear recoil can be measured using the COLTRIMS technique and does not require detection of the electrons at all, making such a determination an attractive target for future experiments. We intend to extend this work on two-photon double ionization to molecular hydrogen. A key physical feature that makes H_2 potentially more interesting than helium is the fact that with hydrogen, there is a range of energies below the sequential threshold where the first photon can excite an autoionizing state which can then either absorb a second photon or autoionize before double ionization is possible. In the atomic case, the autoionizing states lie above the sequential threshold and the sequential double ionization process is so dominant that the role of autoionizing states become less important.

Two-photon double ionization of helium at 44, 52 and 58 eV. ionization (54,4 eV). The energy-integrated nuclear recoil cross sections show a characteristic change in shape as the SI threshold is approached.

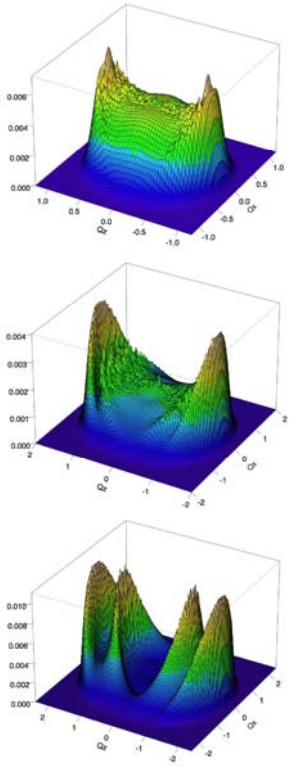

We have made substantial progress on implementing exterior complex scaling with a hybrid method that combines a grid-based discrete variable representation (DVR) with Gaussian functions. To test the method on a realistic case where a purely grid-based, single-center approach would be infeasible, we used a frozen-core model to calculate differential cross sections for ionization of Li_2^+, which has a large equilibrium bond distance at R=5.86 bohr (ref . 25). This large bond distance has several novel consequences: a dominance of f-wave scattering, even close to threshold, and diffraction-like patterns in the photoelectron angular distributions at low energies. We expect this program of research to take us all the way to the first calculations of double photo-ionization of many-electron molecules.

Recent COLTRIMS experiments on H_2 using circularly polarized light at 160 and 240 eV have suggested that two-slit interference effects can also be found in the double ionization, when one electron is much faster than the other and the slow electron is not observed. We have carried out precise quantum mechanical calculations that reproduce the experimental findings, but show that the interpretation in terms of classical diffraction is only appropriate at substantially higher photon energies (ω > 375 eV). At the energies considered in the experiment, the angular distributions simply reflect the mixing of two nondiffractive contributions by circularly polarized light. This work has been submitted to Physical Review Letters (ref. 27).

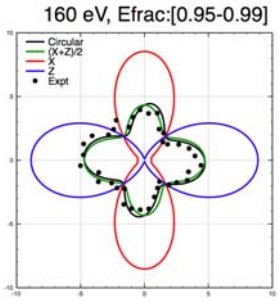

Doubly differential cross section for H_2 double ionization at 160 eV. Measured electron has 95-99% of the total energy. Cross sections using linear polarization are compared with circular polarization results.

Treating ionization with the inclusion of nuclear motion beyond the Born-Oppenheimer approximation is a central challenge for *ab initio* theory. It is also relevant to ultrafast experiments on molecules using X-ray pulses. To test the feasibility of such calculations and to pave the way for future studies in the ultrafast program, we have undertaken a study of intense field ionization of H_2^+ using grid-based methods. Exterior complex scaling can be employed to remove the effects of reflection from the end of a finite grid by applying correct outgoing boundary conditions at its edges, but only if the problem is formulated in the radiation gauge, where the perturbation is $\mathbf{A}(t)\cdot\mathbf{p}$. We have also found that a proper choice of coordinate systems can impact the feasibility of the calculations. Prolate spheroidal coordinates present unique advantages for diatomic targets, can be used in connection with finite elements and the discrete variable representation and will be applicable to many-electron diatomic targets. We intend to pursue these initial studies with the goal of an essentially exact treatment of H_2^+ strong field ionization beyond the Born-Oppenheimer approximation.

2. Electron-Molecule Collisions

Since resonance processes in electron-molecule collisions play a key role in the channeling of electronic energy into vibrational excitation and dissociation, we have spent some time examining the underpinnings of various complex potential models. Our earlier study of the local complex potential model (ref. 6) has been extended to include the non-local complex potential model for resonance collisions of electrons with diatomic molecules and was published in Phys. Rev. A (ref. 20). We plan to extend this work to study the role of non-Born-Oppenheimer effects in threshold

vibrational excitation of polar molecules as well as direct- and non-direct mechanisms in dissociative recombination of electrons with molecular ions.

Our benchmark study of dissociative electron attachment (DEA) to water (refs. 8, 14, 15) succeeded in explaining most of the experimentally observed phenomena, with two notable exceptions. We found no production of O^-+H_2 through, although this minor channel has been seen in previous experiments and we significantly underestimated the cross section for O^- production through the $^2B_2$ resonance. To address these problems, we are studying the role of three-body breakup into O^-+H+H, which was not treated in our earlier study, as the Jacobi coordinate systems we used are only appropriate for two-body channels. New calculations in hyperspherical coordinates enable us to compute the total reactive flux into all channels. Subtracting the known two-body components from the total would then give a result for the three-body cross section. The studies will complete the picture for DEA to water and will complement ongoing COLTRIMS measurements of DEA angular distributions in the AMO experimental program at LBNL.

Previously, we unraveled the mechanism for dissociative electron attachment to formic acid (HCOOH), which involves a complex symmetry-breaking process to produce a formate anion ($HCOO^-$) plus a hydrogen atom (ref. 7). We have initiated a new study the hydroxyl formyl anion $HOCO^-$, another isomeric form of the formate anion, since it has been the focus of a number of recent experimental studies using angular resolved laser photodetachment techniques. These studies have revealed several striking features, namely, a sharp threshold peak that produces an apparently isotropic distribution of photoelectrons and a second low-energy peak that produces a dipole pattern of photoelectrons aligned along the polarization direction of the laser. To understand these features, we are carrying out electron scattering studies on the HOCO radical using the fixed-nuclei, complex Kohn variational method. We plan to use the scattering wave functions from these initial studies to compute the photodetachment cross sections and photoelectron angular distributions from fixed-in-space $HOCO^-$ anions.

Publications (2006-2008):

1. F. Martín, D. A. Horner, W. Vanroose, T. N. Rescigno and C. W. McCurdy, "First Principles Calculations of the Double Photoionization of Atoms and Molecules using B-splines and Exterior Complex Scaling", Proceedings of the Thirteenth International Symposium on Polarization and Correlation in Electronic and Atomic Collisions and the International Symposium on (e,2e), Double Photoionization and Related Topics, Buenos Aires, 2005 (American Institute of Physics, 2006).
2. T. N. Rescigno, D. A. Horner, F. L. Yip and C. W. McCurdy, "A Hybrid Approach to Molecular Continuum Processes Combining Gaussian Basis Functions and the Discrete Variable Representation ", *Phys. Rev. A* **72**, 052709 (2005).
3. C. S. Trevisan, A. E. Orel and T. N. Rescigno, "Resonant Electron-CF Collision Processes" , *Phys. Rev. A* **72**, 062720 (2005).
4. Wim Vanroose, F. Martín, T. N. Rescigno and C. W. McCurdy, "Complete Photofragmentation of the H_2 Molecule as a Probe of Molecular Electron Correlation", *Science* **310**, 1787 (2005).
5. T. N. Rescigno and C. W. McCurdy (with B. C. Garrett *et al.*), "Role of Water in Electron-Initiated Processes and Radical Chemistry: Issues and Scientific Advances" *Chemical Reviews* **105**, 355-389 (2005).
6. K. Houfek, T. N. Rescigno and C. W. McCurdy, "A Numerically Solvable Model for Resonant Collisions of Electrons with Diatomic Molecules ", *Phys. Rev. A* **73**, 032721 (2006).
7. T. N. Rescigno, C. S. Trevisan and A. E. Orel, "Dynamics of Low-Energy Electron Attachment to Formic Acid", *Phys. Rev. Lett.* **96**, 213201 (2006).

8. D. J. Haxton , C. W. McCurdy and T. N. Rescigno, "Angular Dependence of Dissociative Electron Attachment to Polyatomic Molecules: Application to the $^2B_1$ Metastable State of the H_2O and H_2S Anions", *Phys. Rev. A* **73**, 062724 (2006).
9. C. S. Trevisan, A. E. Orel and T. N. Rescigno, "Elastic scattering of low-energy electrons by tetrahydrofuran", *J. Phys. B* **39**, L255 (2006).
10. Wim Vanroose, D. A. Horner, F. Martín, T. N. Rescigno and C. W. McCurdy, "Double Photoionization of Aligned Molecular Hydrogen", *Phys. Rev. A* **74**, 052702 (2006).
11. T. N. Rescigno, Wim Vanroose, D. A. Horner, F. Martín and C. W. McCurdy , "First Principles Study of Double Photoionization of H_2 Using Exterior Complex Scaling", *J. Elec. Spectros., Rel. Phenom.* **161**, 85 (2007).
12. C.S. Trevisan, A.E. Orel and T. N. Rescigno), Low-energy Electron Scattering by Formic Acid, *Phys. Rev. A* **74**, 042716 (2006).
13. D. A. Horner, W. Vanroose, T. N. Rescigno, F. Martin and C. W. McCurdy, Role of Nuclear Motion in Double Ionization of Molecular Hydrogen by a Single Photon, *Phys. Rev. Lett.* **98**, 073001 (2007).
14. D. J. Haxton , C. W. McCurdy and T. N. Rescigno Dissociative Electron Attachment to the H_2O molecule I: Complex-valued Potential Energy Surfaces for the $^2B_1$, $^2A_1$ and $^2B_2$ Metastable States of the Water Anion, *Phys. Rev. A.* **75,** 012710.
15. D. J. Haxton, T. N. Rescigno and C. W. McCurdy, Dissociative Electron Attachment to the H_2O molecule II: Nuclear Dynamics on Coupled Electronic Surfaces Within the Local Complex Potential Model, *Phys. Rev. A.* **75,** 012711.
16. F. L. Yip, D. A. Horner, C. W. McCurdy and T. N. Rescigno, Single and Triple Differential Cross Sections for Double Photoionization of H^-, *Phys. Rev. A.* **75**, 042715 (2007).
17. D. J. Haxton, C. W. McCurdy and T. N. Rescigno, Comment on "A Wave Packet Method for Treating Nuclear Dynamics on Complex Potentials" , *J. Phys. B* **40**, 1461 (2007).
18. D. A. Horner, F. Morales, T. N. Rescigno, F. Martin and C. W. McCurdy, Two-Photon Double Ionization of Helium Above and Below the Threshold for Sequential Ionization, *Phys. Rev. A* **76**, 030701(R) (2007)
19. T. N. Rescigno, C. W. McCurdy, D. J. Haxton, C. S. Trevisan and A. E. Orel, Nuclear Dynamics in Resonant Electron Collisions with Small Polyatomic Molecules, *J. Phys. Conference Series* **88**, 012011 (2007).
20. K. Houfek, T. N. Rescigno and C. W. McCurdy, Probing the Nonlocal Approximation to Resonant Collisions of Electrons with Diatomic Molecules, *Phys. Rev. A* **77**, 012710 (2008).
21. M. S. Schoeffler, J. Titze, N. Petridis,T. Jahnke, D. Akoury, K. Cole, L. Ph. H. Schmidt, A. Czasch, O. Jagutzki, N. A. Cherepkov, S. K. Semenov, C. W. McCurdy, T. N. Rescigno, C. L. Cocke, T. Osipov, S. Lee, M. H. Prior, A. Belkacem, A. Lander, H. Schmidt-Boecking, Th. Weber, and R. Doerner, Ultrafast probing of core hole localization in N_2, Science **320,** 920 (2008)
22. T. Osipov, T. N. Rescigno, T. Weber, S.Miyabe, T.Jahnke, A. Alnaser, M. Hertlein, O. Jagutzki, L. Schmidt, M. Schoeffler, L. Foucar, S. Schoessler, T. Havermeier, M. Odenweller, S. Voss, B. Feinberg, A. Landers, M. Prior, R. Doerner, C. L. Cocke and A. Belkacem, Fragmentation Pathways for Selected Electronic States of the Acetylene Dication, *J. Phys. B* **41**, 091001 (2008)
23. P. L. Bartlett, A. T. Stelbovics, T. N. Rescigno and C. W. McCurdy, Application of Exterior Complex Scaling to Positron-Hydrogen Collisions Including Rearrangement, *Phys. Rev. A* **77**, 032710 (2008).
24. D. A. Horner, T. N. Rescigno and C. W. McCurdy, Decoding sequential vs non-sequential two-photon double ionization of helium using nuclear recoil, *Phys. Rev. A.* **77**, 030703(R) (2008).
25. F. L. Yip, C. W. McCurdy and T. N. Rescigno, A hybrid Gaussian-discrete variable representation approach to molecular continuum processes II: application to photoionization of diatomic Li_2^+ *Phys. Rev. A* (submitted).
26. D. A. Horner, T. N. Rescigno and C. W. McCurdy ,Triple Differential Cross sections and Nuclear Recoil in Two-Photon Double Ionization of Helium, *Phys. Rev. A* (submitted).
27. D. A. Horner, S. Miyabe, T. N. Rescigno , C. W. McCurdy, F. Morales and F. Martin, Classical Two-Slit Interference Effects in Photo-double Ionization of Molecular Hydrogen at High Energies, *Phys. Rev. Lett.* (submitted).

Ultrafast X-ray Science Laboratory

C. William McCurdy (Director), Ali Belkacem, Oliver Gessner, Martin Head-Gordon, Stephen Leone, Daniel Neumark, Robert W. Schoenlein, Thorsten Weber

Chemical Sciences, Lawrence Berkeley National Laboratory, Berkeley, CA 94720

CWMcCurdy@lbl.gov, ABelkacem@lbl.gov, OGessner@lbl.gov, MHead-Gordon@lbl.gov, SRLeone@lbl.gov, DMNeumark@lbl.gov, RWSchoenlein@lbl.gov, TWeber@lbl.gov

Program Scope: This program seeks to bridge the gap between the development of ultrafast X-ray sources and their application to understand processes in chemistry and atomic and molecular physics that occur on both the femtosecond and attosecond time scales. Current projects include: (1) The construction and application of high harmonic generation sources in chemical physics, (2) Applications of a new ultrafast X-ray science facility at the Advanced Light Source at LBNL to solution-phase molecular dynamics, (3) Time-resolved studies and non-linear interaction of femtosecond x-rays with atoms and molecules (4) Theory and computation treating the dynamics of two electrons in intense short pulses, and the development of tractable theoretical methods for treating molecular excited states of large molecules to elucidate their ultrafast dynamics.

Recent Progress and Future Plans:

1. Soft X-ray high harmonic generation and applications in chemical physics

This part of the laboratory is based on a unique high repetition rate femtosecond VUV pulse source. It will provide light pulses in the VUV- and soft X-ray regime with pulse durations on the sub-40 fs timescale and repetition rates up to 3 kHz. The source will be complemented by state-of-the-art photoelectron and photoion detection schemes. It is based on HHG with an IR fundamental in gaseous media. The driving IR laser provides pulses of 25 fs duration at 3 kHz repetition rate with pulse energies up to 5 mJ. After separation from the fundamental, a narrow band of high harmonic photon energies is selected by means of filters, multilayer mirrors, and gratings. The first beamline providing ultrashort pulses at 23.7 eV photon-energy is operational and first femtosecond VUV pump - femtosecond IR probe photoelectron images have been recorded with an estimated apparatus-limited time resolution of ≤40 fs (FWHM).

The first experiments focus on the ionization dynamics of pure and doped Helium droplets. An existing experimental setup consisting of a helium cluster source and a velocity-map-imaging photoelectron spectrometer, have been modified to record femtosecond time-resolved photoelectron energy- and angular-distributions. Synchrotron based studies have revealed the emission of extremely slow (<1 meV) electrons by Helium droplets that are excited ~1 eV below the atomic helium ionization threshold. Furthermore, the photoelectron spectra of doped helium droplets show a rich structure that depends on the photon energy and cluster size. We are currently using a femtosecond VUV pump - femtosecond IR probe scheme in order to directly probe the poorly understood decay dynamics of the VUV-excited helium droplets in the time domain. First pump-probe time-delay dependent photoelectron images have been recorded, which show evidence for a short-lived neutral intermediate droplet state and

possibly the emergence of neutral atomic fragments in highly excited Rydberg states as observed before in synchrotron-based energy-domain studies.

Ultimately, the high-repetition high harmonics source will be equipped with 3 beam lines in order to make optimum use of the femtosecond driving laser. Photoelectron-photoion coincidence imaging experiments and transient X-ray absorption experiments will be installed at the additional beam lines. We will generate and utilize femtosecond soft X-ray pulses with photon energies reaching the water window (290eV-540eV). Finally, the investigator team is applying for time at the LCLS to study inner shell ionization of field-ionized rare gas atoms.

2. Applications of the new femtosecond undulator beamline at the Advanced Light Source to solution-phase molecular dynamics

The objective of this research program is to advance our understanding of solution-phase molecular dynamics using ultrafast x-rays as time-resolved probes of the evolving electronic and atomic structure of solvated molecules. Two new beamlines have been constructed at the Advanced Light Source, with the capability for generating ~200 fs x-ray pulses from 200 eV to 10 keV. The soft x-ray beamline is operational. The hard x-ray beamline has been commissioned, and will soon be operational. We have also developed a new capability for transmission XAS studies of thin liquid samples in the soft x-ray range, based on a novel Si_3N_4 cell design with controllable thickness <1 μm.

Present research is focused on charge-transfer processes in solvated transition-metal complexes, which are of fundamental interest due to the strong interaction between electronic and molecular structure. In particular, Fe^{II} complexes exhibit strong coupling between structural dynamics, charge-transfer, and spin-state interconversions. We previously reported the first time-resolved EXAFS measurement of the atomic structural dynamics associated with the Fe^{II} spin-crossover transition, showing the dilation of the Fe-N bond distance by ~0.2 Å within 70 ps of photoexcitation into the $MLCT^1$ state. This year we have focused on understanding the evolution of the valence electronic structure, and the influence of the ligand field dynamics on the Fe *3d* electrons, using time-resolved XANES measurements at the Fe L-edge. Our recent picosecond results show a clear 1.6 eV dynamic shift in the Fe-L_3 absorption edge with the ultrafast formation of the high-spin state. This reflects the evolution of the ligand-field splitting, and is the first time-resolved solution-phase transmission spectra ever recorded in the soft x-ray region. Femtosecond x-ray studies of these dynamics are now underway.

A second area of focus during this past year has been on the structural dynamics of liquid water following coherent vibrational excitation of the O-H stretch (in collaboration with A. Lindenberg et al. at Stanford). Preliminary time-resolved results at the O K-edge show distinct changes in the near-edge spectral region that are consistent with a weakening of the hydrogen bonds and increased disorder of the hydrogen bond network upon vibrational excitation. Experiments are underway to understand new unexplained features in the picosecond spectra. Femtosecond XANES measurements will elucidate the dynamics of vibrational energy redistribution and its effects on the hydrogen bonding. An important goal is to apply time-resolved X-ray techniques to understand the structural dynamics of more complicated reactions in a solvent environment. Of current interest is the photochemical reaction dynamics of aqueous chlorine dioxide (O-Cl-O) which exists in stratospheric polar clouds and plays a significant role in sunlight-induced atmospheric chemistry due to its ability to produce atomic Cl.

3. Time-resolved studies and non-linear interaction of femtosecond x-rays with atoms and molecules:

An extension of non-linear processes to the XUV spectral region was until recently considered unfeasible due to a lack of sufficiently intense short-wavelength radiation sources. In recent years, higher-order harmonic generation has reached intensities high enough as to induce two or three photon ionization processes. The design and construction of our intense XUV source is based on scaling-up in energy of the loose focusing high harmonic generation scheme. The laser system consists of a mode locked laser oscillator, pulse stretcher, regenerative amplifier operating at 1 kHz, a home built 4-pass amplifier and a pulse compressor. The pulse energy output of the system is 30 mJ at 10 Hz and 35 fs pulse width. The high harmonics are focused by a 5-cm focal length spherical mirror into a pulsed molecular beam over an ion time of flight mass spectrometer. Peaks in the time of flight spectrum due to non-linear ionization are distinguished from linear ionization from intensity dependence. We clearly achieved the intensity regime where two-photon double-ionization of Ar can be produced. We are also able to produce Ne^{2+} and Xe^{3+} through multiphoton ionization at a rate of 0.2 events per XUV pulse. We have attained a regime where the XUV beam ionizes almost every atom in the interaction region.

The design and ordering phase of the Momentum Imaging Spectroscopy for TimE Resovled Studies (MISTERS) apparatus consisting of an ultrahigh vacuum COLTRIMS system, capable to measure 3d momenta of electrons and ions in coincidence, is almost complete. By now several components are manufactured in and out of LBNL; the assembling and testing phase will start in the second half of 2008. In the beginning the setup will be optimized for two-photon double ionization of helium atoms and hydrogen molecules using the high harmonics sources of the UXSL. We intend to measure one ion and one electron in coincidence in order to get access to key values like the momentum vector of the di-electron in the case of helium and the kinetic energy release (KER) in the photo ionization of hydrogen molecules. This will enable us to distinguish between sequential and non-sequential processes and understand the mechanisms behind.

4. Theory and computation

An initial focus of our work is the development of computational methods that will allow the accurate treatment of multiple-ionization of atoms and molecules by short pulses in the VUV and soft X-ray regimes. We have extended our numerical methods based on the finite-element discrete variable representation to the essentially exact time-dependent treatment of two electron atoms in a radiation field. A central challenge for the theory of time-dependent multiple ionization processes, that we have recently solved [10], is the rigorous extraction of the amplitudes for ionization from these wave packets, and the separation of single and double ionization probabilities. These developments have been applied to short pulse single and double ionization of helium [11] in initial tests. Applications to pump/probe investigation of correlation in the doubly excited states of helium are in progress using a new time propagation scheme that involves simultaneous explicit and implicit steps. The extension of these methods to many-electron atoms is being accomplished by the construction of orbitals from the DVR basis functions in the first finite element of our grids.

We are developing tractable theories for molecular excited states, including bright and dark states and their intersections. A new quasi-degenerate perturbation theory building upon single excitation CI has been, formulated, implemented and tested [12]. It is self-interaction-free, and efficient enough to apply to systems in the 50-100 atom regime. Work is in progress on the formulation of its analytical gradient to permit the exploration of excited potential surfaces. Additionally, we have formulated new spin-flip model that can properly treat low-lying dark excited states that have large double excitation contributions [13], with computational cost that is proportional to single excitation CI.

Publications (2006-2008)

1. M.P. Hertlein, H. Adaniya, J. Amini, C. Bressler, B. Feinberg, M. Kaiser, N. Neumann, M.H. Prior and A. Belkacem, "Inner-shell ionization of potassium atoms ionized by femtosecond laser", Phys. Rev. A 73, 062715 (2006).
2. M. Khalil, M.A. Marcus, A.L. Smeigh, J.K. McCusker, H.H.W. Chong, and R.W. Schoenlein, "Picosecond x-ray absorption spectroscopy of a photoinduced iron(II) spin crossover reaction in solution," *J. Phys. Chem. A*, **110**, pp. 38-44 (2006).
3. A.Cavalleri, M.Rini, R.W. Schoenlein, "Ultra-broadband femtosecond measurements of the photo-induced phase transition in VO_2: From the mid-IR to the hard x-rays" *J. Phys. Soc. Jap.*, **75**, p. 011004, (2006).
4. J.M. Byrd, Z. Hao, M.C. Martin, D.S. Robin, F. Sannibale, R.W. Schoenlein, A.A. Zholents, and M.S. Zolotorev, "Tailored Terahertz Pulses from a Laser-Modulated Electron Beam," *Phys. Rev. Lett.*, **96**, 164801, (2006).
5. A. Cavalleri, S. Wall, C. Simpson, E. Statz, D.W. Ward, K.A. Nelson, M.Rini, and R.W. Schoenlein, "Tracking the motion of charges in a terahertz light field by femtosecond X-ray diffraction," *Nature*, **442**, 664 (2006).
6. J. M. Byrd, Z. Hao, M. C. Martin, D.S. Robin, F. Sannibale, R.W. Schoenlein, A. A. Zholents, M.S. Zolotorev, "Laser seeding of the storage ring microbunching instability for high-power coherent terahertz radiation," *Phys. Rev. Lett.*, **97**, 074802, (2006).
7. M. Khalil, M.A. Marcus, A.L. Smeigh, J.K. McCusker, H.H.W. Chong, and R.W. Schoenlein, "Picosecond x-ray absorption spectroscopy of photochemical transient species in solution," in **Ultrafast Phenomena XV**, Springer Series in Chemical Physics , **88**, P. Corkum, D. Jonas, D. Miller, A.M. Weiner, Eds., Springer-Verlag, (2007).
8. Y.M. Rhee and M. Head-Gordon, "Scaled second order perturbation corrections to configuration interaction singles: efficient and reliable excitation energy methods", J. Phys. Chem. A 111, 5314 (2007).
9. C. C. Wang, O. Kornilov, O. Gessner, J. H. Kim, D. S. Peterka, and D. M. Neumark, "Photoelectron Imaging of Helium Droplets Doped with Xe and Kr Atoms", J. Phys. Chem. A, *in press* (2008).
10. A. Palacios, C. W. McCurdy and T. N. Rescigno, Extracting Amplitudes for Single and Double Ionization from a Time-Dependent Wavepacket, *Phys. Rev. A* **76**, 043420 (2007).
11. A. Palacios, T. N. Rescigno and C. W. McCurdy, Cross Sections for Short-Pulse Single and Double Ionization of Helium, *Phys. Rev. A* **77**, 032716 (2008).
12. D. Casanova, Y.M. Rhee and M. Head-Gordon, "Quasidegenerate scaled opposite spin second order perturbation corrections to single excitation configuration interaction", J. Chem. Phys. 128, 164106 (2008)
13. D. Casanova and M. Head-Gordon, "The spin-flip extended single excitation configuration interaction method", J. Chem. Phys. (submitted, 2008).

2008 DOE/BES RESEARCH MEETING OF THE ATOMIC, MOLECULAR, AND OPTICAL SCIENCE (AMOS) PROGRAM

to be held at the
Airlie Conference Center
Warrenton, Virginia

September 14-17, 2008

ABSTRACTS

"OAK RIDGE NATIONAL LABORATORY ATOMIC AND MOLECULAR PHYSICS RESEARCH"

Oak Ridge National Laboratory
Physics Division, P. O. Box 2008
Oak Ridge, TN 37831-6372

Submitted to: Division of Chemical Sciences
U.S. Department of Energy

July 16, 2008

ATOMIC AND MOLECULAR PHYSICS RESEARCH AT OAK RIDGE NATIONAL LABORATORY

David R. Schultz, Group Leader, Atomic Physics
[schultzd@ornl.gov]
ORNL, Physics Division, P.O. Box 2008
Oak Ridge, TN 37831-6372

Principal Investigators

M. E. Bannister, M. R. Fogle, Jr.* C. C. Havener, H. F. Krause, J. H. Macek,
F. W. Meyer, C. Reinhold, D. R. Schultz, C. R. Vane, and H. Zhang*

*Postdoctoral Fellow

The OBES atomic physics program at ORNL has as its overarching goal the understanding of states and interactions of atomic-scale matter. These atomic-scale systems are composed of multiply charged ions, charged and neutral molecules, atoms, atomic ions, electrons, solids, and surfaces. Particular species and interactions are chosen for study based on their relevance to gaseous or plasma environments of basic energy science interest such as those in fusion energy, gas phase chemistry, and plasma processing. Towards this end, the program has developed and operates the Multicharged Ion Research Facility (MIRF) which has recently undergone a broad, multi-year upgrade. Work is also performed as needed at other facilities such as ORNL's Holifield Radioactive Ion Beam Facility (HRIBF) and the CRYRING heavy-ion storage ring in Stockholm. Closely coordinated theoretical activities support this work as well as provide leadership in complementary or synergistic research.

Low-Energy Ion-Surface Interactions – *F. W. Meyer, H. F. Krause, M. J. Lance, H. M. Meyer III, and H. Zhang*

Ion-surface interactions play an essential role in many applications ranging from semiconductor device technology to thermonuclear fusion physics, since many physicochemical reactions occur on and near the surface during plasma exposure. In the case of present and future fusion experiments, the choice of the plasma-facing material is critical due to high heat and particles fluxes arriving on the walls, in particular atomic and molecular ions of deuterium (D) and tritium (T). Carbon materials are good plasma-facing materials (PFM's) because of their thermo-mechanical properties and low atomic number.[1] However, one of the main difficulties to overcome in fusion experiments that employ graphite as PFM is the negative consequences of the plasma–wall interaction, namely, chemical erosion and H-species retention.[2, 3]

We recently initiated an experimental research program to study the interactions of slow ions with surfaces underlying chemical sputtering of fusion-relevant graphite surfaces. Our measurements concentrated on the region of very low impact energies (i.e., below 10 eV/D), where there is currently no available experimental data, and which is the anticipated regime of operation of the ITER divertor.[4] Due to the high D^+ currents obtainable with our ECR ion source, and the highly efficient beam deceleration optics employed at the entrance to our floating scattering chamber, comparison between same velocity atomic and molecular ion impact was possible with our apparatus at energies as low as 10 eV/D. These measurements permitted a test of the commonly made assumption that atomic and molecular species of the same velocity lead to identical sputtering yields when normalized to the number of D atoms in the incident projectiles.[5] We found projectile dependent yields below ~60 eV/D, where the D^+ projectile had the smallest yields and D_3^+ projectiles had the largest yields. A similar enhancement was found in molecular

dynamics (MD) simulations carried out in parallel with our measurements.[5, 6] At higher energies, where immediate dissociation of incident molecular projectiles is highly probable, the observed yields for equivelocity incident atomic and molecular ions are the same, as was noted in previous work.[7]

During the past year, we have obtained production yields of methane and heavier hydrocarbons for hydrogen and deuterium atomic and molecular ions incident on ATJ graphite, HOPG, and a-C:D thin films in the energy range 5 – 250 eV/H(D). The yields were determined at sufficient accumulated ion beam fluences that steady-state conditions were reached. By summing the different hydrocarbon yields, estimates could be obtained of the total erosion of graphite by chemical sputtering processes, which dominate at low energies, i.e., below the physical sputtering threshold. These estimates also permitted comparison with ellipsometry measurements of D^+ ion beam induced crater volumes in a:C-D thin films, work performed in collaboration with Wolfgang Jacob's Reactive Plasma Group at IPP Garching.

In addition to steady-state chemical sputtering yields, we have studied[8] transient hydrocarbon production and hydrogen (deuterium) re-emission from pre-loaded graphite surfaces immediately after the start of beam irradiation. When the surfaces were prepared by irradiation to saturation with lower energy hydrogen (deuterium) beams, transient hydrocarbon and re-emission yields significantly larger than steady-state values were observed, which exponentially decayed as a function of beam fluence. The initial yield values are related to the starting hydrocarbon and hydrogen (deuterium) densities in the prepared sample, while the exponential decay constants provide information on the hydrocarbon kinetic release and hydrogen (deuterium) detrapping cross sections.

To obtain further insights into the chemical sputtering process, we have continued investigations of the graphite surface morphology, and chemical/structural modifications occurring during H and D beam exposure using Scanning Electron Microscopy (SEM), and Raman and Auger Electron Spectroscopy (AES) diagnostics.[9] For example, we have performed Raman spectroscopy of graphite samples exposed to high fluences of D^+ and D_3^+ beams at high and low energies, to compare damage production by isovelocity atomic and molecular deuterium ion beams. While the two high-energy beam-exposed spots showed similar damage, the low-energy molecular-beam-exposed spot showed slightly more damage than the corresponding D^+ beam exposed spot.[10]

1. R. Parker, G. Janeschitz, H. D. Pacher, D. Post, S. Chiocchio, G. Federici, P. Ladd, J. Nucl. Mater. **241–243**, 1 (1997).
2. E. Vietzke, A. A. Haasz, in *Physical Processes of the Interaction of Fusion Plasmas with Solids*, Editors, W. O. Hofer and J. Roth, Academic Press, London, 1996.
3. R. Ruggie´ri, E. Gauthier, J. Hogan, J. M. Layet, and T. Loarer, J. Nucl. Mater. **266–269**, 660 (1999).
4. G. Federici, Phys. Scr. **T124,** 1 (2006).
5. L. I. Vergara, F. W. Meyer, H. F. Krause, P. Träskelin, K. Nordlund, and E. Salonen, J. Nucl. Mater. **357**, 9 (2006).
6. P. S. Krstic, C. O. Reinhold, and S. J. Stuart, New J. Phys. **9**, 209 (2007).
7. M. Balden and J. Roth, J. Nucl. Mater. **280**, 39 (2000).
8. H. Zhang and F. W. Meyer, *Proceedings,18th International Conference on Plasma Surface Interactions, Toledo, Spain, May 25-30, 2008*, to be published in J. Nucl. Mater.
9. H. Zhang, F. W. Meyer, H. M. Meyer III, M. J. Lance, Vacuum **82**, 1285 (2008).
10. F. W. Meyer, H. Zhang, M. J. Lance, and H. F. Krause, Vacuum **82**, 880 (2008).

Production of D_2^- in Grazing Alkali Halide Surface Scattering – *F. W. Meyer,* C. *C. Havener, H. Zhang, and D. G. Seely*

From previous studies, it is known that grazing ion alkali halide surface collisions can lead to very high negative scattered projectile charge fractions.[1,2] We have continued our investigation of molecular hydrogen and deuterium anion production in grazing collisions of H_2^+, H_3^+, D_2H^+, D_2^+, and D_3^+ ions with alkali halide surfaces. Such molecular anions are one of the most fundamental metastable molecular ions and are important intermediate states in processes such as dissociative attachment, vibrational excitation, associative detachment, and collisional detachment.[3] While the predicted short-lived molecular ion was suspected to exist for many years, only recently was there direct, conclusive evidence for the anion's production with μs lifetimes in a sputter ion source.[4]

In addition to the KCl single crystal surface investigated last year, we have extended our measurements this year to KBr and LiF single crystal surfaces. With the latter alkali halides, we were able to measure the ratio of molecular to atomic anions down to 1.25 keV/u.[5] Within the scatter of the data, all three alkali halide surfaces lead to the same negative ion yields over the investigated energy range. For all three surfaces, both the atomic and molecular anion yields increase with decreasing energy. At the lowest energy investigated, we found D_2^-/D^- ratios as high as 10^{-4}, about an order of magnitude higher than that obtained by Golser *et al.* [4] using a sputter ion source. This indicates that grazing ion alkali halide surface collisions provide an efficient means for production of such molecular anions.

For production of H_2^- from incident H_2^+ or H_3^+ ions, we found that D contamination in the incident beams (in the form of D^+ and DH^+, respectively) gave H_2^- yields that were too large by factors of two to an order of magnitude due to varying levels of D^- in the scattered H_2^- component. The D contamination arose not only from the .015% natural abundance of D_2 in H_2 source gas, but also from source memory effects, and further depended on source tuning conditions. For production of D_2^- from incident D_2^+, D_2H^+, and D_3^+, He is a possible contaminant (in the form of He^+, HeH^+, and HeD^+, respectively). However, auxiliary measurements using an incident He^+ beam showed negligible He^- production in the grazing He ion alkali halide collisions.

1. H. Winter, C. Auth, and A. G. Borisov, Nucl. Instrum. Methods Phys. Res. B **115**, 133 (1996).
2. F. W. Meyer, Q. Yan, P. Zeijlmans van Emmichoven. I. G. Hughes, and G. Spierings, Nucl. Instrum. Methods Phys. Res. B **125**, 138 (1997).
3. M. Cizek, J. Horacek, and W. Domcke, J. Phys. B **31**, 2571 (1998).
4. R. Golser *et al.*, Phys. Rev. Lett. **94**, 223003 (2005).
5. D. G. Seely, F. W. Meyer, H. Zhang, and C. C. Havener, invited talk, CAARI-2008, to be published in AIP conference proceedings.

Low-Energy Collisions Using Merged-Beams – *C. C. Havener, D. G. Seely, and C. R. Vane*

An upgraded merged-beams apparatus, together with the intense molecular and atomic ion beams, made available from ECR ion sources provides a unique opportunity at ORNL to provide benchmark measurements to test our understanding of low-energy (meV/u – keV/u) collision processes. The higher velocity, more intense, and less divergent beams from the new MIRF High-Voltage (HV) platform enable a new class of measurements[1,2] exploring charge transfer and (for molecular ions) dissociative charge transfer for atomic and molecular ions with neutrals. Our first successful merged-beams experiment [3] using the higher velocity beams was for Ne^{2+} + D, extending our previous merged-beams measurements below 200 eV/u and resolving discrepancies with previous measurements.

Measurements completed during last year extend the merged-beam technique to a variety of atomic and molecular ions. Measurements[4] for Si^{3+} + H (40-2500 eV/u) span an energy range in

which both molecular orbital close coupling (MOCC) and classical trajectory Monte Carlo (CTMC) calculations are available. The influence of the quantum mechanical effects of the ionic core as predicted by MOCC is clearly seen in our results. However, discrepancies between our experiment and the MOCC results toward higher collision energies are observed. At energies above 1000 eV/u, good agreement is found with CTMC calculations.

The higher velocity ion beams now available from the platform have permitted charge-exchange measurements with both H and D at eV/u energies and below to directly observe isotope effects.[1] Isotopic differences in the charge-exchange cross section are the result of trajectory effects caused by the ion-induced dipole potential. Our measurements now benchmark the strong isotope effect predicted[5] for the Si^{4+} + H(D) system (a factor of two at meV/u energies), while our measurements for N^{2+} + H(D) show no isotope effect at low energies. A recent theoretical investigation of the He^{2+} + H(D) system by Stolterfoht et al.[6] predicts unusually large isotope effects for this fundamental system where rotational coupling is the dominant process for charge transfer. However, our current investigation of C^{4+} + H(D), where rotational coupling is also dominant, shows no difference in the cross section for H and D. In addition, structure observed in our previous measurements[7] of C^{4+} + D, not understood by current theory, has also been seen in the current C^{4+} + H measurements. These results are being prepared for publication. Measurements have now expanded to molecular ions; charge transfer and dissociative charge transfer measurements for the fundamental system H_2^+ + H are underway. Required low signal/noise levels have necessitated additional H_2 pumping, which has been accomplished with the addition of titanium sublimators and getter pumps.

The intense beams from the HV platform will also be used to perform a benchmark study of low-energy charge exchange for fully stripped and H-like ions on atomic hydrogen. While there have been numerous studies at keV/u energies, there is a real lack of total and state-selective data and appropriate quantal theory at eV/u energies and below. X-ray emission measurements are planned for a variety of bare and H-like ions (e.g., C, N, O) + H. For charge transfer at low energies, capture to non-statistical angular momentum states leads to observable signatures in the subsequent X-ray emission. Such measurements are possible using a high efficiency detector mounted directly above the merge path. The sounding rocket X-ray calorimeter at the University of Wisconsin[7] is being considered for these measurements. The X-ray detector is characterized by a high-energy resolution (5 – 12 eV FWHM) along with high throughput (1000 times greater than dispersive X-ray detectors).

1. C. C. Havener *et al*., Nucl. Instrum. Methods Phys. Res. B **261**, 129 (2007).
2. D. G. Seely, H. Bruhns, D. W. Savin, T. J. Kvale, E. Galutschek, H. Aliabadi and C. C. Havener, Nucl. Instrum. Methods Phys. Res. A **585**, 69 (2008).
3. B. Serendyuk, H. Bruhns, D. W. Savin, D. Seely, H. Aliabadi, E. Galutschek, and C. C. Havener, Phys. Rev. A **75**, 054701 (2007).
4. H. Bruhns, H. Kreckel, D. W. Savin, D. G. Seely, and C. C. Havener, Phys. Rev. A **77**, 064702 (2008).
5. M. Pieksma, M. Gargaud, R. McCarroll, and C. C. Havener, Phys. Rev. A **54**, R13 (1996).
6. N. Stolterfoht et al., Phys. Rev. Lett. **99**, 103201 (2007).
7. F. W. Bliek, R. Hoekstra, M. E. Bannister, and C. C. Havener, Phys. Rev. A **56**, 426 (1997).
8. D. McCammon *et al*., Astrophys. J **576**, 188 (2002).

Electron-Molecular Ion Interactions – *M. E. Bannister, C. R. Vane, and M. Fogle*

Electron-molecular ion recombination, dissociation, and excitation and ionization processes are fundamentally important, especially in that they provide a testable platform for investigating and fully developing our understanding of the mechanisms involved in electronic energy redistribution in fragmenting many-body quantum mechanical systems. These processes are also

important practically in that electron-ion collisions are in general ubiquitous in plasmas and molecular ions can represent significant populations in low to moderate temperature plasmas. Neutral and charged radicals formed in dissociation of molecules in these plasmas represent some of the most highly reactive components in initiating and driving further chemical reaction pathways. Thus electron-molecular ion collisions are important in determining populations of some of the most reactive species in a wide variety of environments, such as the divertor and edge regions in fusion reactors, plasma enhanced chemical vapor deposition reactors, environments where chemistries are driven by secondary electron cascades, for example in mixed radioactive waste, the upper atmospheres of planets, and cooler regions of the solar or other stellar atmospheres. To correctly model these environments it is absolutely essential to know the strengths (cross sections and rates), branching fractions, and other kinematical parameters of the various possible relevant collision processes.

Dissociative Excitation and Ionization: Measurements of cross sections for electron-impact dissociative excitation (DE) and dissociative ionization (DI) of molecular ions have continued using the MIRF crossed-beams apparatus.[1] In coordination with our dissociative recombination (DR) investigations of di-hydride ions, we have continued a systematic study of the DE and DI channels for these ions. Experiments during this period included measurements on heavy-fragment ion channels of FD_2^+. Above the DI threshold, the cross sections for dissociation of FD_2^+ ions forming FD^+ fragments are nearly identical to those measured previously for the XD^+ fragment produced by dissociation of XD_2^+ (X=N,O). In the DE-only portion of the cross section, a small peak is observed near 20 eV, similar to that seen for the $OD_2^+ \rightarrow OD^+$ cross section. For the XH^+/XD^+ fragment channel in DE/DI of di-hydrides XH_2^+/XD_2^+ (X=C,N,O,F), it was found that for energies above four times the dissociation threshold E_{th} the cross sections follow the scaling[2] given by $\sigma(E/E_{th}) \propto (1/E_{th})\, f(E/E_{th})$ for a smooth function f(x). This scaling does not hold as well for the X^+ fragment channel. However, the $FD_2^+ \rightarrow F^+$ results did continue the trend that the cross section decreases for the $XD_2^+ \rightarrow X^+$ channel as the electronegativity of X increases for X = C, N, O, and F.

Preliminary measurements have also been completed for the dissociation of CD_3^+ producing the CD_2^+ fragment ion. Above the DI threshold, the cross section for this channel was found to follow the scaling noted above. At lower energies, a large peak was measured in the 10-15 eV range, reminiscent of the peaks observed in the $DCO^+ \rightarrow CO^+$ and $CH_2^+ \rightarrow CH^+$ data.[3,4] However, further measurements are needed to map out the details of this cross section feature.

The dissociation experiments discussed above used molecular ions produced by the ORNL MIRF Caprice ECR ion source,[5] but other cooler sources will also be used in order to understand the role of electronic and ro-vibrational excited states. A second ion source, a hot-filament Colutron ion source, is presently online and expected to produce fewer excited molecular ions. An even colder pulsed supersonic expansion ion source, very similar to the one used for measurements[6] on the dissociative recombination of rotationally cold H_3^+ ions at CRYRING, is under development for use at the ORNL MIRF. Additionally, work continues on a similar supersonic source that uses a piezoelectric mechanism for more reliable pulsed valve operation. With this range of molecular ion sources, one can study dissociation with both well-characterized cold sources and with hotter sources that better approximate the excited state populations in plasma environments found in applications such as fusion, plasma processing, and aeronomy.

---

1. M. E. Bannister, H. F. Krause, C. R. Vane, N. Djuric, D. B. Popovic, M. Stepanovic, G. H. Dunn, Y.-S. Chung, A. C. H. Smith, and B. Wallbank, Phys. Rev. A **68**, 042714 (2003).
2. M. E. Bannister *et al*., "Experiments on Interactions of Electrons with Molecular Ions in Fusion and Astrophysical Plasmas," in *Atomic Processes in Plasmas*, edited by J. D. Gillaspy, J. J. Curry, and W. L. Wiese (AIP Press, Melville, NY, 2007), pp. 197-205.
3. E. M. Bahati, R. D. Thomas, C. R. Vane, and M. E. Bannister, J. Phys. B **38**, 1645 (2005).

4. C. R. Vane, E. M. Bahati, M. E. Bannister, and R. D. Thomas, Phys. Rev. A **75**, 052715 (2007).
5. F. W. Meyer, "ECR-Based Atomic Collision Research at the ORNL MIRF," in *Trapping Highly Charged Ions: Fundamentals and Applications*, edited by J. Gillaspy (Nova Science, Huntington, NY, 1997), p. 117.
6. B. J. McCall *et al.*, Nature **422**, 500 (2003).

Dissociative Recombination: The process of dissociative recombination (DR) of relatively simple three-body molecular ions is being studied in our ongoing collaboration with Prof. Mats Larsson and colleagues at the Manne Siegbahn Laboratory (MSL), Stockholm University. Absolute cross sections, branching fractions, and detailed measurements of the dissociation kinematics, especially of the three-body breakup channel, are being investigated at zero relative energy for a variety of light and heavy vibrationally-cold triatomic di-hydrides and other molecular ions with three-body channels. This research is carried out using the MSL CRYRING heavy ion storage ring facility, which will continue to be available for our electron-molecular ion measurements at least through calendar year 2009.

In the last year, we have performed studies of the di-hydride system BH_2^+. These experiments are a continuation of previous measurements concerning the DR of similar molecules, such as H_2O^+, NH_2^+, CH_2^+, SD_2^+, and O_3^+ that have all revealed three-body break-up as the dominant reaction channel.[1-6] In order to study the three body break-up dynamics in detail, a high-resolution imaging technique is used to measure the displacement of the fragments from the center of mass of the molecule.[7] The displacements are related to the kinetic energies of the fragments and therefore information on the dynamics involved in the process can be obtained, e.g., the internal state distribution of the fragments. These event-by-event measurements yield information about how the kinetic energy made available by neutralization through electron capture is distributed between the two light fragments and the angular distribution of the dissociating molecules. In all of the covalently bonded triatomic di-hydride systems previously studied, the branching fractions showed very roughly (7:2:1) ratios for (X + H + H; XH + H: X + H_2), while the observed energy sharing and angular distributions of the three-body breakup product channel could depend heavily on the structure, bonding and charge center of the parent molecular ion. Experiments during this review period concentrated on measurements of cross sections, branching fractions, and three-body breakup dynamics of BH_2^+ undergoing dissociative recombination (DR) with zero-eV electrons. Interestingly, it was found that this ion dissociates preferentially (56%) into BH + H. Surprisingly, about a third (35%) proceeds through three-body decay to B + H + H, which for almost all other tri-atomic dihydrides is the dominant channel. The two-body B + H_2 channel contributes less than 9%. Despite the relatively small fraction of fragmentation leading to three-body breakup, this channel was investigated with the imaging technique described above. The dynamics were observed to be very similar to the other covalently bonded di-hydride ions, with the kinetic energy almost randomly distributed between the H atoms while the dissociation occurs predominantly from open- and closed-geometry states, that is, with the angle between the bonds at the time of dissociation near 180 or 0 degrees, respectively. Recently, results have been accepted for eight publications.

Investigations of DR of molecular ions have also continued on the merged electron-ion beams energy-loss (MEIBEL) apparatus[9] at ORNL. The fragment imaging technique for MEIBEL has been refined by the addition of a segmented photomultiplier tube (PMT) to trigger the image-intensified camera only when a two-particle event is detected on the phosphor screen of the detector by two segments of the PMT. Subsequent measurements on the DR of H_2^+ indicate that the vibrational distribution for these ions follows essentially a Franck-Condon one and peaks at about v=1 or 2. The dissociation of H_2^+ near zero energy was also investigated using both a solid-state surface-barrier detector as well as a discrete-dynode detector to count the neutrals produced. Because of the non-negligible contribution of DE at low energies for H_2^+ ions with a "hot" initial

vibrational distribution, the measured rates using discrete dynode detector included the sum of the DR and DE channels. However, using the energy-sensitive solid-state detector, we were able to separate the DE (one H atom) and DR (two H atoms) contributions. The measured DR rate coefficients are in excellent agreement with previously measured ones[10,11] for "hot" H_2^+ ions with a Franck-Condon vibrational distribution. Good agreement is also found between the measured DE rate coefficients and those published by Yousif and Mitchell[12] for energies above 50 meV. These studies are made possible by the 250-kV high voltage platform with an all-permanent magnet ECR ion source at the ORNL MIRF. The cold molecular ion sources being commissioned on the HV platform as discussed above are also being adapted for possible use in these DR studies at MEIBEL.

1. R. Thomas *et al*., Phys. Rev. A **71**, 032711 (2005).
2. M. Larsson and R. Thomas, Phys. Chem. Chem. Phys. **3**, 4471 (2001).
3. Å. Larson *et al*., Astrophys. J. **505**, 459 (1998).
4. S. Rosén *et al*., Faraday Discussions **115**, 295 (2000).
5. F. Hellberg *et al.*, J. Chem. Phys. **122**, 224314 (2005).
6. V. Zhaunerchyk *et al.*, Phys. Rev. Lett. **98**, 223201 (2007).
7. R. Thomas *et al*., Phys. Rev. A **66**, 032715 (2002).
8. V. Zhaunerchyk *et al.*, Phys. Rev. A (Rapid Communication) **78** (2008).
9. E. W. Bell *et al*., Phys. Rev. A **49**, 4585 (1994).
10. B. Peart and K. T. Dolder, J. Phys. B **7**, 236 (1974).
11. D. Auerbach *et al*., J. Phys. B **10**, 3797 (1977).
12. F. B. Yousif and J. B. A. Mitchell, Z. Phys. D **34**, 195 (1995).

Molecular Ion Interactions (COLTRIMS and ICCE Trap Developments) – *C. R. Vane, M. E. Bannister, C. C. Havener, H. F. Krause, F. Meyer, and M. Fogle*

Dissociative Electron Capture (COLTRIMS): Using both warm and cold target aspects of the MIRF Cold Target Recoil Ion Momentum Spectroscopy (COLTRIMS)[1] endstation, we are performing studies involving electron capture by molecular projectile ions from atomic targets, leading to molecular dissociation that yields neutral and/or ionic fragments. The process, labeled Dissociative Electron Capture (DEC) or Electron Capture Dissociation (ECD) has been previously investigated using a number of experimental techniques,[2-7] and is technically important in the field of mass spectroscopy of heavy molecules, where it is used as a method of fragmenting gas phase ions for tandem mass spectrometric analysis, giving unique structural information for complex species up to biomolecules.[8] DEC studies also give information complementary to our MIRF and CRYRING measurements of dissociative ionization, excitation, and recombination (DI, DE, and DR) occurring in molecular ion interactions with free electrons for the same molecular ion species. In cool, dense regions of any plasmas, there may be significant populations of all the available components necessary for DEC; i.e., localized high constituent densities of neutral atoms, molecules, and their ions, as well as a variety of their neutral and ionic fragments. Such environments naturally arise in a number of plasma-to-gas or plasma-to-surface transition regions, such as in plasma processing reactors and at the diverter edges of fusion plasma containment devices where the neutral components can present significant target densities for collisions with electrons and/or atomic and molecular ions. Dissociative fragmentation of molecular ions through DEC processes provides channels for significant production of a variety of highly reactive neutral and ionic species.

The ORNL COLTRIMS endstation has been fitted with fragment analysis detectors including a special, energy sensitive detector for determination of chemical branching fractions, and a 3-D (2-D spatial + time) imaging detector system permitting multi-hit coincident detection and position sensitive capability for studies of the dynamics of energy sharing in DEC.

Measurements have been performed for DEC by diatomic and simple triatomic molecular ions in static gas targets and the results compared with branching fractions and kinematics observed for dissociative recombination, dissociative excitation and dissociative ionization measured at CRYRING and at the MIRF electron-ion crossed beams apparatus for similar ion species. Chemical branching fractions resulting from DEC by H_2^+, HD^+, H_3^+, and O_2^+ from the HV platform ECR ion source interacting with H_2, He, N_2, and argon targets have been measured using the partial transmission grid method,[9] and a special ultra-thin window, energy sensitive silicon detector. These 100% detection efficiency measurements are made possible by the higher available energies per unit mass afforded by the MIRF high voltage platform and beamlines. Future DEC studies, especially for triatomic dihydrides XH_2^+ for which we have extensive DR, DE, and DI data, will be carried out with rotationally cold ions from Cold Molecular Ion Sources (CMIS) mounted on the HV platform, and also using the COLTRIMS technique in coincidence with fragment imaging measurements to permit identification of the specific Q-value channels of electron capture leading to dissociation. Integration of the recoil ion COLTRIMS data and the DEC neutral fragment imaging detector data is being assisted by collaboration with Dr. Richard Thomas from Stockholm University, who has developed the multi-hit imaging data analysis software. Neutral atomic beam targets will also be added later in 2009-2010 to permit studies of DEC by molecular ions interacting with highly collimated beams of H, Li, Na, and Cs.

1. J. Ullrich *et al*., Comments At. Mol. Phys. **30**, 285 (1994).
2. C. L. Cocke *et al*., Phys. Rep. **205**, 153 (1991).
3. V. Mergel *et al*., Phys. Rev. Lett. **74**, 2200 (1995).
4. G. W. McClure, Phys. Rev. **140**, A769 (1965).
5. B. Meierjohann and M. Volger, J. Phys. **B**: At. Mol. Phys. **9**, 1801 (1976).
6. D. P. de Bruijn *et al*., Chem. Phys. **85**, 215 (1984).
7. C. M. Laperle *et al*., Phys. Rev. Lett. **93**, 153202 (2004).
8. R. A. Zubarev *et al*., J. Am. Chem. Soc. **120**, 3265 (1998).
9. S. Datz *et al*., Phys. Rev. Lett. **74**, 896 (1995).

Development of the Ion Cooling and Characterization Endstation (ICCE Trap): A significant portion of our effort this last year has been devoted to development and implementation of a number of enhanced experimental capabilities designed specifically to enable expanded, more sophisticated molecular ion research at the MIRF. Measurements with more complex systems require increased levels of control over internal state populations of the reacting partners, as well as more detailed information from analysis and detection systems for rational interpretation of results. To this end we have developed and installed a new electrostatic reflecting ion trap endstation on the MIRF high energy beamline that permits storage, cooling, and characterization of molecular cations, effectively independent of the mass of the ion. These ion beams are produced in several molecular ion sources being mounted on the high voltage platform, including the permanent magnet ECR ion source for 'hot' atomic and molecular ions, and pulsed, supersonic expansion discharge sources for internally 'cold' molecular ions. A first version of the supersonic expansion CMIS is presently undergoing commissioning, being tested for production of rotationally cold molecular ions (e.g., H_2^+, O_2^+, and O_3^+) for use in studies of dissociative electron capture (DEC) and electron impact dissociation using 3-D fragment imaging analysis on the COLTRIMS, MEIBEL, and TRAP endstations. As previously noted, this CMIS is a similar design to that used recently for cold H_3^+ dissociative recombination studies at CRYRING.[1]

The complete ion cooling and characterization endstation (ICCE trap) as shown in Fig. 1 consists of a new ultra-high vacuum transport beamline and chambers with computer controlled, fast-reaction electrostatic deflection and focusing elements, a fully electrostatic mirror trapping system,[2] and a newly developed high-current, low-energy (5-100 eV) crossed electron beam

target located between the trap mirrors.[3] The apparatus is instrumented with a number of beam diagnostic and product characterization components, including two imaging detectors for analysis of neutral fragments arising from fragmentation of the trapped molecular ions, either by collisions with gas (collisional dissociation (CD) and dissociative electron capture (DEC)) or with the electrons (dissociative excitation or ionization (DE, DI), and less likely, dissociative recombination (DR)). Presently, the trap region operates at room temperature with vacuum at ~ 10^{-10} Torr and ion internal state cooling proceeding through radiative decay is limited to 300°K. We plan to lower the beam exposed surfaces of the trap region to less than 70°K through installation next year of an overall copper liner cooled to <70°K with stirling cryocoolers,[4] and connection of one of the mirrors and its shroud ('cold' mirror in Fig. 1) to a 4°K helium cryocooler.[5] Development of the ICCE trap apparatus is in direct support of our mission goal of establishing experimental capabilities necessary for state-selectively producing and manipulating atomic and molecular ions to implement studies of a broad range of plasma relevant ion-interactions in as controlled a manner as possible.

In initial commissioning, relatively intense beams of 10-keV O_2^+ ions from the high-voltage platform ECR ion source were produced, transported, and tuned through the ICCE trap, and neutral O and O_2 products were imaged in the detectors. Lower intensity beams of O_3^+ have also been extracted from the ECR and development is proceeding on enhancing intensity from the ECR, as well as producing 'cold' O_3^+ ions from the supersonic expansion source. Initial work will concentrate on trapping and cooling of these ozone ions and on measurements of DEC from background gas (primarily H_2) and electron impact dissociation (DE, DI, and DR) as a function of electron energy for various trapping/cooling times. These measurements will be compared with our prior O_3^+ DR measurements at CRYRING,[6] that somewhat surprisingly indicated almost complete (94%) 3-body dissociation at zero electron energy, forming predominantly electronically excited O(^{3}P and ^{1}D) fragment atoms.

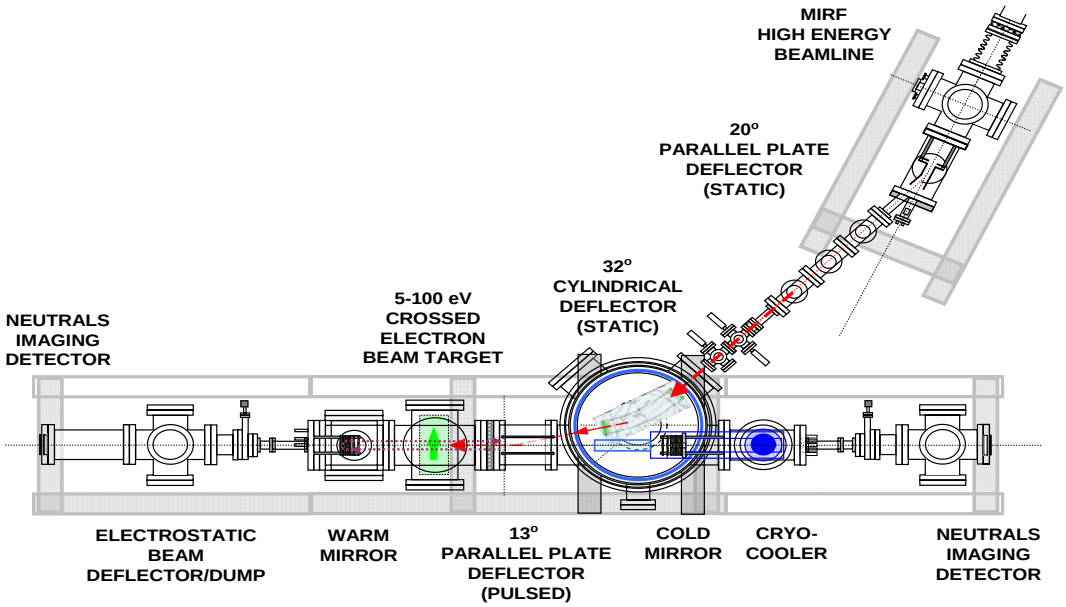

Figure 1. Schematic of the MIRF Ion Cooling and Characterization Endstation (ICCE trap) showing the beamline layout including 20° extraction and 45° injection (32° + 13°) electrodes, crossed low-energy electron target, warm and cold (4°K) trap mirrors, and imaging detectors for analysis of neutral fragments escaping from dissociated ions.

1. B. J. McCall *et al*., J. Phys.: Conf. Ser. **4,** 92 (2005); and Nature **422**, 500 (2003).
2. H. F. Krause *et al*., AIP Conf. Proc. **576** (AIP, New York 1994), pp. 126-129.
3. O. Heber *et al*., Rev. Sci. Instrum. **76**, 013104 (2005).
4. Sunpower Corp., Athens, OH 45701.
5. Janis Research Co., Wilmington, MA 01887.
6. V. Zhaunerchyk *et al*., Phys. Rev. A **77**, 022704 (2008).

Manipulation and Decoherence of Rydberg Wavepackets – *C. O. Reinhold*

Engineering the quantum states of microscopic and mesoscopic objects is a long sought after goal in many current fields of research. Atoms in Rydberg states with large values of principal quantum number (*n>300*) provide a valuable laboratory in which to manipulate quantum states of mesoscopic size (~micrometers). This is achieved using commercially available-pulse generators whose strengths are comparable to the Coulomb electric fields (~mV/cm) and whose time scales (picoseconds) are shorter than the classical orbital period of the atom (~nanoseconds). Such giant atoms can be manipulated using tailored sequences of half-cycle pulses (HCPs) and field steps. These are relative recent additions to the arsenal of short electromagnetic pulses now available in several laboratories and their effect is quite different from that of laser or microwave pulses. Our recent work demonstrates the remarkable level of time-resolved control and imaging of the electronic states that can be achieved.[1-4] One practical limitation for manipulating Rydberg atoms is that these are extremely fragile objects and can be easily altered by their environment.[5] This has opened up new challenges that can be profitably explored to study the quantum-to-classical crossover and decoherence at a level of detail difficult to achieve in other systems. Study of decoherence of the internal state of atoms and ions has been a second focus our work and has been intimately related to our simulations of the time evolution of the internal state of fast ions traversing solids.[6] Rydberg wavepackets provide a partially controlled laboratory to study decoherence. A controlled "amount" of noise can be added to the system in the form of random fluctuations of the electromagnetic pulses to study the rate of decoherence as a function of the "amount" or "color" of noise.[7] Noise might also be introduced experimentally by adding a dilute gas of particles into the experimental chamber. In the long term, we would like to extend the present techniques to engineer two-electron wavepackets involving distant electrons in two interacting Rydberg atoms and planetary atoms. This work is performed in collaboration with the groups of F. B. Dunning (Rice University) and J. Burgdörfer and S. Yoshida (Vienna University of Technology).

1. J. J. Mestayer *et al.*, Phys. Rev. Lett. **100**, 243004 (2008).
2. J. J. Mestayer *et al.*, Phys. Rev. Lett. **99**, 183003 (2007).
3. S. Yoshida *et al.*, Phys. Rev. Lett. **98**, 203004 (2007).
4. W. Zhao *et al.*, Phys. Rev. Lett. **97**, 253003 (2006); Phys. Rev. Lett. **95**, 163007 (2005).
5. C. O. Reinhold *et al.*, J. Phys. Conf. Ser. **88**, 012030 (2007).
6. M. Seliger *et al.*, Phys. Rev. A **75**, 032714 (2007).
7. S. Yoshida *et al.*, Phys. Rev. A **75**, 013414 (2007).

Molecular Dynamics Simulations of Chemical Sputtering – *C.O. Reinhold and P.S. Krstic*

Physical and chemical processes resulting from the interaction of hydrogen isotopes with carbon surfaces are of significant importance within the fusion community. These interactions lead to surface erosion and particle deposition, which degrades fusion performance and produce long-term particle retention. Considerable information is available in the literature at high impact energies (above ~50eV) where the interactions can be modeled using two-body potentials such as those in the TRIM code. In contrast, little is known for low impact energies where chemical

processes dominate, thereby increasing the complexity of the interactions. These can be modeled by large scale molecular dynamics (MD) simulations using many-body reactive potentials. We have recently undertaken a series of such MD simulations for 1-30 eV D and D_2 impact of carbon[1-3] in parallel to experiments at ORNL by Fred Meyer and co-workers. We have shown that the large yields of saturated hydrocarbons typically observed in experiments are not the result of single impacts but rather the consequence of multiple cumulative impacts. We are currently investigating the isotope dependence of surface erosion (i.e., H, D, or T impact). We are also studying the sensitivity of the results with respect to the many-body interaction potentials used in the simulations. We use two types of reactive bond-order potentials: REBO and AIREBO. Most of our simulations have been performed using the first potential that is the simplest and provides a good empirical description of covalent bonds for nonpolar systems. The second potential, AIREBO, is more advanced and includes better descriptions of non-bonded interactions, including torsions and van der Waals. Our work is performed in collaboration with S. Stuart (Clemson University) who is one of the developers of these potentials. In the longer term, we plan to extend our simulations to address the interest within the Fusion community to study materials different from pure carbon.

1. P. S. Krstic, C. O. Reinhold, and S. J. Stuart, New J. Phys. **9**, 219 (2007).
2. P. S. Krstic, C. O. Reinhold, and S. J. Stuart, Europhys. Lett. **77**, 33002 (2007).
3. C. O. Reinhold, P. S. Krstic, and S. J. Stuart, Nucl. Instrum. Methods Phys. Res. B **258**, 274 (2007).

Development of Theoretical Methods for Atomic and Molecular Collisions – *D. R. Schultz, T. Minami, T.-G. Lee, M. S. Pindzola, J. H. Macek, and S. Yu. Ovchinnikov*

Plasma science applications, such as fusion energy, material processing, and the chemistry of the upper atmosphere, continue to drive the study of atomic and molecular collisions. Furthermore, control of atomic-scale dynamics, ultrafast phenomena, and complex behavior provide increasingly strong fundamental motivation to study such atomic and molecular interactions. These research areas in turn demand the development of theoretical methods to either reach new levels of accuracy for fundamental systems or novel completeness for complex systems. Over the past year projects have been undertaken along both these lines.

To begin with, the ongoing quest for more accurate methods, which has motivated development of computational approaches such as the lattice, time-dependent Schrodinger equation (LTDSE) method over the past decade, has enabled the completion of several projects aimed at providing benchmark atomic collision data required in plasma modeling.[1] In addition, collaborations have led to a new computational approach incorporating LTDSE (see the section by Macek and Ovchinnikov) that has led to the surprising observation of vortices in the electronic probability distribution in atomic collisions, which play a significant role in the dynamics of angular momentum transfer not previously appreciated.[3]

Along different lines, work was initiated using a molecular dynamics approach to treat much more complex atomic-scale interactions such as the fragmentation of molecular ions. This work is aimed at providing physical interpretation of experimental measurements ongoing in the Multicharged/Molecular Ion Research Facility. Rather than treating a small number of electrons and nuclei with a fine-grained computational approach solving an *ab initio* equation of motion, a much larger number of electrons and nuclei are treated more approximately with an emphasis on description of the dynamics resulting from the interaction of many more particles.

1. T. Minami, M. S. Pindzola, T.-G. Lee, and D. R. Schultz, J. Phys. B **40**, 3629 (2007).
2. T. Minami, T.-G. Lee, M. S. Pindzola, and D. R. Schultz, J. Phys. B **41**, 134201 (2008).

3. J. H. Macek, J. S. Sternberg, S. Yu. Ovchinnikov, T.-G. Lee, and D. R. Schultz (2008), in preparation.

Computation of Ionization in Ion-Atom Collisions – *J. H. Macek and S. Yu. Ovchinnikov*

Benchmark computations of ionization in ion-atom atom collisions applicable to plasma diagnostics are needed over a wide energy range, namely, from 1 keV to tens of MeV. For some purposes cross sections accurate to 1% are desired. It is impossible, at the present time, to measure ion-atom-ionization cross sections to that accuracy, however calculations can aspire it. This level of accuracy is normally not a goal of atomic collision calculations since it is not needed for comparison with experiment; however, the steady increase of computer speed and memory makes it feasible to design such computational methods for one-electron species.

We are collaborating with D. R. Schultz to adapt the Lattice Time Dependent Schrödinger Equation method (LTDSE) for the calculation of ionization cross sections for proton-hydrogen collisions at the 1% level. The method adapted to ionization is called the Regularized Lattice Time-Dependent Schrödinger Equation method (RLTDSE). Our first computations use unitarity to extract the ionization component. For this purpose it is necessary to compute elastic scattering cross sections accurate to 0.1%. The main accomplishment in the past year is that some proof-of-principal calculations have achieved this accuracy.

We will compute total ionization cross sections using the new RLTDSE method for one-electron model systems over a broad energy range. Total ionization will be computed using unitarity and integration over the electron momentum distribution. Different methods to extract the momentum distribution will be tested for accuracy.

References to Publications of DOE Sponsored Research from 2006-2008 (descending order)

Year 2008 publications

"Rotating Dual-Wire Beam Profile Monitor Optimized for Use in Merged-Beams Experiments," D. G. Seely, H. Bruhns, D. W. Savin, T. J. Kvale, E. Galutschek, H. Aliabadi, and C. C. Havener, Nucl. Instrum. Methods Phys. Res. **585**, 69 (2008).

"Chemical Sputtering and Surface Damage by Low-Energy Atomic and Molecular Hydrogen and Deuterium Projectiles," F. W. Meyer, H. Zhang, M. J. Lance, and H. F. Krause, Vacuum **82**, 880 (2008).

"Surface Modification and Chemical Sputtering of Graphite Induced by Low-Energy Atomic and Molecular Deuterium Ions," H. Zhang, F. W. Meyer, H. M. Meyer III, M. J. Lance, Vacuum **82**, 1285 (2008).

"Electron-Impact Ionization of Be-like C III, N IV, and O V," M. R. Fogle, E. Bahati Musafiri, M. E. Bannister, C. R. Vane, S. D. Loch, M. S. Pindzola, C. P. Ballance, R. D. Thomas, V. Zhaunerchyk, P. Bryans, W. Mitthumsiri, and D. W. Savin, Astrophys. J. Suppl. Ser. **175**, 543 (2008).

"Dissociative Recombination Dynamics of the Ozone Cation," V. Zhaunerchyk, W. Geppert, F. Österdahl, M. Larsson, R. D. Thomas, E. Bahati Musafiri, M. E. Bannister, M. R. Fogle, and C. R. Vane, Phys. Rev. A **77**, 022704 (2008).

"Realization of Localized Bohr-like Wavepackets," J. J. Mestayer, B. Wyker, J. C. Lancaster, F. B. Dunning, C. O. Reinhold, S. Yoshida, and J. Burgdörfer, Phys. Rev. Lett. **100**, 243004 (2008).

"Occupation of Fine-Structure States in Electron Capture and Transport," M. Seliger, C. O. Reinhold, T. Minami, D. R. Schultz, S. Yoshida, J. Burgdörfer, E. Lamour, J.-P. Rozet, and D. Vernhet, Phys. Rev. A **77**, 042713 (2008).

"Total and State-Selective Charge Transfer in He^{2+} + H Collisions," T. Minami, T.-G. Lee, M. S. Pindzola, and D. R. Schultz," J. Phys. B **41**, 134201 (2008).

"Time-Dependent Lattice Methods for Ion-Atom Collisions in Cartesian and Cylindrical Coordinate Systems," M. S. Pindzola and D.R. Schultz, Phys. Rev. A **77**, 014701 (2008).

"Transferring Rydberg Wavepackets between Islands across the Chaotic Sea," S. Yoshida, C. O. Reinhold, J. Burgdörfer, J. J. Mestayer, J. C. Lancaster, and F. B. Dunning, Phys. Rev. A **77**, 013411 (2008).

"Low-Energy Charge Transfer for Collisions of Si^{3+} with Atomic Hydrogen," H. Bruhns, H. Kreckel, D. W. Savin, D. G. Seely, and C. C. Havener, Phys. Rev. A **77**, 064702 (2008).

Year 2007 publications

"Ion Atom Merged-Beams Experiments," C. C. Havener, E. Galutschek, R. Rejoub, and D. G. Seely, Nucl. Instrum. Methods Phys. Res. B **261**, 129 (2007).

"Three-Step Resonant Photoionization Spectroscopy of Ni and Ge: Ionization Potential and Odd-Parity Rydberg Levels," T. Kessler, K. Bruck, C. Baktash, J. R. Beene, C. Geppert, C. C. Havener, H. F. Krause, Y. Liu, D. R. Schultz, D. W. Stracener, C. R. Vane, and K. Wendt, J. Phys. B **40**, 4413 (2007).

"The ORNL Single-Pass Ion-Atom Merged-Beam Experiment," C. C. Havener, [Invited] *Proceedings, 2nd International Workshop on Electrostatic Storage Devices, July 17-21, 2007, Stockholm, Sweden*.

"Experiments on Interactions of Electrons with Molecular Ions in Fusion and Astrophysical Plasmas," M. E. Bannister, H. Aliabadi, E. Bahati Musafiri, M. R. Fogle, P. S. Krstic, C. R. Vane, A. Ehlerding, W. Geppert, F. Hellberg, V. Zhaunerchyk, M. Larsson, and R. D. Thomas, Book Chapter - *Atomic Processes in Plasmas: The 15th International Conference on Atomic Processes in Plasmas* **926**, 195-205 (2007).

"Low-Energy Electron Capture by Ne^{2+} Ions from H(D)," B. Seredyuk, H. Bruhns, D. W. Savin, D. G. Seely, H. Aliabadi, E. Galutschek, and C. C. Havener, Phys. Rev. A **75**, 054701 (2007).

"Quantum and Classical Transport of Excited States of Ions," C. O. Reinhold, M. Seliger, T. Minami, D. R. Schultz, J. Burgdörfer, E. Lamour, J.-P. Rozet, and D. Vernhet, Nucl. Instrum. Methods Phys. Res. B **261**, 125 (2007).

"Angular Distribution of Ions Transmitted by an Anodic Nanocapillary Array," H. F. Krause, C. R. Vane, F. W. Meyer, and H. M. Christen, *Proceedings, 13th International Conference on the Physics of Highly Charged Ions, Belfast, Northern Ireland, UK*, J. Phys.: Conf. Ser. **58**, 323 (2007).

"Electron-Impact Ionization of Be-like, C^{2+}, N^{3+}, and O^{4+}," M. E. Bannister, E. Bahati Musafiri, C. P. Balance, M. R. Fole, S. D. Loch, W. Mitthumsiri, M. S. Pindzola, D. W. Savin, R. D. Thomas, C. R. Vane, and V. Zhaunerchyk, *Proceedings, XXV International Conference on Photonic, Electronic and Atomic Collisions, Freiburg, Germany, July 25-31, 2007.*

"Dissociative Excitation of Diatomic and Polyatomic Molecular Ions Producing Heavy Fragment Ions," M. E. Bannister, E. Bahati Musafiri, M. R. Fogle, P. S. Krstic, M. Larsson, R. D. Thomas, C. R. Vane, and V. Zhaunerchyk, *Proceedings, XXV International Conference on Photonic, Electronic and Atomic Collisions, Freiburg, Germany, July 25-31, 2007.*

"Electron-Impact Dissociation of CH_2^+ Ions: Measurement of CH^+ and C^+ Fragment Ions," C. R. Vane, E. Bahati Musafiri, M. E. Bannister, and R. D. Thomas, Phys. Rev. A **75**, 052715 (2007).

"Atomic Collisions at Ultrarelativistic Energies," C. R. Vane and H. F. Krause, Nucl. Instrum. Methods Phys. Res. B **261**, 244 (2007).

"Three-Body Breakup in Dissociative Recombination of the Covalent Triatomic Molecular Ion O_3^+," V. Zhaunerchyk, W. D. Geppert, M. Larsson, R. D. Thomas, E. Bahati, M. E. Bannister, M. R. Fogle, C. R. Vane, and F. Österdahl, Phys. Rev. Lett. **98**, 223201 (2007).

"Ions Transmitted through an Anodic Nanocapillary Array," H. F. Krause, C. R. Vane, and F. W. Meyer, Phys. Rev. A **75**, 042901 (2007).

"The New ORNL Multicharged Ion Research Facility Floating Beamline," F. W. Meyer, M. R. Fogle, and J. W. Hale, *Proceedings, 22nd Particle Accelerator Conference (PAC'07), Albuquerque, NM, June 25-29, 2007*.

"Merged-Beams Measurements of Absolute Cross Sections for Electron-Impact Excitation of S^{4+} ($3s^2\ ^1S \rightarrow 3s3p\ ^1P$) and S^{5+}($3s\ ^2S \rightarrow 3p\ ^2P$)," B. Wallbank, M. E. Bannister, H. F. Krause, Y.-S. Chung, A.C.H. Smith, N. Djuric, and G. H. Dunn, Phys. Rev. A **75**, 052703 (2007).

"Low-Energy Chemical Sputtering of ATJ Graphite by Atomic and Molecular Deuterium Ions," F. W. Meyer, P. S. Krstic, L. I. Vergara, H. F. Krause, C. O. Reinhold, and S. J. Stuart, Phys. Scr. **T128**, 50 (2007).

"Chemical Sputtering of Room Temperature ATJ Graphite and HOPG by Slow Atomic and Molecular Ions," F. W. Meyer, H. Zhang, L. I. Vergara, and H. F. Krause, Nucl. Instrum. Methods Phys. Res. B **258**, 264 (2007).

"Chemical Sputtering from Amorphous Carbon under Bombardment by Deuterium Atoms and Molecules," P. S. Krstic, C. O. Reinhold, and S. J. Stuart, New J. Phys. **9**, 219 (2007).

"Regge Oscillations in Electron-Atom Elastic Cross Sections," D. Sokolovski, Z. Felfli, S. Yu. Ovchinnikov, J. H. Macek, and A. Z. Msezane, Phys. Rev. A **76**, 1 (2007).

"Transporting Rydberg Electron Wavepackets with Chirped Trains of Pulses," J. J. Mestayer, W. Zhao, J. C. Lancaster, F. B. Dunning, C. O. Reinhold, S. Yoshida, and J. Burgdörfer, Phys. Rev. Lett. **99**, 183003 (2007).

"Electric Dipole Echoes in Rydberg Atoms," S. Yoshida, C. O. Reinhold, J. Burgdörfer, W. Zhao, J. J. Mestayer, J. C. Lancaster, and F. B. Dunning, Phys. Rev. Lett. **98**, 203004 (2007).

"Quantum Treatment of Continuum Electrons in the Fields of Moving Charges," T.-G. Lee, S. Yu. Ovchinnikov, J. Sternberg, V. Chupryna, D. R. Schultz, and J. H. Macek, Phys. Rev. A **76**, 050701 (2007).

"The Time-Dependent Close-Coupling Method for Atomic and Molecular Collision Processes," M. S. Pindzola, F. Robicheaux, S. D. Loch, J. C. Berengut, T. Topcu, J. Colgan, M. Foster, D. C.

Griffin, C. P. Ballance, D. R. Schultz, T. Minami, N. R. Badnell, M. C. Witthoeft, D. R. Plante, D. M. Mitnik, J. A. Ludlow, and U. Kleiman, J. Phys. B **40**, R39 (2007).

"Electric Dipole Echoes and Noise-Induced Decoherence," J. J. Mestayer, W. Zhao, J. C. Lancaster, F. B. Dunning, C. O. Reinhold, S. Yoshida, and J. Burgdörfer, J. Phys. Conf. Ser. **88**, 012055 (2007).

"Open Quantum System Approach in Multiple Atomic Collisions in Solids and Gases," C. O. Reinhold, M. Seliger, T. Minami, S. Yoshida, J. Burgdörfer, J. J. Mestayer, W. Zhao, J. C. Lancaster, and F. B. Dunning, J. Phys. Conf. Ser. **88**, 012030 (2007).

"Low-Energy Chemical Sputtering of ATJ Graphite by Atomic and Molecular D Ions," F. W. Meyer, P. S. Krstic, L. I. Vergara, H. F. Krause, C. O. Reinhold, and S. J. Stuart, Phys. Scr. **T128**, 50 (2007).

"Time Scales of Chemical Sputtering of Carbon," C. O. Reinhold, P. S. Krstic, and S. J. Stuart, Nucl. Instrum. Methods Phys. Res. B **258**, 274 (2007).

"Chemical Sputtering by Impact of Excited Molecules," P. S. Krstic, C. O. Reinhold, and S. J. Stuart, Europhys. Lett. **77**, 33002 (2007).

"Numerical Study of Charge Transfer in $H^+ + He^+$ and $He^{2+} + Li^{2+}$ Collisions," T. Minami, M .S. Pindzola, T.-G. Lee, and D. R. Schultz, " J. Phys. B **40**, 3629 (2007).

"Capture and Transport of Electronic States of Fast Ions Penetrating Solids: An Open Quantum System Approach with Sinks and Sources," M. Seliger, C. O. Reinhold, T. Minami, D. R. Schultz, M. S. Pindzola, S. Yoshida, J. Burgdörfer, E. Lamour, J.-P. Rozet, and D. Vernhet, Phys. Rev. A **75**, 032714 (2007).

"Dephasing of Stark Wavepackets Induced by Colored Noise," S. Yoshida, C. O. Reinhold, J. Burgdörfer, W. Zhao, J. J. Mestayer, J. C. Lancaster, and F. B. Dunning, Phys. Rev. A **75**, 013414 (2007).

"Methane Production by Deuterium Impact at Carbon Surfaces," S. J. Stuart, P. S. Krstic, T. A. Embry, and C. O. Reinhold, Nucl. Instrum. Methods Phys. Res. B **255**, 202 (2007).

Year 2006 publications

"Methane Production from ATJ Graphite by Slow Atomic and Molecular D Ions: Evidence for Projectile Molecule-Size-Dependent Yields at Low Energies," L. I. Vergara, F. W. Meyer, H. F. Krause, P. Träskelin, K. Nordlund, and E. Salonen, J. Nucl. Mater. **357**, 9 (2006).

"Recent ORNL Measurements of Chemical Sputtering of ATJ Graphite by Slow Atomic and Molecular D Ions," F. W. Meyer, L. I. Vergara, and H. F. Krause, *Workshop on New Directions for Advanced Computer Simulations and Experiments in Plasma Surface Interactions, March 21-23, 2005*, Phys. Scr. **T124**, 44 (2006).

"Measurement of the Plasma Potential in the Edge Plasma of the ORNL CAPRICE ECR Ion Source," H. J. You, K. S. Chung, and F. W. Meyer, J. Korean Phys. Soc. **49**, 1470 (2006).

"Deduction of Edge Electron Density with Multiply Charged Ions in the ORNL Volume-Type Electron Cyclotron Resonance Ion Source," H. J. You, H. J. Woo, K. S. Chung, Y. Liu, F. W. Meyer, T. Lho, and M. J. Lee, Rev. Sci. Instrum. **79**, 02A319 (2006).

"Dipole Polarization Effects on Highly-Charged Ion-Atom Electron Capture," C. C. Havener and R. Rejoub, p. 522, *Proceedings, International Conference on Photonic, Electronic, and Atomic Collisions, Rosario, Argentina, July 20-26, 2005* (World Scientific, 2006).

"Laser Ion Source Tests at the HRIBF on Stable Sn, Ge, and Ni Isotopes," Y. Liu, C. Baktash, J. R. Beene, H. Z. Bilheux, C. C. Havener, H. F. Krause, D. R. Schultz, D. W. Stracener, C. R. Vane, K. Breuck, Ch. Geppert, T. Kessler, K. Wendt, Nucl. Instrum. Methods Phys. Res. B **243**, 442-452 (2006).

"The ORNL Multicharged Ion Research Facility Upgrade Project," F. W. Meyer, M. E. Bannister, D. Dowling, J. W. Hale, C. C. Havener, J. W. Johnson, R. C. Juras, H. F. Krause, A. J. Mendez, J. Sinclair, A. Tatum, C. R. Vane, E. Bahati Musafiri, M. Fogle, R. Rejoub, L. Vergara, D. Hitz, M. Delaunay, A. Girard, L. Guillemet, and J. Chartier, *Proceedings, 14th International Conference on Ion Beam Modification of Materials*, Asilomar, *CA, Sept. 5-10, 2004*, Nucl. Instrum. Methods Phys. Res. B **242**, 71 (2006).

"Realization of the Kicked Atom at High Scaled Frequencies," C. O. Reinhold, S. Yoshida, J. Burgdörfer, W. Zhao, J. J. Mestayer, J. C. Lancaster, and F. B. Dunning, Phys. Rev. A **73**, 033420 (2006).

"Influence of a DC Offset Field on Kicked Quasi-One-Dimensional Rydberg Atoms: Stabilization and Frustrated Field Ionization," S. Yoshida, C. O. Reinhold, J. Burgdörfer, W. Zhao, J. J. Mestayer, J. C. Lancaster, and F. B. Dunning, Phys. Rev. A **73**, 033411 (2006).

"Correlated Electron Detachment in H^- - He Collisions," G. N. Ogurtsov, V. M. Mikoushkin, S. Yu. Ovchinnikov, and J. H. Macek, Phys. Rev. A**74**, 042720 (2006).

"Bidirectionally Kicked Rydberg Atoms: Population Trapping near the Continuum," W. Zhao, J. J. Mestayer, J. C. Lancaster, F. B. Dunning, C. O. Reinhold, S. Yoshida, and J. Burgdörfer, Phys. Rev. A **73**, 015401 (2006).

"The Kicked Rydberg Atom," F. B. Dunning, J. C., Lancaster, C. O. Reinhold, S. Yoshida, and J. Burgdörfer, Adv. At. Mol. Phys. **52**, 49 (2006).

"Lattice, Time-dependent Schrödinger Equation Approach for Charge Transfer in Collisions of Be^{4+} with Atomic Hydrogen," T. Minami, M. S. Pindzola, T.-G. Lee,, and D. R. Schultz, J. Phys. B **39**, 2877 (2006).

"Collisions of Slow Highly Charged Ions with Surfaces," J. Burgdörfer, C. Lemell, C. O. Reinhold, K. Schiessl, B. Solleder, K. Tokesi, and L. Wirtz, p. 30, *Proceedings, International Conference on Photonic, Electronic, and Atomic Collisions, Rosario, Argentina, July 20-26, 2005* (World Scientific, 2006).

"Navigating Localized Wavepackets in Phase Space," W. Zhao, J. J. Mestayer, J. C. Lancaster, F. B. Dunning, C. O. Reinhold, S. Yoshida, and J. Burgdörfer, Phys. Rev. Lett. **97**, 253003 (2006).

"Chemical Sputtering of Fusion Plasma-Facing Carbon Surfaces," P. S. Krstic, S. J. Stuart, and C. O. Reinhold, *Proceedings, 23rd Summer School and International Symposium on the Physics of Ionized Gases, Aug.28 – Sept. 1, 2006, Kopaonik, Serbia*, AIP Conf. Proc. **876**, 201 (2006).

"Charge Transfer and Ionization by Intermediate-Energy Heavy Ions," L. H. Toburen, S. L. McLawhorn, R. A. McLawhorn, N. Evans, E.L.B. Justiniano, J. L. Shinpaugh, D. R. Schultz, and C. O. Reinhold, Rad. Prot. Dosim. **122**, 26 (2006).

"State-to-State Rotational Transitions in H_2+H_2 Collision at Low Temperatures," T.-G. Lee, N. Balakrishnan, R. C. Forrey, P. C. Stancil, D. R. Schultz, and G. J. Ferland, J. Chem. Phys. **125**, 114302 (2006).

PULSE: The Stanford Photon Ultrafast Laser Science and Engineering Institue

PULSE Primary Investigators: Y. Acremann, P.H. Bucksbaum, M. Fayer, D. Fritz, J. Hajdu, B. Hedman, K. Hodgson, K. Gaffney, A. Lindenberg, H. Siegmann, J. Stohr

PULSE mission: The Stanford PULSE Institute conducts research in areas of ultrafast science at SLAC that support the research program of the LCLS. PULSE has initiated research in ultrafast materials science, condensed matter physics, molecular physics, physical chemistry, atomic physics, structural biology, electron beams and x-ray laser physics. PULSE also maintains close links to areas of ultrafast science that are critically served by LCLS, but which lie outside the scope of mission activities in BES. These include plasma physics and high energy density physics.

BES funding of PULSE research: PULSE BES activities have divided funding. Four tasks are funded by Chemical Sciences: Attosecond and femtosecond vuv spectroscopy; strong-field molecular wave packet dynamics and quantum control; ultrafast x-ray studies of chemical processes; and coherent x-ray imaging. Other PULSE programs are funded by the Materials Science Division, in the areas of ultrafast magnetic materials and THz-induced materials science. High energy density science and ultrafast source science are pursued with funding outside of these two research divisions of BES. This abstract book will only summarize the AMOS-funded activities. Kelly Gaffney is the coordinator for those activities. The task PI's are Bucksbaum for the atomic and molecular projects E.2.a and E.2.b, Gaffney for chemistry E.3, and Hodgson (acting) for biomolecular imaging E.4.

PULSE laboratory renovation in FY08: PULSE was originally to have been housed in the LCLS Central Laboratory and Office Complex, but plans for this building were removed from the LCLS project in 2006. An alternative location was found in the SLAC Central Laboratory. Partial funds for renovation were approved by Congress in the FY08 budget, and the remainder are in the FY09 Presidential Budget Request for the Department of Energy. The renovation is now underway, and will be completed in about thirty months from now, at the end of CY10. An initial phase will be completed in early CY09, which will enable the establishment of some biomolecular imaging laboratories and some materials science laboratories.

PULSE facilities: PULSE occupies temporary space at SSRL, until our laboratory renovation at SLAC is completed. PULSE also has research in laboratories in the Varian Physics Building and in the Durand Materials Science Engineering Building on the Stanford main campus. PULSE plans to occupy some space in the LCLS Near Experimental Hall on a temporary basis as well. PULSE maintains a number of ultrafast sources and capabilities, including a CEP stabilized laser, a high harmonics source of ultrafast vuv, and laboratories for ultrafast chemistry, materials science, magnetic materials studies, and atomic physics. Immediate future plans include adding a biochemistry laboratory, a cluster computer for computational chemistry, and a laboratory e-beam-based x-ray source, to be located initially in the Near Experimental Hall.

PULSE Institute received its initial funding just one year ago, in July 2007. The initial funding of four programs in Chemical Sciences will be described in abstracts following this general summary. This is summarized in the organization chart (Fig. 1).

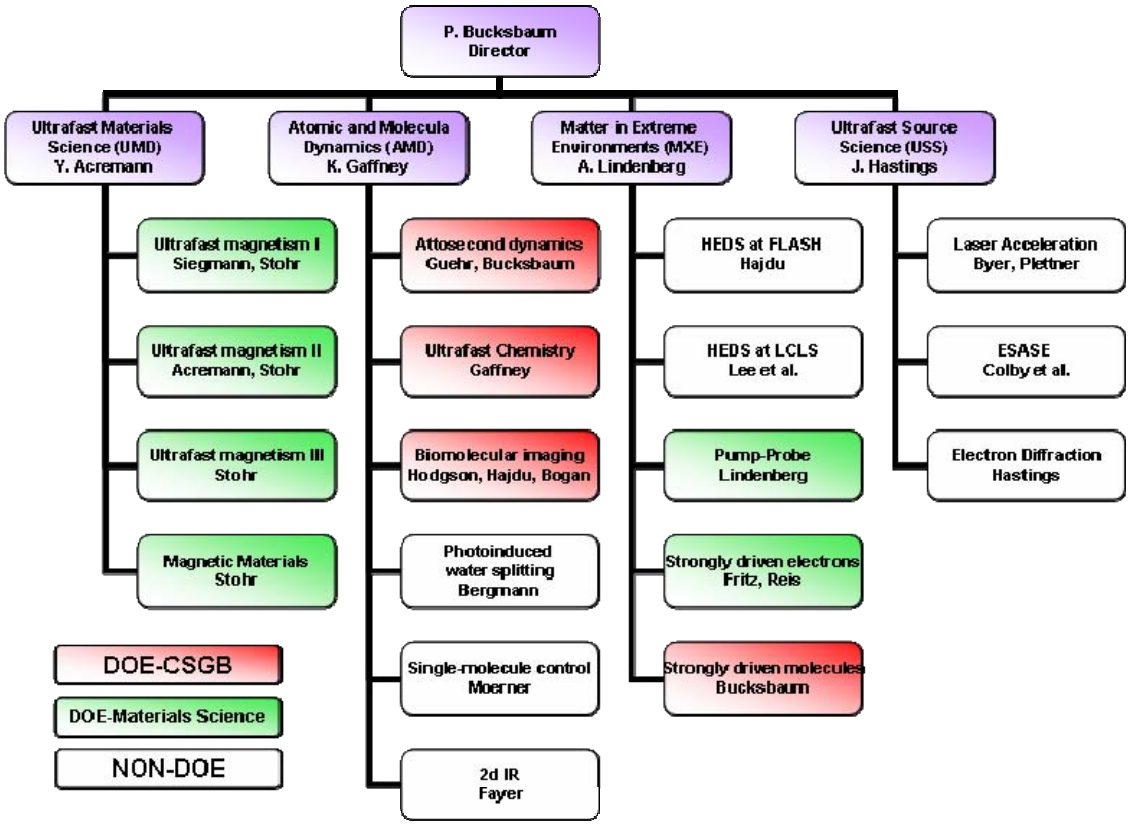

Fig. 1: PULSE organization chart. Tasks funded under DOE/CSGB are shaded red.

Other areas:

Ultrafast source science: This area is presently unfunded, but there are plans to collaborate with the accelerator group at SLAC to compete for future advanced accelerator R&D funding, as well as any future LDRD program, should one be established at SLAC. A third important group for collaboration is LCLS operations. The LCLS operations budget line will not receive full funding until FY09, and at that time we will pursue joint funding in this area. The Hastings project on ultrafast electron diffraction was rejected by BES for budget reasons after there were earlier indications that it might be funded, but there is still strong interest in pursuing it in future years. PULSE also intends to build a table-top ultrafast x-ray source.

High Energy Density Science: BES will not fund this, so we are establishing an international collaborative program in this area, with major funding from Europe, and utilization of LCLS governed by the LCLS access policy devised by their management. US partners include LLNL and U.C. Berkeley. We hope to establish an experimental

program on LCLS, which will complement other research on materials in extreme environments.

Ultrafast Materials Science: PULSE has six tasks in this area, all funded by the BES Division of Materials Science. These were described in abstracts in the DOE x-ray and neutron scattering contractor's meeting last year. The tasks cover investigations of ultrafast magnetic and dielectric properties of materials.

Fig. 2: 2008 PULSE Ultrafast X-ray Summer School during a break.

PULSE Central Activities Central management of the PULSE Institute pays for an administrator, shared safety coordinator, shared IT support, and a visitors program.

PULSE Summer School*:* The Stanford Dean of Research sponsored our second annual Ultrafast X-ray Summer School at the Kavli Institute on the SLAC campus in June. Professor Kelly Gaffney of PULSE was the Summer School Chair. The school was attended by approximately 100 students and postdocs. Information is on the following website: http://www-conf.slac.stanford.edu/uxss/2008/.

PULSE Visitors Program: PULSE maintains a visitors program to enable researchers from around the world to work in our center. Visitors next year will include Ken Schafer, Mette Gaarde, and Jon Marangos, as well as others.

PULSE plans for LCLS: PULSE encouraged and assisted LCLS in the formation of a strong user access policy, and we also participated in the proposal writing workshops, which were held in June 2008. PULSE has now formed three teams to write proposals for LCSL general user time, in the areas of AMO Physics, Soft X-ray Physics, and

Ultrafast X-ray Scattering, and we will continue to form more groups for LCLS in the future.

PULSE priorities for the coming year. PULSE has two areas that must be established in the coming year: theory; and ultrafast x-ray scattering. We have been working with Stanford to recruit two faculty in these areas. They will be appointed jointly in Photon Science, and in either Chemistry or Applied Physics. Stanford is making major commitments to their startup, and we have been discussing with DOE their role in the PULSE mission.

ULTRA-FAST COHERENT IMAGING OF NON-PERIODIC STRUCTURE

Janos Hajdu[1,2] and Mike Bogan[1]
1. Stanford PULSE Center, Stanford Linear Accelerator Center, Menlo Park, CA 94025
2. Laboratory of Molecular Biophysics, Department of Cell and Molecular Biology, Uppsala University, Husargatan 3 (Box 596), SE-751 24 Uppsala, Sweden.
Email: janos@xray.bmc.uu.se, mbogan@slac.stanford.edu

PROGRAM SCOPE

Our ultra-fast imaging program at PULSE is part of an international collaboration whose goal is to perform coherent X-ray imaging of non-periodic structures using X-ray Free Electron Lasers (XFELs), such as the Linac Coherent Light Source (LCLS). Coherent diffraction imaging overcomes the restrictions of limited-resolution X-ray lenses, offering a means to produce images of general non-crystalline objects at a resolution only limited in principle by the X-ray wavelength and by radiation-induced changes of the sample during exposure. The use of this imaging technique with X-ray pulses from an FEL will allow structures of biological and other materials to be determined at atomic resolution, with ultrafast time resolution and represent a breakthrough for many areas of science. While we are primarily motivated to image biological macromolecules, the general imaging techniques, diagnostics and optics, sample manipulation, and understanding of materials in intense X-ray fields, are of fundamental importance to ultrafast x-ray science and cut across all areas of research of the PULSE Center. We propose to continue development of the high-resolution imaging techniques with emphasis on imaging single cells, nanomaterials and viruses in the first period. We also plan to undertake time-resolved imaging studies of the LCLS-matter interaction, investigate the fundamentals of biological sample manipulation to enable substrate-free imaging and other diagnostics, and perform LCLS imaging of aligned nanoparticles.

Coherent diffraction imaging is elegant in its experimental simplicity: a coherent x-ray beam illuminates the sample and the far-field diffraction pattern of the object is recorded on an area detector. These measured diffraction intensities are proportional to the modulus squared of the Fourier transform of the wave exiting the object. An inversion of the diffraction pattern to an image in real space requires the retrieval of the phases of the diffraction pattern. This can be achieved by iterative transform algorithms if the object is isolated and the diffraction pattern intensities are adequately sampled (an approach known as oversampling). Our shrinkwrap algorithm is particularly robust and practical. The algorithm reconstructs images ab initio which overcomes the difficulty of requiring knowledge of the high-resolution shape of the diffracting object. This lensless imaging technique can be scaled all the way to atomic resolution, but in practice the resolution of the image of a single object is restricted by x-ray damage to the sample.

With a quasi-continuous synchrotron source it should be possible to image frozen biological cells to a resolution of about 10 nm, and perhaps 1 nm for radiation-tolerant inorganic materials. Ultrashort hard X-ray pulses from LCLS offer a means of vastly increasing the dose that can be applied to a specimen before damage effects the measurement. Simulations based on molecular dynamics and hydrodynamic models indicate that a few Ångström resolution could be achieved in single pulse X-ray diffraction experiments. The success of the technique requires the scattering measurement to be completed before the X-ray ionized protein undergoes a Coulomb explosion.

Achieving the goal of coherent diffractive imaging of a single particle requires extensive technical and theoretical advances. This will be achieved through a combination of simulation and experiments. The experiments will be carried out at synchrotron sources, the currently operational soft-X-ray FEL at DESY called FLASH, and the LCLS as it becomes operational in 2009. Our technical experience in coherent imaging experiments and FLASH results currently guide the development of the coherent X-ray imaging (CXI) endstation at LCLS as well as other experiments where high-resolution structural information is acquired. The theoretical models and simulations of the interaction of particles in intense XFEL beams will be compared and tested with short-pulse coherent imaging, holographic, and scattering experiments at FLASH and eventually the LCLS. This program will be complemented with the experimental investigation of aerosol nano-engineering methods and nanoscale template

design to deliver encapsulated biomolecules to the FEL and optimize diffraction pattern acquisition. A third component of the project is the development of laser alignment of molecules and particles using intense near-IR lasers which will be done in conjunction with other efforts in the Center.

RECENT PROGRESS

Our main focus has been continuing our program of coherent diffraction imaging at FLASH. We have produced rapid innovations of imaging instrumentation that have defined unforeseen new classes of imaging experiments. We continue to establish the modeling, simulations, and image reconstruction algorithms necessary for a robust imaging program. We succeeded in testing a second prototype single-particle injector system, co-designed by current PULSE staff, to place single cells and various nanoparticles in the path of the FEL beam, and collected diffraction patterns from which the objects could be reconstructed. We performed the first ultrafast optical pump-FEL probe experiments and helped implement a new form of pump-probe experiment called time-delay X-ray holography. Below is a subset of recent results.

Femtosecond time-delay X-ray holography to monitor sample explosion: Conventional time-resolved optical methods require highly synchronized photon pulses to initiate a transition and then probe it at a precisely defined time delay. In the X-ray regime, these methods are challenging since they require complex optical systems and diagnostics. We have helped develop a holographic measurement scheme, inspired by Newton's "dusty mirror" experiment to monitor the X-ray-induced explosion of microscopic objects. The time delay is encoded in the diffraction pattern to an accuracy of better than one femtosecond, and the sample depth is holographically recorded to sub-wavelength accuracy. We applied this technique to follow the X-ray induced explosion of a sample irradiated by an intense pulse from FLASH, and observed that sample explosion occurs picoseconds after the femtosecond X-ray pulse traversed the sample. By varying the distance between the reflecting multilayer and the object, different time delays can be set (a new sample is needed for each shot). The current time resolution of this holographic diffraction method is better than one femtosecond. These results gave the first glimpses into early steps of plasma formation by X-rays.

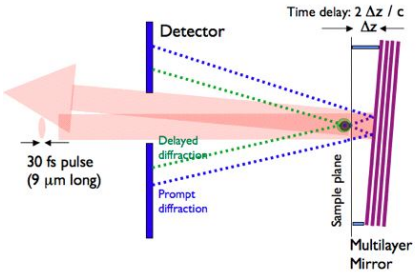

Fig 1. Schematic of a femtosecond time-delay x-ray holography experiment

Ultrafast single-shot diffraction imaging of nanoscale dynamics - Studies on light-induced periodic structures: Optical pump and FEL probe experiments were used to follow laser-induced structural changes in a silicon nitride membrane, into which a small pattern was etched. For each shot, a new sample was used. The diffraction patterns show measured single shot X-ray patterns at 10, 15, 20, 40, and 140 ps after irradiation with an excitation laser pulse at optical frequencies. Immediately visible is the loss of information at high scattering angles, corresponding to loss of mesoscale order as the sample disintegrates due to the laser pulse. At the same time, new structure is induced in the silicon nitride material by the excitation photon pulse. The evolution of this structure produces additional speckles, primarily in the direction of the pump laser polarisation. Additionally, a pair of strong diffraction peaks emerged at longer delays, indicative of a light-induced periodic structure in the foil. Each image was also reconstructed, enabling high spatial and temporal resolution visualization of the dynamics of the nanoscale object. We plan to extend this technique to near atomic resolution using LCLS.

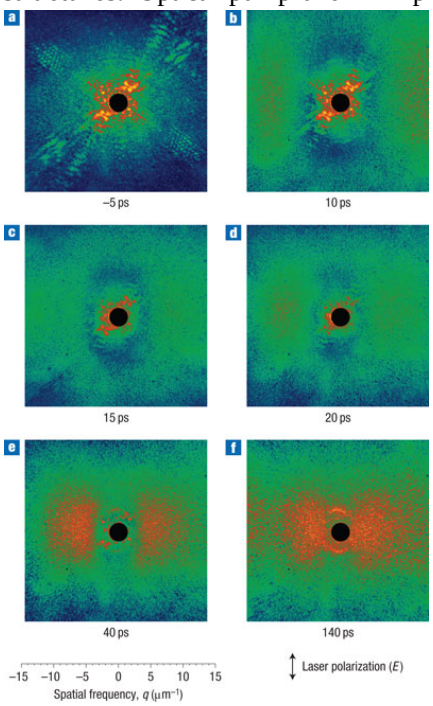

Fig 2 a–f, Measured single-shot diffraction patterns at –5 ps (a), the object just before the laser pulse, and diffraction patterns from the same object at 10 ps (b), 15 ps (c), 20 ps (d), 40 ps (e) and 140 ps (f) after the laser pulse. Gradual

Single Particle X-ray Diffractive Imaging – Sugar encapsulated DNA injected into the FEL pulse: When the number of atoms in a substrate becomes much larger than the number of atoms in the supported sample itself, such as in the case of isolated biomolecules on a membrane, the background signal is expected to dominate the CCD detector. This motivates the development of sample handling systems free of supporting membranes, such as particle beams, for introducing particles and biomolecules into the X-ray beam. We have demonstrated for the first time that particles can be injected into the FEL beam 'on the fly' to perform substrate-free imaging. We used electrospray-based aerosol nano-engineering to create hybrid particles composed of a megadalton DNA complex encapsulated by sucrose. To deliver the particles into the FEL we used an aerodynamic lens system designed and tested at LLNL that can create narrow particle beams of a wide range of particle sizes (1 nm to 10 μm). We demonstrated an imaging resolution of better than 40 nm by diffractive imaging with the single X-ray pulse and further characterized the interaction by mass spectrometry. In the example above, two particles were hit by a single FEL pulse. The structure of the two particles was reconstructed from this pattern and showed that the two particles were in contact and had likely agglomerated during the particle injection process. This method can be used to image any aerosol particles created at atmospheric pressure.

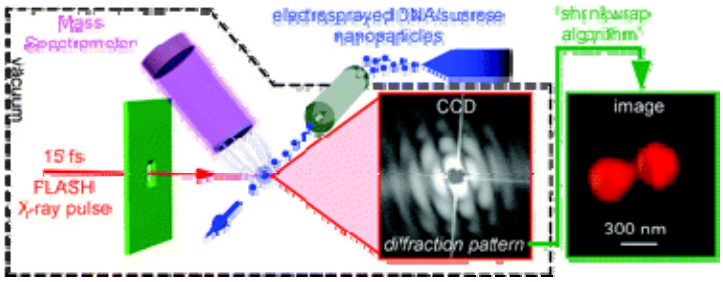

First diffraction experiments on live cells injected into the FEL pulse: We have successfully injected live picoplankton and other cells into the FEL beam under conditions where they were alive. The quality of the diffraction patterns permits reconstruction, and the reconstructed images show no signs of damage (work in progress, manuscripts in preparation). We intend to drive these experiments to near atomic resolutions when short wavelength FEL pulses become available from the LCLS. Picoplankton samples used in the present studies came from fresh water lakes and from the Arctic and Antarctic Polar Oceans where we have a research programme on photosynthetic carbon fixation by picoplankton. We have also studied marine viruses. Viruses are eminently suitable for first experiments on reproducible samples in biology; they are big and can give rise to strong diffraction patterns. We proposed to use viruses for first LCLS experiments (*LCLS - The First Experiments*, 2000). This work has now started at FLASH where we have successfully obtained the very first diffraction patterns from live marine viruses. These viruses were chosen because they infect the picoplankton that we study. The combined system will give us the opportunity to follow the infection process later. We electrosprayed virus particles into the FEL beam, and collected single shot diffraction images. The diffraction signal is strong and reasonably clean. Initial attempts at image reconstruction gave surprisingly good results (work in progress).

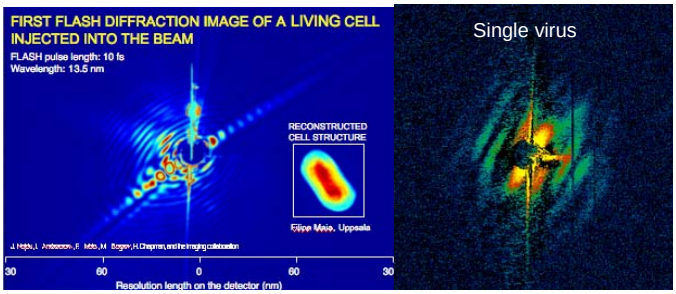

Fig 4. Single-pulse diffraction patterns and example reconstruction of single living marine microorganisms injected into the FLASH beam

FUTURE PLANS

Expected Progress in FY2009: We will continue our efforts at FLASH and plan to perform the first single particle x-ray diffractive imaging experiments at LCLS in mid-2009. We will utilize our experience from FLASH and work in conjunction with LCLS staff to design the LCLS CXI instrument. We will continue to develop the particle beam generation and diagnostics instrumentation necessary to perform any experiments utilizing laser interactions with single particles. We plan to recruit, train, and retain outstanding young talent necessary to support the rapidly growing coherent diffraction imaging of non-periodic structures program at PULSE.

Expected Progress in FY2010: Our efforts will concentrate on completing, commissioning and performing first experiments on single particles and biomolecules on LCLS. We will also provide the

scientific conduit to any imaging experiments at the CXI other end stations. We will interface with beamline/end station scientists and users/collaborators to ensure highly successful experimental campaigns at LCLS.

COLLABORATIONS: This work is done with colleagues from Uppsala, LLNL, SLAC, LBNL, Berlin, and DESY (Hamburg).

Selected Publications from DOE sponsored research in 2007-2008

1. Marchesini, S.; Boutet, S.; Sakdinawat, A.; Bogan, M.; *et al.*: Massively parallel fourier transform X-ray holography, ***Nature Photonics,* 2008**, in press.
2. Benner, W; Bogan, M.; *et al.:* Nondestructive characterization and alignment of aerodynamically focused particle beams by single particle charge detection, ***J. Aerosol Sci.,* 2008**, in press.
3. Boutet, S; Bogan, M.; *et al.:* Ultrafast soft x-ray scattering of spherical polystyrene nanoparticles, ***J. Electron Spectrosc. Rel. Phenom.,* 2008**, in press.
4. Barty, A., Boutet, S., Bogan, M.J., *et al.:* Ultrafast single-shot diffraction imaging of nanoscale dynamics. ***Nature Photonics*, 2008,** 2, 415-419.
5. Hajdu, J., Maia, F.: Clarity through a keyhole. ***Nature Physics,* 2008,** 4, 351-353.
6. Bogan M., *et al.*: Single particle X-ray diffractive imaging. ***Nano Letters,* 2008,** 8, 310-316.
7. Bajt, S., Chapman, H., Spiller, E. *et al.*: A camera for coherent diffractive imaging and holography with a soft-X-ray free electron laser. ***Applied Optics,* 2008,** 47, 1673-1683.
8. Gabrysch, M., Marklund, E., Hajdu, J., et al.: Formation of secondary electron cascades in single-crystalline plasma-deposited diamond upon exposure to femtosecond x-ray pulses, ***J. Appl. Phys.,* 2008**, 103, 064909.
9. Andersson I. *et al* Structure and function of Rubisco.***Plant Physiol. Biochem,* 2008,** 46, 275-291.
10. Andersson, I. Catalysis and regulation in Rubisco. ***J. Exp. Bot.,* 2008,** 59, 1555-1558.
11. H.N. Chapman, S.P. Hau-Riege, M. Bogan, *et al.:* Femtosecond time-delay X-ray holography. ***Nature,* 2007,** 448, 676–679.
12. Bogan, M, Benner, H., *et al.* "Aerosol sample preparation methods for X-ray diffractive imaging: Size-selected nanoparticles on silicon nitride foils," ***J. Aerosol Sci.,* 2007,** 38, 1119-1128.
13. S.P. Hau-Riege, H.N. Chapman, J. Krzywinski, *et al.* "Interaction of nanometer-scale multilayer structures with x-ray free-electron laser pulses," ***Phys Rev. Lett.,* 2007,** 98 145502.
14. Bogan, M.; Benner, WH.; Frank, M.; Chapman, HN.; Woods B.; Boutet, S.; Hajdu, J. "Method and apparatus for x-ray imaging of free nanoscale biomaterials" Record of Invention: **2007**.
15. Hau-Riege, S.; London, R.; Bogan, M. *et al.* "Damage-resistant single-pulse optics for x-ray free electron lasers", Damage to VUV, EUV, and X-ray Optics, Proc. SPIE Vol. 6586, 65860T, **2007**.
16. K. Gaffney and H.N. Chapman, "Imaging Atomic Structure and Dynamics with Ultrafast X-ray Scattering," ***Science,* 2007,** 316, 1444-1448.
17. Dey A, Francis EJ, Adams MWW, et al., Solvent tuning of electrochemical potentials in the active sites of HiPIP versus ferredoxin, ***Science,* 2007,** 318, 1464-1468.
18. D. M. Fritz, D. A. Reis, B. Adams, *et al.* Ultrafast Bond Softening in Bismuth: Mapping a Solid's Interatomic Potential with X-rays. ***Science,* 2007,** 315, 633 – 636.
19. P. B. Hillyard, K. J. Gaffney, A. M. Lindenberg, *et al.* Carrier-Density-Dependent Lattice Stability in InSb. ***Phys. Rev. Letts.,* 2007,** 98, Art. No. 125501.
20. J. Chalupsky, L. Juha, J. Cihelka, *et al.* Characteristics of focused soft X-ray free-electron laser beam determined by ablation of organic molecular solids. ***Optics Express*, 2007,** 15, 6036-6043.
21. Cramer, J.F., Nordberg, P.A., Hajdu, J. *et al.* Crystal structure of a bacterial albumin-binding domain at 1.4 angstrom resolution. ***FEBS Letts.,* 2007,** 581, 3178-3182.
22. Cicero, G., Carbonera, C., Valegård, K. *et al.* Study of the Oxidative Half-Reaction Catalyzed by a Non-Heme Ferrous Catalytic Center by Means of Structural and Computational Methodologies. ***Int. J. Quant. Chem,* 2007,**. 107, 1514–1522.
23. Szoke, A., van der Spoel, D., Hajdu, J.: Energy Utilization, Catalysis and Evolution - Emergent Properties of Life. ***Current Chemical Biology,* 2007,** 1, 53-57.
24. Karkehabadi, S., Satopagan, S., Taylor, T. C., *et al.* Structural analysis of altered large-subunit loop-6/carboxy-terminus interactions that influence catalytic efficiency and CO_2/O_2 specificity of ribulose 1,5-bisphosphate carboxylase/oxygenase. ***Biochemistry,* 2007,** 46, 11080-11089.
25. S.P. Hau-Riege, R.A. London, H.N. Chapman *et al.* "Methods to reduce the effect of damage in x-ray diffraction imaging of single biological molecules," ***Phys. Rev. Lett.,* 2007**, 98, 198302.

PULSE Task E.3.a: High harmonic generation in molecules

Markus Gühr and Philip H. Bucksbaum
Stanford PULSE Institute, Stanford Linear Accelerator Center, Menlo Park, CA 94025
and
Physics Department, Stanford University, Stanford, CA 94305

Scope

The goal of this project is the understanding of high harmonic generation (HHG) in molecules. We explore not only the amplitude of the emitted light but also its phase by applying interferometric techniques. We find multiple orbital contributions to HHG in N_2. Not only the highest occupied molecular orbital (HOMO) contributes to HHG but also a lower bound HOMO-1 orbital. This opens the way for molecular electronic dynamics imaging with sub-angstrom precision on a sub-femtosecond time scale.

Recent Progress

B. K. McFarland, J. P. Farrell, P. H. Bucksbaum and Markus Gühr

a) Phase measurements in N_2 molecules and Ar atoms

In the three step model of high harmonic generation (HHG) [1,2], a portion of the highest occupied orbital of an atom or molecule tunnels into the continuum and is accelerated in a strong oscillating optical field. This continuum part of the wave function is treated as a free electron wave packet which interferes coherently with the bound part of the highest occupied orbital when it returns to the molecule, thus creating a time varying dipole that radiates the harmonic light.
Depending on the orbital symmetry, characteristic maxima or minima appear in the harmonic spectrum due to interference effects, whereas the minimum is accompanied by a phase jump. Amplitude minima are known from the reverse process of photoelectron emission [3] whereas the phase jumps in the harmonic light have been predicted recently for atoms [4] and molecules [5]. In particular, a π phase jump has been predicted at the harmonic with minimal amplitude of the H_2 molecule.

We measured the relative phase between the harmonics emitted by N_2 and Ar. We mixed Ar with N_2 in a ratio of 1:1 and expanded it out of a small nozzle to reach a vibrational cooling for N_2. An ultrashort laser pulse from a Ti:Sapphire amplifier interacts with the anisotropic polarizability of N_2 molecules in a supersonic jet and creates a rotational wave packet that results in molecular alignment at wave packet revivals. At 4.1 ps after the alignment pulse, the molecular ensemble is aligned along the pulse polarization with a prolate distribution and a second laser pulse with a higher intensity generates high harmonics in the aligned molecules. The HHG beam passes through a thin Al filter and aperture which reject the fundamental as well as harmonics from long electron trajectories. The remaining harmonics are dispersed by a flat-field grating and detected by a MCP-phosphor screen unit. The intensity I_{mix} for a particular harmonic is given by

$$Imix = p_{Ar} I_{Ar} + p_{N2} I_{N2} + 2 (p_{Ar} p_{N2} I_{Ar} I_{N2})^{1/2} \cos\varphi, \qquad (1)$$

where p_{Ar}, p_{N2} are the partial pressures of the respective species and I_{Ar}, I_{N2} their respective intensities. Perfoming experiments with the pure gases at the partial pressures and with the gas mixtures allows for the determination of the relative phase between the Ar and N_2 harmonic from harmonic intensities.

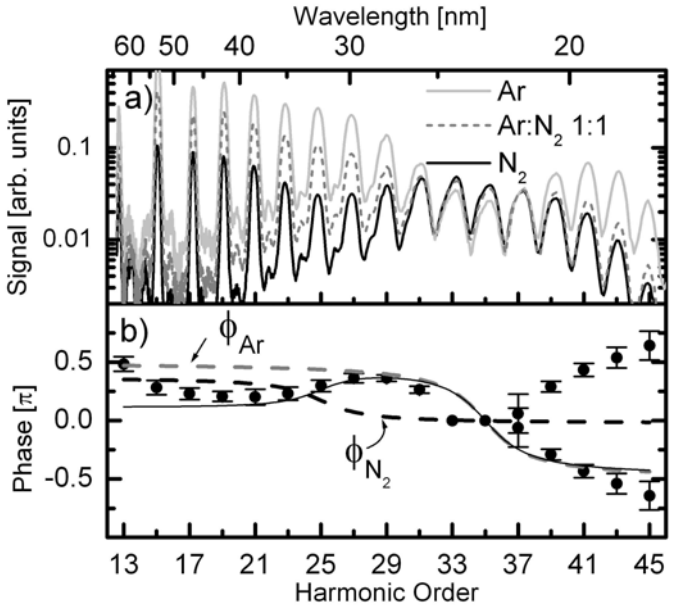

Figure 1: a) High harmonic spectra for Ar (light grey), N2 (black) and a 1:1 mixture of both (dashed grey) from harmonic 13 to 45. Applying Eq. 1 leads to the relative phase plotted as the solid circles in b). For harmonics larger than the 35th the phase is also plotted negative (see text). We decompose the relative phase into phase components of Ar and N2 by fitting it as a sum of two atan functions. The curve for Ar (grey dashed) shows a phase jump of π at harmonic 35, the fit for N2 shows a phase jump of 0.4 π centred around harmonic 25.

Figure 1 a) shows the measured harmonic intensities for pure Ar (solid grey), pure N_2 (solid black) and the 1:1 mixture (dashed grey). From the intensities, we deduce the relative phase plotted as the circles in Fig. 1b). The sign of the phase is not determined since it's the argument of the even cos function in Eq. 1. Since we expect a phase jump at the 35th harmonic for Ar, we plot the phase negative for higher harmonics. The phase jump for Ar is expected at the minimum of the spectrum, lying at harmonic 35. The N2 minimum lies at harmonic 25. Since the expected positions of the phase jumps are well separated, we decompose the relative phase in Ar and N_2 contributions. We fit the relative phase by a sum of two atan functions, one for Ar (dashed grey) and a second for N_2 (dashed black). The sum is given as the solid black line and fits the relative phase well. The magnitude of the Ar phase jump at the 35th harmonic is π in agreement with the expectations from the literature, it reflects a sign change of the transition dipole. The phase jump of N_2 around the 25th harmonic is 0.4 π, which does not agree with the prediction for a simple H_2 molecule [5]. However, the actual molecular axis distribution needs to be taken into account in the model, which can pissibly reduce the theoretical phase shift.

b) High harmonic generation from multiple orbitals

Tomographic imaging of molecules using high harmonic generation has attracted wide interest since its inception [6]. The high temporal and spatial resolution of the method may enable ultrafast movies of molecular orbital dynamics; however to date, only stationary highest occupied molecular orbital (HOMO) states have been imaged. Observing electron dynamics would require the participation of multiple stationary states in HHG. We find first direct experimental evidence for the participation of more deeply bound electrons in the HHG process.

We excite a rotational wave packet leading to field free alignment as above under a). The evolving molecular ensemble of N_2 takes a prolate shape after 4.1 ps and an oblate shape after 4.3 ps (see top of Fig. 2a). The generation laser pulse is polarized orthogonally to the generation polarization, denoted on top of Fig. 2a). For the lower harmonics from 15-25, the harmonic intensity is weak at 4.1 ps, when most of the molecules are standing parallel to the generation polarization. At 4.3 ps, when some molecules of the oblate ensemble are standing parallel to the generation polarization, the signal is strengthened. We analyze the signal with the help of the orbital shape. Figure 2b) shows the orbital shape of the HOMO and HOMO-1 with respect to the

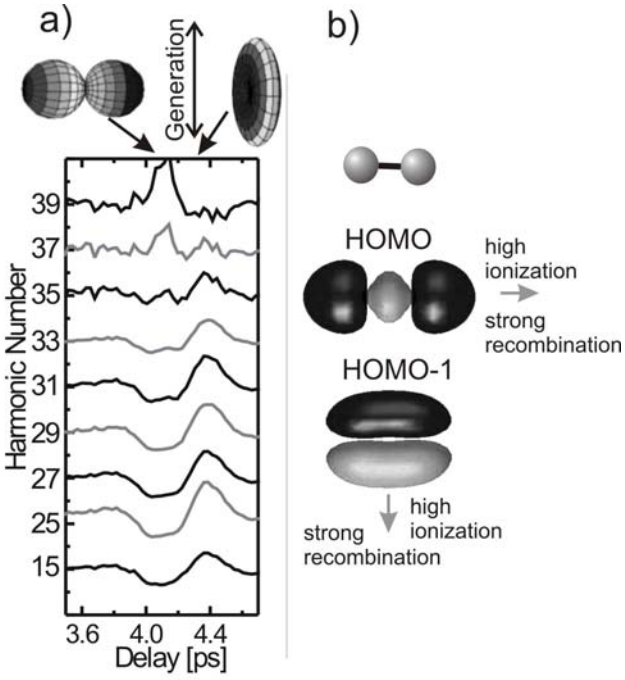

Figure 2: a) Top: Shapes of the aligned molecular ensemble with respect to the generation polarization at 4.1 and 4.3 ps after the alignment pulse. Below: Harmonic signals from 15 to 39 for a generation laser intensity of 2.3×10^{14} W/cm^2. The signal suppression at 4.1 ps for low harmonics turns into an enhancement at the higher harmonics. The harmonic signals are normalized on the unaligned ensemble. b) Shape of the HOMO and next lower bound HOMO-1 of N_2. Tunnelling ionization and the recombination dipole are strong parallel to the internuclear axis for the HOMO and perpendicular to it for the HOMO-1.

internuclear axis. The first step of HHG, namely the tunnelling ionization, is sensitive on the parts of the wave function being far away from the nuclei [7]. The HOMO extends far out from the nuclei in the direction parallel to the internuclear axis and will therefore ionize easily if the field is polarized in that direction. Recombination to the HOMO gives rise to a large dipole since the expectation value of d=er can vary all along the long axis of the HOMO. This explains the signal enhancement at 4.3 ps, when some of the molecules are standing parallel to the generation laser polarization. If the electric field of the generation laser is polarized perpendicular to the molecular axis, the HOMO gives rise to a reduced signal because of reduced tunnelling ionization and recombination in the squeezed direction of the orbital. We thus associate the features at harmonics 15-25 to HHG from the HOMO.

For harmonics 25 and greater a peak grows out of the minimum at 4.1 ps and the revival character seen in the lower harmonics begins to vanish with increasing harmonic order. This transformation is most pronounced in the cut off at harmonic 39 where the revival structure is inverted compared to harmonic 15, resulting in a peak at 4.1 ps for perpendicular HHG laser polarization and molecular alignment and a slight minimum at 4.3 ps for molecules aligned in the oblate shape. The peak is indicative of HHG from the HOMO-1 since both ionization and recombination are stronger for the molecular ensemble oriented 90° to the HHG laser polarization than for the HOMO. The HOMO-1 extends much further out than the HOMO in the direction perpendicular to the internuclear axis. The revival structures in harmonics 25-35 show attributes of both HOMO and HOMO-1 harmonic generation where the HOMO contribution is strongest for the low harmonics and the contribution from the HOMO-1 becomes prominent in the high harmonics.

Future Plans

M. Gühr and P. H. Bucksbaum

a) Chemical imaging

Electron dynamics involves several coherently coupled electronic states. As shown above, we can now monitor several electronic orbitals of a molecule and thus have access to electronic dynamics with a high temporal resolution due to the sub-cycle timescale of HHG and a high spatial resolution determined by the shortest de Broglie wavelength of the recolliding electron wave packet.

We plan to use this ability to look at coherently coupled orbitals where the coupling is either introduced during HHG or by a different laser pulse that is advanced in time. Of special importance in this context are so called conical intersections (CI) [8]. The conical intersections are crucial for biological processes such as light harvesting, primary visual processes and UV stabilization of DNA and for chemical processes in the earth's atmosphere. A wave packet excited by an ultrafast laser pulse explores the potential landscape of the excited state and reaches the conical intersection, where it can change its electronic state very quickly. We want to monitor this multiple state electronic dynamics using high harmonic generation on the photoexcited molecules.

Apart from this, we also want to utilize our knowledge of molecular HHG and our expertise in measuring the harmonic phase for attosecond pulse shaping. The interferences between returning electron wave and molecular electronic states shape the amplitude and phase of the harmonics, which in case of a few cycle laser pulses unite to one attosecond pulse.

References

[1] P. B. Corkum, Phys. Rev. Lett., **71**, 1994 (1993)
[2] J. L. Krause, K. J. Schafer, and K. C. Kulander, Phys. Rev. Lett., **68**, 3535 (1992)
[3] J. W.Cooper, Phys. Rev., **128**, 681 (1962)
[4] J. 4, M. B. Gaarde, K. J. Schafer, Phys. Rev. A, **72**, 013401 (2005)
[5] M. Lein *et al.*, Phys. Rev. A, **66**, 023805 (2002)
[6] J. Itatani *et al.*, Nature, **432**, 867, (2004)
[7] X. M. Tong and Z. X. Zhao and C. D. Lin, Phys. Rev. A, **66**, 33402 (2002)
[8] D. R. Yakorny, J. Phys. Chem. A, **105**, 6277, (2001)

Publications and Conference Contributions

1) M. Gühr, B. K. McFarland, J. P. Farrell and P. H. Bucksbaum, High harmonic generation on N2 and CO_2 beyond the two point model, J. Phys. B: At. Mol. Opt. Phys., **40**, 3745-3755 (2007)
2) M. Gühr, Coherent Dynamics of Halogen Molecules in Rare Gas Solids, in Coherent Vibrational Dynamics, Eds.: S. DeSilvestri, G. Cerullo and G. Lanzani, Taylor and Francis 2008
3) M. Gühr, M. Bargheer, M. Fushitani, T. Kiljunen and N. Schwentner, Ultrafast dynamics of halogens in rare gas solids, Phys. Chem. Chem. Phys, **9**, 779-801, (2007)
4) Philip Bucksbaum, The future of attosecond spectroscopy, Science **317**, 766 (2007)
5) M. Gühr, B. K. McFarland, J.P. Farrell and P. H. Bucksbaum, High harmonic generation from multiple molecular orbitals of N2, Ultrafast Phenomena XVI, Springer 2008
6) B. K. McFarland, J.P. Farrell, P. H. Bucksbaum and Markus Gühr, High Harmonic Generation from multiple orbitals, submitted 2008

PULSE Task E.3.b: Laser Control of Molecular Alignment and Bond Strength

Philip H. Bucksbaum and Ryan N. Coffee
Stanford PULSE Center, Stanford Linear Accelerator Center, Menlo Park, CA 94025

Scope:
This project investigates coherent processes in atoms and molecules that are of value as either LCLS experiments or ultrafast x-ray diagnostics. One of our immediate goals is to obtain and study ro-vibrational control in small molecules in preparation for one of the first experiments in the AMO hutch of the LCLS. This LCLS experiment will focus on the laser induced alignment of molecular gases at densities conducive to x-ray absorption and scattering. To enhance this effort, we are currently in collaboration with LBNL and CEA Saclay to investigate angle resolved soft x-ray absorption and photo-electron spectroscopy. In the VUV regime, we are pursuing selective nonlinear absorbers as a possible means for LCLS beam conditioning. We are currently collaborating with the PULSE E2a project to use the HHG source as a probe of ultrafast resonant EIT. Also, in collaboration with project E2a, we are pursuing the natural molecular alignment produced in a poled polymer environment. We have performed preliminary x-ray scattering experiments and plan to use the scheme for studying chemical dynamics via time-resolved x-ray scattering at the LCLS.

Recent Progress:

Molecular Alignment
Doug Broege. James Cryan, Ryan N. Coffee, and Phil H. Bucksbaum

We investigated impulsive laser alignment of molecular iodine at a density of ~10^{18} molecules/cm^3 and a temperature of 120 C using a 1.5 mJ 40 fs 800 nm laser system [1]. In this experiment, we split the 1.5mJ beam into two arms. One arm is sent through a 250mm BBO crystal and produces ~20uJ of 400nm light. A polarizer ensures that this beam is horizontally polarized. The other arm serves as the laser alignment pulse. The alignment arm is polarization rotated to 45 degrees to the horizontal. This induces a transient birefringence in the gas cell. We observe this transient birefringence by measuring the amount of 400 nm light exiting the cell with vertical polarization. In Figure 1 we show the half- and full-revivals for iodine. The oscillatory signal is due to the strong effect of centrifugal distortion that exists for such a thermally hot ensemble of rotors.

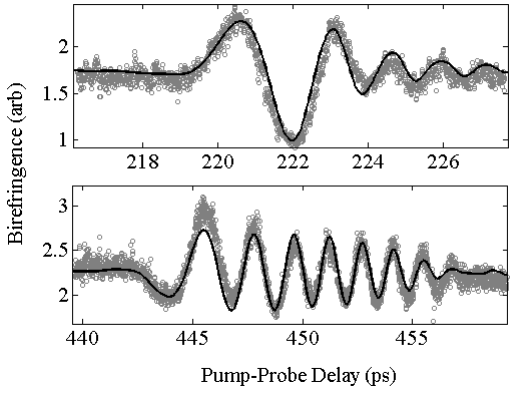

Figure 1Transient birefringence I2 following impulsive excitation with 800 nm, 40 fs pulses. Data are represented by gray circles and the semi-classical simulation is represented by the solid line.

We have also begun a program to produce and detect impulsive molecular alignment *along* the direction of laser propagation. We have constructed an interferometric technique that is capable of detecting molecular alignment in a gas cell that does *not* produce a birefringence signal. This technique is run in parallel to the previously developed birefringence technique of Ref. [1] and allows us to measure and distinguish molecular alignment along any of the lab-fixed directions with only one, co-propagating, probe beam. This experiment is nearing completion. Upon final development of this technique, it will be used to produce laser aligned molecules at the LCLS where the alignment axis can be switched in real time from X to Y to Z for scattering experiments.

We have recently purchased and installed a 3.5 mJ 35fs laser amplifier in the E2b lab in building 130 at SLAC. in this lab we are currently constructing a pulse stacking scheme that will be used for improved molecular alignment by a train of off resonant pulses. We are working to develop a 16 pulse analog of Ref [4] for use in a proposed LCLS experiment that aims to measure the angular distribution for photo-electrons by measuring many PE events per shot for lab-fixed molecules (see below).

XFEL Cleaning with EIT
Mike Glownia, Markus Guehr, Hamed Merdji, Ryan N. Coffee and Phil H. Bucksbaum

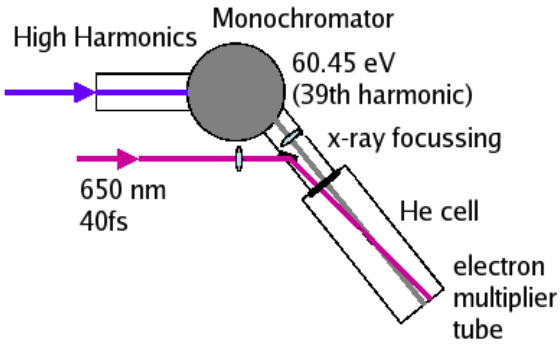

Figure 2 Use of the E2a HHG beam, monochromatized, for EIT in He.

We are currently pursuing electromagnetically induced transparency (EIT) in atomic He. We will conduct a proof of principle experiment using an existing high harmonic light source of sub-task E2a to evaluate the scalability to high intensity and hard x-ray sources such the LCLS. A new multi-pass amplifier is currently under construction in the E2a lab in Varian Physics. Upon completion of the multi-pass we will construct a high power visible NOPA to pump the EIT system on resonance. We will then investigate the effects of driving the transparency with strong resonant fields, with strong fields detuned from resonance, and with driving fields that have a shorter duration than the probe pulse. This last test is in the spirit of cleaning the LCLS pulses that span many tens of femtoseconds with a ~10fs EIT field gas in a cell.

I_3^- in polymer matrix – joint with E2a,.
Limor Spector, Ryan Coffee, Markus Guehr, David Reis (University of Michigan), Phil Bucksbaum

In this study, we will combine ultrafast x-ray measurements with femtosecond pump-

probe spectroscopy of I_3^- embedded in a polymer matrix. The tri-iodide molecule is a prototypical reactive system for photoinduced fragmentation. I_3^- is particularly interesting because its gas and condensed phase photofragmentation differ dramatically. This makes the system well-suited for a study of the effects of the environment in photochemistry. For the case of x-ray diffraction, I_3^- has several advantages. Low frequency motions are well-suited to the anticipated x-ray pulse durations. A large number of electrons in the iodine atomic core enhances the x-ray scattering signal and provides a high contrast between the chromophore and the surrounding polymer matrix. Finally, this system provides an opportunity for a high density of isolated and aligned chromophores, in which alignment is achieved simply by stretching the polymer.

In a recent run on the SPEAR3 Beamline 11.3 WAXS instrument, we investigated both liquid and polymer solutions of the I_3^- anion in preparation for hard x-ray scattering of polymer based aligned molecular systems.

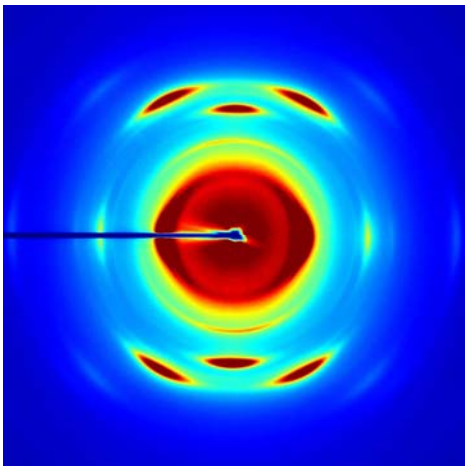

Figure 3 Typical WAXS image of I_3^- doped to 333mM concentration in a stretched PVDF polymer.

Future Prospects:

Angle Resolved photo-electron Spectroscopy of Aligned Molecules
Hamed Merdji, Ryan N. Coffee, and Phil H. Bucksbaum
We are working in collaboration with the group of Hamed Merdji from Saclay and Ali Belkacem from (LBNL) to perform angle resolved photo-electron spectroscopy to image the electron orbitals of simple molecules. This experiment will serve as a preliminary experiment for the angle resolved photo-electron spectroscopy experiment we are currently proposing for the initial phase of the LCLS.

An LCLS Proposal
Ryan Coffee, John Bozek, Linda Young, Robin Santra, Christian Buth, Steve Southworth, Nora Berrah, Lou DiMauro, Ali Belkacem, Marcus Hertein, Hamed Merdji, Markus guehr, Janos Hajdu, and Phil Bucksbaum

The goal of this proposal is to develop laser alignment techniques for molecular gas-phase experiments at LCLS. The ability to spatially align target molecules provides benefits for x-ray-based techniques such as (a) measurement of photoelectron angular

distributions with respect to the molecular frame and (b) electronically elastic x-ray diffraction. The advantage of laser alignment in both cases lies in the suppression of rotational averaging. While (b) is sensitive to molecular geometry, (a) is sensitive to the molecular electronic structure as well its configuration.

LCLS is the first x-ray source that will allow one to exploit impulsive alignment for gas-phase x-ray applications. Transient alignment persists for a time that is prohibitively short for the x-ray pulses available at third-generation synchrotron sources . In order to take x-ray snapshots of transiently aligned molecules, a pulse duration of 1 ps or shorter is required. Currently, the only synchrotron-based sources that provide such short pulses exploit laser slicing. However, gas-phase experiments using slicing sources are generally photon-starved. At LCLS, we will have ~10^{13} photons per pulse at a repetition rate of 120 Hz, making it feasible to measure photoelectron angular distributions for transiently aligned molecules.

Wave-packet interferometry
James Cryan, Ryan N. Coffee and Phil H. Bucksbaum

An amplitude shaped visible spectrum NOPA is currently under construction in the E2b lab in building 130 at SLAC. This NOPA will be used to perform molecular wave-packet interferometry (WPI) in systems where de-coherence or dissociation prohibit the more traditional WPI technique of Ref. [5] by using pulses separated in frequency rather than time. It has been shown that WPI can be used to completely reconstruct both the amplitude and the phase of a molecular vibrational wave-packet. This new scheme would allow the reconstruction of dissociating wave-packets or those with fast decoherence. Although the initial experiment will use white light absorption as a probe to prove the principle, the ultimate goal is to use the hard x-ray end station of the LCLS as a probe.

Recent Publications and Conference Abstracts
[1] Broege, D.W. and Coffee, R.N. and Bucksbaum, P.H., *Strong-field impulsive alignment in the presence of high temperatures and large centrifugal distortion*, Phys. Rev. A, in review, (2008)

[2]. Douglas W. Broege, Ryan N. Coffee, Phil H. Bucksbaum, "*Impulsive Alignment of Hot, Centrifugally Distorted Molecules*," CLEO Abstract CWA4, 2008.

[3]. Douglas Broege, Ryan Coffee, Philip Bucksbaum, *"Strong field impulsive alignment in the presence of high temperatures and large centrifugal distortion,"* Bull. Am. Phys. Soc. **53**, No. 7, DAMOP Abstract: K6.00004 (2008), http://meetings.aps.org/Meeting/DAMOP08/Event/84874

References:
[4] Leibscher, M. and Averbukh, I. Sh. and Rabitz, H., *Molecular Alignment by Trains of Short Laser Pulses,* Phys. Rev. Lett. **90**, 213001, (2003)
[5] Jeffrey A. Cina, *Nonlinear wavepacket interferometry for polyatomic molecules,* J. Chem. Phys., **113,** 9488 (2000)

Structural Dynamics in Chemical Systems

Stanford Synchrotron Radiation Laboratory
Stanford Linear Accelerator Center

Principal Investigator

Kelly J. Gaffney, PULSE Institute, Photon Science, SLAC,
Stanford University, Menlo Park, CA 94025
Telephone: (650) 926-2382
Fax: (650) 926-4100
Email: kgaffney@slac.stanford.edu

I. Program Scope: The research funded by this grant will focus on understanding the fundamental structural and dynamical properties that influence light harvesting efficiency and solar energy conversion in photo-catalysis. A natural connection exists between ultrafast experimental techniques with sub-picosecond resolution and photochemical reactivity because the initial events in molecular light harvesting invariably occur on the ultrafast time scale. Acquiring a better understanding of the fundamental events that shape photochemical reaction mechanisms will assist in the acquisition of affordable and renewable energy sources.

Developing and utilizing ultrafast x-ray pulses for the study of chemical dynamics represents a core objective of this research program. Our efforts had focused on the Sub-Picosecond Pulse Source (SPPS), a linear accelerator derived femtosecond hard x-ray source at SLAC. With the decommissioning of the SPPS, our efforts turn to preparing for the arrival of the Linac Coherent Light Source (LCLS), an x-ray free electron laser being built at SLAC. These ultrafast x-ray studies will be complemented by ultrafast vibrational and electronic spectroscopic studies of electron transfer dynamics, as well as ground state x-ray absorption and emission studies of electronic structure. These combined efforts will address fundamental questions regarding the interplay of electronic and molecular structure and dynamics in electron transfer complexes.

The current research being conducting in my research group extends beyond the areas currently funded from DOE to the PULSE Institute. These efforts have been supported by non-DOE funding sources, and primarily have paid for postdoctoral and graduate student salaries. These additional funds have supplemented and utilized equipment purchased with DOE funding, and rely of SLAC infrastructure supported by DOE. **III.A.** in the **Scientific Progress Section**, represents the primary DOE supported activity in my research group.

II. Infrastructure development: The past year has seen significant development of the infrastructure necessary for conducting experimental studies of chemical dynamics at the Stanford Synchrotron Radiation Laboratory (SSRL) and the Stanford Linear Accelerator Center (SLAC). SLAC completed the laboratory space and building infrastructure for an ultrafast chemical dynamics laboratory in March 2007. During the past 18 months we have established two independent experiments based on a single Ti:sapphire regeneratively amplified femtosecond laser. One experiment uses tuneable UV/visible light to excite chemical dynamics, and probe these dynamics with white light. The other experiment is designed for multidimensional vibrational correlation spectroscopy, and for probing photochemical dynamics with vibrational spectroscopy. The first experimental set-up has just begun collecting preliminary data as the final stage of commissioning, while the vibrational spectroscopy experimental set-up is fully commissioned and we are currently writing our first paper on data collected with this system.

III. Scientific Progress: The successful achievement of the scientific objectives of the 'Structural Dynamics in Chemical Systems' grant requires the development of experimental techniques and tools applicable to a wide range of ultrafast x-ray science. The LCLS will produce intense

femtosecond x-ray pulses with a first harmonic upper energy range up to 8 keV, a narrow spectral width of ~20 eV FWHM, and limited frequency tuning capability in the beginning. All of these attributes make x-ray emission spectroscopy (XES), x-ray absorption near edge spectroscopy (XANES), and resonant inelastic x-ray scattering (RIXS) the preferred spectroscopic techniques for the LCLS. These techniques are ideally suited to studying electron transfer in organometallic compounds because they provide easily interpretable information about the oxidation state, spin multiplicity, and the local coordination of the metal centers in these complexes.

III.A. ***X-ray spectroscopy studies of electron dynamics in organometallic chemistry*****:** A key component of our research will be utilizing x-ray spectroscopy to probe the charge, spin, and covalency dynamics in photoexcited organometallic complexes. Organometallic structures catalyze a wide range of chemical reactions, most prominently in metallo-enzymes, but the time evolution of the electronic structure during photochemical reactions cannot be robustly determined with standard UV/visible spectroscopy. We have decided to emphasize manganese and iron based complexes given their prominence and diversity in metallo-enzymatic systems, as well as the compatibility of their x-ray absorption K-edges with the energy range of the LCLS.

This project has been focusing on two key developments. Firstly, the construction of an ultrafast laser system for probing photochemical dynamics with time resolved electronic and vibrational spectroscopy. As discussed in the **Infrastructure Development** section, we are finalizing the commissioning of the UV/visible pump-probe set-up with our first test experiment, and we have already begun collecting data with our ultrafast vibrational spectroscopy set-up. Secondly, developing the ability to perform and interpret x-ray emission and resonant inelastic x-ray scattering (RIXS) experiments. We have made significant progress in this area as well, having submitted our first x-ray spectroscopy manuscript in 2008.

Our initial RIXS studies have investigated $RbMnFe(CN)_6$, a model photoelectron transfer system for developing time resolved XES spectroscopy. $RbMnFe(CN)_6$ undergoes a thermal phase transition from the Mn^{2+}(S=5/2)-NC-Fe^{3+}(S=1/2) cubic high temperature (HT) phase to the Mn^{3+}(S=2)-NC-Fe^{2+}(S=0) tetragonal low temperature (LT) phase caused by the electron transfer between Mn to Fe and a Jahn-Teller distortion around the Mn^{3+} ion. The high temperature phase can also be transiently photo-excited to the high temperature phase well below the phase transition temperature. This photo-induced phase transition has been attributed to a metal-to-metal photoelectron transfer from Fe^{2+} to Mn^{3+}. We have chosen a solid state photoinduced phase transition sytem, rather than a solution phase chemical system, to investigate initially because it will optimize the concentration of excited states and consequently the transient changes in the XES spectrum. At the LCLS, where the laser coincident x-ray flux greatly exceeded that achievable at current synchrotrons, solution phase studies will be possible and we will be able to observe the time evolution of the spin multiplicity of photon induced spin crossover complexes.

We have completed our steady state XES and RIXS measurements of the high and low temperature phases in $RbMnFe(CN)_6$. This detailed characterization of the electronic structure in this compound paves the way for our studies of the photo-induced phase transition. to study the thermal phase transition, and will be initiating optical transient absorption measurements following the construction of our laser laboratory. The equilibrium and photoexcited phases have distinct spectra in the visible and the mid-IR, making these promising measurements that will effectively complement the time resolved x-ray studies. By combining a variety of time resolved techniques and methods, including time resolved powder diffraction, we have the potential to track structural and electronic degrees of freedom, making it possible to investigate their interdependence.

III.B. ***Vibrational spectroscopy studies of dynamics in ionic solutions*****:** Aqueous ionic solutions lubricate the chemical machinery of natural and biological systems and electrical energy storage devices currently rely on organic solvents with high concentrations of dissolved salts. We utilize time resolved vibrational spectroscopy to study the dynamics on these ionic solutions.

We initiated our investigations with aqueous sodium perchlorate solutions. In these studies we have utilized multidimensional vibrational correlation spectroscopy (MVCS) to study the exchange between water-water hydrogen bonds and water-ion hydrogen bonds. Aqueous perchlorate solutions have a hydroxyl stretch absorption spectrum that has a peak that originates from hydroxyl groups that donate a hydrogen bond to a perchlorate ion and a peak that originates from hydroxyl groups that donate a hydrogen bond to another water molecule. With MVCS we can characterize the dynamics of each of these sub-ensembles separately, as well as determine how quickly these sub-ensembles interconvert. These studies have demonstrated that water molecules equilibrate within there local hydrogen bond structure before exchanging hydrogen bond environments. We have established a collaboration with Micheal Odelius of Stocklholm University to conduct ab initio molecular dynamics simulations of the system aqueous sodium perchlorate. We are currently writing a manuscript describing our first results in this system.

III.C. ***Carrier dynamics in photovoltaic materials*****:** We have also initiated studies of carrier dynamics in photovoltaic systems. We have initiated collaborations with Professors Mike McGehee and Yi Cui at Stanford University to study carrier dynamics in organic and nano-structured inorganic semiconductors. Our initial studies have focused on determining the magnitude of the carrier multiplication that occurs in low band gap nanocrystalline materials when excited with UV light. If more than one exciton can be generated from a single UV photon this has significant potential to enhance the efficiency of photovoltaic devices. Klimov and Nozik have both reported high efficiencies, but these claims have been highly controversial. Our first goal has been to investigate the magnitude of the carrier multiplication by probing excitons with the excited state absorption in the mid-IR. This parallels work performed by Nozik, but we will be spectrally resolving the mid-IR signal. We believe this to be a critical aspect to the measurement, because prior investigations have shown that the mid-IR absorption depends upon the number of excitons present in a single nanocrystal. Our longer term goal is to investigate and understand the exciton-exciton interactions that lead to carrier multiplication and how these interactions depend upon the size and shape of the nano-structured semiconductor.

In addition to optical laser based probes of carrier dynamics in photovoltaics, we are using ultrafast soft x-ray spectroscopy to study excited state dynamics in photovoltaic materials. These studies will use the laser slicing source at the Advanced Light Source (ALS). We have conducted initial experiments on laser generated carriers in Cu_2O, where we photo-excited the sample with 400 nm pulses from a femtosecond laser source synchronized to the ALS storage ring and then probed the changes in the x-ray absorption at both the Cu L_3-edge and the O K-edge. Ultrafast core hole spectroscopy provides the opportunity to map the excited-state electronic structure with atomic resolution. Performing time resolved measurements at absorption edges for all the atomic species involved in the laser excited state represents a novel approach to characterizing excited state structure that we will be pursuing.

III.D. ***Carrier induced crystal instabilities in semiconductor crystals*****:** We have continued to investigate the role of carrier induced vibrational softening as a mechanism for crystal disordering and melting. This research project started at the SPPS, and we have conducted theoretical studies to clarify how electronic excitation changes the potential energy surface in semiconductor crystals. We have also initiated studies of carrier dynamics in photovoltaic systems. We have initiated collaborations with Professors Mike McGehee and Yi Cui at Stanford University to study carrier dynamics in organic and nano-structured inorganic semiconductors. Our initial studies have focused on determining the magnitude of the carrier multiplication that occurs in low band gap nanocrystalline materials when excited with UV light. If more than one exciton can be generated from a single UV photon this has significant potential to enhance the efficiency of photovoltaic devices. Klimov and Nozik have both reported high efficiencies, but these claims have been highly controversial. Our first goal has been to investigate the magnitude of the carrier multiplication by probing excitons with the excited state absorption in the mid-IR. This parallels

work performed by Nozik, but we will be spectrally resolving the mid-IR signal. We believe this to be a critical aspect to the measurement, because prior investigations have shown that the mid-IR absorption depends upon the number of excitons present in a single nanocrystal. Our longer term goal is to investigate and understand the exciton-exciton interactions that lead to carrier multiplication and how these interactions depend upon the size and shape of the nano-structured semiconductor.

Publications:

1. Clocking Femtosecond X-rays: A.L. Cavalieri, *et al.Phys. Rev. Lett.* **94**, 114801(2005).
2. Atomic-scale Visualization of Inertial Dynamics: A.M. Lindenberg, *et al. Science* **5720**, 392 (2005).
3. Observation of Structural Anisotropy and the Onset of Liquid-like Motion During the Nonthermal melting of InSb: K.J. Gaffney, *et al.*, *Phys. Rev. Lett.* **95**, 125701 (2005).
4. Ultrafast X-ray Science at the Sub-Picosecond Pulse Source: K.J. Gaffney for the SPPS Collaboration, *Synchro. Rad. News* **18**, 32 (2005).
5. Opportunities and Challenges Using Short-Pulse X-ray Sources: J. Larsson, *et al., J. Phys.* **21**, 87 (2005).
6. Ultrafast X-ray Studies of Structural Dynamics at SLAC: K.J. Gaffney, *et al.*, *Proc. SPIE* **5917**, 59170D1 (2005).
7. Ultrafast Dynamics of Laser-Excited Solids: D.A. Reis, K.J. Gaffney, G.H. Gilmer, D. Torralva, *Mat. Res. Soc. Bull.* **31**, 1 (2006).
8. Ultrafast Bond Softening in Bismuth: Mapping a Solid's Interatomic Potential with X-rays: D.M. Fritz, *et al. Science* **315**, 633 (2007).
9. Carrier Density Dependent Lattice Stability in InSb: P.B. Hillyard, *et al. Phys. Rev. Lett.* **98**, 125501 (2007)**.**
10. Imaging Atomic Structure and Dynamics with Ultrafast X-ray Scattering: K.J. Gaffney, H.N. Chapman, *Science* **316**, 1444 (2007).
11. X-ray Diffuse Scattering Measurements of Nucleation Dynamics at Femtosecond Resolution: A.M. Lindenberg, *et al.Phys. Rev. Lett.* **100**, 135502 (2008).
12. Ultrafast Carrier Induced Disordering in InSb Studied with Density Functional Perturbation Theory: P.H. Hillyard, D.A. Reis, K.J. Gaffney, *Phys. Rev. B* **77**, 195213 (2008).

University Research Summaries
(by PI)

PROBING COMPLEXITY USING THE ALS and LCLS

Nora Berrah
Physics Department, Western Michigan University, Kalamazoo, MI 49008
e-mail:nora.berrah@wmich.edu

Program Scope

The objective of our research program is to carry out experiments that will further our understanding of *fundamental interactions between photons and gas-phase systems*. The unifying theme of this program is to probe the frontiers of *complexity* by investigating quantitatively how atoms, molecules, clusters and their ions respond to two classes of VUV-X-ray photon sources. We presently are using photons from the Advanced Light Source (ALS) to study single photon absorption of atoms, molecules clusters and their anions. We will also use in 2009 the linac coherent light source (LCLS), the first x-ray ultra-fast free electron laser (FEL) facility to study multiple and multi-photon ionization of gas-phase systems. Preparations are underway to be ready to use the LCLS.

Our studies include investigation of multi-electron interactions and of energy transfer processes within atoms, molecules, clusters and their ions which will advance our understanding of single photon and in the near future of multiple photon absorption or scattering. Furthermore, most of our work is carried out in a strong partnership with theorists.

This year we have improved our coincidence experimental system by combining our momentum imaging spectrometer with two electron time-of-flight spectrometers. This new system allows us to probe selectively cluster fragmentation by targeting either the surface- or bulk- cluster ionization since the e-TOFs provide very good kinetic energy resolution. In addition, a movable ion-photon beamline (MIPB) in the collinear geometry has been commissioned for the photodetachment and photoionization studies of ions.

We present here results completed and in progress this past year and plans for the immediate future.

Recent Progress

1. Inner-Shell Double Photoionization: Coincident Energy and Angular Distributions in Xenon $4d_{5/2}$

Photo double-ionization (PDI), the emission of two electrons resulting from single photon absorption, has been intensively studied by many research groups over the past two decades since it is related to two important topics of modern atomic physics, namely electron correlations and the three-body Coulomb problem. Understanding the role of both effects in the PDI process can be achieved through a detailed description of the Triply Differential Cross Section (TDCS), which can only be carried out through coincidence measurements between two of the ionization fragments.
In sequential PDI, such as the $4d_{5/2}$ inner-shell ionization in Xenon with subsequent

$N_5O_{2,3}O_{2,3}$ Auger decay the singly charged intermediate 4d core hole can decay via an Auger process into a doubly charged final state. The two outgoing electrons are correlated via the intermediate state, and further through the final states under particular experimental conditions, such as both electrons having similar kinetic energy or ejection direction. Because electrons are indistinguishable, it is necessary to describe the Auger electron as a resonance embedded in the PDI continuum. The striking theoretical prediction within this model [a] of strong interference effects in the TDCS for the case when both free electrons have the same kinetic energies has caught researchers attention and was investigated experimentally in the valence outer-shell PDI of Neon and Xenon. Earlier experimental work has also shown how the spin state determines the constructive or destructive nature of the interference, which is a consequence of a general selection rule [b] already verified in direct PDI of Helium. With three charged particles in the final state, PDI requires in addition a detailed delineation of Coulomb interactions in the resulting few body system, also called Post Collision Interactions (PCI). The common manifestations of PCI in non-coincident measurements are significant shifts of the atomic lines whose tails also become asymmetric. While these effects disappear in photoionization experiments when the difference in velocities between photo and Auger electron is large, they are always present if the incident particle is charged. The influence of PCI on angular distributions of the emitted electrons and the dependence of the post collision interaction on the inter electron angle were studied separately, all requiring coincidence experiments for an accurate description.

We have carried out the first kinetic energy and angular distributions for the Auger decay from Xenon $4d_{5/2}$ photoionization leading to $^3P_2$, $^1D_2$ final state of the $N_5O_{2,3}O_{2,3}$ Auger decay. We have also shown that it is possible to adequately describe the coincident angular distributions using a two-step model approach. Furthermore, the angular distribution data allows one to extract some information about the amplitude and phases of the emitted Auger electron and photoelectrons [1].

We have used an instrument that consists of a set of four rotating electron time-of-flight (TOF) energy analyzers, well suited to perform coincident measurements. These detectors are ideal since they can detect easily the kinetic energy of the two emitted electrons which spreads out over a wide kinetic energy range. The four TOF analyzers are placed in a plane perpendicular to the direction of the incident light which crosses an effusive gas beam. Mechanical constraints (size of the vacuum vessel) limit the length of the drift tube of the analyzers to 12.5 cm.

We measured the triply differential cross section of previously unexplored doubly charged Xe^{2+} states ($^1D_2$, $^3P_{2)}$ by coincident measurements of the $N_5O_{2,3}O_{2,3}$ Auger electrons with the $4d_{5/2}$ photoelectron for the two final states ($^1D_2$) and ($^3P_2$) of the doubly charged ion. We found a very good agreement between our measurements and the theoretical models of the PCI effect given by both Kammerling et al. [c] as well as Sheinerman and Schmidt [d]. Furthermore, the two-step model is applicable for inner electron angles in the range of 35° to 180° if the energy separation between the two electrons is larger than the intrinsic level width of the intermediate state. Moreover, we measured the first angular distribution pattern of the TDCS for these two final states and

were able to reproduce them by a semi empirical model which describes the transitions populating these two states in the non-relativistic dipole approximation [1].

2. Shape Resonances in *K*-shell Photodetachment of Small Size-Selected Clusters: Experiment and Theory

Traditionally, resonances emerging from photodetachment or electron-atom scattering were divided into two classes; Feshbach and shape resonances which are both important since they reveal the position of the states with respect to the parent atom. We have conducted both an experimental and theoretical study of *K*-shell photodetachment of the size-selected clusters B_2^- and B_3^- to explore possible resonance trends in small cluster systems. In addition, our measurements allow a qualitative measurement of the photo-fragmentation process in both B_2^- and B_3^-. The motivation for this work stems from the fact that although there is much sophisticated molecular and cluster anions laser photodetachment work there is no information on inner-shell photodetachment and fragmentation of cluster and molecular anions to date.

The experimental absolute photodetachment cross sections exhibit bound resonances below threshold and two shape resonances above the *K*-shell threshold. Similar results were obtained for all of the cationic products observed, B^+ and B_2^+ from B_2^-, as well as B^+, B_2^+, and B_3^+ from B_3^-. The overall agreement between measured and calculated photodetachment cross sections is very good. However, the theoretical study yielded additional bound resonances not observed in the experimental data [2].

3. Multi-User Movable Ion Beamline

We have designed and built a portable ion beamline (MIPB) to complement the existing one fixed at the ALS beamline 10.0.1. The instrument will enable us (and any user) to exploit the capabilities of other ALS beamlines, below 9 eV and above 340 eV photon energies not available on BL10.0.1, including tunable circularly polarized light for the study of negative and positive ions. In addition, the instrument can be used at any other facility such as the LCLS at SLAC, Stanford University.

Future Plans.

The principal areas of investigation planned for the coming year are to:
1) Contribute to the commissioning of the AMO instrument using the LCLS. The ultrafast light source is scheduled to start in July 2009 with beamtime available for commissioning during the summer and fall of 2009. Atomic, molecular and cluster multiple ionization and multiphoton ionization are planned. 2) Continue the experimental Coulomb explosion investigations of molecules and clusters using the ALS as well as continue the analysis of the fragmentation studies of molecules and clusters using coincidence techniques that utilizes the ion imaging and two time-of-flight spectrometers. 3) Carry out photodetachment experiments in the carbon anions cluster chain using the movable ion beamline with ALS beamline 8.0.1 allowing access to higher photon energies. 4) Continue our collaborative efforts with the Technical University cluster group (Moeller et al.) at the FLASH facility until the LCLS is fully operational.

References

[a] L.Vegh and J. H. Macek, *Phys. Rev. A* **50**, 4031 (1994); J H *Phys. Rev. A* **50**, 4036 (1994).
[b] F. Maulbetsch and J. S. Briggs, *J. Phys. B: At. Mol. Opt. Phys.* **28**, 551 (1995).
[c] B. Kammerling and V. Schmidt 1991 *Phys. Rev. Lett.* **67**, 1848 (1991); .*J. Phys. B:* **26**, 261 (1993).
[d] S. A. Sheinerman and V. Schmidt *J. Phys. B: At. Mol. Opt. Phys.* **30**, 1677 (1997).

Publications from DOE Sponsored Research.

1. M. Wiedenhoeft, A. A. Wills, X. Feng, S. Canton, J. Viefhaus, T. Gorczyca, U.Becker, and N. Berrah "Exchange and PCI effects on Angular Distribution in Xe $4d_{5/2}$" J. Phys. B. **41** 095202, (2008).
2. N. Berrah, J. D. Bozek, R. C. Bilodeau G. D. Ackerman, "Inner-Shell Photodetachment and Fragmentation of small clusters B_2^-, B_3^-", Phys. Rev. A. **76**, 042709 (2007).
3. G. Turri, B. Lohmann, B. Langer, G. Snell, U. Becker and N. Berrah, "Spin polarization of the Ar^* $2p^{-1}{}_{1/2}4s$, and $2p^{-1}{}_{1/2}3d$ Auger decay" J. Phys. B **40**, 3453 (2007).
4. N. Berrah , R.C. Bilodeau, I. Dumitriu, J.D. Bozek,G.D. Ackerman, O. T. Zatsarinny and T. W. Gorczyca "Shape resonances in K-shell photodetachment of B^-: Experiment and Theory" Phys. Rev. A **76,** 032713 (2007).
5. L. F. DiMauro, J. Arthur, N. Berrah, J. Bozek, J. N. Galayda and J. Hastings,**"**Progress report on the LCLS XFEL at SLAC"**,** . *Phys.: Conf. Ser.* **88**, 012058 (2007).
6. D. Rolles, Z. D. Peˇsi´c,1 H. Zhang,, R. C. Bilodeau, J. D. Bozek, and N. Berrah, "Size effects in van der Waals clusters studied by spin and angle-resolved electron spectroscopy and multi-coincidence ion imaging" *J. Phys.: Conf. Ser.* **88** 012003, (2007).
7. E. Sokell, A. A. Wills, M. Wiendenhoeft, X. Feng, D. Rolles and N. Berrah, "Inner-shell photoionization of molecules using a two-dimensional imaging technique" *J. Phys.: Conf. Ser.* **88** 012007 (2007).
8. D. Rolles, H. Zhang, A. Wills, R. Bilodeau, E. Kukk B. Rude, G. Ackerman, J. Bozek and N. Berrah "Size effects in Van der Waals clusters using angle resolved photoelectron spectroscopy, Phys. Rev. A, Rap Com. **75**, 032101(R) (2007).
9. D. Rolles , Z. D. Pešić, M. Perri, R. Bilodeau, G. Ackerman, B. Rude, D. Kilcoyne, J. D. Bozek, and N. Berrah "A velocity map imaging spectrometer for electron-ion and ion-ion coincidence experiments with synchrotron radiation, (Nucl. Instr. and Meth. **B 261**, 170 (2007).
10. Z. D. Pešić, D. Rolles, M. Perri, R. C. Bilodeau, G. D. Ackerman, B. S. Rude, A. L. D. Kilcoyne, J. D. Bozek, and N. Berrah, "Studies of Molecular Fragmentation using Velocity Map Imaging Spectrometer and Synchrotron Radiation", J. Elect. Spec. and Rela. Phen, **155**, 155 (2007)
11. D. Cubaynes, H-L Zhou, N. Berrah, J-M. Bizau, J. D. Bozek, S. Canton, S. Diehl, X-Y Han, A. Hibbert, E. T. Kennedy, S. T. Manson, L. VoKy,F. Wuilleumier, "Dynamical and relativistics effects in experimental and theoretical studies of innershell photoionization of sodium", J Phys B **40**, F121, (2007).
12. R. C. Bilodeau, C. W. Walter, I. Dumitriu, N. D. Gibson, G. D. Ackerman, J. D. Bozek, B. S. Rude, R. Santra, L. S. Cederbaum, and N. Berrah "Photo Double Detachment of CN^-: Electronic Decay of an Inner-Valence Hole in Molecular Anions, Chem. Phys. Lett. **426**, 237(2006)
13. R. C. Bilodeau, J. D. Bozek, A. Agular, G. D. Ackerman, and N. Berrah, "Photodetachment of He^- near the 1s threshold: Absolute cross section measurements and post-collision interactions" Phys. Rev. A **73**, 034701 (2006).
14. X. Feng, A. A. Wills, E. Sokell, M. Wiedenhoeft, and N. Berrah, "Study of Auger decay in core-excited HBr by angle-resolved two-dimensional photoelectron spectroscopy" Phys. Rev. A **73** 012716 (2006).
15. C. W. Walter, N.D. Gibson, R.C. Bilodeau, N. Berrah, J.D. Bozek, G.D. Ackerman, and A. Aguilar, "Shape Resonance in K-Shell Photodetachment from C¯", Phys. Rev. A **73**, 062702 (2006)
16. N. Berrah, R. C. Bilodeau, J.D. Bozek, C.W. Walter, N.D. Gibson,and G.D. Ackerman, "Double Auger decay, and shape resonances in negative ions" Radiat. Phys. Chem. **75,** 1447 (2006).

Strongly Anisotropic Bose and Fermi Gases

Principal Investigator
John Bohn
JILA, UCB 440
University of Colorado
Boulder, CO 80309
Phone (303) 492-5426
Email bohn@murphy.colorado.edu

Program Scope

This program focuses on the fundamental properties of dilute quantum degenerate gases whose constituent particles possess dipole moments. It is concerned with the implications of the dipole-dipole interactions on the structure, dynamics, and control of these gases, as well as their ability to provide prototypes for novel condensed matter systems and potentially useful materials. The properties of the gas are tunable to a high degree, by varying such quantities as the density of the gas, the orientation of the dipoles, the scattering length of the constituents, and the anisotropy of the trap in which they are held.

Recent Progress

In the previous funding cycle we had built expertise in calculations of dipolar BEC, both the mean-field ground state and the collective excitations as described by the Bogoliubov-deGennes equations. These calculations, further refined in the present funding cycle, can now stably make calculations that exploit cylindrical symmetery (easy and quick) or that do not possess this symmetry (slower, but still tractable); they can also find stationary states, or can follow the time evolution of the BEC upon perturbation.

Using this suite of codes makes us flexible enough to calculate observables directly relevant to the world's only (so far) experiment on dipolar BEC, namely, that of the Pfau group in Stuttgart. In work to be submitted, we assess the stability of a dipolar BEC as a function of the aspect ratio of the trap in which it is held. This result is shown in the figure below, where the critical scattering length for stability (tunable in the experiment) is plotted versus trap aspect ratio λ. The shaded region at the top represents stable condensates, while the white region below represents unstable ones. For prolate traps (left end of graph), the trap shape encourages the dipoles to align in a head-to-tail orientation, where attractive interactions would overwhelm the kinetic energy of trap confinement and cause the BEC to implode. However, a large positive scattering length can defeat this tendency and stabilize the condensate. For more oblate traps, the trap shape encourages repulsion between dipoles, and a smaller scattering length suffices to stabilize the BEC.

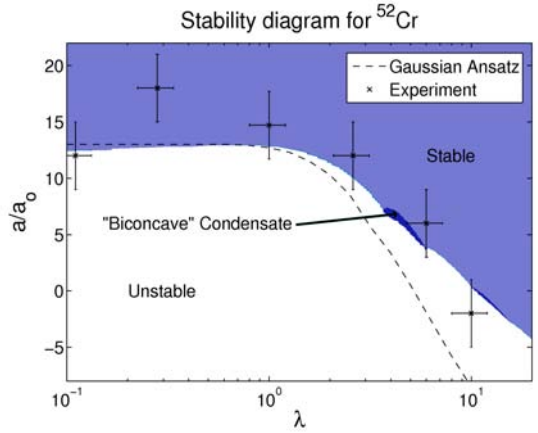

Figure. Stability diagram for a BEC of Cr atoms, which possess a 6 Bohr magneton magnetic moment. In a prolate trap (small aspect ratio λ), the BEC is stable against collapse only for a large positive scattering length. The division between stable (shaded) and unstable (white) regions is calculated in mean-field theory. Data are from the Stuttgart group [T. Koch et al., Nature Physics doi:10.1038/nphys887].

Additionally, we seek novelties in ground and excited states of dipolar BEC. We have studied, for example, the structure of a vortex core in a rotating dipolar BEC, finding a direct link between this structure and a set of "roton-like" excited modes that we have previously identified. This link has been made previously in studies of superfluid helium, via detailed density functional calculations. In a dipolar BEC, we can obtain results exactly within mean field theory, and even make semiqantitative arguments using perturbation theory. This result points to the utility of using dipolar BEC as a testbed for understanding in detail unusual superfluid properties. This work has generated a recent Physical Review Letter, and a more detailed follow-up is being written now.

Future Plans

The success of identifying excited modes that are the trapped-gas analogues of rotons strengthens the analogy between this canonical condensed matter system and the dilute, readily-controlled dipolar BEC gas. The most striking result to follow from the roton minimum in helium is the superfliud velocity, below which the fluid can flow with no dissipative losses. In the dipolar BEC, not only can the superfluid velocity be controlled, it will also be anisotropic due to the anisotropy of the dipolar interaction. Moreover, we continue to discuss physics with the Stuttgart group, seeking ways to observe unusual behavior in the dipolar gas.

DOE-supported publication in the past year

Manifestations of the Roton Mode in Dipolar Bose-Einstein Condensates
R. M. Wilson, S. Ronen, J. L. Bohn, and H. Pu, Phys. Rev. Lett. **100**, 245302 (2008).

Atomic and Molecular Physics in Strong Fields

Shih-I Chu
Department of Chemistry, University of Kansas
Lawrence, Kansas 66045
E-mail: sichu@ku.edu

Program Scope

In this research program, we address the fundamental physics of the interaction of atoms and molecules with intense ultrashort laser fields. The main objectives are to develop new theoretical formalisms and accurate computational methods for *ab initio* nonperturbative investigations of multiphoton quantum dynamics and very high-order nonlinear optical processes of one-, two-, and many-electron quantum systems in intense laser fields, taking into account detailed electronic structure information and many-body electron-correlated effects. Particular attention will be paid to the exploration of the effects of electron correlation on high-harmonic generation (HHG) and multiphoton ionization (MPI) processes, time-frequency spectrum, and coherent control of HHG processes for the development of tabletop x-ray laser light sources, and attosecond AMO processes, etc.

Recent Progress

1. *Ab initio* Theoretical Investigation of the Frequency Comb Structure and Coherence in the VUV-XUV Regimes via High-Order Harmonic Generation

In the last several years, femtosecond laser-based optical frequency combs have led to remarkable advancements in ultrafast science [1], high-precision optical frequency measurement and synthesis [2], and enabled optical atomic clocks [3]. As a universal optical frequency comb synthesizer, this method provides a direct link between optical and microwave frequencies. More recently, there is substantial experimental interest in the exploration of the feasibility of generating frequency comb in the extreme ultraviolet (xuv) and vacuum ultraviolet (vuv) regimes at a repetition frequency of more than 100 MHz via high-order harmonic generation (HHG) [4,5]. At such a repetition rate, the mode spacing of the frequency comb is large enough for high-resolution spectroscopy. Although such a comb structure has been anticipated, there are currently experimental difficulties in the observation of the frequency comb structure within each harmonic, with the exception of the third-order harmonic case [5].

To advance this field, we have recently presented the first fully *ab initio* quantum investigation of the frequency comb structure and coherence within each order of the high-order harmonic generation spectrum in the high-frequency vuv-xuv regime [6]. The HHG spectrum driven by a train of equal-spacing short laser pulses is calculated by propagating the time-dependent Schrödinger equation (TDSE) accurately and efficiently by means of the time-dependent generalized pseudospectral (TDGPS) method [7]. We explore the comb structure and coherence by varying the laser pulse separation τ, the number of pulses N, and the laser intensity. We found that a nested comb structure appears within each of the harmonics, ranging from the first harmonic all the way to the cutoff harmonic, and this global pattern persists regardless of the values of τ and N used. Finally, the frequency comb structure prevails even in the presence of appreciable ionization.

2. Many-Mode Floquet Theoretical Approach for the Exploration of Coherent Control of Multiphoton Dynamics Driven by Intense Frequency-Comb Laser Fields

We extend the many-mode Floquet theorem (MMFT) [8,9] for the nonperturbative investigation of multiphoton resonance dynamics driven by intense frequency-comb laser fields [10]. The frequency comb structure generated by a train of short laser pulses can be exactly represented by a combination of the main frequency and the repetition frequency. MMFT allows non-perturbative and exact treatment of the

interaction of a quantum system with the frequency-comb laser fields. We explore multiphoton resonance processes between a two-level system and frequency-comb laser. We found that the multiphoton processes can be coherently controlled by tuning the laser parameters such as the carrier-envelope phase (CEP) shift. In particular, high-order harmonic generation shows immense enhancement by tuning the CEP shift, due to simultaneous multiphoton resonances [10].

3. Effect of Electron Correlation on High-Order-Harmonic Generation of Helium Atoms in Intense Laser Fields [11]

We present a *time-dependent generalized pseudospectral* (TDGPS) approach in hyperspherical coordinates for fully *ab initio* and nonperturbative treatment of high-order harmonic generation (HHG) processes of atomic systems in intense laser fields. The procedure is applied to a detailed investigation of HHG processes of helium atoms in ultrashort laser pulses at a KrF wavelength of 248.6 nm. The six-dimensional coupled hyperspherical-adiabatic-channel equations are discretized and solved efficiently and accurately by means of the TDGPS method. The effects of electron correlation and doubly excited states on HHG are explored in detail. A HHG peak with Fano line profile is identified which can be attributed to a broad resonance of doubly excited states.

4. Coherent Control of a Single Attosecond XUV Pulse by Few-Cycle Intense Laser Pulses

We perform *ab initio* quantum and classical investigations of the production and control of a single attosecond pulse by using intense few-cycle laser pulses as the driving field [12]. The time-frequency characteristics of the attosecond xuv pulse are analyzed in detail by means of the wavelet transform of the time-dependent induced dipole. To better understand the physical processes, we also perform classical trajectory simulation of the strong-field electron dynamics and electron returning energy map. We found that the quantum and classical results provide complementary information regarding the underlying mechanisms responsible for the production of the coherent attosecond pulse. For few-cycle (5 fs) driving pulses, it is shown that the emission of the consecutive harmonics in the super continuum cutoff regime can be synchronized and locked in phase resulting in the production of a coherent attosecond pulse. Moreover, the time profile of the attosecond pulses can be controlled by tuning the carrier envelope phase.

5. Extension of High-order Harmonic Generation Cutoff via Coherent Control of Intense Few-Cycle Chirped Laser Pulses

We present an *ab initio* quantum exploration of the HHG cutoff extension mechanisms controlled by a few cycle *chirped* laser pulse [13]. It is shown that significant cutoff extension can be achieved through the optimization of the chirping rate parameters. The HHG power spectrum is calculated by solving accurately and efficiently the TDSE by means of the TDGPS method and the time-frequency characteristics of the HHG power spectrum are analyzed in detail by means of the wavelet transform of the time-dependent induced dipole acceleration. It is found that the quantum and classical results provide consistent information regarding the underlying mechanisms responsible for the substantial extension of the cutoff region. Furthermore the time duration of the emitted attosecond bursts produced by the chirped laser pulse is significantly reduced from that of the chirp-free laser pulses.

6. Precision Studies of MPI/HHG of H_2^+ in Intense Laser Fields

a) Recently we developed a *time-dependent* non-Hermitian Floquet approach [14] for the fully *ab initio* investigation of MPI/HHG and their correlation in H_2^+. The procedure involves the *complex-scaling* generalized pseudospectral spatial discretization of the time-dependent Hamiltonian and non-Hermitian time propagation of the time-evolution operator in the *energy* representation. The new procedure is applied to a precision calculation of MPI and HHG rates of H_2^+ in linearly polarized laser fields with wavelength 532 nm and several laser intensities, as well as various internuclear distances R in the range between 2.0 and 17.5 a.u. We found that both the MPI and HHG rates are strongly dependent on *R*. Further, at some internuclear separations *R*, the HHG productions are strongly enhanced and this

phenomenon can be attributed to the resonantly enhanced MPI at these *R*. Finally, the enhancement of higher harmonics is found to take place mainly at larger *R*. Detailed study of the correlation between the behavior of MPI and HHG phenomena is presented.

b) More recently we present a fully *ab initio* and high-precision 3D study of the orientation effects in MPI and HHG of H_2^+ subject to intense laser pulses [15]. The orientation of the molecular axis with respect to the polarization of the laser field can be arbitrary. The calculations were performed for the ground and two first excited electronic states of H_2^+ at the internuclear separation R = 2.0 a.u. The dependence of MPI and HHG behavior on the orientation angle is analyzed. We found that orientation effects are strongly affected by the symmetry of the wave function and the corresponding distribution of the electron density. While the anisotropy of MPI and HHG is rather weak for the $1\sigma_g$ state, both processes are suppressed at the orientation angle 90° for the $1\sigma_u$ state and at the angle 0° for the $1\pi_u$ state. We discuss the multiphoton resonance and two-center interference effects in the HHG spectra which can lead both to enhancement and suppression of the harmonic generation.

7. Development of *Self-Interaction-Free* Time-Dependent Density Functional Theory (TDDFT) for Nonperturbative Treatment of Multiphoton Processes of Many-Electron Systems in Intense Pulsed Laser Fields

Recently we have continued the development of *self-interaction-free* time-dependent density functional theory (TDDFT) [16-19] for accurate and efficient treatment of strong-field AMO physics, taking into account both electron correlations and detailed electronic structure. Given below is a brief summary of the progress in 2005-2008.

a) Very- High-Order Harmonic Generation of Ar Atoms and Ar^+ Ions in Superintense Pulsed Laser Fields: An All-Electron Ab Initio Study

Recently it has been demonstrated experimentally [20] that the generation of very high-order harmonics (HHG), up to 250 eV, can be obtained by using the Ar gas. To explore the underlying quantum dynamics responsible for the production of the very-high-order harmonics, we performed an *all-electron* treatment of the response of Ar and Ar^+ systems to superintense laser fields [18] by means of the self-interaction-free TDDFT. In our study, all the valence electrons are treated explicitly & their partial contributions to the ionization are analyzed. Further, by introducing an effective charge concept, we can study at which laser intensity the contribution to the high-energy HHG from Ar^+ ions precede over the Ar atoms. Comparing the HHG power spectrum from Ar and Ar^+, we conclude that the high-energy HHG observed in the experiment [20] originated from the ionized Ar atoms.

b) Role of the Electronic Structure and Multi-electron Response in Ionization Mechanisms and HHG of Diatomic Molecules in Intense Laser Fields

Recently there has been much experimental and theoretical interests in the study of strong-field molecular ionization and HHG. Most theoretical studies in the recent past are based on approximate models such as the ADK model, strong-field approximation, etc. These models usually assume that ionization rates depend only upon laser wavelength and intensity, and the *field-free* ionization potential of the species of interest and consider only the response of the highest occupied molecular orbital (HOMO). The effects of detailed electronic structure and multi-electron responses are ignored. Although these models have some partial success in weaker field processes, they cannot provide an overall consistent picture of the ionization and HHG behavior of different molecules.

We have recently further developed the *self-interaction-free* TDDFT [17] for nonperturbative investigation of the ionization mechanisms as well as the HHG power spectra of homonuclear (N_2, O_2, and F_2) and heteronuclear (CO) diatomic molecules in intense ultrashort lasers [16,17,19]. A *time-dependent two-center generalized pseudospectral method* is developed for accurate and efficient treatment of the TDDFT equations in space and time. The procedure allows *nonuniform* and optimal

spatial grid discretization of the Hamiltonian in prolate spheroidal coordinates and a split-operator scheme in the *energy representation* is used for the time propagation of the individual molecular spin-orbital. Our studies reveal several intriguing behaviors of the nonlinear responses of molecules to intense laser fields: (a) It is found that detailed electron structure and correlated multielectron responses are important factors for the determination of the strong-field ionization behavior. Further, it is not adequate to use only the HOMO for the description of the ionization behavior since the inner valence electrons can also make significant or even dominant contributions. Finally, the ionization potential (IP) is laser-intensity and frequency dependent and it is also not the only major factor determining the molecular ionization rates. (b) We predict substantially different nonlinear optical response behaviors for homonuclear (N_2) and heteronuclear (CO) diatomic molecules, despite the fact that CO has only a very small permanent dipole moment. In particular, we found that the MPI rate for CO is higher than that of N_2. Furthermore, while laser excitation of the homonuclear N_2 molecule can generate only odd harmonics, both even and odd harmonics can be produced from the heteronuclear CO molecule [19].

c) An invited review article for a special issue of the Journal of Chemical Physics, entitled "Recent development of self-interaction-free time-dependent TDDFT for nonperturbative treatment of atomic and molecular multiphoton processes in intense laser fields," has been published [17].

Future Research Plans

In addition to continuing the ongoing researches discussed above, we plan to initiate the following several new project directions: (a) Exploration of 3D orientation dependent MPI/HHG processes of diatomic molecules in intense laser pulses. (b) Development of TDGPS method and extension of self-interaction-free TDDFT to triatomic molecular systems for the study of the MPI mechanisms and HHG phenomena in strong fields. (c) Development of spin-dependent *localized* Hartree-Fock (LHF)-DFT method for the study of singly, doubly, and triply excited states of Rydberg atoms and ions as well as inner shell excitations [21]. (d) Coherent control of rescattering and attosecond phenomena in strong fields.

References Cited (* Publications supported by the DOE program in the period of 2005-2008.)

[1] M. Hentschel *et al.*, Nature (London) **414**, 509 (2001); M. Drescher *et al.*, Science **291**, 1923 (2001).
[2] M. Fischer *et al.*, Phys. Rev. Lett. **92**, 230802 (2004); H. S. Margolis *et al.*, Science **306**, 1355 (2004).
[3] M. Takamoto *et al.*, Nature (London) **435**, 321 (2005); S. A. Diddams *et al.*, Science **293**, 825 (2001).
[4] C. Gohle, *et al.*, Nature (London) **436**, 234 (2005).
[5] R. J. Jones, *et al.*, Rev. Lett. **94**, 193201 (2005).
*[6] J. J. Carrera, S. K. Son, and S. I. Chu, Phys. Rev. A **77**, 031401(R) (2008).
[7] X. M. Tong and S. I. Chu, Chem. Phys. **217**, 119 (1997).
[8] T. S. Ho, S. I. Chu, and J. V. Tietz, Chem. Phys. Lett. **96**, 464 (1983); T. S. Ho and S. I. Chu, Phys. Rev. A **31**, 659 (1985).
[9] S. I. Chu and D. A. Telnov, Phys. Rep. **390**, 1-131 (2004).
*[10] S.-K. Son and S. I. Chu, Phys. Rev. A **77**, 063406 (2008).
*[11] X. X. Guan, X. M. Tong, and S. I. Chu, Phys. Rev. A **73**, 023406 (2006).
*[12] J. Carrera, X. M. Tong, and S. I. Chu, Phys. Rev. A **74**, 023404 (2006).
*[13] J. Carrera and S. I. Chu, Phys. Rev. A **75**, 033807 (2007).
*[14] D. Telnov and S. I. Chu, Phys. Rev. A**71**, 013408 (2005).
*[15] D. A. Telnov and S. I. Chu, Phys. Rev. A **76**, 043412 (2007).
[16] X. Chu and S. I. Chu, Phys. Rev. A**70**, 061402 (R) (2004).
*[17] S. I. Chu, J. Chem. Phys. **123**, 062207 (2005).
*[18] J. Carrera, X. M. Tong, and S. I. Chu, Phys. Rev. A**71**, 063813 (2005).
*[19] J. Heslar, J. Carrera, D. Telnov, and S. I. Chu, Int. J. Quantum Chem. **107**, 3159 (2007).
[20] E. A. Gibson, *et al.*, Phys. Rev. Lett. **92**, 033001 (2004).
*[21] Z.Y. Zhou and S. I. Chu, Phys. Rev. A**75**, 014501 (2007).

Formation of Ultracold Molecules

Robin Côté

Department of Physics, U-3046
University of Connecticut
2152 Hillside Road
Storrs, Connecticut 06269

Phone: (860) 486-4912
Fax: (860) 486-3346
e-mail: rcote@phys.uconn.edu
URL: http://www.physics.uconn.edu/∼rcote

Program Scope

Current experimental efforts to obtain ultracold molecules (*e.g.*, photoassociation (PA), buffer gas cooling, or Stark deceleration) raise a number of important issues that require theoretical investigations and explicit calculations.

This Research Program covers interconnected topics related to the formation of ultracold molecules. We propose to investigate schemes to form ultracold molecules, such as homonuclear alkali metal dimers using stimulated and spontaneous processes. We will also study heteronuclear molecules, in particular alkali hydrides; these polar molecules have very large dipole moments. In addition, we will investigate the enhancement of the formation rate via Feshbach resonances, paying special attention to quantum degenerate atomic gases, and how STIRAP (Stimulated Raman Adiabatic Passage) could be optimized by using a chainwise multi-step approach. Finally, we will explore the possible formation of a new and exotic type of molecules, namely ultralong-range Rydberg molecules.

Recent Progress

Since the start of this Program (August 1st 2005), we have worked on the following projects:

• Formation of alkali hydrides

We explored the formation of alkali hydrides from one- and two-photon photoassociative processes. We found that the one-photon formation rate for LiH and NaH in their $X^1\Sigma^+$ ground electronic state is sizable in the upper ro-vibrational states $|v'', J = 1\rangle$; assuming conservative values for the atom densities (10^{12} cm^{-3}), temperature (1 mK), laser intensity (1000 W/cm^2), and the volume illuminated by it (10^{-6} cm^3), the rate coefficients are of the order 3×10^{-13} cm^3/s, leading to about 30,000 molecules per second [1]. We also found that all of those molecules would populate a narow distribution of J-states in the $v'' = 0$ vibrational level by spontaneous emission cascading (see Fig.1); the momentum transfer due to the photon emission is not large enough for remove the molecules from traps deeper than 10 μK or so. In the two-photon case, we calculated the formation rate of LiH into the singlet ground state via the $B^1\Pi$ excited state. This excited electronic state has only three bound levels (in the $J = 1$ manifold) and a fairly good overlap with the $X^1\Sigma^+$ ground electronic state. We found rate coefficients about 1000 times larger [2]. However, the constraints brought by the possibility of back-stimulation from a bound state to the continuum

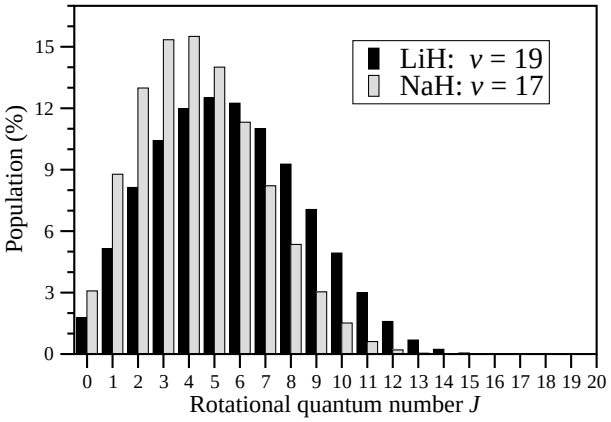

Figure 1: Distribution into the J states of the $v = 0$ manifold starting from $v = 19, J = 1$ for LiH and $v = 17, J = 1$ for NaH. In both cases, we observe that the maximum population is achieved around $J \sim 5$.

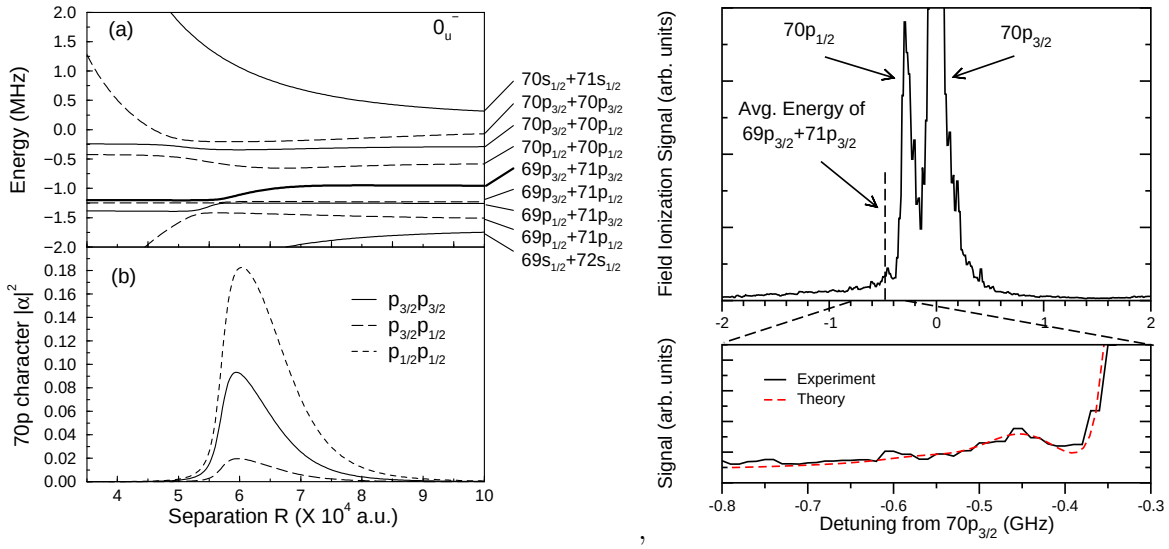

Figure 2: Left panel: (a) Potentials for the 0_u^- symmetry for asymptotes between $70s + 71s$ and $69s+72s$ (zero of energy set at the $70p_{3/2}+70p_{3/2}$ asymptote). (b) Fraction of $70p$ character $|\alpha|^2$ for $p_{3/2}p_{3/2}$, $p_{3/2}p_{1/2}$, and $p_{1/2}p_{1/2}$ mixtures of the $69p_{3/2} + 71p_{3/2}$ curve. Right panel: Experimental spectrum near the $70p$ atomic resonance. Zoom: comparison between experiment and theory (assuming a 120 MHz laser bandwidth, and contributions from the 0_g^+, 0_u^-, and 1_u symmetries).

limits these larger rates to values of the same order as the single photon process via an excited state [2].

More recently, we also explored the formation of LiH molecules in the $a^3\Sigma^+$ electronic state [3]. It is predicted to support one ro-vibrational level, leading to a sample in a pure single ro-vibrational state. We found that very large rate coefficients ca be obtained by using the $b^3\Pi$ excited state, which supports only five or six bound levels. Because of the extreme spatial extension of their last "lobe", the wave functions of the two uppermost bound levels have large overlap with the $(v = 0, J = 0)$ bound level of $a^3\Sigma^+$, leading to branching ratios ranging from 1% to 90%. This property implies that large amounts of LiH molecules could be produced in a single quan tum state, a prerequisite to study degenerate molecular gases [3].

• Rydberg-Rydberg interactions

We began working on the Rydberg-Rydberg interactions to explain some spectral features observed in ^{85}Rb experiments. We calculated the long-range molecular potentials between two atoms in $70p$ in Hund's case (c), by diagonalization of an interaction matrix. We included the effect of fine structure, and showed how the strong ℓ-mixing due to long-range Rydberg-Rydberg interactions can lead to resonances in excitation spectra. Such resonances were first reported in S.M. Farooqi *et al.*, Phys. Rev. Lett. **91** 183002, where single UV photon excitations from the $5s$ ground state occurred at energies corresponding to normally forbidden transitions or very far detuned from the atomic energies. We modeled a resonance correlated to the $69p_{3/2} + 71p_{3/2}$ asymptote by including the contribution of various symmetries (see Fig. 2): the lineshape is reproduced within the experimental uncertainties [4]. More recently, we extended this work to the case of strong resonances observed near the $69d + 70s$ asymptote [5]. In addition to the lineshape, we also computed the n-scaling of the signal size. We found that our theoretical results are in good agreement with the observations of our colleagues at UConn.

• **Evanescent-wave mirrors**

In [6], we investigated the interaction of an ultracold diatomic polar molecule with an evanescent-wave mirror (EWM). Several features of this system were explored, such as the coupling between internal rovibrational states of the molecule and the laser field. Using numerical simulations under attainable physical conditions, we found that the reflection/transmission coefficient depends on the internal (rovibrational) states of the molecules. Such molecular optics components could facilitate the manipulation and trapping of ultracold molecules, and might serve in future applications in several fields, e.g., as devices to filter and select state for ultracold chemistry, to measure extremely low temperatures of molecules, or to manipulate states for quantum information processing.

We extended this work from the static case, where the optical fields have constant intensities, to the time-varying case. We found that in addition to trapping molecules, one could use such devices to also cool them [7].

• **Degenerate Fermi gas**

In [8], we worked on the spectroscopic signature of Cooper pairs in a degenerate Fermi gas, namely ^{6}Li. We calculated two-photon Raman spectra for fermionic atoms with interactions described by a single-mode mean-field BCS-BEC crossover theory. By comparing calculated spectra of interacting and non-interacting systems, we found that interactions lead to the appearance of correlated atomic pair signal - due to Cooper pairs; splitting of peaks in the spectroscopic signal - due to the gap in fermionic dispersion; and attenuation of signal - due to the partial conversion of fermions into the corresponding single-mode dimer. By exploring the behavior of these features, on can obtain quantitative estimates of the BCS parameters from the spectra, such as the value of the gap as well as the number of Cooper pairs.

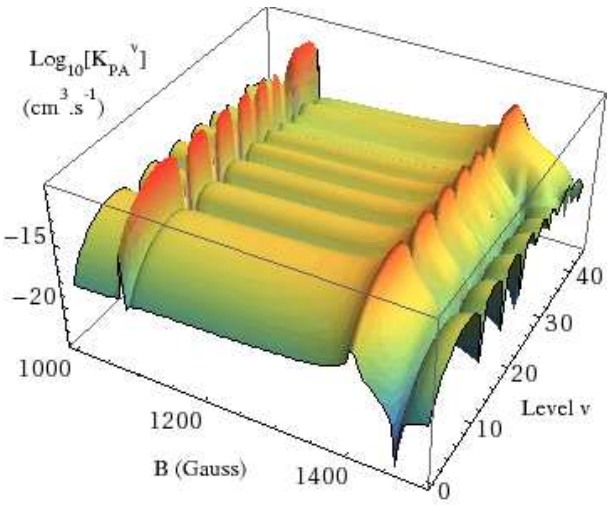

Figure 3: Rate coefficient (log-scale) in cm^3/s as a function of the B-field for various $v = 0 - 42$ of the singlet state of LiNa. The rate coefficient increases drastically in the vicinity of the two Feshbach resonances shown here.

• **Feshbach Optimized Photoassociation (FOPA)**

We have started to investigate the formation of polar molecules using photoassociation of atoms in mixtures in the vicinity of Feshbach resonances [9]. We calculated the rate coefficients K_v to form singlet molecules of LiNa using this Feshbach Optimized Photoassociation (FOPA) mechanism, and found that they increase by 10^{3-4} when compared to the off-resonance rate coefficients $K_v^{\rm off}$ (see Fig. 3). We also formulated a simple treatment based on two coupled channels, and found that FOPA follows

$$K_v = K_v^{\rm off} \left|1 + C_1 \tan\delta + C_2 \sin\delta\right|^2 \ ,$$

where δ is the resonant phase shift, and C_1 and C_2 depend on the overlap of the initial scattering state and target state v.

We also applyed FOPA to the homonuclear case of ^{7}LI$_2$ [10], for which measurement have recently been carried on by the group of R. Hulet at Rice university.

• **Chainwise multi-steps STIRAP**

We explored a multi-state chainwise STIRAP approach to bring a molecule to the ground state through a series of intermediate vibrational states coupled by optical fields. We analyzed a five-level model (see Fig. 4). At least two vibrational levels $|e_1\rangle$ and $|e_2\rangle$ in the excited electronic state are required, with good Franck-Condon overlaps with the initial $|g_1\rangle$ and target $|g_3\rangle$ states, respectively. The goal is to efficiently transfer population from the state $|g_1\rangle$ (a high-lying state produced, *e.g.*, by magneto-association) to the target state $|g_3\rangle$ (*e.g.*, the $v = 0$ level). We found that using a dark state that does not populate $|e_1\rangle$ and $|e_2\rangle$ allows for ~ 90 % transfer efficiency in $^{87}Rb_2$ [11].

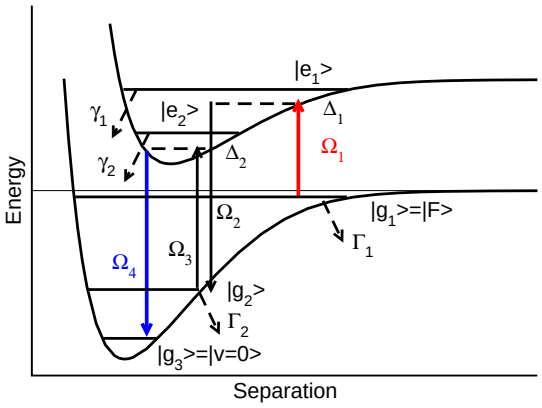

Figure 4: Five-level STIRAP scheme.

Future Plans

In the coming year, we plan to continue the alkali hydride work, and extend it to other polar molecules relevant to the experimental community, such as LiCs, LiRb, etc. We also plan to continue our work on FOPA as well as multi-steps STIRAP, and extend them to other systems.

We expect to carry more calculations on Rydberg-Rydberg interactions and explore the possibility of forming metastable long-range doubly-excited Rydberg molecules as well as the experimental signature to be expected.

Publications sponsored by DOE

1. E. Juarros, P. Pellegrini, K. Kirby, and R. Côté, *One-photon-assisted formation of ultracold polar molecules.* Phys. Rev. A **73**, 041403(R) (2006).
2. E. Juarros, K. Kirby, and R. Côté, *Laser-assisted Ultracold Lithium-hydride Molecule Formation: Stimulated vs. Spontaneous Emission.* J. Phys. B **39**, S965 (2006).
3. E. Juarros, K. Kirby, and R. Côté, *Formation of ultracold molecules in a single pure state: LiH in* $a^3\Sigma^+$. In preparation.
4. J. Stanojevic, R. Côté, D. Tong, S.M. Farooqi, E.E. Eyler, and P.L. Gould, *Long-range Rydberg-Rydberg interactions and molecular resonances.* Eur. Phys. J. D **40**, 3 (2006).
5. J. Stanojevic, R. Côté, D. Tong, S.M. Farooqi, E.E. Eyler, and P.L. Gould, *Long-range potentials and* $(n-1)d+ns$ *molecular resonances in an ultracold Rydberg gas.* Submitted to Phys. Rev. A.
6. K. Shimshon, B. Segev, and R. Côté, *Evanescent-Wave Mirror for Ultracold Diatomic Polar Molecules.* Phys. Rev. Lett. **95**, 163005 (2005).
7. K. Shimshon and R. Côté, *Trapping and controlling molecules with Evanescent-Wave Mirrors.* Submitted to Phys. Rev. A.
8. M. Koštrun and R. Côté, *Two-color spectroscopy of fermions in mean-field BCS-BEC crossover theory.* Phys. Rev. A **73**, 041607(R) (2006).
9. P. Pellegrini, M. Gacesa, and R. Côté, *Giant formation rates of ultracold molecules via Feshbach Optimized Photoassociation.* Accepted in Phys. Rev. Lett.
10. P. Pellegrini and R. Côté, *Probing the unitarity limit at low laser intensities.* Submitted to Phys. Rev. Lett..
11. E. Kuznetsova, P. Pellegrini, R. Côté, M.D. Lukin, and S.F. Yelin, *Formation of deeply bound molecules via chainwise adiabatic passage.* Accepted in Phys. Rev. A.

Exciton Fine Structure in CdSe Nanocrystals Revealed by High Magnetic Field and Single-Dot Spectroscopies

Scott Crooker & Victor Klimov
National High Magnetic Field Laboratory (MS-E536) & Chemistry Division (MS-J567)
Los Alamos National Laboratory; Los Alamos, New Mexico 87545
crooker@lanl.gov & klimov@lanl.gov

1. Program Scope

Semiconductor quantum dots are often regarded as model candidates for spin-based "qubits" – the building blocks of quantum computing – due to their discrete, atomic-like density of states, the relative ease of generating single spin-polarized electrons per dot, and the long lifetimes and coherence times of these spins. In quantum dots grown by molecular beam epitaxy, prototype designs for generating, manipulating, and detecting coherent superpositions of electron and/or exciton spin states have been recently reported and have attracted considerable interest. In this project we investigate electron spin and exciton spin phenomena in *nanocrystal quantum dots* (NQDs) grown by colloidal chemistry, which provides an alternative route toward quantum-confined charges and spins in semiconductors. In contrast with epitaxially-grown dots, NQDs are nearly spherical in shape and generally provide much stronger quantum confinement (radii down to 10 Å), and are free from the straining influence of an adjacent substrate. Importantly, colloidal NQDs can also be chemically assembled, post-synthesis, into two- and three dimensional functional structures, with sizes and shapes flexibly controlled during growth. Using the ultrahigh magnetic fields available at the National High Magnetic Field Laboratory, we perform polarization-resolved magneto-optical spectroscopy of NQD ensembles to study the spin structure of the ground-state exciton. We also use magnetic fields in conjunction with single-dot spectroscopy to investigate Zeeman energies and spin-polarized exciton states in individual CdSe nanocrystals. And finally, magnetic circular dichroism studies are used to reveal magnetic exchange coupling in magnetically-doped core/shell nanocrystals.

2.1 Recent Progress I: Revealing exciton fine structure in CdSe nanocrystals

Of particular interest for quantum information processing are entanglement schemes that exploit the distinct exciton eigenstates that occur naturally in quantum dots due to shape anisotropy (elongation) of the dot, and its associated anisotropic exchange. This anisotropy mixes the lowest optically-allowed (spin ±1) bright excitons, giving a 'fine structure' of two eigenstates, $|X,Y\rangle = (|+1\rangle \pm |-1\rangle)/\sqrt{2}$, that are linearly and orthogonally polarized. In these first experiments we demonstrated the existence of an |X,Y> bright exciton fine structure in CdSe NDQ ensembles through the use of ultrahigh magnetic fields **B** to 33 Tesla. When the magnetic Zeeman energy ($g\mu_B B$) exceeds any fine-structure splitting of bright excitons (Δ_{XY}), the |X> and |Y> states evolve into eigenstates quantized along **B**, which couple to circularly

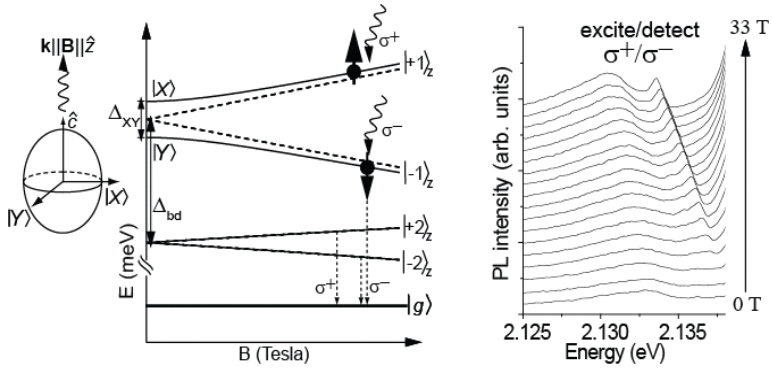

Figure 1. Revealing an intrinsic |X,Y> fine structure of bright excitons in CdSe nanocrystals by using ultrahigh magnetic fields.

polarized light. The exciton eigenenergies do not evolve linearly with B but rather as $\pm\frac{1}{2}\sqrt{\Delta_{XY}^2+(g\mu_B B)^2}$, as depicted in Figure 1. In an ensemble of NQDs, monitoring the energy difference between these levels provides a measure of the average characteristic fine-structure splitting of bright excitons. In these studies we resonantly excite (and selectively analyze emission from) spin-up or spin-down excitons. At magnetic fields exceeding ~10 T, the resonant emission spectra develop a narrow, circularly polarized peak due to spin-flipped bright excitons, as shown in Figure 1. Its evolution with magnetic field directly reveals a large (1-2 meV), intrinsic fine-structure splitting of bright excitons, due to anisotropic exchange. The magnitude of the fine structure splitting scales inversely with the nanocrystal volume, in agreement with theories that ascribe Δ_{XY} in these wurtzite NQDs to long-range, anisotropic electron-hole exchange interaction.

2.2 Recent Progress II: Magneto-optical spectroscopy of single nanocrystals

In parallel with our high-field studies of nanocrystal ensembles, we have also focused on spectroscopy from individual nanocrystals. We have recently measured for the first time the circularly-polarized photoluminescence from *individual* CdSe nanocrystals in applied magnetic fields. As shown in the data of Figure 2, single nanocrystals having a small bright exciton fine structure splitting (Δ_{XY}<0.5 meV) exhibit a 'conventional' left- and right-circularly polarized Zeeman PL doublet in applied magnetic fields, allowing a measurement of the exciton *g*-factor in single colloidal nanocrystals. In contrast, nanocrystals with large Δ_{XY} (>1 meV) show a highly anomalous magneto-PL polarization, wherein the lower-energy peak becomes circularly polarized with increasing field, while the higher-energy peak *remains linearly polarized*. This unusual behavior arises from strong mixing between the absorbing and emitting bright exciton levels due to strong anisotropic exchange interactions, and a theoretical model of these effects is found to be in good agreement with the experimental data.

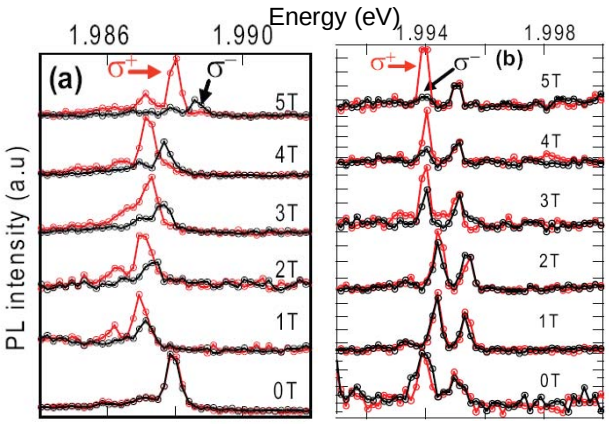

Figure 2. Circularly-polarized magneto-PL from *single* CdSe NQDs at 4K, from 0-5 T. a) This dot shows no intrinsic |XY> fine structure, and develops a 'conventional' Zeeman spltting. b) This dot has an intrinsic |XY> fine structure (clearly visible as two peaks at B=0), and exhibits a correspondingly anomalous circular polarization in applied magnetic field.

To perform these experiments we built a low-temperature, single-dot magneto-PL system that allows for simultaneous detection of both orthonormal PL polarization components. This system largely mitigates the undesirable effects of PL line wandering (spectral diffusion) and intensity fluctuations (blinking) that are typical in single-NQD studies. Dilute dispersions of CdSe/ZnS core/shell NQDs in polymethylmethacrylate are deposited onto quartz substrates (<0.5 nanocrystals/μm^2), and mounted in a 4 K optical cryostat in the room-temperature bore of a 5 T superconducting magnet. The NQDs are excited by a continuous wave 532 nm laser through a 40X objective (0.4 numerical aperture), and PL from individual NQDs is collected by the same objective. A quarter-wave plate then converts right- and left-circularly polarized PL to horizontal- and vertical polarizations, which are then spatially separated by a Wollaston prism and directed through an imaging spectrometer onto the upper and lower halves of a cooled charge-coupled device. In this way, both σ^+ and σ^- PL spectra are acquired simultaneously.

2.2 Recent Progress III: Tunable magnetic interactions in Mn-doped nanocrystals

Magnetic doping of semiconductor nanostructures is actively pursued for applications in magnetic memory and spin-based electronics. Central to these efforts is a drive to control the interaction strength between carriers (electrons and holes) and the embedded magnetic atoms. In this respect, colloidal nanocrystal *heterostructures* provide great flexibility via growth-controlled 'engineering' of electron and hole wavefunctions within individual nanocrystals. We have very recently demonstrated a widely tunable magnetic *sp-d* exchange interaction between electron-hole excitations (excitons) and paramagnetic manganese ions using 'inverted' core-shell nanocrystals composed of Mn^{2+}-doped ZnSe cores overcoated with undoped shells of narrower-gap CdSe (see Fig. 3). Magnetic circular dichroism studies reveal giant Zeeman spin splittings of the band-edge exciton that, surprisingly, are tunable in both magnitude *and sign*. Effective exciton *g*-factors are controllably tuned from -200 to +30 at low temperatures solely by increasing the CdSe shell thickness, demonstrating that strong quantum confinement and wavefunction engineering in heterostructured nanocrystal materials can be utilized to manipulate carrier-Mn^{2+} wavefunction overlap *and* the *sp-d* exchange parameters themselves.

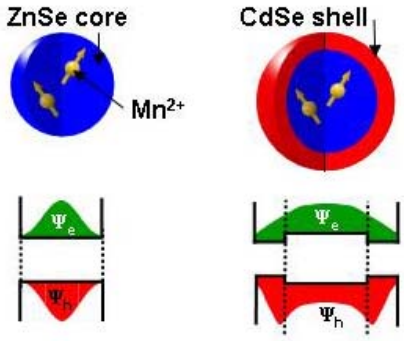

Figure 3. Mn^{2+}-doped ZnSe/CdSe 'inverted' core/shell nanocrystals, which allow for electron and hole wavefunction engineering.

While magnetically-doped monocomponent NCs are well established, wavefunction engineering using magnetic multi-component colloidal *heterostructures* has not been extensively explored. One new class of NC heterostructure that holds promise for tuning *sp-d* exchange interactions are 'inverted' core-shell designs, wherein wide-gap semiconductor cores are overcoated with narrower-gap shells. With increasing shell thickness, the electron and hole envelope wavefunctions, $\Psi_{e,h}(\boldsymbol{r})$, migrate towards the NC periphery (albeit at different rates), thus tuning their overlap with magnetic atoms located, for example, in the core alone (Fig. 3). We investigated precisely this type of wavefunction engineering and exchange interaction control using 'inverted' ZnSe/CdSe core/shell NCs whose cores are doped with paramagnetic, spin-$\frac{5}{2}$ Mn^{2+} ions. Magnetic circular dichroism spectroscopy at the NC absorption edge reveals a giant *sp-d* exchange interaction that *inverts sign* with increasing shell thickness as shown in Figure 4, suggesting confinement-induced sign inversion of the electron-Mn^{2+} exchange constant, α, accompanied by significant reduction of the hole-Mn^{2+} overlap due to wavefunction engineering.

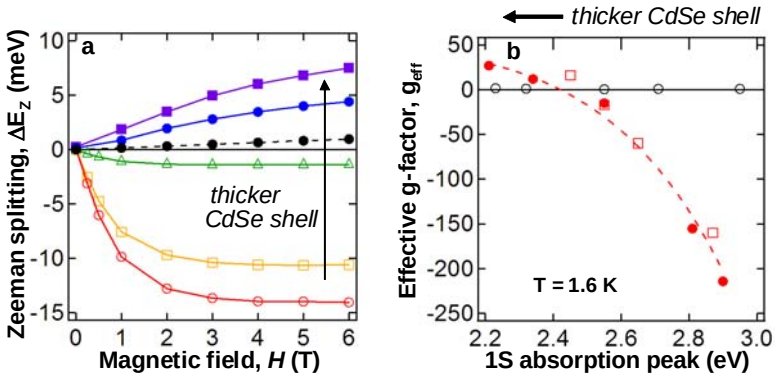

Fig. 4. The measured Zeeman splitting and effective exciton *g*-factor in Mn-doped inverted ZnSe/CdSe core/shell nanocrystals. Note inversion of magnetic *sp-d* exchange interaction when CdSe shell thickness>2 Å.

3. Future Plans

Our future work will focus on bringing these two parallel research efforts together, so as to enable polarization-resolved magneto-optical spectroscopy of *single nanocrystals* that contain *single* Mn^{2+} *ions*. In this way we aim to investigate how individual electron-hole excitations interact with individual magnetic spins in single nanocrystals. Both aspects of this planned work (single-dot spectroscopy, and doping of nanocrystals ensembles having - statistically - one Mn^{2+} ion/dot) have already been demonstrated as described above. A primary aim of these studies is to utilize the emission from these individual nanocrystals to "read out" the spin orientation of the single Mn^{2+} atom, by taking advantage of the large *sp-d* exchange interaction in these systems wherein the Mn^{2+} spin orientation directly influences the emission energy of photoexcited excitons. A second aspect of our future work will focus on disentangling the relative contributions of the electron-Mn^{2+} (*s-d*) exchange interaction from the hole-Mn^{2+} (*p-d*) exchange interaction in Mn^{2+}-doped nanocrystals, through the use of core-shell nanocrystal heterostructures and careful wavefunction engineering. By localizing the electron and hole wavefunctions $\Psi_{e,h}(\boldsymbol{r})$ in different parts of the nanocrystal (core versus shell, for example), it will be possible to isolate the effects of the *s-d* (or *p-d*) exchange interaction alone if the Mn^{2+} spins are embedded in, e.g., only the core. These new structures will permit an investigation of the effects of quantum confinement on the exchange parameters themselves

4. Publications

[1] M. Furis, H. Htoon, M. A. Petruska, V. I. Klimov, T. Barrick, and S. A. Crooker, Bright exciton fine structure and anisotropic exchange in CdSe nanocrystal quantum dots. *Phys. Rev. B Rapid Comm.* **73**, 241313 (2006).

[2] M. Furis, J. A. Hollingsworth, V. I. Klimov, and S. A. Crooker, Time- and polarization-resolved optical spectroscopy of colloidal CdSe nanocrystal quantum dots in high magnetic fields. *Journal of Physical Chemistry B* **109**, 15332 (2005).

[3] H. Htoon, M. Furis, S. A. Crooker, S. Jeong, and V. I. Klimov, Linearly-polarized 'fine-structure' of the bright exciton state in individual CdSe nanocrystal quantum dots, *Physical Review B* **77**, 035028 (2008).

[5] H. Htoon, M. Furis, S. A. Crooker, S. Jeong, Al. L. Efros, and V. I. Klimov, Magneto-photoluminescence of single CdSe nanocrystal quantum dots: Anisotropic exchange and anomalous circular polarization. *Under review.*

[4] D. A. Bussian, S. A. Crooker, M. Yin, M. Brynda, Al. L. Efros, and V. I. Klimov, Tunable magnetic interactions in Mn-doped inverted core-shell ZnSe/CdSe nanocrystals. *Under review.*

Optical Two-Dimensional Spectroscopy of Disordered Semiconductor Quantum Wells and Quantum Dots

Steven T. Cundiff
JILA, University of Colorado and NIST, Boulder, CO 80309-0440
cundiff@jila.colorado.edu

July 16, 2008

Program Scope: The goal of this program is to implement optical 2-dimensional Fourier transform spectroscopy and apply it to electronic excitations, including excitons, in semiconductors. Specifically of interest are quantum wells that exhibit disorder due to well width fluctuations and quantum dots. In both cases, 2-D spectroscopy will provide information regarding coupling among excitonic localization sites.

Progress: During the last year, our efforts have focused on developing a new apparatus with improved performance and capabilities. The apparatus is now working and routinely generating 2D Fourier transform spectra. We have begun studying quantum wells that display inhomogeneous broadening due to disorder and localized states in natural quantum dots. We also demonstrated a new 2D Fourier transform technique that can isolate Raman coherences.

In an inhomogeneously broadened system, the homogeneous linewidth cannot be determined from a linear spectrum, but rather requires the use of a nonlinear technique. The ability to determine the homogeneous linewidth was a motivation for using transient four-wave-mixing (TFWM), which can produce a photon-echo, to study semiconductor nanostructures. However the decay of the TFWM signal depends on whether or not the sample is inhomogeneously broadened, which can lead to ambigiuity in some cases. Furthermore, interference effects can cause the TFWM signal to decay anomalously fast [1].

Our theory collaborators in Marburg showed that it was possible to unambiguously and simultaneously determine both the homogeneous and inhomogeneous linewidths from the 2D Fourier transform spectra [H]. Our original experimental 2D spectra showed very little inhomogeneous broadening because the high excitation density and the free-carriers excited because of the large bandwidth of the incident pulses, both of which increases the dephasing rate and tends to "homogenize" the sample. By improving our signal-to-noise ratio, we were able to lower the excitation density and obtain spectra that showed a larger inhomogeneous linewidth than the inhomogeneous width [J]. Interestingly, these results showed that the inhomogeneous width of the light-hole exciton is less than that of the heavy-hole exciton. We tentatively attribute this result to the differences in their Bohr radii, which changes how they sensitive they are to disorder.

We are also working with a theory group at UC-Irvine. This collaboration produced a theoretical analysis of the 2D spectra using double sided Feynman diagrams [F]. The Feynman diagram analysis led to the insight that the spectrum $S_I(\tau, \omega_T, \omega_t)$ isolates Raman coherences as individual peaks. Raman coherences are non-radiative coherences that are established between two states of similar energy, for example the heavy and light hole excitons. We implemented the ability to measure this spectrum and acquired spectra that are consistent with the theory [K].

During the last year, we have developed a new apparatus for taking optical 2D Fourier transform spectra. There were three motivations for developing this apparatus: (i) Measuring the long dephasing times of localized states requires long delays and high stability; (ii) Probing two-quantum coherences requires all three excitation pulses to be phase locked; (iii) Decomposition into real and imaginary parts for cross-polarized and two-quantum spectra requires a technique other than comparison to spectrally-resolved transient absorption.After careful consideration, we concluded that the original apparatus could not meet these requirements, or that the modifications were so extensive that it would be equivalent to rebuilding the apparatus. Thus we decided the best approach was to build a new apparatus that would incorporate many "lessons learned" over the several years of using the original setup.

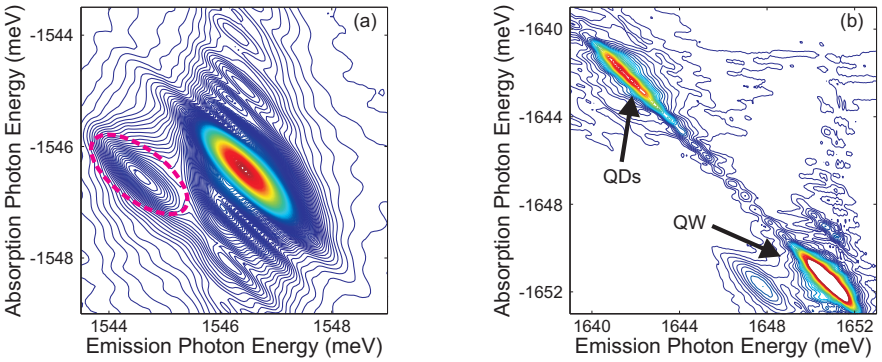

Figure 1: 2D Fourier transform spectra taken with the new apparatus. For both spectra, the excitation pulses are co-linearly polarized. (a) HH exciton resonance for excitation by narrow band pulses at low density. Inhomogeneous broadening due to well width fluctuations and the inhomogeneously broadened biexction resonance (dashed circle) are evident . (b) Natural quantum dot sample showing resolution limited diagonal feature due to QDs. Both spectra are taken at a sample temperature of 5K.

The second motivation actually influenced our design the most, so it will be discussed first. Two-quantum pathways are in a coherence during all time periods, thus all delays must be interferometrically stabilized. Locking both excitation delays in our original apparatus could not be easily implemented. However we realized that it was possible to lock four pulses together (3 delays) by building a nested interferometer. This design consists of an interferometer where each of the arms was itself an interferometer similar to the one that we used to lock the delay between the first two pulses in the original apparatus. Once the interferometers in each of the arms was locked, then they could be locked together. While only three phase locked pulses are required to excite the sample, we realized that the fourth pulse could be put to use in optically determining the overall phase of the signal.

Clearly the new apparatus would need to be very stable. The long dephasing times of quantum dots means that small phase fluctuations would result in unacceptable broadening of the corresponding very narrow spectral features. The use of nested interferometers also puts stringent requirements on the stability. Rather than build the apparatus up from an optical table as normal, we instead built it using thick cast aluminum plates that were machined to allow the translation stages to recessed into them. There are two plates, each of which was a single interferometer to generate a pulse pair. One of these plates was flipped upside down on top of the other, making the entire apparatus very compact and reducing the length of the beam paths between the two interferometers.

As a first test of the new apparatus, we examined a 4 layer 10 nm GaAs/AlGaAs quantum well. We also added a band pass filter, between the laser and the 2D apparatus to excite only the hh exciton and avoid creating lh excitons or, more importantly, free electron hole pairs. The intrinsic stability of the new apparatus allowed us to go to lower excitation density than before. At lower excitation density and no free electrons, the excitation induced dephasing was greatly reduced. The heavy hole exciton peak was strongly elongated along the diagonal due to inhomogeneous broadening from well width fluctuations (see Fig. 1(a)).The observation of a diagonally elongated exciton peak is significant as it means that many-body interactions among excitons localized on different sites are minimal. Interactions among localized excitons has been the subject of some controversy [2].

In addition to seeing inhomogeneous broadening of the hh exciton, we also saw a clear inhomogeneously broadened biexciton peak. Previously, we had seen evidence for biexcitons as a low energy shoulder along the emission axis for cross-polarized excitation [G]. This spectrum is the first time we have seen the biexcitonic contribution for co-linearly polarized pulses. It is observable here because the low excitation density and narrow bandwidth result in a narrow enough homogeneous width so that the exciton and biexciton can be resolved. This spectrum shows one of the powerful features of 2D spectroscopy – the exciton peak and biexciton peak are completely resolved in the 2D spectrum, while for an absorption spectrum (projection on left axis) the two peaks would be completely overlapped and for an emission spectrum (projection on bottom axis) they would be partially overlapped. It is not immediately obvious that the biexciton peak in a disordered quantum well should be diagonally elongated. Diagonal elongation shows that

biexcitons are predominately forming from two excitons on the same, or energetically similar, localization sites. In principle, biexcitons could also form from excitons localized on sites with differing energy, which would result in a circular feature, not an diagonally elongated one. The clear separation of the biexciton peak from the exciton peak allows us to measure the biexciton binding energy and the biexciton linewidth as a function of localization energy. We find that the biexciton binding energy varies significantly across the inhomogeneous line. While there was previous evidence that localization increases the biexciton binding energy [3], it was not know that it such a strong effect that the binding energy actually changed significantly within a single disordered quantum well. The strong variation of the binding energy will disrupt rephasing of the inhomogeneity in a photon echo experiment and may explain past observations that the temporal characteristics of the TFWM signal depended on intensity [4] and polarization [5].

As a first attempt to study quantum dots (QDs) using 2DFTS, we chose to look at "natural" QDs, which are localized states in thin quantum wells [6]. The sample was provided by Dr. Gammon from the Naval Research laboratories. It included 5 single quantum wells of decreasing thickness. The narrower wells clearly show two distinct peaks in the photoluminescence spectrum. The higher energy peak is ascribed to "quantum well" states and the lower energy peak is ascribed to "quantum dot" states (note there is a close analogy to the wetting layer and QD states, respectively, in a sample of self-organized quantum dots). We have obtained 2D Fourier transform spectra of all but the thinnest of the quantum wells in the sample.

The 2D Fourier transform spectrum of a narrow quantum well is shown in Fig. 1(b). Two peaks appear along the diagonal, a higher energy peak corresponding to the quantum well states and a lower energy peak due to the quantum dot states. The QD peak is strongly spread along the diagonal, due the size dispersion, and has a resolution-limited cross-diagonal width. The cross diagonal width corresponds to the homogeneous linewidth, which has been found to be 10's of μeV range in single dot photoluminescence studies [6]. We estimate our spectral resolution to be approximately 50 μeV, limited by the pixel size of the CCD camera used to collect the spectral interferograms.

Future Plans: The interplay and competition between many-body interactions and localization of the electronic wavefunction due to structure will be the scientific focus of our work in the near future. Our work to date has focused on the regime where many-body interactions dominate the optical response of semiconductor nanostructures. As the center-of-mass wavefunction of the electron-hole pair becomes increasing localized, whether it be purposeful due to the fabrication of structures that provide three-dimensional confinement or due to inevitable disorder that is inherent to all nanostructures, the effect of many-body interactions diminishes and the electron-hole pairs act more as if they were in an atom rather than as an extended state in a solid. Consequently, quantum dots are often called "artificial atoms" and their optical properties described using transitions between discrete states. However even for quantum dot states, many-body interactions will still occur because excitations can also occur in the surrounding medium [7].

A truly isolated nanostructure is not particularly useful. For example, it must be possible to inject carriers into a nanostructure being used for solid state lighting, similarly it must be possible to extract carriers in solar energy devices, and in more exotic applications such as quantum information, interactions between qubits is required. The injection or extraction of carriers can occur by coupling to continuum states in the surrounding material or to discrete states in other nanostructures, for example tunnel injection in QD lasers [8]. 2DFTS can characterize either type of coupling, and thus provide information that is directly relevant to device performance. Furthermore, 2DFTS can characterize coupling that may not be directly involved in device operation, but may well influence the device operating parameters.

The first step will be to demonstrate a method of determining the overall phase of the 2D spectrum based solely on optical measurements of the excitation and reference beams. Once this method is established, we will be able to concentrate on physics. Understanding how localized excitons interact is an important topic, and thus we will carefully study the best example we have so far for such interactions – the biexcitonic feature in Fig. 1(a). We will also study two-quantum transitions, which provide a new avenue for understanding the interactions between optical excitations in matter. We will apply all of the tools we have developed to study natural quantum dots. We will also try studying self-organized quantum dots, however, we have not yet shown that we can obtain a measurable signal from a self-organized quantum dot sample.

Publication during the last 3 years from this project:

A. T. Zhang, C.N. Borca, X. Li, and S.T. Cundiff, "Optical two-dimensional Fourier transform spectroscopy with active interferometric stabilization," Opt. Express **13**, 7432 (2005).

B. C.N. Borca, T. Zhang, X. Li, and S.T. Cundiff, "Optical two-dimensional Fourier transform spectroscopy of semiconductors," Chem. Phys. Lett. **416**, 311 (2005). (Item

C. X. Li, T. Zhang, C.N. Borca, and S.T. Cundiff, "Many-Body Interactions in Semiconductors Probed by Optical Two-Dimensional Fourier Transform Spectroscopy," Phys. Rev. Lett. **96**, 057406 (2006).

D. I. Kuznetsova, P. Thomas, T. Meier, T. Zhang, X. Li, R.P. Mirin, S.T. Cundiff, "Signatures of many-particle correlations in two-dimensional Fourier-transform spectra of semiconductor nanostructures," Sol. State Commun. **142**, 154 (2007).

E. A. G. V. Spivey and S. T. Cundiff, "Inhomogeneous dephasing of heavy-hole and light-hole exciton coherences in GaAs quantum wells," J. Opt. Soc. Am. B **24**, 664 (2007).

F. L. Yang, I. V. Schweigert, S. T. Cundiff, and S. Mukamel, "Two-dimensional optical spectroscopy of excitons in semiconductor quantum wells: Liouville-space pathway analysis," Phys. Rev. B **75**, 125302 (2007).

G. T. Zhang, I. Kuznetsova, T. Meier, X. Li, R.P. Mirin, P. Thomas and S.T. Cundiff, "Polarization-dependent optical 2D Fourier transform spectroscopy of semiconductors," Proc. Nat. Acad. Sci. **104**, 14227 (2007).

H. I. Kuznetsova, T. Meier, S.T. Cundiff, and P. Thomas, "Determination of homogeneous and inhomogeneous broadening in semiconductor nanostructures by two-dimensional Fourier-transform optical spectroscopy," Phys. Rev. B **76**, 153301 (2007).

I. A. G. V. Spivey, C. N. Borca and S. T. Cundiff, "Correlation coefficient for dephasing of light-hole excitons and heavy-hole excitons in GaAs quantum wells," Solid State Commun. **145**, 303 (2008).

J. I. Kuznetsova, P. Thomas, T. Meier, T. Zhang, and S. T. Cundiff,"Determination of homogeneous and inhomogeneous broadenings of quantum-well excitons by 2DFTS: An experiment-theory comparison," to appear in Physica Status Solidi (c) (2008).

K. L. Yang, T. Zhang, A.D. Bristow, S.T. Cundiff and S. Mukamel, "Isolating excitonic Raman coherence in semiconductors using two-dimensional correlation spectroscopy," submitted to J. Chem. Phys. (2008).

References

[1] S. T. Cundiff, M. Koch, W. H. Knox, J. Shah, and W. Stolz, "Optical coherence in semiconductors: Strong emission mediated by nondegenerate interactions," Phys. Rev. Lett. **77**, 1107–1110 (1996).

[2] A. Euteneuer, E. Finger, M. Hofmann, W. Stolz, T. Meier, P. Thomas, S. W. Koch, W. W. Rühle, R. Hey, and K. Ploog, "Coherent excitation spectroscopy on inhomogeneous exciton ensembles," Phys. Rev. Lett. **83**, 2073–2076 (1999).

[3] T. F. Albrecht, K. Bott, T. Meier, A. Schulze, M. Koch, S. T. Cundiff, J. Feldmann, W. Stolz, P. Thomas, S. W. Koch, and E. O. Göbel, "Disorder mediated biexcitonic beats in semiconductor quantum wells," Phys. Rev. B **54**, 4436–4439 (1996).

[4] M. D. Webb, S. T. Cundiff, and D. G. Steel, "Observation of time-resolved picosecond stimulated photon-echoes and free polarization decay in GaAs/AlGaAs multiple quantum-wells," Phys. Rev. Lett. **66**, 934–937 (1991).

[5] S. T. Cundiff, H. Wang, and D. G. Steel, "Polarization-dependent picosecond excitonic nonlinearities and the complexities of disorder," Phys. Rev. B **46**, 7248–7251 (1992).

[6] D. Gammon, E. Snow, B. Shanabrook, D. Katzer, and D. Park, "Homogeneous linewidths in the optical spectrum of a single gallium arsenide quantum dot," Science **273**, 87–90 (1996).

[7] H. Schneider, W. Chow, and S. Koch, "Many-body effects in the gain spectra of highly excited quantum-dot lasers," Phys. Rev. B **64** (2001).

[8] P. Bhattacharya, S. Ghosh, S. Pradhan, J. Singh, Z. Wu, J. Urayama, K. Kim, and T. Norris, "Carrier dynamics and high-speed modulation properties of tunnel injection InGaAs-GaAs quantum-dot lasers," IEEE J. Quantum Electr. **39**, 952–962 (2003).

July 2008

Theoretical Investigations of Atomic Collision Physics

A. Dalgarno

Harvard-Smithsonian Center for Astrophysics
Cambridge, MA 02138
adalgarno@cfa.harvard.edu

The research develops and applies theoretical methods for the interpretation of atomic, molecular and optical phenomena and for the quantitative prediction of the parameters that characterize them. The program is responsive to experimental advances and influences them. A particular emphasis has been the study of collisions in ultracold atomic and molecular gases.

There is considerable experimental interest in collisions of ytterbium atoms and ions in cold ytterbium gas and we have initiated a theoretical study of them. Ion-atom scattering at low and ultralow temperatures is dominated by the long range interaction which for an atom in a state of zero orbital angular momentum decreases at large internuclear distances R as C_4R^{-4} where $C_4 = -\alpha/2$, α being the static electric polarizability of the neutral atoms. We have tried a variety of theoretical methods for calculating alpha including full four-component and approximate relativistic models. Our recommended polarizability is 143 atomic units, a value consistent with other published values to within their probable error. Atom-atom scattering is controlled at ultralow temperatures by the long range van der Waals interaction which varies as the inverse sixth power of R if at least one of the atoms is in an S state. An estimate of the coefficient C_6 can be obtained from the polarizability calculations using the Cauchy moments from linear coupled cluster theory. We found that C_6 = 2062(200) atomic units.

We decided to employ several of the other available methods for directly calculating C_6 to try to assess their accuracy when applied to a complex atom like ytterbium. After extensive experimentation, we concluded that high precision could be obtained for Yb-Yb using time-independent linear response coupled cluster theory. Our recommended theoretical value is 2070 atomic units to within a probable error of 10%. Other calculations yield values in the range from 2400 to 2800 atomic units. There are two empirical estimates. Enomoto et al. derive C_6 = 2300 (250)from an analysis of photodissociation spectra and Kitigawa et al. derive C_6 = 1932(30)from a fitting of the vibrational level structure of Yb_2.The agreement is satisfactory but could perhaps be improved by including the Casimir force in the model potential used in the fit. With this in mind, we calculated the Casimir potential. We also evaluated the next term in the interaction, C_8R^{-8}. We predict $C_8 = 20.23 \times 10^4$ atomic units compared to the empirical $19(5) \times 10^4$ atomic units of Kitigawa et al. We have in progress a full ab initio quantum chemistry calculation of the entire potential energy of the ground state of Yb_2^+.

Measurements of the cross sections of charge exchange in collisions between ^{174}Yb and ^{172}Yb+ are being carried out by Grier et al. The charge exchange cross sections depend on the potential energy curves of the lowest Σ_g and Σ_u states of the molecular ion Yb_2^+. We have used elaborate quantum chemistry codes to compute the potentials taking particular care to achieve sufficient accuracy to ensure the potentials behave correctly at large distances. The polarizability derived from fitting the long range form agrees with the polarizability of 143 atomic units we had calculated earlier. We have computed the cross sections for elastic

scattering and for charge exchange scattering, initially neglecting the small change in energy that arises because of the different ionization energies of the different isotopes. However the difference though small has profound consequences at ultralow energies. Theoretically there occurs a radial coupling of the electronic and nuclear motion which depends on the isotope masses and there is a failure of the Born-Oppenheimer approximation. We explored ways of generalizing the conventional theories and constructed a method which took into account mass-dependent adiabatic corrections and scaling to ensure the correct energies were reproduced. The fundamental data are available for the case of H+ colliding with D and there are earlier calculations of the cross sections at energies above 10^{-5} eV that provided a check. The scattering length is a complex number. For the real part we obtained 15.3 a.u. and for the imaginary part 30.6 a.u. The imaginary part corresponds to a rate coefficient at zero temperature of 1.9×10^{-9} cm^3s^{-1}. The cross section for charge exchange of H^+ with D follows Wigner's law below 10^{-6} eV. We are now engaged in a study of the nuclear-electronic coupling for the isotopes of Y_b^+.

The ab initio quantum chemistry calculations become inaccurate at large R because they involve the subtraction of two large numbers to derive a small number. Because charge exchange is sensitive to the difference of the gerade and ungerade states of the molecular ion it poses a still more severe problem. The Holstein-Herring formula may offer a procedure for overcoming the difficulties. It expresses the difference of the two potentials as a direct integral and is valid at large R where the variational methods fail. We have extended a formula due to Bardsley et al. and we are testing it by comparison with some model potential data for Cs^+-Cs.

Theoretical and experimental studies of cold collisions of spin-polarized metastable hydrogen H(2s) atoms have been performed. The computed trap loss rate coefficients are a factor of two to three times larger than the measured values and show little variation with temperature where the experiments indicate a significant increase. The trap loss may occur by single and double charge transfer and by associative and Penning ionization. The theory omits a coupling term arising from interaction with the doubly excited autoionizing states separating to the H(n=2) + H(n'=2) product states. The theory also used the coupled states approximation to solve the scattering equations. We extended the calculations to include the coupling and a more complete description of the scattering but the discrepancies persisted. The results are useful nevertheless in indicating the relative magnitudes of the several channels that contribute to the quenching of the metastable atoms.

Because of its astrophysical significance the rotational excitation of carbon monoxide by hydrogen atoms has been investigated in many papers. It was accepted that the rate coefficients obtained with a potential surface that was consistent with the spectroscopic data on HCO were reliable. However the rate coefficients departed significantly from the expected propensity rule that emphasizes even changes in the rotational excitation transitions. A group that had been involved in the calculations of potential energy surfaces and scattering calculations assembled to try to resolve the apparent contradiction, With improved potential energy surfaces particularly at large distances we found that the original results that were consistent with the even j propensity rule were correct. We also found that the cross sections are sensitive to the fine details of the interaction.

In plasmas created by photodissociation or photoionization or particle bombardment the ions and atoms are often initially energetic with energies of the order of electron volts. The hot atoms may participate in chemical reactions that are otherwise inaccessible. There may occur a hot atom chemistry with unique consequences. Their

significance depends on the rate at which they thermalize. The possibilities have been explored but with an assumption that the thermalization is complete after some small number of collisions. There appears to have been no systematic exploration of the thermalization process. At best the discussions adopt a thermalization cross section but no prescription is advanced for its definition or calculation except to assume hard sphere collisions or to arbitrarily adopt the momentum transfer or diffusion cross section. The studies based on the hard sphere approximation have led to the view that there are clear differences between thermalization in a Rayleigh gas in which the mass of the bath gas atoms is much smaller than the mass of the hot particles and in a Lorentz gas in which the opposite is the case. We have carried out a comprehensive study for energetic nitrogen atoms moving in a thermal bath of helium atoms and of argon atoms. We began by calculating the interaction potentials at a level of accuracy that ensured that at large internuclear distances they tend to the correct van der Waals form. With the actual potentials we computed the energy loss distribution as a function of collision energy and of scattering angle. The distributions are markedly different from those given by the hard sphere approximation and emphasize the importance of small angle collisions. We then set up and solved the time-dependent linear Boltzmann transport equation for the velocity distribution as it evolved from some chosen initial spatially isotropic distribution that corresponded to that occurring in laboratory measurements by Y.Matsumi, T.Nakayama and K.Takahashi in Japan. The theoretical results reproduced the experimental data. The collisions first bring about a bimodal structure but with time the velocity profile becomes Gaussian and remains so until it reaches thermal equilibrium at the bath gas temperature. At least two time scales are needed to characterize the thermalization. One is the time to relax to a Maxwellian shape and the second to cool continuously to the bath temperature. The two stage evolution applies to the Lorentz gas and to the Rayleigh gas. Relaxation proceeds somewhat more efficiently in the heavier bath gas because energy transfer is more rapid in argon than in helium. The scattering is dominated by small angle collisions driven by the long range van der Waals and the energy relaxes through a large number of small energy transfer collisions. The behavior is very different from that predicted by the hard sphere model for which a substantial difference occurs between the heavier and lighter gases.

The thermalization process occurs in experiments in which the bath gas is cold helium and we propose to carry out similar calculations. We received an inquiry from Claudio Lenz Cesar who is interested in the behavior of hot hydrogen atoms in a gas of neon atoms. We have completed calculations of the H-Ne interaction and we are in a position to examine the details of the thermalization. In helium, neon and argon only elastic collisions can occur but in atoms with internal structure and in molecules inelastic collisions contribute to energy loss. We propose to explore the velocity distributions in some such cases. It may be possible to infer the inelastic cross sections from velocity data. In molecular gases chemical reactions may take place and may also provide information about chemical rate coefficients.

Publications 2006-2008

C.M. Dutta, C. Oubre, P. Nordlander, M. Kimura and A. Dalgarno, Charge Transfer Cross Sections in Collisions of Ground State Ca and H^+, Phys. Rev. A 73, 032714 , 2006.

M P.J. van der Loo, G.C. Groenenboom, M. J. Jamieson and A. Dalgarno, Raman Association of H_2 in The Early Universe, Disc. Farad Soc. 133, 43, 2006.

Y. V. Vanne, A. Saenz, A. Dalgarno, R.C. Forrey, P. Froelich and S. Jonsell, Doubly Excited Autoionizing States of H_2 Converging to the H(n=2)+H(n´=2) Limit, Phys. Rev. A 73, 2706, 2006.

A. Dalgarno and M.P.J. van der Loo, Recombination of H_2 by Raman Association in the Early Universe, ApJ Letters, 646 L91, 2006.

E. Abrahamsson, R.V. Krems and A. Dalgarno, Fine Structure Excitation of OI and CI by Impact with Atomic Hydrogen, ApJ 654, 1171, 2007.

Xi Chu, Alexander Dalgarno and Gerrit C. Groenenboom, Dynamic polarizabilities of an eye as he he he and his or her in a atoms and dispersion coefficients for their interaction with helium atoms Phys. Rev. A. 75, 032723, 2007.

P. Zhang, V. Kharchenko and A. Dalgarno, Thermalization of super thermal N(^{4}S) atoms in He and Ar gases, Molec. Phys. 105, 1487, 2007.

G. C. Groenenboom, X. Chu and R.V. Krems, Electronic and Anisotropy between Open Shell Atoms in First and Second Order Perturbation Theory, J. Chem. Phys.126 204306, 2007.

B.C. Shepler, B. H. Yang, T. J. Dhilip Kumar, P.C. Stancil, J. M. Bowman, N. Balakrishnan, P. Zhang, E. Bodo, and A. Dalgarno, Low Energy H+CO Scattering Revisited: CO Rotational Excitation with New Potential Surfaces, A&A 475, L15-L18, 2007.

Peng Zhang and A. Dalgarno Static Dipole Polarizability of Ytterbium, J. Phys. Chem. A, 111, 12471, 2007.

P. Zhang, V. Kharchenko, A. Dalgarno, Y. Matsumi, T. Nakayama and K. Takahashi, Approach to Thermal Equilibrium in Atomic Collisions, Phys. Rev. Lett. 100, 103001, 2008.

E. Bodo, P. Zhang and A. Dalgarno, Ultracold Ion-Atom Collisions: near Resonant Charge Exchange, New J. Phys. 033024, 2008.

P. Zhang and A. Dalgarno, Long-Range Interactions of Ytterbium Atoms Molec. Phys. in press 2008.

Production and trapping of ultracold polar molecules

D. DeMille
Physics Department, Yale University, P.O. Box 208120, New Haven, CT 06520
e-mail: david.demille@yale.edu

Program scope: The goal of our project is to produce and trap polar molecules in the ultracold regime. Once achieved, a variety of physical effects associated with the low temperatures and/or the polar nature of the molecules should be observable for the first time. We will build on recent results from our group, in which we form and trap ultracold RbCs. We plan to transfer the vibrationally excited molecules currently trapped into their absolute internal ground state and then study the resulting sample of polar molecules. We will investigate a variety of techniques for manipulating and probing this sample, including methods for "distilling" a pure ground-state sample, imaging detection, etc.

Our group has pioneered techniques to produce and state-selectively detect ultracold heteronuclear molecules. These methods yielded RbCs molecules at translational temperatures $T < 100$ μK, in any of several desired rovibronic states—including the absolute ground state, where RbCs has a substantial electric dipole moment. Our method for producing ultracold, ground state RbCs consists of several steps. In the first step, laser-cooled and trapped Rb and Cs atoms are bound together into an electronically excited state, via the process known as photoassociation (PA).[1] These states decay rapidly into a few, weakly bound vibrational levels in the ground electronic state manifold.[2] By proper choice of the PA resonance, we form metastable molecules exclusively in the $a\ ^3\Sigma^+$ level. We also demonstrated the ability to transfer population from these high vibrational levels, into the lowest vibronic states $X\ ^1\Sigma^+(v=0,1)$ of RbCs[3] using a laser "pump-dump" scheme. Two sequential laser pulses drove population first "upward" into an electronically excited level, then "downward" into the vibronic ground state. In these initial experiments, the vibronic ground-state molecules were spread over a small number (2-4) of the lowest rotational levels, determined by the finite spectral resolution of the pump/dump lasers. We state-selectively detect ground-state molecules with a two-step, resonantly-enhanced multiphoton ionization process (1+1 REMPI) followed by time-of-flight mass spectroscopy.[4]

In more recent work, we have incorporated a CO_2-laser based 1D optical lattice into our experiments. This makes it possible to trap and accumulate vibrationally-excited RbCs molecules as they are formed. (Previously, the molecules were not subject to the magneto-optic trapping forces that held the atoms.) In this optical trap, we have demonstrated the ability to hold the precursor Rb and Cs atoms with long lifetimes ($\gtrsim$5 s). We also have the ability to selectively remove either atomic species by resonant push-beams. We measure molecule number in individual states, using the same methods as earlier. We used these capabilities to measure inelastic (trap loss) cross-sections for individual RbCs vibrational levels on both Rb and Cs atoms in the ultracold regime.[5] We also developed a simple theoretical model for these collisions which matches our data reasonably well. We hope to observe molecule-molecule collisions in the near future, once molecular densities are fully optimized.

We are now preparing to transfer this sample of trapped molecules to their absolute internal ground state. In this X(v=0, J=0) state the molecules should be immune to all (two-body) inelastic collisional loss processes, and should also possess a sizeable dipole moment (~1.3 D).

To accomplish this, we plan to use an improved version of the method we demonstrated earlier for producing (untrapped) ground-state molecules. A pair of lasers, tuned to the same transitions as used before, will again be used for the transfer. However, here we plan to use a coherent (STIRAP, STimulated Raman Adiabatic Passage) process rather than the incoherent, stepwise method as before. Use of STIRAP is made possible by the small size of our sample and the resulting high Rabi frequencies attainable by tight focusing of single-mode diode lasers. We estimate transfer efficiencies of ~80% should be possible even with "standard" lasers (~0.5 MHz linewidth).

We have carefully considered limitations on STIRAP due to details of the molecular levels due to e.g. hyperfine and rotational structure. We find that high efficiency of ground-state molecule production almost certainly requires full control of all degrees of freedom, including nuclear spins. This analysis was deepened and informed by our recent experiments studying the level structure of deeply-bound Cs_2 ground-state molecules.[6] To address this issue, we now optically pump our trapped atoms to spin-stretched states, and plan to use appropriate laser polarizations and transitions to remain in a stretched state throughout the PA and STIRAP processes. Identification of the correct transitions requires knowledge of the hyperfine structure in each electronic level of the process, and we will use the first STIRAP laser to measure this structure in sufficient detail.

Once we have demonstrated the STIRAP transfer to the ground state, we plan to develop a variety of techniques for manipulating and studying this sample. Among the first questions will be the collisional stability of the ground-state molecules. Of particular concern is loss due to collisions with residual, vibrationally excited molecules. We plan to selectively re-introduce both Rb and Cs atoms to the trap to address this problem: based on our measurements of "maximal" (i.e., unitarity-limited) elastic cross-sections for the vibrationally excited molecules, it appears viable to use a high-density atom cloud as a "scrubber" to eliminate the troublesome species. An interesting side benefit is the possibility to observe chemical reactions between atoms and ground-state molecules (which are allowed only with Rb, not Cs atoms).

We also plan to develop methods for imaging detection of the ground-state molecules. This is far more difficult than for atoms, because of the lack of cyling optical transitions. However, the experience of the community studying quantum-degenerate atomic gases makes it plain that imaging detection is a tool so powerful it must be maintained. Here we plan to build on our experience with REMPI detection, and replace our simple channeltron detector with an imaging ion detection setup (microchannel plate + phosphor screen + fiber optic image conduit + CCD camera).[7] Once this method is established, we can effectively study the variety of interesting two-body and many-body physics associated with polar molecules. These include phenomena such as ultra-long range "field-linked" states of polar molecules in an external electric field,[8] extraordinarily large (~10^8 Å^2) elastic collision rates with nontrivial dependence on the strength of a polarizing electric field,[9,10] many-body states such as liquid-crystal-like chains[11] or dipolar crystals;[12] etc.

References

[1]A.J. Kerman *et al.*, Phys. Rev. Lett. **92**, 033004 (2004).

[2]T. Bergeman *et al.*, Eur. Phys. J. D **31**, 179 (2004).

[3]J.M. Sage, S. Sainis, T. Bergeman, and D. DeMille, Phys. Rev. Lett. **94**, 203001 (2005).

[4]A.J. Kerman *et al.*, Phys. Rev. Lett **92**, 153001 (2004).

[5] Eric R. Hudson, Nathan B. Gilfoy, S. Kotochigova, Jeremy M. Sage, and D. DeMille. Inelastic collisions of ultracold heteronuclear molecules in an optical trap. Phys. Rev. Lett. **100,** 203201 (2008). [DOE SUPPORTED]

[6] D. DeMille, S. Sainis, J. Sage, T. Bergeman, S. Kotochigova, and E. Tiesinga. Enhanced sensitivity to variation of me/mp in molecular spectra. Phys. Rev. Lett. **100**, 043202 (2008). [DOE SUPPORTED]

[7] D.W. Chandler and P.L. Houston, J. Chem. Phys. **87**, 1445 (1987); A.J.R. Heck and D.W. Chandler, Annu. Rev. Phys. Chem. **46**, 335 (1995).

[8]A.V. Avdeenkov and J. L. Bohn, Phys. Rev. Lett. **90**, 043006 (2003); A.V. Avdeenkov, D.C.E. Bortolotti and J.L. Bohn, Phys. Rev. A **69**, 012710 (2004).

[9]D. DeMille, D.R. Glenn, and J. Petricka, Eur. Phys. J. D **31**, 275 (2004).

[10]M. Kajita, Eur. Phys. J. D **20**, 55 (2002); C. Ticknor, Phys. Rev. A **76**, 052703 (2007).

[11] D.-W. Wang, M.D. Lukin, and E. Demler, Phys. Rev. Lett. **97**, 180413 (2006).

[12] H. P. Buechler *et al.*, arXiv:cond-mat/0607294 (2006).

ATTOSECOND AND ULTRA-FAST X-RAY SCIENCE

Louis F. DiMauro
Department of Physics
The Ohio State University
Columbus, OH 43210
dimauro@mps.ohio-state.edu
co-PI: Pierre Agostini (OSU Physics)

1. PROJECT DESCRIPTION

1.1 PROGRESS IN FY08

This document describes the BES funded project (grant #: DE-FG02-04ER15614) entitled "Attosecond & Ultra-Fast X-ray Science" at The Ohio State University (OSU). Over the past few years, we have developed the tools, skills and metrology necessary to conduct the proposed attosecond experiments. Progress over the past year includes (1) implementation of an all-optical method for spectral phase measurements of high harmonic light for fundamental wavelengths as long as 2 μm, (2) construction of an attosecond beamline/end-station for RABBITT phase measurements for attosecond science and (3) design of a 2π magnetic bottle electron spectrometer for use at OSU and the AMOS end-station at the LCLS XFEL at SLAC.

The original proposal outlines an experimental program designed to study high harmonic generation in gases and attosecond synthesis using long wavelength laser sources. The objective is to explore the scaling of the intense laser-atom interaction and provide a potential path towards the production of *light pulses with both the time-scale and the length-scale each approaching atomic dimension*. In other words, the formation of kilovolt x-rays bursts with attosecond (10^{-18} s) duration.

Over the past year we have performed both experimental and theoretical studies that verify the efficacy of this approach. The near future will see the applications of these advances for investigating electron dynamics.

Spectrally resolved high harmonic radiation generated by driving wavelengths of 0.8 μm, 1.3 μm and 2 μm. The high harmonics from various inert gases were explored using different fundamental wavelengths. The 2 μm observations were particularly important since the unique scaling strategy discussed in the proposal exploits the behavior of an atom in long wavelength ($\lambda > 1$ μm) fields. For example, our 2 μm measurements establish that high harmonic generation in argon extends to a photon energy of 220 eV, validating the scaled physics. The findings of this work have been published in Nature Physics in 2008.

Measurement of the wavelength dependence of the attochirp. The above study established that long wavelength fundamental fields can generate a higher photon energy cutoff in the spectrum. However, the critical information needed for complete description of an attosecond pulse is the phase of the different spectral components. In absence of complete characterization, the minimal information set is the relative phase between the adjacent harmonic orders. Various methods based on two-color photoionization have been developed for this measurement. Upon completion, the OSU attosecond beamline/end-station apparatus will have the ability to implement a number of these schemes.

In order to gain some initial insight into the relative phase of the high harmonic spectrum we started measurements using an all-optical method introduced by Dudovich *et al.* [1]. In this measurement, harmonics are generated using a two-color field composed of an intense fundamental field (ω) and a weak

2ω field. The 2ω field is derived using 2nd harmonic generation in a standard nonlinear crystal and sufficiently weak not to cause HHG alone. The two colors have a defined phase relationship that is controlled by introducing a differential optical path length. The spectrum is composed of intense odd-order (H39-H61) harmonics and weaker even-orders (H40-H62). The phase information is obtained by analyzing the relative phase shift in the oscillating amplitude between successive even harmonics orders.

We have demonstrated the efficacy of this method at three different fundamental wavelengths (0.8 μm, 1.3 μm and 2 μm) and on two different inert gas atoms (argon and xenon). This has allowed us to make the first experimental measurement of the attochirp as a function of fundamental wavelength. This work is being prepared for publication in Science.

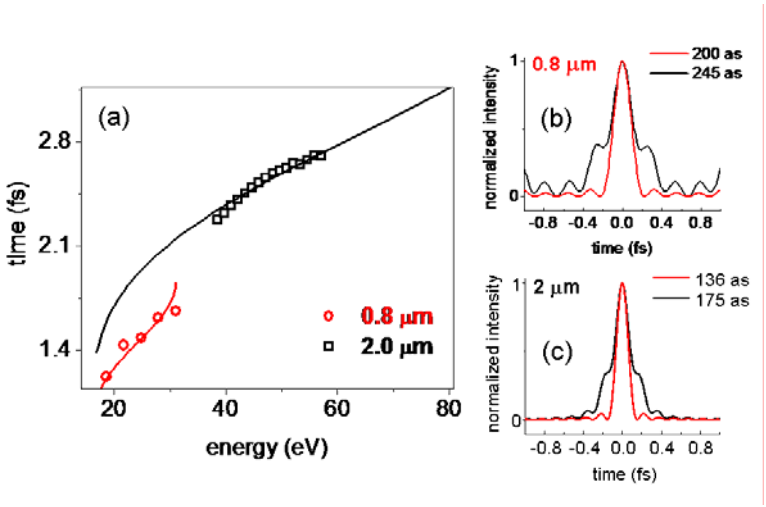

Figure 1: The wavelength dependence of the attochirp. Plot (a) is the emission time as a function of harmonic order for 0.8 μm (red circles) and 2 μm (black squares) fundamental fields at constant intensity. Plots (b) and (c) are the reconstructed pulses (black line) using the phases in (a).

Figure 1 shows that result of our analysis of the attochirp for argon atoms at 0.8 μm and 2 μm. The comparison is performed at constant intensity. Figure 1(a) shows the interpolated recombination time (phase) derived from the all-optical measurement plotted as a function of frequency (harmonic order). The figure is essentially a dispersion plot, and for the two wavelengths shown the dispersion is positive. The attribute to note is that the slope is smaller for the 2 μm fundamental field than 0.8 μm field, e.g. less dispersion. This was the critical feature predicted by us and now has been experimentally verified: longer wavelength fundamental fields produce inherently shorter attosecond burst. Figures 1(b) and (c) are the attosecond pulses reconstructed from the measured phase and amplitude. The results verify the reduction in pulse duration at 2 μm compared to 0.8 μm. Note, the all-optical measurement retrieves the phase in the generation gas source and thus any external dispersion management cannot be measured but the figures does show (red line) the ultimate duration expect with metal filter compensation. The more precise measurement will be performed with the RABBITT method, described in the next section.

OSU attosecond beamline/end-station for RABBITT measurements. The RABBITT method [2], developed by Agostini and collaborators, is a more direct and reliable measurement of the spectral phase. This method was used to measure the first attosecond pulses. The method is a two-color, pump-probe interferometric technique based on photoionization. The spectral phase is directly extracted from the experiment.

The OSU attosecond beamline/end-station will be capable of conducting RABBITT measurements. The apparatus is under construction and operations are expected by November 2008. The apparatus

consists of three vacuum chambers (left to right in Fig. 2): harmonic generation source, XUV focusing and electron spectrometer. The optical system of the apparatus has interferometric stability for attosecond precision.

In the harmonic source chamber, high harmonics are generated in by a high density gas jet interacting with an intense (10^{14} W/cm^2) laser pulse. The size of the harmonic source chamber is sufficient to support a variety of optical geometries and different wavelength (0.8-2 μm) operation. A RABBITT probe beam (yellow beam) is derived by splitting a small fraction (~5 %) of the fundamental beam (red beam).

The differential pumped XUV focusing chamber allows spectral and spatial filtering and contains a toroidal mirror for focusing the harmonic beam (blue) and a spherical mirror for focusing the RABBITT probe beam. Both the focused harmonic and probe beams spatially overlap in the UHV electron spectrometer chamber. The electron spectrometer is a 2π-magnetic bottle design with a 1.5 meter flight tube. This design provides efficient electron collection (2π-angular acceptance) and excellent energy resolution (2-3 %) over a large energy range for the RABBITT measurement. A suitable inert gas atom is leaked into the electron spectrometer for the RABBITT measurement and the attosecond pump-probe delay is introduced by a delay line located in the harmonic source chamber. The electron spectrometer is designed and constructed by a graduate student (Chris Roedig) and will be tested in late August 2008. This spectrometer will be the prototype for a similar instrument for initial experiments at the LCLS XFEL in collaboration with Dr. John Bozek (SLAC).

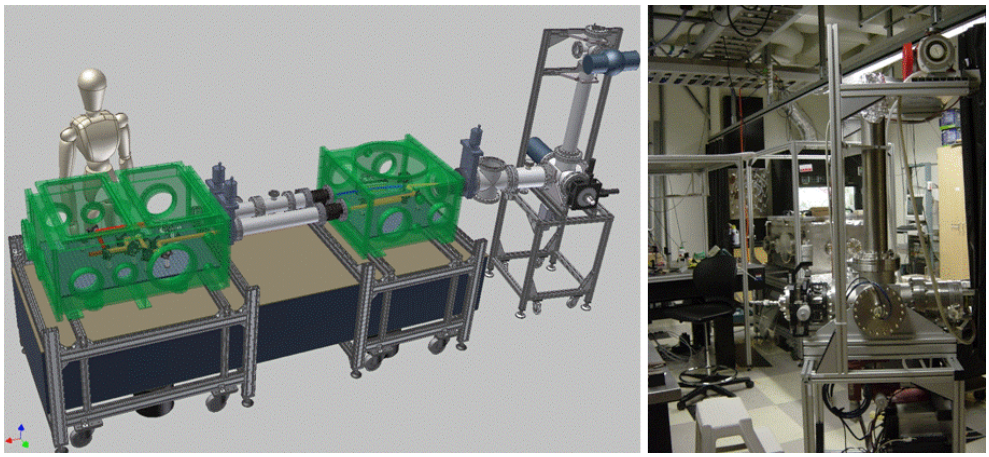

Figure 2: Shown on the left is the CAD layout of the OSU attosecond beamline/end-station apparatus for measuring the spectral phase by the RABBITT method. Shown on the right is the construction as of July 2008. In the foreground is the 2π electron spectrometer while in the background is the harmonic source chamber positioned over the optical table. The toroidal mirror focusing chamber is being fabricated in the OSU physics machine shop.

1.2 PROPOSED STUDIES IN FY09

The following is a brief description of experimental plans in FY09:

1. Finish construction of the OSU attosecond beamline/end-station apparatus.
2. Begin RABBITT measurements on argon using 0.8 μm, 1.3 μm and 2 μm fundamental fields.
3. Begin FROG measurements using the Keldysh scaled systems and compare to current theoretical models of strong-field harmonic generation.

1.3 REFERENCES CITED

[1] N. Dudovich *et al.*, Nature Phys. **2**, 781 (2006).
[2] P. Paul *et al.*, Science **292**, 1689 (2001).

1.4 PUBLICATION RESULTING FROM THIS GRANT

1. L. F. DiMauro, J. Arthur, N. Berrah, J. Bozek, J. N. Galayda and J. Hastings, "Progress Report on the LCLS XFEL at SLAC", J. Phys. **88**, 012058 (2007).
2. P. Colosimo *et al.*, "Scaling strong-field interactions towards the classical limit", Nature Phys. **4**, 386 (2008).
3. O. Guyetand *et al.*, "Complete Momentum Analysis of Multi-Photon Photo-Double Ionization of Xenon by XUV and Infrared Photons", J. Phys. B **41**, 065601 (2008).
4. P. Agostini and L. F. DiMauro, "Atoms in high intensity mid-infrared pulses", Contemp. Phys., in press.

IMAGING OF ELECTRONIC WAVE FUNCTIONS DURING CHEMICAL REACTIONS

Louis F. DiMauro
Department of Physics
The Ohio State University
Columbus, OH 43210
dimauro@mps.ohio-state.edu
co-PIs: Pierre Agostini (OSU Physics) & Terry A. Miller (OSU Chemistry)

1. PROJECT SCOPE

Our research aims to develop experimental methods, and the theory to support them, for imaging electronic dynamics. The ultimate goal is to meet the challenge of "watching" and "clocking" the electron motion during chemical bond breaking. The program is built on two seminal technical advances made over the past few years. The first is the realization of attosecond (10^{-18} s) burst of XUV light (the electronic "clock") and the second is the method of tomographic imaging of the molecular wave function (the detector to "watch"). A novel aspect of our approach is the combination of these techniques using long wavelength light thereby exploiting the fundamental scaling principles of strong-field physics,

2. RECENT PROGRESS

Over the first two years of this project we have developed the tools, skills and metrology necessary to conduct the proposed imaging experiments using high harmonic generation. Achievements include (1) implementation of a new method for spectral phase measurements of high harmonic light for fundamental wavelengths as long as 2 μm, (2) construction of a kilohertz repetition rate pulsed valve for pre-cooling molecules prior to impulsive alignment and harmonic generation and (3) initial construction of an attosecond beamline/end-station for RABBITT phase measurements [1] for tomographic imaging. During the past year, we also began to investigate high harmonic generation from simple liquids, e.g. water, methanol, using ultra-short 3.6 μm pulses, with the aim of developing techniques to explore the feasibility of imaging solution dynamics.

The original proposal outlines an experimental program designed to meet the challenge of “watching” and “clocking” the electron motion during chemical bond breaking. The program is built on recent technical advances. The first is the realization of attosecond (10^{-18} s) bursts of light and the second is tomographic imaging of the molecular wave function (the detector to “watch”). Our approach is to combine these techniques while exploiting the fundamental scaling principles of strong-field physics. Specific achievements are detailed below.

Spectrally resolved high harmonic radiation generated by driving wavelengths of 0.8 μm, 1.3 μm and 2 μm. The high harmonics from various inert gases and nitrogen were explored using different fundamental wavelengths. The 2 μm observations were particularly important since our scaling strategy exploits the behavior of a molecule in long wavelength ($\lambda > 1$ μm) fields. Our 2 μm measurements (published in Nature Physics in 2008) establish that high harmonic generation in argon extends to a photon energy of 220 eV, validating the scaled physics.

Measurement of the harmonic spectral phase using an all-optical technique. Central to the tomographic reconstruction of a molecular orbital image is the measurement of the spectral phase and the high harmonic spectrum as a function of the molecular alignment. We originally proposed to perform these measurements using the RABBITT method, and progress on constructing an apparatus for these measurements will be described in the next section.

To expedite initial insight into the relative phase of the high harmonic spectrum we started measurements using an all-optical method recently introduced by Dudovich *et al.* [2]. In this measurement, harmonics are generated using a two-color field composed of an intense fundamental field

(ω) and a weak 2ω field. Referring to Fig. 1, the 2ω field is derived using 2nd harmonic generation in a standard nonlinear crystal and sufficiently weak not to cause HHG alone. The two colors have a defined phase relationship that is controlled by introducing a differential optical path length (wedges). Figure 1 shows a contour plot of a portion of the argon harmonic spectrum as a function of delay between the two colors (2 μm and 1 μm). The spectrum is composed of intense odd-order (H39-H61) harmonics (saturated scale) and weaker even-orders (H40-H62). The phase information is obtained by analyzing the relative phase shift in the oscillating amplitude between successive even harmonics orders.

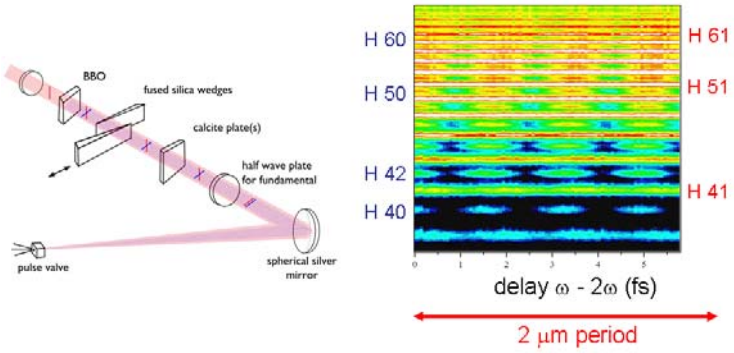

Figure 1: The optical setup used for all-optical spectral phase measurements. A BBO crystal generates a second harmonic pulse. Temporal overlap is realized with birefringent calcite plates and a pair of wedges is used to fine tune the delay. The pulses are focused with a 45 cm mirror on the pulsed valve target. The red and blue lines show the progression of polarization for the ω and 2ω beams, respectively. The contour plot shows the argon harmonic photon energy as a function of delay between an intense 2 μm and weak 1 μm fields.

We have demonstrated the efficacy of this method at three different fundamental wavelengths (0.8 μm, 1.3 μm and 2 μm) and on two different inert gas atoms (argon and xenon). This has allowed us to make the first experimental measurement of the attochirp as a function of fundamental wavelength. This work is being prepared for publication in Science or PRL as part of our DOE attosecond program. We are now ready to apply this all-optical method to impulsively aligned nitrogen molecules. The experiment will first be benchmarked at 0.8 μm before moving towards longer wavelength.

However, our experiments have revealed a number of short comings in this approach which will significantly hamper our progress in ultra-fast tomography. On the practical side, our measured spectral range was limited by the resolution and throughput of our x-ray spectrometer, and not the extent of the harmonic plateau. Furthermore, our set-up's optical loss results in significant reduction in the fundamental pulse energy, limiting harmonic generation. Fundamentally, the phase method depends upon *a priori* knowledge of the harmonic process and thus is model dependent. Our current experiments already show a breakdown in the method at the harmonic cutoff.

OSU attosecond beamline/end-station for RABBITT measurements. As detailed above, a more robust, direct and reliable method for measuring the spectral phase is needed for tomography, especially since *a priori* knowledge of the *molecular* harmonic process may not exist. The RABBITT method [1], developed by Agostini and collaborators, was used to measure the first attosecond pulses. The method is a two-color, pump-probe interferometric technique based on photoionization. The spectral phase is directly extracted from the experiment.

The OSU attosecond beamline/end-station will be capable of conducting RABBITT measurements. The apparatus is under construction and operation is expected later this year. The apparatus consists of three vacuum chambers (left to right in Fig. 2): harmonic generation, XUV focusing and electron spectrometer. The optical system of the apparatus has interferometric stability for attosecond precision.

In the harmonic chamber, molecules exiting from a pulsed valve are aligned by a moderately intense ($10^{12\text{-}13}$ W/cm^2) laser pulse. A delayed, intense (10^{14} W/cm^2) laser pulse interacts with the aligned

molecules generating high harmonics. The polarization of the intense pulse is kept fixed and the polarization of the alignment laser is varied. The size of the harmonic chamber is sufficient to support a variety of optical geometries and different wavelength (0.8-2 μm) operation. A RABBITT probe beam (yellow beam) is derived by splitting a small fraction (~5 %) of the fundamental beam (red beam).

The differential pumped XUV focusing chamber allows spectral and spatial filtering and contains a toroidal mirror for focusing the harmonic beam (blue) and a spherical mirror for focusing the RABBITT probe beam. Both the focused harmonic and probe beams spatially overlap in the UHV electron spectrometer chamber. The electron spectrometer is a magnetic bottle design with a 1.5 meter flight tube. This design provides efficient electron collection (2π-angular acceptance) and excellent energy resolution (2-3 %) over a large energy range for the RABBITT measurement. A suitable gas is introduced into the electron spectrometer for the RABBITT measurement and the attosecond pump-probe delay is introduced by a delay line located in the harmonic chamber.

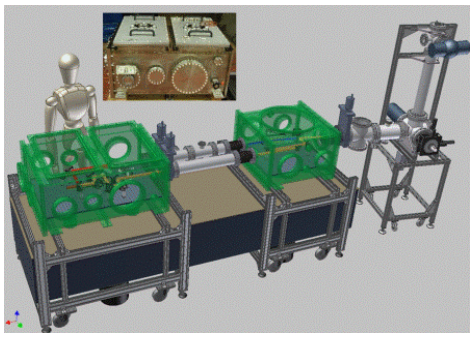

Figure 2: The layout of the OSU attosecond beamline/end-station apparatus for measuring the spectral phase by the RABBITT method. The inset is the newly constructed harmonic chamber.

High harmonics from liquids driven by ultra-fast 3.6 μm pulses. One novel aspect from driving strong field interactions with long wavelength ($\lambda > 3$ μm) laser sources is that the emitted high harmonic radiation falls into the visible and near-UV spectral region. We have begun experiments (see Fig. 3[a]) that exploit this point for investigating harmonics generated from liquids at room temperature, which typically absorb at UV and shorter wavelengths. A wire guided fluid jet creates thin (100-150 μm) flowing samples of various fluids. A 100 fs, 3.6 μm, 1 kHz repetition rate fundamental pulse is focused on the fluid with a maximum intensity of 5×10^{13} W/cm^2. The radiation emitted along the forward direction is analyzed in an optical spectrometer.

The emission in the forward direction is dominated by coherent, odd-order harmonic light. There is no evidence for the more commonly observed super-continuum generation [3]. This may be caused by the thickness of the sample, focusing conditions and material properties which limit nonlinear propagation effects to a minimum. The total nonlinear phase from self phase modulation is less than 1 radian.

Odd harmonics from samples of water, heavy water and several alcohols have been examined. Figures 3(b) and (c) show a quantitative comparison of the spectra obtained from water (H_2O) and isopropyl alcohol (C_3H_8O). The differences in energy per harmonic cannot be explained by bulk transmission properties of the respective fluids. For the collections shown in Fig. 3 the 7th harmonic of C_3H_8O has a peak height 130 times that of H_2O. In addition the conversion of the fundamental field to harmonic is ~10^{-5} for C_3H_8O (5th through 9th harmonic) and ~10^{-7} for H_2O (5th through 11th harmonic).

The data shown in Fig. 3 raises some intriguing questions. In the gas-phase, one envisions the production of harmonics as a field-atom rescattering phenomenon. Here we must consider the fact that the significant electron excursion (~10 nm for an isolated molecule/atom in the presence of the intense 3.6 μm laser field) in a condensed phase system may require concepts such as effective mass, nearest neighbor, and limited band structure [4-5] to describe the molecule-field interaction. These initial and

unexpected results have the potential for transforming how tomographic imaging and ultra-fast dynamics can be performed in condensed phase systems and particularly in chemically relevant environments.

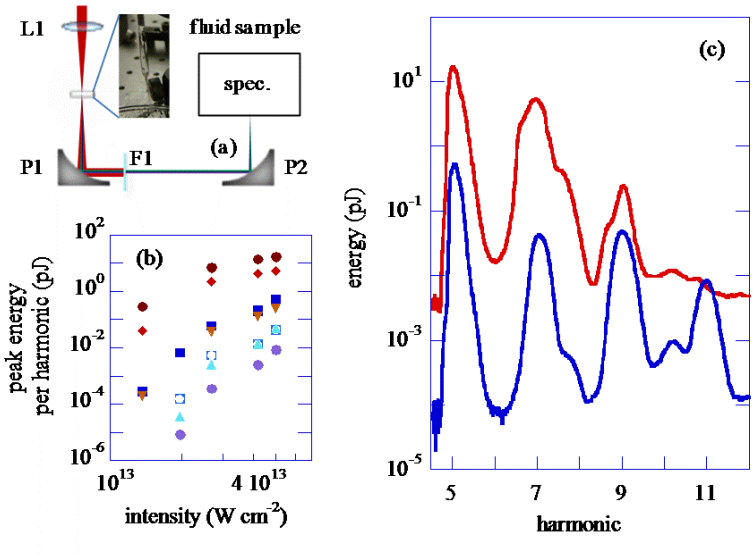

Figure 3: (a) Schematic, not to scale, of the apparatus with a picture of the fluid jet shown in inset. Intensity scaling (b) of the harmonics from H_2O 5th (■), 7th (▫), 9th (▲) & 11th (●) and C_3H_8O 5th (●), 7th (♦) & 9th (▼). (c) Typical wavelength spectra, plotted as harmonic order, of C_3H_8O (red) and H_2O (blue) at 5×10^{13} W/cm^2.

3. Future Plans

In the coming year, we hope to test and compare the degree of molecular alignment using both the static cell and pulsed valve and measure the generated high harmonic spectrum as a function of alignment angle for N_2 molecules using 0.8 μm, 1.3 μm and 2 μm fundamental fields. We will apply the all-optical phase metrology for measuring the phase of high harmonic generation from aligned molecules produced by these wavelengths. We plan to evaluate the RABBITT technique for phase measurement once the OSU attosecond beamline and end-station becomes operational. We plan to continue to study the fundamental physics responsible for high harmonic generation from liquid samples and evaluate the potential for ultra-fast studies in solution dynamics, including chemical reactions.

References Cited

[1] P. Paul *et al.*, Science **292**, 1689 (2001).

[2] N. Dudovich *et al.*, Nature Phys. **2**, 781 (2006).

[3] R. Alfano, *The Supercontinuum Laser Source*, (Springer-Verlag, New York, 1989).

[4] B. M. Smirnov, Phys.-Uspekhi **45**, 1251 (2002).

[5] I. T. Steinberger, J. Chimie Physique et Physico-Chimie Biologique **90**, 681 (1993).

Publications Resulting from this Grant

P. Colosimo *et al.*, "Scaling strong-field interactions towards the classical limit", Nature Phys. **4**, 386 (2008).

P. Agostini and L. F. DiMauro, "Atoms in high intensity mid-infrared pulses", Contemp. Phys., in press.

High Intensity Femtosecond XUV Pulse Interactions with Atomic Clusters

Project DE-FG02-03ER15406
Abstract (Summer 2008)

Principal Investigator:
Todd Ditmire
The Texas Center for High Intensity Laser Science
Department of Physics
University of Texas at Austin, MS C1600, Austin, TX 78712
Phone: 512-471-3296
e-mail: tditmire@physics.utexas.edu

Collaborators: J. W. Keto, B. Murphy and K. Hoffman

Program Scope:

The nature of the interactions between high intensity, ultrafast, near infrared laser pulses and atomic clusters of a few hundred to a few thousand atoms has come under study by a number of groups world wide. Such studies have found some rather unexpected results, including the striking finding that these interactions appear to be more energetic than interactions with either single atoms or solid density plasmas and that clusters explode with substantial energy when irradiated by an intense laser. Under this phase of BES funding we have extended investigation in this interesting avenue of high field interactions by undertaking a study of the interactions of intense extreme ultraviolet (XUV) pulses with atomic clusters. These experiments have been designed to look toward high intensity cluster interaction experiments on the Linac Coherent Light Source (LCLS) under development at SLAC. The goal of our program is to extend experiments on the explosion of clusters irradiated at 800 nm to the short wavelength regime (10 to 100 nm). The clusters studied range from a few hundred to a few hundred thousand atoms per cluster (ie diameters of 1-30 nm). Our studies with XUV light are designed to illuminate the mechanisms for intense pulse interactions in the regime of high intensity but low ponderomotive energy by measurement of electron and ion spectra. This regime of interaction is very different from interactions of intense IR pulses with clusters where the laser ponderomotive potential is significantly greater than the binding potential of electrons in the cluster. With our XUV studies we are mimicing closely the low ponderomotive potential, high intensity short wavelength conditions expected in the focus of the LCLS beam.

We have been conducting these studies by converting a high-energy (1 J) femtosecond laser to the short wavelength region through high order harmonic generation. These harmonics are focused into a cluster jet and the ion and electrons ejected are analyzed by time-of-flight methods. We have been studying van der Waals clusters and are moving toward studies of solid-state clusters, including metallic clusters in the coming year. The latter targets will be studied with an eye toward understanding the consequences of irradiating metal clusters chosen such that the intense XUV pulse rests at a wavelength that coincides with the giant plasma resonance of the cluster.

Progress During the Past Year

During the past year, we concluded a campaign of experiments using our femtosecond laser-driven high harmonic source beamline constructed in the first year of this present funding period. In this campaign we concentrated on studies of XUV driven explosions of noble gas clusters, particularly Xe clusters as these are easy to produce and have been well studied by our group and others when irradiated by intense IR pulses. An illustration of our beam line is shown in figure 1. Production of harmonic radiation is accomplished by

loosely focusing with a MgF f/60 lens the compressed output of the 20 TW, 40 fs THOR Ti:sapphire laser into a jet of argon at 200 psi. We separated the harmonics from the IR by imaging an annular beam mask in the infrared beam before the focusing lens onto an aperture after the focus, taking advantage of the fact that the XUV harmonics have substantially less divergence than the infrared beam. This allows the removal of most of the infrared radiation. To reject scattered infrared light and to pass high harmonics with the energies between 15 eV and 73 eV an additional a 200 nm thin Al filter was used. To select a single XUV harmonic we then employed a specially designed Sc/Si short focal length multilayer mirror optimized for the 21st harmonic at 32.5 eV (38.1 nm) at close to normal incidence. (This mirror was fabricated at the Lebedev Physical Institute in Moscow). The harmonic focus was characterized by a scanning knife edge measurement and an AXUV-10 diode (IRD Inc.). Results from this focal scan are reproduced in figure 2. These data show that we were able to produce an 8µm spot with the 38 nm pulse, yielding a a focal intensity of ~ 10^{11} W/cm^2 assuming an XUV pulse duration of 20 fs.

These harmonics were then focused into the plume of a second, low density Xe cluster jet. This cluster interaction region was located in a separated vacuum chamber. A Wiley McLaren time-of -flight (TOF) spectrometer was used to extract positive ions after photo ionization of the Xe clusters. Typical TOF spectra for various cluster sizes are shown in figure 3. Though the photon energy is sufficient only to ionize electrons by direct photo ionization up to Xe^{3+}, in fact we observe strong signal in charge states up to Xe^{5+} and a small number of charge states up to Xe^{+8} at the largest cluster sizes. Similar charge states were reported earlier from measurements performed at the DESY FEL at longer wavelength but at two-orders oif magnitude higher intensity [1]. The authors of that paper interpreted the high charge states accompanied by high kinetic ion energies in the keV range as a result of cluster disintegration by Coulomb explosion. We, however, believe that these high Xe charge states result from electron collisional ionization in a warm nanoplasma created by XUV irradiation of the Xe cluster.

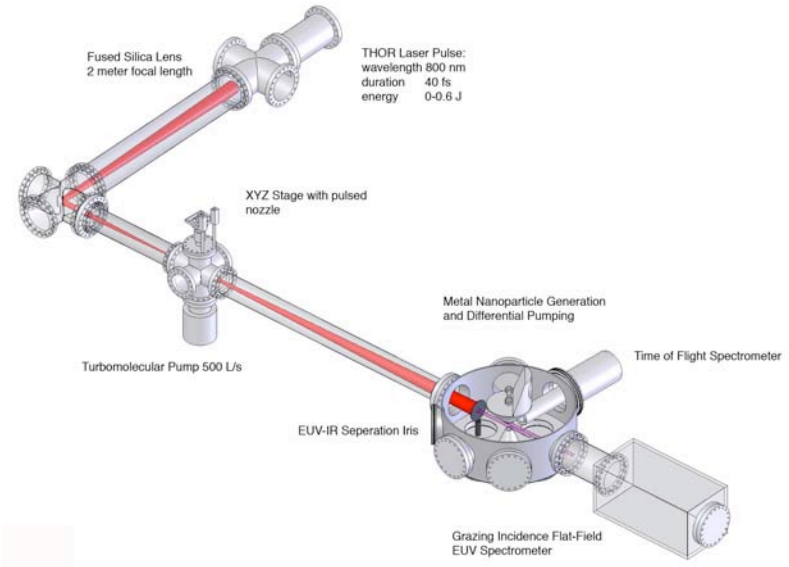

Figure 1: Schematic and specs of the new HHG cluster beamline on the THOR 20 TW laser

We surmise that the high charge states we observe in Xe are a consequence of plasma continuum lowering in the dense nanoplasma that is produced by the initial photo ionization of the Xe clusters. The dense plasma environment of the Xe cluster may lower the ionization potential of the ions in the cluster by as much as 25 eV, permitting direct, single photon ionization up to Xe^{5+}. The small number of higher charge

[1] H.Wabnitz et al., "Multiple ionization of atom clusters by intense soft X-rays from a free electron laser", *Nature (London)* **420**, 482 (2002).

states, then appear to be created by collisional ionization of the highly charge ions produced by photo-ionization.

Evidence for the production of a Xe nanoplasma also comes from measurements that we have made of the Xe cluster ion spectrum. By removing the TOF extraction and acceleration grids, kinetic energy measurements were made of the released ions by field-free time-of-flight. The ion spectrum derived in this way from the explosions of ~30,000 atom clusters is illustrated in figure 3. This broad energy spectrum is characteristic of a plasma explosion and exhibits ion temperature much colder than would be expected from Coulomb explosion. We calculated the spectrum expected from Coulomb exploding clusters by convolving the spectrum of a single Coulomb exploding cluster with a log-normal cluster size distribution. The calculated spectrum for Coulomb exploding clusters with $<N>=30,000$ (and $Z\sim1$) is illustrated in figure 4. This distribution is very different than the observed spectrum, peaking well above 2 keV. For comparison, the spectrum from a best fit distribution with $<N>=100$ is also illustrated in this figure. Such a Coulomb explosion distribution accurately matches the shape of the ion spectrum peak at 100 eV but does not accurately match the tail of the energy distribution. On the other hand, we also fitted our observed ion spectrum to that of a hydrodynamically expanding quasi-neutral cluster nanoplasma. This best fit is shown in figure 4 and passes through the data over the entire energy range from 10 eV to 600 eV. This spectrum is consistent with an initial electron temperature in the Xe cluster plasmas of 8 eV.

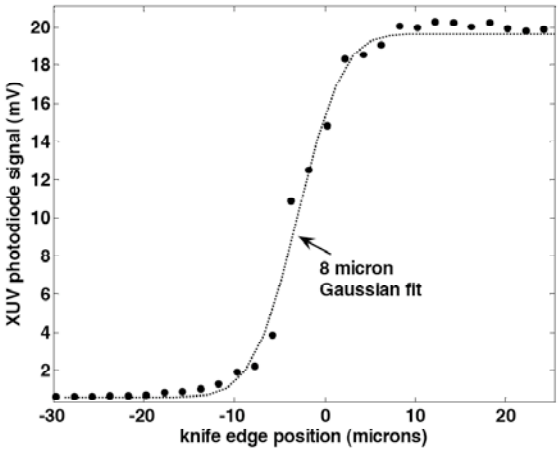

Figure 2: Measured signal in an XUV sensitive photodiode at the XUV pulse focus passing around a razor blade as a function of blade position in the focus. The solid line is a fit of an 8 μm ($1/e^2$) Gaussian focus.

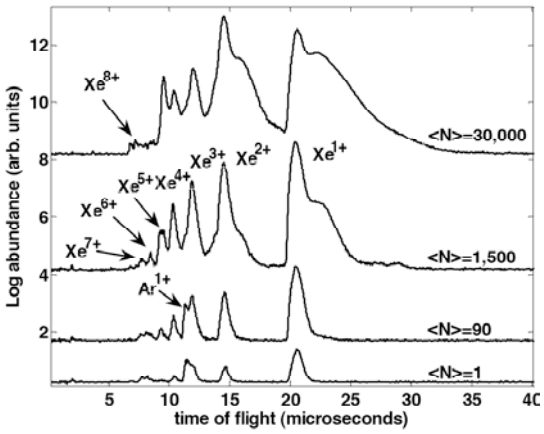

Figure 3: Ion charge state time-of-flight spectra for various cluster sizes.

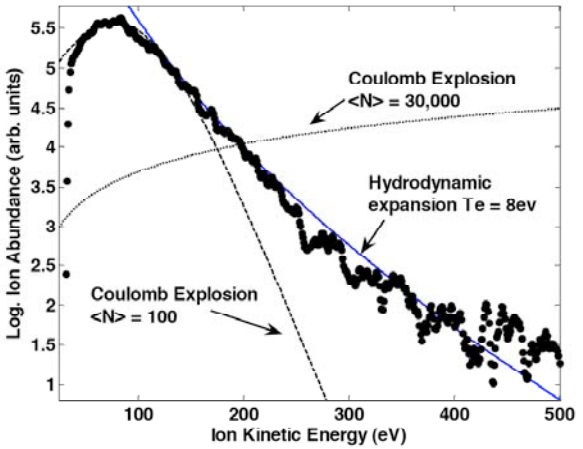

Figure 4: Xe ion kinetic energy spectrum from field-free time-of-flight of the exploding cluster ion. The spectrum is fit to a model of Coulomb explosion of large clusters (dotted line) and small clusters (dashed line), as well as the spectrum of a quasineutral expansion of a spherical cluster with an initial temperature of 8eV (solid line).

Future Research Plans

Our future plans will now shift to the study of mixed species clusters, such as methane. The explosions of clusters such as methane in intense XUV fields is of interest because these more closely approximate the organic based large molecular targets that will ultimately be studied at the LCLS. We will also begin study of solid material clusters irradiated at 38 nm. We are in the process of fabricating an add-on chamber that will allow us to create metal clusters via the laser ablation of micro-particles technique [2]. We will start by investigating Ag clusters, which exhibit interesting absorption resonances at around 20-30 eV attributed to giant collective plasma resonance of both s and d electrons.

Refereed papers published on work supported by this grant during the past three years:

1) B. F. Murphy, K. Hoffmann, A. Belilopetski, J. Keto, and T. Ditmire, "Explosion of Xenon Clusters Driven by Intense Femtosecond Pulses of Extreme Ultraviolet Light" *Phys. Rev. Lett.* submitted.
2) S. Kneip, B. I. Cho , D. R. Symes, H. A. Sumeruk, G. Dyer, I. V. Churina, A. V. Belolipetski, A.S. Henig, T. D. Donnelly, and T. Ditmire "K-shell Spectroscopy of Plasmas Created by Intense Laser Irradiation of Micron-scale Cone and Sphere Targets" *J. High Energy Density Physics.* **4**, 41 (2008).
2) D. R. Symes, M. Hohenberger, A. Henig, and T. Ditmire, "Anisotropic Explosions of Hydrogen Clusters under Intense Femtosecond Laser Irradiation" *Phys. Rev. Lett.* **98**, 123401 (2007).
3) B. Shim, G. Hays, R. Zgadzaj, T. Ditmire, and M. C. Downer, "Enhanced harmonic generation from expanding clusters" *Phys. Rev. Lett.* **98**, 123902 (2007).
4) H. A. Sumeruk, S. Kneip, D. R. Symes, I. V. Churina, A. V. Belolipetski, T. D. Donnelly, and T. Ditmire, "Control of Strong-Laser-Field Coupling to Electrons in Solid Targets with Wavelength-Scale Spheres" *Phys. Rev. Lett.* **98**, 045001 (2007).
5) H. A. Sumeruk, S. Kneip, D. R. Symes, I. V. Churina, A. V. Belolipetski, G. Dyer, J. Landry, G. Bansal, A. Bernstein, T. D. Donnelly, A. Karmakar, A. Pukhov and T. Ditmire "Hot Electron and X-ray Production from Intense Laser Irradiation of Wavelength-scale Polystyrene Spheres" *Phys. Plas.* **14**, 062704 (2007).
6) D. R. Symes, J. Osterhoff, R. Fäustlin, M. Maurer, A. C. Bernstein, A. S. Moore, E. T. Gumbrell, A. D. Edens, R. A. Smith, and T. Ditmire "Production of periodically modulated laser driven blast waves in a clustering gas", *J. of High Energy Density Phys.* **3**, 353 (2007).
7) M. Hohenberger, D. R. Symes, K. W. Madison, A. Sumeruk, and T. Ditmire, "Dynamic Acceleration Effects in Explosions of Laser Irradiated Heteronuclear Clusters", *Phys. Rev. Lett.* **95**, 195003 (2005).
8) F. Buersgens, K. W. Madison, D. R. Symes, R. Hartke, J. Osterhoff, W. Grigsby, G. Dyer and T. Ditmire , "Angular distribution of neutrons from deuterated cluster explosions driven by fs-laser pulses", *Phys. Rev. E*, **74**, 016403 (2006)
9) R. Hartke, D. R. Symes, F. Buersgens, L. Ruggles, J. L. Porter, T. Ditmire, "Neutron Detector Calibration using a table-top laser heated plasma neutron source" *Nuc. Inst. And Methods A* **540**, 464 (2005).
10) T.D. Donnelly, J. Hogan, A. Mugler, M. Schubmehl, N. Schommer, Andrew J. Bernoff, S. Dasnurkar and T. Ditmire, "Using ultrasonic atomization to produce an aerosol of micron-scale particles", *Rev. Sci. Instr.* **76**, 113301 (2005).

[2] W.T. Nichols, D.E. Henneke, G. Malyavanatham, M.F. Becker†, J.R. Brock, and J.W. Keto, and H. D. Glicksman, "Large scale production of nanocrystals by laser ablation of aerosols of microparticles," *Appl. Phys. Lett.* **78**, 1128 (2001).

Ultracold Molecules: Physics in the Quantum Regime

John Doyle
Harvard University
17 Oxford Street
Cambridge MA 02138
doyle@physics.harvard.edu

1. Program Scope

Our research encompasses a unified approach to the trapping of both atoms and molecules. Our goal is to extend our work with CaH to NH and approach the ultracold regime. Our plan is to trap and cool NH molecules loaded directly from a molecular beam, and measure elastic and inelastic collisional cross sections. Cooling to the ultracold regime will be attempted. We note that as part of this work, we are continuing to develop an important trapping technique, buffer-gas loading. This method was invented in our lab and is able to cool large numbers of atoms and molecules.

2. Recent Progress

Milestones for this project include (x indicates complete):

x–spectroscopic detection of ground-state NH molecules via LIF
x–production of NH in a pulsed beam
x–spectroscopic detection of ground-state NH molecules via absorption
x–injection of NH beam into cryogenic buffer gas (including LIF and absorption detection)
x–realization of 4 T deep trap run in vacuum
x–injection of NH molecules into cryogenic trapping region
x–loading of NH molecules into cryogenic buffer gas with 4 T deep trap
x–trapping of NH
x–measurement of spin-relaxation rate of NH with He
o–removal of buffer gas after trapping of NH
o–measurement of elastic and inelastic cross sections
o–attempt evaporative cooling

NH, like many of the diatomic hydrides, has several advantages for molecular trapping including large rotational constant and relatively simple energy level structure. Some of the several key questions before us when this project began were: Could we produce enough NH using a pulsed beam? Is it possible to introduce a large number of NH molecules into a buffer gas? Would the light collection efficiency be enough for us to adequately detect fluorescence from NH? Could we get absorption spectroscopy to work so that absolute number measurements could be performed? Could we achieve initial loading of NH into the magnetic trap? Will the spin relaxation rates with helium be low enough for us to remove the buffer gas? We have now answered these questions, all to the positive. In addition, we have added something very new to the technical arsenal, co-trapping of N with NH.

There are important questions left. For example, will the NH-NH or NH-N collision rates be adequate for evaporative cooling or sympathetic cooling into the ultracold regime? What will be the nature of an ultracold dense sample of heteronuclear molecules. Specifically, what about the hydrides, with their large rotational constants? These questions are still open and answering them are some of the stated long-term goals of this work.

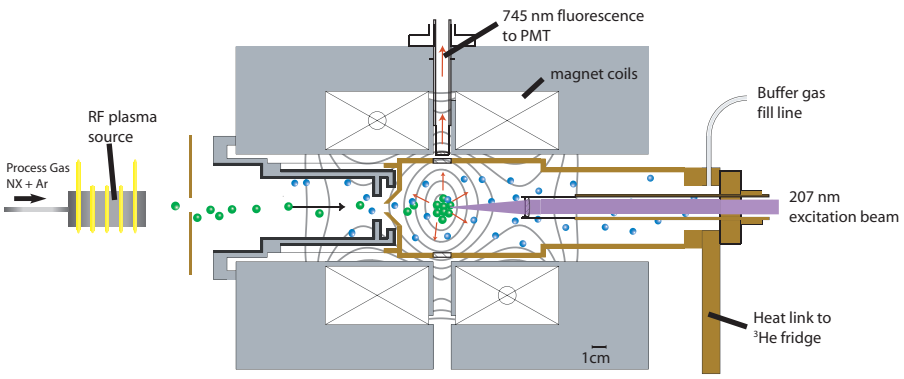

Figure 1: Schematic of current molecule trapping apparatus. Essentially arbitrary mixtures of gases can be discharged in either a plasma source or RF pulsed glow discharge. The molecules travel into the trapping region where they are thermalized with the buffer gas and trapped. Detection of NH and N is done spectroscopically and simultaneously.

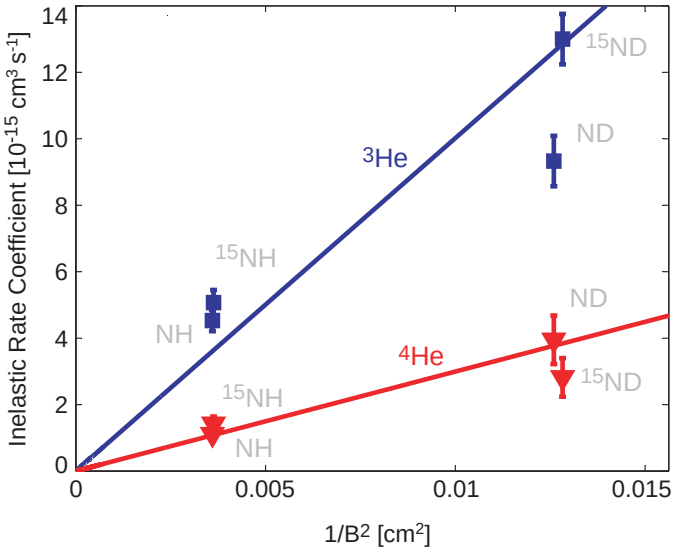

Figure 2: Plot of measured spin relaxation rates for collisions of NH with helium. All possible stable isotopic combinations were used. These values are plotted versus the inverse of the square of the magnetic field. The theory of Krems and co-workers indicates that spin relaxation should scale with the square of the magnetic field due to the fundamental source of coupling in Σ triplet molecules, the spin-spin interaction.

Summary of Status of Project

The heart of the apparatus is a beam machine that we use to produce pulsed NH – alone or in combination with atomic N – in a beam (see figure 1). (Figure 3 shows a photo of the internals of the apparatus.) We have used two types of sources successfully, an "RF Plasma Source (CW)" and a "Glow Discharge Source (Pulsed)". The plasma source is a commercial source used typically in MBE machines. The design of the pulsed source is based on the production of OH via DC discharge as executed by Nesbitt.

This beam is directed toward our trapping magnet, inside of which is a cryogenic buffer-gas cell. This cell can be cooled to as low as 500 mK by a He^3 refrigerator. An entrance orifice of a few mm in diameter to allow the beam of NH to enter the cell. Thus, buffer-gas cooling of the NH and/or N takes place. Several windows exist for the introduction and collection of light.

The basic experimental procedure is as follows. The source beam is directed toward the trap for times from about 10-100 ms. This long pulse beam travels about 10 cm to the face of the cell where some portion enter through the orifice and into the cell. The NH and/or N are then cooled by the buffer gas to their ground state. In our latest experiments we have been using fluorescence and absorption spectroscopy to detect the NH in the trapping region and pulsed TALIF to detect atomic N. We have been able to observe trapped NH molecules for longer than a second (1/e lifetimes as long as 900 ms) and N for many seconds (due to its higher magnetic moment). With such long trap lifetimes we are able to make measurements of key spin relaxation cross sections of NH and compare with theory. This was recently published as *Magnetic Trapping and Zeeman Relaxation of NH*, W.C. Campbell, E. Tsikata, H. Lu, L.D. van Buuren, and J.M. Doyle, Physical Review Letters, 98, 213001 (2007) and a second preprint.

3. Future Plans

We continue on our program of trapping of NH. The next step is to lower the background He gas pressure by cryogenic pump out of the helium. We expect to first see a dramatic lengthening of the trap molecule lifetime to greater than 100 seconds. This should allow us to start seeing NH-NH collisional processes and determine the NH-NH spin relaxation rates. This will naturally lead to attempting evaporative cooling. It is our hope to increase the number of trapped NH molecules to make this regime even more accessible.

This will be done by using a cell that is essentially "open", with a 6 cm diameter hole in the side facing a cryopump. We will then "puff" a short burst of cryogenic helium into the cell, load the molecules and then wait for a short time as the helium flows out of the open cell and into the cryopumps.

Figure 3:

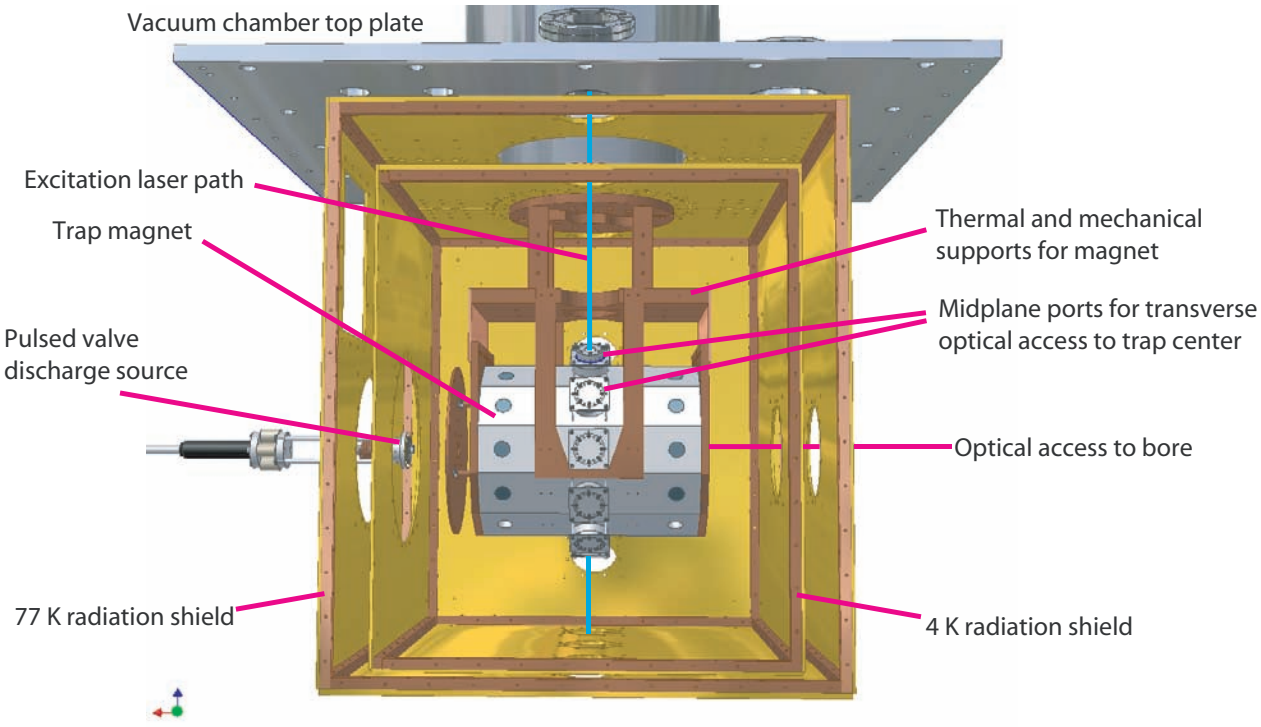
Vacuum chamber top plate
Excitation laser path
Trap magnet
Pulsed valve
discharge source
77 K radiation shield
Thermal and mechanical
supports for magnet
Midplane ports for transverse
optical access to trap center
Optical access to bore
4 K radiation shield

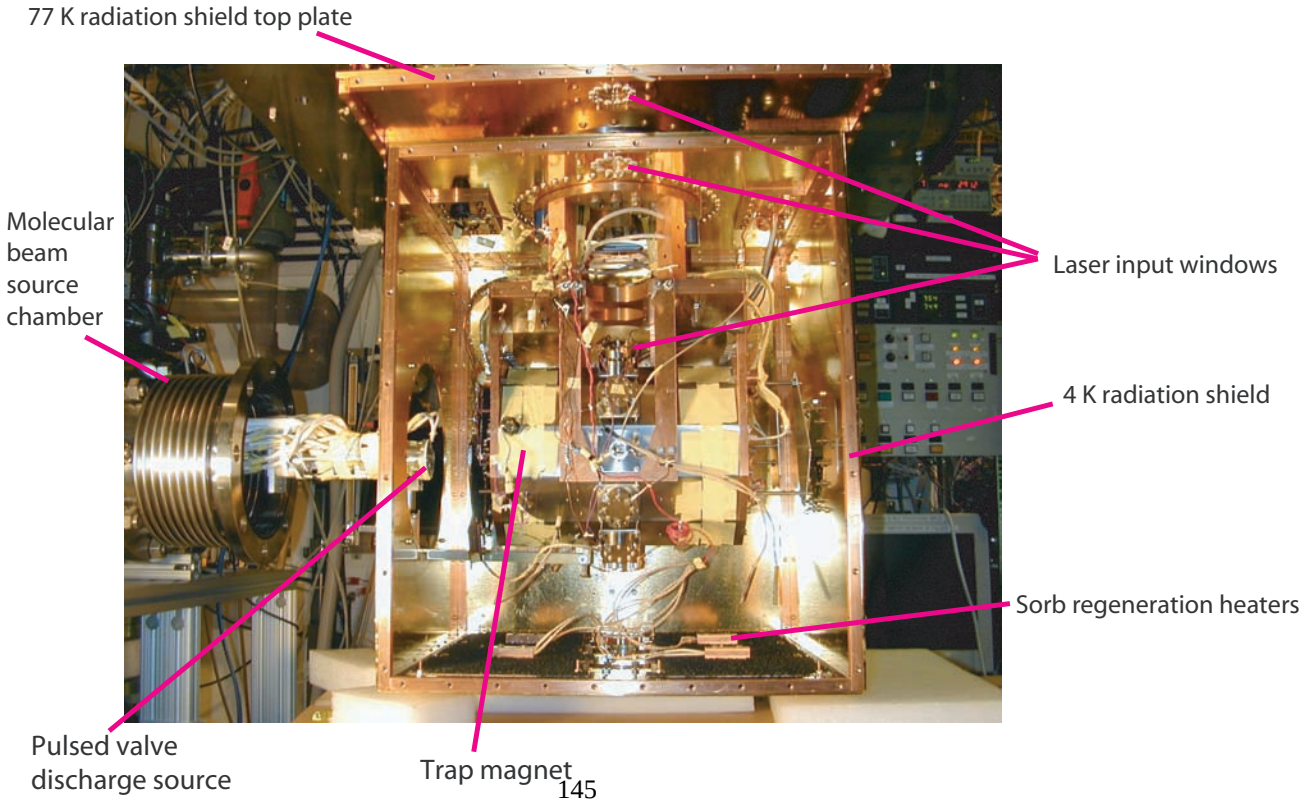
77 K radiation shield top plate
Molecular
beam
source
chamber
Laser input windows
4 K radiation shield
Sorb regeneration heaters
Pulsed valve
discharge source
Trap magnet

Atomic Electrons in Strong Radiation Fields

J. H. Eberly
Department of Physics and Astronomy
University of Rochester, Rochester, NY 14627
eberly@pas.rochester.edu

July 18, 2008

Scope: Electron Correlation under Strong Laser Fields

We are interested to understand how very intense laser light couples to multi-electron atoms and molecules. Substantial challenges to theoretical study arise from the fully phase-coherent character as well as the rapid time-dependence, of femtosecond-scale laser pulses that can exert electric eld forces on electrons that are on par with nuclear coulomb forces and the pairwise electron-electron repulsive force at atomic distances. An important additional challenge arises when there is a need to account accurately for more than one dynamically active electron, as there is in situations of recent experimental activity.

During 2007-08 we obtained results from a large-scale extension of our fully classical ensemble method (summarized previously). Our current work follows a track outlined and published in several intervening reports [1, 2, 3, 4, 5]. We are now exploiting systematic calculations for two, three and four active atomic electrons in strong time-dependent and phase-coherent elds. We are also beginning to systematize direct comparisons of the classical ensemble approach with both experimental data and with existing so-called S-matrix calculations.

Recent Progress #1: Extended Dimensionality

In the context of NSDI we now use both planar and three-dimensional geometries in employing the two-particle ensemble method developed earlier within the aligned-electron approximation (AEA). We have devoted some effort to determining how much difference exists between two-dimensional and three-dimensional treatments, and in many case the distinction is not great, as shown in Fig. 1, where 2d, 3d and experimental results are compared.

The extended dimensionality this year permitted the rst direct comparison of optical double ionization and triple ionization in the same species with the same laser parameters [6]. In addition, we were able to capture trajectories in triple ionization showing both Coulomb focusing and a kind of “thermalization” in which the recolliding single electron was able to share its energy with the two bound electrons and create a triple-escape trajectory [4]. We clearly saw that the sharing process of energy equalization can take place in 20-30 attoseconds.

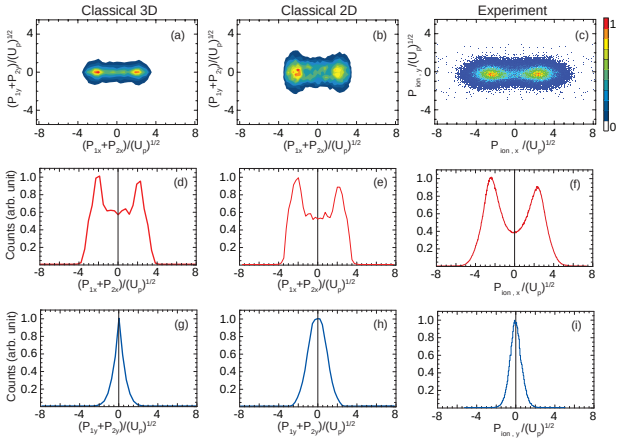

Figure 1: Momentum distributions of the recoil ion (total two-electron) obtained from (a) 3-D and (b) 2-D classical ensemble theory and (c) COLTRIMS measurement. The results in the first and second columns are calculated with 56466 and 71790 2-e classical NSDI trajectories respectively, in which all the trajectories are obtained at $I = 0.3$ PW/cm^2. The COLTRIMS experimental data are obtained by subjecting Ne targets to 795-nm laser pulses at $I = 1.5$ PW/cm^2, as in the 2006 report of Zrost, et al. [7]. The data are plotted here in momentum units $(U_p)^{1/2}$. The top row shows recoil-ion momentum distributions, the component parallel (x) vs. the component perpendicular (y) to the laser polarization axis. The middle and bottom rows show the distributions of recoil-ion momentum components parallel and perpendicular to the polarization axis respectively. From P.J. Ho, Ph.D. thesis [8].

Recent Progress #2: Momentum Distribution Shape Dependences

We have found it useful to recall that even within the one-dimensional aligned electron approximation (AEA), many aspects of NSDI [9, 10, 11, 12] were found to be mainly reproduced by a classical treatment, and a labelling scheme was found useful, which Fig. 2 exhibits. The "Z" and "NZ" labels refer to zero and non-zero ion momenta, intuitively implying that ejection of the NSDI electrons on opposite sides of the nucleus imparts approximately zero ion momentum and same-side ejection imparts non-zero ion momentum. The existing experimental reports were open to such an analysis as shown in Fig. 2. The AEA two-electron simulations as reported in [1] were in satisfactory agreement, showing clear peaks that could also be called "Z" and "NZ" at the same momentum values.

These pictures are not new, but the Z and NZ labels are now useful in connection with open questions about atomic species dependences in NSDI data. The panels in the figure show what can

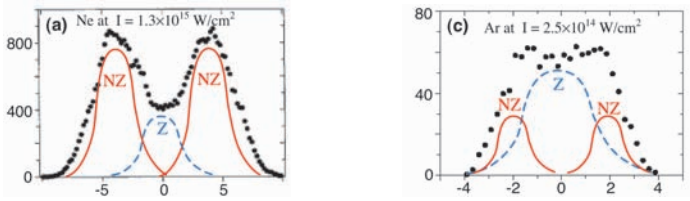

Figure 2: Data points give final ion momenta of neon [9] and argon [11] measured using COLTRIMS. In each panel, there are two solid curves and a dashed curve drawn under the experimental data. These curves are inserted by hand to show the contributions of two groups of NSDI trajectories. In particular, one group gives a distribution peaked at Zero (Z) momentum, and the other gives distributions peaked at two different Non-Zero (NZ) momenta. Whether the overall shape, i.e., the mix of Z and NZ trajectories, in each distribution depends on the atomic species is the open question.

be called generic “neon-type” and “argon-type” distributions, with a rather deep central depression in the first case, and a fairly flat top in the second case. These are persistently observed shapes, confirmed in a number of experimental studies. A conjecture about their origin has been mentioned, assigning the tendency toward these shapes to atomic species differences.

We believe that the explanation is somewhat simpler. Our analysis suggests that the ionization dynamics, reflecting electron trajectory behavior rather than structural differences due to species differences, provides an explanation as soon as the single-ionization saturation intensity (SISI) for each species is taken into account. This is largely a matter of the ionization energies and not a subtle structural feature. We have suggested an experimental test of this hypothesis [13].

Future Plans

The extension of the classical approach to 2d and 3d has opened the domain of elliptical polarization to study, and that topic will be pursued. The same is true of molecular multi-electron ionization. Neither of these is restricted to two electrons, although we'll begin there.

The state of theoretical work on two-electron ionization of atoms in linearly polarized fields has become quasi-stable in the past 2-3 years, and comparitive assessments can begin to be made. Three main themes are on the verge of maturity in regard to NSDI studies: (i) solution of the two-electron TDSE, exactly for helium and in various approximations for other atoms, (ii) diagramatically guided SFA (strong field approximation) theory, sometimes labelled as S-matrix theory, and (iii) classical theory for very large ensembles of two-electron trajectories obeying Newtonian equations. In cooperation with the MBI-Berlin theory group of Wilhelm Becker we are preparing an assessment of these three approaches for Reviews of Modern Physics [14].

More speculative work is being contemplated in regard to one of the mysteries of NSDI. That is, there is no explanation yet for the increasingly likely conclusion that the strong electron correlation in NSDI has a mostly classical origin. Such classical dominance is almost certainly not inevitable in extreme environments. The distinction between classical and quantum correlation is a matter of the degree of state entanglement between electrons, but here it is non-local entanglement rather than the highly local entanglement of atomic orbitals that is at work. This raises important questions about issues of specifically quantum complexity under extreme conditions, and the dynamics of entanglement. We are planning that a fraction of our effort going forward will be devoted to an examination of questions related to this.

We continue to value our cooperation on multi-electron strong-field effects with the group of S.L. Haan at Calvin College [15].

Acknowledgment

Publications marked with *** in the listing below have been supported by DOE Grant DE-FG02-05ER15713.

References

[1] Phay J. Ho, R. Panfili, S. L. Haan and J. H. Eberly, *Phys. Rev. Lett.* **94**, 093002 (2005).

[2] Phay J. Ho, *Phys. Rev. A* **74**, 045401 (2005).

[3] ***Phay J. Ho and J.H. Eberly, *Phys. Rev. Lett.* **95**, 193002 (2005).

[4] ***Phay J. Ho and J.H. Eberly, *Phys. Rev. Lett.* **97**, 083001 (2006).

[5] ***S.L. Haan, L. Breen, A. Karim, and J. H. Eberly, *Phys. Rev. Lett.* **97**, 103008 (2006) [also selected for Virtual Journal of Ultrafast Science].

[6] ***Phay J. Ho and J. H. Eberly, *Optics Expr.* **15**, 1845-1850 (2007).

[7] K. Zrost, A. Rudenko, Th. Ergler, B. Feuerstein, V. L. B. de Jesus, C. D. Schröter, R. Moshammer and J. Ullrich, *J. Phys. B* **39**, S371 (2006).

[8] P.J. Ho, Dissertation submitted to the Department of Physics and Astronomy, University of Rochester (2007), in ful llment of requirements for the Ph.D. degree.

[9] R. Moshammer *et al.*, *Phys. Rev. Lett.* **84**, 447 (2000).

[10] Th. Weber *et al.*, *Phys. Rev. Lett.* **84**, 443 (2000).

[11] Th. Weber *et al.*, *J. Phys. B* **33**, L127 (2000).

[12] For example, see S. Palanaiyappan, et al., *Phys. Rev. Lett.* **94**, 243003 (2005).

[13] ***Phay J. Ho and J.H. Eberly, submitted to *Phys. Rev. Lett.*

[14] ***Phay J. Ho, X. Liu, W. Becker, and J.H. Eberly, *Rev. Mod. Phys.* in preparation.

[15] ***S.L. Haan, L. Breen, A. Karim and J.H. Eberly, "Recollision Dynamics and Time Delay in Strong-Field Double Ionization," *Optics Expr.* **15**, 767 (2007).

Few-Body Fragmentation Interferometry

Department of Energy 2008-2009

James M Feagin

Department of Physics
California State University–Fullerton
Fullerton CA 92834
jfeagin@fullerton.edu

We continue two parallel efforts with (i) emphasis on *detection interferometry* while (ii) pursuing longtime work on *collective Coulomb excitations*. We thus continue our ongoing DOE work to extract basic understanding and quantum control of few-body microscopic systems based on our practiced experience with more conventional studies of correlated electrons and ions. We have transitioned our efforts from few-body Coulomb dynamics and reaction detection—a longstanding theme of the BES program—to a somewhat broader perspective of reaction imaging interferometry.

Although trapped-ion and atom interferometry have proven over the past decade to be powerful tools for establishing quantum control, the essential system entanglements have been achieved almost exclusively with scattered photons. There thus remains fundamental interest in demonstrating analogous levels of entanglement and control using scattered electrons and ions, however, the experiments remain very difficult due to the intrinsically short deBroglie wavelengths involved. Nevertheless, remarkable progress has been recently achieved in experiments by Th. Weber, M. Schöffler, L. Cocke and coworkers at the LBNL ALS involving the photo double ionization of molecular hydrogen.[1] In particular, two-center electron interference with which-path marking via the outgoing electron-pair entanglement has been observed. These and related experiments of our colleagues in this country and internationally involving atom and molecule fragmentation are opening a new genre of charged-particle collision physics and strongly motivate our work here.

Einstein's Recoiling-Slit Experiment

Some time ago, Wootters and Zurek[2] revisited the Einstein recoiling-slit gedanken experiment to analyze Young's double-slit interferometry to include in detail the photon which-path information stored in the recoiling entrance slit. They assumed an entrance slit cut into a spring-mounted plate that could be treated as a quantum oscillator under the action of a passing photon. They then considered alternative position and momentum measurements of the plate and the effect of the measurements on the photon interference. Wootters and Zurek thus exploited the underlying photon-plate entanglement to formulate quantitative statements about wave-particle duality, and their work became one of the first major publications on the subject.

We have analyzed photon scattering by a trapped ion as a modern realization of Wootters and Zurek's quantum analysis of the recoiling-slit experiment.[3] While a harmonically trapped ion provides a perfect quantum realization of a spring-mounted plate and entrance slit, we find that a coherent-state measurement of the recoiling ion, besides likely having experimental advantages, can mimic both position and momentum measurements of the ion in full analogy with Wootters and Zurek. One readily identifies the resulting photon fringe visibility as the

---

[1] D. Akoury et al., Science **318**, 949 (2007); K. Kreidi et al., Phys. Rev. Lett. **100**, 133005-1 (2008).
[2] W. K. Wootters and W. H. Zurek, Phys. Rev. D**19**, 473 (1979).
[3] R. S. Utter and J. M. Feagin, Phys. Rev. A **75**, 062105 (2007). (**Utter** *was a CSUF masters degree student. This work was highlighted in the June 2007 issue of the Virtual Journal of Quantum Information,* vjquantuminfo.org.)

overlap of recoil-ion marker states describing a photon scattered towards one or the other slit. When the overlap vanishes, the direction of the scattered photon can in principle be determined via the photon-ion entanglement by a measurement of the recoil ion, blocking an interference effect. On the other hand, when the overlap is perfect the interference is as well, and neither the direction of the recoiling ion nor of the scattered photon is discernible. The intermediate stage of duality characterized by moderate overlap continues to warrant further study.

Trapped-ion interferometry has advanced extraordinarily in recent years. Young's fringes formed by photons scattered by a pair of harmonically trapped $^{198}Hg^{+}$ ions have been observed and analyzed in detail by Wineland, Itano, and co-workers at NIST-Boulder.[4] Coherent and squeezed states[5] as well as double-humped *Schrödinger-cat* superpositions of displaced coherent states[6] of (external) motion of a harmonically trapped $^{9}Be^{+}$ ion have been engineered by Monroe, Meekhof, Wineland, and coworkers. Entanglement analogous to the photon-ion-CM entanglement we have considered has been observed between the *internal* states of a trapped ion and a polarization-analyzed fluorescence photon by Blinov, Monroe, and co-workers at Michigan.[7] And in a recent tour de force, quantum teleportation between three trapped ions has been achieved by Wineland, Itano, and coworkers at NIST[8] and independently by Blatt and coworkers at the Universität Innsbuck.[9]

In order for the photon phase relations characterizing the system entanglement to remain accessible for local observation and interference, the ion-CM-recoil marker states must overlap. Otherwise, the ion recoil could be cleanly measured and the photon path (which port entered) determined unambiguously. If the overlap is perfect the fringes will be perfect, and if the overlap vanishes the fringes will as well. The ion recoil thus stores information on the port and path taken by the scattered photon. As articulated originally by Wootters and Zurek, the question becomes what goes on between these two extremes. For a given fringe visibility, how reliably can the photon path be predicted?

Although there is no definitive answer to this question, a straightforward estimate is simply to evaluate the difference between the joint probabilities for scattering the photon into one or the other port while detecting the recoiling ion summed over all possible recoil-ion measurement outcomes, the so called classical *trace distance*, or what Englert has referred to as the *which-path knowledge*.[10] One is thus led to consider the quantum trace distance, or distinguishability of the ways, as an upper bound on the classical trace distance, and we thereby recover Englert's duality relation between the distinguishability and the fringe visibility.

Hardy Nonlocality

In parallel work, we have analyzed[11] the detection of a pair of recoiling reaction fragments, each by its own interferometer, to demonstrate Hardy's contradiction between quantum mechanics and local hidden variables.[12] Hardy's theorem sidesteps Bell's inequality by establishing the contradiction with just four measurement outcomes on two system fragments. Whereas Bell's theorem involves fully statistical violations of the quantum description, the Hardy result is simpler and hinges on essentially perfect correlations to establish nonlocality. Our interferometry is

---

[4] U. Eichmann et al., Phys. Rev. Lett. **70**, 2359 (1993); W. Itano et al., Phys. Rev. A**57**, 4176 (1998).
[5] D. M. Meekhof, C. Monroe, W. Itano and D. J. Wineland, Phys. Rev. Lett. **76**, 1796 (1996).
[6] C. Monroe, D. M. Meekhof, B. E. King and D. J. Wineland, Science **272**, 1131 (1996).
[7] B. B. Blinov, D. L. Moehring, L.-M. Duan, and C. Monroe, Nature **428**, 153 (2004) and also E. Polzik, Nature **428**, 129 (2004).
[8] M. D. Barrett et al., Nature **429**, 737 (2004).
[9] M. Riebe, H. Häffner, C. F. Roos, W. Hnsel, J. Benhelm, G. P. T. Lancaster, T. W. Körber, C. Becher, F. Schmidt-Kaler, D. F. V. James and R. Blatt, Nature 429, 734 (2004).
[10] B.-G. Englert, Phys. Rev. Lett. **77**, 2154 (1996); Zeit. f. Naturforschung, **54a**, 11 (1999).
[11] J. M. Feagin, Phys. Rev. A **69**, 062103 (2004). (*This work was highlighted in the June 2004 issue of the Virtual Journal of Quantum Information,* vjquantuminfo.org.)
[12] L. Hardy, Phys. Rev. Lett. **71**, 1665 (1993)

based on the projectile-target momentum entanglement and is independent of the identity and internal state of the fragments. Although no doubt a very difficult experiment, our approach is thus relatively straightforward, at least conceptually.

We have recently revisited the Hardy theorem as a possible application of trapped-ion interferometry. Hardy nonlocality has thus far only been verified with down-converted and polarization-entangled photon pairs. Our current efforts have been to extend Hardy's analysis to the nonorthogonal coherent CM states of the trapped ion we used to analyze Einstein's recoiling-slit experiment, as described above.

Two-Center Interferometry

It is natural to regard the position of a macroscopic object to be quasi-sharply defined: if a cat is sleeping in the chair, we don't consider for a moment that she may in fact be out on a bench in the garden. Yet, quantum mechanics encourages us to superpose displaced and narrow wavepackets to describe states of a single 'sleeping cat' that could be either in the chair or on a bench. This quantum reality and the wider notion of entanglement (something bumps the cat and adds bench and chair markers) are profound and continue to generate debate over what the wavefunction actually describes. Nevertheless, it is now widely recognized that interactions with the environment and their inevitable entanglements can dephase the quantum superpositions. The resulting decoherence eliminates macroscopic interferences and thereby restores a natural sense of reality. Our interest in this problem is an outgrowth of our general considerations of scattering interferometry and two-center interference effects from extended targets.[13]

Advances in atom interferometry and ion trapping now afford systematic study of quantum interferences in mesoscopic systems with parameters that can be tracked from quantum towards macroscopic limits. Along with the double-humped Schrödinger-cat CM states of a trapped ion engineered by Monroe and coworkers in Boulder,[5] Pritchard and coworkers at MIT[14] observed the interference fringes of a sodium atom passing through the two arms of a Mach-Zehnder interferometer and scattering a photon. Besides their novelty in traditional AMO collision physics, such target systems allow one to study quantum correlations in well controlled environments with relatively few quantum parameters. Within the impulse approximation, we have developed a framework[15] to connect these and related experiments including the observation of Young's fringes with photons scattered by a *pair* of trapped ions.[16]

Collective Coulomb Excitations

These projects continue to link to our more conventional and longtime work in the AMO field of collective Coulomb excitations.[17,18] We have recently extended the above impulse approximation to a description of the electron-pair interferences observed in the pioneering photo double ionization experiments on molecular hydrogen of Th. Weber, M. Schöffler, L. Cocke and coworkers at the LBNL ALS.[1] We thus express the cross section as a product of a single-center (helium) double ionization cross section multiplied by a form factor describing the two-center Bragg-like diffraction of the electron pair. We find this description to characterize the original observations as well as new data for a variety of molecular orientations and photon polarization geometries.[19] We also predict an isotope dependence in the exploding ion-pair angular

---

[13] J. M. Feagin and S. Han, Phys. Rev. Lett. **86**, 5039 (2001); Phys. Rev. Lett. **89**, 109302 (2002). (**Han** *was a CSUF masters degree student.*)
[14] M. S. Chapman et al., Phys. Rev. Lett. **75**, 3783 (1995); D. A. Kokorowski et al., Phys. Rev. Lett. **86**, 2191 (2001).
[15] J. M. Feagin, Phys. Rev. A **73**, 022108 (2006).
[16] W. Itano et al., Phys. Rev. A **57**, 4176 (1998).
[17] A. Knapp et al, J. Phys. B: At. Mol. Opt. Phys. **35**, L521 (2002). (*Feagin is a coauthor.*)
[18] Th. Weber et al., Phys. Rev. Lett. **92**, 163001 (2004) and references therein. (*Feagin is a coauthor.*)
[19] J. M. Feagin, S. Raj, R. Gibson, Th. Weber and M. Schöffler, Phys. Rev. Lett., submitted (2008).

distribution, which is being tested in new experiments on D_2.[20]

Parallel to these interests, but at much lower photon energies, we have revisited our description of molecular photo double ionization based closely on an analogous double-ionization model we established for helium.[21] This lowest-order approximation based on ${}^1P^o$ outgoing electron pairs has the advantage of providing approximate dynamical quantum numbers and propensity rules for excitation of a given molecular fragmentation configuration.[22] Our predictions have recently been studied in detail experimentally by T. Reddish and A. Huetz and coworkers in Paris.[23] Their results and comparisons with state-of-the-art close-coupling[24] and exterior complex-scaling[25] numerical computations show strong evidence for contributions to the fragmentation from higher electron-pair angular momenta.

We have thus generalized our electron-pair *momentum* states, based on the outgoing electron-pair center of mass momentum $\mathbf{k}_+ = \mathbf{k}_1 + \mathbf{k}_2$ and a z axis along the pair's relative momentum $\mathbf{k}_- = (\mathbf{k}_1 - \mathbf{k}_2)/2$, to total angular momentum $L > 1$. In addition, we require these states to have a definite *saddle-inversion* symmetry under $\mathbf{k}_+ \to -\mathbf{k}_+$ as well as a reflection symmetry in the plane of the molecular axis and the photon (linear) polarization. Saddle-inversion symmetry has been shown to be a key approximate quantum number in describing electron-pair dynamics in helium and in H^- above and below the double ionization threshold.[22] We are finding that superpositions of just two of these states ${}^1P^o + {}^1D^o$ give a remarkably good description of a variety of observed molecular fragmentation configurations.[26] These states should thus prove useful in improving and interpreting convergence in numerical computations as well as in modeling a variety of proposed double ionization studies of complex molecules and surfaces.[27]

Recent Publications and Submissions

Impulse-Approximation Description of Electron-Pair Interferences in Molecular Hydrogen Photoionization, J. M. Feagin, S. Raj, R. Gibson, Th. Weber and M. Schöffler, Phys. Rev. Lett., submitted (2008). (**Raj** *and* **Gibson** *are CSUF masters degree students.*)

Electron-Pair Collective Excitations in Molecular Hydrogen Photo Double Ionization, J. M. Feagin, J. Colgan, A. Huetz, and T. Reddish, Phys. Rev. Lett., submitted (2008).

Trapped-Ion Realization of Einstein's Recoiling-Slit Experiment, R. S. Utter and J. M. Feagin, Phys. Rev. A **75**, 062105 (2007). (**Utter** *was a CSUF masters degree student. This work was highlighted in the June 2007 issue of the Virtual Journal of Quantum Information,* vjquantuminfo.org.)

Two-Center Interferometry and Decoherence Effects, J. M. Feagin, Phys. Rev. A **73**, 022108 (2006).

Hardy Nonlocality via Few-Body Fragmentation Imaging, J. M. Feagin, Phys. Rev. A**69**, 062103 (2004). (*This work was highlighted in the June 2004 issue of the Virtual Journal of Quantum Information,* vjquantuminfo.org.)

Fully Differential Cross Sections for Photo Double Ionization of Fixed-in-Space D_2, Th. Weber et al, Phys. Rev. Lett. **92**, 163001 (2004). (*Feagin is a coauthor.*)

(**Raj** *and* **Gibson** *are CSUF masters degree students.)*

[20] R. Dörner, private communication, July (2008)

[21] J. M. Feagin, J. Phys. B: At. Mol. Opt. Phys. **31**, L729 (1998); T. J. Reddish and J. M. Feagin, J. Phys. B: At. Mol. Opt. Phys. **32**, 2473 (1999).

[22] M. Walter, J. S. Briggs and J. M. Feagin, J. Phys. B: At. Mol. Opt. Phys. **33**, 2907 (2000).

[23] M. Gisselbrecht et al., Phys. Rev. Lett. **96**, 153001 (2006).

[24] J. Colgan, M. S. Pindzola and F. Robicheaux, Phys. Rev. Lett. **98**, 153001 (2007).

[25] W. Vanroose, F. Martin, T. N. Rescigno and C. W. McCurdy, Science **310**, 1787 (2005); Phys. Rev. A**74**, 052702 (2006); C. W. McCurdy, private communication.

[26] J. M. Feagin, J. Colgan, A. Huetz, and T. Reddish, Phys. Rev. Lett., submitted (2008).

[27] Th. Weber, private communication, May (2008).

Studies of Autoionizing States Relevant to Dielectronic Recombination

T.F. Gallagher
Department of Physics
University of Virginia
P.O. Box 400714
Charlottesville, VA 22904-4714
tfg@virginia.edu

Two electron atoms, alkaline earth atoms to be precise, constitute the focus of this research program. Much, but not all of the work is concentrated on the doubly excited autoionizing states. The practical motivation of direct interest to the Department of Energy is that a systematic study of autoionization allows us to understand the reverse process, dielectronic recombination (DR), i.e., recombination of ions and electrons via intermediate autoionizing states. DR provides an efficient recombination mechanism for both laboratory and astrophysical plasmas.[1-3] The most important pathway for DR in high temperature plasmas, such as fusion plasmas, is through the autoionizing Rydberg states converging to the lowest lying excited states of the parent ion. As a result of passing through Rydberg states, DR rates are profoundly influenced by small electric and magnetic fields, which can originate in the charged particles of the plasma or be externally applied.

In the past year we have completed measurements of the effects of combined electric and magnetic fields on DR, explored above threshold DR in the presence of a strong microwave field, and conducted microwave resonance experiments on bound Rydberg states to extract the ionic matrix elements.

In our experiments we do not study DR but a process which we term DR from a continuum of finite bandwidth. In DR from a continuum of finite bandwidth we replace the true continuum with a continuum of finite bandwidth, the broad $6p_{3/2}8g$ ionizing state straddling the Ba^+ $6p_{1/2}$ limit.[4] Specifically, we have examined the process

$$\text{Ba } 6p_{3/2}8g \rightarrow \text{Ba } 6p_{1/2}\,ng \rightarrow \text{Ba } 6s\,ng + h\nu . \tag{1}$$

An atom in the $6p_{3/2}8g$ state makes the interchannel transition to the degenerate $6p_{1/2}ng$ state ($20 < n < \infty$). If it decays radiatively to the bound $6s_{1/2}ng$ state, DR has occurred. The primary attractions of this technique are the energy resolution of ~ 0.5 cm^{-1} (< 0.1 meV), the fact that the experiments can be done in zero electric and magnetic field, and that the partial wave of the entrance channel has a well defined ℓ. In true DR all incoming ℓ channels are allowed, but the capture rate from high ℓ states is low. As a result, DR from a continuum of finite bandwidth is very similar to true DR. Nonetheless, the control of the incoming channel gives us more detailed insight into the process. In the continuum of finite bandwidth experiments the $8g$ electron makes about twenty orbits and collides with the Ba^+ core twenty times before it autoionizes. Our experiments are similar to DR experiments done in storage rings,[5] in which the electrons have many opportunities to collide and recombine with the ions.

Enhancement of the process of Eq. (1) occurs at very low electric fields, those exceeding

$$E = \frac{3\delta_g}{2n^5}, \tag{2}$$

where δ_g is the quantum defect of the $6s_{1/2}ng$ state. The enhancement occurs because for fields in excess of this field the $n\ell$ states of $\ell \geq 4$ are converted to nk Stark states, all of which can contribute to DR.[6] Note that m remains a good quantum number in the electric field. In general we see an enhancement of DR by a factor of twenty. Adding a magnetic field which is parallel to the electric field has no effect, but adding one which is not parallel to the electric field leads to a mixing of the Stark states of different m, which leads to a further enhancement of the DR rate.[7] Our measurements with perpendicular electric and magnetic fields show that there are three requirements for enhancement of the DR rate by the magnetic field. The magnetic coupling must exceed the separation between adjacent Stark states, it must exceed the radiative decay rate, and it must exceed the autoionization rate. The first requirement had been appreciated for some time, but the second and third had not been considered previously. Our work has shown them to be important. In one theoretical analysis it was predicted that the maximum enhancement of the DR rate would occur when the electric and magnetic fields were not perpendicular,[8] but we found that the maximum enhancement always occurs when they are perpendicular, which seems more intuitive.

Together with R. R. Jones we have examined DR from a continuum of finite bandwidth in the presence of a high frequency, 40 GHz, microwave field and observed what might be called above threshold recombination. In zero field the DR signal is observed when the exciting laser is tuned within 0.5 cm^{-1} of the Ba^+ $6p_{1/2}$ limit. In the presence of fields as small as 100 mV/cm the DR signal extends several wavenumbers below the limit, so to actually realize a 0.5 cm^{-1} wide peak requires that the fields be kept below 10 mV/cm. If DR occurs in the presence of a 40 GHz microwave field clearly resolved replicas of the zero field DR peak are observed at multiples of the microwave frequency both above and below the limit. The extent of the replicas is proportional to the microwave field. This observation is counter to the intuitive expectation, based on the Simpleman's model,[9,10] that the energy spread should be proportional to the ponderomotive energy, which is proportional to the power. Not only is the extent of the replicas not proportional to the microwave power, but it is a factor of fifty larger than the ponderomotive energy. The explanation for these observations is that DR occurs in the combined Coulomb-microwave field, not simply the microwave field. Thus the dominant energy transfer occurs near the ion and varies as the product of the microwave field and the Coulomb field. It is the first cycle of the microwave field which is most important. The physics of this problem is very similar to laser assisted Auger decay and ionization by a half cycle pulse.[11,12] A report of this work has been prepared for publication.

We have made measurements of the intervals between the Sr 5*snf*, 5*sng*, 5*snh*, and 5*sni*, levels with the goal of extracting the polarizabilities of the Sr^+ core and, more important the dipole and quadrupole matrix elements connecting the Sr^+ 5*s* state to the 4*d* and 5*p* states. The quadrupole 5*s*-4*d* matrix element is important for it determines the radiative lifetime of the ionic 4*d* state, which may be important in clocks and parity violation measurements.[13] It has long been known that the polarizabilities can be extracted from the $\Delta\ell$ intervals using the adiabatic model of Mayer and Mayer,[14] and this approach has been used with great success for the alkali atoms. For the alkaline earth atoms non adiabatic effects come into play, and they must be taken into

account.[15-16] In the alkaline earth atoms the high ℓ states are split , which we term the K splitting, and Lundeen et al correctly interpreted this splitting as arising from a combination of the nonadiabatic core polarization effects and the fine structure splitting of the ion.[17] We realized that much of the K splitting is due to the lowest ionic dipole and quadrupole matrix elements, and showed that values could be extracted from the K splitting using the extant data for the Ba 6snℓ states.[18]

The Sr measurements have been made by exciting Sr using three pulsed dye lasers via the route

$$5s5s \rightarrow 5s5p \rightarrow 5s5dnl \rightarrow 5snf, \qquad (3)$$

and then driving the one, two, and three photon microwave transitions to the higher 5*sn*ℓ states. The higher ℓ states were detected by delayed field ionization or the fact that their ionizing fields are lower than the ionization fields of the 5*snf* states. The measurements covered the $18 \leq n \leq 22$ states, and the frequencies used were between 13 and 38 GHz. To extract the ionic matrix elements we must calculate the $1/r^2$ and $1/r^3$ matrix elements for the Rydberg electron, and this process is currently underway.

In the coming year we plan to finish work on the relative enhancement of DR passing through the *ng* states and *nd* states in linearly polarized microwave fields. We plan to begin to study the autoionization rates of high angular momentum states states converging to the Ba^+ $6p_{3/2}$ limit in low electric fields and attempt to mimic magnetic fields strong enough to undo the mixing produced by the electric field. To do the latter experiment we plan to use a circularly polarized microwave field, which has the same effect as a magnetic field, except that there is no diamagnetism. Finally, we hope to begin to explore the above threshold recombination both using other frequencies, and eventually in conjunction with excitation using a laser of roughly 5 ps duration which is synchronized with the microwave field.

References

1. A. Burgess, Astrophys. J. 139, 776 (1964).
2. A.L. Merts, R.D. Cowan, and N.H. Magee, Jr., Los Alamos Report No. LA-62200-MS (1976).
3. S. B. Kraemer, G. J. Ferland, and J. R. Gabel, ApJ. 604 556 (2004).
4. J.P. Connerade, Proc. R. Soc. London, Ser. A, 362, 361 (1978).
5. G. Kilgus, J. Berger, P. Blatt, M. Grieser, D. Habs, B. Hochadel, E. Jaeschke, D. Kramer, R. Neumann, G. Neureither, W. Ott, D. Schwalm, M. Steck, R. Stokstad, E. Smolza, A. Wolf, R. Schuch, A. Muller, and M. Wagner, Phys. Rev. Lett. 64, 737 (1990).
6. V. L. Jacobs, J. L. Davis, and P. C. Kepple, Phys. Rev. Lett. 37, 1390 (1976).
7. F. Robicheaux and M. S. Pindzola, Phys. Rev. Lett. 79, 2237 (1997).
8. K. LaGattutua and B. Borca, J. Phys. B 31, 4781 (1998).
9. H. B. van Linden van den Heuvell and H. G. Muller, in Multiphoton Processes, edited by S. J. Smith and P. L. Knight (Cambridge University Press, Cambridge, 1988).
10. T. F. Gallagher, Phys. Rev. Lett.. 61, 2304 (1988).
11. J. M. Schins,P. Breger, P. Agostini, R. C. Constantinescu, H. G. Muller, A. Antonetti, and A. Mysyrowicz, , Phys. Rev. Lett. 73, 2180 (1994).
12. R. R. Jones, Phys. Rev. Lett.. 61, 2304 (1996).
13. T. W. Koerber, M. Schacht, W. Nagourney, and E. N. Fortson, J. Phys. B 36, 637 (2003).
14. J. E. Mayer and M. G. Mayer, Phys. Rev. 431, 605 (1933).
15. J. H. Van Vleck and N. G. Whitelaw, Phys. Rev. 44, 551 (1933).
16. T. F. Gallagher, R. Kachru, and N. H. Tran, Phys. Rev. A 26, 2611 (1982).
17. S. R. Lundeen, in Advances in Atomic , Molecular, and Optical Physics, edited by P. Berman and C. Lin (Elsevier Academic Press, San Diego, 2005).
18. E. S. Shuman and T. F. Gallagher, Phys. Rev. A 74, 022502 (2006).

Publications 2006-2008

1. E. S. Shuman and T. F. Gallagher, "Microwave Spectroscopy of autoionizing Ba $5d_{3/2}n\ell$ states" Phys. Rev. A 73, 032511 (2006).
2. E. S. Shuman and T. F. Gallagher, "Ionic dipole and quandrupole matrix elements from nonadiabatic core polarization" Phys. Rev. A 74, 022502 (2006).
3. W. Yang, E. S. Shuman, and T. F. Gallagher, "Spectral hole burning in the dielectronic recombination from a continuum of finite bandwidth," Phys. Rev. A 75, 023411 (2007).
4. E. S. Shuman, J. Nunkaew, and T. F. Gallagher, "Two-photon spectroscopy of Ba $6sn\ell$ states," Phys. Rev. A 75, 044501 (2007).
5. E. S. Shuman, W. Yang, and T. F. Gallagher, "Magnetic field enhancement of dielectronic recombinmation from a continuum of finite bandwidth ," Phys. Rev. A 76, 031401 (2007).
6. E. S. Shuman, W. Yang, and T. F. Gallagher, "Enhancement of dielectronic recombiniation in combined electric and magnetic fields," Phys. Rev. A 77, 063419 (2008).

Experiments in Ultracold Collisions and Ultracold Molecules

Phillip L. Gould
Department of Physics U-3046
University of Connecticut
2152 Hillside Road
Storrs, CT 06269-3046
<phillip.gould@uconn.edu>

Program Scope:

Ultracold atoms and, more recently, ultracold molecules have become important topics in modern atomic, molecular and optical (AMO) physics. A number of techniques for producing ultracold samples have emerged, such as laser cooling, buffer gas cooling, electrostatic slowing, and evaporative cooling. At the same time, various schemes for trapping these cold atoms and molecules have been developed, including magneto-optical traps, laser dipole traps, magnetic traps, and electrostatic traps. This combination of cooling and trapping techniques has enabled numerous applications such as: precision measurements and atomic clocks; quantum optics and cavity QED; quantum degenerate gases (bosons, fermions, and mixtures); atom optics and interferometry; quantum and nonlinear atom optics; targets for ionization studies; quantum computation; optical lattices and quantum simulations; ultracold plasmas; ultracold chemistry; and ultracold collisions. Because these applications typically involve conditions of high density and low temperature, the various interactions which can occur between the particles are important to understand and, hopefully, control. For example, inelastic collisions can cause undesirable heating and/or loss in high-density samples. On the other hand, processes such photoassociation and magnetoassociation (sweeping a magnetic field through a Feshbach resonance) allow the formation of ultracold molecules from the constituent atoms. The main goal of our experimental program is to use frequency-chirped laser light to coherently control ultracold collision dynamics, including the process of photoassociative formation of ultracold molecules.

Our ultracold collision experiments use frequency-stabilized diode lasers at 780 nm to form a magneto-optical trap (MOT) for Rb atoms. Rb is the atom of choice based on several factors: 1) the convenient match of its resonance lines to readily available diodes lasers; 2) the existence of two stable and abundant isotopes (^{85}Rb and ^{87}Rb); 3) ^{87}Rb is the most widely-used atom for BEC studies; and 4) significant knowledge exists regarding the photoassociative formation of ultracold Rb_2 molecules. We use a phase-stable MOT in our experiments and, in order to maintain a very low background pressure, we load this MOT with a slow atomic beam generated from a secondary "source" MOT. To date, our experiments have involved inelastic trap-loss collisions. Rate constants are determined by measuring the density-dependent loss rate of atoms from the trap.

Recent Progress:

Recently, we have made progress in three areas: the effects of nonlinear frequency chirps on ultracold trap-loss collisions; the production of short (few

nanoseconds) pulses of chirped light; and the installation of a pulsed laser for ultracold molecule detection.

For the case of laser-induced collisions, the dominant long-range interaction between the two colliding atoms, separated by R, is the $1/R^3$ dipole-dipole potential. The detuning of the light relative to the atomic resonance determines the Condon radius R_c, the separation at which the atom pair is resonantly excited to this potential. If the excited pair subsequently gains sufficient kinetic energy (e.g., >1 K) in rolling down the attractive potential, the atoms will be lost from the trap. By "chirping" the light, i.e., changing its frequency as a function of time, atom pairs spanning a wide range of R can be excited and caused to undergo inelastic trap-loss collisions. One advantage of using chirped light is that for sufficiently high intensities, the population transfer to the excited state can be adiabatic, and therefore efficient and robust. Also, if the time scale of the chirp is comparable to that of the atomic motion, the collision can be controlled by the details of the chirp.

We previously examined the dependence of the trap-loss collision rate on chirp direction and found interesting differences. In particular, at certain center detunings of the chirp, the negative (blue-to-red) chirp yields a significantly smaller collision rate than the positive (red-to-blue) chirp. We attribute this difference to the fact that excited atom pairs always accelerate inward on the attractive potential, while the Condon radius R_c moves either inward (negative chirp) or outward (positive chirp), depending on the sign of the chirp. In the latter case, only the initial excitation is important since an atom pair, once excited, does not further interact with the positively chirped light. In the former case, however, the Condon radius and the trajectory of the excited atom pair both proceed inward and further interactions between the light and the atom pair are therefore possible. These multiple interactions can lead to destructive interference, or "coherent collision blocking", resulting in a reduction in the collisional flux reaching short range in the excited state. This larger collisional rate for positive versus negative chirps observed in the experiment is also seen in classical Monte-Carlo simulations as well as quantum mechanical ones.

These previous results involved linear frequency chirps. In an effort to exert a higher degree of coherent control over collisions induced by negatively-chirped light, we use nonlinear frequency chirps. For comparison purposes, we fix the beginning and ending frequencies of the chirp, as well as the total time duration, but vary the shape of the chirp. Starting with a linear chirp, we superimpose a nonlinear variation with either positive curvature (concave-up) or negative curvature (concave-down). This is done by controlling the injection current to an external-cavity diode laser with an arbitrary waveform generator. For negative chirps, we find a small but significant difference in collision rates for the concave-up versus concave-down shapes. We believe that this is due to details of the matching of the temporal evolution of the Condon radius to the atom-pair trajectories. For the positive chirp, we see no significant difference. This is expected because after the initial excitation, there are no further interactions between the light and the atom pair.

To date, our experiments have used frequency-chirped light (e.g., 1 GHz in 100 ns) generated by a current-ramped external-cavity diode laser and amplified by a separate "slave" laser. We have developed a new technique based on a fiber-based electro-optic phase modulator driven by an arbitrary waveform generator. In this scheme, a pulse of

light from a diode laser is sent through the modulator multiple times, acquiring the prescribed phase shift during each pass. Each time it emerges from the fiber loop, the light is re-injected into the initial laser to boost the power. We realize much higher chirp rates (e.g., 1 GHz in 10 ns) and have the ability to produce chirps of arbitrary shape. We are also utilizing a similar fiber-based electro-optic modulator to control the intensity. This allows us to produce pulses of with intensities of arbitrary shape on the nanosecond time scale.

Some of our upcoming experiments will involve ultracold molecule formation, so we have installed a new pulsed dye-laser system for state-selective ionization detection of the resulting ground-state molecules. The necessary ion detector and ion optics are also being incorporated into the apparatus.

Future Plans:

We will exploit the capabilities of our new chirping method in order to vary the chirp shape and study the influence of these variations on trap-loss collisions. This will resemble a short-pulse coherent control experiment, but where the time scale is nanoseconds instead of femtoseconds. Such long time scales allow the pulse shaping to be done directly in the time domain instead of the frequency domain. We are ultimately interested in applying our techniques to coherently control the formation of ultracold molecules. Once we have developed the capability for molecular ionization detection, we will investigate the use of chirped photoassociation, as well as photoassociation enhanced by chirped long-range excitation, to optimize the production of ground-state molecules. In general, we anticipate that our ability to control the temporal variation of both the laser frequency (by chirping) and amplitude (by pulsing) will open up new opportunities in the manipulation of ultracold collisions and molecule formation.

Recent Publications:

"Control of Ultracold Collisions with Frequency-Chirped Light", M.J. Wright, S.D. Gensemer, J. Vala, R. Kosloff, and P.L. Gould, Phys. Rev. Lett. **95**, 063001 (2005).

"Probing Ultracold Collisional Dynamics with Frequency-Chirped Pulses", M.J. Wright, J.A. Pechkis, J.L. Carini, and P.L. Gould, Phys. Rev. A **74**, 063402 (2006).

"Coherent Control of Ultracold Collisions with Chirped Light: Direction Matters", M.J. Wright, J.A. Pechkis, J.L. Carini, S. Kallush, R. Kosloff, and P.L. Gould, Phys. Rev. A **75**, 051401(R), (2007).

"Generation of Arbitrary Frequency Chirps with a Fiber-Based Phase Modulator and Self-Injection-Locked Diode Laser", C.E. Rogers III, M.J. Wright, J.L. Carini, J.A. Pechkis, and P.L. Gould, J. Opt. Soc. Am. B **24**, 1249 (2007).

Physics of Correlated Systems

Chris H. Greene
Department of Physics and JILA
University of Colorado, Boulder, CO 80309-0440
chris.greene@colorado.edu

Program Scope

The quantum mechanical description of atoms, molecules, photons, and their mutual interactions is comparatively straightforward when those interactions are weak or perturbative. As the interaction strength grows, however, it becomes extremely difficult to treat the most interesting and important systems exhibiting chemical and physical richness. The major goal of this project is the development of techniques that extend the types of such systems that are amenable to realistic theoretical description. We concentrate on problems residing at the cusp of current theoretical capabilities for handling such strongly-interacting or strongly-correlated systems. The relevance to the mission of the Department of Energy lies in the fact that all processes involving energy control and transfer, as well as all chemical rearrangement processes, must inherently involve such correlations. As a result, our theoretical progress on the problems being studied will ultimately add to our capabilities to control the energy flow and rearrangement reactions associated with complex physico-chemical environments, and hopefully spawn a deeper understanding of the potentially damaging effects of radiation damage or energy transmutation.

Recent Progress

The past year of support by this grant has enabled us to make headway on several different specific prototype examples of correlated systems. One topic tackled in the past year, in collaboration with S. R. Leone's group at Berkeley, was a combined theoretical and experimental study of the interaction between XUV photons and the infrared-laser-dressed doubly-excited states of atomic helium.[1] With the imminent arrival of fourth-generation free-electron lasers providing intense radiation in the X-ray range, the exploration of nonlinear photon-atom and photon-molecule coupling is becoming increasingly important to understand in detail.

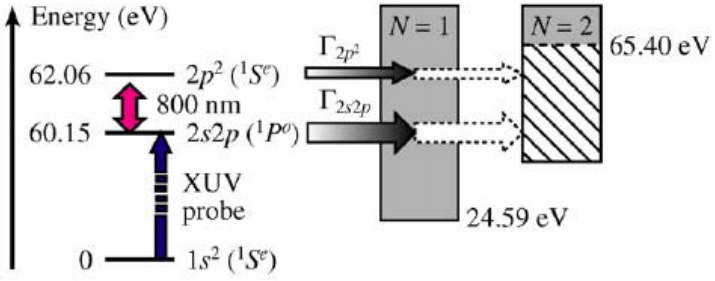

Fig.1. Scheme for the Ref.[1] experiment, in which the 2s2p $^1P^o$ and $2p^2$ $^1S^e$ helium doubly-excited states are coupled or dressed by an 800 nm laser, and then probed using XUV high-harmonics generated by the same laser source.

In this particular study [1], femtosecond high-order harmonic transient absorption spectroscopy has been utilized to probe EIT-like behavior in laser-dressed helium. The 800 nm dressing laser is seen to cause both enhanced transparency at some probe wavelengths, and enhanced absorption at other wavelengths near the minimum of the unperturbed Fano lineshape because the bare Fano *q*-parameter is finite. One goal of this line of research is to see whether an infrared laser can serve as a kind of X-ray switch, which can make a gas suddenly transparent or else suddenly opaque to energetic photons in some range of energies. The present system is only a comparatively inefficient switch, but the study would seem to confirm that this type of manipulation of X-ray absorption in a gas is at least a possibility. A phenomenological model developed by Zoller and Lambropoulos, after generalization to allow for an

additional ionization pathway opened up by the presence of the dressing laser, provides a reasonably successful theoretical description in accord with the experimental observations.

One of the recent developments from the Ottawa group of Villeneuve, Corkum, and coworkers, which has stirred the imagination of the whole community, has been the idea of using energetic high-harmonic generation photons, emitted from an oriented molecule subjected to a strong infrared laser pulse, to form an image of a molecular electron orbital. An idea somewhat conceptually simpler, proposed by Santra, has been to carry out the tomographic reconstruction using instead the time reverse of the final recombination step of HHG, namely angle-resolved photoelectron angular distribution spectroscopy. This removes one complexity present in the HHG experiments, which is the distortion of the interacting electron-ion wavefunction by the intense laser field. A new model study with examples in both one and three dimensions [2] explores the limitations of the plane-wave approximation as it is commonly used in such tomographic reconstructions. The main upshot of that study has been to document something that was expected by a number of researchers in the field: under typical conditions for which current-generation tomographic experiments have been operating, i.e. with rescattering electrons in the energy range 20-50 eV, the molecular field distorts the wavefunction of the returning electron dramatically and the plane-wave approximation cannot be expected to give a faithful reconstruction. In cases where the reconstruction appears to have been successful, this means that it is quite likely a fortuitous example. Our main conclusion is that the original idea of tomographic reconstruction of molecular electron wavefunctions is only likely to be useful if the theory is improved in a nontrivial manner, or if the recolliing energies have one or two orders of magnitude higher energy than in present-day experiments.

Another case we recently studied was high-harmonic generation in the polyatomic molecule SF_6, which is induced by a strong laser pulse that follows a weak Raman-excitation laser pulse. This molecule provides a highly stringent test of theory, partly because of the large number of atoms, partly because of electronic structure issues such as the unbound, triply-degenerate electronic state of the ion after one electron is ripped out by the strong laser pulse. To date only relatively crude approximations have been applied to the rescattering electron, such as the plane-wave or strong-field approximation. In an effort to improve on such restricted theoretical methods, we have formulated an alternative scheme: following the active electron tunneling, its acceleration and subsequent return to the molecule is described using a semiclassical approximation.[3] This semiclassical returning wave is then joined onto a realistic zero-field wavefunction that includes the nonperturbative modification of the de Broglie waves by the molecular field. The last step of the recombination calculation involves the use of this highly-distorted wavefunction to determine the electric dipole matrix element for emission of a photon as the electron fills the hole from which it was initially ejected. It is hoped that this more realistic description of the different portions of the electron motion, while still approximate and piecemeal, should give a qualitative improvement over descriptions that omit the important electron-molecule interaction physics. The resulting comparison with the Murnane-Kapteyn group experiment [Wagner et al. Proc. Nat'l. Acad. Sci. 103, 13279 (2006)] shows encouraging agreement with the general magnitude of the HHG vibrational modulations observed, but at the same time, this level of theory has still failed to achieve quantitative agreement. In particular, the triply-degenerate Raman-active vibrational modulation amplitude is underestimated by an order of magnitude, so future improvements in the theoretical description remain necessary. Note that this theoretical work has relied heavily on previous headway made in this DOE-supported project, through the development of a finite-element R-matrix treatment of electron-molecule scattering at the one-electron level of approximation.[4,5,6]

During the past year we have also made extensive headway on calculations of the dissociative recombination (DR) that occurs when an electron collides with NO_2^+, the neutral species of which is an atmospheric pollutant that is an extremely challenging system for theory to tackle. Despite the fundamental importance of this molecule in atmospheric physics, even a quantity as basic as its total thermally-averaged dissociative recombination rate has apparently never been measured or calculated. Since this is one of the most "chemically-relevant'' molecules that we have ever treated, it has posed new challenges to our theoretical capabilities. One challenge is that there are some "direct" DR pathways, while at the same time some extensive spectroscopic information exists about the Rydberg states of NO_2

at energies near the ionization threshold, and with postdoctoral associate D. Haxton we have been attempting to formulate a unified theoretical treatment that treats the full dimensionality of nuclear motion and which moreover includes the competition and coupling between the direct and indirect paths. This project is getting close to being ready to submit for publication, and in parallel, the difficulty of these calculations has led us to apply the theory to a few simpler molecules to make sure the theory is on solid footing and to improve and generalize it.

Immediate Plans

In the next funding period, we intend to continue our investigations into the single and multiphoton ionization of atomic species that exhibit nonperturbative channel interactions. One of the systems that is planned for study is atomic barium, where the group of Elliott has some challenging experimental measurements of both one-photon and two-photon ionization of the state formed by resonance excitation of barium. This experimental group also has information about the interference of one- and two-photon processes, and our treatment should be able to compute some of those related observables as well. Some preliminary calculations for that system are already encouraging. Another problem that will receive continued interest in the next funding period is the interaction of XUV or X-ray photons with laser-dressed atoms, a topic of importance for the upcoming round of experiments in the next year or two at the FLASH and LCLS free-electron laser facilities. In the area of multiphoton processes, effort is also still underway to try to identify the extent to which zero-field atomic properties, such as Cooper minima and shape resonances, will have their imprint identifiable in the spectrum of photons emitted in a high-harmonic generation experiment. The work on dissociative recombination of diatomic and triatomic ions, especially aiming towards atmospherically-relevant species such as NO2+, will continue as well. Finally, our attempts to model electron scattering from the DNA bases, when they are arranged into a DNA helical twist in the A or B form, will continue and this is expected to result in at least one publication of the P.I. in collaboration with coauthors Tonzani, Caron, and Sanche during the coming year.

Papers published since 2006 that were supported at least in part by this grant

[1] *Femtosecond induced transparency and absorption in the extreme ultraviolet by coherent coupling of the He 2s2p ($^1P^o$) and 2p^2 ($^1S^e$) double excitation states with 800 nm light,* Zhi-Heng Loh, C. H. Greene, and S. R. Leone, Chem. Phys. **350**, 7-13 (2008). (This study and the next two below were supported partially by DOE and partially by NSF.)

[2] *Limits of the plane wave approximation in the measurement of molecular properties,* Z. B. Walters, S. Tonzani and C. H. Greene, J. Phys. Chem. A (in press, 2008); see also arXiv:0804.1958

[3] *High harmonic generation in SF_6: Raman-excited vibrational quantum beats,* Z. B. Walters, S. Tonzani, and C. H. Greene, J. Phys. B **40**, F277 (2007).

[4] *FERM3D: A finite element R-matrix general electron molecule scattering code,* S. Tonzani, Comp. Phys. Commun. **176**, 146-156 (2007).

[5] *Radiation damage to DNA: electron scattering from the backbone subunits.* S. Tonzani and C. H. Greene, J. Chem. Phys. **125**, 094504-1 to -7 (2006).

[6] *Low energy electron scattering from DNA and RNA bases: shape resonances and radiation damage,* S. Tonzani and C. H. Greene, J. Chem. Phys. **124**, 054312-1 to -11 (2006).

[7] *Theoretical progress and challenges in H_3^+ dissociative recombination,* C. H. Greene and V. Kokoouline, Phil. Trans. R. Soc. A **364**, 2965-2980 (2007). (This study was supported partially by DOE and partially by NSF).

[8] *Interaction of intense VUV radiation with large xenon clusters,* Z. B. Walters, R.

Santra, and C. H. Greene, Phys. Rev. A **74**, 043204-1 to -14 (2006).

[9] *Lebedev discrete variable representation*, D. J. Haxton, J. Phys. B **40**, 4443 (2007).

[10] *Comment on 'A wave packet method for treating nuclear dynamics on complex potentials'*, D. J. Haxton, C. W. McCurdy, and T. N. Rescigno, J. Phys. B **40**, 1461 (2007).

Strongly-Interacting Quantum Gases

Principal Investigator: Murray Holland

murray.holland@colorado.edu

440 UCB, JILA, University of Colorado, Boulder, CO 80309-0440

Research Program

The dilute quantum gas has proved to be a useful quantum system in which to study and investigate strongly-interacting many-body phenomena in both the equilibrium and dynamic regimes. This research program aims to pursue theoretically some of the most interesting and fundamental aspects of these systems, with particular emphasis on the proposal of atomic and molecular experiments. The fact that there are many example systems across physics which exhibit strongly-interacting phenomena—in nuclear and particle physics, in condensed matter physics, in atomic physics, and in astrophysics—means that the interesting issues are universal, widely applicable, and of general interest. Although the diluteness of a gas often implies a weakly-interacting quantum system, there are two basic possibilities which lead to the strongly-interacting regime; either the interactions between the particles can be resonantly enhanced through application of a Feshbach resonance, shape resonance or similar, or the effective dimensionality can be reduced by confining the atoms in a periodic optical lattice in all three dimensions. The strongly-interacting atomic gas is a particularly interesting system to consider since the microscopic elements can be controlled as a function of time, in contrast to nuclear matter or condensed matter where the structural parameters are time-invariant.

Over this past year, we have extended our studies in a few specific directions. These include the rapidly rotating gas, Bragg spectroscopy of the Bose-Einstein condensate in the Feshbach resonance regime, the strongly-correlated nonequilibrium physics of atomtronics, and interacting photonic systems in the presence of optical cavities.

Bose-Einstein condensates in a rotating optical lattice

One of the paradigm examples of many-body physics in condensed matter is the fractional quantum Hall effect. Some of the most well-known features include the non-abelian nature and fractional particle statistics. The fractional quantum Hall effect is produced by confining electrons in two-dimensions and subjecting them to a very strong magnetic field. It turns out that this system maps almost exactly onto a rapidly rotating atomic gas, since in both cases the same underlying vector potential arises. Achieving the interesting parameter regime experimentally, by directly spinning the atomic gas, is a substantial challenge. We proposed an alternate approach to realizing the fractional Quantum Hall effect physics in cold gases by examining cold bosons confined to a rotating optical lattice [11]. We derived a modified Bose-Hubbard Hamiltonian to study the system in the tight-binding limit and thereby developed analogies to Bloch electrons in the presence of a magnetic field. One possible approach to

generating a rotating optical lattice is utilizing the method developed in the laboratory of Cornell at JILA, as shown in Fig. 1.

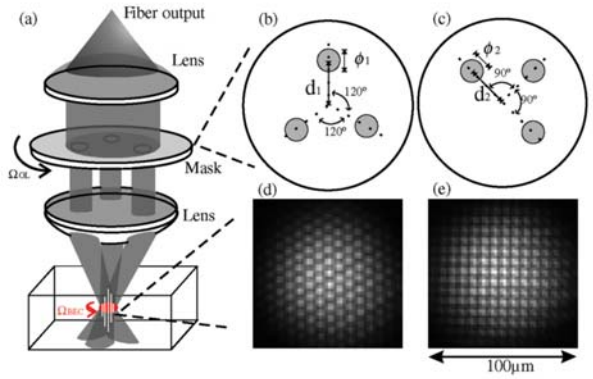

Figure 1. (a) Schematic diagram of the setup used in the Cornell lab at JILA for the rotating quasi-2D optical lattice. Triangular (b) and square masks (c) are used for triangular (d) and square (e) optical lattices respectively.

We studied hardcore bosons by diagonalizing the Hamiltonian in the Fock basis and showed how vorticity can be characterized in this system by the quasiangular momentum [5]. A linear analysis of the system's response to an AC perturbation showed that the system does indeed display characteristics of the fractional quantum Hall effect, as shown in Fig. 2 [6].

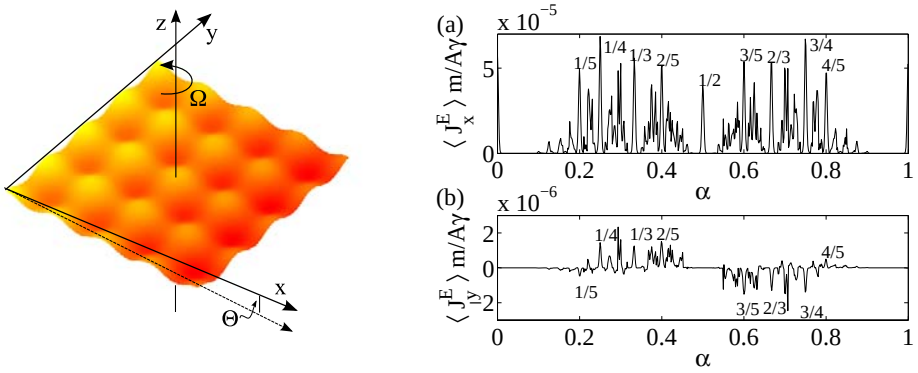

Figure 2. (Left) Our proposed scheme for creating a perturbative linear gradient potential. The lattice potential is tilted by a sinusoidally modulated angle. (Right) The resulting particle currents (transverse top and longitudinal bottom) at the edge of the lattice as function of the angular rotation rate α, for a single particle in a 40×40 lattice. The peaks in the transverse response are quantum Hall states of fractional statistics, and the associated fractional quantum numbers are shown.

Bragg spectroscopy of a strongly-interacting Bose-Einstein condensate

We studied the Bragg spectroscopy of a strongly interacting Bose-Einstein condensate using time-dependent Hartree-Fock-Bogoliubov theory and included the effect of the momentum dependent scattering amplitude which is shown to be the dominant factor in determining the spectrum for large momentum Bragg scattering [1]. The condensation of the Bragg scattered atoms significantly alters the observed excitation spectrum by creating a new pairing channel

of mobile pairs. These calculations were motivated by and are directly applicable to ongoing experiments on Rb-85 at JILA.

Atomtronic circuits and devices

A major research direction has been an investigation of a dynamic strongly-correlated physical system, a topic we have termed *atomtronics* [8]. Atomtronics focuses on establishing ultracold atom analogs of electronic circuits and devices. We have now demonstrated complete atomtronic circuits, rather than atomtronic devices, by implementation of power supplies, connections, and components for ultracold atoms, as illustrated in Fig. 3 [3]. Our approach required developing a theoretical method for solving the dynamics of strongly-interacting many-body, *open* quantum systems. Open quantum systems are those in which a small quantum system of interest is connected to a large reservoir characterised by thermodynamic quantities. Using these results we have been able to explore the analogies to semiconductor device physics—in particular diodes, transistors, logic gates, and memory elements—implemented via the physical system of ultracold atoms and optical lattices.

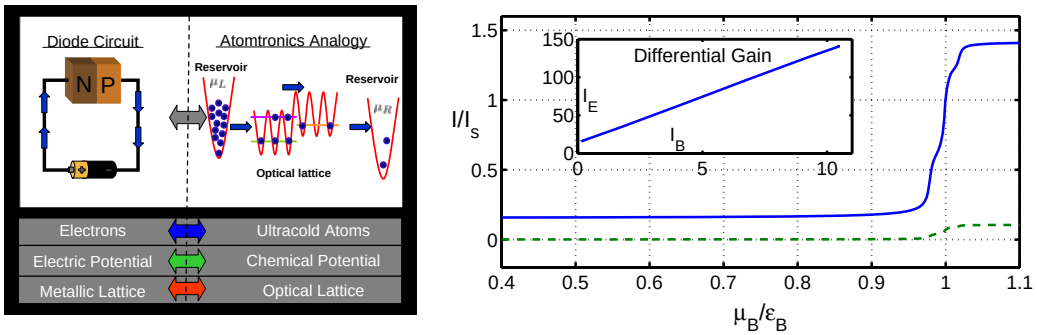

Figure 3. (left) Conventional circuit and atomtronic analogies. (right) Our calculation of the current response of the atomtronic transistor as well as the differential gain. The transistor has three optical lattice wells and three reservoirs model the transistor legs. The middle reservoir has one-fifth the coupling strength of the left and right reservoirs. For a fixed chemical potential difference across the device, we vary the middle potential and record the response of currents leaving the system from both the right site or emitter (solid curve) as well as out of the middle site or base (dashed curve). The large potential differential gain indicates the possibility for utilizing the transistor as an amplifier.

Strongly-correlated photonic systems

We have begun to explore the possibility for generating and analysing complex and collective phenomena in photonic systems, which would open up a new area for future research in this field. For example, we have applied the method of evaporative cooling to a photon fluid confined to a nonlinear Fabry-Perot cavity [2]. A photon fluid is a collection of interacting photons that exhibit fluidic hydrodynamical properties. The photons interact through the presence of a medium such as an atomic Rydberg gas or nonlinear optical crystal. The effects of photon collisions through their atom-mediated interactions and evaporation with an energy dependent reflectivity of the cavity can lead to Bose amplified stimulated emission into the lowest energy mode, as occurs in the Bose-Einstein condensation of ultracold atoms.

Future outlook

In future work, we will extend our atomtronic devices to consider collective effects in mesoscopic systems, as to date most of our studies have been limited to small devices. We will focus our research on rotating optical lattices to consider the experimental implementation possibilities and the important observable and measurable quantities. We will also continue to pursue collective phenomena in photonic systems, building further on the analogy between atoms in optical cavities and ultracold atomic systems.

Publications in peer-reviewed journals on DOE supported research

[1] J. J. Kinnunen, M. J. Holland, *Bragg spectroscopy of a strongly interacting Bose-Einstein condensate*, arXiv:0807.2602 (under review 2008).

[2] B. T. Seaman, M. J. Holland, *Evaporative Cooling of a Photon Fluid to Quantum Degeneracy* , arXiv:0807.1356 (under review 2008).

[3] R. A. Pepino, J. Cooper, D. Z. Anderson, M. J. Holland, *Atomtronic circuits of diodes and transistors*, arXiv:0705.3268 (under review 2008).

[4] D Meiser, Jun Ye and M J Holland, *Spin squeezing in optical lattice clocks via lattice-based QND measurements*, New J. Phys. 10 073014 (17pp) (2008).

[5] B. Peden, R. Bhat, M. Krämer, M. Holland, *Quasi-angular momentum of Bose and Fermi gases in rotating optical lattices*, J. Phys. B: At. Mol. Opt. Phys. **40**, 3725 (2007).

[6] Rajiv Bhat, M. Krämer, J. Cooper, and M. J. Holland, *Hall effects in Bose-Einstein condensates in a rotating optical lattice*, Phys. Rev. A 76, 043601 (2007).

[7] B. T. Seaman, L. D. Carr, and M. J. Holland, *Reply to comment on 'Nonlinear band structure in Bose-Einstein condensates: Nonlinear Schrödinger equation with a Kronig-Penney potential'* , Phys. Rev. A 76, 017602 (2007).

[8] B. T. Seaman, M. Krämer, D. Z. Anderson, and M. J. Holland, *Atomtronics: Ultracold-atom analogs of electronic devices*, Phys. Rev. A 75, 023615 (2007).

[9] R. Bhat, B. Peden, B. Seaman, M. Krämer, L. Carr, M. Holland, *Quantized vortex states of strongly interacting bosons in a rotating optical lattice*, Phys. Rev. A 74, 063606 (2006).

[10] M.L. Chiofalo, S. Giorgini, and M. Holland *Released momentum distribution of a Fermi gas in the BCS-BEC crossover*, Phys. Rev. Lett. 97, 070404 (2006).

[11] R. Bhat, M. Holland, and L. Carr, *Bose-Einstein Condensates in Rotating Lattices*, Phys. Rev. Lett. **96**, 060405 (2006).

[12] L. Carr, M. Holland, B. Malomed, *Macroscopic quantum tunneling of Bose-Einstein condensates in a finite potential well*, J. Phys. B: At. Mol. Opt. Phys. **38**, 3217 (2005).

[13] C. A. Regal, M. Greiner, S. Giorgini, M. Holland, and D. S. Jin *Momentum distribution of a Fermi gas of atoms in the BCS-BEC crossover*, Phys. Rev. Lett. **95**, 250404 (2005).

[14] B. T. Seaman, L. D. Carr, and M. J. Holland *Period doubling, two-color lattices, and the growth of swallowtails in Bose-Einstein condensates*, Phys. Rev. A **72**, 033602 (2005).

[15] L. D. Carr and M. J. Holland *Quantum phase transitions in the Fermi-Bose Hubbard model*, Phys. Rev. A 72, 033602 (2005).

[16] B. T. Seaman, L. D. Carr, M. J. Holland *Nonlinear Band Structure in Bose Einstein Condensates: The Nonlinear Schrödinger Equation with a Kronig-Penney Potential*, Phys. Rev. A **71**, 033622 (2005).

[17] B. T. Seaman, L. D. Carr, M. J. Holland *Effect of a potential step or impurity on the Bose-Einstein condensate mean field*, Phys. Rev. A **71**, 033609 (2005).

Using Intense Short Laser Pulses to Manipulate and View Molecular Dynamics

Robert R. Jones, Physics Department, University of Virginia
382 McCormick Road, P.O. Box 400714, Charlottesville, VA 22904-4714
rrj3c@virginia.edu

I. Program Scope

This project focuses on the exploration and control of non-perturbative dynamics in small molecules driven by strong laser fields. Intense non-resonant laser pulses can radically affect molecules, both in internal and external degrees of freedom. The energy and angular distributions of electrons, ions, and/or photons that are emitted from irradiated molecules contain a wealth of information regarding molecular structure and field-driven dynamics. Not surprisingly, a molecule's alignment with respect to the laser polarization is a critical parameter in determining the effect of the field, and information encoded in photo-fragment distributions may only be interpretable if the molecular axis has a well-defined direction in the laboratory frame. Moreover, even molecules which possess a symmetry axis that can be aligned at a well-defined angle relative to the laser polarization are typically not symmetric with respect to inversion along that axis. Such asymmetric molecules may respond very differently to the alternating positive and negative half-cycles of the electric field in an intense laser pulse. The ability to identify or optically control the head vs. tail orientation of molecules in the laboratory frame is, therefore, critical for observing and characterizing an asymmetric response to standard, symmetric laser fields.

Alternatively, by using 2-color ($1\omega+2\omega$) fields with well-defined relative phases, or few-cycle laser pulses with well-defined carrier-envelope (CE) phase, molecules can be exposed to intense oscillating fields in which there is a pronounced difference in the peak amplitude in one direction over another. Such fields make it possible to induce and/or exploit directional asymmetries within atoms or molecules. For example, charge-localization induced by an asymmetric field can be used to control directional dissociative ionization (i.e. ion ejection up or down) of symmetric molecules [1]. Alternatively, such fields can exploit native charge localization in asymmetric targets, selectively ionizing or fragmenting molecules with specific orientations from within a random ensemble. More generally, strong asymmetric fields used in combination with preferentially oriented targets will enable experiments seeking to probe structure/dynamics or to control photoprocesses by driving molecular electrons in specific directions. Accordingly, our recent work has focused on field-free laser alignment and orientation of molecular targets, characterization of molecular ionization, fragmentation, and high-harmonic generation (HHG) from aligned targets in symmetric and asymmetric fields, and the re-examination of the influence of the atomic/molecular potential on laser-driven continuum electron dynamics.

II. Recent Progress

During the past year we have obtained results from a variety of experiments which are summarized below. First, we have continued to investigate the use of 2-color ($1\omega+2\omega$) laser fields to control directional fragmentation following strong-field dissociative ionization of diatomic molecules. Second, we have demonstrated that, beyond preparation of target molecules for subsequent experiments, transient field-free alignment can be used as a tool for measuring molecular polarizability anisotropies. Third, we have employed counter-propagating laser beams to examine the HHG efficiency from a periodic array of aligned molecules in a hollow-core waveguide. Fourth, in collaboration with Tom Gallagher's group, we have studied multi-photon assisted recombination and found that the parent ion potential enables an oscillating microwave

field to extract far more energy from a continuum electron than is predicted by the standard "Simpleman's" model.

A. Controlled Directional Dissociation in an Asymmetric 2-Color Laser Field

We have studied intense laser dissociative ionization of N_2, CO, and HBr in the presence of an intense, weakly-asymmetric 35 fsec laser pulse. Rather than use few cycle CE phase stabilized pulses [2], we employ a two-color field consisting of two relatively weak ($I < 10^{14}$ W/cm^2), temporally overlapped, "pump" pulses at 400 nm and 800 nm as well as a more intense ($I < 10^{15}$ W/cm^2) "probe." The relative optical phase, φ, between the two pump pulses is controlled using a pair of rotating glass plates in the collinear beams. The pump and probe lasers cross at a small angle in the interaction region such that the relative phases between the pump beams and the probe vary by several full cycles across the interaction region. Thus, φ serves as the only relevant control knob for tuning the relatively small field asymmetry.

For all molecules studied, the yields of atomic ion fragments, A^{+m} and B^{+n} with total charge $(m+n) > 2$ and $A^{+m} \neq B^{+n}$, show a pronounced, φ-dependent forward/backward asymmetry along the spectrometer axis. For all fragments, the maximum ion asymmetry is observed at φ_{max}, for which the field has the greatest asymmetry. In all fragment pairs, the sign of the forward/backward asymmetry is the same for those ions whose creation requires the largest intensity. Similar results are obtained with linearly and circularly polarized pump fields as both result in a net optical field with a phase-dependent directional asymmetry. This indicates that electron rescattering does not play a dominant role in the ionization process.

Instead, our measurements are consistent with a control mechanism based on enhanced sequential ionization at a critical internuclear separation, R_c, as the molecule dissociates [3,4]. Higher charged states are most likely produced when (i) the dissociating molecule has expanded to R_c, and (ii) at the field maximum, weakly bound electrons are trapped on the uphill side of the combined molecular and optical potential due to native or field-induced charge localization. Following the removal of 3 or more electrons, the atomic ions rapidly move apart on repulsive Coulombic potentials. Accordingly, the ion angular distributions at the detector reflect their orientation at the instant of ionization. Thus, the direction of the maximum in the asymmetric field determines the preferred emission direction for the two ions in each fragment channel. A manuscript describing this work is in preparation. It is worth noting that the asymmetric dissociation is robust. Its observation requires only a standard time-of-flight spectrometer and a modest field asymmetry. We intend to explore whether it might find application as a single-shot CE-phase detector for few cycle pulses.

B. Measurement of Polarizability Anisotropies from Transient Alignment Dynamics

Transient laser alignment of linear molecules is a well-established technique for producing ensembles of molecules which preferentially align along a laboratory fixed axis at well-defined times [5]. In essence, a short laser pulse gives the molecules an angular impulse, creating a rotational wavepacket which exhibits periodic angular localization along the laser polarization. The impulse is the result of a time-averaged interaction potential, $U(\theta) \sim -\Delta\alpha\, I(t) \cos^2\theta$, due to the potential energy of the induced molecular dipole in the laser field. Here, I(t) is the temporal intensity envelope of the laser, θ is the angle between the laser field and the molecular axis, and Δα is the molecular polarizability anisotropy. Δα specifies the degree to which a molecule's electron distribution is distorted by an applied electric field. Although Δα impacts a wide range of molecular properties, accurate measurements are not always available in the literature. For

example, it determines the relative intensities of rotational Raman transitions, plays an important role in intermolecular forces, and is required for the calculation of molecular quadrupole moments.

We recently showed that for a known aligning laser intensity, the polarizability anisotropy and the rotational temperature of a molecular ensemble can be determined by comparing time-dependent alignment measurements to quantum rigid rotor simulations. Specifically, we employed identical 40 fsec ultrafast laser pulses to dynamically align N_2 and HBr. We monitored the ensemble alignment via Coulomb explosion using intense 40 fsec probe pulses. We then incorporated the known rotational constant and polarizability anisotropy for N_2 in a rigid-rotor simulation. Comparison of the simulation results to the experimental data enabled us to determine the rotational temperature of the N_2 sample as well as the peak aligning pulse intensity used for both molecules. We then used this intensity determination and the known rotational constant for HBr in an analogous fit of the HBr alignment data. The rotational temperature of the HBr beam as well as the first experimental determination of $\Delta\alpha_{HBr} = 1.7$ (+0.5, -0.2) a.u., were extracted from the fit. A manuscript describing the measurement has been accepted for publication in the Journal of Chemical Physics.

C. HHG from a Periodic Array of Aligned Molecules in a Hollow-Core Fiber

It is well documented that the efficiency of high-harmonic generation from a molecular gas depends dramatically on the molecular alignment relative to the polarization of the drive laser [6]. Co-propagation of alignment and harmonic generating beams ensures that molecules throughout a spatially extended sample are at the same phase of their rotational evolution when they emit harmonics. However, spatial variations in the harmonic generation efficiency can be used to enhance the HHG yield via quasi-phase matching [7,8]. Accordingly, we recently investigated the use of spatially varying molecular alignment to increase the net harmonic yield.

One method for quasi-phase matching HHG involves the use of counter-propagating laser pulses to disrupt the harmonic generation in certain regions along the length of a hollow core fiber [8]. The formation of standing waves at locations where the counter-propagating pulses temporally overlap suppresses harmonic emission from those zones [8]. We also use counter-propagating pulses in a gas filled hollow-core waveguide for our experiments. We first employed co-propagating alignment and harmonic generating pulses in N_2 filled fiber to characterize the variation in harmonic yield as a function of molecular sample alignment. We then reversed the direction of travel of the alignment pulse in the fiber and measured the HHG efficiency in Ar and N_2. In accord with the previous results [8], for both gases we find that temporal overlap of the counter-propagating pulses results in an enhancement or suppression of the harmonic yield, depending on the duration of the laser pulse and the location of the overlap within the guide.

To determine if periodic molecular alignment alone might enable phase-matching, the harmonic generating pulse was delayed so that there was no temporal overlap between it and the aligning pulse within the waveguide. Since Ar and N_2 have very similar pressure tuned phase-matching curves, we consider the effect of the counter-propagating pulse on ratio of the harmonic yield in N_2 to that in Ar. This normalizes out small changes in the harmonic efficiency caused by the small increase in free electrons in the fiber due to ionization by the alignment pulse. As expected, we found that relatively long counter-propagating pulses (1.5 psec), which do not alignN_2, do not affect the N_2:Ar HHG yield ratio. However, relatively short pulses (100 fsec) which do align N_2 molecules result in a small increase (5-10%) in the N_2:Ar HHG yield ratio. At this point it is not clear if this enhancement is due to quasi-phase matching associated with the periodic variation in

molecular alignment along the fiber, or if it is the result of a simple enhancement in the N_2 HHG yield due to time-independent, "incoherent" alignment [5]. Our analysis is continuing.

D. Energy Exchange Between an Oscillating Field and an Electron in an Atomic Continuum
The "Simpleman's Model" was introduced approximately 20 years ago to explain the range of electron energies observed from above threshold ionization (ATI) in intense oscillating fields. It accurately predicts the high-energy cut-off in HHG and has recently been used to describe the influence of few-cycle laser fields on attosecond photoelectron wavepackets [9,10]. In its standard form the Simpleman's model completely neglects the atomic potential. This is a good approximation at the very high electron energies which are typically of interest in ATI and HHG studies. However, it breaks down for the case of low energy photoelectrons driven by fairly weak oscillating fields. This regime has been explored in recent attosecond experiments [10].

In collaboration with Tom Gallagher's group, we have examined energy exchange, in the form of multi-photon recombination, between continuum electrons and a fairly weak microwave field. Energy extraction, far greater than that predicted by the standard Simpleman's model, is observed. The experimental data are in excellent agreement with another, "Simplerman's model," which provides analytic expressions for the maximum energy exchange between an electron and an oscillating field. The model neglects the pondermotive energy of the electron, rather than the atomic potential. This work is described in a manuscript submitted to Physical Review Letters.

III. Future Plans
We are continuing our efforts to observe transient field-free orientation of molecules using unipolar pulses or two-color laser fields. Both of these asymmetric fields are capable of creating rotational wavepackets with non-definite parity. In addition, we have purchased an optical frequency comb laser and are working to improve its CE-phase stability before installing it as the seed for one of our Ti:Sapphire amplifiers. We then plan to employ a fiber compressor to generate few-cycle CE-phase controlled pulses for exploring molecules in strong asymmetric fields.

IV. Publications from Last 3 Years of DOE Sponsored Research (July 2005- July 2008)

i) D. Pinkham, T. Vogt, and R.R. Jones, "Extracting the Polarizability Anisotropy from the Transient Alignment of HBr," J. Chem. Phys. (in press).
ii) D. Pinkham, K. E. Mooney, and R.R. Jones, "Optimizing Dynamic Alignment in Room Temperature CO," Physical Review A **75**, 013422 (2007).
iii) D. Pinkham and R.R. Jones, "Intense Laser Ionization of Transiently Aligned CO," Physical Review A **72,** 023418 (2005).
iv) E. Wells, K.J. Betsch, C.W.S. Conover, M.J. DeWitt, D. Pinkham, and R.R. Jones, "Closed-Loop Control of Intense-Laser Fragmentation of S_8," Physical Review A **72,** 063406 (2005).

References

1. M.F. Kling *et al.*, Science **312**, 246 (2006); V. Roudnev et al., Phys. Rev. Lett. **93**, 163601 (2004).
2. T. Seideman, M.Yu. Ivanov, and P.B. Corkum, Phys. Rev. Lett. **75**, 2819 (1995).
3. G. L. Kamta and A.D. Bandrauk, Phys. Rev. A **76**, 053409 (2007).
4. H. Stapelfeldt and T. Seideman, Rev. Mod. Phys.**75**, 543 (2003) and references therein.
5. Itatani *et al*., Nature **432**, 867 (2004).
6. E. Gibson et al., Science **302**, 95 (2003).
7. A.L. Lytle et al., Phys. Rev. Lett. **98**, 123904 (2007).
8. R. Keinberger et al., Science **297**, 1144 (2002) .
9. J. Mauritsson et al., Phys. Rev. Lett. **100**, 073003 (2008).

Ultrafast Atomic and Molecular Optics at Short Wavelengths

P.I.s: Henry C. Kapteyn and Margaret M. Murnane
University of Colorado at Boulder, Boulder, CO 80309-0440
Phone: (303) 492-8198; E-mail: kapteyn@jila.colorado.edu

The goal of this work is to develop novel short wavelength probes of materials and of molecules. We have made exciting advances in several experiments in recent months in developing methods to probe molecular and materials dynamics.

1. Molecular recollision interferometry (Publications 8, 14, 15): In work just published in Physical Review Letters and illustrated in Fig. 1, we made the first direct and unambiguous observation of the π phase shift in high harmonic emission due to the structure of a molecule. As a result, we directly confirmed the simple two-charge center interference model that predicts such a π phase shift in harmonic emission from CO_2. In our experiment, we interfered harmonic emission from randomly oriented molecules with harmonic emission from a molecular sample that was aligned. At a certain harmonic order and molecular orientation, the phase of the HHG emission changes by π, and the resultant interference fringes shift.
Moreover, by fitting the HHG emission as a function of time within a rotational revival to the two-charge center interference model convolved with the rotational distribution, we can extract the dispersion of the returning electron wavepacket due to the influence of the molecular potential. These results have important implications for extracting molecular structure from measurements of HHG from molecules, and can be used to benchmark realistic theories of molecules in strong fields. In related work published in Phys. Rev. A, we measured the phase of the harmonic emission by interfering HHG beams from a gas mixture of Argon and CO_2.

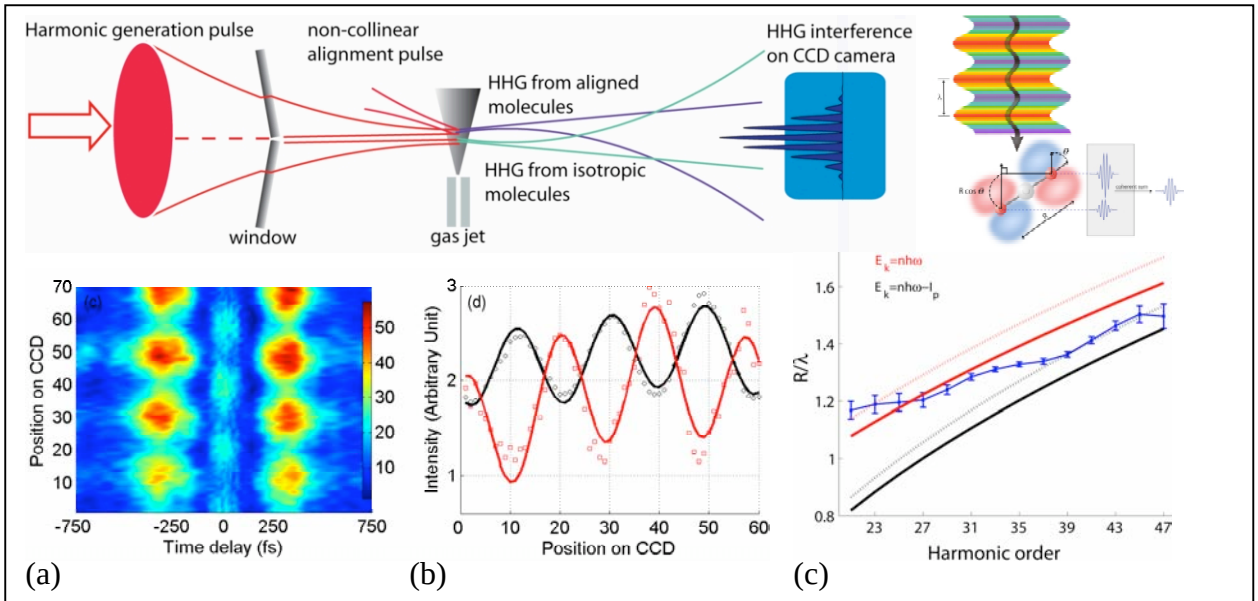

Figure 1: (top left) Setup for directly measuring the intensity and phase of HHG from molecules. HHG from aligned and randomly oriented CO_2 molecules from two different regions in a gas jet interfere in the far field. At a certain harmonic order and molecular orientation, the phase of the HHG emission changes by π, and the resultant interference fringes shift. (top right) Schematic of two charge center model of harmonic emission from CO_2. (bottom) (a, b) Interferences fringes showing a π phase shift in HHG emission due to the molecular structure. (c) Dispersion of the recolliding electron wavepacket as a function of harmonic order. Extracted value of R/λ versus harmonic order (blue squares with error bar). The calculated value of R/λ is also shown for two different dispersion relationships and internuclear separations: Ek = nhω - Ip and R=2.32 Å (black solid line), R=2.45 Å (black dashed line); Ek = nhω and R=2.32 Å (red solid line), R=2.45 Å (red dashed line).

Future work in collaboration with theorists will explore other molecules driven by infrared light to observe more harmonic orders and to explain why no phase shifts are observed in some symmetric molecules such as N_2, but are observed from anti-symmetric molecules.

2. Time-resolved Probing of Dynamics in Polyatomic Molecules using High Harmonic Generation (Publications 19): In this work we performed the first time-resolved study of large-amplitude dynamics in a polyatomic molecule using high harmonic generation. We showed for the first time both theoretically and experimentally that, in order to understand harmonic generation from molecules during a chemical reaction or other large change in configuration, multiple ionization continua must be considered. After exciting large amplitude vibrations in an N_2O_4 dimer molecule, we found that bright bursts of soft x-rays are emitted only at the outer turning point of the vibration, while emission at the inner turning point is much weaker. Theoretical calculations reveal that at the inner turning point, tunnel ionization favors the first electronically excited state (B_{2g}) of the cation, which is "dark" for harmonic emission. At the outer point, the "bright" A_g ground state of N_2O_4 dominates. This work uncovers new understanding of how molecular structure and dynamics can influence high harmonic generation. (see Fig. 2) This work was done in collaboration with Albert Stolow from NRC Canada. Future work will explore dissociating and conformational dynamics in molecules.

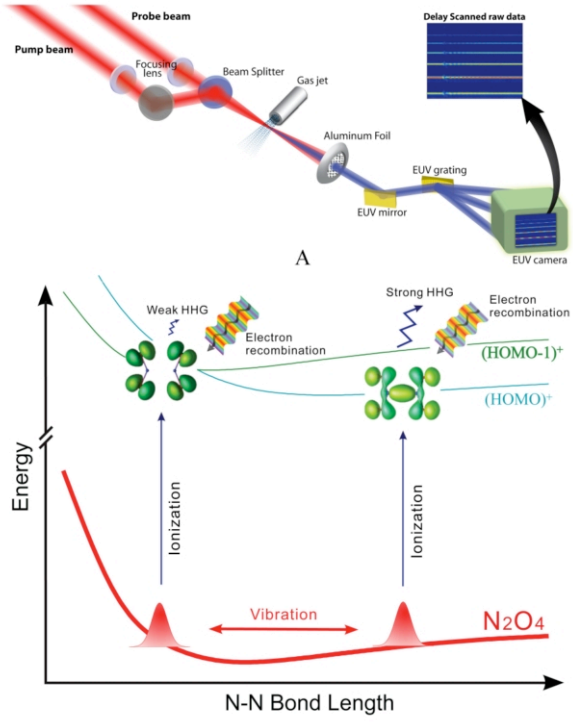

Fig. 2: (top) N_2O_4 molecules are impulsively excited using ultrafast 800nm laser pulses. A more intense, collinear, probe pulse generates harmonics from the vibrationally excited dimer. (bottom) Schematic of the potential energy curves for N_2O_4 as a function of N-N bond length. At the outer turning point, the "bright" ground state Ag continuum is accessed, for which the structural ionization factor and recombination dipole are high, leading to bright x-ray emission. At the inner turning point, the "dark" first excited B_{2g} state is accessed, with low structural ionization factor and recombination dipole.

3. Observation of x-ray driven shake-up and autoionizing dynamics in N_2 and O_2 (Publications 12, 16, 20): In this work we studied and controlled highly excited states of nitrogen and oxygen in the time domain, that result from molecular photoionization. We demonstrated the existence of negative binding energy in a neutral oxygen atom arising from Feshbach resonances. Then, by combining momentum imaging coincident detection (COLTRIMS) with an ultrafast soft x-ray high harmonic source, we used this process to study autoionization in O_2^+. The use of electron-ion coincidence detection makes it possible to uniquely identify and study the autoionizing states. Finally, by introducing an infrared laser pulse coincident with the soft x-ray ionizing pulse, we controlled the dissociation pathway of the

ionized oxygen molecule. This work was done in collaboration with Robin Santra at Argonne National Lab. and with Lew Cocke at Kansas State. Future work will explore fast electronic dynamics in molecules.

4. First observation of elliptically polarized harmonic emission from molecules driven by linearly-polarized light (Publication 21): In very recent work presented as a postdeadline presentation at the International Conference on Ultrafast Phenomena, we reported that elliptically polarized HHG beams can be generated from N_2 molecules even when driven by linearly polarized lasers. These findings shed new understanding of HHG from molecules, and will be very useful to benchmark new and more complete theories of molecules in strong fields. Moreover, our results present a straightforward and efficient way to generate circular polarized harmonic beams for applications in molecular and materials science. Our findings differ from previously published results because we achieve stronger molecular alignment and we achieve a better signal-to-noise ratio. Future work will explore other molecules and compare with theory.

5. Direct Measurement of Angular Dependent Ionization Cross-section for Single Photon Ionization of N2 and CO2 (Publication 17): In work in collaboration with Steve Pratt form Argonne National Laboratory and published in J. Phys. Chem. A, by combining a state-of-the-art high-harmonic ultrafast soft x-ray source with field-free dynamic alignment, we mapped the angular dependence of molecular photoionization yields for the first time for a non-dissociative molecule. The observed modulation in ion yield as a function of molecular alignment was attributed to the molecular frame transition dipole moment of single photon ionization to the X, A and B states of N_2^+ and CO_2^+. Our data show that the transition dipoles for single photon ionization of N_2 and CO_2 at 43 eV have larger perpendicular components than parallel ones. A direct comparison with published theoretical partial wave ionization cross-sections confirm these experimental observations - which are the first results to allow such comparison with theory for bound cation states. The results provide the first step towards a novel method for measuring molecular frame transition dipole matrix elements.

6. Progress in other areas (Publications 1-7, 9-11, 13, 18): In work done in collaboration with Keith Nelson at MIT, we probed thin film thermoacoustic responses and nano-thermal heat transport using spatially coherent EUV beams for the first time. In work done in collaboration with Jorge Rocca at Colorado State University, we significantly extended the energy range of high harmonic generation from Ar ions to 450eV, and demonstrated full phase matching in Ar and Ne at energies of 100eV and 200eV for the first time. We also developed new phase matching schemes for the hard-x-ray region.

Publications as a result of DOE support since 2005

1. Henry C. Kapteyn, Margaret M. Murnane and Ivan P. Christov, "Coherent X-Rays from Lasers: Applied Attosecond Science", invited article, Physics Today, page 39 (March 2005).
2. L. Misoguti, I.P. Christov, S. Backus, M. M. Murnane, and H. C. Kapteyn, "Nonlinear wavemixing processes in the extreme ultraviolet", Physical Review A 72, 063803 (2005).
3. A. Paul, E. Gibson, X. Zhang, A. Lytle, T. Popmintchev, X. Zhou, M. Murnane, I. Christov, H. Kapteyn, "Phase matching techniques for coherent soft-x-ray generation", ***invited paper***, IEEE J. Quant. Electron. **42**, 14 (2006).
4. D. Gaudiosi, E. Gagnon, A. Lytle, J. Fiore, M. Murnane, H. Kapteyn, R. Jimenez, S. Backus, "Scalable multi-kHz Ti:sapphire amplifier based on down-chirped pulse amplification", Opt. Express **14**, 9277 (2006).
5. N. Wagner, A. Wüest, I. Christov, T. Popmintchev, X. Zhou, M. Murnane, H. Kapteyn, "Monitoring Molecular Dynamics using Coherent Electrons from High-Harmonic Generation", *PNAS* **103**, 13279 (2006).
6. D. Gaudiosi, B. Reagan, T. Popmintchev, M. Grisham, M. Berril, O. Cohen, B. Walker, M. Murnane, H. Kapteyn, J. Rocca, "HHG from ions in a capillary discharge", Phys. Rev. Lett. **96**, 203001 (2006).

7. R. Tobey, M. Siemens, M. Murnane, H. Kapteyn, K. Nelson, "Ultrasensitive Transient Grating Measurement of Surface Acoustic Waves in Thin Metal Films with EUV Radiation ", Appl. Phys. Lett. **89**, 091108 (2006).
8. N. Wagner et al., "High-Order X-Ray Raman Scattering using Coherent Electrons from High Harmonic Generation", "Optics in 2006", Optics and Photonics News pp 43 (Dec. 2006). *Also featured on cover*.
9. D. Gaudiosi et al., "HHG from ions in a capillary discharge", "Optics in 2006", Optics and Photonics News, pp 44 (Dec. 2006).
10. Ra'anan I. Tobey, Mark E. Siemens, Oren Cohen, Margaret. M. Murnane, and Henry C. Kapteyn "Ultrafast Extreme Ultraviolet Holography: Dynamic Monitoring of Surface Deformation", Optics Letters **32**, 286 (2007).
11. B.A. Reagan et al., "Enhanced High Harmonic Generation from Xe, Kr, and Ar in a Capillary Discharge", Physical Review A **76**, 013816 (2007).
12. Etienne Gagnon, Predrag Ranitovic, Ariel Paul, C. Lewis Cocke, Margaret M. Murnane, Henry C. Kapteyn, and Arvinder S. Sandhu, "Soft X-ray driven femtosecond molecular dynamics," *Science* **317**, 1374 (2007).
13. Henry C. Kapteyn, Oren Cohen, Ivan Christov, Margaret M. Murnane, "Harnessing Attosecond Science in the Quest for Coherent X-Rays," *Science* **317**, 775 (2007).
14. N. Wagner et al."Extracting the Phase of High Harmonic Emission from a Molecule using Transient Alignment in Mixed Samples," Phys. Rev. A **76**, 061403(R) (2007).
15. Xibin Zhou, Robynne Lock, Wen Li, Nick Wagner, Margaret. M. Murnane, Henry C. Kapteyn, "Molecular Recollision Interferometry in High Harmonic Generation," Physical Review Letters **100**, 073902 (2008).
16. E. Gagnon, A. Paul, A. Czasch, T. Jahnke, K. Hagen, B. Walker, P. Ranitovic, C.L. Cocke, M. Murnane, H. Kapteyn, A. Sandhu, "Time-resolved momentum imaging system for molecular dynamics studies using a tabletop ultrafast extreme-ultraviolet light source," Rev. Sci. Instrum. **79**, 063102 (2008).
17. .I. Thomann, R. Lock, V. Sharma, E. Gagnon, S. Pratt, H. Kapteyn, M. Murnane, W. Li, "Direct Measurement of the Transition Dipole for Single-Photon Photoionization of N_2 and CO_2," to be published, J. Phys. Chem. A (2008).
18. T. Tenio Popmintchev, M.C. Chen, O. Cohen, M.E. Grisham, J.J. Rocca, M.M. Murnane, H.C. Kapteyn, "Phase-Matching of High Harmonics Driven by Mid-Infrared Light," submitted to Optics Letters (2008). Also presented as a Postdeadline presentation, CLEO/QELS Conference.
19. Wen Li, Xibin Zhou, Robynne Lock, Henry C. Kapteyn, and Margaret M. Murnane "Time-resolved Probing of Dynamics in Polyatomic Molecules using High Harmonic Generation", in preparation (2008).
20. E. Gagnon, V. Sharma, W. Li, A.S. Sandhu, R. Santra, P. Ranitovic, C.L. Cocke, M.M. Murnane, H.C. Kapteyn, "Control of Dissociation and Autoionization using the Negative Binding Energy of Feshbach Resonances in Oxygen," in preparation (2008).
21. Xibin Zhou, Robynne Lock, Henry C. Kapteyn, and Margaret M. Murnane, "Observation of Elliptically Polarized High Harmonic Emission from Molecules Driven by Linearly Polarized Light," Postdeadline Paper, Ultrafast Phenomena XVI (Springer Series in Chemical Physics) to be published (2009).

Detailed Investigations of Interactions between Ionizing Radiation and Neutral Gases

Allen Landers

landers@physics.auburn.edu
Department of Physics
Auburn University
Auburn, AL 36849

Program Scope

We are investigating phenomena that stem from the many body dynamics associated with ionization of an atom or molecule by photon or charged particle. Our program is funded through a new Department of Energy EPSCoR Laboratory Partnership Award in collaboration with Lawrence Berkeley National Laboratory. We are using variations on the well established COLTRIMS technique to measure ions and electrons ejected during these interactions. Photoionization measurements take place at the Advanced Light Source at LBNL. Additional experiments on charged particle impact are conducted locally at Auburn University with a 2MV tandem NEC Pelletron accelerator. Finally, a new experiment has been developed that allows the investigation of ion production following ionization of atoms and molecules by low energy electron impact. Presented here is a report of recent work at the ALS-LBNL and future directions along with a brief report on the collisions work at Auburn.

Recent Results

Breakdown of the Two-step Model in Core-level Photoionization of Neon.

For a single multi-level atom such as neon, the photoionization process is yet to be understood in full detail. In particular, just above the core photoionization threshold two interesting phenomena can occur: (1) the three body post-collision interaction (PCI) between the photoelectron, residual ion and subsequent Auger electron; and (2) the possible recapture of the photoelectron. Both processes are associated with the change in potential caused by the fast Auger decay of the core-excited Ne^{*+} that occurs after photoionization. Shortly after emerging from the atom, the outgoing photoelectron is subject to a change in potential associated with the change of parent ion from Ne^{*+} to Ne^{2+}. Within the sudden approximation, the loss in energy (in atomic units) of the photoelectron is simply the change in potential energy given by 1/r, where r is the distance traveled from the ion before Auger decay occurs. If this energy loss is less than the original continuum energy, then the electron simply remains in the continuum with reduced kinetic energy (process 1). In this case, all three bodies can exchange momentum and energy. If, however, the energy loss is greater than the photoelectron's initial energy, the electron can be recaptured into Rydberg state orbiting the Ne^{2+} core (process 2).

At the LBNL-ALS in Berkeley, California, we have used the COLTRIMS technique to investigate in detail both processes (1) and (2) above along with the associated fundamental physics. We have measured the full momentum vectors of both the slow photoelectron and the recoiling neon ion in coincidence. For case (1), the momentum of the faster Auger electron has been determined by conservation laws, giving us the full momentum vectors three-body continuum state in coincidence.

A CTMC calculation by Robicheaux is used to model the interaction between the photoelectron and Auger electron. Because the De Broglie wavelengths differ by a factor of 23, their interaction in the continuum should be well approximated classically. Each event in the calculation consisted of the emission from the origin of a 1.36 eV electron followed by the

emission of an 800 eV Auger electron in a random direction after a random time delay with and exponential distribution determined by the Auger lifetime. For the calculations, we assume no correlation between the original outgoing directions of the two electrons. Once both electrons are launched, he solves the classical time dependent equation of motion to determine the final momenta of the two electrons. Thus, the full electron-electron interaction in the field of the ion is incorporated in this classical calculation. The three components of each electron's momentum were stored in list mode, which allowed for the same sorting analysis of the CTMC data as was used in the analysis of the experimental data. This allowed for a realistic modeling of the experimental resolution.

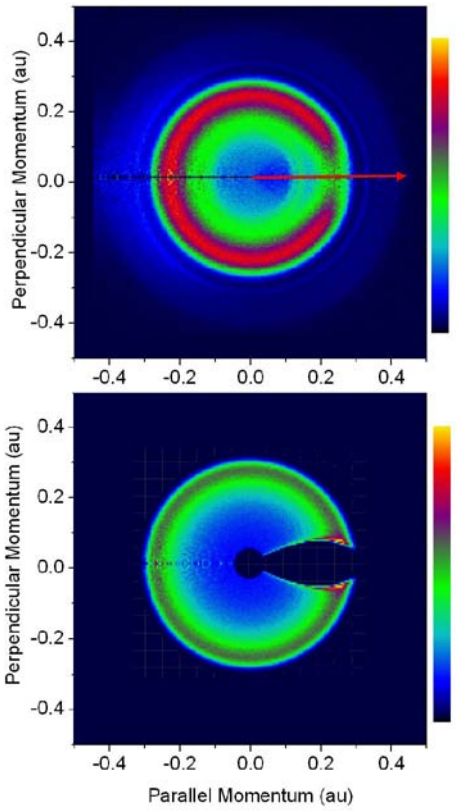

Figure 1: Momentum image of the photoelectron in a frame defined with axes parallel and perpendicular to the Auger emission direction (indicated by the red arrow). The color scale is linear and represents the number of events. The top panel shows the experimental result for low energy electrons in coincidence with the Auger electron. The isotropic discreet rings correspond to a separate recapture/re-emission process. The lower panel shows 2-step CTMC result (Robicheaux) in the same format. Note: The pileup along the edge of the opening of the "C" is not present in the experimental data.

The primary result that has stemmed from this work is the following: Within the two step model, the initial photoelectron flux is diverted away from the Auger emission direction, as can be seen in the calculation Robicheaux in the lower panel of Fig 1. However, in the measurement, we find that the photoelectrons emitted along the Auger direction are not diverted, but rather, they don't come out at all. This is a strong indication that initial state correlation plays a critical role in this photoionization/Auger process and the 2-step picture of the emission of one electron preceding that of the other doesn't fit for the small amount of phase space where the two are emitted in the same direction.

This effect can be seen more clearly in Figure 2, where the cosine of the relative angle between the emission directions of the photo- and Auger- electron is plotted. Here isotropy corresponds to a flat distribution. Here we show the data and CTMC calculation as a function of the cosine of the angle between the two electrons. The CTMC calculation is shown in three curves. The first is the model alone, and the other two correspond to including the 1x and 2x momentum resolution of the experiment in the initial conditions of the CTMC calculation. The calculated pile up of flux is not an effect of the classical treatment of the final state correlation. Such a redistribution rather than suppression of flux is a consequence of the two-step assumption.

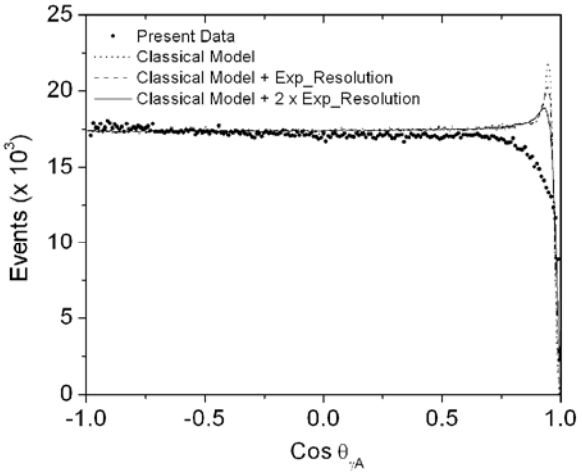

Figure 2: Distribution in cosine of the angle between the Auger electron and photoelectron. Closed circles (•) represent experiment data. Dashed and solid lines correspond to a two-step CTMC calculation (Robicheaux), including cases where the experiment resolution and twice the experiment resolution have been folded into the calculation. The calculation clearly shows a redistribution of photoelectron flux, while it can be seen from the data the flux is actually lost.

Future Plans

There is a small probability (~6%) that the $Ne(1s^{-1})^+$ hole state will decay via double Auger electron emission. In this decay channel, the final state includes the photoelectron, two Auger electrons and the residual Ne^{3+} ion. This relaxation pathway has been investigated previously through use of a magnetic bottle spectroscopy technique [3]. However, to date no measurement exists of the angular correlation between the three continuum electrons. Such a measurement would allow, for example, a study of how the relationship between the photoelectron momentum and the momentum sum of the two Augers as function of the energy sharing between the two electrons, which would lead to significant further insight into the roles of initial- and final-state correlation in core-photoionization.

We plan to pursue a coincidence momentum imaging experiment, measuring three electrons e^- and a recoiling Ne^{3+} ion in coincidence following the core-photoionization of neon. Recognizing that the two-step interpenetration is at heart of this investigation, we still use this model to describe the process:

$$Ne + h\nu(870\text{-}890eV) \rightarrow Ne(1s^{-1})^+ + e^-_{photo} \text{ (photoelectron emission)}$$
$$Ne(1s^{-1})^+ + e^-_{photo} \rightarrow Ne(1s^{-1})^{3+} + e^-_{photo} + e^-_{Auger} + e^-_{Auger} \text{ (Double Auger decay)}$$

The aim is to explore the entangled angular distribution of the three emitted electrons with respect one another. Such a simultaneous vector momentum measurement of three continuum electrons will enable a deeper understanding of the relaxation processes in excited atoms. We plan to pursue these measurements in the spring 2009 two-bunch mode operation at the Advanced Light Source at LBNL.

Goal 1: Investigation of the correlated Auger-electron emission. We will be able to explore, for example, the simultaneous angular and energy correlation between the two Auger electrons to deepen our understanding of this highly-correlated decay pathway. We suspect that the double-Auger decay is in many ways similar to the well documented direct double photoionization (one photon in, two electrons out) of say, helium. For roughly equal energy sharing, there might a strong correlation between the two Auger electrons as in a knock-out type mechanism; and for strongly asymmetric energy sharing, there might be little or no correlation between the two electrons as in a shake-off type mechanism.

Goal 2: Understanding the role of initial and final state correlation in core-level photoionization. As discussed above, one primary motivation of the experiment is to shed further light on the breakdown of the two-step model in describing photo-ionization and (successive?) Auger-decay. A strong initial-state effect might be observed in the correlation between sum momentum of the two Augers and the photoelectron. It might be that such an effect is observed to vary with different energy sharing between the Augers.

Onsite Research at AU: Ionization of Molecules through Collisions with Ions and Electrons

We are also pursuing a local research program at Auburn University that allows for the training of students in a hands-on environment. We have built an electron-molecule collision experiment that uses a pulsed COLTRIMS technique that allows for momentum imaging of molecule fragments after dissociative ionization by electrons with energies from 10eV up to 2000 eV. Preliminary experiments focus on isotope effects in the dissociative ionization of HD. We have also built a pulsed chopper apparatus for the Auburn ion-accelerator, where we are pursuing orientation effects in dissociative ionization of small molecules.

References

[1] A. Russek and W. Mehlhorn, *J. Phys. B* **19** 911 (1986), and references therein.

[2] T. W. Gorczyca, O. Zatsarinny, H.-L. Zhou, S. T. Manson, Z. Fel and A. Z. Msezane, *Phys Rev A* **68**, 050703(R) (2003).

[3] Y Hikosaka, T Aoto, P Lablanquie, F Penent, E Shigemasa and K Ito, *J. Phys. B* **39** 2006 3457-64).

Co-authored Publications over past 2 years (Present funding began Feb 2007)

7. **Angular Correlation between Photo- and Auger electrons from K-Shell Ionization of Neon** A.L. Landers, F. Robicheaux, T. Jahnke, M. Schöffler, T. Osipov, J. Titze, S.Y. Lee, H. Adaniya, M. Hertlein, P. Ranitovic, I. Bocharova, D. Akoury, A. Bhandary, Th. Weber, M.H. Prior, C.L. Cocke, R. Dörner, and A. Belkacem (described above, submitted to PRL).
6. **Ultrafast Probing of Core Hole Localization in N_2** M. S. Schöffler, J. Titze, N. Petridis, T. Jahnke, K. Cole, L. Ph. H. Schmidt, A. Czasch, D. Akoury, O. Jagutzki, J. B. Williams, N. A. Cherepkov, S. K. Semenov, C. W. McCurdy, T. N. Rescigno, C. L. Cocke, T. Osipov, S. Lee, M. H. Prior, A. Belkacem, A. L. Landers, H. Schmidt-Böcking, Th. Weber, and R. Dörner, Science, **320**, 920 (2008).
5. **Interference in the collective electron momentum in double photoionization of H_2** Kreidi K, Akoury D, Jahnke T, Weber T, Staudte A, Schoffler M, Neumann N, Titze J, Schmidt LPH, Czasch A, Jagutzki O, Costa Fraga RA, Grisenti RE, Smolarski M, Ranitovic P, Cocke CL, Osipov T, Adaniya H, Thompson JC, Prior MH, Belkacem A, Landers AL, Schmidt-Bocking H, and Dorner R., Phys. Rev. Lett., **100**, 133005 (2008).
4. **A two-electron double slit experiment: interference and entanglement in photo double ionization of H_2** D. Akoury, K. Kreidi, T. Jahnke, Th. Weber, A. Staudte, M. Schöffler, N. Neumann, J. Titze, L. Ph. H. Schmidt, A. Czasch, O. Jagutzki1, R.A. Costa Fraga1, R. Grisenti, R. Diez Muino, N. Cherepkov, S. Semenov, P. Ranitovic, C.L. Cocke, T. Osipov, H. Adaniya, M.H. Prior, A. Belkacem, A. Landers, H. Schmidt-B¨ Böcking, and R. Dörner, Science, **318**, 949 (2007).
3. **Single Photon-Induced Symmetry Breaking of H_2 Dissociation** F. Martín, J. Fernández, T. Havermeier, L. Foucar, Th. Weber, K. Kreidi, M. Schöffler, L. Schmidt, T. Jahnke, O. Jagutzki, A. Czasch, E. P. Benis, T. Osipov, A. L. Landers, A. Belkacem, M. H. Prior, H. Schmidt-Böcking, C. L. Cocke, R. Dörner, Science **315**, 629 (2007).
2. **Nondipole effects in the angular distribution of photoelectrons from the C K shell of the CO molecule** K. Hosaka, J. Adachi, A. V. Golovin, M. Takahashi, T. Teramoto, N. Watanabe, T. Jahnke, Th. Weber, M. Schöffler, L. Schmidt, T. Osipov, O. Jagutzki, A. L. Landers, M. H. Prior, H. Schmidt-Böcking, R. Dörner, A. Yagishita, S. K. Semenov, and N. A. Cherepkov, Phys. Rev. A **73**, 022716 (2006).
1. **Momentum-imaging investigations of the dissociation of D_2^+ and the isomerization of acetylene to vinylidene by intense short laser pulses** Alnaser AS, Litvinyuk I, Osipov T, Ulrich B, Landers A, Wells E, Maharjan CM, Ranitovic P, Bochareva I, Ray D, Cocke CL. J. Phys. B 39, 485 (2006).

Resonant and Nonresonant Photoelectron-Vibrational Coupling

Robert R. Lucchese, Department of Chemistry, Texas A&M University, College Station, TX, 77843, lucchese@mail.chem.tamu.edu

Erwin Poliakoff, Department of Chemistry, Louisiana State University, Baton Rouge, LA 70803, epoliak@lsu.edu

Program Scope

Molecular photoionization provides an ideal means of studying correlations between electronic and vibrational degrees of freedom. In our research, resonant and nonresonant photoionization are studied for systems ranging from diatomics to large polyatomic systems. High resolution photoelectron spectroscopy measurements at the Advanced Light Source provide the experimental data, and we employ frozen-core Hartree-Fock single-center expansion calculations to provide a theoretical foundation for the analysis. The goal is to develop an understanding of how photoelectrons traverse anisotropic molecular frameworks and exchange energy with vibrations. This research benefits the goals of the Department of Energy because the results elucidate structure/spectra correlations that will be indispensable for probing complex and disordered systems of DOE interest such as clusters, catalysts, reactive intermediates, transient species, and related species.

Recent Progress

In the molecular photoionization process, both the electronic degrees freedom and the vibrational degrees of freedom can be excited. The coupling between these two degrees of freedom can be well described by the adiabatic approximation. Expanding the fixed-nuclei amplitude, $f\left(\vec{k},\hat{n},q\right)$, about a fixed value of the nuclear coordinate, q_0, then gives a photoionization amplitude of the form

$$f^{(f\leftarrow i)}\left(\vec{k},\hat{n}\right) = f\left(\vec{k},\hat{n},q_0\right)\left\langle \chi_{v'}^{(f)}(q)\middle|\chi_{v}^{(i)}(q)\right\rangle_q + \left.\frac{\partial f}{\partial q}\right|_{q_0}\left\langle \chi_{v'}^{(f)}(q)\middle|(q-q_0)\middle|\chi_{v}^{(i)}(q)\right\rangle_q + \cdots$$

where $\chi_v^{(i)}(q)$ and $\chi_{v'}^{(f)}(q)$ are the initial and final state vibrational wave functions, and q represents a vibrational coordinate. Retaining only the first term in this expansion gives the Franck-Condon approximation. If ratios of the cross sections leading to different final vibrational states are made, then one obtains branching ratios. Within the Franck-Condon approximation such branching ratios are independent of the photon energy, whereas when there is a breakdown in the Franck-Condon approximation there can be significant variation of the branching ratios with photon energy.

We have studied a number of cases where the Franck-Condon approximation breaks down. One such case in the photoionization of polyatomic molecules is when the Franck-Condon term is identically zero. This can occur when the vibrational mode under consideration has an antisymmetric character in the point group of the molecule [1]. A second case is when the geometry dependence of the transition amplitude is large, i.e.

when $\partial f/\partial q$ is large. This case often occurs when there is a resonant process whose energy and or width is sensitive to the value of the coordinate, q [5]. A third case of deviations from the Frank-Condon approximation occurs when one of the larger transition matrix elements contributing to a process has a zero as a function of energy, i.e. when there is a Cooper minimum, and when the location of the Cooper minimum varies with q. Finally, there can be other q dependent variations of the cross section with energy at high photon energy that can also lead to deviations from the Franck-Condon approximation. Some recent examples of systems we have studied with these different Franck-Condon breakdown modes are considered here.

Computational study of the $(b_{2u})^{-1}$ photoionization of C_6F_6

Experimental results on the $(b_{2u})^{-1}$ photoionization of C_6F_6 have been previously published [3]. We have now performed a corresponding computational study on this system. We have focused on the excitation of two different symmetric stretching modes in this system, ν_1 which is the symmetric C-F stretching mode and ν_2 which is the symmetric ring-breathing mode. In the computed photoionization cross section there are two prominent shape resonances that occur at about 19 eV and 21 eV. The resonant cross sections respond differently to the two symmetric stretching modes. The C-F stretch dramatically affects the heights of the peaks in the cross sections and their widths, however that mode has only a limited effect on the positions of the resonances. In contrast, the ring breathing mode shifts the positions of the resonances with only a minimal influence on the peak heights or widths.

The strong geometry dependence found in the fixed nuclei calculations results in significant deviations from constant branching ratios expected in the Franck-Condon approximation as seen in figure 1. We considered one-dimensional treatments, where each mode was treated separately, and a two-dimensional treatment where the fixed-nuclei results were computed on a two-dimensional grid of points and all vibrational integrals were performed in two dimensions. Although the level of agreement between

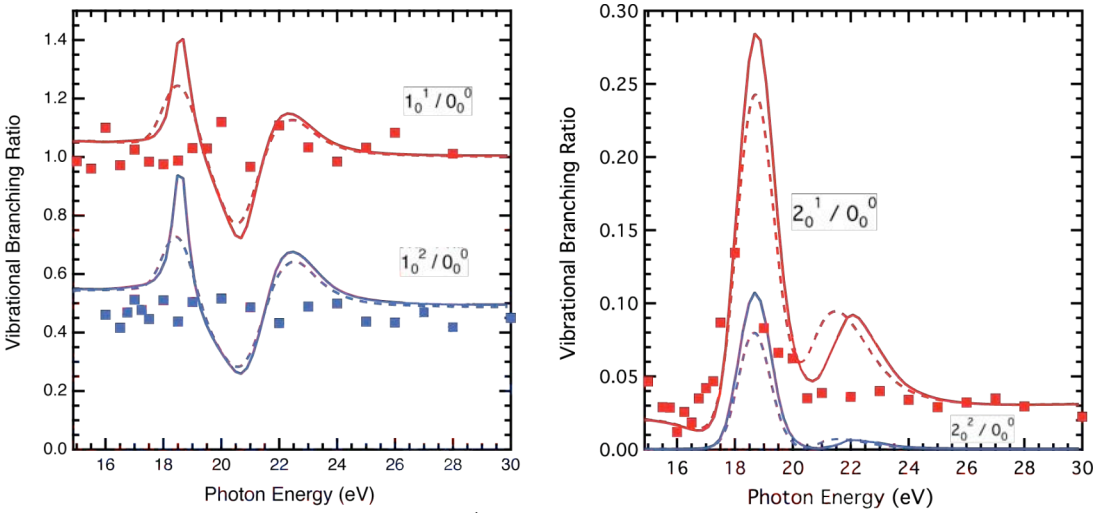

Figure 1. Branching ratios for $(b_{2u})^{-1}$ photoionization of C_6F_6. Left frame is for ν_1 and right frame is for ν_2. Solid lines are from one-dimensional treatments and the dashed lines are the corresponding two-dimensional results.

theory and experiment is not quantitative, there is significant qualitative agreement. Both theory and experiment show marked peaks in the $2_0^1/0_0^0$ branching ratios at about 18.5 eV that is not seen in the $1_0^1/0_0^0$ branching ratio. The distinctive line shape seen in the computed $1_0^1/0_0^0$ branching ratio results from the fact that the C-F stretch does not shift the positions of the resonances but only changes the heights and widths of the cross section features. The qualitative features seen in these branching ratios can be understood using the simple model that the resonant ke_{2g} state is a particle on a ring. In this model, the ν_1 mode does not change the size of the ring but does change the coupling to the continuum, thus this mode does not change the positions of the resonances but does change their widths and peak cross sections. The ν_2 mode changes the size of the ring, and thus shifts the energies of the resonances.

Branching ratios in the $(8\sigma)^{-1}$ ionization of OCS

The branching ratios for all three vibrational modes have been measured and computed for the photoionization of OCS leading to the $(8\sigma)^{-1}$ state of OCS^+. In this system the most dramatic fixed-nuclei effects are seen when the ν_3 mode, the C-O stretching mode, is considered. For motion in that mode, significant shifts in intensities and widths are seen for the broad shape resonances in the continuum. Much weaker effects are seen in response to the C-S stretch (ν_1) and the bending mode (ν_2). However, when the branching ratios are computed and measured, the most significant non-Franck-Condon effects are seen in the branching ratios for the bending mode. In the Franck-Condon approximation the cross section for excitation of the bending mode is zero. Thus any observed intensity in the (010) state is necessarily due to a breakdown in the Franck-Condon approximation. In this system, the non-Franck-Condon effects are further enhanced by the presence of two broad shape resonances in the continuum.

Branching ratios in the $(7\pi)^{-1}$ ionization of ICN

We have also studied experimentally and computationally the $(7\pi)^{-1}$ ionization of ICN leading to the $X\ ^2\Pi_{1/2}$ and $X\ ^2\Pi_{3/2}$ states of ICN^+. In this system, the cross section is featureless in the photon energy range of 20-80 eV, with a nearly exponential falloff across this range of energies. We have considered the vibrationally specific cross sections for excitation of the two stretching modes, ν_1, the C-N stretch, and ν_3, the C-I stretch. The branching ratios are overall nearly flat as a function of energy indicating that the Franck-Condon approximation is accurate.

One interesting feature of this system is that the two spin-orbit states have substantially different branching ratios. For excitation of the ν_1 mode, the (100)/(000) branching ratio for the $X\ ^2\Pi_{1/2}$ state is ~0.12 and for the $X\ ^2\Pi_{3/2}$ state it is ~0.04. This substantial difference can attributed to a difference in equilibrium geometry for the two ion states. Good agreement between theory and experiment can be obtained if we assume that the equilibrium value of R(C-N) in the two ion states differ by ~0.009Å. A similar analysis of the ν_3 branching ratios lead to the conclusion that the shift in R(C-I) in the two spin-orbit ion states is also ~0.009 Å.

Another interesting feature of the ν_1 branching ratio is that it is slowly rising over the range of 40 eV to 80 eV. This behavior of the computed results is due to the fact that

the fixed nuclei cross section is exponentially decaying with a characteristic decay constant that is dependent on the value of q_1. The fixed nuclei cross section can be well represented by the function

$$\sigma = \exp\left[\left(1.717029 - 0.038086E\right) + q_1\left(0.050121 + 0.001261E\right)\right].$$

Inserting amplitudes derive from this expression into the vibrational integral leads to branching ratios that match those obtained in the full calculation.

Future Plans

For the resonant processes, we will develop methods for the proper computational treatment of symmetry breaking vibrations for systems of high symmetry, in particular for degenerate vibrational modes. These methods will be applied to systems such as BF_3, C_6F_6, and CF_4. We will also pursue experimental and theoretical studies of electron-nuclear coupling in low symmetry systems where both the electronic state and vibrational modes are localized in particular regions of the molecule. An example of such a system is the uracil molecule. Finally, we will include multi-channel effects in the scattering calculations to allow for the treatment of vibrational effects in Feshbach-type two-electron resonances for which we already have some experimental evidence.

References

It the last three years, the following eight papers have been published based on our DOE funded research.

[1] G. J. Rathbone, E. D. Poliakoff, J. D. Bozek, and R. R. Lucchese, "Electronically forbidden ($5\sigma_u \rightarrow k\sigma_u$) photoionization of CS_2: Mode-specific electronic-vibrational coupling," *J. Chem. Phys.* **122**, 064308:1-9 (2005).

[2] G. J. Rathbone, E. D. Poliakoff, J. D. Bozek, D. Toffoli, and R. R. Lucchese, "Photoelectron trapping in N_2O $7\sigma \rightarrow k\sigma$ resonant ionization," *J. Chem. Phys.* **123**, 014307:1-9 (2005).

[3] A. Das, E. D. Poliakoff, R. R. Lucchese, and J. D. Bozek, "Launching a particle on a ring: $b_{2u} \rightarrow ke_{2g}$ ionization of C_6F_6," *J. Chem. Phys.* **125**, 164316:1-5 (2006).

[4] E. D. Poliakoff and R. R. Lucchese, "Evolution of photoelectron-vibrational coupling with molecular complexity," *Phys.Scr.* **74**, C71-C79 (2006).

[5] R. Montuoro, R. R. Lucchese, J. D. Bozek, A. Das, and E. D. Poliakoff, "Quasibound continuum states in SiF_4 $\tilde{D}\,^2A_1$ photoionization: Photoelectron-vibrational coupling," *J. Chem. Phys.* **126**, 244309:1-9 (2007).

[6] A. Das, J. S. Miller, E. D. Poliakoff, R. R. Lucchese, J. Bozek, "Vibrationally resolved photoionization dynamics of CF_4 in the $D\,^2A_1$ state," *J. Chem. Phys.* **127**, 044312:1-6 (2007).

[7] R. R. Lucchese, J. Söderström, T. Tanaka, M. Hoshino, M. Kitajima, H. Tanaka, A. De Fanis, J.-E. Rubensson, and K. Ueda, "Vibrationally resolved partial cross sections and asymmetry parameters for nitrogen K-shell photoionization of the N_2O molecule," *Phys. Rev. A* **76**, 012506:1-8 (2007).

[8] M. Hoshino, R. Montuoro, R. R. Lucchese, A. De Fanis, U. Hergenhahn, G. Prümper, T. Tanaka, and K. Ueda, "Vibrationally resolved partial cross sections and asymmetry parameters for nitrogen K-shell photoionization of the NO molecule," *J. Phys. B* **41**, 085105:1-7(2008).

Program Title:

"Properties of actinide ions from measurements of Rydberg ion fine structure"

Principal Investigator: Stephen R. Lundeen,
Dept. of Physics
Colorado State University
Ft. Collins, CO 80523
Lundeen@Lamar.colostate.edu

Program Scope:

Measurements of the fine structure of non-penetrating, high-L Rydberg states of atoms or ions can be used to deduce polarizabilities and permanent moments of the positive ions that form the cores of these Rydberg systems. Special experimental techniques developed under previous DOE support now make it possible to carry out such studies in a wide range of elements and charge states. The current goal of this project is the application of these techniques to measure some properties of chemically interesting actinide ions, such as U^{6+}, Th^{4+}, and other open shell U and Th ions. Since *a-priori* prediction of the properties of such highly relativistic ions is very challenging but still much simpler than predicting their behavior in chemical compounds, it is hoped that such measurements will contribute to improved understanding of actinide chemistry.

Recent Progress:

Work on this project takes place at two locations. At Colorado State University (CSU), we carry out studies of neutral Rydberg systems, with the aim of testing and improving the theoretical framework used to relate the measured fine structure patterns to positive ion properties. At Kansas State University (KSU), we share the use of ECR sources producing beams of multiply-charged ions needed to study Rydberg ion fine structure. A new permanent magnet ECR source capable of producing the beams of U and Th ions needed for this program is currently being installed at KSU and should be in operation by the end of the summer 2008.

At KSU, our progress this year has been the purchase and delivery of the new ECR source, and the planning and construction of the new beamlines needed to bring it into operation. In order to make the shared use of the source more convenient for users of the KLS laser source, the beamlines have been lowered to the height of the the KLS beam and reoriented in the lab floor plan. These changes should make the new source more productive over the long run, although they have slightly extended the installation time. Our hope, at present, is to have operational beamlines by September, 2008 and actinide beams by December, 2008. Our first studies will be of the Rn-like ions U^{6+} and Th^{4+}.

At CSU this year, we completed a RESIS/microwave study of Rydberg states of argon. Since Ar^+ is a $^2P_{3/2}$ ion with a non-zero quadrupole moment, the fine structure of argon Rydberg states is much more complex than that of atoms like Ba that have $^2S_{1/2}$ cores, though still not as complex as the structure expected for Rydberg levels bound to open shell actinide ions like Th^{3+}. The argon study will be only the second extensive study of a high-L Rydberg system with anisotropic ion core, and it should help to stimulate the development of the theoretical tools needed to understand these systems in detail. In connection with this study, we carried out a complete theoretical derivation of

the long-range potential seen by an electron in the vicinity of a J=3/2 positive ion. A complete report of this work is nearly ready for publication.

A second project at CSU is in its initial stages. We have recently obtained the first RESIS spectra of Nickel Rydberg states, showing many lines in the pattern of 10 to 31 excitation of Ni. The Ni^+ ion is has a $^2D_{5/2}$ ground state, so its Rydberg fine structure patterns are even more complex than Ar, and comparable in complexity to that expected for the Th^{3+} ion, with it's $^2F_{5/2}$ ground state. We have not yet succeeded in making unambiguous identifications of the lines and so do not yet have any conclusions about the properties of the Ni^+ ion. This work is continuing.

Immediate Plans:.

At KSU, we will complete the construction of new beamlines and begin studies of Rydberg ions bound to the Rn-like ions U^{6+} and Th^{4+}. These studies should be no more difficult than our completed studies of Kr^{6+}, and depending on the beam intensities and beam quality obtained with the new ECR source, could be much easier. Within the year, we also hope to begin exploring the RESIS spectra produced by Rydberg ions bound to open shell U and Th ions.

At CSU, our primary experimental project will be the continuation of the study of Nickel Rydberg fine structure. This will also involve extension of the theoretical model relating ion properties to Rydberg fine structure to include core ion angular momentum as large as 5/2.

Another project will involve further theoretical analysis of the spin splittings observed in Rydberg states of Ba, and documented in a recent publication.

Recent Publications:

"Ion Properties from High-L Rydberg Fine Structure: Dipole Polarizability of Si^{2+}" R.A. Komara, M.A. Gearba, C.W. Fehrenbach, and S.R. Lundeen, J. Phys. B. At. Mol. Opt. Phys. 38, S87 (2005)

"Stark-induced X-ray emission from H-like and He-like Rydberg ions", M.A. Gearba, R.A. Komara, S.R. Lundeen, C.W. Fehrenbach, and B.D. DePaola, Phys. Rev A 71, 013424 (2005)

"Determination of dipole and quadrupole polarizabilities of Ba^+ by measurement of the fine structure of high-L, n=9 and 10 Rydberg states of Barium" E.L. Snow, M.A. Gearba, W.G. Sturrus, and S.R. Lundeen, Phys. Rev A 71, 022510 (2005)

"Fine Structure in High-L Rydberg states: A Path to Properties of Positive Ions" in *Advances in Atomic, Molecular, and Optical Physics*, Vol. 52 edited by Chun C. Lin and Paul Berman (Academic Press, 2005)

"Relative charge transfer cross section from Rb(4d)", M.H. Shah, H.A. Camp, M.L. Trachy, X. Flechard, M.A. Gearba, H. Nguyen, R. Bredy, S.R. Lundeen, and B.D. DePaola, Phys. Rev. A 72, 024701 (2005)

"Optical spectroscopy of high-L Rydberg states of Argon" L.E. Wright, E.L. Snow, S.R. Lundeen, and W.G. Sturrus, Phys. Rev. A 75, 022503 (2007)

"Higher-order contributions to fine structure in high-L Rydberg states of Si^{3+}", E.L. Snow and S.R. Lundeen, Phys. Rev. A 75, 062512 (2007)

"Polarizability of Kr^{6+} from High-L Kr^{5+} Fine Structure Measurements", S.R. Lundeen and C.W. Fehrenbach, Phys. Rev. A 75, 032523 (2007)

"Fine Structure Measurements in high-L, n=17 and n=20 Rydberg states of Barium", E.L. Snow and S.R. Lundeen ,Phys. Rev. A, 76, 052505 (2007)

"Determination of dipole and quadrupole polarizabilities of Mg^{+} by fine structure measurements in high-L, n=17 Rydberg states of Mg", E.L. Snow and S.R. Lundeen, Phys. Rev. A 77, 052501 (2008)

Theory of threshold effects in low-energy atomic collisions

J. H. Macek

Department of Physics and Astronomy,
University of Tennessee, Knoxville, Tennessee and
Oak Ridge National Laboratory, Oak Ridge, Tennessee
email:jmacek@utk.edu

1 Program scope

Developing methods for benchmark calculations of time-dependent atomic processes is the chief focus of this work. In particular, we will compute cross sections for ionization of atomic hydrogen by proton impact with an accuracy goal of 1%. Such accuracy cannot be obtained by measurements, however, it is possible, at least in principle, to achieve such accuracy by numerical solution of the Schrödinger equation to ionization processes. Indeed, our project is predicated upon the view that developing methods for highly accurate calculations of ion-atom collisions is a timely task for atomic theory since the interactions are known, they are relatively simple, numerical methods such as the Lattice-Time-Dependent-Schrödigner equation are approaching high accuracy, and cross sections accurate at the 1% level are needed to characterize hydrogen atom beams used in plasma diagnostics.

To achieve high accuracy in numerical calculations it is essential to understand all of the physical processes that occur in time-dependent quantum processes. A second goal of our work is to interpret structure in the electron momentum distribution $P(\boldsymbol{k})$ and identify essential physical processes involved in ionization. To do this we have developed a method to extract $P(\boldsymbol{k})$ from time-dependent wave functions that allow us to trace structure in $P(\boldsymbol{k})$ to structure in atomic wave functions when target and projectile are strongly interacting. In this way we have found, apparently for the first time, that free vortices are formed in one-electron wave functions. Calculations are under way to study how these vortices may be observed.

We also continue our research into structure related to threshold phenomena. The projects listed in this abstract are sponsored by the Department of Energy, Division of Chemical Sciences, through a grant to the University

of Tennessee. The research is is carried out in cooperation with Oak Ridge National Laboratory under the ORNL-UT Distinguished Scientist program.

2 Recent progress

The Lattice-Time-Dependent-Schrödinger equation method has been adapted to the computation of ionization processes [8]. The adaptation recognizes that standard numerical methods cannot correctly treat ionization because the electron wave function has an essential singularity at infinite distances. A method to factor out the essential singularity has been developed. One surprising consequence of this factorization is the "imaging theorem", namely $P(\boldsymbol{k})$ images the *coordinate* space wave function according to

$$P(\boldsymbol{k}) = \lim_{t\to\infty} \left[|\psi(\boldsymbol{r},t)|^2\right]_{\boldsymbol{r}=\boldsymbol{k}t} \tag{1}$$

where it is understood that $\boldsymbol{r} \neq \boldsymbol{r}_Q$ where $\boldsymbol{r}_Q$ is any potential center. It follows from Eq. (1) that structure in $P(\boldsymbol{k})$ can be traced to structure in $\psi(\boldsymbol{r},t)$ at earlier times. Using this theorem we have investigated a suggestion by B. D. Esry that "holes" in our computed momentum distributions are due to free vortices. The "holes" are traced to a single hole which dominates the wave function at earlier times. The electron current is found to circulate around this hole indicating that it is a free vortex.

Since such vortices have not been identified earlier we have checked whether they occur in the universally accepted Born theory of $P(\boldsymbol{k})$. We find vortices in the impact parameter Born amplitude $A(\boldsymbol{b},\boldsymbol{k})$, even though they are absent in the usual plane wave theory.

To see if the vortices are observable, at least in principle, the impact parameter amplitude is transformed to physical space by the transformation

$$A^{CB}(\boldsymbol{K},\boldsymbol{k}) = (2\pi)^{-1} \int A(\boldsymbol{b},\boldsymbol{k}) b^{2iZ_P/v} \exp(-i\boldsymbol{K}_\perp \cdot \boldsymbol{b}) d^2b \tag{2}$$

where $\boldsymbol{K}$ is the momentum transfer and $\boldsymbol{K}_\perp$ is its component perpendicular to the initial velocity vector. Because the coulomb interaction between the target and projectile nucleus is taken into account, the amplitude is indicated with the superscript CB for "Coulomb Born". The corresponding $P(\boldsymbol{k})$ has been found to have vortices even though the standard Born amplitude does not. Since the CB amplitude is more correct, it is apparent that even well-known approximate theories may show vortices if analyzed using the imaging theorem.

Preliminary results indicate that the vortices may be observable. For example, contour plots of the electron momentum distribution were computed using Eq. (2) for and incident energy of 400 keV and a perpendicular momentum transfer of Z_T/v for proton impact on atomic hydrogen. A hole appears in the distribution at $k_y/v = 0.25$ and $k_x/v = 0.4$. This hole is a vortex minimum as verified by a plot of the electron current. In addition, this structure is sufficiently pronounced that it should be observable. Observation of such structure would be the first indication that vortices in atomic wave functions play an important role in ionization processes.

Other projects investigate structure that appears in elastic scattering [1,5,7,9], charge exchange reactions [2], low energy three-body interactions [4,6] and ionization by positron impact [10]. The threshold ionization cross section obeys the extended threshold law proposed earlier by us and verified by convergent close coupling model calculations. We find some unanticipated structure owing to hidden crossings of hyperspherical adiabatic potential energy curves.

3 References to DOE sponsored research that appeared in 2006-2008

1. Oscillations in the Integral Cross Sections for Scattering of Protons by Inert Gas Atoms, S. Yu. Ovchinnikov, P. S. Krstic and J. H. Macek, *Phys. Rev. A* **74**, (2006), Accepted for Publication.

2. Quantum Phase Interference Effects in Anion to Dianion Charge-exchange Collisions, S. Yu. Ovchinnikov, J. H. Macek, A. A. Tuinman, J. D. Steil, R. N. Compton, P. Hvelplund, I. S. Holm, S. S. Nielsen and M. B. Nielsen, *Phys. Rev. A* **73**, 064704 (2006).

3. Exact Solution for Three Particles Interacting via Zero-range Potentials, J. H. Macek, S. Yu. Ovchinnikov and G. Gasaneo, *Phys. Rev. A* **73**, 032704 (2006).

4. Properties of Pseudopotentials for Higher Partial Waves, J. H. Macek and J. Sternberg, *Phys. Rev. Lett.* **97**, 023201 (2006).

5. What can one do with Regge poles?, D. Sokolovski, A. Z. Msezane, Z.

Felfli, S. Yu. Ovchinnikov, and J. H. Macek, Nuc. Inst. Meth. B, **261**, 133 (2007).

6. Efimov states: what are they and why are they important?, J. H. Macek, Phys. Scr. **76**, C3 (2007).

7. Feshbach resonances in Atomic Structure and Dynamics, J. H. Macek in Quantum Few-Body Systems, Proceedings of the joint physics/mathematics workshop on quantum few-body systems. Aahus Denmark 19-20 March 2007, Ed. Jacob S. Moller and Dmitri Fedorov, AIP conference proceedings **998**, pages 59-69, (2007).

8. Quantum treatment of continuum electrons in the fields of moving charges,Teck-Ghee Lee, S. Yu. Ovchinnikov, J. Sternberg, V. Chupryna,3 D. R. Schultz, and J. H. Macek, A **76**, 050701R (2007).

9. Regge oscillations in electron-atom elastic cross sections, D. Sokolovski,1 Z. Felfli,2 S. Yu. Ovchinnikov,3 J. H. Macek,4 and A. Z. Msezane2, Phys Rev. A **76**, 012705 (2007).

10. Near-threshold positron impact ionization of hydrogen, S. J. Ward, Krista Jansen, J. Shertzer, and J. H. Macek, Nuc. Inst. Meth. B, **266**, 410 (2008).

Photoabsorption by Free and Confined Atoms and Ions

Steven T. Manson, Principal Investigator
Department of Physics and Astronomy, Georgia State University, Atlanta, Georgia 30303
(smanson@gsu.edu)

Program Scope

The goals of this research program are: to provide a theoretical adjunct to, and collaboration with, the various atomic and molecular experimental programs that employ third generation light sources, particularly ALS and APS; to generally enhance our understanding of the photoabsorption process; and to study the properties (especially photoabsorption) of confined atoms and ions. To these ends, calculations are performed employing and enhancing cutting-edge methodologies to provide deeper insight into the physics of the experimental results; to provide guidance for future experimental investigations; and seek out new phenomenology, especially in the realm of confined systems. The general areas of programmatic focus are: manifestations of nondipole effects in photoionization; photodetachment of inner and outer shells of atoms and atomic ions (positive and negative); exploratory studies of atoms endrohedrally confined in buckyballs, C_{60}. Flexibility is maintained to respond to opportunities that present themselves as well.

Highlights of Recent Progress

1. Confined Atoms

The study of confined atoms is in it's in its infancy. There are a handful of theoretical investigations of various atoms endohedrally confined in C_{60} [1], but not much in the way of experiment as yet. Thus, we are involved in a program of exploratory calculations aimed at providing a compendium of the properties of such systems, especially photoionization, to tempt the experimental community. Among our recent results, we have found that a huge transfer of oscillator strength from the C_{60} shell, in the neighborhood of the giant plasmon resonance, to the encapsulated atom for both $Ar@C_{60}$ [2] and $Mg@C_{60}$ [3]. For example, the Ar 3p oscillator strength in the region up to 50 eV increases from just under 6, for the free atom, to about 60 in the confined case. This occurs owing to a *coherent* interchannel coupling interaction between the photoionization channels of the atom and C_{60}. Qualitatively, the phenomenon is independent of the nature of the confined atom, but quantitatively, the dependence is quite strong, contradicting a recent semi-classical study [4].

In addition, a new type a resonance has been discovered, termed a correlation confinement resonance [5]. Confinement resonances occur in the photoionization of an endohedral atom owing to the interferences of the photoelectron wave function for direct emission with those scattered from the surrounding carbon shell. We have found that the confinement resonances in the dominant subshell cross section can be transferred to other subshell cross sections *via* interchannel coupling.

The photoionization of endohedral atoms within nested fullerenes, called buckyonions, has also been investigated [6]. It is found that, as a result of the multi-

walled confining structures, the confinement resonances become considerably more complicated.

2. Atomic Photoionization

The study of photoionization of atoms, particularly open-shell atoms, leads to results of great complexity. Our effort is to perform state-of-the-art calculations, in concert with high-resolution synchrotron experiments, to understand this complexity. This philosophy has been applied to inner-shell photoionization of Sc^{++}, the simplest system containing a d-electron. Experimental measurements had been performed [7] which have defied the efforts of theorists to provide an accurate calculation—until now. Using the Breit-Pauli R-matrix approach, we have succeeded in reproducing the experimental result with excellent accuracy [8], with one proviso. The calculated cross section is about 60% larger than the experimental result. A sum rule analysis of the results suggests that it experiment that is substantially too low, and this is being looked into right now. These results demonstrate the predictive/corrective power of theory and experiment working collaboratively.

3. Nondipole Effects in Atoms

Up until relatively recently, the conventional wisdom was that nondipole effects in photoionization were of importance only at photon energies of tens of keV or higher, despite indications to the contrary more than 35 years ago [9]. The last decade has seen an upsurge in experimental and theoretical results [10] showing that nondipole effects in photoelectron angular distributions could be important down to hundreds [11] and even tens [12] of eV. Our recent work included a combined calculational and laboratory investigation that has provided the first experimental evidence for a quadrupole Cooper minimum, a phenomenon that had been predicted to exist much earlier [13], revealed in studies of nondipole effects in Xe 5*s* and 5*p* [14]. While the evidence is much "cleaner" for the 5*s* case, the 5*p* case shows how much can be learned by a careful analysis of a combined theoretical and experimental investigation.

Future Plans

Fundamentally our future plans are to continue on the paths set out above. In the area of nondipole effects the inner subshells of Hg will be investigated to try to unravel the combined effects of many-body correlation effects and relativistic interactions. In addition, the search for cases where nondipole effects are likely to be significant, as a guide for experiment, and quadrupole Cooper minima, will continue. The study of the photodetachment of C^- shall move on to the photoabsorption in the vicinity of the K-shell edge of both the ground ^4S and exited ^2D states in order to understand how the slight excitation of the outer shell affects the inner-shell photoabsorption and to pave the way for experiment, in addition to further study of Na^-. Further, build upon our previous work, we shall attack the problem of inner-shell Photoionization of the Sc atom. Additionally, a study of the photoionization of confined Hg atoms will be pursued in order to learn how the much larger relativistic effects in heavy systems affect the photoabsorption properties of caged atoms.

Publications Citing DOE Support Since November, 2006

- "Strong Final-State Term-Dependence of Nondipole Photoelectron Angular Distributions from Half-Filled Shell Atoms," V.K. Dolmatov and S. T. Manson, Phys. Rev A **74**, 032705-1-7 (2006).
- "Resonance Induced Deviations of β from 2.0 for Rare Gas s-Subshell Photoionization," S. B. Whitfield, R. Wehlitz, H. R. Varma, T. Banerjee, P. C. Deshmukh and S. T. Manson, J. Phys. B **39**, L335-L343 (2006).
- "New Correlation Effects in the Photoionization of Atoms and Ions," S. T. Manson, Radiation Phys. Chem. **75**, 2119-2123 (2006).
- "Spin-Polarized Photoelectrons from Half-Filled Shell Atoms," V. K. Dolmatov and S. T. Manson, Phys. Rev. A **75**, 022701-1-4 (2007).
- "Dipole and Quadrupole Cooper Minima and their Effects on Dipole and Nondipole Photoelectron Angular Distributions in Hg 6s," T. Banerjee, P. C. Deshmukh and S. T. Manson, Phys. Rev. A **75**, 042701-1-8 (2007).
- "Dynamical and Relativistic Effects in Experimental and Theoretical Studies of Inner-Shell Photoionization of Sodium," D. Cubaynes, H. L. Zhou, N. Berrah, J.-M. Bizau, J. D. Bozek, S. Canton, S. Diehl, X.-Y. Han, A. Hibbert, E. T. Kennedy, S. T. Manson, L. VoKy and F. J. Wuilleumier, Phys. Rev. A **40**, F121-F129 (2007).
- "Confinement, Correlation and Relativistic Effects on the Photoionization of the 6s Subshell of Hg," H. R. Varma, T. Banerjee, S Sunil Kumar, P. C. Deshmukh, V. K. Dolmatov and S. T. Manson, J. Phys. Conf. Ser. **80**, 012025-1-5 (2007).
- "Krypton E2 Photoionization Cross-sections and Angular Distribution of Photoelectrons," T. Banerjee, P. C. Deshmukh and S. T. Manson, J. Phys. Conf. Ser. **80**, 012001-1-8 (2007).
- "Correlation and Relativistic Effects in the Photoionization of Confined Atoms," H. R. Varma, P. C. Deshmukh, V. K. Dolmatov and S. T. Manson, Phys. Rev. A **76**, 012711-1-7 (2007).
- "Photoionization of Hydrogen-like Ions Surrounded by a Charged Spherical Shell," A. S. Baltenkov, S. T. Manson and A. Z Msezane, Phys. Rev. A **76**, 042707-1-6 (2007).
- "'Reading' the Photoelectron β-Parameter Spectrum in a Resonance Region," V. K. Dolmatov, E. Guler and S. T. Manson, Phys. Rev. A **76**, 032704-1-5 (2007).
- "Ionization in Fast Atom-Atom Collisions: the Influence and Scaling Behavior of Electron-Electron and Electron-Nuclear Interactions," J. M. Sanders, R. D. DuBois, S. T. Manson, S. Datz, E. F. Deveney, H. F. Krause J. L. Shinpaugh and C. R. Vane, Phys. Rev. A **76**, 062710-1-7 (2007).
- "Spectacular Enhancement in Low Energy Photoemission of Ar Confined in C_{60}," M. E. Madjet, H. S. Chakraborty and S. T. Manson, Phys. Rev. Letters **99**, 243003-1-4 (2007).
- "Theoretical and Experimental Demonstration of the Existence of Quadrupole Cooper Minima," P. C. Deshmukh, T. Banerjee, H. R. Varma, O. Hemmers, R. Guillemin, D. Rolles, A. Wolska, S. W. Yu, D. W. Lindle, W. R. Johnson, and S. T. Manson, J. Phys. B **41**, 021002-1-5 (2008).
- "Photoionization of C_{60}: A Model Study," M. E. Madjet, H. S. Chakraborty, J. M. Rost and S. T. Manson, J. Phys. B **41**, 105101-1-8 (2008).

• "Theoretical Studies of Photoabsorption By Atomic Systems," S. T. Manson, W.-C. Chu, A. M. Sossah and H.-L. Zhou, *Frontiers in Atomic Molecular and Optical Physics* (in press).
• "Dynamical Effects of Confinement on Atomic Valence Photoionization in $Mg@C_{60}$," M. E. Madjet, H. S. Chakraborty, J. M. Rost and S. T. Manson, Phys. Rev. A (in press).
• "Photoionization of Atoms Confined in Giant Spherical Buckyballs and Buckyonions," V. K. Dolmatov, P. Brewer and S. T. Manson, Phys. Rev. A (in press).
• "Relativistic-Random-Phase Approximation Calculations of Atomic Photoionization: What We Have Learned," S. T. Manson, Can. J. Phys. (in press).
• "Electron-Impact Ionization of Atoms: Secondary Electron Angular Distributions and Drag Currents," A. S. Baltenkov, S. T. Manson and A. Z. Msezane, Phys. Rev. A (submitted).
"Relaxation Effects in Photodetachment of Intermediate p shells of the Chlorine and Bromine Negative Ions," V. Radojevic, J. Jose, G. B. Pradhan, P. C. Deshmukh and S. T. Manson, Can. J. Phys. (in press).
• "Correlation confinement resonances in photoionization of endohedral atoms: $Xe@C_{60}$," V. K. Dolmatov and S. T. Manson, J. Phys. B (submitted).
• "Electron-Impact Ionization of Atoms: Secondary Electron Angular Distributions and Drag Currents," A. S. Baltenkov, S. T. Manson and A. Z. Msezane, Phys. Rev. A (submitted).

References

[1] V. K. Dolmatov, A. S. Baltenkov, J.-P. Connerade and S. T. Manson, Radiation Phys. Chem. **70**, 417 (2004).
[2] M. E. Madjet, H. S. Chakraborty and S. T. Manson, Phys. Rev. Letters **99**, 243003 (2007).
[3] M. E. Madjet, H. S. Chakraborty, J. M. Rost and S. T. Manson, Phys. Rev. A (in press).
[4] S. Lo, A. V. Korol and A. V. Solov'yov, J. Phys. B **40**, 3973 (2007).
[5] V. K. Dolmatov and S. T. Manson, J. Phys. B (submitted).
[6] V. K. Dolmatov and S. T. Manson, J. Phys. Rev. A (in press).
[7] S. Schippers, et al, Phys. Rev A **67**, 032702 (2003).
[8] A. M Sossah, H.-L. Zhou and S. T. Manson, Bull. Am. Phys. Soc. **53** (7), 36 (2008).
[9] M. O. Krause, Phys. Rev. 177, 151 (1969).
[10] O. Hemmers, R. Guillemin and D. W. Lindle, Radiation Phys. and Chem. **70**, 123 (2004) and references therein.
[11] O. Hemmers, R. Guillemin, E. P. Kanter, B. Kraessig, D. W. Lindle, S. H. Southworth, R. Wehlitz, J. Baker, A. Hudson, M. Lotrakul, D. Rolles, W. C. Stolte, I. C. Tran, A. Wolska, S. W. Yu, M. Ya. Amusia, K. T. Cheng, L. V. Chernysheva, W. R. Johnson and S. T. Manson, Phys. Rev. Letters **91**, 053002 (2003).
[12] V. K. Dolmatov and S. T. Manson, Phys. Rev. Letters **83**, 939 (1999).
[13] L. A. LaJohn and R. H. Pratt, Radiation Phys. and Chem. **61**, 365 (2001); **71**, 665 (2004); and references therein.
[14] P. C. Deshmukh, T. Banerjee, H. R. Varma, O. Hemmers, R. Guillemin, D. Rolles, A. Wolska, S. W. Yu, D. W. Lindle, W. R. Johnson, and S. T. Manson, J. Phys. B **41**, 021002 (2008).

Combining High Level *Ab Initio* Calculations with Laser Control of Molecular Dynamics

Thomas Weinacht
Department of Physics and Astronomy
Stony Brook University
Stony Brook, NY
tweinacht@ms.cc.sunysb.edu

and

Spiridoula Matsika
Department of Chemistry
Temple University
Philadelphia, PA
smatsika@temple.edu

Program Scope

We use intense, shaped, ultrafast laser pulses to control molecular dynamics and high level *ab initio* calculations to interpret and guide the control. In particular, we are interested in controlling bond breaking and isomerization by tailoring the phase and amplitude of ultrafast laser pulses which drive the reaction dynamics. A learning algorithm inside a learning control loop is used to discover optimal pulse shapes for control, and *ab initio* calculations are used to interpret the control and guide further control experiments. Ultimately, we are interested in developing new techniques for molecular wave function imaging and pulse shape spectroscopy based upon our control experiments.

Recent Progress

Molecular ionization by a strong-field, ultrafast laser pulse is typically accompanied by wave packet motion on ionic potential energy surfaces (PESs) of the molecule since the equilibrium configuration of the ion generally differs from that of the neutral. These wave packet dynamics in the ionic PESs can have a significant effect on the fragmentation of the molecule, particularly if there are low-lying ionic states that are accessible from the ground state of the ion with a subsequent laser pulse (via single-photon absorption in the visible or near infrared 1.5 - 3 eV). The importance of ionic resonances has been debated in the literature, with recent work highlighting the importance of wave packet motion across resonances in determining molecular fragmentation patterns.

High-level, *ab initio* electronic structure calculations have been used to interpret the fragmentation dynamics of $CHBr_2COCF_3$ following excitation with an intense ultrafast laser pulse. The potential energy surfaces of the ground and excited cationic states along the dissociative C-CF_3 bond have been calculated using multireference second-order perturbation theory methods. The calculations confirm the existence of a charge-transfer resonance during the evolution of a dissociative wave packet on the ground state potential energy surface of the molecular cation and yield a detailed picture of the dissociation dynamics observed in earlier work. Comparisons of the ionic spectrum for two similar molecules, $CHBr_2COCF_3$ and CH_3COCF_3, support a general picture in which molecules are influenced by dynamic resonances in the cation during dissociation.

Future Plans

Ionic resonances as a function of molecular geometry are not only important and useful for control, but can also be very useful for following dynamics since they can have a significant effect on the fragmentation of a molecule exposed to a strong field laser pulse. Tunnel ionization at a geometry where there is a resonance between the ground ionic state and higher lying ionic states can be followed by rapid excitation to dissociative ionic states which leads to the production of many small fragment ions. We are using this to monitor control over the isomerization of molecules such as cyclohexadiene (CHD) in the gas phase. The experiments make use of our recently developed shaped ultrafast UV laser pulses followed by a strong field IR pulse which probes the geometry via dissociative ionization. We have demonstrated control over the ring opening in CHD and are now working on understanding the dynamics underlying control.

We are also making use of dynamic ionic resonances to characterize electronic and vibrational wave packets generated in small polyatomic molecules via both tunnel and multiphoton ionization. We are interested in measuring the phase and amplitude of these wave functions as a function of time via holographic techniques (wave packet interference).

Publications

- "Interpreting Ultrafast Molecular Fragmentation Dynamics with *ab initio* Calculations", C. Trallero, B. J. Pearson, T. Weinacht, K. Gilliard and S. Matsika, *J. Chem. Phys.*, **128**, 124107, (2008)

PROGRESS REPORT

ELECTRON-DRIVEN PROCESSES IN POLYATOMIC MOLECULES

Investigator: Vincent McKoy

A. A. Noyes Laboratory of Chemical Physics
California Institute of Technology
Pasadena, California 91125

email: mckoy@caltech.edu

PROJECT DESCRIPTION

The focus of this project is the continued development, extension, and application of accurate, scalable methods for computational studies of low-energy electron–molecule collisions, with emphasis on larger polyatomics relevant to materials-processing and biological systems. Because the required calculations are highly numerically intensive, efficient use of large-scale parallel computers is essential, and the computer codes developed for the project are designed to run both on tightly-coupled parallel supercomputers and on workstation clusters.

HIGHLIGHTS

Over the past year we have gained deeper insight into the interactions of slow electrons with biological molecules while engaging in fruitful collaborations with experimental groups. Principal developments include:

- A systematic study of elastic electron scattering by methyl phosphate esters and phosphoric acid, which are models for phosphate moiety in the DNA backbone
- A joint experimental and theoretical study of elastic electron scattering by 3-hydroxytetrahydrofuran, a model for the sugar moiety in the DNA backbone
- A collaborative study of elastic electron scattering by CF_2, in which our calculations supported the first quantitative measurements of the elastic cross section for a radical
- A joint experimental/theoretical study of electron-impact excitation of C_2H_4 to the $\tilde{a}\ ^3B_{1u}$ state
- First results, for methanol and ethanol, from an ongoing collaboration with experimentalists and other theorists on alcohols and other biologically relevant molecules

ACCOMPLISHMENTS

During 2008, we pursued our examination of electron collision processes involving DNA by taking a closer look at possible mechanisms for temporary electron trapping on the phosphate-sugar backbone. Recent experimental studies [1–5] have suggested that temporary anion states (resonances) exist through which slow electrons can attach directly to the DNA backbone and promote strand breaking. Such a direct path would call into question the model of Simons and coworkers [6–9], in which electrons first attach through a π^* resonance on one of the nucleobases before undergoing transfer to the backbone. To investigate this possibility, we studied [10] elastic scattering by a series of compounds that model the phosphate moiety, starting with phosphoric acid, H_3PO_4, and progressively adding methyl groups to form the mono-, di-, and trimethylphosphate esters, $(CH_3)_xH_{3-x}PO_4$, x=1–3. Our results for H_3PO_4 are qualitatively similar to those computed by Tonzani and Greene [11], while overall, our calculations reveal strong similarities among the scattering cross sections of these compounds and indicate the presence of several broad shape resonances at higher collision energies. However, our calculations do not produce any narrow, low-energy shape resonances that could account for dissociative attachment below 5 eV. Our results are consistent with the absence in these molecules of low-lying, empty valence orbitals that can temporarily trap an electron; in particular, they support the view that the phosphoryl bond is not a true σ, π double bond and does not

have a conjugate π^* orbital associated with it, as also argued by Burrow *et al.* [5]. On the other hand, open questions remain about the origin of low-energy features seen in the dissociative attachment [4] and electron transmission [5] spectra of phosphate esters.

In a second study related to the DNA backbone [12], we collaborated with experimentalists to determine differential and integral elastic cross sections for electron scattering by 3-hydroxytetrahydrofuran (3-OH-THF), a model for the deoxyribose moiety. This study was a follow-on to earlier work by each group on the simpler model compound tetrahydrofuran (THF) [13,14]. On the whole, the cross sections for 3-OH-THF proved very similar to those for THF, with broad shape resonances above 5 eV but no indication of narrow or low-lying resonances that might promote dissociative attachment. One puzzling feature was that our calculation indicated a slightly larger cross section for 3-OH-THF than for THF, consistent with its larger physical size, while the experiment indicated the opposite trend, i.e., a smaller cross section for 3-OH-THF than for THF.

Over the past year we also pursued productive collaborations on smaller systems, including a study of CF_2 that involved the first quantitative measurements of differential elastic cross sections for electron scattering by a radical [15] and a re-examination, together with Michael Allan of Fribourg, of the cross section for electron-impact excitation of ethylene (C_2H_4) to its lowest excited electronic state, $\tilde{a}\ ^3B_{1u}$ [16]. The latter work resolved a long-standing discrepancy between theory and experiment by showing that correct positioning of the elastic-channel shape resonance, which lies below the triplet threshold, is essential to obtaining the correct magnitude for the near-treshold excitation cross section. We also obtained the first results from an experimental-theoretical collaboration initiated last year to study alcohols and other small molecules, publishing a combined study of the elastic electron cross sections of methanol and ethanol [17].

PLANS FOR COMING YEAR

In the coming year, we plan to continue work now under way to examine resonant channel coupling in the DNA and RNA nucleobases. In this work, we are looking at the effect of coupling between the elastic channel and low-lying $\pi \rightarrow \pi^*$ triplet excited states on the character of resonances seen in the elastic cross section. Previous calculations on pyrazine [18,19], a high-symmetry analogue of the pyrimidine bases, showed that the third π^* shape resonance was strongly mixed with core-excited resonances built on triplet states, and we expect similar channel mixing to occur in the nucleobases themselves. Preliminary calculations have been carried out for uracil, but the results indicate the need for further extension of the capabilities of our scattering codes before definitive results can be obtained. Those extensions are under way. Last year, we recoded the portion of our scattering program that generates and transforms Gaussian integrals to make it more efficient and easier to parallelize. We are currently recoding the section that generates many-electron integrals from those matrix elements as a distributed-memory parallel code in order to allow larger matrix dimensions. With the new code we expect scattering calculations with $\sim 10^5$ configurations in the variational space should be possible.

Also in the coming year, we expect to wrap up a collaborative study of 1-propanol and 1-butanol that is nearing completion and and begin studies, together with the same collaborators, of inelastic processes in water. Time permitting, we would also like to begin investigations in which we look at nuclear motion in connection with electron-collision dynamics in order to understand resonance-driven dissociative attachment processes.

REFERENCES

[1] P. Sulzer, S. Ptasinska, F. Zappa, B. Mielewska, A. R. Milosavljevic, P. Scheier, T. D., Märk, I. Bald, S., Gohlke, M. A.. Huels, and E. Illenberger, J. Chem. Phys. **125**, 044304 (2006).

[2] I. Bald, J. Kopyra, and E. Illenberger, Angew. Chem. Int. Ed. **45**, 4851 (2006).

[3] I. Bald, J. Kopyra, I. Dąbkowska, E. Antonsson, and E. Illenberger, J. Chem. Phys. **126**, 074308 (2007).

[4] C. König, J. Kopyra, I. Bald, and E. Illenberger, Phys. Rev. Lett. **97**, 018105 (2006).
[5] P. D. Burrow, G. A. Gallup, and A. Modelli, J. Phys. Chem. A **112**, 4106 (2008).
[6] R. Barrios, P. Skurski, and J. Simons, J. Phys. Chem. B **106**, 7991 (2002).
[7] J. Berdys, I. Anusiewicz, P. Skurski, and J. Simons, J. Phys. Chem. A **108**, 2999 (2004).
[8] J. Berdys, P. Skurski, and J. Simons, J. Phys. Chem. B **108**, 5800 (2004).
[9] I. Anusiewicz, J. Berdys, M. Sobczyk, P. Skurski, and J. Simons, J. Phys. Chem. A **108**, 11381 (2004).
[10] C. Winstead and V. McKoy, Int. J. Mass Spectrom. (in press).
[11] S. Tonzani, C. H. Greene, J. Chem. Phys. **125**, 094504 (2006).
[12] V. Vizcaino, J. Roberts, J. P. Sullivan, M. J. Brunger, S. J. Buckman, C. Winstead, and V. Mckoy, New J. Phys. **10**, 053002 (2008).
[13] C. Winstead and V. McKoy, J. Chem. Phys. **125**, 074302 (2006).
[14] C. J. Colyer, V. Vizcaino, J. P. Sullivan, M. J. Brunger, and S. J. Buckman, New J. Phys. **9**, 41 (2007).
[15] T. M. Maddern, L. R. Hargreaves, J. R. Francis-Staite, M. J. Brunger, S. J. Buckman, C. Winstead, and V. McKoy, Phys. Rev. Lett. **100**, 063202 (2008).
[16] M. Allan, C. Winstead, and V. McKoy, Phys. Rev. A **77**, 042715 (2008).
[17] M. A. Khakoo, J. Blumer, K. Keane, C. Campbell, H. Silva, M. C. A. Lopes, C. Winstead, V. McKoy, R. F. da Costa, L. G. Ferreira, M. A. P. Lima, and M. H. F. Bettega, Phys. Rev. A **77**, 042705 (2008).
[18] C. Winstead and V. McKoy, Phys. Rev. Lett. **98**, 113201 (2007).
[19] C. Winstead and V. McKoy, Phys. Rev. A **76**, 012712 (2007).

PROJECT PUBLICATIONS AND PRESENTATIONS, 2006–2008

1. "Low-Energy Electron Collisions with Fullerene, C_{60}," C. Winstead and V. McKoy, Phys. Rev. A **73**, 012711 (2006).

2. "Total Dissociation Electron Impact Cross Sections for C_2F_6," D. W. Flaherty, M. A. Kasper, J. E. Baio, D. B. Graves, H. F. Winters, C. Winstead, and V. McKoy, J. Phys. D **39**, 4393 (2006).

3. "Electron Collisions with Large Molecules: Computational Advances," V. McKoy, American Chemical Society National Meeting, Atlanta, March 28, 2006 *(invited talk).*

4. "Low-Energy Electron Scattering by N_2O," M. H. F. Bettega, C. Winstead, and V. McKoy, Phys. Rev. A **74**, 022711 (2006).

5. "Low-Energy Electron Collisions with Gas-Phase Uracil," C. Winstead and V. McKoy, submitted to J. Chem. Phys. **125**, 174304 (2006).

6. "Low-Energy Electron Scattering by Deoxyribose and Related Molecules," C. Winstead and V. McKoy, J. Chem. Phys. **125**, 074302 (2006).

7. "Electron Collisions with Large Molecules," C. Winstead, Colloquium, Department of Physics, Federal University of Paraná, Curitiba, Brazil, July 27, 2006.

8. "Interaction of Low-Energy Electrons with the Purine Bases, Nucleosides, and Nucleotides of DNA," C. Winstead and V. McKoy, J. Chem. Phys. **125**, 244302 (2006).

9. "Electron-Driven Processes in Polyatomic Molecules," V. McKoy, XVI National Conference on Atomic and Molecular Physics, Tata Institute of Fundamental Research, Mumbai, India, 8–11 January, 2007 *(invited talk).*

10. "Resonant Channel Coupling in Electron Scattering by Pyrazine," C. Winstead and V. McKoy, Phys. Rev. Lett. **98**, 113201 (2007).

11. "Interactions of Slow Electrons with Biomolecules," V. McKoy, Molecular Theory for Real Systems Program, University of Tokyo, Japan, 18–19 March, 2007 *(invited talk).*

12. "Recent Computations of Electron Collisions with Large Molecules," V. McKoy, EIPAM 07 (Electron Induced Processes at the Molecular Level), Hveragerđi, Iceland, 25–29 May, 2007 *(invited talk).*

13. "Interactions of Slow Electrons with Biomolecules," V. McKoy, XXV International Conference on Photonic, Electronic, and Atomic Collisions, Freiburg, Germany, 25–30 July, 2007 *(invited talk).*

14. "Electron Collisions with Biomolecules," V. McKoy, Fifteenth International Symposium on Electron–Molecule Collisions and Swarms, Reading, United Kingdom, 1–4 August, 2007 *(invited talk).*

15. "Low-Energy Electron Scattering by Pyrazine," C. Winstead and V. McKoy, Phys. Rev. A **76**, 012712 (2007).

16. "Interaction of Low-Energy Electrons with the Pyrimidine Bases and Nucleosides of DNA," C. Winstead, V. McKoy, and S. d'A. Sanchez, J. Chem. Phys. **127**, 085105 (2007).

17. "Resonant Interactions of Slow Electrons with DNA Constituents," C. Winstead, ASR 2007 (International Symposium on Charged Particle and Photon Interactions with Matter), JAEA Advanced Science Research Center, Tokaimura, Japan, 6–9 November, 2007 *(invited talk).*

18. "Interactions of Slow Electrons with Biomolecules," V. McKoy and C. Winstead, J. Phys. Conf. Ser. **88**, 012072 (2007).

19. "Absolute Elastic Differential and Integral Cross Sections for Electron Scattering from the CF_2 Radical," T. M. Maddern, L. R. Hargreaves, J. R. Francis-Staite, M. J. Brunger, S. J. Buckman, C. Winstead, and V. McKoy, Phys. Rev. Lett. **100**, 063202 (2008).

20. "Interactions of Slow Electrons with DNA," V. McKoy, Chemistry Department Seminar, University of Alabama, Tuscaloosa, Alabama, February 28, 2008.

21. "Low Energy Elastic Electron Scattering from Methanol and Ethanol," M. A. Khakoo, J. Blumer, K. Keane, C. Campbell, H. Silva, M. C. A. Lopes, C. Winstead, V. McKoy, R. F. da Costa, L. G. Ferreira, M. A. P. Lima, and M. H. F. Bettega, Phys. Rev. A **77**, 042705 (2008).

22. "Electron Scattering in Ethene: Excitation of the $\tilde{a}\ ^3B_{1u}$ State, Elastic Scattering and Vibrational Excitation," M. Allan, C. Winstead, and V. McKoy, Phys. Rev. A **77**, 042715 (2008).

23. "Elastic Electron Scattering from 3-Hydroxytetrahydrofuran: Experimental and Theoretical Studies," V. Vizcaino, J. Roberts, J. P. Sullivan, M. J. Brunger, S. J. Buckman, C. Winstead, and V. Mckoy, New J. Phys. **10**, 053002 (2008).

24. "Interactions of Slow Electrons with DNA," V. McKoy, Physics Department Seminar, Federal University of Juiz de Fora, Juiz de Fora, Brazil, June 11, 2008.

25. "Interaction of Slow Electrons with Methyl Phosphate Esters," C. Winstead and V. McKoy, Int. J. Mass Spectrom. (in press).

26. "Resonant Interactions of Slow Electrons with DNA Constituents," C. Winstead and V. McKoy, Radiat. Phys. Chem. (in press).

27. "Electron Collisions with Biomolecules," V. McKoy and C. Winstead, J. Phys. Conf. Ser. (in press).

28. "Electron-Impact Dissociation of Oxygen-Containing Molecules—A Critical Review," J. W. McConkey, C. P. Malone, P. V. Johnson, C. Winstead, V. McKoy, and I. Kanik, Phys. Rep. (in press).

ELECTRON/PHOTON INTERACTIONS WITH ATOMS/IONS

Alfred Z. Msezane (email: amsezane@cau.edu)

Clark Atlanta University, Department of Physics and CTSPS, Atlanta, Georgia 30314

PROGRAM SCOPE

We develop methodologies for calculating Regge pole trajectories and residues for both singular and nonsingular potentials, important in heavy particle collisions, chemical reactions and atom-diatom systems. Methods are developed for calculating the generalized oscillator strength (GOS), useful in probing the intricate nature of the valence- and open-shell as well as inner-shell electron transitions. Standard codes are used to generate sophisticated wave functions for investigating CI mixing and relativistic effects in atomic ions. The wave functions are utilized in exploring correlation effects in dipole and non-dipole photoionization studies. Regge trajectories probe the near-threshold formation of negative ions as Regge resonances in electron scattering, revealing new and interesting manifestations and yielding a better understanding of the underlying physics in this energy region.

RECENT PROGRESS

A. COMPLEX ANGULAR MOMENTUM METHODS AND APPLICATIONS TO COLLISIONS

In the following sections we briefly describe our accomplishments in this area for the current funding period.

A.1 Simple Method for Electron Affinity Determination: Results for Ca, Sr and Ce

Benchmarking the recently developed Regge-pole methodology [1] for electron-atom elastic scattering on the most recently measured electron affinity (EA) of the Ca atom, we illustrate the predictive power of the methodology, when used with a Thomas-Fermi type potential that incorporates the vital core polarization interaction, by calculating the binding energy of the tenuously bound negative ion Sr^- and predicting the value of 0.61 eV for the binding energy of the ground state of the very complicated Ce^- ion, with f- and d- open sub-shells, a shape resonance at 0.37 eV and a Ramsauer-Townsend minimum at about 0.09 eV [2]. Our calculated EA value for the Ce atom favors the latest theoretical [3] and experimental [4] values rather than the measured one by Davis and Thompson [5].

A.2 Dramatic Resonances in Low- Energy Electron Scattering from Rb, Cs and Fr Atoms: Signatures of Electron Affinities

We predict [6]dramatic resonances in low-energy electron elastic total cross sections for Rb, Cs and Fr atoms, whose energy positions are identified with the electron affinities (EA's) for these atoms, preceded by shape resonances and Ramsauer-Townsend minima. This provides a new powerful theoretical method of determining unambiguous EA values for atoms. The extracted EA values for Rb and Cs atoms agree very well with the most recently measured values, but our value for Fr disagrees significantly with existing calculated values. The calculation used the recent Regge-pole methodology [1] with a Thomas-Fermi type potential incorporating the vital core-polarization interaction.

A.3 Near-Threshold Resonance Structures in Electron Elastic Scattering Cross Sections for Au and Pt Atoms: Identification of Electron Affinities

The recent Regge-pole methodology has been employed together with a Thomas-Fermi potential which incorporates the vital core polarization interaction to investigate the near-threshold electron attachment in Au and Pt as Regge resonances [7]. The resultant stable negative ion states are found to

have the discernable characteristic of very small imaginary parts of the Regge poles, which translates into long-lived resonances. The near-threshold electron elastic total cross sections are characterized by multiple resonances from which we extract the EA values through the careful scrutiny of the imaginary part of the relevant complex angular momentum, L. For the Au^- and Pt^- negative ions the extracted BE's of 2.262 eV and 2.163 eV, respectively are in excellent agreement with the most recently measured EA values for Au and Pt. Ramsauer-Townsend minima, shape resonances and the Wigner threshold behavior are identified in both Au^- and Pt^- ions.

A.4 Low-Energy Electron Elastic Scattering Cross Sections for Lanthanide Atoms

Total and Mulholland partial cross sections for the elastic scattering of electrons from the lanthanide atoms La to Lu are calculated [8] for the electron impact energy range $0 \leq E \leq 1$ eV using the recently developed Regge-pole methodology [1] under similar conditions as in Section A.1 above. Dramatically sharp resonances are found to characterize the near-threshold electron elastic scattering total and Mulholland partial cross sections, whose energy positions are identified with the EA's of these atoms through a close scrutiny of the imaginary part of the complex angular momentum, L. The unambiguous extracted EA values of the lanthanide atoms vary from a low value of 0.016 eV for the Tm atom to a high value of 0.631 eV for the Pr atom; none is predicted to have a lower EA value than the former. These EA values have been compared with available experimental and other theoretical values.

All the negative ions of the lanthanide atoms can be classified through their BE's as weakly bound negative ions (BE's < 1.0 eV), while only three qualify for classification as tenuously bound (EA's < 0.1 eV). Ramsauer-Townsend minima, shape resonances and the Wigner threshold behavior for these lanthanides are also determined. In particular, our extracted EA value for the Ce atom agrees excellently with the most recently measured [4] and calculated [3] values, while for Nd the agreement with the calculated [9] value is outstanding. These agreements give great credence to the already demonstrated predictive power of the Regge-pole methodology to extract unambiguous and reliable binding energies for tenuously bound and complicated open-shell atomic systems, requiring no *a priori* knowledge of the EA values whatsoever. All fourteen of the fifteen low-energy electron elastic scattering cross sections for the lanthanides have never been published before; only those for the Ce atom are available. This new perspective to the EA determination of atoms from low-energy electron scattering resonances promises future accurate and reliable theoretical EA values, even for small molecules and clusters.

B. RANDOM PHASE APPROXIMATION WITH EXCHANGE FOR ATOMS WITH AN INNER OPEN-SHELL

A random phase approximation with exchange method has been developed for the photoionization of atoms (ions) with an inner open-shell [10]. The method allows for the inclusion of both the intra-shell and the inter-shell correlations in the calculation and has been used to study the photoelectron asymmetry parameter and the photoionization cross sections of the Sc 4s in which the Sc 3p-3d transition has been successfully included. The results demonstrate that the inclusion of the 3p - 3d transitions is extremely important in the inter-shell coupling, which significantly influences the calculated asymmetry parameter and the cross sections for the Sc 4s photoionization. Comparisons of our calculated asymmetry parameter and the cross sections with the measured data and available calculation are made and discussed. Possible improvements to the present calculated data are offered as well.

C. FINE-STRUCTURE ENERGIES, OSCILLATOR STRENGTHS AND LIFETIMES

C.1 Fine-Structure Energy Levels, Oscillator Strengths and Lifetimes for Co XV

Excitation energies from ground state for 98 fine-structure levels as well as oscillator strengths and radiative decay rates for all electric-dipole-allowed and intercombination transitions among the fine-structure levels of the terms belonging to the $(1s^2 2s^2 2p^6)3s^2 3p$, $3s3p^2$, $3s^2 3d$, $3p^3$, $3s3p3d$, $3p^2 3d$, $3s3d^2$, $3s^2 4s$, $3s^2 4p$, $3s^2 4d$, $3s^2 4f$, and $3s3p4s$ configurations of Co XV are calculated [11], using extensive

configuration-interaction (CI) wave functions, obtained with Program CIV3 of Hibbert. The important relativistic effects in intermediate coupling are included through the Breit-Pauli approximation via spin-orbit, spin-other-orbit, spin-spin, Darwin and mass correction terms. Small adjustments to the diagonal elements of the Hamiltonian matrices have been made. Our calculated excitation energies, including their ordering, are in excellent agreement with the experimental results and the compiled energy values of NIST wherever available. The mixing among several fine-structure levels is found to be very strong, with most of the strongly mixed levels belonging to the $(1s^2 2s^2 2p^6)3p^2 3d$ and $3s3d^2$ configurations. The strong mixing among several fine-structure levels makes it very difficult to identify them uniquely. We have also calculated radiative lifetimes of some fine-structure levels and also predict new data for several fine-structure levels.

C.2 Oscillator Strengths and Lifetimes in Ge XXI

We have calculated energy splittings of 53 fine-structure levels as well as oscillator strengths and radiative decay rates for all electric-dipole-allowed and intercombination transitions among the $(1s^2 2s^2 2p^6)3s^2(^1S)$, $3s3p(^{1,3}P^o)$, $3s3d(^{1,3}D)$, $3s4s(^{1,3}S)$, $3s4p(^{1,3}P^o)$, $3s4d(^{1,3}D)$, $3s4f(^{1,3}F^o)$, $3p^2(^1S, ^3P, ^1D)$, $3p3d(^{1,3}P^o, ^{1,3}D^o, ^{1,3}F^o)$, $3p4s(^{1,3}P^o)$, and $3d^2(^1S, ^3P, ^1D, ^3F, ^1G)$ states of Ge XXI [12], using extensive CI wave functions, obtained with the CIV3 computer code of Hibbert. The important relativistic effects in intermediate coupling are incorporated by means of the Breit-Pauli Hamiltonian. In order to keep our calculated energy splittings as close as possible to the experimental values, we have made small adjustments to the diagonal elements of the Hamiltonian matrices. Our excitation energies, including their ordering, are in excellent agreement with the available experimental results. From our transition probabilities, we have also calculated radiative lifetimes of some fine-structure levels. Our calculated oscillator strengths and the lifetimes agree very well with other available theoretical results. New data for several fine-structure levels are also predicted.

FUTURE PLANS

The development and application of the CAM theory continue, particularly in chemical reactions and electron-atom/ion collisions. From the resonances in the near-threshold electron elastic scattering TCS's, reliable EA's for tenuously bound and complicated atoms can be extracted through the close scrutiny of the imaginary part of the CAM value. Other research activities, such as GOS and photoionization of inner-shell of open-shell atoms (ions) investigations continue, including the probing of correlations. Extension of the Regge pole approach to the interesting and challenging multichannel case is advancing.

REFERENCES AND SOME PUBLICATIONS

1. D. Sokolovski, Z. Felfli, S. Yu. Ovchinnikov, J. H. Macek and A. Z. Msezane, Phys. Rev. A **76**, 012705 (2007)
2. Z. Felfli, A.Z. Msezane and D. Sokolovski, J. Phys. B **41**, 041001 (2008) (FAST TRACK)
3. S. M. O'Malley and D. R. Beck, Phys. Rev. A **74**, 042509 (2006)
4. W. Walter, N. D. Gibson, C. M. Janczak, K. A. Starr, A. P. Snedden, R. L. Field III, and P. Andersson, Phys. Rev. A **76**, 052702 (2007)
5. V. T. Davis and J. S. Thompson, Phys. Rev. Lett. **88**, 073003 (2002)
6. A.Z. Msezane, Z. Felfli and D. Sokolovski, Chem. Phys. Lett. **456**, 96 (2008)
7. A.Z. Msezane, Z. Felfli and D. Sokolovski, J. Phys. B **41**, 105201 (2008)
8. Z. Felfli, A.Z. Msezane and D. Sokolovski, Phys. Phys. A, Submitted (2008)
9. M. O'Malley and D.R. Beck, Phys. Rev. A**77**, 012505 (2008)
10. Zhifan Chen and A.Z. Msezane, Phys. Rev. A **77**, 042703 (2008)
11. G. P. Gupta and A. Z. Msezane, European Physical Journal D, At Press (2008).
12. G. P. Gupta and A. Z. Msezane, Physica Scripta **77**, 035303 (2008).

SOME ADDITIONAL PUBLICATIONS 2006 – 2008

1. "Modification of the Xe 4d Giant Resonance by the C_{60} Shell in Molecular Xe@C_{60}", M. Ya. Amusia, A.S. Baltenkov, L.V. Chernysheva, Z. Felfli and A.Z. Msezane, Journal of Experimental and Theoretical Physics **102**, 53 (2006)
2. "Main Universal Features of the ^{3}He Experimental Temperature–Density Phase Diagram", V.R. Shaginyan, A.Z. Msezane. K.G. Popov and V.A. Stephanovich, Phys. Rev. Lett. **100**, 096406 (2008)
3. "Soft X-ray Emission Lines of Fe XV in Solar Flare Observations and the Chandra Spectrum of Capella", F.P. Keenan, J.J. Drake, S. Chung, N.S. Brickhouse, K.M. Aggarwal, A.Z. Msezane, R.S.I. Ryans and D.S. Bloomfield, ApJ **449**, 1203 (2006)
4. "Oscillator Strengths and Lifetimes in Kr XXV", G.P. Gupta and A.Z. Msezane, Physica Scripta **73,** 556 (2006)
5. "Near-Threshold Behaviour of Electron Elastic Scattering Cross Sections for Fr: A Regge Pole Analysis" , Z. Felfli , A.Z. Msezane and D. Sokolovski, J. Phys. B **39**, L353 (2006)
6. "Quasiparticles and Quantum Phase Transition in Universal Low-Temperature Properties of Heavy Fermion Metals", V.R Shaginyan, A.Z. Msezane, V.A. Stephanovich and E.V. Kirichenko, Europhys. Lett. **76**, 898 (2006)
7. "Oscillator Strengths and Lifetimes in Ge XXI", G. P. Gupta and A. Z. Msezane, Physica Scripta **77**, 035303 (2007).
8. "Photoelectron Spectra of N@C60 Molecule on Crystalline Si Surface", A.S. Baltenkov, U. Becker, S.T. Manson and A.Z. Msezane, Phys. Rev. B**73**, 075404 (2006)
9. "Universal Cause of High-Tc Superconductivity and Anomalous Behavior of Heavy Fermion Metals", V.R. Shaginyan, M.Ya. Amusia, A.Z. Msezane and K.G. Popov, *in Recent Developments in Superconductivity Research* (NOVA Science, New York, 2006) Ed. B.P. Martins pp. 275-337
10. "Generalized Oscillator Strengths for the 3d Electrons of Cs, Ba, and Xe: Effects of Spin-Orbit-Activated Interchannel Coupling", M. Ya. Amusia, L.V. Chernysheva, Z. Felfli, A.Z. Msezane, Phys. Rev. A**73**, 062716 (2006)
11. "Near-Threshold Electron Attachment as Regge Resonances: Cross Sections for K, Rb and Cs Atoms", A.Z. Msezane, Z. Felfli and D. Sokolovski, J. Phys. Chem. A **112**, 10, 199 (2008)
12. "Fine-Structure Energy Levels, Oscillator Strengths and Lifetimes in Mn XIII", G. P. Gupta and A. Z. Msezane, Physica Script **76**, 225 (2007).
13. "What can one do with Regge Poles?" D. Sokolovski, A.Z. Msezane, Z. Felfli, S.Yu. Ovchinnikov and J.H. Macek, Nucl. Instr. and Meth. B **261**, 133 (2007).
14. "Energy Levels and Radiative Rates for Transitions in Co XI", F.P. Keenan, K.M. Aggarwal and A.Z. Msezane, Astronomy & Astrophysics **473**, 995 (2007).
15. "Octupole Contributions to the Generalized Oscillator Strengths of Discrete Dipole Transitions in Noble Gas Atoms", M. Ya. Amusia, L.V. Chernysheva, Z. Felfli and A.Z. Msezane, Phys. Rev. A**75**, 062703 (2007).
16. "Photoionization of Hydrogen-Like Ions Surrounded by Charged Spherical Shell", A. S. Baltenkov, S. T. Manson and A. Z. Msezane, Phys. Rev. A **76**, 042707 (2007)
17. "Elastic Electron Scattering From Multicenter Potentials", A. S. Baltenkov, S. T. Manson and A.Z. Msezane, J. Phys. B **40**, 769 (2007)
18. "Ionization of Sodium by the Impact of Alpha Particles", S. Bhattacharya, K.B. Choudhury, N.C. Deb, C. Sinha, K. Roy and A.Z. Msezane, Eur. Phys. J. D **47**, 335 (2008)
19. "Fine-Structure Energy Levels, Oscillator Strengths and Lifetimes in Co XV", G. P. Gupta and A. Z. Msezane, European Physical Journal D, At Press (2008).
20. "Random Phase Approximation with Exchange for Inner-Shell Electron Photoionization", Zhifan Chen and A.Z. Msezane, in Contemporary Problems in Mathematical Physics, Eds. J. Gavaerts, M.N. Hounkonnou and A.Z. Msezane (World Scientific, 2006) page 198

Theory and Simulations of Nonlinear X-ray Spectroscopy of Molecules

Shaul Mukamel
University of California, Irvine, CA 92697

Progress Report 2008 DOE DE-FG02-04ER15571

Program Scope

Design principles and computational tools are developed for time-domain experiments that employ sequences of attosecond x-ray and femtosecond optical pulses in order to probe electronic and nuclear dynamics in molecules. Such experiments will be made possible by new bright, coherent ultrafast sources for soft and hard x-rays. The nonlinear response formalism widely used in optical spectroscopy is extended to the x-ray regime. A hierarchy of possible techniques which involve an increasing number of x-ray beams are considered. The simplest, optical pump/x-ray probe technique does not require phase control or coherence whereas all- x-ray four-wave mixing will require four beams with phase control. Models for predicting the various signals and assessing their sensitivity and information content are developed. The roles of the pulse carrier-frequencies, phases, bandwidths, and envelopes are analyzed using closed expressions derived for resonant coherent multidimensional spectra.

Two-dimensional x-ray coherent correlation spectra (2DXCS) obtained by varying two delay periods between pulses show off-diagonal crosspeaks induced by coupling of core transitions of two different types. The frequencies and dipole moments of ground-to-core and valence-to-core electronic transitions are calculated using time-dependent density-functional theory within the equivalent-core approximation. The state-to-state transitions are obtained by projecting TDDFT transition density matrices onto the configuration-interaction-singles (CIS) states. N1s x-ray absorption and resonant x-ray emission signals of molecules with amine, imine, nitroso, and nitrile groups are simulated and compared to spectra obtained with single-electron approaches and with experiment. Nonadditive effects of functional groups in the stimulated Raman signal of conjugated molecules are predicted. Coherent nonlinear optical spectra of excitons in semiconductor nanostructures are used to test simulation algorithms and laser pulse sequences and gain insights for the design and analysis of their x-ray counterparts.

Recent Progress

The impulsive stimulated x-ray Raman signal from quinolinol (Fig.1) was simulated and analyzed using the doorway-window representation of pump-probe spectroscopy. The pump creates an electronic wavepacket, whose components include the ground, valence-excited and core-excited states. Recording the signal for various delays gives time-resolved snapshots of this wavepacket in the vicinity of the atoms contributing to the probe absorption. Signals involving electron wavepackets created by attosecond pulses can be described by extending concepts used for vibrational wavepackets in the femtosecond regime. A valence electronic wave packet prepared by the pump, tuned on resonance with a given core-hole, is localized in the vicinity of a selected atom and probed by a window localized on a different atom, selected by the probe pulse. All valence electronic states spanned by the pulse bandwidths can be observed with high spatial and temporal resolution, by monitoring the variation of the signal with the delay between the pulses. The natural-orbital representation of the reduced single electron density matrix is used to visualize the dynamics of the valence wave packet, described as a linear combination of determinants made of occupied and unoccupied Kohn-Sham orbitals. Like RIXS, the coherent Raman signal can be expressed in a generalized Kramers-Heisenberg form. However, the additional control offered by the pulses allows to monitor the excitation dynamics in the desired region of space and time.

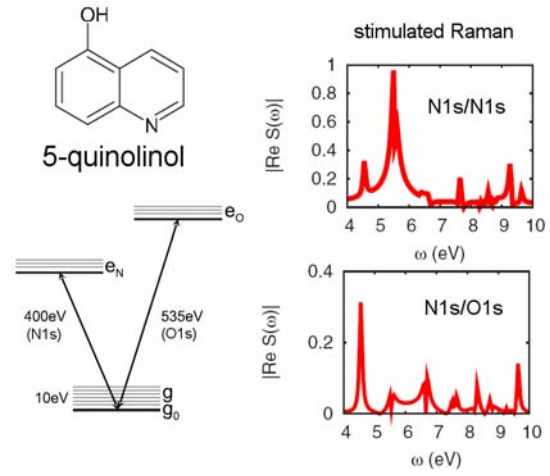

Fig. 1: The coherent stimulated x-ray Raman signal of 5-quinolinol(upper left) can be described in terms of valence electronic states with differing core-occupations(lower left). Peaks in the one-(upper right) and two-color (lower right) frequency domain spectra represent valence excitations, weighted by their projections onto the nitrogen and oxygen [P13]

Simulations of 2DXCS demonstrate its capacity to probe multiple core-hold interactions in the nitrogen K-edge of isolated DNA bases and Watson-Crick basepairs, which contain multiple absorbing nitrogen atoms (Figs.2 and 3). This technique is an analogue of homonuclear NMR. Simulations employed methods based on the equivalent-core approximation, in which core excited states are described as valence excitations of the equivalent-core molecule with an additional valence electron. The same level of quantum chemistry is applied to both valence and core transitions. Changes in crosspeak intensities between hydrogen-bonded and stacked basepairs are identified. Nucleobase analogues are proposed for investigating base-stacking and hydrogen bonding interactions.

The excited states were expanded in singly and doubly excited Slater determinants of the ground state Kohn-Sham orbitals. The nitrogen atoms in each nucleobase can be divided into two types: double-bonded imine and the trivalent amine. The amine 1s orbital lies lower in energy than the imine nitrogen, blue-shifting core-to-valence transitions from this nitrogen. The dominant features in XANES and 2DXCS are the valence band are π^* and σ^* type excitations.

Single- basepair hydrogen bonds enhance the intensity of imine crosspeaks. The same imine crosspeaks are broader in the stacked based than the separated case.

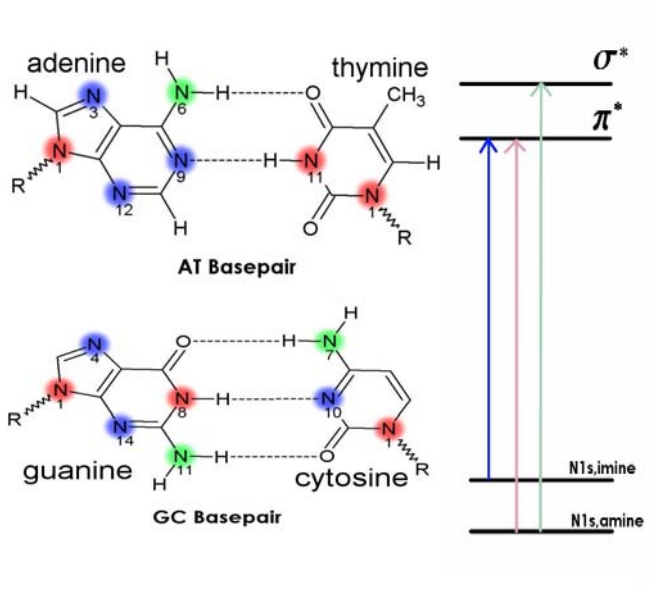

Fig 2: (Left) the structure of the nucleobases, with imine(blue), amine(red) and –NH2(green) nitrogens color-coded. (Right) A level scheme for x-ray transitions in the nucleobases.

Future Plans

Effort will focus on developing higher - level electronic-structure methods for multiple core transitions and introducing nuclear dynamics and core migration. Studies of 2D spectra in semiconductor nanostructures will be used to develop and test exciton models and new pulse configurations. Several categories of computational approaches of core excited states will be explored. The first employs rigorous many-body expansions such as the polarization propagator or the equation-of-motion coupled-cluster formalism to calculate the core excited states explicitly. The second category of methods avoids the explicit calculation of core excitations. Instead, they use a ground-state-like self-consistent field approach where the effect of promoting core electrons is accounted for via modified orbital occupations. A third category neglects the many-electron interactions between the core and valence electrons and describes the core transition as the response of valence electrons to an either adiabatically or instantly switched core-hole potential. These methods were successful in describing the Fermi-edge singularities and Anderson catastrophe in the x-ray absorption spectra of metallic systems.

The optical response may be alternatively described in terms of quasiparticles (QP), which avoid the expensive computation of many-electron eigenstates. Instead, signals are calculated by solving equations of motion for a proper hierarchy of dynamical variables. A Bethe-Salpeter approach for two-excitons could provide an efficient computational tool. Closed expressions for optical 2D spectra derived by solving the Nonlinear Exciton Equations (NEE) are given in terms of the single exciton Green's function and the exciton scattering matrix. The QP expressions provide complementary view to the sum over states into the origin of features seen in 2D spectrograms. A unified description is obtained for electron-hole excitations in semiconductors, Frenkel excitons in molecular aggregates (Paulions), and anharmonic vibrations (bosons). This formalism will be extended to multiple core-hole excitations. Since the core holes are well localized, we only need consider the delocalization of the valence electrons. This makes it simpler than Wannier excitons in semiconductors. 2DCXS has the potential to provide some unique insights into carrier dynamics in semiconductors, complementing nonlinear optical experiments which provide information about many-exciton states such as biexcitons, their interactions, relaxation and dissociation.

A three-pulse coherent optical signal generated in the direction $\mathbf{k_1 + k_2 + k_3}$ is particularly sensitive to two-exciton correlations. Two Liouville-space pathways for the density matrix contribute to this double-quantum-coherence signal, creating a characteristic highly resolved pattern. This level of detail is not available from

conventional 1D four-wave mixing or other 2D signals. Applications to GaAs Quantum wells and pairs of quantum dots show that it can fully resolve the pure heavy-hole, pure light-hole, and the mixed two excitons. The Time-Dependent -Hartree–Fock approximation, where the two-exciton variables are factorized, misses some important many-body effects, attributed to correlated electron–hole pairs. Contributions of different types of two excitons may be completely separated from higher-order Coulomb correlations by specific pulse polarization configurations. This technique will be extended to the x-ray regime.

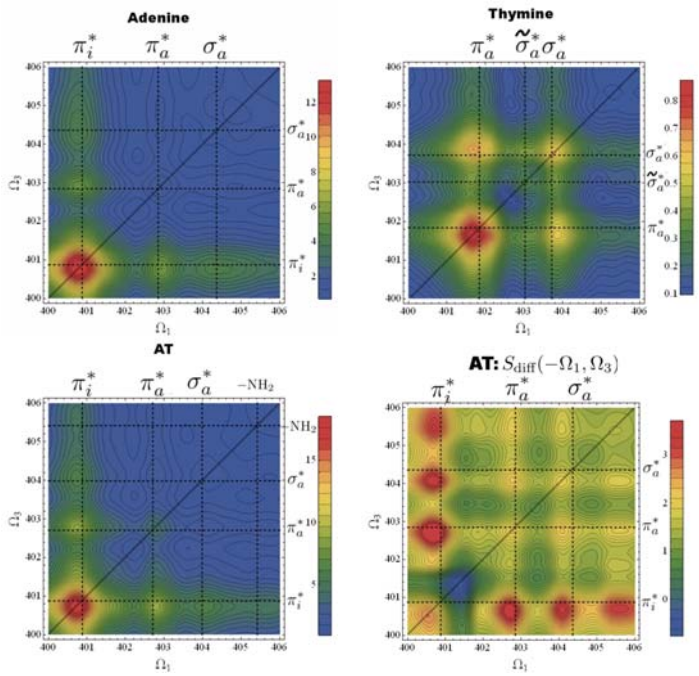

Fig 3: 2DXCS for adenine, thymine, the hydrogen bonded basepair, and the difference between the basepair and the sum of the bases(lower right). Dashed lines give the peak assignments for each transition. The difference spectra show that the imine π_i^* crosspeaks gain intensity, when the bases are hydrogen-bonded. [P17, P19]

2DXCS simulations of double-stranded DNA should allow the probing of fluctuating electronic states of the nucleobases in solid or solvent environments in a single experiment. The current simulations of the smaller nucleobase and basepair systems containing several nitrogen atoms, provide a key ingredient for addressing large polymer systems. Some features of 2DXCS for a basepair can be used to assign the relative orientation of the bases. The melting curve for a given sequence of DNA can be described using the dynamics of transient hydrogen-bond breaking between paired nucleobases, which takes place on timescales comparable to the period of the hydrogen bond vibration (~13fs). A simplified effective Hamiltonian of the double-stranded system should allow a wide range of simulations of larger systems. We have proposed a family of chirality-induced nonlinear techniques and developed coupled exciton models in the visible and infrared. These will be extended to the 2DXCS of DNA. Optically-excited DNA is known to rapidly relax into non-radiative states. It is unknown whether this relaxation is through vibrational relaxation, as in the monomer, excimer formation between stacked basepairs, or delocalization of the electronic wavepacket over many basepairs. Optical-pump X-ray -probe experiments may find evidence of delocalized, dark states which form an important step in the ultrafast energy transfer pathways. Two other nitrogen-containing polymeric systems will be examined. Polyaniline is a linear polymer of aniline subunits, which alternates between the imine and amine form of nitrogen along the strand. It is much better characterized than DNA and could serve as model for 2DXCS in 1D conductive systems. Melanin is a two dimensional disordered polymer which mixes the imine and amine forms of nitrogen, composed of the same subunits that make up porphyrin rings. Prior XANES studies on melanin clusters in the retina have identified differences in the XANES for melanine granules in mutated cells.

Publications Resulting from the Project

[P1] “Coherent-Control of Pump-Probe Signals of Helical Structures by Adaptive Pulse Polarizations," D. Voronine, D. Abramavicius, S. Mukamel, J. Chem. Phys. 124, 034104 (2006)

[P2] “Anomalous continuous-time-random-walk spectral diffusion in coherent third order optical response," F. Sanda, S. Mukamel, Phys. Rev. E 73, 011103 (2006)

[P3] “Multiple Core-Hole Coherence in X-Ray Four-Wave-Mixing-Spectroscopies," S. Mukamel, Phys. Rev. B 72, 235110 (2005)

[P4] “Simulation of XANES and X-ray Fluorescence Spectra of Optically Excited Molecules," . R.K. Pandey and S. Mukamel, J. Chem, Phys 124, 094106 (2006)
[P5] \Quantum Master Equation for Electron Transport Through Quantum Dots and Single Molecules", U. Harbola, M. Esposito and S.Mukamel. Phys. Rev. B. 74,235309 (2007)
[P6] “Manipulating Multidimensional Electronic Spectra of Excitons by Polarization Pulse-Shaping," D. Voronine, D. Abramavicius, S. Mukamel, J.Chem. Phys. 126,044508(2007)
[P7] “Manipulating Multidimensional Nonlinear Spectra of Excitons by Coherent Control with Polarization Pulse Shaping," D. Voronine, D. Abramavicius and S. Mukamel. In Ultrafast Phenomena XV, R.J.D. Miller, A.M. Weiner, P. Cornum and D.M. Jonas (editors) Springer Verlag (2006)
[P8] “Multipoint Correlation Functions for Photon Statistics in Single Molecule Spectroscopy;Stochastic Dynamics in Liouville Space," F. Sanda and S. Mukamel. In "Theory, Modeling and Evaluation of Single-Molecule Measurements", Editors E. Barkai, F. Brown, M. Orrit and H. Yang, World Scientific, (2007).
[P9] “Simulation of X-ray Absorption Near Edge of Organ Metallic Compounds in the Ground and Optically Excited States," R. Pandey and S. Mukamel., J.Phys.Chem.A. 111,805-816 (2007).
[P10] “Two-Dimensional Optical Spectroscopy of Excitons in Semiconductor Quantum Wells: Liouville-Space Pathways Analysis," L. Yang, I.V. Schweigert, S. Cundiff and
S. Mukamel, Phys.Rev.B., 75,125302(2007).
[P11] Comment on “Failure of the Jarzynski Identify for a Simple Quantum System," S.Mukamel. Cond-mat/0701003vl, Dec. 30, 2006.
[P12] “Two-Dimensional Infrared Surface Spectroscopy for CO on Cu(100):Detection of Intermolecular Coupling of Adsorbates," Y. Nagata, Y. Tanimura and S. Mukamel J.Chem.Phys. 126, 204703 (2007).
[P13] “Probing Valence ElectronicWavepacket Dynamics by all X-ray Stimulated Raman Spectroscopy; A Simulation Study," I.V. Schweigert and S. Mukamel Phys. Rev. A.76, 0125041 (2007).
*[P14] “Partially-Time-Ordered Keldysh-Loop expansion of Coherent Nonlinear Susceptibilities," S. Mukamel, Phys. Rev.A., 77, 023801, 2008.
*[P15] “Two-Dimensional Correlation Spectroscopy of Two-Exciton Resonances in Semi-conductor Quantum Wells," L. Yang and S. Mukamel, Phys. Rev. Lett, 100, 057402, 2008.
*[P16] “Ultrafast Optical Spectroscopy of Spectral Fluctuations in a Dense Atomic Vapor," V.O. Lorenz, S. Mukamel, W. Zhuang and S.T. Cundiff, Phys. Rev. Lett., 100, 013603, 2008.
*[P17] “Coherent Ultrafast Core-hole Correlation Spectroscopy: X-ray Analogues of Multidimensional NMR," I. Schweigert and S. Mukamel, Phys. Rev. Lett , 99, 163001, 2007.
**[P18] “Simulating Multidimensional Wave Optical Mixing Signals with Finite Pulse Envelopes”, I. Schweigert and S. Mukamel, Phys. Rev. A., 77, 33802, 2008.
*[P19] “Probing Interactions Between Core-Electron Transitions by Ultrafast Two Dimensional X-Ray Coherent Correlation Spectroscopy”, I.V. Schweigert and S. Mukamel, J.Chem.Phys. 128, 184307 (2008).
*[P20] “Revealing Exciton-Exciton Couplings in Semiconductors by Multidimensional Four Wave Mixing Signals”, L. Yang and S. Mukamel, Phys. Rev. B., 77, 075335 (2008).
*[P21] “Many-body Effects in 2-D Optical Spectra of Semiconductor Quantum-Dot Pairs; TDHF approximation and Beyond”, R. Oszwaldowski, D. Abramavicius and S. Mukamel, J. Phys. Cond. Matt. 20, 045206 (2008).
*[P22] “Probing Multiple Core-hole Interactions in the Nitrogen K-edge of DNA Basepairs by multidimensional X-ray Spectroscopy; A Simulation Study”, D. Healion, I. Schweigert and S. Mukamel, J. Phys. Chem.(Submitted, 2008).
*[P23]“Dissecting Quantum Pathways in Two-dimensional Correlation Spectroscopy of Semiconductors”, L. Yang and S. Mukamel, J. of Physics (Submitted, 2008).

Nonlinear Photoacoustic Spectroscopies Probed by Ultrafast EUV Light

Keith A. Nelson
Department of Chemistry
Massachusetts Institute of Technology
Cambridge, MA 02139
Email: kanelson@mit.edu

Henry C. Kapteyn
JILA
University of Colorado and National Institutes of Technology
Boulder, CO 80309
E-mail: kapteyn@jila.colorado.edu

Margaret M. Murnane
JILA
University of Colorado and National Institutes of Technology
Boulder, CO 80309
E-mail: murnane@jila.colorado.edu

Program Scope

This project is aimed at direct spectroscopic characterization of phenomena that occur on mesoscopic (nanometer) length scales and ultrafast time scales in condensed matter, including non-diffusive thermal transport and the high-wavevector acoustic phonon propagation that mediates it, complex structural relaxation and the density and shear dynamics that comprise it. The primary effort in the project is directed toward nonlinear time-resolved spectroscopy with coherent soft x-ray, or extreme ultraviolet (EUV), wavelengths. Time-resolved four-wave mixing, or transient grating (TG), measurements are conducted in order to directly define an experimental length scale as the interference fringe spacing λ (or wavevector magnitude $q = 2\pi/\lambda$) formed by two crossed excitation pulses. [1] The dynamics of material responses at the selected wavevector, including thermoelastically induced surface acoustic waves and thermal diffusion or non-diffusive thermal transport, are recorded through time-resolved measurement of coherent scattering, i.e. diffraction, of variably delayed probe pulses from the transient grating pattern. In complementary measurements [2], the frequency rather than the wavevector of an acoustic response is specified by using a sequence of femtosecond excitation pulses at a specified repetition rate, with each pulse thermoelastically driving a single acoustic cycle. In this case the acoustic wave propagates through the sample rather than along the surface, and detection is carried out at the opposite sample surface, i.e. multiple-pulsed excitation is at the front and detection is at the back of the sample.

The EUV measurements have been made possible by continued progress in high harmonic generation [3] which has yielded femtosecond soft x-ray pulses with nanojoule energies and excellent spatial coherence and focusability. The possibility of intensity levels comparable to those used in much of condensed matter nonlinear spectroscopy encourages the effort to extend the spectroscopic methods to EUV wavelengths. Transient grating measurements with EUV excitation and probe pulses will provide fringe spacings in the range of a few tens of

nanometers. EUV probe pulses also offer important advantages for probing thermoelastic responses at moderate wavevectors, induced by visible or UV excitation pulses, as described below.

Recent Progress

We previously demonstrated the use of HHG beams to probe the changing diffraction in micro-patterned surfaces due to surface acoustic waves with high sensitivity [4], and in a Gabor holography geometry to interferometrically observe laser-induced thermoelastic surface displacements on the picometer scale. [5]. In new experiments [6] that facilitate access to the ballistic regime of heat transport, we used sapphire as the substrate material under nano-patterned nickel because the mean free path of the dominant heat-carrying phonons is long (150 nm at room temperature, and much longer at lower temperatures) and because sapphire is transparent to the 800 nm optical pumping wavelength. A nano-grating pattern of thin nickel lines (20 nm high and between 70 nm and 1 μm wide) was fabricated on the surface by electron beam lithography and liftoff by collaborators at LBL (Eric Anderson and his group). The nickel was heated by an 800-nm pulse from a Ti:Sapphire laser amplifier. The laser-induced thermal excitation and subsequent cooling of the nickel lines can be probed by measuring the diffraction of a 30 nm HHG beam from the sample (see Fig. 1a). The diffraction efficiency of the nickel grating depends strongly on small thermally-induced changes in the height of the nickel lines. By assuming a linear coefficient of thermal expansion, we can determine the temperature change corresponding to a given change in diffraction.

By monitoring the change in the probe diffraction from the grating as a function of pump-probe delay, we obtain a transient signal shown in Figure 1b. The oscillation is due to surface acoustic wave (SAW) propagation initiated by the patterned surface strain caused by heating of the nickel. The SAW frequency matches that predicted for sapphire at this wavevector, and is independent of sample temperature and pump intensity. The signal also includes a non-oscillatory component that decays exponentially due dissipation of the heat deposited in the nickel lines into the sapphire substrate. This thermal decay is an indicator of phonon energy transport efficiency between the nickel lines and the sapphire substrate, which depends in turn on heat transport within the sapphire from regions near the metal lines to regions farther from them.

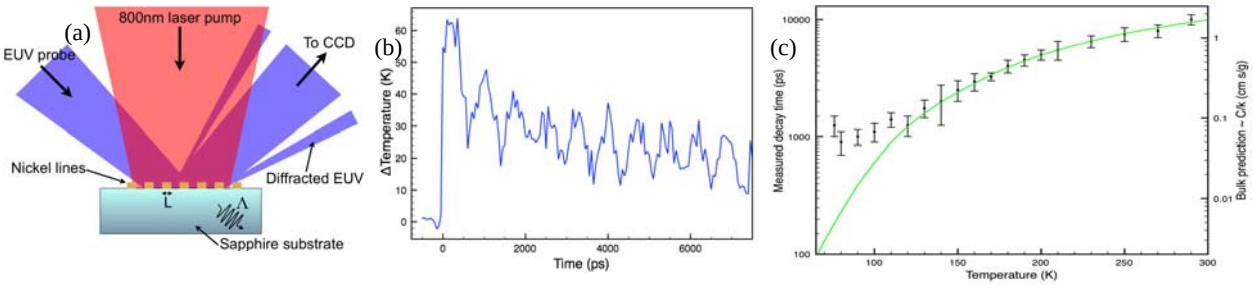

Figure 1. (a) Experimental geometry: a sample consisting of nickel lines of width L = 1 μm on sapphire is illuminated with an 800 nm pump pulse and probed using EUV light. (b) Time-resolved signal from the nickel lines at room temperature. Surface acoustic wave oscillations at 1.34 GHz and a non-oscillatory thermal component are observed. (c) Exponential decay time of thermal signal component as a function of temperature (points; left axis), and predicted behavior for bulk sapphire (solid curve; right axis).

At room temperature, heat transport in this sample is diffusive since the characteristic length (nickel wire width L = 1 μm) is much greater than the phonon mean free path (Λ ~ 150 nm) in sapphire at room temperature. In the 76-300 K temperatures range, the phonon mean

free path varies as $\Lambda \sim 1/T$ [7,8] (e.g. $L/\Lambda \approx 1$ at 110 K), so at reduced temperatures quasi-ballistic heat transport is expected. To reveal the transition between heat transport regimes, we fit the non-oscillatory thermal signal component at each temperature to a single-exponential decay. The decay times $\tau(T)$ are plotted in Fig. 3 as the points with error bars. According to Newton's law of cooling, which is based on diffusive heat transport, the decay time should be inversely proportional to the thermal diffusivity $K = k/C = v\Lambda/3$ [7], where C is the sapphire volumetric specific heat, k is the thermal conductivity, and v is the sound speed. This prediction is depicted in Fig. 1c as the solid curve. At temperatures above 130 K, the decay times we measure show the trend predicted based on diffusive transport in bulk sapphire. Below 130 K, we observe significant deviation from diffusive behavior, consistent with a transition to the quasi-ballistic regime of heat transport. ~ 500 nm in sapphire at 130 K, so the onset of quasi-ballistic transport occurs when $L/\Lambda \sim 2$.

Thermal transport in insulators is mediated by longitudinal and transverse acoustic phonons of all wavevectors, weighted by the density of states $\rho_{ph} \sim q^2$ and by the mean free path which decreases with increasing wavevector in a complex and temperature-dependent manner. A microscopic description of thermal transport requires knowledge of the q-dependent longitudinal and transverse acoustic phonon mean free paths. (Note that the parameter Λ used above is a weighted average over acoustic wavevectors and polarizations.) Our approach, in which timed sequences of femtosecond optical excitation pulses are absorbed in a metal film at the front of a substrate to launch frequency-tunable acoustic waves that are detected optically at the back [2,9], can provide this information in the high wavevector range of greatest interest. See Fig. 2.

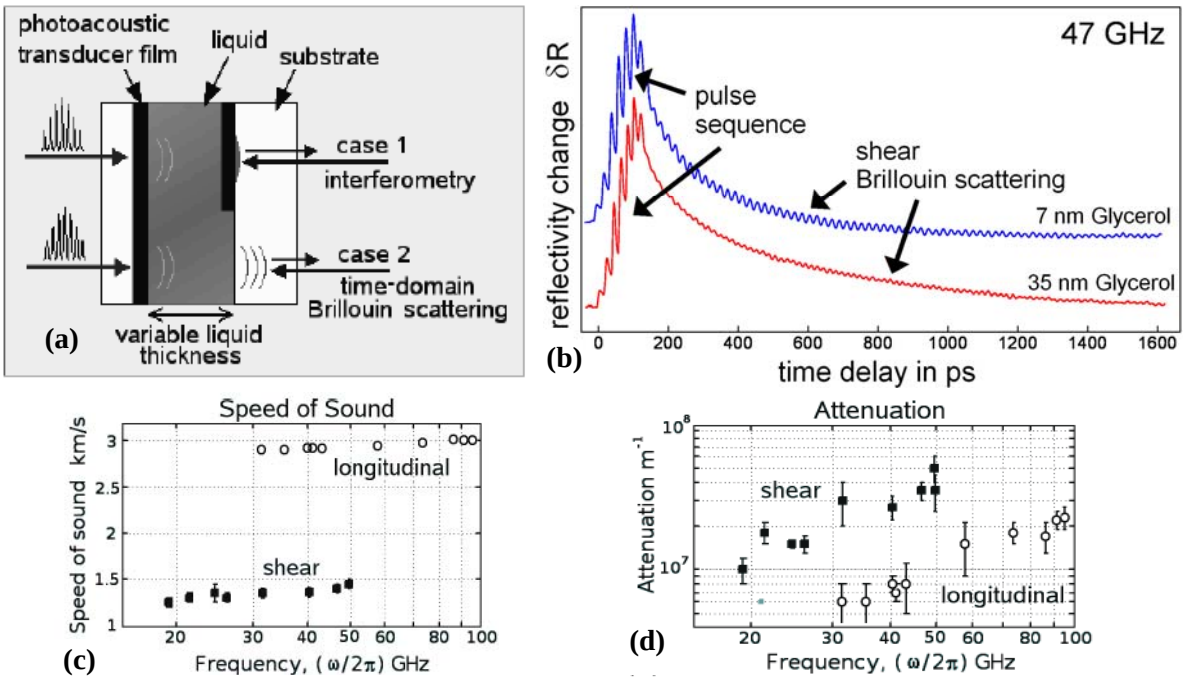

Figure 2. (a) Experimental geometry: an Al or crystallographically canted Fe film is irradiated by a femtosecond pulse sequence, thermoelastically launching a longitudinal or transverse acoustic wave that passes through the liquid sample and is detected interferometrically at the back of a second Al film (case 1) or through coherent depolarized Brillouin scattering in a sapphire substrate (case2) respectively. (b) Time-resolved signal from shear acoustic waves after passing through glycerol liquid layers of different thickness. The differences in arrival time and amplitude yield the sound speed and attenuation rate respectively. (c,d) Longitudinal and shear acoustic speeds and attenuation rates in glycerol at room T.

Figure 2 shows data from shear waves and results for both shear and longitudinal wave speeds and attenuation rates (i.e. mean free paths) in the glass-forming liquid glycerol at room temperature. This demonstration shows that even for viscous samples with extremely strong acoustic damping rates, it is now possible to characterize phonon mean free paths in the high-wavevector range of greatest interest for thermal transport. In solid samples, longitudinal acoustic frequencies over 300 GHz have been characterized [2].

Future Plans

Coherent HHG provides a sensitive probe of nanoscale dynamics, including thermal transport and surface acoustic wave propagation. We plan to extend the study of quasi-ballistic heat transport to nanoscale wire arrays and other complex nanoscale structures. For example, we plan to study acoustic dispersion using dynamic EUV diffraction, and to combine dynamic photoacoustic and photothermal techniques with coherent imaging techniques that we have also recently demonstrated in the lab using high-harmonic sources [10,11]. Optical multiple-pulse excitation and EUV TG measurements will be used for acoustic phonon characterization in the high-wavevector range to achieve a full microscopic description of thermal transport in insulating materials. These experiments will further our understanding of heat transport fundamentals and thermal management at nanoscale dimensions.

References

1. "Impulsive stimulated light scattering from glass-forming liquids: I. Generalized hydrodynamics approach; II. Salol relaxation dynamics, nonergodicity parameter, and testing of mode coupling theory," Y. Yang and K.A. Nelson, *J. Chem. Phys*. **103**, 7722-7731; 7732-7739 (1995).
2. "Generation of ultrahigh frequency tunable acoustic waves," J. D. Choi, T. Feurer, M. Yamaguchi, B. Paxton, and K. A. Nelson, *Appl. Phys. Lett*. **87**, 081907 (2005).
3. "Phase-matched generation of coherent soft-x-rays," A. Rundquist, C. Durfee, Z. Chang, S. Backus, C. Herne, M. M. Murnane and H. C. Kapteyn, *Science* **280**, 1412 – 1415 (1998).
4. R. I. Tobey, E. H. Gershgoren, M. E. Siemens, M. M. Murnane, H. C. Kapteyn, T. Feurer, and K. A. Nelson, "Nanoscale photothermal and photoacoustic transients probed with extreme ultraviolet radiation," *Appl. Phys. Lett.* **85**, 564-566 (2004).
5. "Ultrafast extreme ultraviolet holography: Dynamic monitoring of surface deformation", M.E. Siemens, R.I. Tobey, O. Cohen, M. M. Murnane, H. C. Kapteyn, and K.A. Nelson, *Opt. Lett.* **32**, 286-288 (2007).
6. "Nanoscale Heat Transport Probed with Ultrafast Soft X-Rays," M. Siemens, Q. Li, M. Murnane, H. Kapteyn, R. Yang, and K. Nelson, in *Ultrafast Phenomena XVI*, Stresa, Italy, 2008, p. TBP.
7. G. Chen, *Nanoscale Energy Transport and Conversion*. Oxford: Oxford University Press, 2005.
8. G. Chen, D. Borca-Tasuica, and R. G. Yang, "Nanoscale Heat Transfer," *Encyclopedia of Nanoscience and Nanotechnology*, vol. 7, pp. 429-459, 2004.
9. "Picosecond photoexcitation of acoustic waves in locally canted gold films," T. Pezeril, F. Leon, D. Chateigner, S.Kooi, and K.A. Nelson, *Appl. Phys. Lett*. **92**, 061908 (2008).
10. "Lensless diffractive imaging using tabletop coherent high-harmonic soft-x-ray beams," R. L. Sandberg, A. Paul, D. A. Raymondson, S. Hadrich, D. M. Gaudiosi, J. Holtsnider, R. I. Tobey, O. Cohen, M. M. Murnane, and H. C. Kapteyn, *Phys. Rev. Lett.* **99**, 098103 (2007).
11. "High numerical aperture tabletop soft x-ray diffraction microscopy with 70-nm resolution," R. L. Sandberg, C. Y. Song, P. W. Wachulak, D. A. Raymondson, A. Paul, B. Amirbekian, E. Lee, A. E. Sakdinawat, C. La-O-Vorakiat, M. C. Marconi, C. S. Menoni, M. M. Murnane, J. J. Rocca, H. C. Kapteyn, and J. W. Miao, *Proc. Nat'l. Acad. Sci. USA* **105**, 24-27 (2008).

Antenna-Coupled Emission from Single Quantum Systems

Lukas Novotny (novotny@optics.rochester.edu)
University of Rochester, The Institute of Optics, Rochester, NY, 14627.

1 Program Scope

The goal of this project is the control of a single quantum emitter by use of an optical antenna. More specifically, we are developing and studying optical antennas to selectively influence the stimulated emission rate and the excited state lifetime of an electronic multilevel system (atom, ion, molecule, defect center).

In the past project period we employed nonlinear laser spectroscopy to understand the optical response of different antenna structures, such as noble metal particles, rods, and tips. It is well known that surface plasmons in metal nanostructures can bring out a strongly enhanced local field. Less known is the nonlinear response of these plasma oscillations, such as harmonic generation, wave mixing, and continuum generation. We have established that the nonlinear response of metal nanostructures is very sensitive to changes in the local environment. For example, we have measured nonlinear four-wave mixing (4WM) as a function of the distance between a pair of gold nanoparticles and found that the 4WM yield increases by 4 orders of magnitude within the last two nanometers near touching contact [4]. To establish a quantitative understanding of 4WM in metal nanostructures we have studied nonlinear surface plasmon excitation in thin gold films as described below [1].

2 Recent Progress

In the past project period we have demonstrated nonlinear excitation of surface plasmons on a gold film by optical four-wave mixing (4WM). Two excitation beams of frequencies ω_1 and ω_2 are used in a modified Kretschmann configuration to induce a nonlinear polarization at frequency $\omega_{4\mathrm{wm}} = 2\omega_1 - \omega_2$, which gives rise to surface plasmon excitation at frequency $\omega_{4\mathrm{wm}}$. We observed a characteristic plasmon dip at the Kretschmann angle and explained its origin in terms of destructive interference [1]. Despite of a non-vanishing bulk response, surface plasmon excitation by four-wave mixing is dominated by a nonlinear *surface* polarization.

In our experiments we used a gold film of thickness $\sim 52\,\mathrm{nm}$ (roughness 1 nm rms, prepared by e-beam evaporation on glass) excited in a modified Kretschmann configuration (c.f. Fig. 1) by two incident laser beams of frequencies ω_1 and ω_2, respectively. The metal's third-order susceptibility $\chi^{(3)}$ gives rise to a nonlinear polarization at frequency $\omega_{4wm} = 2\omega_1 - \omega_2$, which leads to scattered radiation at the same frequency. The two laser beams are generated by a Ti:Sapphire laser providing pulses of duration $\sim 200\,\mathrm{fs}$ and wavelength $\lambda_1 = 810\,\mathrm{nm}$, and an optical parametric oscillator (OPO) providing pulses of the same duration and wavelength $\lambda_2 = 1162\,\mathrm{nm}$. Both lasers have a repetition rate of 76 MHz, and the average powers are 3 mW and 12 mW, respectively. The spot diameters at the gold surface are $1.2\,\mu$m and $4\,\mu$m, respectively. The scattered light at the four-wave mixing frequency ω_{4wm} has a wavelength of $\lambda_{4wm} = 613\,\mathrm{nm}$.

As shown in Fig. 1, we use an oil-immersion objective of numerical aperture $NA = 1.3$ and magnification $M = 40$ to focus the incident laser beams on the metal surface and to collect the generated light at the four-wave mixing frequency. The different wavelengths are spectrally separated by optical filters (two bandpass filters $500\,\mathrm{nm} < \lambda < 700\,\mathrm{nm}$, two shortpass filters $\lambda < 750\,\mathrm{nm}$, a line filter $\lambda = 620 \pm 20\,\mathrm{nm}$, and a dichroic beamsplitter reflecting $\lambda > 725\,\mathrm{nm}$). The angular resolution of the experiments is defined by the diameter of the incident laser beams relative to the size of the back aperture (13 mm) of the objective lens. The angle of emission is measured by projecting the scattered beam at ω_{4wm} on a thermoelectrically cooled CCD. Thus, the displacement Δx of the detected spot on the CCD measured from the optical axis is a direct measure for the transverse wavevector $k_x = (k/f)\Delta x$, with f being the focal length of the objective

and $k = n\,\omega_{4wm}/c$ being the wavevector of the emitted radiation.

The third-order susceptibility $\chi^{(3)}$ giving rise to four-wave mixing is a tensor of rank three. Although the symmetry of our experimental configuration allows many components of the tensor to be eliminated the number of unknowns remains high. Furthermore, in addition to the bulk response we have to take into consideration the surface-specific response. It can be expected that the bulk response strongly dominates over the surface response and hence it is not a priori clear how effective third-order surface plasmon excitation is.

To understand the surface-specific response we consider 4WM by two collinear excitation beams incident at the angle θ as shown in Fig. 1(b). The surface polarization at the 4WM frequency on the bottom interface acts as a source current and gives rise to a scattered field. As illustrated in Fig. 1(c), the field radiated into the upper space is reflected from the top boundary and then superimposed to the field emitted into the lower space. The interference of these two fields gives rise to a 'plasmon dip' at the Kretschmann angle. Our goal was to experimentally demonstrate this dip, and to prove that despite of the bulk contribution of $\chi^{(3)}$, surface plasmons at the frequency $\omega_{4\mathrm{wm}}$ are efficiently excited by a nonlinear surface polarization at the glass-metal interface.

As shown in Fig. 2, we clearly observe the predicted plasmon dip in the emission patterns. In Fig. 2a,b we expanded the incident excitation beams in order to cover a broad range of angles θ. Both incident beams are p polarized in Fig. 2a, and s polarized in Fig. 2b. Evidently, the dip is only observed for p polarized excitation, which proves that a surface plasmon is excited at the four-wave mixing wavelength $\lambda_{4wm} = 613\,\mathrm{nm}$. For s-polarized excitation the 4WM signal is still measurable but the dip is not present anymore. The 4WM signal exists even if the excitation beams are centered on the optical axis (moved towards the cross-hair in Fig. 2a,b), which suggests that both bulk *and* surface nonlinearities are involved in the four-wave mixing mechanism. Fig. 2(c) plots the normalized 4WM signal over the entire range of incident angles θ. The graph represents the ratio of four-wave mixing intensity generated by p-polarized excitation (I_p) and four-wave mixing intensity generated by s-polarized excitation (I_s). The normalization is performed in order to remove any possible artifacts due to diffraction at the rims of the backaperture and

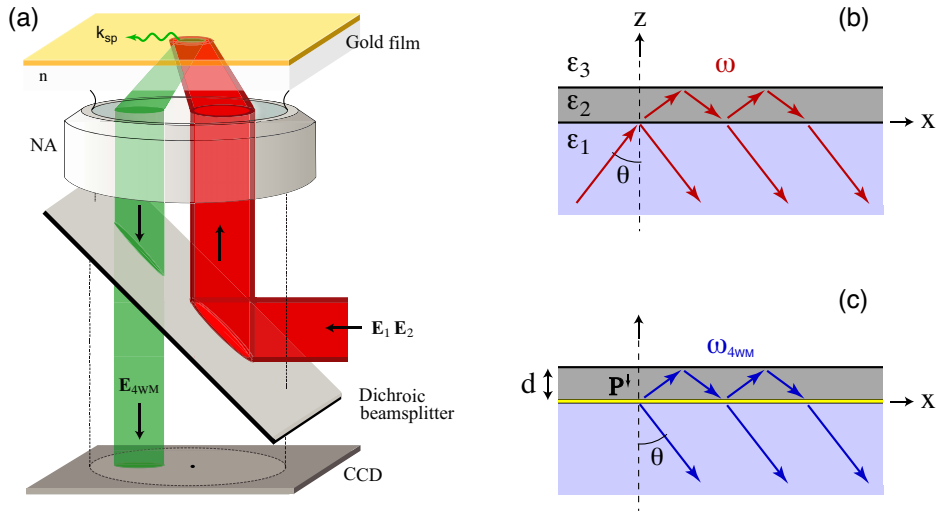

Figure 1: *Nonlinear excitation of surface plasmons. (a) Two incident beams at frequencies ω_1 and ω_2 give rise to four-wave mixing at a gold film and generate an outgoing beam at frequency $\omega_{4wm} = 2\omega_1$ - ω_2, which is projected onto a CCD. The lateral CCD coordinates correspond to the transverse wavevector k_x. (b) The incident laser field generates nonlinear surface polarizations at the lower and upper gold interfaces. (c) The nonlinear polarization $\mathbf{P}^{\downarrow}$ at the lower interface acts as a source for a secondary field at the nonlinear frequency $\omega_{4\mathrm{WM}}$*

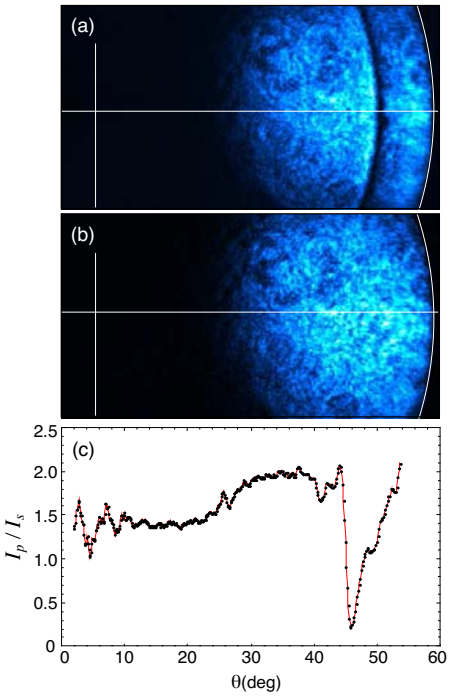

Figure 2: *Nonlinear four-wave mixing at a 52nm gold film on a glass substrate. (a,b) CCD images using expanded excitation beams. (a) p polarized excitation beams; (b) s polarized excitation beams. (c) Angular dependence of four-wave mixing radiation ($\lambda_{4wm} = 613\,nm$). The curve shows the ratio of four-wave mixing intensity generated by p-polarized excitation (I_p) and four-wave mixing intensity generated by s-polarized excitation (I_s).*

due to spectral and angular variations of the objective's transmissivity. Interestingly, the emitted 4WM radiation is predominantly p polarized even if the incident waves are s polarized. Additionally, for p polarized excitation the total emitted intensity at ω_{4wm} is approximately twice as strong as the intensity generated by s polarized excitation. These observations indicate that the third-order *surface* polarization is a dominant contribution in nonlinear four-wave mixing at metal films.

The strongest evidence for a third-order *surface* nonlinearity is provided by the observed plasmon dip at the Kretschmann angle. This dip originates from a nonlinear surface polarization at the lower gold interface. The nonlinear polarization gives rise to radiation at frequency $\omega_{4\mathrm{wm}}$ emitted both into the lower half-space (glass substrate) and the metal film. The latter excites surface plasmons at the upper gold interface and the resulting leakage radiation interferes destructively with the radiation emitted directly into the lower half-space. This interference is phase-sensitive and the appearance of a dip requires a clear phase separation between the two interfering components. No dip would be expected if the third-order nonlinearity were entirely associated with a bulk response. We hence conclude that surface plasmon excitation by four-wave mixing is dominated by a third-order *surface* nonlinearity.

3 Future Plans

In our future work we will generate four-wave mixing at the apex of an optical antenna. We will investigate the possibility of performing absorption spectroscopy on single molecules using the localized 4WM emission as an excitation source. In parallel, we will develop optimized antenna geometries to independently enhance the stimulated and spontaneous emission rate of single quantum emitters.

DOE Sponsored Publications (2005-2008)

[1] S. Palomba and L. Novotny, "Nonlinear excitation of surface plasmon polaritons by four-wave mixing," *Phys. Rev. Lett.* in print (2008).

[2] L. Novotny and C. Henkel, "Van der Waals versus optical interaction between metal nanoparticles," *Opt. Lett.* **33**, 1029 (2008).

[3] R. J. Moerland, T. H. Taminiau, L. Novotny, N. F. van Hulst, and L. Kuipers, "Reversible polarization control of single molecule emission," *Nano Lett.* **8**, 606 (2008).

[4] M. Danckwerts and L. Novotny, "Optical frequency mixing at coupled gold nanoparticles," *Phys. Rev. Lett.* **98**, 026104 (2007).

[5] P. Anger, P. Bharadwaj, and L. Novotny, "Nanoplasmonic enhancement of single molecule fluorescence," *Nanotechnology* **18**, 044017 (2007).

[6] L. Novotny, "The history of near-field optics," *Progress in Optics* **50**, 137-180, E. Wolf (ed.), Elsevier, Amsterdam (2007).

[7] H. Gersen, L. Novotny, L. Kuipers, and N. F. van Hulst, "On the concept of imaging nanoscale vector fields," *Nature Photonics* **1**, 242 (2007).

[8] L. Novotny and A. Bouhelier, "Near-field optical excitation and detection of surface plasmons," in *Surface Plasmon Nanophotonics*, M. Brongersma (ed.), Kluwer Academic (2007).

[9] P. Bharadwaj and L. Novotny, "Spectral dependence of single molecule fluorescence enhancement," *Opt. Express* **15**, 14266 (2007).

[10] R. Kappeler, D. Erni, C. Xudong, and L. Novotny, "Field computations of optical antennas," *J. Comp. Theor. Nanosc.* **4**, 686 (2007).

[11] P. Anger, P. Bharadwaj, and L. Novotny, "Enhancement and quenching of single molecule fluorescence," *Phys. Rev. Lett.* **96**, 113002 (2006).

[12] N. Anderson, A. Bouhelier and L. Novotny, "Near-field photonics: tip-enhanced microscopy and spectroscopy on the nanoscale," *J. Opt. A: Pure Appl. Opt.* **8**, S227 (2006).

[13] M. R. Beversluis, L. Novotny, and S. J. Stranick, "Programmable vector point-spread function engineering," *Opt. Express* **14**, 2650 (2006).

[14] L. Novotny and S. J. Stranick, "Near-field optical microscopy and spectroscopy with pointed probes," *Ann. Rev. Phys. Chem.* **57**, 303 (2006).

[15] A. Hartschuh, H. Qian, A. J. Meixner, N. Anderson, and L. Novotny "Tip-enhanced optical spectroscopy for surface analysis in biosciences," *Surface and Interface Analysis* **38**, 1472 (2006).

[16] H. Qian, T. Gokus, N. Anderson, L. Novotny, A. J. Meixner, and A. Hartschuh, "Near-field imaging and spectroscopy of electronic states in single-walled carbon nanotubes," *Phys. Stat. Sol. (b)* **243**, 1 (2006).

[17] A. Hartschuh, H. N. Pedrosa, J. Peterson, L. Huang, P. Anger, H. Qian, A. J. Meixner, M. Steiner, L. Novotny, and T. D. Krauss, "Single carbon nanotube optical spectroscopy," *ChemPhysChem* **6**, 1 (2005).

[18] A. Hartschuh, H. Qian, A. J. Meixner, N. Anderson, and L. Novotny, "Nanoscale optical imaging of excitons in single-walled carbon nanotubes," *Nano Lett.* **5**, 2310 (2005).

Electron-Driven Excitation and Dissociation of Molecules

A. E. Orel
Department of Applied Science
University of California, Davis
Davis, CA 95616
aeorel@ucdavis.edu

Program Scope

This program will study how energy is interchanged in electron-polyatomic collisions leading to excitation and dissociation of the molecule. Modern *ab initio* techniques, both for the electron scattering and the subsequent nuclear dynamics studies, are used to accurately treat these problems. This work addresses vibrational excitation, dissociative attachment, and dissociative recombination problems in which a full multi-dimensional treatment of the nuclear dynamics is essential and where non-adiabatic effects are expected to be important.

Recent Progress

We have carried out a number of calculations studying low-energy electron scattering from polyatomic systems leading to vibrational excitation and dissociative attachment. Much of this work has been done in collaboration with the AMO theory group at Lawrence Berkeley Laboratory headed by T. N. Rescigno and C. W. McCurdy. As a result of this collaboration one of my students is doing his thesis work with the AMO experimental group headed by A. Belcamen. He is currently carrying out experiments on dissociative attachment of systems where we have carried out calculations, both on NO and C_2H_2.

Dissociative Attachment of Acetylene

The acetylene molecule has been studied extensively in the literature both experimentally and theoretically; however, less work has been done on its negative ion and its decay. Early dissociative electron attachment (DEA) experiments showed that in the 0-3 eV collision energy range the main products were H and C_2H^- fragments in their ground electronic states. The corresponding DEA cross section showed a pronounced peak around 3 eV with a non-vertical onset at around 2.6 eV. The DEA process is given by the following the mechanism:

$$C_2H_2\ (X^1\Sigma_g^+) + e^-(E) \rightarrow (C_2H_2^-)^*(^2\Pi_g) \rightarrow C_2H^-(^1\Sigma^+) + H(^2S)$$

which suggests that a symmetry-breaking event takes place along this reaction pathway. Note that the initially formed negative ion is a π^*-shape resonance with $^2\Pi_g$ symmetry and thus does not correlate with the fragments C_2H_2 ($X^1\Sigma_g^+$) and H(^{2}S) in their totally symmetric representations. This implies that a one-dimensional study of this system is inadequate to describe the dissociation dynamics and that bending must be taken into consideration. This is similar to what was seen in earlier studies of DEA in formic acid (Publication 3).

We have carried out *ab initio* calculations for elastic electron scattering from acetylene using the complex Kohn variational method. We identified the responsible negative ion state as a transient π^*- anion with the electron temporarily trapped in the CC antibonding π orbital. These calculations and additional quantum chemistry calculations were used to map out the resonance surface and autoionization width keeping on C-H distance fixed, reducing the problem to three dimensions, the C-CH distance (r), the distance from the other hydrogen atom to the center of mass (R) and the angle in-between them (θ). We then carried out MultiConfiguration Time-Dependent Hartree (MCTDH) calculations [1] to track the dissociation dynamics and obtain the dissociative attachment cross sections. We found that the molecule must first bend, followed by stretching of the CH bond leading to dissociation. The calculated cross section agrees quite well with most recent experimental results of May *et al*[2].

The results of the calculation are described in a paper published in Physical Review A (Publication 7)

Dissociative Electron Attachment to HCN and HNC

Previously we have carried out studies on DEA of ClCN and BrCN (Publication 5). We have extended these calculations to HCN and its isomer HNC. These molecules are known to be among the initial species that drive synthesis of amino acids in the interstellar media. Previous experimental and theoretical studies have indicated low-lying Σ and Π resonances. These resonant states are expected to depend on stretching and bending of the molecule and lead to competition (CN^- + H) and (CN + H^-) products. We have carried out electron scattering calculation using the complex Kohn variational method as a function of the three internal degrees of freedom to obtain the resonance energy surface and autoionization widths. We used this as input to a dynamics calculation using the MCTDH approach [1]. In contrast to acetylene, instead of bending, the H atom tunnels through the barrier to dissociation. The DEA cross section and branching ratios were compared to available experiment and theory.

The results of the calculation are described in a paper to be submitted to in Physical Review A (Publication 9)

FUTURE PLANS

Electron interactions with CF_x radicals

Previously, we have studied the dissociative attachment of CF, the process, $e^- + CF \rightarrow F^- + C$. It was found not to produce significant F^-(Publication 2). The dissociative recombination of the cation CF^+ is interesting since ion-pair formation, the process, $e^- + CF^+ \rightarrow F^- + C^+$ is possible. This has been suggested as a possible source of F^- in these fluorocarbon plasmas. Experiments on the dissociative recombination have been carried out on both the ASTRID and CRYRING storage rings [3].

We will performed extensive structure calculations coupled with electron scattering calculations to characterize both the Rydberg states converging to the ground and low-

lying excited states of the ion, as well as the resonant states and their autoionization widths as a function of internuclear separation. This data will be used in an MQDT study of the dissociative recombination as well as a wave packet study of resonant dissociative excitation. The results can then be compared to the recent experiments and used to explain the experimental results. We have carried out some preliminary calculations on this system and compared to some more recent experimental results [4].

In collaboration with T.N. Rescigno, LBL, we have begun a study of the radical CF_2. We have performed fixed-nuclei scattering calculations using the Complex Kohn variational method and extracted the resonance parameters, for each geometry of interest, by analyzing the energy dependence of the eigenphase sums. These preliminary calculations have showed a single resonance at low energy that at the static exchange level is unbound at the equilibrium geometry of the ground state. However, at the relaxed SCF level of calculation, which correctly balances the anion and target correlation and has been used previously with great success to study similar resonances, the anion is bound at the equilibrium geometry. This is in contrast to the R-matrix calculations [5] that show the anion to be unbound at the equilibrium geometry. These calculations have only been performed as a function of one variable, one C--F distance, with all other degrees of freedom frozen at their equilibrium values. We have also carried out one-dimensional wave packet calculations using the potential energy curves and couplings at each level of calculation. The addition of polarization at the relaxed SCF level increases the cross section by several orders of magnitude. It is necessary to carry out calculations allowing the other degrees to vary to see how the cross section is affected. We are currently extending these one-dimensional calculations to a full three-dimensional study of this process at both the static exchange and relaxed SCF level.

Dissociative Attachment of Acetylene

Recent experimental work shows that at a higher energy (>7 eV) the channel, which fragments into C_2^- and H_2, becomes open. This reaction proceeds through a higher-lying Feshbach resonance, and involves a dramatic change in geometry to proceed to products. We have begun a series of *ab initio* calculations, with a number of open electronic channels for electron scattering from acetylene using the Complex Kohn variational method. These calculations have shown, not only a series of Feshbach resonances, but also the higher lying shape resonances in the system. More work is needed to study the potential energy surfaces for these states and identify which of these states are involved in the dissociation process. It is possible that more than one state is involved and that interaction between the states must be included. We propose to study this and calculate the multi-dimensional dynamics leading to dissociation.

Dissociative Attachment in Halogenated Molecules

There have been no theoretical systematic studies of dissociative attachment in organic molecules. There have been some such experimental studies, but these have been limited [6,7,8]. We have begun a series of calculations on mono-substituted organic compounds to look for general trends and to better understand what controls the energy flow leading to dissociation in these systems. We have chosen the systems, HCCCl, H_3CCCl, H_5CCCl, showing a series from triple, double to single bond respectively.

We started calculations on ClCCH, chloroactylene. In our first calculations, the molecule was studied as a pseudo-diatomic, varying the Cl--C internuclear separation and keeping all other bond distances fixed. If the molecule is bent there is coupling between channels arising from σ^* and π^* antibonding orbitals. We are investigating this effect by carrying out the scattering for the bent structure. We are also looking at variations as other bonds are modified. In our studies of ClCN and BrCN (Publication 5), there was no significant mixing between the σ^* and π^* channels. However, in acetylene (Publication 8), it was that coupling that allowed dissociation to occur. We have completed the one- and two-dimensional studies of this system and are now investigating the effect of bending. In addition, we have begun one-dimensional studies of the H_3CCCl (double-bond case) and H_5CCCl (the single bond case) systems.

REFERENCES

1. M. H.Beck, A. Jackle, G.A. Worth and H. –D. Meyer, Phys. Rep., 324 (2000).
2. O. May, J. Fedor, B. C. Ibanescu and M. Allan, Phys. Rev. A. **77**, 040701 (2008).
3. O. Novotny et al, J. Phys. B, **38**, 1471 (2005)
4. O. Novotny et al, J. Phys. Conf. Series, **XX**, XX (2008).
5. I. Rozum, N. J. Mason and Jonathan Tennyson, *J. Phys. B*, **35**, 1583 (2002).
6. D. M. Pearl and P. D. Burrow, *J. Chem. Phys.*, **101**, 2940 (1994).
7. K. Aflatooni and P. D. Burrow, *J. Chem. Phys.*, **113**, 1455 (2000).
8. G. A. Gallup, K. Aflatooni and P. D. Burrow, *J. Chem. Phys.*, **118**, 2562 (2003).

PUBLICATIONS

1. A nonlocal *ab initio* model of dissociative electron attachment and vibrational excitation of NO, C. S. Trevisan, Karel Houfek, Zhiyong Zhang, A. E. Orel, C. W. McCurdy, and T. N. Rescigno, Phys. Rev. A, **71,** 052714 (2005).
2. Resonant electron-CF collision processes, C. S. Trevisan, A. E. Orel, and T. N. Rescigno, Phys. Rev. A, **72,** 627720 (2005).
3. Dynamics of Low-Energy Electron Attachment to Formic Acid, T. N. Rescigno, C. S. Trevisan and A. E. Orel, Phys. Rev. Lett. **96** 213201 (2006).
4. Elastic Scattering of Low-energy Electrons by Tetrahydrofuran, C. S. Trevisan, A. E. Orel and T. N. Rescigno, J. of Phys. B **39** L255 (2006).
5. Dissociative Attachment of ClCN and BrCN, J. Royal and A. E. Orel, J. Chem. Phys, **125** 214307 (2006).
6. Low-Energy Electron Scattering by Formic Acid, C. S. Trevisan, A. E. Orel and T. N. Rescigno, Phys. Rev. A **74** 042716 (2006).
7. Electron-induced resonant dissociation and excitation of NeH+ and NeD+, V.Ngassam, A. I. Florescu-Mitchell, and A. E. Orel, Phys.Rev. A, 77, 042706 (2008)
8. Dissociative Electron Attachment of Acetylene, S. Chourou and A. E. Orel, Phys.Rev. A, 77, 042709 (2008)
9. Dissociative Electron Attachment of HCN and HNC, S. Chourou and A. E. Orel, (to be submitted) Phys.Rev. A

"Low-energy electron interactions with interfaces and biological targets"

Thomas M. Orlando *(Thomas.Orlando@chemistry.gatech.edu), School of Chemistry and Biochemistry and School of Physics, Georgia Institute of Technology, Atlanta, GA 30332*

Program Scope: The primary objectives of this program are to investigate the fundamental physics and chemistry involved in low-energy (1-250 eV) electron interactions with i) condensed films of water co-adsorbed with solvated ions and biologically relevant molecules, ii) condensed samples of complex biological targets such as deoxyribonucleic acids (DNA) and iii) aqueous solution surfaces and interfaces containing solvated ions and biomolecules. The program concentrates on the important issues dealing with electron initiated damage and energy exchange in the deep valence and shallow core regions of the collision targets.

Recent Progress: We have completed four major tasks related to understanding the interaction of low-energy electrons and ultraviolet photons with complex targets. The first task focused on experimental studies of low-energy electron interactions with water adsorbed on rare gas overlayers and water adsorbed on TiO_2 surfaces. The second task extended the Coulomb exchange model developed in task 1 and focused on photoionization of aqueous salt solution interfaces. The third task involved further experimental and theoretical work on diffraction effects in stimulated desorption (DESD). The fourth focused on applying these scattering calculations to DNA targets and to the development of experimental approaches for examining electron-induced damage of DNA.

Project 1. The interaction of low-energy electrons and cluster ion ejection from water covered insulator surfaces. We have examined the electron-stimulated production and removal of water cluster ions from water covered surfaces. The cluster ion yields were then modeled with a simple screened hole-hole interaction theory which leads to an intermolecular Coulomb repulsion effect.

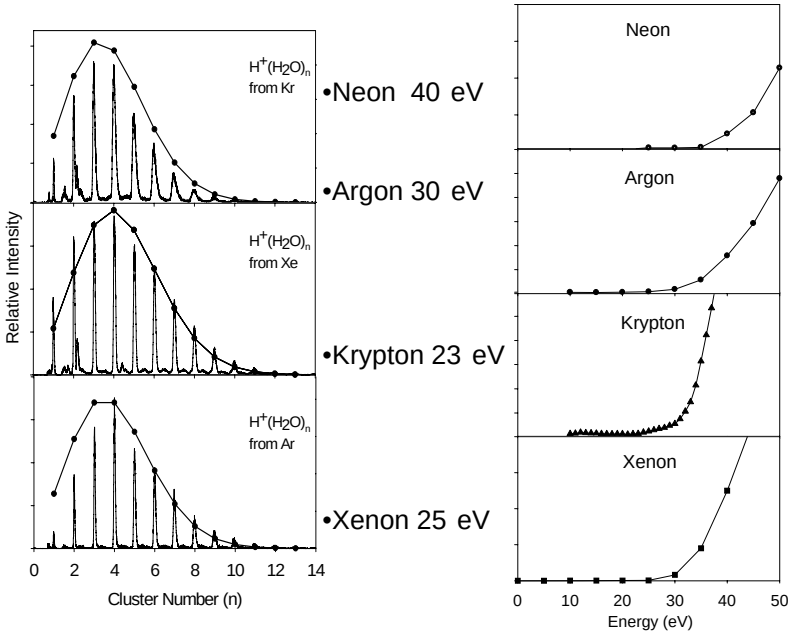

Figure 1. (Left) Cluster ion distributions observed during 100 eV electron-beam irradiation of water adsorbed on rare gas substrates. (Right) The threshold energy for producing the cluster ions are 25, 23, 30 and 40 eV for Xe, Kr, Ar, and Ne, respectively. These correspond to shallow core levels of the underlying rare gases

The cluster ion yields are very sensitive to local hydrogen bonding interactions and are very good probes of hole exchange. Specifically, when water is co-adsorbed with rare gases such as Xe, Ar Kr and Ne, cluster ion production and escape is greatly enhanced. The yields, threshold energies and velocities indicate that cluster ion formation and removal involves hole mediated

intermolecular Coulomb exchange. Our work has been the first to experimentally demonstrate this phenomenon with chemically important molecular collision targets.

Project 2. Laser stimulated processes at aqueous surfaces. We have employed a liquid microjet to examine the gas/liquid interface of aqueous sodium halide (Na^+X^-, X=Cl, Br, I) salt solutions. Laser excitation at 193 nm produced and removed cations of the form $H^+(H_2O)_n$ and $Na^+(H_2O)_m$ from liquid jet surfaces containing either NaCl, NaBr or NaI. The protonated water cluster yield varied inversely with increasing salt concentration, while the solvated sodium ion cluster yield varied by anion type. The distribution of $H^+(H_2O)_n$ at low salt concentration is identical to that observed from low-energy electron irradiated amorphous ice and the production of these clusters can be accounted for using a localized ionization/Coulomb expulsion model. Production of $Na^+(H_2O)_m$ is not accounted for by this model but required ionization of solvation shell waters and a contact ion/Coulomb expulsion mechanism. The reduced yields of $Na^+(H_2O)_m$ from high concentration (10^{-2} and 10^{-1} M) NaBr and NaI solutions indicate a propensity for Br^- and I^- at the solution surfaces and interfaces. This is supported by the observation of multiphoton induced production and desorption of Br^+ and I^+ from the 10^{-2} and 10^{-1} M solution surfaces.

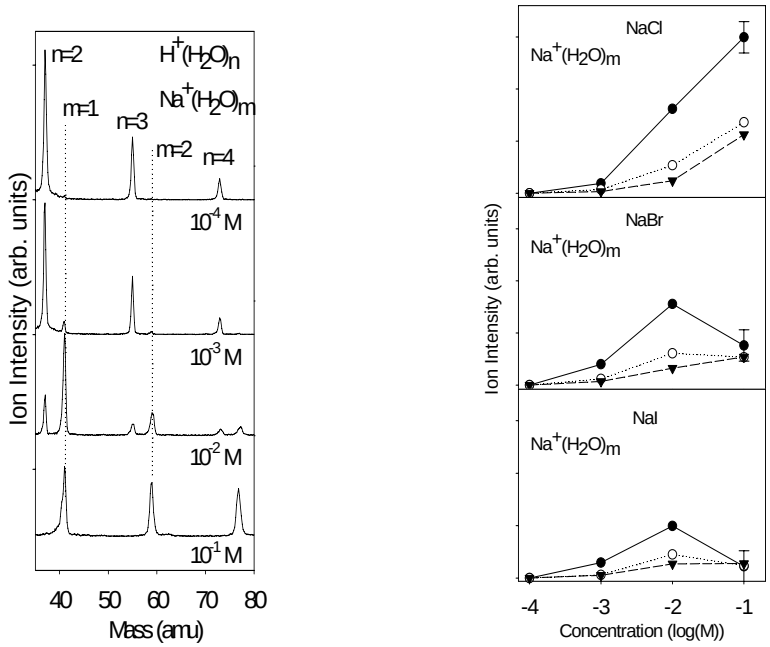

Figure 2: (Left) Time-of-flight spectra obtained during photoionization of NaCl solutions with concentrations ranging from 10^{-4} to 10^{-1} M. (Right) Experimentally observed cluster ion yields as a function of concentrations for NaCl (top panel), NaBr, (middle panel), and NaI (bottom panel) solutions.

We have also completed studies on the role of aqueous interfaces and intrinsic ions in surface assisted laser desorption. These experiments were carried out, in part, to develop analysis techniques necessary for studies on electron beam damage of DNA.

Project 3. A theoretical description and experimental demonstration of diffraction in electron stimulated desorption (DESD). The role of diffraction in electron-stimulated desorption (DESD) was re-examined and described theoretically. Specifically, initial state effects in DESD of Cl^+

from Si(111)-(1×1):Cl and Si(7×7):Cl was examined and the theory was expanded to encompass spherical-wave and multiple scattering effects of low-energy incident electrons by introducing a separable propagator method. The scattering amplitude was calculated and compared with a plane-wave approximation. Qualitative analysis of Cl^+ desorption shows that the initial excitation occurring on the Si(111)-(1×1):Cl surface primarily involves the Si. Two desorption mechanisms were proposed, i) ionization of the Si(3s) level followed by Auger cascading from the σ-bonding surface state and shake-up of an electron in the non-bonding π-level and ii) direct ionization of the Si-Cl σ-bonding state. For the case of Si(7×7) surfaces, a propensity for the removal of Cl^+ from the unfaulted region was observed. Finally, temperature effects on DESD rates were analyzed and modeled.

Project 4. Low-energy electron-induced damage of DNA We have examined theoretically the elastic scattering of 5-30 eV electrons within the B-DNA 5'-CCGGCGCCGG-3' and A-DNA 5'-CGCGAATTCGCG-3' sequences using the separable representation of a free-space electron propagator and a curved wave multiple scattering formalism. The disorder brought about by the surrounding water and helical base stacking leads to featureless amplitude build-up of elastically scattered electrons on the sugars and phosphate groups for all energies between 5-30 eV. However, some constructive interference features arising from diffraction were revealed when examining the structural waters within the major groove. These appear at 5-10, 12-18 and 22-28 eV for the B-DNA target and at 7-11, 12-18 and 18-25 eV for the A-DNA target. Though the diffraction depends upon the base-pair sequence, the energy dependent elastic scattering features are primarily associated with the structural water molecules localized within 8-10 Å spheres surrounding the bases and/or the sugar-phosphate backbone.

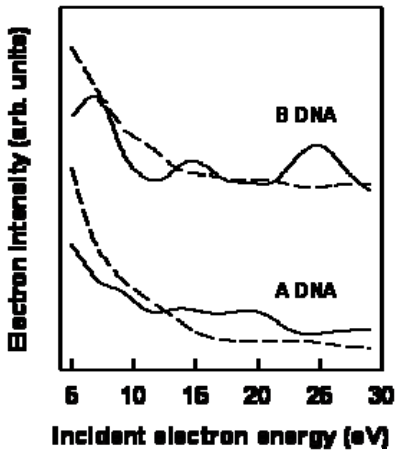

Figure 3. A comparison of the calculated electron intensities associated with the structural waters located within the major (solid line) or minor (dashed line) groove of B-DNA 5'-CCGGCGCCGG-3' and A-DNA 5'-CGCGAATTCGCG-3' targets as a function of incident electron energy.

The electron density build-up occurs in energy regimes associated with dissociative electron attachment resonances, direct electronic excitation and dissociative ionization. We have used post-irradiation gel electrophoresis to measure the single and double strand breaks. Comparison of this data with the scattering calculation implies that compound H_2O:DNA states may contribute to the energy dependent low-energy electron induced break probability.

We have also utilized a vacuum ultraviolet (VUV) laser source using third-harmonic generation in rare gases to detect the neutral fragments released during the low-energy electron beam induced damage of DNA plasmids physisorbed on graphite substrates. The results support the contention that dissociative electron attachment (DEA) resonances localized on DNA sub-units can lead to damage, especially at energies below the ionization threshold. Damage also occurs due to direct dissociative excitation and dissociative ionization.

Future Plans: Our future investigations should be particularly fruitful in extracting important details regarding the roles of counter ions, interfacial energy exchange, and molecular structure in non-thermal damage of hydrated biological interfaces. Specifically, we intend to:

- Investigate low-energy electron interactions with water co-adsorbed with biologically relevant molecules (i.e. phosphate-linked sugars, nucleic acids, nucleotides and nucleosides).
- Investigate low-energy electron induced damage of DNA.
- Expand multiple scattering calculations with biological targets to include more realistic potentials which include core holes and counter ions.
- Probe ion-solvation at liquid surfaces using electron-irradiation of micro-jets.

Presentations from this project during 2005-2008

1. Y. Chen, C. Sullards, T. Huang, S. May, and T. M. Orlando, "Analysis of Metabolites by Laser Desorption Single Photon Ionization Mass Spectrometry", PITTCON05, Orlando, FL, March 2005.
2. T. M. Orlando, J. Herring Captain, A. Alexandrov and G. A. Grieves, "Non-thermal Processes on Low-Temperature Ice Surfaces", Atmospheric Chemistry Gordon Conference, Sept. 4-9, 2005.
3. T. M. Orlando, "The Formation of Reactive Atomic Fragments via Dissociative Recombination, Dissociative Electron Attachment and Coulomb Explosions", European Group on Atomic and Molecular Physics, Ischia, Italy 2006.
4. Y. Chen, C. Santai, N. Hud, and T. M. Orlando, "Low-energy Electron-induced Damage and Desorption of Hydrated DNA", International Workshop on Desorption Induced by Electronic Transitions (DIET XI), Berlin, March 11-16, 2007.
5. G. A. Grieves and T. M. Orlando, "Low-energy (5-250 eV) Electron Stimulated Desorption of Cluster ions from Water Adsorbed on Rare-gas Overlayers", International Workshop on Desorption Induced by Electronic Transitions (DIET XI), Berlin, March 11-16, 2007.
6. C. Lane, T. M. Orlando, N. Petrik and G. A. Kimmel, "Oxidation of the TiO2(110) Surface during Electron Irradiation of an Adsorbed Water Monolayer", International Workshop on Desorption Induced by Electronic Transitions (DIET XI), Berlin, March 11-16, 2007.
7. T. M. Orlando, D. Oh, Y. Chen, and A. Alexandrov, "Low-energy Electron Diffraction and Induced Damage in Hydrated DNA", Radiation Chemistry Gordon Conference, July 7-12, 2008.

Publications from this project during 2005-2008.

1. J. Herring-Captain, G.A. Grieves, A. Alexandrov, M.T. Sieger, H.-Y. Chen and T.M. Orlando, "Low-energy (5-250 eV) Electron Stimulated Desorption of H^+, H_2^+ and $H^+(H_2O)_n$ from Low-temperature Water Ice Surfaces," *Phys. Rev. B* 72, 035431 (2005).
2. Y. Chen, C. Sullards, T. Huang, S. May and T. M. Orlando, "Analysis of Organoselenium and Organic Acid Metabolites by Laser Desorption Single Photon Ionization Mass Spectrometry", *Anal. Chem.* 78 (24), 8386 (2006).
3. D. Oh, M. T. Sieger and T. M. Orlando, "Zone Specificity in the Low-energy Electron Stimulated Desorption of Cl^+ from Reconstructed Si(111)-7×7 surfaces", *Surf. Sci.*, 600(19), L245-L249 (2006).
4. C. D. Lane, N. G. Petrik, T. M. Orlando and G. A. Kimmel, "Electron-Stimulated Oxidation of Thin Films of Water Adsorbed on TiO_2(110)", *J. Phys. Chem. C*, 111, 16319 (2007).
5. C. D. Lane, N. G. Petrik, T. M. Orlando and G. A. Kimmel, "Site-Dependent Electron-Stimulated Reactions in Water Films on TiO_2(110)", *J. Chem. Phys.*, 127, 224706, (2007).
6. Y. Chen, H. Chen, A. Aleksandrov and T. M. Orlando, "The Roles of Water, Acidity and Surface Morphology on Surface Assisted Laser Desorption Ionization of Amino Acids", *J. Phys. Chem. C.* 112, *(*2008).
7. G. A. Grieves, N. Petrik, J. Herring-Captain, B. Olanrewaju, A. Aleksandrov, R. G. Tonkyn, S. A. Barlow, G. A. Kimmel, and T. M. Orlando, "Photoionization of Sodium Salt Solutions in a Liquid Jet", *J. Phys. Chem. C*. 112, 8359 (2008).
8. T. M. Orlando, D. Oh, Y. Chen, and A. Alexandrov, "Low-energy Electron Diffraction and Induced Damage in Hydrated DNA", *J. Chem. Phys*. 128, 195102 (2008).
9. Y. Chen, A. Aleksandrov and T. M. Orlando, "Probing low-energy electron induced damage of DNA using single-photon ionization mass spectrometry", *Int. J. of Mass Spec. and Ion Physics (in press).*

Energetic Photon and Electron Interactions with Positive Ions

Ronald A. Phaneuf,
Department of Physics /220
University of Nevada
Reno NV 89557-0058
phaneuf@physics.unr.edu

Program Scope

This experimental program investigates photon and electron initiated processes leading to ionization of positive atomic and molecular ions. The objective is a deeper understanding of both ionization mechanisms and electron-electron interactions in ions of atoms, molecules and nano-scale molecular clusters. Monoenergetic beams of photons and electrons are merged or crossed with mass/charge analyzed ion beams to probe their internal electronic structure as well as the dynamics of their interaction. Of particular interest are highly-correlated processes such as collective electron excitations that are manifested as giant dipole resonances in the ionization of atomic ions and also of fullerene ions, whose unique cage structure characterizes them as intermediates between individual molecules and solids. In addition to precision spectroscopic data for understanding ionic structure and interactions, high-resolution measurements of absolute cross sections for photoionization and electron-impact ionization provide critical benchmarks for testing theoretical approximations such as those used to generate opacity databases. Improving their accuracy is critical to modeling and diagnostics of astrophysical, fusion-energy and laboratory plasmas. Of particular relevance to DOE are those produced by the Z pulsed-power facility at Sandia National Laboratories, the world's brightest and most efficient x-ray source, and the National Ignition Facility at Lawrence Livermore National Laboratory, the world's most powerful laser. Both are dedicated to high-energy-density science and fusion-energy research.

Recent Progress

The major thrust is the application of an ion-photon-beam (IPB) research endstation to experimental studies of photoionization of singly and multiply charged positive ions using monochromatized synchrotron radiation at the Advanced Light Source (ALS). The high photon beam intensity and energy resolution available at ALS undulator beamline 10.0.1.2 make photoion spectroscopy a powerful probe of the internal electronic structure of atomic and molecular ions, permitting tests of sophisticated structure and dynamics computer codes at unprecedented levels of detail and precision. Measurements using the IPB endstation at ALS still define the current state of the art worldwide in energy resolution available to studies of photon-ion interactions. This program led the development and continues to have primary responsibility for maintenance and upgrade of this permanently installed multi-user research endstation at the ALS.

- Due to their large number of atoms, size and hollow cage structure, fullerene molecular ions are of interest as structural intermediates between individual molecules and solids. As is the case for conducting solids, their large number of valence electrons may be collectively excited in plasmon modes, whereas the excitation of core electrons is localized and of molecular character. Unusual physical

properties of fullerene molecules containing trapped atoms within their hollow carbon cage structures have been predicted by several recent theoretical studies. Phenomena related to resonant interactions of these so-called endohedral fullerenes with ultraviolet light remain essentially untested by experiments. To explore their physical properties and to assess the validity of these predictions, a program of photoionization measurements with endohedral fullerene molecular ion beams was recently initiated with German collaborators from Giessen (A. Müller and S. Schippers) and Dresden (L. Dunsch). Because of the availability of samples, initial proof-of-principle measurements were made of photoionization of $Sc_3N@C_{80}^+$ and $Ce@C_{82}^+$ with ion beam currents of only a few picoamperes. Both sets of measurements indicated clear signatures of the encaged molecule or atom [12]. A series of follow-up measurements on $Ce@C_{82}^+$ was successful in quantifying the Ce 4d inner-shell excitation contributions. They indicated a dramatic reduction and redistribution of the 4d oscillator strength to additional decay channels, and on the basis of accompanying measurements on Ce atomic ions (below), determined the valency of the encaged Ce atom to be +3. A report on this work was submitted to Physical Review Letters [13].

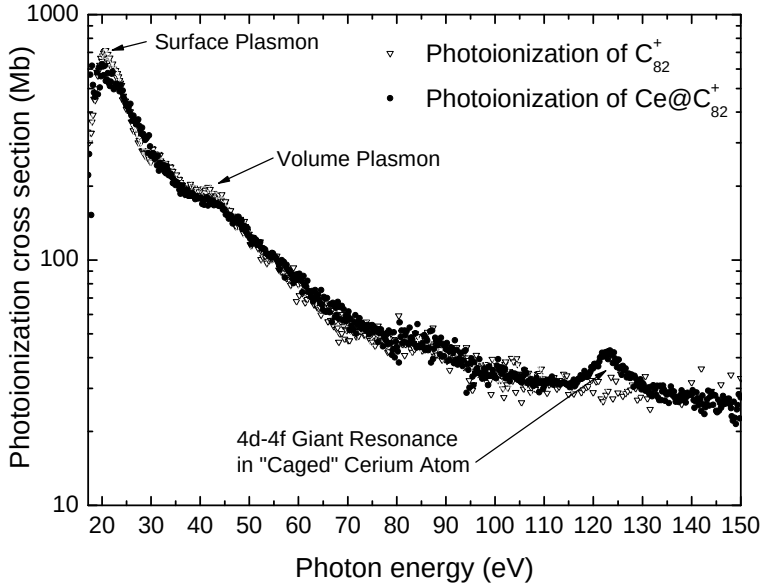

Measured cross sections for photoionization of empty C_{82}^+ and endohedral $Ce@C_{82}^+$ indicating surface and volume plasmon resonances of the fullerene cage and the 4d giant dipole resonance of the caged Ce atom.

- A systematic series of absolute photoionization measurements for ions of the Ce isonuclear sequence (Ce^+ through Ce^{9+}) was completed in the energy range of the 4d giant dipole resonance (110 – 150 eV). The measurements included both single and double photoionization of Ce^+, Ce^{2+} and Ce^{3+}, and single photoionization of Ce^{4+} – Ce^{9+}. As the initial ion charge state increases, the transition of 4d excitations from continuum to discrete final 4f states is evident in the measured widths of the resonance features in this energy range. This systematic investigation constitutes part of the Ph.D. dissertation research of M. Habibi.

- Absolute measurements of photoionization of Se^+, Se^{2+} and Se^{3+} are in progress in collaboration with A. Aguilar of LBNL and N. Sterling of NASA Goddard Space Flight Center. Complementary measurements of electron-impact ionization of Se^{3+} were also completed at the University of Nevada. This investigation constitutes part of the Ph.D. dissertation research of D. Esteves.

Future Plans

In addition to completing ongoing investigations, research is planned in three new directions.

- Photoionization measurements with doubly charged $Ce@C_{82}^{2+}$ ions are planned to probe the effect of net fullerene charge on the valency of the caged Ce atom and on the chemical stability of the endohedral molecule. Determining the energy position and strength of the Ce 4d giant dipole resonance will be the primary objectives of this investigation in collaboration with A. Müller, S. Schippers and L. Dunsch.

- Although they are the focus of most current theoretical work, noble-gas endohedral fullerenes are not currently available as solid samples in quantities sufficient for evaporation into an ion source. Their production within a discharge as well as in collisions of a fullerene ion beam with a noble gas has been reported. Both methods for *in situ* production of rare-gas endohedral fullerene ion beams will be tested at ALS and if successful, a program will be initiated to study photoionization and photo-fragmentation of $Ne@C_{60}^+$, $Ar@C_{60}^+$ and $Xe@C_{60}^+$ endohedral fullerene ions. The measurements will focus on the effect of the caged Ne, Ar or Xe atom on the C_{60}^+ surface and volume plasmon resonances observed near 22 eV and 38 eV. Measurements on photoionization of $Xe@C_{60}^+$ will also key on the energy range of the broad Xe 4d giant dipole resonance (75 – 150 eV), which is predicted to be split into four narrow components due to reflection of photoelectron waves by the fullerene shell [Amusia et al., J. Phys. B: At. Mol. Opt. Phys. **38**, L169 (2005)]. Measurements on $Ar@C_{60}^+$ will investigate a predicted order-of-magnitude enhancement in the Ar 3p photoionization cross section in the 19 – 35 eV photon energy range and an attenuation of the of the surface plasmon resonance [Madjet et al, Phys. Rev. Let. **99**, 243003 (2007)]. Measurements on $Ne@C_{60}^+$ will search for signatures of 2s-np excitation-autoionization resonances in Ne and Ne^+ in the 40 – 50 eV range to determine the valency of the caged Ne atom.

- Photoionization of the fullerene fragment ions C_{58}^+, C_{56}^+, C_{54}^+… is of interest to explore the effects of the size and symmetry of the molecular cage structure on the collective plasmon resonances and on the chemical stability of these ions. Such measurements will be compared with existing data for C_{60}^+, C_{70}^+, C_{80}^+, C_{82}^+ and C_{84}^+ in order to systematically explore the cross-section scaling with the number of carbon atoms, as well as effects of the cage symmetry and size on the plasmon resonances.

References to Publications of DOE-Sponsored Research (2006-2008)

1. *Photoionization and electron-impact ionization of multiply charged krypton ions*, Miao Lu, Ph.D. Dissertation, University of Nevada, Reno (2006).

2. *Photoionization and electron-impact ionization of Kr^{5+}*, M. Lu, M.F. Gharaibeh, G. Alna'Washi, R.A. Phaneuf, A.L.D. Kilcoyne, E. Levenson, A.S. Schlachter, A. Müller, S. Schippers, J. Jacobi and C. Cisneros, Phys. Rev. A 74, 012703 (2006).

3. *Photoionization and electron-impact ionization of Kr^{3+}*, M. Lu, G. Alna'Washi, M. Habibi, M.F. Gharaibeh, R.A. Phaneuf, A.L.D. Kilcoyne, E. Levenson, A.S. Schlachter, C. Cisneros and G. Hinojosa, Phys. Rev. A 74, 062701 (2006).

4. *Absolute photoionization cross sections for Xe^{4+}, Xe^{5+} and Xe^{6+} near 13.5 nm: Experiment and theory*, A. Aguilar, J.D. Gillaspy, G.F. Gribakin, R.A. Phaneuf, M.F. Gharaibeh, M.G. Kozlov, J.D. Bozek and A.L.D. Kilcoyne, Phys. Rev. A 74, 032717 (2006).

5. *Interaction of photons with ionized matter*, Ronald A. Phaneuf, p.p. 171-175 in McGraw-Hill Yearbook of Science and Technology 2006, McGraw-Hill, New York (2006).

6. *Doubly excited resonances in the photoionization spectrum of Li^+: experiment and theory*, S.W.J. Scully, I. Álvarez, C. Cisneros, E.D. Emmons, M.F. Gharaibeh, D. Leitner, M.S. Lubbell, A. Müller, R.A. Phaneuf, R. Püttner, A.S. Schlachter, S. Schippers, W. Shi, C.P. Balance and B.M. McLaughlin, J. Phys. B: At. Mol. Opt. Phys. 39, 3957 (2006).

7. *Photoionization and Electron-impact Ionization of Ar^{5+}*, Jing Cheng Wang, M.S. Thesis, University of Nevada, Reno (2006).

8. *Photoionization and electron-impact ionization of Ar^{5+}*, Jing Cheng Wang, M. Lu, D. Esteves, M. Habibi, G. Alna'Washi, R.A. Phaneuf and A.L.D. Kilcoyne, Phys. Rev. A 75, 062712 (2007).

9. *Colliding-beams Experiments for Studying Fundamental Atomic Processes*, 13th International Conference on the Physics of Highly Charged Ions, Belfast, Northern Ireland, August 28, 2006; J. Phys. Conf. Ser. 58, 1 (2007).

10. *Photoionization of Cl-like K^{2+} and Ca^{3+}*, Ghassan Alna'Washi, Ph.D. Dissertation, University of Nevada, Reno (2007)

11. *Reply to Comment on photoexcitation of a volume plasmon in C_{60} ions*, S.W.J. Scully, E.D. Emmons, M.F. Gharaibeh, R.A. Phaneuf, A.L.D. Kilcoyne, A.S. Schlachter, S. Schippers, A. Müller, H.S. Chakraborty, M.E. Madjet and J.M. Rost, Phys. Rev. Lett. 98, 179602 (2007).

12. *Photoionization of the endohedral fullerene ions $Sc_3N@C_{80}^+$ and $Ce@C_{82}^+$ by synchrotron radiation*, A. Müller, S. Schippers, R.A. Phaneuf, M. Habibi, D. Esteves, J.C. Wang, A.L.D. Kilcoyne, A. Aguilar, S. Yang and L. Dunsch, XXV International Conference on Photonic, Electronic and Atomic Collisions, Freiburg, Germany, July 25-31, 2007; J. Phys. Conf. Ser. 88, 02138 (2007).

13. *Significant redistribution of Ce 4d oscillator strength observed in photoionization of endohedral $Ce@C_{82}^+$ ions*, A. Müller, S. Schippers, M. Habibi, D. Esteves, J.C. Wang, R.A. Phaneuf, A.L.D. Kilcoyne, A. Aguilar and L. Dunsch, Physical Review Letters (submitted, June 2008).

Control of Molecular Dynamics: Algorithms for Design and Implementation

Herschel Rabitz and Tak-San Ho, Princeton University
Frick Laboratory, Princeton, NJ 08540, hrabitz@princeton.edu, tsho@princeton.edu

A. Program Scope

This research is concerned with the conceptual and algorithmic developments addressing control over quantum dynamics phenomena. The research is theoretical and computational in nature, with a particular focus towards exploring basic principles of importance for laboratory studies, especially in conjunction with the use of optimal control theory and its realization in closed-loop learning experiments. This research program involves a set of interrelated components aiming at developing a deeper understanding of quantum control and providing new algorithms to extend the laboratory control capabilities.

B. Research Progress

In the past year several projects were pursued and the results are summarized below.

1. **Revealing the factors contributing to the optimization complexity of controlling quantum phenomena[1]** It has been widely observed in optimal control simulations and experiments that state preparation is surprisingly easy to achieve, regardless of the dimension of the system Hilbert space. This work performed a large number of optimal control calculations for state preparation to assess the scaling of effort particularly in relation to the landscape features [7-12]. Importantly, the collective studies reveal essentially an invariant scaling of effort for reaching optimal yields, regardless of the system Hilbert space dimension. This dramatic behavior is directly connected with the topology of quantum control landscapes. Furthermore, it was found that the actual path length traversed in going from a trial control to its optimal form is typically only modestly larger than the Euclidean distance between the initial and final control. These collective results bode well for the future identification of successful quantum controls in the laboratory. The full implications of these findings for the most efficient execution of laboratory experiments will be pursued in the planned research ahead.
2. **Optimally controlled preparation of high fidelity quantum gates with suppression of decoherence[2-4]** Perhaps the most challenging goal for quantum control is its application to the creation of quantum gates for ultimate functional operation in quantum information sciences. The highest degree of gate fidelity is demanded including while fighting against decoherence phenomena. A series of optimal control simulations were carried out exploring this prospect, and a new computational technique was introduced to permit taking a homotopy excursion along a geodesic to reach the final target unitary transformation. By operating in this fashion, control fields were found that produced

gate transformations to machine precision. Although decoherence can mitigate such high yields, excellent degrees of control were attained in multiqubit systems.

3. **Advanced algorithms for performing quantum control experiments[5]** In the laboratory, virtually all of the adaptive feedback quantum control experiments operate with guidance from genetic algorithms (GA). Although these algorithms can be effective, in recent years a number of advanced evolutionary strategies (ES) have been developed particularly including with covariance matrix adaptation (CMA-ES). This work considered the latter algorithm in competition with standard GAs and other evolutionary strategies. Both simulations and laboratory experiments were carried out for this purpose on second harmonic generation and state preparation in Rb vapor. The CMA-ES algorithm was shown to be over an order of magnitude faster than previous techniques. Further research is planned to test this algorithm on other demanding quantum control applications.
4. **On the diversity of controls for achieving molecular alignment[6]** The laboratory attainment of molecular alignment is a subject of considerable interest as it can lead to well defined conditions for subsequent further manipulation of the aligned molecules. This work explored the diversity of controls that can achieve alignment for diatomic molecules as well as the effect of field constraints on the attainable level of alignment. It was found that optimized alignment yields can reach extremely high values even with severe field constraints being present. A variety of effective controls were identified along with the mechanisms through which they operate.
5. **The topology of quantum control landscapes[7-12]** The ultimate success of laboratory quantum control experiments depends critically on the relationship between the observable and the underlying control field. This relationship defines a quantum control landscape. Through a series of works we have been able to show that the underlying topology of quantum control landscapes is generic to all quantum systems, although the detailed nature of any successful control field sensitively depends on the system Hamiltonian and environmental interactions. The topological structure of quantum control landscapes has important implications for the practical ability to perform successful quantum control experiments. In this aspect of the research, a series of investigations were carried out exploring the landscapes for state-to-state transitions and general quantum observables as well as the landscapes for quantum systems interacting with an environment. The primary focus of these investigations was on identifying the so-called critical topology of the landscapes, which corresponds to revealing whether the landscape extrema are minima, maxima or saddles. Most striking, the broad conclusion from all of these studies is that quantum control landscapes inherently contain no false traps to impede adequately flexible control fields from taking the observable to its highest attainable value. These collective works reveal that any intermediate landscape critical points strictly correspond to saddles, which inherently cannot trap the controlled dynamics. A number of additional conclusions follow from the landscape analyses including the existence of multiple solutions at any elevation on the control landscape as

well as at the absolute maximum. The fundamental nature of these landscape features is receiving experimental attention for confirmation. The ensuing DOE research will perform advanced landscape analyses including for their implications for accelerating the search on effective quantum controls.

C. Future Plans

The research in the coming year will mainly focus on the fundamental nature of quantum control landscapes – the map between the control field and the laboratory observable. Understanding the properties of control landscapes provides the basis to (a) explain the success of emerging quantum control experiments and (b) predict future promising directions for the field. Previous studies have focused on constraint-free landscapes for state-to-state transitions and other observables. The general finding is that these landscapes are trap free, which is consistent with the relative ease of controlling broad classes of quantum phenomena. Many experiments achieve optimal control upon comparison of one observable value to another, and the experiments inevitably operate with various types of constraints placed on the controls. A careful study will be undertaken on the structure of control landscapes for multiple observables including in the presence of realistic laboratory constraints. Preliminary work on multi-observable control landscapes indicates the existence of very favorable topology, and the full nature of these structures will be investigated. Along with this mathematical analysis of the control landscape topologies, a practical means for taking excursions over these landscapes will be developed for purposes of simulation as well as ultimate transfer to the laboratory. The research will also seek out the nature of systematic rules for controlling quantum phenomena with photonic reagents in analogy with the existence of such rules when performing chemical transformations with ordinary reagents. The identification of systematic rules will be explored to seek control fields that produce similar outcomes when operating over homologous families of physical systems (Hamiltonians).

D. References

1. On the relationship between quantum control landscape structure and optimization complexity, K. Moore, M. Hsieh, and H. Rabitz, J. Chem. Phys., **128**, 154117 (2008).

2. Optimal control of quantum gates and suppression of decoherence in a system of interacting two-level particles, M. Grace, C. Brif, H. Rabitz, I. Walmsley, R. Kosut, D. Lidar, J. Phys. B-Atom. Mole. Opti. Phys. **40** S103-S125 (2007).

3. Fidelity of optimally controlled quantum gates with randomly coupled multiparticle environments, atthew D. Grace, Constantin Brif, Herschel Rabitz, Daniel A. Lidar, Ian A. Walmsley, and Robert L. Kosut, J. of Modern Optics, **54**, 2339 (2007).

4. Optimal control of high-fidelity quantum gates in the presence of decoherence, M. Grace, C. Brif, H. Rabitz, I. Walmsley, R. Kosut and D. Lidar, Phys. Rev. A, submitted 2008.

5. Performance analysis of derandomized evolution strategies in quantum control experiments, O. Shir, J. Roslund, T. Back and H. Rabitz (in preparation).

6. On the diversity of multiple optimal controls for quantum systems, O M Shir, V Beltrani, Th Bäck, H Rabitz and M J J Vrakking, J. Phys. B., **41**, 074021 (2008).

7. Topological and statistical properties of quantum control transition landscapes, Michael Hsieh, Rebing Wu, Carey Rosenthal and Herschel Rabitz, J. Phys. B., **41**, 074020 (2008).

8. Control landscapes for observable preparation with open quantum systems, Rebing Wu, Alexander Pechen, Herschel Rabitz, Michael Hsieh, and Benjamin Tsou, J. Math. Phys. **49**, 022108 (2008).

9. Control landscapes for two-level open quantum systems, Alexander Pechen, Dmitrii Prokhorenko, Rebing Wu and Herschel Rabitz, J. Phys. A: Math. Theor., **41**, 045205 (2008).

10. Characterization of the critical submanifolds in quantum ensemble control landscapes, R. B. Wu, H. Rabitz, and M. Hsieh, J. Phys. A: Math. Theor., **41**, 015006 (2008).

11. Exploring families of quantum controls for generating unitary transformations, J. Dominy and H. Rabitz, J. Phys. A, **41** ,205305 (2008).

12. Controllability of open quantum systems with Kraus-map dynamics, R. Wu, A. Pechen, C. Brif, H. Rabitz, J. Phys. A-Math. Theo. Phys., **40**, 5681-5693 (2007).

13. Controlling quantum dynamics regardless of laser beam spatial profile and molecular orientation, H. Rabitz and G. Turinici, Phys. Rev. A. **75**, 043409 (2007).

14. Foundations for cooperating with control noise in the manipulation of quantum dynamics, F. Shuang, H. Rabitz, M. Dykman, Phys. Rev. E, **75**, 021103 (2007).

15. Global analytical potential energy surfaces for $H_2(\tilde{X}^2A'')$ based on high-level ab initio calculations, D. Q. Xie, C. X. Xu, T.-S. Ho, H. Rabitz, et al., J. Chem. Phys., **126**, 074315 (2007).

16. The topology of optimally controlled quantum mechanical transition probability landscape, H. Rabitz, T.-S. Ho, M. Hsieh, B. Kosut, and M. Demiralp, Phys. Rev. A, **74**, 012721 (2006).

17. Optimal control landscapes for quantum observables, H. Rabitz, M. Hsieh, and C. Rosenthal, J. Chem. Phys. **124**, 204107 (2006)

18. Revealing the key variables and states in optimal control of quantum dynamics, M. Artamonov, T.-S. Ho, and H. Rabitz, Chem. Phys. Lett. **421**, 81 (2006).

19. Quantum optimal control of molecular isomerization in the presence of a competing dissociation channel, M. Artamonov, T.-S. Ho, and H. Rabitz, J. Chem. Phys. **124**, 064306 (2006)

Interactions of Cold Rydberg Atoms in a High-Magnetic-Field Atom Trap

G. Raithel, University of Michigan
4255 Randall Laboratory, Ann Arbor, MI 48109, e-mail: graithel@umich.edu

1 Program Scope

Highly magnetized, cold Rydberg-atom gases and magnetized plasmas are investigated. We use a particle trap that operates at magnetic fields up to 6 Tesla and that can simultaneously function as a ground-state atom trap, Rydberg-atom trap and nested Penning ion and electron trap. Ground-state atom clouds collected in the trap are laser-excited into clouds of magnetized Rydberg atoms or cold plasmas. The combination of low temperatures, strong magnetic fields, and substantial collision rates leads to a rich variety of atomic and plasma processes; these are the focus of this project. Our studies relate to the physics of atoms and plasmas in astrophysical environments, in magnetized man-made plasmas, in anti-hydrogen research, and in quantum information processing.

In studies of low-angular-momentum Rydberg atoms directly excited by high-resolution narrow-band lasers, we are interested in coherent single-atom dynamics and in coherent interactions in many-body Rydberg-atom systems. Coherent effects of the internal motion include spin oscillations of the Rydberg electron induced by spin-orbit coupling. Investigations of coherent interactions and correlations in cold, magnetized many-body Rydberg systems rely on spatially resolved Rydberg-atom detection, which is possible in the utilized setup. At higher Rydberg-atom or plasma densities, collisions and / or recombination lead to the formation of atoms in gyration-center states (=drift states), which exhibit distinct cyclotron, bounce and magnetron motions of the Rydberg electron. These drift-state atoms have large z-components of the angular momentum, high densities of states, long lifetimes, and are suitable for magnetic trapping. Using our recently demonstrated capability to magnetically trap such atoms, we intend to measure their properties. We further prepare cold plasmas in nested Penning traps by photo-ionization of trapped ground-state atoms, and study the coupled dynamics of the ion and electron components of these plasmas. Employing the capability of our apparatus to combine Rydberg-atom and Penning traps, we study Rydberg-atom-electron collisions and recombination in strong-magnetic-field environments.

2 Recent Work

2.1 Two-component plasma trap

One of the outstanding goals in the field of cold plasmas is to reach the regime of strong coupling for both the electronic and ionic components. A possible avenue to reach this goal will be the trapping of both plasma components in a strong magnetic field, which affords long confinement times and cyclotron cooling. In this work, cold, strongly magnetized two-component plasmas have been excited and confined in a Penning trap with a strong bias magnetic field [6]. The expansion of the plasmas is essentially one-dimensional, leading to confinement times of several milliseconds, which is one to two orders of magnitude longer than that in magnetic-field-free cold-plasma experiments conducted elsewhere. We further observe a modulation in the effective electron trapping potential, caused by space-charge oscillations of the ionic component. Measurements of the electron temperature reveal that the electron component undergoes significant cooling. The observed cooling rate is much faster than the cyclotron cooling rate. We have identified several possible causes for the electron cooling; this issue is still under investigation.

2.2 Recombination experiments

Studies of three-body recombination (TBR) in cold, magnetized plasmas are of fundamental interest and are relevant in ongoing efforts to form and trap anti-hydrogen. The decay of the recombined atoms is at the focus of current theoretical work elsewhere. To study recombination in cold, magnetized plasmas, we excite the plasmas in shallow two-component traps as discussed in Section 2.1. The bound-state Rydberg-atom population that forms via recombination is analyzed using state-selective electric-field ionization (FI). The FI pulse is applied at a variable delay time after plasma generation. The plasma trapping conditions are varied from closed and symmetric (blue curve in Fig. 1) to fully open (red curve). Recent results of recombination measurements are shown in Fig. 2. In the case of an open trap, the time window of overlap between ionic and electron components of the plasma is limited to several tens of μs. We observe considerable build-up of a recombination signal between 0 and 32 μs. The signal develops from the high-electric-field side, corresponding

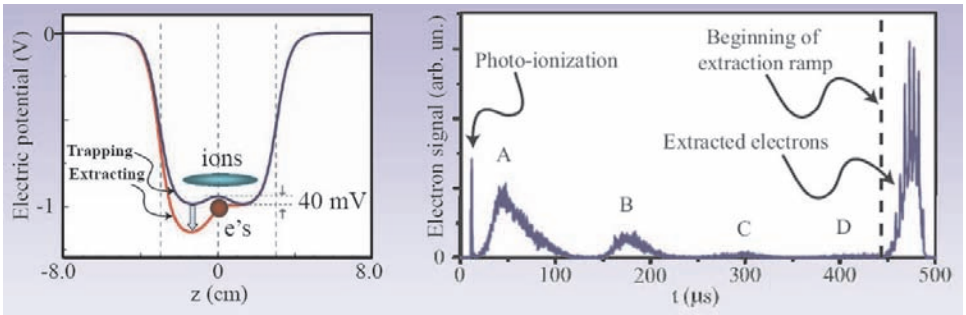

Figure 1: Left: Trapping potential (blue curve) along the magnetic-field axis. Electrons are trapped at the center, while ions are trapped in the wider double-well structure. The trap can be distorted (red curve) to extract and measure the electron component of the plasma. Right: Measured electron shake-off signal caused by coupled space-charge oscillations of the electron and ion components of the trapped plasma. The shake-off maxima (A-D) occur at the ion breathing-mode frequency. At 450 μs an electron extraction ramp is applied. The extracted electron signal at $t > 450$ μs is used to determine the electron temperature.

to deeply bound states, and gradually progresses towards the continuum. It appears that at short times any recombined atoms are mostly re-ionized due to ongoing electron-Rydberg-atom collisions. These collisions may also drive a fraction of the recombined atoms into lower-lying states that are de-coupled from further collision-induced dynamics because of small collision cross sections. Any low-lying atoms should rapidly decay into the ground state. As the electron density gradually drops, more recombined Rydberg atoms remain, culminating in a peak of about 15 detected Rydberg atoms per shot at 32 μs (lower left in Fig. 2). Due to detection inefficiencies, this number corresponds to an actual number of about 200 Rydberg atoms, corresponding to about 1% of the initially ionized atoms. The Rydberg atom yield may be higher, as we only detect Rydberg atoms with binding energies less than about $hc \times 80$ cm^{-1}. At times after 32 μs, all electrons have been extracted from the plasma, and the Rydberg atom population gradually decays (mostly due to electromagnetic decay). Atoms close to the ionization limit decay more slowly, leading to a gradual increase of the relative fraction of loosely bound Rydberg atoms divided by the total Rydberg-atom number.

In closed traps (right column in Fig. 2), we observe very small numbers of recombined Rydberg atoms. The few atoms that are detected have rather high binding energies. These observations are consistent with re-ionization and / or collisional de-excitation of recombined Rydberg atoms due to the persistently dense electron component of the plasma. In closed traps, the small observed Rydberg-atom component increases over the whole investigated range of the delay time (256 μs in Fig. 2). This is attributed to partial separation of the electron and ion components of the plasma in the nested Penning trap, which occurs on a time scale on the order of the ion breathing-mode period (100 μs in Fig. 1). Partially open traps exhibit a recombination behavior that is in-between the extreme cases of fully closed and open traps, as expected (see middle column in Fig. 2). In the near future, it is planned to quantitatively compare these and other data with theory.

2.3 High resolution spectroscopy

We have recently observed Landau quantization effects in the photo-, auto- and field-ionization behavior of magnetized Rydberg atoms [3]. The observed phenomena include multiple ionization potentials, meta-stable states embedded in the continuum, and indications of coherent spin oscillations caused by spin-orbit coupling. To study the excitation spectra, the decay and field ionization behavior, coherent spin-flip dynamics, and electric multi-pole interactions of magnetized Rydberg atoms prepared in individual quantum states, we have recently installed a narrow-linewidth Rydberg excitation laser (wavelength $\sim$ 480 nm, linewidth several MHz). To perform controlled high-resolution scans, a new pressure-tuned, temperature-stabilized Fabry-Perot interferometer has been built. To perform a scan, the laser is locked to the Fabry-Perot while the pressure inside the Fabry-Perot is scanned in a well-defined manner. In Fig. 3 we show first results obtained with this system.

Atoms are excited in a two-step process from 5S via 5P into diamagnetic Rydberg levels using coincident laser pulse of about 5 μs duration. The lower-transition pulse is on-resonant with the $5S_{1/2}$ $|m_J = 1/2\rangle \rightarrow$ $5P_{3/2}$ $|m_J = 3/2\rangle$ transition (wavelength 780 nm), while the upper-transition pulse (wavelength $\approx$ 480 nm)

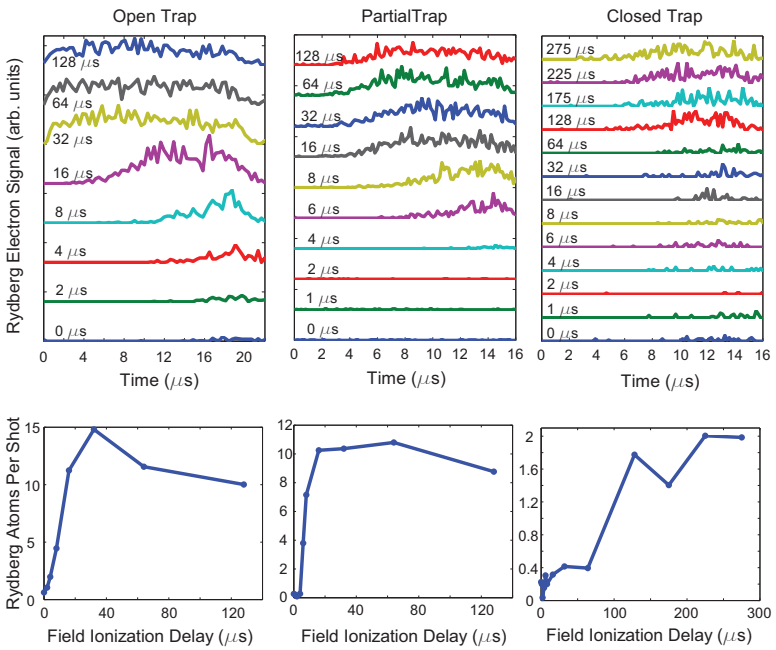

Figure 2: Top row: Bound-state field ionization signal for the indicated values of the delay time between plasma excitation and application of the field ionization ramp. The ionization electric field increases linearly from zero to about 200 V/cm over the time interval displayed on the time-axes. Bottom row: Number of recombined atoms per shot vs delay time, obtained by integrating the traces shown in the top row. The electron trap conditions range from symmetric and closed (left column) through partially closed (middle column) to entirely open (right column). The number of initially generated electron/ion pairs is of order 10^4.

is scanned in frequency. We record field ionization (FI) traces as a function of the frequency of the upper-transition laser and plot the results in two-dimensional false-color plots. An example of such a plot is shown in the upper left of Fig. 3. There, the frequency is varied over several hundred MHz, and the Rydberg FI signal is shown over a time interval in which the electric field of the FI pulse rises linearly from about 10 V/cm to 40 V/cm. Typically, at fixed frequency the FI signal exhibits peaks at several values of the FI electric field (two in the upper left plot in Fig. 3). These fields correspond to different orbital and spin magnetic quantum numbers m and m_s of the Rydberg electron. The quantum numbers corresponding to the strongest FI peak follow from the selection rules for the laser excitation from the intermediate 5P state, while the less strong FI peaks result from mixing due to spin-orbit coupling and m-mixing (which results from stray electric fields and possibly atom-atom interaction). The integrals of the FI-traces yield the total Rydberg atom number as a function of laser frequency (*i.e.* an ordinary "spectral line"). Typically, individual spectral lines exhibit an asymmetric structure that is due to the magnetic dipole moment of the excited Rydberg state and the magnetic-field inhomogeneity in the trap (see upper left in Fig. 3). At an energy of about -18 cm^{-1} relative to the field-free ionization energy, longer scans reveal diamagnetic Rydberg lines at a density of about 1 per GHz, as seen in the lower panel of Fig. 3. For most of these lines, we have obtained two-dimensional false-color plots analogous to the one shown in Fig. 3. A complete analysis of these plots is in progress.

Diamagnetic Rydberg states have substantial electric-quadrupole moments. The resultant electrostatic interaction between nearby Rydberg atoms is expected to cause excitation saturation effects. Measuring the number of Rydberg counts vs power of the excitation laser for a diamagnetic Rydberg state, we observe a clear saturation trend (upper-right plot in Fig. 3). This data may be the first observation of a quadrupole Rydberg excitation blockade.

3 Plans

Recombination of strongly magnetized, cold plasmas into Rydberg atoms will be investigated in more detail. The measured quantities will include state distributions and recombination rates, magnetic moments of the

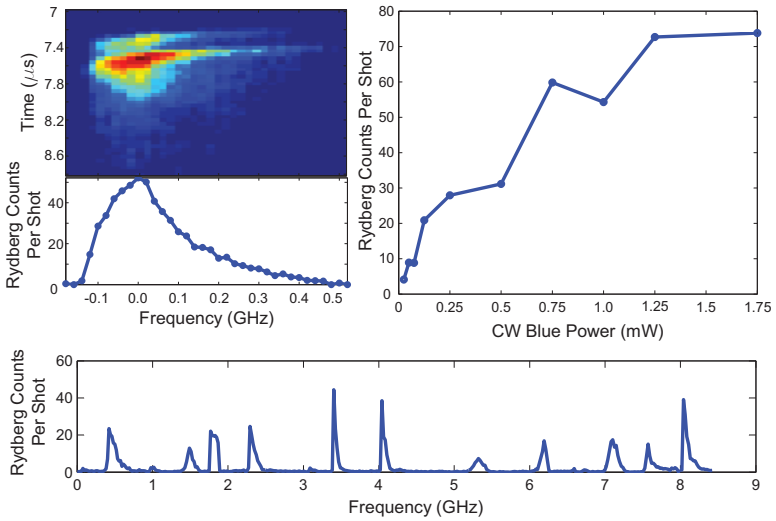

Figure 3: Upper left: Diamagnetic Rydberg line at B=2.8 T and energy -18.4 cm^{-1} vs the frequency offset of the excitation laser. The false-color field ionization plot is explained in the text. Upper right: Peak count on the Rydberg line vs power of the blue excitation beam. The data exhibit a clear saturation trend. Bottom: Rydberg excitation spectrum starting at -17.6 cm^{-1} vs frequency offset of the excitation laser.

recombined Rydberg atoms, the fraction of recombined Rydberg atoms that can be magnetically trapped, and the fraction of recombined atoms that decay into a magnetically trapped ground-state. Experimental results will be compared with theory (Robicheaux et al., Pohl et al.). We will continue high-resolution spectroscopy and studies of coherent dynamics of laser-excited, highly magnetized Rydberg atoms. The internal degrees of freedom of these atoms are coupled through non-adiabatic mixing, spin-orbit coupling and electric-field-induced m-mixing, leading to interesting coherent **single-atom** dynamics. Specifically, coherent spin oscillations of the Rydberg electron induced by spin-orbit coupling are investigated. In high-resolution studies of **many-body** Rydberg systems, coherent electrostatic interactions of two or more magnetized Rydberg atoms will be investigated. Topics of interest include interaction-induced excitation saturation, spatial correlations between Rydberg excitations, and quantum excitation hopping in cold atom ensembles. Further, the currently employed Penning trap will be upgraded with an improved electrode insert. The improvements will lead to a higher intrinsic plasma confinement time, which will be sufficiently long to take advantage of cyclotron cooling of electrons and sympathetic cooling of ions.

4 Recent Papers

[1] "Laser cooling and magnetic trapping at several Tesla," J. R. Guest, J.-H. Choi, E. Hansis, A. P. Povilus and G. Raithel, Phys. Rev. Lett. **94**, 073003 (2005).
[2] "Coherent population transfer of ground-state atoms into Rydberg states", T. Cubel, B. K. Teo, V. S. Malinovsky, J. R. Guest, A. Reinhard, B. Knuffman, P. R. Berman, and G. Raithel Phys. Rev. **A 72**, 023405 (2005).
[3] "Time dependence and Landau quantization in the ionization of cold, magnetized Ryberg atoms," J.-H. Choi, J. R. Guest, E. Hansis, A. P. Povilus, and G. Raithel, Phys. Rev. Lett. **95**, 253005 (2005).
[4] "Magnetic trapping of long-lived cold Rydberg atoms," J.-H. Choi, J. R. Guest, A. P. Povilus, E. Hansis, and G. Raithel, Phys. Rev. Lett. **95**, 243001 (2005).
[5] "Magnetic Trapping of Strongly-Magnetized Rydberg Atoms," J.-H. Choi, J. R. Guest, G. Raithel, European Physics Journal **D 40**, 19 (2006).
[6] "Trapping and evolution dynamics of ultracold two-component plasmas," J.-H. Choi, B. Knuffman, X. Zhang, A. P. Povilus, and G. Raithel, Phys. Rev. Lett., (2008).
[7] "Cold Rydberg Atoms," (*Book article*) J.-H. Choi, B. Knuffman, T. Cubel Liebisch, A. Reinhard, G. Raithel, in Advances in Atomic, Molecular and Optical Physics vol. 54, p. 131-202, eds. E. Arimondo and P. Berman (Elsevier, 2007).

Dual Quantum Gases of Bosons: From Atomic Mixtures to Heteronuclear Molecules

Principal Investigator:

Dr. Chandra Raman
Associate Professor
School of Physics
Georgia Institute of Technology Atlanta, GA 30332-0430
craman@gatech.edu

Program Scope:

This program centers on creating a dual species atomic Bose-Einstein condensate of ^{23}Na and ^{87}Rb. The eventual goal is to synthesize heteronuclear molecules of the two species. Our approach takes advantage of the large trapped atom number technology available for Na atoms using a Zeeman slower and a dark MOT to sympathetically cool a relatively smaller sample of Rb. Molecules will be created in the vicinity of a Feshbach resonance (see PRA 72, 062505 (2005) for some recent predictions). A future thrust of the molecular effort will be to create a dipolar superfluid, a novel strongly correlated quantum system.

Each atomic mixture is unique. Measurement of the Na-Rb interatomic potentials is necessary to predict all properties of the mixture. Locating Feshbach resonances will be of key importance in this regard, as one can identify the bound states of the interatomic potentials. The Na-Rb system is versatile, as both ^{87}Rb-Na and ^{85}Rb-Na mixtures can be explored, each with their own distinctive properties.

Recent Progress:

- **New apparatus.** A new atomic beam apparatus for the study of trapped ultracold sodium-rubidium mixtures has come online in the past 12 months. The machine incorporates a single atomic beam containing both species Na and Rb, dual species Zeeman slowing magnets and a quartz vacuum cell in ultra-high vacuum conditions for good optical access to the two species. In addition, we have implemented a new magnetic trap with separate coils that will allow us to search for Feshbach resonances at magnetic bias fields up to 1 kiloGauss.

- **Dual species magnetic trapping.** We have achieved the first magnetic trapping of Na-Rb atomic mixtures. Atoms were loaded from a dual MOT (magneto-optical trap). When loaded separately, we obtained 10^9 Na and 10^8 Rb atoms in the quadrupole magnetic trap, both in the hyperfine state F=1, M_F = -1. In addition, we have demonstrated species-selective evaporation of Na atoms (the coolant) from our magnetic trap by driving the Na hyperfine transition near 1.77 GHz. Experiments are ongoing to optimize the loading sequence to initiate evaporative cooling.

Ultrafast X-Ray Coherent Control*

D. A. Reis†

Department of Physics, University of Michigan, 450 Church Street, Ann Arbor, MI 48109-1040. 734-763-9649, dreis@umich.edu

P. H. Bucksbaum

PULSE Center and Department of Physics, Applied Physics, Photon Science, Stanford University, 2575 Sand Hill Rd, Menlo Park, California 94025. 650-926-5337. phb@slac.stanford.edu

This is a program to develop ultrafast x-ray physics using accelerator-based sources. The research currently is carried out primarily at the Advanced Photon Source (APS) sector 7; and is expected to extend to the Linac Coherent Light Source (LCLS). Our research centers on atomic-scale dynamics in AMO and CM physics and builds upon our earlier successes at the APS and SPPS to develop the ultrafast physics and techniques and the associated work on extending the capabilities of existing short pulse 3rd generation facilities, such as the proposed picosecond upgrade to sector 7 and the be prepared to perform world class science using the unprecedented characteristics of the LCLS.

Recent Progress

A. Impulsive softening and Debye Waller Model of ultrafast melting

Intense ultrafst laser excitation can alter the interatomic forces on a time-scale that is short compared to ionic motion. At the SPPS, we used ultrafast diffraction to study two regimes: 1. ultrafast disordering in semiconductors (solid-liquid) (4; 9; 13; 14) and 2. measurement of the excited state potential in bismuth which undergoes softening of bonds and shift in the equilibrium position as it is driven towards a solid-solid transition (10). In Hillyard, Reis and Gaffney (9), we compared density functional perturbation theory calculations (similar to those performed on bismuth in collaboration with the Stephen Fahy under NSF support) of photoexcited InSb with a new formalism that takes into account phonon squeezing to more accurately model the dissordering process, which appears to occur on the sub-picosecond time-scale(14). Interestingly, the results predict that the lattice will first go unstable at the X-point unlike Si which goes unstable at the L-point. It also shows that while powerful, diffraction on its own is not sufficient to identify which modes go unstable and where. For that we propose x-ray diffuse scattering from the nonthermal phonon population using the LCLS for femtosecond studies (and APS for long-time dynamics).

B. X-ray diffuse scattering of nucleation dynamics at SPPS

In the final experiment [Lindenberg et. al., (4)] from the SPPS collaboration, studies on ultrafast disordering in semiconductors (9; 13; 14)were extended to view the early stages of

* Grant Number: DE-FG02-00ER1503

† Principal Investigator

the nonequlibrium liquid state and nucleation process during ablation. These experiments made use of femtosecond pulses from SPPS to perform time-resolved small and wide angle x-ray scattering to probe the formation of nanoscale voids as well as the onset of the pair distribution function, over picoseconds to hundreds of nanoseconds. In the future the use of coherent x-ray scattering from LCLS could allow a much more detailed study of the nucleation process as well as provide substantially more x-rays for probing the non-periodic structure with much better signal to noise. This will be especially important for our studies of nonequilibrium phonon dynamics that we are proposing at the LCLS. We point out that these experiments also made use of our earlier electrooptic sampling technique for timing information for the shortest delay times, where random jitter between the laser and x-ray would otherwise smear out our temporal resolution (10; 15).

C. X-ray probing of Unfolded Phonons

The generation and detection of monochromatic acoustic vibrations (phonons) with nanometer wavelength is of fundamental interest to a wide range of problems in solid state physics ranging from nanoscale heat transport between dissimilar materials to metrology. Long wavelength coherent THz phonons can be generated in artificial superlattices (SL) excited by a femtosecond laser pulse. These phonons, known as folded phonons because the added periodicity of the SL folds the phonon dispersion into a smaller Brillouin zone, can unfold into short wavelength modes upon transmission into the bulk. In Trigo et al., (1), we use the picosecond x rays a the APS to probe the unfolding process in real time as sidebands develop on the an x-ray diffraction peak of the underlying bulk substrate. In this case x-rays are required to detect the bulk modes because the much longer wavelength of the optical radiation makes it blind to the atomic motion. While the x-ray pulse is long compared to a single oscillation period, we nonetheless can detect the phonons through stimulated x-ray Brillouin scattering not as an energy shift, but instead through the momentum transfer imparted to the diffracting x rays. We compare our results with dynamical diffraction simulations of propagating strain which supports this interpretation. In the future, coherent control can be utilized to switch on and off the folded modes, resulting in a specifically tailored acoustic wavepacket being launched into the bulk, or as a means of controlling the x-ray diffraction process to generate a short picosecond switch.

D. Time-resolved x-ray diffraction study of thermal transport across a semiconductor heterostructure

We also utilized time-resolved diffraction at s7 of the APS to study thermal transport in an AlGaAs/GaAs heterostructure(2). This work is a continuation of our work on coherent acoustic pulse propagation (16) except that now we are interested in the propagation of incoherent phonons (heat). In this case, the x rays act as independent and noncontact thermometers of the film and substrate. Even though the two materials are exquisitely lattice matched, the high resolution of the APS allow us to follow minute changes in the temperature of the two materials and upon comparing our results with dynamical diffraction simulations, we are able to extract the thermal conductivity of the film. In materials where a less good interface is present, this technique can also be used to measure the thermal boundary resistance.

E. Molecular alignment towards LCLS

In collaboration with the PULSE Institute at SLAC, we are currently investigating methods to coherently align molecules for x-ray targets. We have begun to plan to use these targets for LCLS high field or time-resolved x-ray scattering work. There are two different results to report in this area. We investigated impulsive laser alignment of molecular iodine at a density of $\sim 10^{18}$ molecules/cm^3, i.e. high enough column densities for elastic scattering experiments at LCLS. Such coherent rotational ensembles maintain alignment for on the order of 0.5ps, which is enough for studies of photo-induced vibration or dissociation. We have also performed x-ray studies at SSRL of the iodine cation trimer I_3^- in solution or in a polymer matrix. In the latter case we can align the trimer by stretching the polymer, and this could be a very interesting method for producing aligned molecules at LCLS.

Future Plans

The sensitivity of time-resolved x-ray scattering has the potential to provide information about the full spectrum of vibrational modes in the excited state of the crystal, with atomic-scale resolution on the time-scale of the fastest processes in solids and molecules. In the near future, we will study the full spectrum of coherent unfolded modes generated in superlattices to study the dynamics of the high wavevector bulk unfolded modes. We are also working on a manuscript which generalizes the diffraction model in the presence of squeezed modes to x-ray diffuse scattering (an important step in our analysis of future experiments). While we do not have a source powerful enough to do the experiments on femtosecond dynamics, we are working on experiments at 100 picosecond resolution near various solid-solid phase transitions. Optical studies on carrier dynamics in photoexcited bismuth have been completed and are writing up the results. These studies are complementary to the structural information that we obtain from x-ray diffraction and are critically important in understanding the electron-phonon coupling mechanisms at high photoexcited densities. We are also designing a unique laboratory based x-ray source that will provide few picosecond x-rays at MHz repetition rate to meet the growing needs of near-equilbrium condensed matter experiments at the atomic scale and complement our existing studies.

Recent Publications

[1] M. Trigo, Y. M. Sheu, D. A. Arms, J. Chen, S. Ghimire, R. S. Goldman, E. Landahl, R. Merlin, E. Peterson, M. Reason, and D. A. Reis. Probing unfolded acoustic phonons with x rays. *Physical Review Letters*, 101(2):025505, 2008.

[2] Y. M. Sheu, S. H. Lee, J. K. Wahlstrand, D. A. Walko, E. C. Landahl, D. A. Arms, M. Reason, R. S. Goldman, and D. A. Reis. Thermal transport in a semiconductor heterostructure, measured by time-resolved x-ray diffraction. *In press, PRB*, 78(4), 2008.

[3] P. B. Hillyard, D. A. Reis, and K. J. Gaffney. Carrier-induced disordering dynamics in insb studied with density functional perturbation theory. *Physical Review B (Condensed Matter and Materials Physics)*, 77(19):195213, 2008.

[4] A. M. Lindenberg, S. Engemann, K. J. Gaffney, K. Sokolowski-Tinten, J. Larsson, et al., X-ray diffuse scattering measurements of nucleation dynamics at femtosecond resolution. *Physical Review Letters*, 100(13):135502, 2008.

[5] D.W. Broege, R.N. Coffee, and P.H. Bucksbaum, , Strong-field impulsive alignment in the presence of high temperatures and large centrifugal distortion *Phys. Rev. A, in review*, 2008.

[6] D. W. Broege, R. N. Coffee, P. H. Bucksbaum, Impulsive Alignment of Hot, Centrifugally Distorted Molecules, *CLEO Abstract CWA4*, 2008.

[7] D. Broege, R. Coffee, P. Bucksbaum, Strong field impulsive alignment in the presence of high temperatures and large centrifugal distortion, *Bull. Am. Phys. Soc. 53, No. 7, DAMOP Abstract: K6.00004*, 2008.

[8] D. A. Reis and A. M. Lindenberg. Ultrafast x-ray scattering in solids. In M. Cardona and R. Merlin, editors, *Light Scattering in Solids IX, Topics in Applied Physics*, volume 108, pages 371–422. Springer, 2007.

[9] P. B. Hillyard, K. J. Gaffney, A. M. Lindenberg, S. Engemann, R. A. Akre, et al., Carrier-density-dependent lattice stability in InSb. *Physical Review Letters*, 98(12):125501, 2007.

[10] D. M. Fritz, D. A. Reis, B. Adams, R. A. Akre, J. Arthur, et al., Ultrafast bond softening in bismuth: Mapping a solid's interatomic potential with x-rays. *Science*, 315:633–636, February 2 2007.

[11] D. A. Reis, K. J. Gaffney, G. H. Gilmer, and B. Torralva. Ultrafast dynamics of laser-excited solids. *MRS bulletin*, 31:601–606, 2006.

[12] B. Lings, J. S. Wark, M. F. DeCamp, D. A. Reis, and S. Fahy. Simulations of time-resolved x-ray diffraction in laue geometry. *J. Phys.: Condens. Matter*, 18:9231–9244, 2006.

[13] K. J. Gaffney, A. M. Lindenberg, J. Larsson, K. Sokolowski-Tinten, C. Blome, et al., Observation of structural anisotropy and the onset of liquidlike motion during the nonthermal melting of InSb. *Physical Review Letters*, 95(12):125701, 2005.

[14] A. M. Lindenberg, J. Larsson, K. Sokolowski-Tinten, K. J. Gaffney, C. Blome, et al., Atomic-scale visualization of inertial dynamics. *Science*, 308:392–395, 2005.

[15] A. L. Cavalieri, D. M. Fritz, S. H. Lee, P. H. Bucksbaum, D. A. Reis, et al., Clocking femtosecond x-rays. *Phys. Rev. Lett.*, 94:114801, 2005.

[16] S. H. Lee, A. L. Cavalieri, D. M. Fritz, M. C. Swan, R. S. Hegde, M. Reason, R. S. Goldman, and D. A. Reis. Generation and propagation of a picosecond acoustic pulse at a buried interface: Time-resolved x-ray diffraction measurements. *Phys. Rev. Lett.*, 95(24):246104, 2005.

[17] M. F. DeCamp, D. A. Reis, D. M. Fritz, P. H. Bucksbaum, E. M. Dufresne, and R. Clarke. X-ray synchrotron studies of ultrafast cyrstalline dynamics. *J. Synch. Rad.*, 12:177–192, 2005.

"Coherent and Incoherent Evolution of Rydberg Atoms"

F. Robicheaux
Auburn University, Department of Physics, 206 Allison Lab, Auburn AL 36849
(robicfj@auburn.edu)

Program Scope

This theory project focuses on the time evolution of Rydberg states. This study is divided into three categories: (1) coherent evolution of highly excited quantum states, (2) incoherent evolution of highly excited quantum states, and (3) the interplay between ultra-cold plasmas and Rydberg atoms. Some of the techniques we developed have been used to study collision processes in ions, atoms and molecules. In particular, we have studied the correlation between two (or more) continuum electrons.

Recent Progress 2007-2008

Photon-atom processes in strong magnetic fields: We studied how the radiative recombination changes in a strong magnetic field.[20] The only previous studies of RR in a strong magnetic field relied on classical estimates. We found that this process is equivalent to the radiative decay rate from positive energy states of a confined atom. Using this formulation, we studied the temperature and magnetic field dependence of RR. We found that the rate was changed only if the energy spacing of the Landau levels was larger than k_BT. When this condition is satisfied, the rate tends to increase with increasing magnetic field strength. The enhancement was mainly for recombination into Rydberg states; unlike the B=0 situation, most of the recombination was into weakly bound states.

Fluorescence as a probe of Ultracold plasmas: In a joint study with Bergeson's experimental group, we studied the fluorescence from an ultracold plasma.[19] The experiment was able to measure the time dependence of light emitted by the plasma. This gives a probe of the time dependence of the atom distribution because the light was from deeply bound states which can only be reached after three body recombination and several collisions between free electrons and Rydberg atoms. We found that a peculiarity of the Ca spectrum (a perturbation in the 4snd series) allowed a probe of weakly bound states as well. We were able to use this to study how the three body recombination develops on time scales less than 1 microsecond. For the lowest temperatures studied, we found a different scaling of the recombination rate with density: the fluorescence rate scaled as density^2 instead of the predicted density^3.

Transitions through a chaotic sea: A recent experiment by T. Gallagher's group showed that it is possible to drive a 10 photon transition in Rydberg states without any of the intermediate photons being resonant. We performed classical and quantum calculations of this system to understand how this process works.[21] Gallagher explained their results as arising from a sequence of avoided crossings. Our quantum calculations were able to reproduce the measurements. Surprisingly, the classical calculations also could reproduce the measurements. The classical mechanism for the transition was an expansion of the chaotic sea to encompass the

starting region of phase space; the surprise was that this mechanism could deliver the electron to a small range of n-states which is possible due to the stickiness of the edge the chaotic regions. Also, we found that the development of the angular momenta strongly depended on the duration of the pulse.

Correlation in electron ejection: In a joint study with an experimental project led by A. Landers, we studied the interaction between a pair of electrons ejected from a Ne atom.[22] In this study, a photon is absorbed by a 1s electron giving a free electron with excess energy of order 1 eV. An Auger process occurs a short time later which gives an outgoing electron with approximately 800 eV. We performed a classical Monte Carlo simulation of this process and were able to successfully describe the energy shift of the slow electron due to the Auger process. Also, we could qualitatively reproduce the angular distribution of the ejected electrons, including a lack of electrons going out in the same direction. However, there was a clear feature in the calculation when the electrons have nearly the same outgoing angle that was not present in the experiment. This feature seems to indicate an unexpected (and currently unexplained) correlation in the ejection angle of the two electrons.

Molecules: Some of the techniques we developed for highly excited atoms can be used to investigate processes in molecules. In Ref. [15], we extended the distorted wave method to compute the electron impact ionization of molecules and obtained results for H_2 and N_2; this perturbative method is crucial for our implementation of the non-perturbative calculations. In Ref. [17], we investigated the double ionization of H_2 molecules by a single photon. In particular, we were interested in how the triple differential cross sections which characterize the energy and direction dependence of the outgoing electron pair evolves with time after the photon is absorbed. In Ref. [18], we computed the 2 photon, double ionization of H_2 by 30 eV photons. We found some similarity with He but also effects specific to molecules. In particular, we found that the cross section strongly varied with the KE released to the protons if the photon polarization is parallel to the internuclear axis but not if it is perpendicular.

Three electron continua: Over the past decade we have performed many calculations of processes involving two electron escape from an atom/ion. The computational tool has been the direct solution of the time dependent Schrodinger equation. We recently extended the calculations to three electrons escaping an atom, but the method was restricted in energy. By extending this technique, we were able to compute the electron impact double ionization of He for energies up to and beyond the peak of the cross section.[16]

Finally, this program has several projects that are strongly numerical but only require knowledge of classical mechanics. This combination is ideal for starting undergraduates on publication quality research. Since 2004, seven undergraduates have participated in this program. Daniel Phalen completed the quantum scattering calculation of Ref. [1] during the summer of 2004. Chris Norton and Michael Wall completed the double charge exchange calculation[3] during spring of 2005; MW later completed a time dependent quantum calculation for a different grant. Michael Wall was one of 5 undergraduates invited to give a talk on their research at the

undergraduate session of the DAMOP 2006 meeting. Michelle Zhang and Christine Taylor completed a project to simulate the motion of an anti-hydrogen atom interacting with the complicated magnetic fields in the proposed anti-hydrogen traps in order to test ideas about measuring whether or not the anti-hydrogen atoms are trapped[9]. Jennifer Hurt and Patrick Carpenter carried out calculations of the scattering of positrons from antiprotons. In addition to these undergraduates, this grant supported the investigations of Turker Topcu who was a graduate student (Ph.D. 8/2007); he completed the investigation of radiative cascade in strong B[6], the component of Ref. [4] related to model double photoionization near threshold, model quantum calculations of electron impact ionization of Rydberg atoms (n~25)[10], the calculation of the time dependent escape of Rydberg electrons in parallel electric and magnetic fields[14], and is currently studying the effect of near resonant microwaves on highly excited states.

Future Plans

Ultra-cold plasmas The recent collaboration with Bergeson's group has raised some interesting questions about the early time evolution of ultracold plasmas. In particular, we plan to study the evolution of the components of the plasmas at very early times.

Anti-hydrogen motivated calculations The next generation of anti-hydrogen experiments are aimed at trapping the anti-hydrogen. To address possible issues, we will investigate processes that arise from this goal. In particular, we plan to: (1) develop a program to compute the spin flip of the positron during a radiative cascade in magnetic field and (2) study the three body recombination rate when all of the particles have the same mass.

Coherent evolution Motivated by the collaboration with Landers, we will devote substantial time to the interaction between two free electrons or the interaction between a free electron and a Rydberg atom. This was the most speculative aspect of the proposal and the last major component of the original proposal that hasn't been investigated.

DOE Supported Publications (7/2005-7/2008)

[1] D.J. Phalen, M.S. Pindzola, and F. Robicheaux, Phys. Rev. A **72,** 022720 (2005).
[2] M.S. Pindzola, F. Robicheaux, and J. Colgan, J. Phys. B **38**, L285 (2005).
[3] M.L. Wall, C.S. Norton, and F. Robicheaux, Phys. Rev. A **72**, 052702 (2005).
[4] U. Kleiman, T. Topcu, M.S. Pindzola, and F. Robicheaux, J. Phys. B **39**, L61 (2006).
[5] F. Robicheaux, Phys. Rev. A **73**, 033401 (2006).
[6] T. Topcu and F. Robicheaux, Phys. Rev. A **73**, 043405 (2006).
[7] M.S. Pindzola, F. Robicheaux, S.D. Loch, and J.P. Colgan, Phys. Rev. A **73**, 052706 (2006).
[8] A. Wetzels, A. Gurtler, L.D. Noordam, and F. Robicheaux, Phys. Rev. A **73**, 062507 (2006).
[9] C.L. Taylor, Jingjing Zhang, and F. Robicheaux, J. Phys. B **39**, 4945 (2006).

[10] T. Topcu, M.S. Pindzola, C.P. Balance, D.C. Griffin, and F. Robicheaux, Phys. Rev. A **74**, 062708 (2006).
[11] F. Robicheaux, J. Phys. B **40**, 271 (2007).
[12] M.S. Pindzola, F. Robicheaux, S.D. Loch, J.C. Berengut, T. Topcu, J. Colgan, M. Foster, D.C. Griffin, C.P. Balance, D.R. Schultz, T. Minami, N.R. Badnell, M.C. Witthoeft, D.R. Plante, D. M. Mitnik, J.A. Ludlow, and U. Kleiman, J. Phys. B **40**, R39 (2007).
[13] J. Colgan, M.S. Pindzola, and F. Robicheaux, Phys. Rev. Lett. **98**, 153001 (2007).
[14] T. Topcu and F. Robicheaux, J. Phys. B **40**, 1925 (2007).
[15] M. S. Pindzola, F. Robicheaux, J. Colgan, and C. P. Balance, Phys. Rev. A **76**, 012714 (2007).
[16] M. S. Pindzola, F. Robicheaux, and J. Colgan, Phys. Rev. A **76**, 024704 (2007).
[17] J. Colgan, M. Foster, M. S. Pindzola, and F. Robicheaux, J. Phys. B **40**, 4391 (2007).
[18] J. Colgan, M. S. Pindzola, and F. Robicheaux, J. Phys. B **41**, 121002 (2008).
[19] S.D. Bergeson and F. Robicheaux, "Recombination Fluorescence in Ultracold Neutral Plasmas," submitted Phys. Rev. Lett. (2008).
[20] F. Robicheaux, "Atomic Processes in Antihydrogen Experiments: A Theoretical and Computational Perspective," submitted to J. Phys. B (2008).
[21] T. Topcu and F. Robicheaux, "Driving Transitions through a chaotic sea" in preparation
[22] A.L. Landers, F. Robicheaux, T. Jahnke, M. Schoffler, T. Osipov, J. Titze, S.Y. Lee, H. Adaniya, M. Hertlein, P. Ranitovic, I. Bocharova, D. Akoury, A. Bhandary, Th. Weber, M.H. Prior, C.L. Cocke, R. Dorner, and A. Belkacem, "Angular Correlation Between Photo- and Auger Electrons from K-Shell Ionization of Neon," submitted Phys. Rev. Lett. (2008).

High Brightness Table-top Sources of Coherent Soft X-Ray Light

Jorge J. Rocca,
Electrical and Computer Eng Department, Colorado State University, Fort Collins, CO 80523-1373
rocca@engr.colostate.edu
Henry C. Kapteyn
JILA/Physics Department, University of Colorado, Boulder, CO 80309-0440
kapteyn@jila.colorado.edu

Program description

This project is exploring the use of a pre-ionized medium created by a compact capillary discharge to guide high intensity laser light over increased distances and extend the cutoff photon energy for high-order harmonic generation (HHG). The discharge reduces ionization-induced defocusing of the driving laser and ionization energy loss. We have extended harmonic emission from Xe up to an unprecedented photon energy of 160 eV [1], and observed photons with energies up to 170 eV from Kr, and 275 eV from Ar [5]. The discharge plasma also provided means to spectrally tune the harmonics by tailoring the initial level of ionization of the medium. We have also employed the complementary technique of using longer wavelength driving light at 1.3 μm to extend full phase matching of high harmonic generation in Ar and Ne to 100 and 200 eV respectively, well beyond the phase-matching limit for 0.8 μm [7]. This opens the possibility of combining these techniques with new phase matching schemes in capillary discharge plasmas to generate significantly increased harmonic flux for applications experiments at much higher photon energies than are currently accessible (100 eV- keV).

In related work we have seeded soft x-ray laser plasma amplifiers with high harmonic pulses to create a fundamentally new regime for the generation of essentially fully coherent short soft x-ray laser pulses with pulsewidths that are governed by the amplifier bandwidth and are independent of the gain duration. We have recently measured that the soft x-ray laser pulses generated by this technique are the shortest soft x-ray pulse duration demonstrated to date from a plasma amplifier [9].

High harmonic generation from ions in a capillary discharge

The highest photon energy that can be produced through HHG is predicted by the cutoff rule to be $h\nu_{max} = I_p + 3.2U_p$, where I_p is the ionization potential of the gas and $U_p \propto I \lambda^2$ is the quiver energy of the liberated electron. In principle, with long wavelength or high field lasers, $h\nu_{max}$ may be as high as 6 keV before relativistic effects suppress rescattering and HHG. To date however, for many experiments the highest harmonic photon energies observed have not been limited by the available laser intensity, but rather by the ionization of the nonlinear medium by the driving laser. The electron density from photoionization refractively defocuses the driving laser, reducing the peak laser intensity and consequently the highest harmonic photon energy observed. Moreover, the loss of the laser energy due to photoionization limits the length in the medium over which a high peak intensity can be maintained. To overcome these limitations, we are investigating the use of a capillary discharge plasma waveguide to create a preformed plasma with a tailored level of ionization. This makes it possible to generate higher photon energies from ionization of ions with correspondingly higher I_p. Additionally, the concave radial electron density profile of the capillary discharge plasma produces an index waveguide that combats additional ionization-induced defocusing of the laser and allows for a decreased laser intensity near the walls of the capillary, making it possible to guide the higher intensities required for shorter wavelength generation without damaging the walls. Using a capillary discharge we have demonstrated that the "cut-off," i.e. the highest observable photon energy

generated through the HHG process, can be extended significantly. In Xe we observed photon energies up to ~160 eV, well above the highest previously observed value of ~70 eV [1]. The harmonic flux near the cutoff was enhanced by nearly two orders of magnitude. Furthermore, the reduced self-phase modulation that results from pre-ionization made it possible to observe clearly resolved harmonic peaks up to 85 eV photon energy. In the cases of Kr and Ar, the observed maximum photon energies were extended further, to 170 eV and 275 eV [5]. Here the emission necessarily originates from ionization of ions. These data indicate that any further extension of the cutoff is primarily limited by the large plasma-induced phase mismatch between the fundamental and harmonic waves. In future work, we plan to develop new phase-matching techniques to further extend the range of photon energies that can be efficiently generated.

High Repetition Rate (200 Hz) Capillary Discharge Plasma Waveguide for HHG

Our experiments to-date on HHG from ions in capillary discharge plasmas were conducted at 10 Hz repetition rate. During the past year we have developed a new capillary discharge plasma that was successfully operated at 200 Hz repetition rate, made possible by employing water cooling of the capillary channel and electrodes (Fig 1a). Figure 1(b) shows the measured transmission of ~28 fs FWHM, 8.5 mJ pulses through a 150 μm diameter capillary filled with 6 Torr of Ar for different time delays between the rise of the current pulse and the injection of the laser pulse, operating the discharge with conditions nearly identical to those we used to optimize HHG in Ar. Without firing the discharge, the laser pulse energy transmission is ~24 %. When the discharge current pulse is initiated, the transmission quickly rises to 65% and remains high at the optimum time delay for HHG. Simultaneously, the laser mode quality at the exit of the capillary is also significantly improved (Fig. 1(c)).

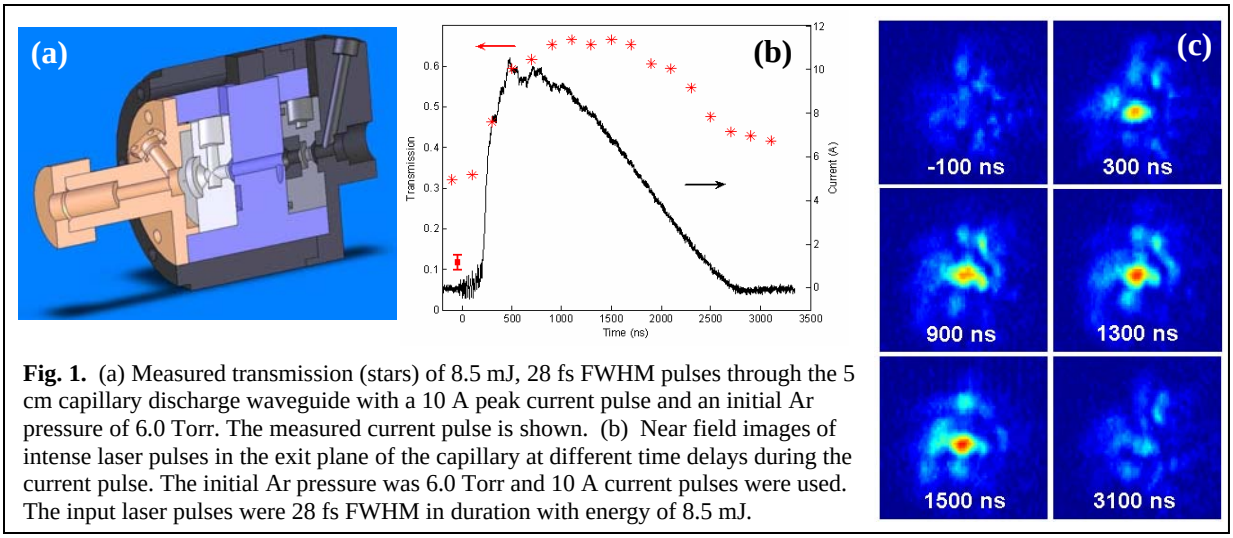

Fig. 1. (a) Measured transmission (stars) of 8.5 mJ, 28 fs FWHM pulses through the 5 cm capillary discharge waveguide with a 10 A peak current pulse and an initial Ar pressure of 6.0 Torr. The measured current pulse is shown. (b) Near field images of intense laser pulses in the exit plane of the capillary at different time delays during the current pulse. The initial Ar pressure was 6.0 Torr and 10 A current pulses were used. The input laser pulses were 28 fs FWHM in duration with energy of 8.5 mJ.

Extended Phase-Matching of High Harmonic driven by Mid-Infrared Light

We have recently showed experimentally and theoretically that it is possible to extend true phase-matching of HHG to significantly higher photon energies (in theory to ≈ 1keV) using long wavelength driving lasers. This increase is a result of the fact that for longer wavelength driving beams, higher energy photons are generated at lower intensities where the medium is much-less ionized. The pressure-length product for phase matching in the waveguide geometry, which is important for increasing the harmonic efficiency when mid-infrared pulses are used, also increases significantly. Thus, mid-IR driving beams will be capable of generating bright short

wavelength harmonics in regions of interest for biological and materials imaging. Using a 1.3 μm driving laser and pressure-tuned phase matching in a hollow waveguide, the perfect phase matching in Ar gas was extended from ≈45 eV (0.8 μm driver) to ≈100eV (Fig 2 a). This is a 2x increase in phase-matching cutoff energy compared with using a 0.8 μm driving laser. In addition, we showed that phase matching is obtained at higher pressures, 100-200 torr, using longer driving wavelengths. Thus, although scaling of the single atom efficiency with driving wavelength corresponds to an 11-18 times weaker emission for 1.3 μm compared with an 0.8 μm driving pulse, because of the ability to phase match the process, the photon flux observed within the 70-100 eV phase-matching region is of comparable intensity to that of the brightest HHG source in the region – phase-matched He at 0.8 μm (Fig. 2.b). At lower pressures and higher peak intensity of the driving pulse (in a non-phase matched regime and for long data integration times), HHG emission from argon driven by 1.3 μm light extends up to 200 eV (Fig. 2.c). These results, combined with the use of capillary discharge waveguides, demonstrates a path for producing bright coherent x-rays for biological and materials imaging up to keV and higher energies.

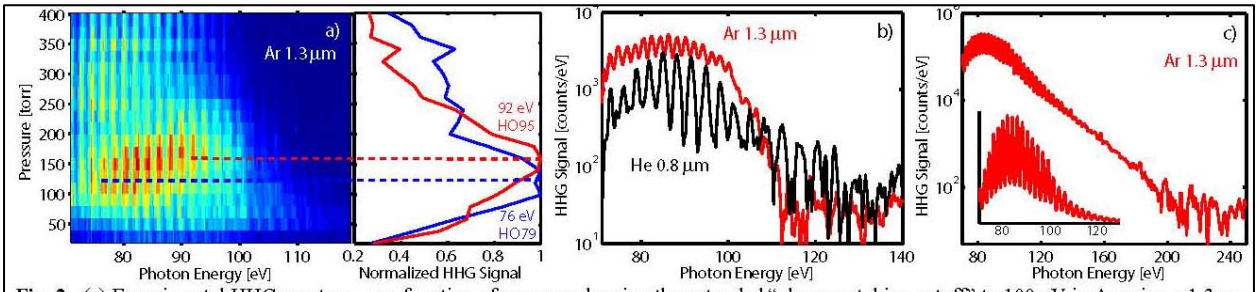

Fig. 2. (a) Experimental HHG spectrum as a function of pressure showing the extended "phase-matching cutoff" to 100 eV in Ar using a 1.3μm driving pulse (b) Comparison between the HHG signal from phase-matched Ar (160 torr) driven by 1.3 μm and from phase-matched He (500 torr) driven by 0.8 μm (3000 laser shots in both cases). A 2.6x higher peak intensity was used at 0.8 μm in order to reach similar cutoff photon energies. (c) Highest cutoff of 200 eV obtained from Ar driven by 4.5×10^{14} W/cm^2, 1.3 μm pulse (linear and log scale, 36000 laser shots).

Demonstration Phase-Coherent Soft X-Ray Laser Pulses of 1 Picosecond Duration by High Harmonic Seeding of a Plasma Amplifier

Soft x-ray lasers (SXRL) are an attractive complement to HHG as source of coherent light at short wavelengths due to their ability to generate pulses with significantly higher pulse energy. There is keen interest in reducing the pulse duration of table-top SXRLs. Until recent experiments, the pulse duration of all SXRLs was determined by the duration of the gain. By injection-seeding soft x-ray laser plasma amplifiers with high harmonic pulses, we have created a fundamentally new regime for the generation of short soft x-ray laser pulses in which the pulse width is governed by the amplifier bandwidth and is independent of the gain duration. In these experiments, high harmonic seed pulses were amplified in a soft x-ray amplifier created by plasma generation from a solid target. Injection-seeding of the SXL amplifier produced intense soft x-ray pulses with full spatial and temporal coherence, low divergence, and defined polarization at wavelengths as short as 13.2 nm. The high density of these SXRL plasma amplifiers results in relatively broad laser line bandwidths that in principle can support the generation of sub-ps SXRL pulses. Although our modeling had indicated that the pulse duration from this setup should be ~ 1 ps, a measurement of the pulsewidth had not been done for comparison. In a recent experiment conducted in collaboration with Kansas State University we have realized the first measurement of the duration soft x-ray laser pulses from such an injection-seeded plasma amplifier created irradiating a solid target [8]. An ultrafast streak camera

developed by Zenghu Chang et al. was used to make single-shot measurements of soft x-ray pulses generated by seeding the 32.6 nm line of Ne-like Ti with the 25th harmonic of a Ti:Sapphire laser (see Fig 3). The measured pulse duration of 1.13 ± 0.47 ps is to our knowledge the shortest soft x-ray laser pulse duration demonstrated to date from a plasma amplifier. In Fig. 3 c, the results are compared with hydrodynamic/atomic physics model computations. Moreover, the results suggest that injection seeding of higher-density soft x-ray laser plasmas will lead to SXRL pulses of a few hundred femtosecond duration.

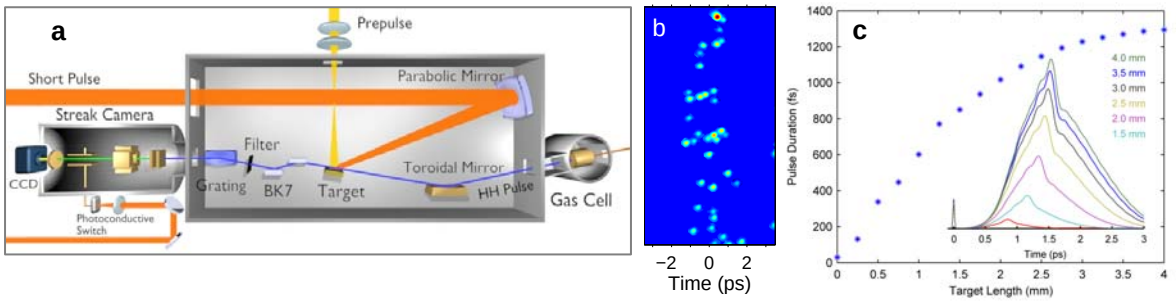

Fig. 3. (a) Set up for the measurement of soft x-ray laser pulse duration using an ultrafast streak camera. (b) streak (the de-convolved pulse width is ~ 1.1 ns wide). C) Computed pulsewidth and pulse profile of amplified seed pulses as a function of soft x-ray laser amplifier length.

Future plans

The remaining barrier to overcome for efficient high harmonic generation at much higher photon energies than are currently useful (~ 100 eV) is to improve phase matching of the process. We will investigate new optical phase matching schemes in capillary discharge plasmas, where intense laser beams can be guided, overcoming limitations due to ionization-induced refraction.

Journal publications from DOE sponsored research 2006-2008

1. D.M. Gaudiosi, B. Reagan, T. Popmintchev, M. Grisham, M. Berrill, O. Cohen, B.C. Walker, M.M. Murnane, H.C. Kapteyn, J.J. Rocca, "High-Order Harmonic Generation from Ions in a Capillary Discharge", Physical Review Letters, **96**, 203001 (2006).
2. J.J. Rocca, H.C Kapteyn, D.T. Attwood, M.M. Murnane, C.S. Menoni, and E. Anderson, "Tabletop Lasers in the Extreme Ultraviolet", (Invited) Optics & Photonics News, **17**, No. 11, pg. 30, (2006).
3. D. Gaudiosi, B. Reagan, T. Popmintchev, M. Grisham, M. Berrill, O. Cohen, B.C. Walker, M.M. Murnane, H.C. Kapteyn, and J.J. Rocca, "High Harmonic Generation from Ions in a Capillary Discharge Plasma Waveguide", Optics & Photonics News , **17**, No. 12, p. 44, (2006).
4. M.A. Larotonda, Y. Wang, M. Berrill, B.M. Luther, J.J. Rocca, Mahendra Man Shakya, S. Gilbertson, and Zenghu Chang , "Pulse duration measurements of grazing incidence pumped high repetition rate Ni-like Ag and Cd transient soft x-ray lasers". Optics Letters, **31**, 3043, (2006).
5. B.A. Reagan, T. Popmintchev, M.E. Grisham, D.M. Gaudiosi, M. Berrill, O. Cohen, B.C. Walker, M.M. Murnane, J.J. Rocca, and H.C. Kapteyn, "Enhanced High Harmonic Generation from Xe, Kr, and Ar in a Capillary Discharge", Physical Review A, 013816, (2007)
6. T. Popmintchev, M.C.Chen, O. Cohen, M. Grisham, J.J. Rocca, M.M. Murnane and H.C. Kapteyn "Extended Phase Matching of High Harmonics Driven by Mid-Infrared Light", Optics Letter, in press (2008)
7. Y.Wang, M. Berrill, F. Pedaci, M.M. Shakya, S. Gilbertson, Zenghu Chang, E. Granados, B.M. Luther, M.A. Larotonda and J.J. Rocca. " Measurement of 1 Picosecond Soft X-Ray Laser Pulses from an Injection-Seeded Plasma amplifier", Phys. Rev. Lett. (submitted)

Ultrafast holographic x-ray imaging and its application to picosecond ultrasonic wave dynamics in bulk materials

Christoph G. Rose-Petruck
** Department of Chemistry, Box H, Brown University, Providence, RI 02912*
phone: (401) 863-1533, fax: (401) 863-2594, Christoph_Rose-Petruck@brown.edu

1 Program Scope

The focus of this work is to develop ultrafast, holographic x-ray imaging methods suitable for use with laser plasma x-ray sources. The methods will image structural dynamics and motions in materials using phase shifts imparted on the x-ray waves as they propagate though the material. The planned work seeks to directly observe, for instance, picosecond phonon wave packets, shock waves, or phonon solitons propagating in the bulk of materials. This work was funded in the spring of 2008.

Imaging of bulk materials relies on Propagation-based Differential Phase Contrast Imaging (PDPCI) which measures the Laplacian of the real part of the index of refraction, n_r, of the material and Talbot Effect imaging (TEI), which measures the 1st spatial derivative of n_r. No x-ray interferometers will be used. The sensitivity to of the measurements to density variations is up to 1000 times larger than that of conventional x-ray absorption based imaging methods.

2 Recent Progress

Our previously completed work focused on the engineering and characterization of laser-driven tabletop, ultrashort pulse, hard-x-ray sources with high brightness.[1-7] Initially, ultrafast x-ray absorption spectra of chemical processes were measured. Based on experiences gained with these measurements, a new laser plasma source with an integrated x-ray goniometer and camera holding arm was constructed with the specific goal to improve x-ray flux, lower the maintenance requirements, and improve the long-term stability of the experiments. The new x-ray source has been designed for time-resolved x-ray absorption spectroscopy as well as imaging applications. This marks the first laser-driven plasma x-ray source that continuously recycles the target material, facilitating nearly maintenance-free operation. As a consequence, this work lays the foundation for the future development of ultrafast x-ray sources that can operate as maintenance-free as conventional x-ray tubes. Simultaneously, the use of mercury as a target material enables the production of x-ray pulses that could theoretically achieve a temporal full width at half maximum (fwhm) of a few tens of femtoseconds. In preparation for this new project introduced in this abstract on phase-contrast image formation, the Hg source was used for in-line holographic imaging applications and first results were shown in last year's abstract.

3 Future plans

The ultrafast laser-driven x-ray source developed during the previous funding cycle will be used for ultrafast holographic x-ray imaging. The goal of this project, that began in the Spring of 2008, is to use the transversal coherence properties of the laser plasma source to the development of ultrafast PDPCI and TEI and to apply them to the imaging of picosecond ultrasonic wave packets propagating in the bulk of materials. Initially, high strain, ultrasonic wave packets, for example in silicon crystals, will be imaged because the results can be compared to diffraction data reported in the literature. However, the sample material's crystal structure is irrelevant for the imaging process and, in the future, applications to materials not accessible to x-ray diffraction will be the major application area. Image contrast caused by x-ray phase shifts is up to a factor 1000 larger than x-ray absorption contrast.

The specific project objectives are:

1. Development and application of ultrafast PDPCI: PDPCI measures under appropriate conditions the Laplacian of real part of the index of refraction, which is proportional to the material's density. The goal of this work is to not just image density variations but to quantify the variations, which, for instance, will enable the measurement of wave functions of ps-ultrasonic waves in crystalline as well

as non-crystalline materials. An analysis method will be developed which equates the measured images with the Laplacian in the ultrasonic wave equations, and applies Fourier transformations to obtain the wave function vs. time. Alternatively, the measured Laplacian can be directly inserted into the wave equations and the potentially noisy calculation of derivatives from experimental data in unnecessary. This can be highly beneficial as this method applies to important physically phenomena such as the Helmholtz equation for diffusion processes, wave equations, Schrödinger equations. PDPCI requires sufficient transversal coherence of the laser plasma source and therefore this study will seek to find most suitable optical parameters, such as the object to image distance, magnification as well as to minimize the source diameter and the interference fringe averaging as demonstrated in the bottom picture of Error! Reference source not found.. This task will require balancing conflicting parameters, such as spatial coherence at the object (which is a function of source-object distance and source size), magnification (a function of the relative source, object, and detector positions), x-ray shot noise (a function of source-detector distance), spatial resolution (a function of magnification and source size), best exploitation of the x-ray polychromaticity (related to the ability to recover the absolute phase shifts from the measured images), etc. The smallest density gradient that can be imaged will be determined.

2. Development and application of ultrafast TEI: TEI measures the 1st spatial derivative of n_r. This method does not require spatial coherence of the x-ray source and in fact it can be carried out with x-ray emitting areas of millimeter diameters. The phase sensitivity is principally independent of the source size although the spatial resolution drops with increasing source size. The absolute phase can be obtained through lateral integration of the signal. While a similar procedure is more difficult for PDPCI, the PDPCI contrast highlights interfaces strongly. Therefore, both phase-sensitive x-ray imaging methods are complementary as they measure different spatial derivatives of n_r, enter differently into wave equations, and have different sensitivity to the spatial frequencies (feature sizes) of the sample.

3. Picosecond ultrasonic phenomena, such as shock wave propagations as well as strain wave focusing in optically opaque materials will be imaged. The imaging of such ultrasonic waves is important because it enables the direct observation of a material's response to high strain rates and amplitudes. The x-ray measurements do not requires any prior knowledge of the materials properties. For instance, time-resolved x-ray diffraction measurements of highly shock-strained silicon found that the diffraction signal disappears beyond a certain strain. The reasons for this disappearance are unknown but phase transitions are the likely cause. Since the ultrasonic properties of the modified silicon are unknown it is desirable to directly image the ultrasonic waves propagation from the original to the newly created phase, which does not require any prior knowledge of the properties of the phase transition. It will be shown that the measurement of the absorption contrast as well as TE and PDPC contrast quantitatively image a material's density distribution, and the 1st and 2nd derivatives of the density. All measurement can be carried out in the same experimental setup. They are mathematically related to each other by Fourier transformations and simple spatial integrations. Thus, all measurements should directly or after data processing yield the same density distribution. This fact will permit checking the consistency of all measurements and data analysis procedures which yields an estimate for the accuracy of the quantitative imaging of strain waves.

While both, TE and PDPC imaging rely on the phase shift of the x-rays passing through the material, the absence of single-crystal interferometers, relieves the project from the construction and mechanical control of sensitive x-ray optical components while promising very alignment-robust imaging methods. Simultaneously, it will be shown that the transmission of the in-line x-ray optical setup is between 25% and close to 100%. Furthermore, it will be shown that most of the contrast features are x-ray wavelength independent which enables the use of the entire x-ray spectrum emitted from the LPS. The combination of

high transmission and broad x-ray bandwidth yields short data acquisitions times that are expected to be on the order of minutes or less per image. Initial experiments will achieve spatial resolutions of several μm.

4 References

1. "Ultrafast x-ray generation from a liquid mercury target," C. Reich, C. M. Laperle, X. Li, B. Ahr, F. Benesch-Lee and C. G. Rose-Petruck, Optics Letters **32** (4), 427 (2007).

2. "Propagation based differential phase contrast imaging and tomography of murine tissue with a laser plasma x-ray source," C. M. Laperle, P. Wintermeyer, J. R. Wands, D. Shi, A. A. Mark, X. Li, B. Ahr, G. J. Diebold and C. Rose-Petruck, Applied Physics Letters **91** (17), 173901 (2007).

3. "Ultrafast XAFS of transition metal complexes," T. Lee, C. Reich, C. M. Laperle, X. Li, M. Grant and C. G. Rose-Petruck, in *Ultrafast Phenomena*, Vol. XV, edited by R.J.D. Miller, A.M. Weiner, P. Corkum, and D.M. Jonas (Springer Verlag, Berlin, 2006), p. 719.

4. "X-ray Phase Contrast Imaging: Transmission Functions Separable in Cartesian Coordinates," G. Cao, T. Hamilton, C. Rose-Petruck and G. J. Diebold, J. Am. Optical Soc. A **24**, 1201 (2006).

5. "Ultrafast tabletop laser-pump-x-ray probe measurement of solvated Fe(CN)(6)(4-)," T. Lee, Y. Jiang, C. G. Rose-Petruck and F. Benesch, Journal of Chemical Physics **122** (8) (2005).

6. "Ultrafast laser-pump x-ray probe measurements of solvated transition metal complexes," T. Lee, F. Benesch, C. Reich and C. G. Rose-Petruck, in *Femtochemistry VII*, edited by Jr. A.W. Castleman and M. Kimble (Elsevier, 2005), p. 23

7. "Acoustically Modulated X-ray Phase Contrast and Vibration Potential Imaging," A. C. Beveridge, C. J. Bailat, T. J. Hamilton, S. Wang, C. Rose-Petruck, V. E. Gusev and G. J. Diebold, in *Photons Plus Ultrasound: Imaging and Sensing 2005*, edited by A.A. Oraevsky and L.V. Wang (SPIE Publishing, Bellingham, WA, 2005), Vol. 5697, p. 90

Auger Recombination and Carrier Multiplication in Semiconductor Nanocrystals

Richard D. Schaller and Victor I. Klimov
Chemistry Division, C-PCS, MS-J567, Los Alamos National Laboratory
Los Alamos, New Mexico 87545
rdsx@lanl.gov & *klimov@lanl.gov*

1. Program Scope

Semiconductor nanocrystals (NCs) are of broad interest due to their designer properties such as tunable energy gap (E_g), range of available compositions, high photoluminescence quantum yields, and optical gain performance. The properties of multiple exciton states (multiple electron-hole pairs) are directly relevant to the performance of optical amplifiers, the brightness of light-emitting diodes in the high current regime, and the potential for enhanced power conversion efficiency single junction photovoltaics. Multiexciton properties appear to differ significantly between NCs and their bulk semiconductor counterparts. The work presented here is aimed at understanding the physics that dictates multiexciton recombination (Auger recombination) and generation properties (carrier multiplication or impact ionization) in semiconductor NCs.

2. Recent Progress

2.1 Auger Recombination in Semiconductor Nanocrystals. In the Auger recombination process, one electron-hole pair (an exciton) non-radiatively recombines and transfers its energy to a third carrier (an electron or a hole), resulting in a net loss in the total number of excited carriers. In bulk semiconductors, this process exhibits an energy barrier that arises from the requirements of energy and translational momentum (p) conservation. In short, the third carrier must gain the energy of the recombined exciton while also conserving the total system momentum. Because energy and momentum are linked, only combinations of carriers with sufficient initial momentum, and therefore energy, can undergo Auger recombination. The energy threshold (E_A) for activating Auger recombination is directly proportional to E_g, ($E_A = \gamma E_g$; where γ is a constant that is determined by details of electronic structure such as the electron, m_e, and the hole, m_h, effective masses), since E_g dictates the momentum acquired by the third carrier. Because of this energy barrier, the Auger recombination rate (k_{AR}) is exponentially dependent upon E_g as $k_{AR} \propto \exp[-\gamma E_g/kT]$, where T is temperature and k is the Boltzmann constant. The Auger recombination activation threshold is observed for bulk semiconductors in temperature-dependent studies of Auger recombination rates and is implicit from the ca. five-orders-of-magnitude per 1-eV variation that is observed in Auger recombination rates for semiconductors as a function of E_g.

The constraints upon Auger recombination in three-dimensionally (3D) quantum-confined semiconductors NCs are expected to be relaxed in comparison to the bulk.

Carriers contained within NCs reside in discrete, atomic-like levels. In spherical NCs, these levels are classified according to angular momentum (M) but not translational momentum. Thus, it is expected that Auger recombination in NCs must conserve total carrier energy and angular momentum. In this case, theoretically, it should occur without an energetic barrier because carrier energy and M are not in direct relationship, and hence, the carrier that is re-excited during Auger recombination can easily access an energy-conserving, higher-lying state with an appropriate value of M. This difference from bulk materials has several important ramifications. The lack of a barrier to Auger recombination in NCs means that: i) excitons in low energy configurations are available for Auger recombination whereas in the bulk they are not, ii) temperature does not influence Auger recombination rates, iii) NC size (which defines the strength of Coulomb coupling) and wavefunction overlap alone determine Auger recombination rates, and iv) the inverse-Auger recombination process of impact ionization should also be barrierless, i.e., can be induced by a carrier with a kinetic energy at the fundamental limit of E_g. Though Auger recombination has been reported in several NC materials, direct experimental evidence in support or opposition to this concept of barrierless Auger recombination in NCs has been notably absent from the literature.

A significant problem in verifying the concept of barrierless Auger recombination in NCs has been the difficulty of decoupling the effects of NC size and energy gap on Auger recombination rates. For a given multi- electron-hole (multiexciton) state, experimentally measured Auger recombination rates exhibit a strong, cubic dependence on NC radius, R. This size dependence can arise from multiple factors including changes in the effective carrier concentration (scales as R^{-3}), the strength of Coulomb coupling (proportional to R^{-1}), the density of the final states for the re-excited carrier, and potentially, the size-dependent energy gap, which in the particle-in-the-box model changes as R^{-2}.

We have begun to use hydrostatic pressure as a tool to tune the NC energy gap via bulk deformation potential without causing significant changes in NC size. Specifically, we use transient absorption to investigate Auger recombination of biexcitons in PbSe NCs contained within a diamond anvil cell (DAC). A DAC is used to isostatically and reversibly apply large pressures (~0.1 to 20 GPa) to NCs that are dissolved in a non-crystallizing solvent. Because deformation potentials and bulk moduli (inverse compressibility) of many semiconductors are quite large, significant shifts in energy can be achieved with only small fractional changes in NC volume, and often without moving the crystal through a phase transition. Because of a large exciton radius (46 nm) in bulk PbSe, sub-10 nm PbSe NCs are ideally suited for investigation of the “quantum-confined” Auger recombination process since for these NC sizes, both electrons and holes are in the regime of strong quantum confinement. We start by confirming the relatively small NC volume change and constancy of crystal phase for a range of pressures using X-ray diffraction (XRD), which implies that carrier mass and Bloch wavefunction properties are not significantly altered. We find that the Auger recombination rate is not dependent upon E_g, in accordance with the concept of barrierless Auger recombination. Finally, we observe a slight reduction in biexciton lifetime with pressure that correlates well with the concomitant slight reduction in NC volume.

2.2 Carrier Multiplication (Multiple Excitons from a Single Photon). Solar cells represent clean source of renewable energy. However, in order to make them competitive with traditional energy sources, the cost-to-efficiency ratio must be reduced appreciably. Increases in efficiency have typically relied on iterative improvements in material quality (for both Si and non-Si systems) and/or device engineering aspects including, e.g., the use of tandem architectures. There exist, however, approaches that can potentially lead to leaps in photovoltaic performance through the use of new principles for conversion of solar energy into electricity. Proposed methods include the development of impurity band and intermediate band devices, hot electron extraction, and carrier multiplication. Carrier multiplication, which was first observed in bulk semiconductors in the 1950s, would provide increased power conversion efficiency in the form of increased solar cell photocurrent. As was first proposed by Nozik, semiconductor NCs might provide a regime where carrier multiplication could be greatly enhanced relative to bulk through processes such as impact ionization scattering. Impact ionization is an Auger-type process whereby a high-energy exciton, created in a semiconductor by absorbing a photon of energy $\geq 2E_g$, relaxes to the band edge via energy transfer of at least $1E_g$ to a valence band electron, which is excited above the energy gap. The result of this energy transfer process is that two excitons are formed for one absorbed photon. Thus, this process converts more of the high photon energy portion of the solar spectrum into usable energy.

One of the barriers to study of carrier multiplication in semiconductor NCs has been the lack of approaches to observe the process. Using our understanding of Auger recombination, we have developed both transient absorption and time-resolved photoluminescence methods for exploring this effect. We have found that NCs do in fact produce multiple excitons upon absorption of single photons of sufficient energy. In 2004, we found for the first time that PbSe NCs undergo carrier multiplication with an energetic onset that is reduced relative to bulk materials and exhibit a photon-energy dependence that is also larger than the bulk. Moreover, using measurements of intraband relaxation rates as well as studies of exciton population buildup times, we have found that the process occurs exceptionally rapidly. From studies of multiple NC material systems, it also appears that the energetic onset of carrier multiplication is likely determined by the disproportionation of photon energy between the electron and the hole (in conjunction with optical selection rules). Furthermore, we have performed theoretical calculations of a viable quantum mechanical mechanism for enhanced carrier multiplication in NCs. In this theory, it is the increased Coulombic interactions between multiple excitons contained within a single NC relative to bulk that causes carrier multiplication to become efficient.

3. Future Plans

Our future work will focus on trying to understand the physics that control both Auger recombination rates and carrier multiplication efficiencies. For instance, reduction in the rates of Auger recombination would lead to improved performance of NC-based optical amplifiers as well as increase the likelihood of realization of carrier multiplication-enhanced photovoltaics. Likewise, we will continue to investigate the factors that dictate the efficiency of carrier multiplication as well as the processes that compete with it.

Concepts we will address also include Auger recombination and carrier multiplication of materials that are in different regimes of quantum confinement (strong, intermediate, and weak).

4. Relevant Publications

[1] V. I. Klimov, J. A. McGuire, R. Schaller, and V. I. Rupasov, Scaling of multiexciton lifetimes in semiconductor nanocrystals, *Phys. Rev. B* **77**, 195324 (2008).
[2] R. D. Schaller, J. M. Pietryga, and V. I. Klimov, Carrier Multiplication in InAs Nanocrystal Quantum Dots with an Onset Defined by the Energy Conservation Limit, *Nano Lett.* **7**, no. 11, 3469 – 3476 (2007)
[3] V. I. Rupasov and V. I. Klimov, Carrier multiplication in semiconductor nanocrystals via intraband optical transitions involving virtual biexciton states, *Phys. Rev. B* **76**, no. 12, 125321 (2007).
[4] X. Jiang, R. D. Schaller, S. B. Lee, J. M. Pietryga, V. I. Klimov, and A. A. Zakhidov, PbSe nanocrystal/conducting polymer solar cells with an infrared response to 2 micron, *J. Mat. Res.* **22**, 8, 2204-2210 (2007)
[5] V. I. Klimov, S. A. Ivanov, J. Nanda, M. Achermann, I. Bezel, J. A. McGuire, and A. Piryatinski, Single-exciton optical gain in semiconductor nanocrystals, *Nature* **447**, 441 (2007).
[6] A. Piryatinski, S. A. Ivanov, S. Tretiak, and V. I. Klimov, Effect of quantum and dielectric confinement on the exciton exciton interaction energy in type II core/shell semiconductor nanocrystals, *Nano Lett.* **7**, 108 (2007)
[7] V. I. Klimov, Spectral and dynamical properties of multiexcitons in semiconductor nanocrystals, *Annu. Rev. Phys. Chem.* **58**, 635 (2007).
[8] J. Nanda, S. A. Ivanov, M. Achermann, I. Bezel, A. Piryatinski, V. I. Klimov Light Amplification in the single-exciton regime using exciton-exciton repulsion in type-II nanocrystal quantum dots, *J. Phys. Chem. B* **111**, 15382 (2007).
[10] V, I. Klimov, Mechanisms for photogeneration and recombination of multiexcitons in semiconductor nanocrystals: Implications for lasing and solar energy conversion, *J. Phys. Chem. B, Feature Article* **110**, 16827 (2006).
[11] R. D. Schaller, M. Sykora, S. Jeong, and V. I. Klimov, High-efficiency carrier multiplication and ultrafast charge separation in semiconductor nanocrystals studied via time-resolved photoluminescence, *J. Phys. Chem. B* **110**, 25332 (2006).
[12] V. I. Klimov, Detailed-balance power-conversion limits of nanocrystal-quantum-dot solar cells in the presence of carrier multiplication, *Appl. Phys. Lett.* **89**, 123118 (2006).
[13] M. Sykora, M. A. Petruska, J. Alstrum-Acevedo, I. Bezel, T. J. Meyer, and V. I. Klimov, Photoinduced charge transfer between CdSe nanocrystalline quantum dots and Ru-polypyridine complexes, *J. Am. Chem. Soc.* **128**, 9984 (2006).
[14] M. Achermann, A. P. Bartko, J. A. Hollingsworth, and V. I. Klimov, The effect of Auger heating on intraband relaxation in semiconductor quantum rods *Nature Physics* **2**, 557 (2006).
[15] R. D. Schaller and V. I. Klimov, Non-Poissonian exciton populations in semiconductor nanocrystals via carrier multiplication, *Phys. Rev. Lett.* **96,** 097402 (2006).
[16] J. Nanda, S. A. Ivanov, H. Htoon, I. Bezel, A. Piryatinski, S. Tretiak, and V. I. Klimov, Absorption cross sections and Auger recombination lifetimes in inverted core/shell nanocrystals: Implications for lasing performance, *J. Appl. Phys.* **99**, 034309 (2006).
[17] R. D. Schaller, M. Sykora, J. M. Pietryga, and V. I. Klimov, Seven excitons at a cost of one: Redefining the limits for conversion efficiency of photons into charge carriers, *Nano Lett.* **6**, 424 (2006).

New Directions in Intense-Laser Alignment

Tamar Seideman
Department of Chemistry, Northwestern University
2145 Sheridan Road, Evanston, IL 60208-3113, t-seideman@northwestern.edu

1. Program Scope

Molecular alignment by moderately-intense laser pulses has developed during the past few years into an exciting field of experimental and theoretical research. This activity has been fueled by appreciation of the rich dynamics displayed by rotational wavepackets, by the development of experimental techniques to visualize and quantify alignment, and by a broad variety of demonstrated and anticipated applications. These range from study and manipulation of chemical reactions and elucidation of molecular structure, through generation of ultra-short light pulses and of high-order harmonics of light, to fundamental studies in coherence and dissipation and new routes to quantum information processing.[9] (Citations refer to the publication list of Sec. 4 and are therefore not in the order cited.)

The main goal of our DOE-sponsored research has been to extend the concept of nonadiabatic alignment from the domain of isolated, rigid diatomic molecules to complex systems, including large polyatomic molecules, solvated molecules, molecular assembly, and molecular junctions. Work toward this goal during the past year includes the development of an alignment-based approach to manipulate transport through molecular junctions, the introduction of a coherent means of inducing toroidal current and associated magnetic fields in oriented molecules, the development of a selective bond-breaking scheme, based on coherent orientation, and the extension of alignment to guide the assembly of molecules, thus producing molecular devices with long range orientational order. These and other recent activities are detailed in Secs. 2.1–2.6 For space considerations, I omit projects discussed in my 2007 AMOS abstract in cases where work during the current year has been essentially an extension.

In related research within the nonadiabatic alignment theme, inspired by experimental research of AMOS colleagues, we developed in 2007 a theoretical framework for the calculation of high harmonic generation (HHG) spectra from nonadiabatically aligned molecules.[6] New results in this area are discussed in Sec. 2.7 and related planned research in collaboration with AMOS experimentalists is outlined in Sec. 3.1.

2. Recent Progress

We begin (Secs. 2.1–2.3) with recent progress on the application of nonadiabatic orientation in different coherent control scenarios, proceed with 3D alignment of isolated large polyatomic systems (Secs. 2.4–2.5) and conclude with applications of feedback control of alignment (Sec. 2.6) and of HHG from aligned molecules(Sec. 2.7) as coherence spectroscopies of dissipative media.

2.1 Orientation control of transport through molecular nano-junctions

In recent work we propose an ultrafast, nanoscale molecular switch based on extension of nonadiabatic alignment to surface-adsorbed molecules. The switch consists of a conjugated organic molecule adsorbed onto a semiconducting surface and placed near a scanning tunneling microscope tip. A low-frequency (sub-bandgap), polarized laser field is used to switch the system by orienting the molecule with the field polarization axis, thereby enabling conductance through the junction. Enhancement and spatial localization of the incident field by the metallic tip allow operation at

low intensities. The principles of nonadiabatic alignment lead to switch on and off time-scales far below rotational time-scales.

2.2 Orientation, toroidal current, and induced magnetic field in polar molecules

In a forthcoming publication, we use half cycle pulses to nonadiabatically orient BeO molecules, and next apply a circularly polarized laser pulse in resonance with an excited, degenerate singlet state to induce unidirectional electric ring current about the axis of the oriented molecule. As a consequence, a strong magnetic field is induced at the oxygen nucleus. Our predictions are based on analysis of the orbital composition of the states involved and are substantiated by high-level electronic structure calculations of the potential and dipole moments and quantum simulations of the laser-driven orientation and the toroidal current excitation.

2.3 Selective bond breaking via nonadiabatic orientation

In another recent application of the nonadiabatic orientation concept, we introduce an approach to selective bond breaking through the combination of an IR and a UV pulses. Field-free orientation of OHF^- is induced by moderately intense half-cycle, IR laser pulses. After the field has been switched off, pronounced molecular orientation is observed for several picoseconds. Subsequently femtosecond few-cycle laser pulses are applied to the oriented system to steer vibrational dynamics and lead to selective bond breaking. The result is spatial separation of the dissociation products in the space-fixed frame.

2.4 Theory of three-dimensional alignment

In Ref. 3, we develop a theoretical framework for study of three-dimensional alignment by moderately intense laser pulses, and discuss it at an elementary level. Several features of formal interest are noted and clarified. Our approach is nonperturbative, treating the laser field within classical, and the material system within quantum mechanics. The theory is implemented numerically using a basis set of rotational eigenstates, transforming the time-dependent Schrödinger equation to a set of coupled differential equation where all matrix elements are analytically soluble. We provide simple numerical examples to illustrate the content of the equations and test the numerical machinery.

2.5 Toward complete control over molecular rotations

The theory outlined in item 2.4 has been applied in three joint studies with an experimental group (H. Stapelfeldt and coworkers, Aarhus). One of these introduces two new approaches to realization of 3D alignment and compares these with two earlier approaches to achieve the same goal. The second study extends the concept of 3D alignment to establish dynamical control over the rotational motions of asymmetric top molecules. Our approach applies two linearly and orthogonally polarized laser pulses, one long and one short with respect to the molecular rotational periods. The long pulse tightly aligns the most polarizable molecular axis along its polarization vector. The subsequent short pulse sets the molecule into coherent revolution about the arrested molecular axis. Our results show that the long pulse constructs a tightly aligned eigenstate of the complete Hamiltonian in the presence of the long pulse field. The short pulse excites this state into a coherent wavepacket of helicity states that subsequently exhibits a revival pattern at a period characterizing the field-free rotational motion. By populating a very broad rotational wavepacket with the long pulse, we are able to near the classical limit of a rigid body held fixed in space and controllably spined about its axis. A preliminary version of this work was published.[4]

2.6 Feedback control of alignment in dissipative media

In Ref. 1, we extend recent work on optimal control of alignment in dissipative media[8] to address several general problems in the controllability of dissipative systems. In addition to investigating the extent to which nonadiabatic alignment can make a useful tool in the presence of deccoherence and population relaxation, we use coherent rotational superpositions as a simple model to explore several general questions in the control of systems interacting with a bath. These include the extent to which a pure state can be created out of a statistical ensemble, the degree to which control theory can develop superposition states that resist dissipation, and the nature of environments that prohibit control. Our results illustrate the information content of control studies regarding the dissipative properties of the bath and point to the strategies that optimize different targets in wavepacket alignment in non-ideal environments.

2.7 On the information content of high harmonics generated from aligned molecules

In Ref. 2, we develop and apply a density matrix formalism to explore high harmonic signals from aligned molecules subject to a dissipative medium. Rotations are taken into account exactly, through an extension of a recently developed theory,[5] leading to an expression for the harmonic signal in terms of a series of rotational expectation values that are determined by the geometry of the experiment and the symmetry of the molecular ground electronic state. A multi-level Bloch model is used to illustrate the imprint of rotational decoherence and relaxation in the harmonic emission. It is shown that the harmonic intensities can be decomposed into two components, each of which carries a different physical interpretation and information content. The usefulness of the decomposition scheme in unraveling the interplay between the different dipole moment components that make the signal, and in relating the observable time dependence of the signal to the underlying electronic-rotational dynamics, is delineated. We show that the phase of the harmonic signal contains unique information regarding the phases of the electronic dipole matrix elements and hence the underlying electronic continuum.

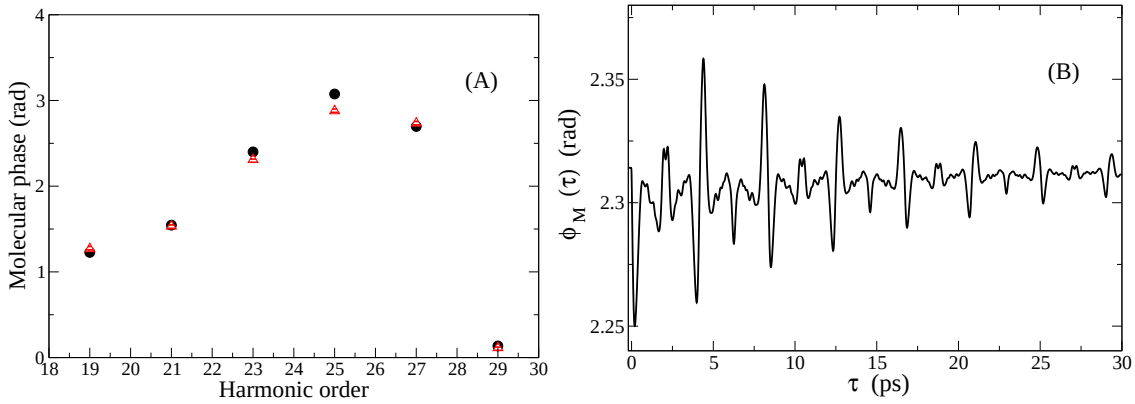

FIG. 1: HHG from aligned molecules as a coherence spectroscopy.(A) Molecular phase spectrum of N_2 molecules in the absence of the alignment pulse (striated triangles) compared with the phase of the dominant electronic dipole, corresponding to a single partial wave of the recombining electron. (B)Phase of the 23rd harmonic from a N_2/Ar system (P = 200 Torr, T=30 K) versus the time delay, τ, between the alignment and the ionization pulses. The alignment pulse intensity is $I = 7.0 \times 10^{13}$ W cm^{-2}.

3. Future Plans

3.1 Our research on the problem of HHG from nonadiabatically-aligned molecules (Sec. 2.7) will be extended in several ways. We will apply the theory developed in Refs. 2,6 in collaborative research

with the group of Kapteyn and Murnane to explore questions raised by recent and ongoing experiments. We will extend the theory from the case of linear molecules subject to co-linearly polarized fields to the case of a general polyatomic subject to a combination of alignment and ionizing pulses of arbitrary polarizations. We will implement a fully quantum mechanical approach for description of the electronic motions, that will go beyond the strong field approximation employed in our previous work.[6] Using HHG spectra from aligned polyatomics, we expect to gain new insights into the dynamics of classically unstable motions.

3.2 Our work on torsional control in general, and its application to charge transfer reactions in particular (discussed in my 2007 AMOS abstract and not included here) will be continued, as current experimental interest in realizing this scheme offers new questions for theoretical research. The concept will be extended from the static (long-pulse-induced, adiabatic alignment) domain to the case of short pulses, where the alignment dynamically entangles with the charge transfer and new opportunities arise, both for analyzing and for controlling charge transfer events.

3.3 Our work on guided molecular assembly (discussed in my 2007 AMOS abstract and not included here) will continue along two routes. First, we will improve our numerical approach to make reliable predictions of the intramolecular forces involved for different molecules of experimental interest. Second, we will continue collaborative research with our experimental coworkers to design improved set-ups for study of different assembly problems.

4. Published and accepted articles from DOE sponsored research, 07/05–07/08

1. A. Pelzer, S. Ramakrishna and T. Seideman, *Optimal Control of Rotational Motions in Dissipative Media*, J. Chem. Phys. , in press.
2. S. Ramakrishna and T. Seideman, *High-Order Harmonic Generation as a Probe of Rotational Dynamics*, Phys. Rev. A, in press.
3. M. Artamonov and T. Seideman, *Theory of Three-Dimensional Alignment by Intense Laser Pulses*, J. Chem. Phys. , **128** 154313 (2008).
4. S. S. Viftrup, V. Kumarappan, S. Trippel, H. Stapelfeldt, E. Hamilton and T. Seideman, *Holding and Spinning Molecules in Space*, Phys. Rev. Lett. **99**, 143602 (2007).
5. S. Ramakrishna and T. Seideman,*On the Information Content of High Harmonics Generated from Aligned Molecules*, Phys. Rev. Lett. **99** 113901 (2007).
6. S. Ramakrishna and T. Seideman, *Torsional Alignment by Intense Pulses*, Phys. Rev. Lett. **99**, 103001 (2007).
7. L. Holmegaard, V. Kumarappan, S. S. Viftrup, C. Z. Bisgaard, H. Stapelfeldt, E. Hamilton and T. Seideman, *Control of Rotational Wavepacket Dynamics in Asymmetric Top Molecules*, Phys. Rev. A **75** 051403 (2007).
8. A. Pelzer, S. Ramakrishna and T. Seideman, *Optimal Control of Molecular Alignment in Dissipative Media*, J. Chem. Phys. **126**, 034503 (2007).
9. T. Seideman and E. Hamilton, *Nonadiabatic Alignment by Intense Pulses. Concepts, Theory, and Directions*, Ad.At.Mol.Opt.Phys. **52**, **52**, 289 (2006) (**invited**).
10. N. Moiseyev and T. Seideman, *Alignment of Molecules by Lasers: Derivation of the Hamiltonian within the (t,t') Formalism*, J.Phys. B:At.Mol.Opt.Phys. **39** L211 (2006).
11. M.D. Poulsen, T. Ejdrup, H. Stapelfeldt, E. Hamilton and T. Seideman, *Alignment Enhancement by the Combination of a Short and a Long Laser Pulse*, Phys. Rev. A **73**, 033405 (2006).
12. S. Ramakrishna and T. Seideman, Dissipative Dynamics of Laser Induced Nonadiabatic Molecular Alignment, J. Chem. Phys. **124**, 034101 (2006).
13. E. Hamilton, T. Seideman, T. Ejdrup, M.D. Poulsen, C.Z. Bisgaard, S. S. Viftrup and H. Stapelfeldt, *Alignment of Symmetric Top Molecules by Short Laser Pulses*, Phys. Rev. A, **72**, 043402 (2005).
14. S. Ramakrishna and T. Seideman, *Intense Laser Alignment in Dissipative Media as a Route to Solvent Properties*, Phys. Rev. Lett. **95**, 113001 (2005).

Ro-vibrational Relaxation Dynamics of PbF Molecules

Neil Shafer-Ray*, Gregory Hall**, and Trevor Sears**
*University of Oklahoma Homer L. Dodge Department of Physics and Astronomy (shaferry@physics.ou.edu)
**Brookhaven National Laboratory

1) Program Scope

In 1950 Purcell and Ramsey[1] suggested that the electron might have a CP-violating electric dipole moment (e-EDM) proportional to its spin angular momentum. This possibility initiated an ongoing hunt for the e-EDM that has been spurred on by the recognition of the importance of CP-violation to the formation of a matter-dominated universe[2] as well as a difference in magnitude of the Supersymmetric[3] and Standard Model[4] prediction for its value. The current limit on the e-EDM is 1.6×10^{-27}e·cm as determined in a Ramsey beam resonance study of the Tl atom[5].

The PbF molecule provides a unique opportunity to measure the e-EDM. The molecule's odd electron, heavy mass, and large internal field combine to give it an intrinsic sensitivity to an e-EDM that is over three orders of magnitude bigger than that of the Tl atom[6]. In addition to this increased intrinsic sensitivity, the ground state of the PbF molecule allows for a "magic" electric field at which the magnetic moment vanishes[7]. All of these advantages create an opportunity to significantly lower the current limit on the e-EDM. These advantages can only be realized if an intense source of ground-state PbF molecules can be created and detected with high efficiency. The scope of this project is to (1) create a rotationally cold molecular beam source of PbF, (2) achieve a continuous ionization scheme for sensitive state selective detection of the PbF molecule.

2) Recent Progress

2.1) Direct measurement of the lifetime of the D state of PbF

The publication listed in section 5 details an extensive investigation of schemes to ionize the PbF molecule carried out over a three year period. This work includes the DOE-sponsored measurement of the lifetime of the D state of PbF described here.

The A state is the only electronically excited state of PbF known to have a lifetime that is sufficiently long to allow for state-selective detection. Unfortunately, direct ionization of this state proves to be impractical: The uv laser radiation required to ionize the A state also directly ionizes the ground state via an efficient $1+1$ ionization process. This non-state-selective one-color process completely swamps any state-selective two-color $1+1$ ionization process that might occur. This fact led us to the $1+1+1$ doubly resonance enhanced ionization scheme

$$X \underset{436\,\mathrm{nm}}{\rightarrow} A \underset{477\,\mathrm{nm}}{\rightarrow} D \underset{532\,\mathrm{nm}}{\rightarrow} PbF^{+}. \qquad (1)$$

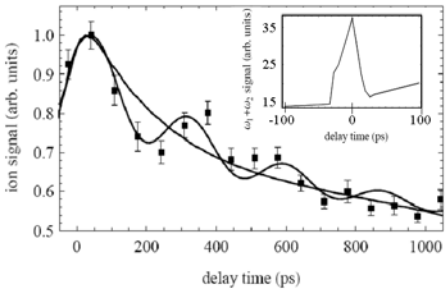

Figure 1: Decay of the D state of PbF

Knowledge of the $D-$state lifetime is critical to the design of an optimal laser system to implement this ionization scheme. Unfortunately the bandwidth of the Nd:YAG pumped dye laser system used to discover the $A \rightarrow D \rightarrow PbF^+$ ionization pathway is not sufficiently narrow to make a conclusive statement about the $D-$state lifetime. For this reason we coaxed our 7-ns Nd:YAG laser system to perform a time domain measurement with picosecond resolution. To accomplish this we took advantage of the temporal mode structure of our unseeded Nd:YAG laser. Specifically, we used the 532-nm output of this laser to pump a dye laser at 863.3 nm. The 1064-nm laser radiation of the Nd:YAG laser was then mixed with the dye laser radiation to create 476.6-nm laser radiation. By creating 476.6-nm laser radiation in this way, the radiation is modulated with the temporal structure of the Nd:YAG laser. This coherence is observed in an auto-correlation measurement that monitors the 251-nm radiation resulting from sum-frequency generation of 532-nm and 476.6-nm laser radiation in a BBO crystal as a function of an optical delay between the two input wavelengths (Figure 1, inset.) The lifetime of the D state of PbF is made by observing the PbF^+ ionization signal as a function of the delay between the 476.6-nm and 532-nm laser radiation. The resulting time-dependent ionization signal is shown in Figure 2 and indicates a lifetime of 250 ± 150 ps.

The $D-$state lifetime is short enough to dramatically reduce the efficiency of an ionization scheme utilizing continuous wave radiation. For this reason, we will employ a pseudo-continuous source of laser radiation producing 6 ps pulses of laser radiation at a repetition rate of 76 MHz.

2.2) Characterization of the $A \rightarrow D$ transition of PbF

We have begun a detailed interpretation of the two-dimensional $X_1\ ^2\Pi_{1/2} \rightarrow A^2\Sigma_{1/2} \rightarrow D$ spectrum shown in Figure 2 and published in the reference listed in section 5. The energy levels of the X_1, A, and D states are well described by the spin rotational Hamiltonian for $\Omega = 1/2$ molecules described by Kopp and Hougen and others[8, 6]. These energy levels are given by Eq 2.

	X_1	A	D	$\beta J(J+1) \pm p(J+\frac{1}{2})$	(2)
p/β	-0.605	2.996	-1.04		

Here β is the rotational constant, J the total angular momentum (excluding nuclear spin) and p the Ω doubling constant. The rotational constant and spin-doubling constant for the X_1 and A states have been measured previously[9][10]. We have found that, for the D state of PbF, $\beta_D = 0.24$ and $p = -0.25$. The fact that $p_D/\beta_D \approx -1.0$ is significant and may help lead to a better understanding of the electronic structure of the ground X_1 state.

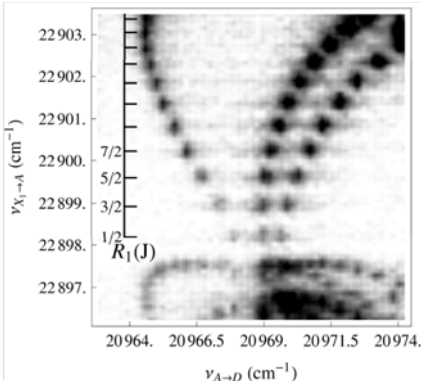

Figure 2: 2-D spectrum of the $X_1 \to A \to D$ transition.

For a $^2\Pi_{1/2}$ molecule, the $J-$labeled energy states are nearly degenerate and $p/\beta << 1$. For the case of a $^2\Sigma_{1/2}$ molecule, $p/\beta \approx -2$ and $N-$labeled energy states are nearly degenerate with energies $\beta N(N+1)$. From the table above, one can see that neither of these conditions are met for any of the states considered. Kopp and Hougen have considered the physics of a mixed $^2\Pi_{3/2}$, $^2\Sigma_{1/2}$, $^2\Pi_{1/2}$ system[8]. Here the value of p is free to take on a range of values, but with the constraint that the sum $(p_1/\beta_1 + p_2/\beta_2) = \pm 2$. It has long been assumed[10] that the $X_1(^2\Pi_{1/2})$, $X_2(^2\Pi_{3/2})$ and $A(^2\Sigma_{1/2})$ state form such a mixed system. However, the $p_1/\beta_1 + p_2/\beta_2$ sum rule is very closely followed by the $A - D$ system. In addition, the $A - D$ energy split is smaller than the $X_1 - A$ energy split. Thus it is likely that the A and D states are strongly mixed along with a yet-to-be-discovered $^2\Pi_{3/2}$ state.

In a separate work we have found that the hyperfine constants of the X_1 state of ^{207}PbF does not agree with that in the literature. Specifically, we find $A_\perp = 7200 \pm 150$ MHz differs in sign from its predicted[6] value . We note that if the parity of the ground state and A state are both incorrect in the literature, then our data would be fit by $A_\perp = -7200 \pm 150$ MHz. Perhaps this disagreement may be explained by the complex interaction between the X_1, A, and D states.

We have observed that R_2 and P_1 branches of the $A \to D$ transition are suppressed in our spectra. This propensity may be understood in terms of a transition dipole moment that violates parity considerations in the simple Born-Oppenheimer picture, but obeys parity selection rules when the complete spin-rotational system is considered. Specifically, overall parity of the spin-rotational wave functions allow for two possible transition dipole moments:

$$\vec{\mu}_{ZY} = \mu_{||}\hat{z}' + i\mu_\perp \hat{y}' \text{ or } \vec{\mu}_X = \mu_\perp \hat{x}'.$$

Here $\hat{z}'$ refers to the internuclear axis, $\hat{y}'$ the molecular fixed coordinate in the plane containing $\hat{z}'$ and the rotational axis. One finds that the R_2 and P_1 transitions may vanish in the $\vec{\mu}_{ZY}$ case. Our data both allows us to conclude that the transition is one of the form $\vec{\mu}_{ZY}$ and to determine the relative value of $\mu_{||}$ and $\mu_{\perp}$. This ratio is sensitive to the details of the electronic nature of the A and D state[8].

3) Future Plans

Rotational cooling of our molecular beam source of PbF has the potential to increase our sensitivity to an e-EDM by as much as a factor of 100 and is a central goal of this research grant. At the onset of this project, our pumping speed was limited by a small foreline pump (originally purchased for a much less demanding pulsed molecular beam experiments.) During this reporting period we have replaced vacuum plumbing and a mechanical pump in order to increase the pumping speed of our forline by a factor of 40. We have almost completed the construction of a larger source chamber pumped by a 10-inch (rather than 6-inch) diffusion pump. This source chamber is scheduled to be installed in September and will allow us to investigate possibility of rotational cooling.

Much of this year has been spent thoroughly characterizing the $A \rightarrow D$ transition. Our current understanding of the line intensities, energy levels, and lifetime of the A and D states has allowed us to optimize the specifications for a laser system to perform state-selective ionization of the molecule. This laser system has been constructed by HighQLaser Inc. At the time of writing this report, this laser system had just arrived to the Physics Department for installation during the second week of July 2008. We look forward to testing this new system in the upcoming months.

4) References

[1] E. Purcell, N. Ramsey, *Phys Rev*, 78 807 (1950).
[2] Sakharov, *JETP Lett*, 5 24 (1967).
[3] R. Arnowitt, B. Dutta, Y. Santoso, *Phys Rev D* 64 113010 (2001).
[4] F. Hoogeveen, *Nuc Phys*, B341 322 (1990).
[5] Regan, Commins, Schmidt, DeMille, *Phys Rev Let* 88 71805 (2002).
[6] Kozlov, Fomichev, Dmitriev, Labzovsky, Titov, *J Phys B* 20 4039 (1987).
[7] N. E. Shafer-Ray, *Phys Rev A* 73 34102 (2006).
[8] I. Kopp, J. Hougen, *Can J Phys* 45 2581 (1967).
[9] Rochester, *Proc R Soc Lon A* 153 407 (1936).
[10] D. Lumley, R. Barrow, *J Phys B* 10 1537 (1977).

5) DOE Sponsored Publication

State-selective detection of the PbF molecule by double resonant multiphoton ionization, P. Sivakumar, C.P. McRaven, Dustin Combs, N.E. Shafer-Ray, and Victor Ezhov, *Phys. Rev. A* 77, 062508 (2008.)

DYNAMICS OF FEW-BODY ATOMIC PROCESSES

Anthony F. Starace

The University of Nebraska
Department of Physics and Astronomy
116 Brace Laboratory
Lincoln, NE 68588-0111

Email: astarace1@unl.edu

PROGRAM SCOPE

The goals of this project are to understand and describe processes involving energy transfers from electromagnetic radiation to matter as well as the dynamics of interacting few-body, quantum systems. Investigations of current interest are in the general areas of strong field physics, attosecond physics, high energy density physics, and multiphoton and double photoionization processes. Nearly all projects under investigation involve large-scale numerical computations for the direct solution of the three-dimensional time-dependent or time-independent Schrödinger equation describing the interaction of atomic systems with electromagnetic radiation. Principal benefits and outcomes of this research are improved understanding of how to control atomic processes with electromagnetic radiation and how to transfer energy from electromagnetic radiation to matter. In some cases our studies are supportive of and/or have been stimulated by experimental work carried out by other investigators funded by the DOE AMO physics program.

RECENT PROGRESS

A. Attosecond Pulse Carrier-Envelope-Phase Effects on Ionized Electron Momentum and Energy Distributions: Roles of Frequency, Intensity, and an Additional IR Pulse

The effects of the carrier-envelope phase (CEP) of a few-cycle attosecond pulse on ionized electron momentum and energy spectra have been analyzed, both with and without an additional few-cycle IR pulse. In the absence of an IR pulse, we find CEP effects on ionized electron momentum distributions produced by attosecond pulses having durations comparable to those obtained by G. Sansone et al. [*Science* **314**, 443 (2006)]. The onset of significant CEP effects is predicted to occur for attosecond pulse field strengths close to those possible with current experimental capabilities. The CEP-induced asymmetries in the ionized electron momentum distributions are found to vary as the 3/2 power of the attosecond pulse intensity, thereby implying an interference of one- and two-photon processes. These asymmetries are also found to satisfy an approximate scaling law involving the frequency and intensity of the attosecond pulse that allows one to predict how CEP effects will change with changes in attosecond pulse frequency or intensity.

In the presence of even a very weak IR pulse (having an intensity of order 10^{11}-10^{12} W cm^{-2}), the attosecond pulse CEP-induced asymmetries in the ionized electron momentum distributions are found to be significantly augmented. In addition, for higher IR laser intensities, we observe for low electron energies peaks separated by the IR photon energy in one electron momentum direction along the laser polarization axis; in the opposite direction, we find structured peaks that are spaced by twice the IR photon energy. Possible physical mechanisms for such asymmetric, low-energy structures in the ionized electron momentum distribution have been put forward and are being explored further. In particular, for short attosecond pulses producing an electron energy spectrum having significant numbers of low-energy electrons, we have shown that the IR field may allow one to explore rescattering of the ionized electron from the ionic core of the ionized atom. Our results are based on single-active-electron solutions of the three-dimensional, time-dependent Schrödinger equation including atomic potentials appropriate for the H and He atoms. (*See references [11] and [12] in the publication list below.*)

B. Threshold-Related Enhancements of Rescattering Plateaus in Laser-Assisted Electron-Atom Scattering

Our recently developed time-dependent effective range [TDER] theory for above-threshold ionization processes [see M.V. Frolov et al., *Phys. Rev. Lett.* **91**, 053003 (2003)] has very recently been extended to give an essentially exact account of laser-assisted, electron-atom scattering (LAES) processes. The TDER theory combines the well-known effective range theory (for electrons interacting with a short-range potential) and the equally well-known Floquet theory (for atomic systems interacting with a monochromatic laser field). Our initial focus has been the study of threshold-related enhancements of the strong-field rescattering plateau in LAES spectra. These threshold phenomena are known to occur in above-threshold ionization as well as in high-order harmonic generation at the closing of a multiphoton ionization channel. Such threshold phenomena can also occur in electron–atom scattering in a laser field, because this process is substantially multichannel in nature: the possible transitions of an electron with momentum p and energy $E=p^2/2m$ to states with energies $E_n=E+n\omega$ correspond to absorption ($n> 0$), elastic scattering ($n= 0$), and induced emission ($n< 0$) of laser field photons. In the latter case, the number of emitted photons is limited by the threshold value $n_{min} = -[E/\omega]$ (where $[x]$ is the integer part of x). In contrast to above-threshold ionization and the generation of high harmonics, the threshold conditions for laser-assisted electron-atom scattering are independent of the field intensity and are achieved by varying either the electron energy E or the field frequency ω so as to satisfy the relation $E=\mu\omega$, where $\mu=1, 2, \ldots$. (Thus, the multiphoton emission threshold corresponds to $n_{min}= -\mu$.) According to general scattering theory, threshold anomalies can exist in all channels with $n>n_{min}$. However, their character and the region of n values in which the threshold modification of the cross sections is significant depend on both the specific process and on the parameters of the problem and thus cannot be determined without a detailed investigation of the particular process being considered.

Whereas in above threshold ionization and in high-order harmonic generation, threshold-related enhancements of strong field rescattering plateaus occur at the closing of either even or odd multiphoton ionization channels, we have found that in laser-assisted electron-atom scattering the enhancements of the plateaus occur at the opening of both even and odd multiphoton channels. These enhancements have been found to increase the electron scattering cross sections with absorption of n laser photons by several orders of magnitude. Our results also show that

threshold phenomena are typical features for the electron rescattering plateau region in the cross sections for all atomic photoprocesses in a strong laser field. Numerical results for e - H and e - F scattering have been investigated thus far. (*See reference [13] in the publication list below*.)

C. Angularly Resolved Electron Spectra of H^- Produced by Few-Cycle Laser Pulses

We have recently investigated the detachment of the H^- negative ion by a linearly-polarized, few cycle laser pulse. The angular distribution of the detached electrons is found to be extremely sensitive to the carrier-envelope phase of the few-cycle laser pulse. Results have been obtained for laser pulses with various pulse widths. The sensitivity of the detached electron momentum distributions thus is shown to provide a measure of the characteristics of the short laser pulse and, in particular, of its carrier-envelope phase. (*See reference [14] in the publication list below*.)

FUTURE PLANS

Our group is currently carrying out research on the following additional projects: (1) Analysis of few-cycle XUV attosecond pulse carrier-envelope-phase effects on ionized electron momentum and energy distributions in the presence of a few-femtosecond IR laser pulse; (2) Modelling of XUV attosecond pulse ionization plus excitation processes in He.

PUBLICATIONS STEMMING FROM DOE-SPONSORED RESEARCH (2005 – 2008)

[1] A.V. Flegel, M.V. Frolov, N.L. Manakov, and A.F. Starace, "Circularly Polarized Laser Field-Induced Rescattering Plateaus in Electron-Atom Scattering," Phys. Lett. A **334**, 197 (2005).

[2] A.Y. Istomin, N.L. Manakov, A.V. Meremianin, and A.F. Starace, "Nondipole Effects in the Triply-Differential Cross Section for Double Photoionization of He," Phys. Rev. A **71**, 052702 (2005).

[3] A.Y. Istomin, A.F. Starace, N.L. Manakov, A.V. Meremianin, A.S. Kheifets, and I. Gray, "Parametizations and Dynamical Analysis of Angle-Integrated Cross Sections for Double Photoionization Including Nondipole Effects," Phys. Rev. A **72**, 052708 (2005).

[4] A.Y. Istomin, N.L. Manakov, A.V. Meremianin, and A.F. Starace, "Non-Dipole Effects in Double Photoionization of He," in *Ionization, Correlation, and Polarization in Atomic Collisions*, ed. A. Lahmam-Bennani and B. Lohmann (A.I.P., Melville, NY, 2006), pp. 18-23.

[5] A.Y. Istomin, A.F. Starace, N.L. Manakov, A.V. Meremianin, A.S. Kheifets, and I. Bray, "Nondipole Effects in Double Photoionization of He at 450 eV Excess Energy," J. Phys. B **39**, L35 (2006).

[6] S.X. Hu and A.F. Starace, "Laser Acceleration of Electrons to GeV Energies Using Highly Charged Ions," Phys. Rev. E **73**, 066502 (2006).

[7] L.Y. Peng, Q. Wang, and A.F. Starace, "Photodetachment of H^- by a Short Laser Pulse in Crossed Static Electric and Magnetic Fields," Phys. Rev. A **74**, 023402 (2006).

[8] A.Y. Istomin, E.A. Pronin, N.L. Manakov, S.I. Marmo, and A.F. Starace, "Elliptic and Circular Dichroism Effects in Two–Photon Double Ionization of Atoms," Phys. Rev. Lett. **97**, 123002 (2006).

[9] L.Y. Peng and A.F. Starace, "Application of Coulomb Wave Function Discrete Variable Representation to Atomic Systems in Strong Laser Fields," J. Chem. Phys. **125**, 154311 (2006).

[10] G. Lagmago Kamta, A.Y. Istomin, and A.F. Starace, "Thermal Entanglement of Two Interacting Qubits in a Static Magnetic Field," Eur. Phys. J. D **44**, 389 (2007).

[11] L.Y. Peng and A.F. Starace, "Attosecond Pulse Carrier-Envelope Phase Effects on Ionized Electron Momentum and Energy Distributions," Phys. Rev. A **76**, 043401 (2007).

[12] L.Y. Peng, E.A. Pronin, and A.F.Starace, "Attosecond Pulse Carrier-Envelope Phase Effects on Ionized Electron Momentum and Energy Distributions: Roles of Frequency, Intensity, and an Additional IR Pulse," New J. Phys. **10**, 025030 (2008).

[13] N.L. Manakov, A.F. Starace, A.V. Flegel, and M.V. Frolov, "Threshold Phenomena in Electron-Atom Scattering in a Laser Field," JETP Lett. **87**, 92 (2008).

[14] L.-Y. Peng, Q. Gong, and A.F. Starace, "Angularly Resolved Electron Spectra of H^- by Few-Cycle Laser Pulses," Phys. Rev. A **77**, 065403 (2008).

FEMTOSECOND AND ATTOSECOND LASER-PULSE ENERGY TRANSFORMATION AND CONCENTRATION IN NANOSTRUCTURED SYSTEMS

DOE Grant No. DE-FG02-01ER15213

Mark I. Stockman, Pi

Department of Physics and Astronomy, Georgia State University, Atlanta, GA 30303
E-mail: mstockman@gsu.edu, URL: http://www.phy-astr.gsu.edu/stockman

Report for the Grant Period of 2006-2008 (Publications 2006-2008)

1 Program Scope

The program is aimed at theoretical investigations of a wide range of phenomena induced by ultrafast laser-light excitation of nanostructured or nanosize systems, in particular, metal/semiconductor/dielectric nanocomposites and nanoclusters. Among the primary phenomena are processes of energy transformation, generation, transfer, and localization on the nanoscale and coherent control of such phenomena.

2 Recent Progress

2.1 Time-Reversal Solution of the Problem of Spatio-Temporal Coherent Control on the Nanoscale [1, 2]

Our research has significantly focused on problem of controlling localization of the energy of ultrafast (femtosecond) optical excitation on the nanoscale. We have proposed and theoretically developed a distinct approach to solving this fundamental problem [3, 4, 5, 6, 7, 8, 9]. This approach, based on the using the relative phase of the light pulse as a functional degree of freedom, allows one to control the spatial-temporal distribution of the excitation energy on the nanometer-femtosecond scale. Following our pioneering work, there has recently been an explosion of activity on both theoretical [10, 11, 12, 13] and experimental [14, 15, 16, 17, 18] investigations of the ultrafast coherent control on the nanoscale. This field will rapidly grow into one of the most important in the nanoscience with application to the nanoscale computations, sensing, spectroscopy, etc. It will require our increased attention to stay at the forefront.

One of the most fundamental problems in nanoplasmonics and nanooptics generally is the spatio-temporal coherent control of nanoscale localization of optical energy. However, a key element was missing: an efficient and robust method to determine a shape of the controlling femtosecond pulse that would compel the femtosecond evolution of the nanoscale optical fields in a plasmonic system to result in the spatio-temporal concentration of the optical energy at a given nano-site within a required femtosecond interval of time. We have solved this problem by using the idea of the time-reversal [1, 2]. We have shown that by exciting a system at a given spot, recording the produced wave in one direction in the far zone, time reversing it and sending the produced plane wave back to the system leads to the required spatio-temporal energy localization. This method can be used both theoretically and experimentally to determined the required polarization, phase and amplitude modulation of the controlling pulses.

2.2 Attosecond Nanoplasmonics [19, 20]

In collaboration with M. Kling, U. Kleineberg, and F. Krausz from Max Plank Institute for Quantum Optics (Garching, Germany), we have theoretically developed a novel concept called Attosecond Nanoplasmonic Field Microscope [19]. It is based on the use of attosecond laser pulses synchronized with an intense, waveform-stabilized optical field driving a nanosystem. The attosecond pulses cause photoemission of electrons in a given phase of the optical excitation, which are accelerated in the local nanoplasmonic fields. These electrons are detected by an energy-resolving photoemission electron microscope (PEEM). The energy of these electrons yields the potential of the local optical fields at the surface of the nanosystem with nanometer spatial resolution and ~ 100 attosecond temporal resolution. This work sets the foundation of a novel direction in nanoplasmonics that is attosecond nanoplasmonics that studies that fastest phenomena existing at the nanoscale.

In a related development, we have shown that the carrier-envelope phase (CEP) of an excitation pulse significantly defines ultrafast responses of metal nanostructures in the regime of the above-threshold ionization (optical field emission) [20]. This suggests a way to build ultrasensitive detectors of the CEP, which is an important problem of the quantum optics.

2.3 Full Spatio-Temporal Control on Nanoscale: Nanoplasmonic Active Phased Array Radar (NAPAR) [21]

In collaboration with K. Nelson (MIT), we have proposed an approach of full coherent control on the nanoscale [21]. This is a nanoplasmonic counterpart of the active phased array radar. It uses excitation of the plasmon polariton waves by independently exciting a set of nanoparticles on a thin metal layer by shaped laser pulses uses an array of pulse shapers. The surface plasmon polariton waves excited in such a way interfere to form a front converging to an arbitrarily defined nanoscale point. This approach can be used for a wide range of applications from ultramicroscopy to controlling computations on the nanoscale.

2.4 Criterion of Negative Refraction with Low Optical Losses [22]

We have derived a novel criterion that defines a possibility of a negative-index material that would have a negligible loss at a given, working frequency [22]. This criterion is rigorous and general, based on the fundamental principle of causality. It shows that to achieve a negative refraction, a significant loss must be present in the vicinity of the working frequency. This criterion will guide the further quest for the low-loss negative index materials worldwide.

2.5 Anomalous Dispersion and Reflection of Surface Plasmon Polaritons at Metal-Dielectric Interfaces [23]

We have predicted a new effect, the total external reflection of surface plasmon polaritons (SPP) for nanometric dielectric films on plasmonic metal [23]. This effect can be used to create efficient SPP mirrors and resonators.

2.6 Octupolar Metal Nanoparticles as Optically Driven, Coherently Controlled Nanorotors [24]

We have proposed that metal nanoparticles with an octupolar symmetry, in particular regular metal nanotriangles and nanotetrahedra, will rotate by a predetermined angle when subjected to the simultaneous action of the fundamental and second harmonic radiations that are circularly polarized in the opposite directions [24]. This angle is coherently control by the phase difference between the fundamental and second harmonic. This project is carried out in collaboration with Prof. Joseph Zyss (ENS Cachan, France).

2.7 Efficient Nanolens [25, 26]

As an efficient nanolens, we have proposed a self-similar linear chain of several metal nanospheres with progressively decreasing sizes and separations [27]. The proposed system can be used for nanooptical detection, Raman characterization, nonlinear spectroscopy, nano-manipulation of single molecules or nanoparticles, and other applications. The second harmonic local fields form a very sharp nanofocus between the smallest spheres where these fields are enhanced by more than two orders of magnitude. This effect can be used for diagnostics and nanosensors. We have also obtained the first results on the Surface Enhanced Raman Scattering (SERS) in the nanosphere nanolens [25] where we show the SERS enhancement facto differ significantly from the commonly used fourth power of the local field enhancement. Recently, we have performed full electrodynamic modeling of the nanolenses [26]. We have confirmed the high predicted level of enhancement and found new electrodynamic resonances where the nanosphere aggregate works both as a plasmonic nanoantenna and as electrodynamic metal antenna.

2.8 Nanoplasmonics at Metal Surface: Enhanced Relaxation and Superlensing [28]

We have considered a nanoscale dipolar emitter (quantum dot, atom, fluorescent molecule, or rare earth ion) in a nanometer proximity to a flat metal surface [28, 29].There is strong interaction of this emitter with unscreened metal electrons in the surface nanolayer that causes enhanced relaxation due to surface plasmon excitation and Landau damping. For the system considered, conventional theory based on metal as continuous dielectric fails both qualitatively and quantitatively.

In a recent development [28], we have considered a principal limitations on the spatial resolution on the nanoscale of the “Perfect Lens” introduced by Pendry, also known as the superlens. In the conventional, local electrodynamics, the superlens builds a 3d image in the near zone without principal limitations on the spatial resolution. We have shown that there is a principal limitation on this resolution, ~5 nm in practical terms, which originates from the spatial dispersion and Landau damping of dielectric responses of the interacting electron fluid in metals.

2.9 Surface Enhanced Raman Scattering (SERS) [30, 31]

We have revisited theory of one of the most important phenomena in nanoplasmonics, Surface Enhanced Raman Scattering [30, 31]. This theory shows that the predicted levels of enhancement in the red spectral region are still several orders of magnitude less than the enhancement factors $\sim 10^{13} - 10^{14}$ observed experimentally. The difference may be due to the effects not taken into account by the theory: self-similar enhancement [27] or chemical enhancement [32].

Recently, an important development of SERS has been achieved with our participation. For the first time, the enhancing effect of nanolenses (see Sec. 2.7) have been observed [31]. This opens up a way to produce a reproducible, robust, and efficient substrate for SERS with very low background.

2.10 Excitation of Surface Plasmon Polaritons (SPPs) by Free Electron Impact [33]

We have provided theoretical support and interpretation for the experimental investigation of the SPP generation by free-electron impact. This effect can be used as a basis of a novel method to visualize eigenmodes of plasmonic nanosystem by exciting them with an electron microscope beam.

3 Future Plans [34, 35, 36]

We will develop both the theory in the directions specified above and the collaborations with the experimental and theoretical groups that we have developed. Among the future projects, we will develop theory of the attosecond nanoplasmonics (see Sec. 2.2), where the corresponding experiments are presently conducted at the Max Born Institute for Quantum Optics (Garching, Germany) and Ludwig Maximilian University (Munich, Germany). Another group of projects is related to the time-reversal coherent control on the nanoscale proposed recently by us (see Sec. 2.1).

Recently, the interest to SPASER, which we introduced in the framework of our first DOE, has tremendously increased. In response to the request by Nature Photonics, we have written a Commentary on SPASER [34]. We intend to revisit and further develop theory of SPASER on the basis of the density matrix approach for quantum dots coupled to the quantized surface plasmon field.

Another field of activity will be study the effects of the proximity to plasmonic systems on the Coulomb interactions in electrons in molecules and semiconductors, i.e., plasmonic resonant renormalization of the Coulomb interactions. We have done preliminary work on this subject published as a preprint recently [35]. The effects of the nanoplasmonic renormalization of the Coulomb interaction are of great importance for electron-interaction effects such as electron scattering, Auger relaxation and ionization, chemical reactions, and many-electron kinetics.

A dramatic development in nonlinear nanoplasmonics reported recently has been the discovery of the high-harmonic generation by radiation from an oscillator (without the commonly used amplifiers) on a table top, using plasmonic enhancement in nanoantenna array [37]. We have recently written a News and Views article requested by Nature [36] describing the stunning horizons that this discovery opens up. A significant activity of our group can be expected in this field.

4 Publications Resulting from the Grant

The major articles published by our group during this Report (2006-2007) period are indicated by bold typeface at the corresponding headings above. These are Refs. [1, 2, 19, 20, 21, 22, 23, 24, 25, 26, 28, 30, 31, 33]. We have also published two editorially-invited articles in Nature [36] and Nature Photonics [34], which are outreach articles promoting the field and the research sponsored by this grant.

References

1. X. Li and M. I. Stockman, *Time-Reversal Coherent Control in Nanoplasmonics*, arXiv:0705.0553 (2007).
2. X. Li and M. I. Stockman, *Highly Efficient Spatiotemporal Coherent Control in Nanoplasmonics on a Nanometer-Femtosecond Scale by Time Reversal*, Phys. Rev. B **77**, 195109-1-10 (2008).
3. M. I. Stockman, S. V. Faleev, and D. J. Bergman, *Coherent Control of Femtosecond Energy Localization in Nanosystems*, Phys. Rev. Lett. **88**, 67402-1-4 (2002).
4. M. I. Stockman, S. V. Faleev, and D. J. Bergman, *Coherently Controlled Femtosecond Energy Localization on Nanoscale*, Appl. Phys. B **74**, S63-S67 (2002).
5. M. I. Stockman, S. V. Faleev, and D. J. Bergman, *Coherently-Controlled Femtosecond Energy Localization on Nanoscale*, Appl. Phys. B **74**, 63-67 (2002).
6. M. I. Stockman, D. J. Bergman, and T. Kobayashi, in Proceedings of SPIE: Plasmonics: Metallic Nanostructures and Their Optical Properties, edited by N. J. Halas, *Coherent Control of Ultrafast Nanoscale Localization of Optical Excitation Energy* (SPIE, San Diego, California, 2003), Vol. 5221, p. 182-196.
7. M. I. Stockman, S. V. Faleev, and D. J. Bergman, in Ultrafast Phenomena XIII, *Coherently-Controlled Femtosecond Energy Localization on Nanoscale* (Springer, Berlin, Heidelberg, New York, 2003).
8. M. I. Stockman, D. J. Bergman, and T. Kobayashi, *Coherent Control of Nanoscale Localization of Ultrafast Optical Excitation in Nanosystems*, Phys. Rev. B **69**, 054202-10 (2004).
9. M. I. Stockman and P. Hewageegana, *Nanolocalized Nonlinear Electron Photoemission under Coherent Control*, Nano Lett. **5**, 2325-2329 (2005).
10. M. Sukharev and T. Seideman, *Phase and Polarization Control as a Route to Plasmonic Nanodevices*, Nano Lett. **6**, 715-719 (2006).
11. M. Sukharev and T. Seideman, *Coherent Control Approaches to Light Guidance in the Nanoscale*, J. Chem. Phys. **124**, 144707-1-8 (2006).

12. T. Brixner, F. J. G. d. Abajo, J. Schneider, C. Spindler, and W. Pfeiffer, *Ultrafast Adaptive Optical near-Field Control*, Physical Review B **73**, 125437 (2006).
13. T. Brixner, F. J. G. d. Abajo, J. Schneider, and W. Pfeiffer, *Nanoscopic Ultrafast Space-Time-Resolved Spectroscopy*, Phys. Rev. Lett. **95**, 093901-1-4 (2005).
14. A. Kubo, K. Onda, H. Petek, Z. Sun, Y. S. Jung, and H. K. Kim, *Femtosecond Imaging of Surface Plasmon Dynamics in a Nanostructured Silver Film*, Nano Lett. **5**, 1123-1127 (2005).
15. A. Kubo, K. Onda, H. Petek, Z. Sun, Y. S. Jung, and H. K. Kim, in Ultrafast Phenomena XIV, edited by T. Kobayashi, T. Okada, T. Kobayashi, K. A. Nelson and S. D. Silvestri, *Imaging of Localized Silver Plasmon Dynamics with Sub-Fs Time and Nano-Meter Spatial Resolution* (Springer, Niigata, Japan, 2004), Vol. 79, p. 645-649.
16. P. v. d. Walle, L. Kuipers, and J. L. Herek, in Ultrafast Phenomena XV, *Coherent Control of Light in Metal Nanostructures* (Pacific Grove, California, 2006), p. Paper TuD3.
17. M. Bauer, D. Bayer, T. Brixner, F. J. G. d. Abajo, W. Pfeiffer, M. Rohmer, C. Spindler, and F. Steeb, in Ultrafast Phenomena XV, *Adaptive Control of Nanoscopic Photoelectron Emission* (Pacific Grove, California, 2006), p. Paper ThB3.
18. M. Aeschlimann, M. Bauer, D. Bayer, T. Brixner, F. J. G. d. Abajo, W. Pfeiffer, M. Rohmer, C. Spindler, and F. Steeb, *Adaptive Subwavelength Control of Nano-Optical Fields*, Nature **446**, 301-304 (2007).
19. M. I. Stockman, M. F. Kling, U. Kleineberg, and F. Krausz, *Attosecond Nanoplasmonic Field Microscope*, Nature Photonics **1**, 539-544 (2007).
20. M. I. Stockman and P. Hewageegana, *Absolute Phase Effect in Ultrafast Optical Responses of Metal Nanostructures*, Appl. Phys. A **89**, 247-250 (2007).
21. M. Durach, A. Rusina, M. I. Stockman, and K. Nelson, *Toward Full Spatiotemporal Control on the Nanoscale*, Nano Lett. **7**, 3145-3149 (2007).
22. M. I. Stockman, *Criterion for Negative Refraction with Low Optical Losses from a Fundamental Principle of Causality*, Phys. Rev. Lett. **98**, 177404-1-4 (2007).
23. M. I. Stockman, *Slow Propagation, Anomalous Absorption, and Total External Reflection of Surface Plasmon Polaritons in Nanolayer Systems*, Nano Lett. **6**, 2604-2608 (2006).
24. M. I. Stockman, K. Li, S. Brasselet, and J. Zyss, *Octupolar Metal Nanoparticles as Optically Driven, Coherently Controlled Nanorotors*, Chem. Phys. Lett. **433**, 130–135 (2006).
25. K. Li, M. I. Stockman, and D. J. Bergman, *Li, Stockman, and Bergman Reply to Comment On "Self-Similar Chain of Metal Nanospheres as an Efficient Nanolens"*, Phys. Rev. Lett. **97**, 079702 (2006).
26. J. Dai, F. Cajko, I. Tsukerman, and M. I. Stockman, *Electrodynamic Effects in Plasmonic Nanolenses*, Physical Review B (Condensed Matter and Materials Physics) **77**, 115419-1-5 (2008).
27. K. Li, M. I. Stockman, and D. J. Bergman, *Self-Similar Chain of Metal Nanospheres as an Efficient Nanolens*, Phys. Rev. Lett. **91**, 227402-1-4 (2003).
28. I. A. Larkin and M. I. Stockman, *Imperfect Perfect Lens*, Nano Lett. **5**, 339-343 (2005).
29. I. A. Larkin, M. I. Stockman, M. Achermann, and V. I. Klimov, *Dipolar Emitters at Nanoscale Proximity of Metal Surfaces: Giant Enhancement of Relaxation in Microscopic Theory*, Phys. Rev. B **69**, 121403(R)-1-4 (2004).
30. M. I. Stockman, in Springer Series Topics in Applied Physics, edited by K. Kneipp, M. Moskovits and H. Kneipp, *Surface Enhanced Raman Scattering – Physics and Applications* (Springer-Verlag, Heidelberg New York Tokyo, 2006), p. 47-66.
31. J. Kneipp, X. Li, M. Sherwood, U. Panne, H. Kneipp, M. I. Stockman, and K. Kneipp, *Gold Nanolenses Generated by Laser Ablation-Efficient Enhancing Structure for Surface Enhanced Raman Scattering Analytics and Sensing*, Anal. Chem. **80**, 4247-4251 (2008).
32. J. Jiang, K. Bosnick, M. Maillard, and L. Brus, *Single Molecule Raman Spectroscopy at the Junctions of Large Ag Nanocrystals*, J. Phys. Chem. B **107**, 9964-9972 (2003).
33. M. V. Bashevoy, F. Jonsson, A. V. Krasavin, N. I. Zheludev, Y. Chen, and M. I. Stockman, *Generation of Traveling Surface Plasmon Waves by Free-Electron Impact*, Nano Lett. **6**, 1113-1115 (2006).
34. M. I. Stockman, *Spasers Explained*, Nature Photonics **2**, 327-329 (2008).
35. M. Durach, A. Rusina, V. Klimov, and M. I. Stockman, *Nanoplasmonic Renormalization and Enhancement of Coulomb Interactions*, arXiv:0802.0229 (2008).
36. M. I. Stockman, *Attosecond Physics - an Easier Route to High Harmony*, Nature **453**, 731-733 (2008).
37. S. Kim, J. H. Jin, Y. J. Kim, I. Y. Park, Y. Kim, and S. W. Kim, *High-Harmonic Generation by Resonant Plasmon Field Enhancement*, Nature **453**, 757-760 (2008).

Molecular Structure and Electron-Driven Processes in a Gas and Liquid phases.

Vladimir Tarnovsky[1]

[1]Department of Physics, Stevens Institute of Technology, Hoboken, NJ 07030

[2]

(vtarnovs@stevens.edu;

Program Scope:

This program is aimed at investigating the molecular structure and the collisional dissociation and ionization of selected molecules and free radicals. The focus areas are (1) ionization studies of selected molecules and free radicals and (2) the study of electron-impact induced neutral molecular dissociation processes. The new direction has also been established where electron-driven processes were applied to a gas/liquid phase. The scientific objectives of the research program can be summarized as follows:

(1) provide the atomic and molecular data that are required in efforts to understand the properties of low-temperature processing plasmas on a microscopic scale

(2) identify the key species that determine the dominant plasma chemical reactions

(3) measure cross sections and reaction rates for the formation of these key species and to attempt to deduce predictive scaling laws

(4) establish a broad collisional and spectroscopic data base which serves as input to modeling codes and CAD tools for the description and modeling of existing processes and reactors and for the development and design of novel processes and reactors

(5) Provide data that are necessary to develop novel plasma applications.

(6) Utilized the data collected on the fast neutral-beam apparatus for developing new types of electrochemical interactions on a gas/liquid interface.

Recent Progress and Ongoing Work:

My recent work moved into an area of plasma interface with liquid solutions. While it is not directly related to main goals of the program, it is a natural expansion of the electron driven processes in a gas phase into area of the gas/liquid interface. In the present abstract is the

summary of the work that has been done during last year in addition to the papers that has been published on the electron – impact ionization cross sections for SiCl3 radicals.

Publications Acknowledging DOE Support (since 2005)

1 S. Matt-Leaner, S. Feel, K. Gluch, J. Fedor, A. Stamatovic, O. Echt, P. Scheier, K. Becker, and T.D. Märk " Energetics, Kinetics, and Dynamics of Decaying Metastable Ions Studied with a High Resolution Three-Sector-Field Mass Spectrometer", Plasma Sources Sci. Techn. 14, 26-30 (2005)

2 H. Deutsch, P. Scheier, S. Matt-Leubner, K. Becker, and T.D. Märk " A Detailed Comparison of Calculated and Measured Electron-Impact Ionization Cross Sections of Atoms Using the Deutsch-Märk (DM) Formalism", Int. J. Mass Spectrom. 243, 215-21 (2005)

3 H. Deutsch, K. Becker, A.N. Grum-Grzhimailo, M. Probst, S. Matt-Leubner, and T.D. Märk, " Calculated Electron Impact Ionization Cross Sections of Excited Ne Atoms Using the DM Formalism", Contr. Plasma Phys. 7, 494-499 (2005)

4 R. Basner, M. Gutkin, J. Mahoney, V. Tarnovsky, H. Deutsch, and K. Becker, " Electron Impact Ionization of Silicon Tetrachloride", J. Chem. Phys. 123, 05313 (2005)

5 H. Deutsch, K.B. MacAdam, K. Becker, H. Zhang, and T.D. Märk, " Calculated Cross Sections for the Electron Impact Ionization of Na(ns) and Na(nd) Rydberg Atoms", J. Phys. B 39, 343-353 (2005)

6 S. Denifl, B. Sonnweber, J. Mack, L. T. Scott, P. Scheier, K. Becker, and T.D. Märk, " Appearance Energies of Singly, Doubly, and Triply Charged Coronene and Corannulene Ions Produced by Electron Impact", Int. J. Mass Spectrom. 249/250, 353-358 (2006)

7 H. Deutsch, K. Becker, P. Defrance, M. Probst, J. Limtrakul, and T.D. Märk, " Newly Calculated Absolute Cross Sections for the Electron Impact Ionization of $C_2H_2^+$", Europ. Phys. J. D 38, 489-493 (2006)

8 K. Becker, J. Mahoney, M. Gutkin, V. Tarnovsky, and R. Basner, " Electron Impact Ionization of $SiCl_x$ and $TiCl_x$ (x = 1-4): Contributions from Indirect Ionization Channels", Jap. J. Appl. Phys. 45, 8818-8891 (2006)

9 J. Lecointre, D.S. Belic, J. Jureta, K. Becker, H. Deutsch, J. Limtrakul, T.D. Märk, M. Probst and P. Defrance, " Absolute cross sections and kinetic energy release for doubly and triply charged fragments produced by electron impact on CO^+", J. Phys. B 39, 85-100 (2006)

10 J. Lecontre, S. Cherkani-Hassani, D.S. Belic, J.J. Jureta, K. Becker, H. Deutsch, T.D. Märk,

M. Probst, R.K. Janev, and P. Defrance, " Absolute Cross Sections and Kinetic Energy Release distributions for Electron Impact Ionization of CD^+" , J. Phys. B 40, 2201-2221 (2007)

1 Deutsch, K. Becker, and T.D. Märk, " Calculated Absolute Cross Sections for the Electron-Impact Ionization of Atoms with Atomic Numbers between 20 and 56 Using the DM Formalism" , Int. J. Mass Spectrom. (2007), submitted

2 H. Deutsch, K. Becker, H. Zhang, M. Probst, and T.D. Märk, " Calculated Absolute Cross Sections for the Electron-Impact Ionization of the Lanthanide Atoms Using the DM Formalism" , Int. J. Mass Spectrom. (2007), submitted

1. H. Deutsch, K. Becker, P. Defrance, M. Probst, J. Limtrakul, and T.D. Märk, " Newly Calculated Absolute Cross Sections for the Electron Impact Ionization of $C_2H_2^+$" , Europ. Phys. J. D 38, 489-493 (2006)

2. K. Becker, J. Mahoney, M. Gutkin, V. Tarnovsky, and R. Basner, " Electron Impact Ionization of $SiCl_x$ and $TiCl_x$ (x=1-4): Contributions from Indirect Ionization Channels" , Jap. J. Appl. Phys. 45, 8818-8891 (2006)

3. J. Lecointre, D.S. Belic, J. Jureta, K. Becker, H. Deutsch, J. Limtrakul, T.D. Märk, M. Probst and P. Defrance, " Absolute cross sections and kinetic energy release for doubly and triply charged fragments produced by electron impact on CO^+" , J. Phys. B 39, 85-100 (2006)

4. J. Lecontre, S. Cherkani-Hassani, D.S. Belic, J.J. Jureta, K. Becker, H. Deutsch, T.D. Märk, M. Probst, R.K. Janev, and P. Defrance, " Absolute Cross Sections and Kinetic Energy Release distributions for Electron Impact Ionization of CD^+" , J. Phys. B 40, 2201-2221 (2007)

5. H. Deutsch, K. Becker, and T.D. Märk, " Calculated Absolute Cross Sections for the Electron-Impact Ionization of Atoms with Atomic Numbers between 20 and 56 Using the DM Formalism" , Int. J. Mass Spectrom. 271, 58-62 (2008)

6. H. Deutsch, K. Becker, H. Zhang, M. Probst, and T.D. Märk, " Calculated Absolute Cross Sections for the Electron-Impact Ionization of the Lanthanide Atoms Using the DM Formalism", Int. J. Mass Spectrom. 271, 63-67 (2008)

187. J. Mahoney, V. Tarnovsky, and K. Becker, " Electron Impact Ionization of $SiCl_2$ and SiCl", Europ. Phys. J. D. 46, 298-293 (2008)

7. J. Mahoney, V. Tarnovsky, and K. Becker, " Electron Impact Ionization of $SiCl_3$ using a Modified Fast-Beam Apparatus", IOP J. Conf. Proc. " XV. Int. Symp. on Electron-Molecule Collisions and Swarms", (2008), in press

8. H. Deutsch, K. Becker, M. Probst, W. Zhu, and T.D. Märk, " Calculated Absolute Cross Sections for the Electron-Induced Detachment of the B2-, O2-, BO-, and CN- Anions Using the DM Formalism", Int. J. Mass Spectrom. (2008), in press (Eugen Illenberger Special Issue)

9. M. Gutkin, J.M. Mahoney, V. Tarnovsky, H. Deutsch, and K. Becker, " Electron-Impact Ionization of the $SiCl_3$ Radical", Int. J. Mass Spectrom. (2008), submitted for publication (Zdenek Herman Special Issue)

The next generation of the organic matter.

Vladimir Tarnovsky

Department of Physics and Engineering Physics, Stevens Institute of Technology,
Hoboken, NJ 07030, USA

Abstract.

The commonly known forms of matter like gas, liquid, and solids belong to what is understood as macro classical objects. These objects, while consisting of atoms and molecules, which are themselves quantum matter, which exists in a superposition of all possible states, the macro states carry no observable signature of its quantum nature.
Until now it was understood that apart from few cases, like low temperature superconductors, or super fluid helium, no known chemical compounds at room temperature expected to exhibit its collective quantum nature in observable way.

These assumptions might be challenged after it was discovered that certain organic materials can be successfully converted through a specific but relatively simple procedure into a crystalline form that appear to exhibit large scale quantum behavior. This manifests itself in a number of highly unusual but extremely useful chemical and electromagnetic properties. The properties to the best of my knowledge never have been observed before, and their discovery could constitute a breakthrough in modern science.
The properties that being observed so far are:

Complete inertness in all existing solvents, from acids, to bases as well.
Possessing extremely strong electric moments.
Ability to be converted into magnetic states
To withstand temperatures up to 2300 K.
Ability to be molded into any shape.

According to a proposed model, the formation of the crystal structure undergoes a chain of reactions that preserves the initial coherent dipole state, through building the carbon cage that shields the dipole as the crystal continues to grow. While the material appears to be a crystal- like, its x-ray diffraction gives no signs of the unit cell structure.
In addition, the electric moments are so large that the crystals will move in a presence of electric potential of only 3000 V. Similarly, it can be converted to a magnetic dipole state as well.
To summarize the available results, the new type of organic matter has been synthesized and its basic properties had been obtained.

Laser-Produced Coherent X-Ray Sources

Donald Umstadter, Physics and Astronomy Department, 212 Ferguson Hall, University of Nebraska, Lincoln, NE 68588-0111, dpu@unlserve.unl.edu

Program Scope

In this project, we experimentally and theoretically explore the physics of novel x-ray sources, based on the interactions of ultra-high-intensity laser light with matter. A promising approach involves the nonlinear or relativistic Thomson scattering of intense laser light from a relativistic electron beam. In this process, 1-eV energy laser light can be Doppler-shifted (by a factor of up to 10^6), to produce a well-collimated, ultrashort-duration, hard x-ray beam. Measurements with such as photon source could provide information on the structure of matter with atomic-scale resolution, on both the spatial and temporal scale lengths–simultaneously. Moreover, because the electron beam is accelerated by the ultra-high gradient of a laser-driven wakefield–via a light pulse from the same laser system that produces the scattering pulse–the combined length of both the accelerator and wiggler regions is only a few millimeters.

The x-ray source design parameters are sub-angstrom wavelength, femtosecond pulse duration, and university-laboratory–scale footprint. The required components, laser system (delivering peak power >100 TW at a repetition rate of 10 Hz) and electron accelerator (delivering beams with energy up to 400 MeV and divergence of 6 mrad) have now been developed and fully characterized. Both have durations less than 30 femtoseconds ($3x10^{-14}$ s).

This project involves the physics at the forefront of relativistic plasma physics and beams, as well as relativistic nonlinear optics. Applications include the study of ultrafast chemical, biological and physical processes, such as inner-shell electronic or phase transitions. Industrial applications include non-destructive evaluation, large-standoff–distance imaging of cracks, remote sensing and the detection of shielded nuclear materials.

Recent Results

Following is a more detailed discussion of the two essential components of a Thomson x-ray source: a high-power laser system and a synchronized laser-driven electron beam.

Diocles high-peak-power laser system – Over the previous two years, construction was completed of a new laboratory, and a high-power laser system. Once characterized and optimized, the laser was demonstrated to achieve unprecedented levels of performance with respect to peak power, as well as stability and reproducibility. Improvements to the system–the implementation of a deformable mirror, in particular–enabled near-diffraction limited focusing, as shown in Fig. 1. The measured laser parameters are shown in Table 1, and a schematic diagram of the system is shown in Fig. 2.

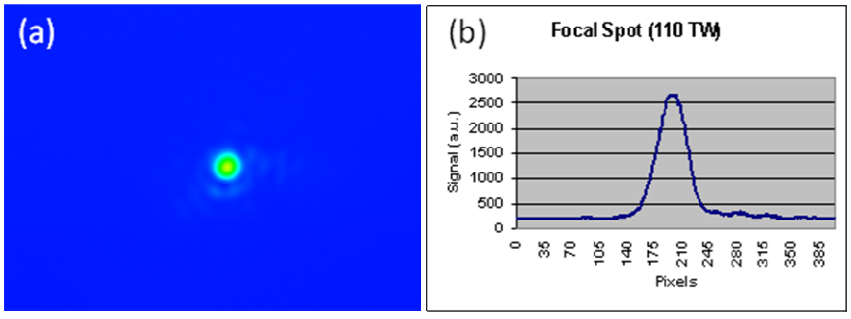

Figure 1: Focal spot of a high power laser pulse with wavefront correction: (a) focal spot obtained with a 1 m focal length paraboloid. The central spot contains 75% of the incident energy (b) lineout indicates a focal spot size of 16 microns.

Laser Parameter	*Measurement*
Peak power	140 TW
Repetition rate	10 Hz (0.1 Hz)
Central wavelength	805 nm
Pulse duration	< 30 fs
Pulse energy	3.5 J (compressed)
Energy stability (8 hours)	0.8% rms, 4.9%
Strehl ratio	0.95
Pointing stability	(1 min): 3.5μrad

Table 1: Laser parameter measured during full-power operation by means of beam sampling.

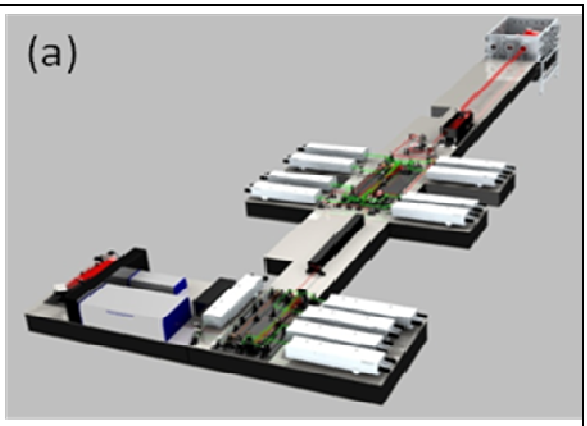

Figure 2: Schematic diagram of the Diocles laser system.

UNL laser wakefield accelerator – During the most recent year of the grant, electron beams accelerated by Diocles-laser–driven wakefields were characterized. Their dependence on laser and plasma parameters, as well as the optimal accelerator operating points, were both determined. It was demonstrated that the highest quality electron beams are produced when the laser and plasma parameters are nearly "matched." Because the laser pulse initially begins the interaction with its pulse duration and focal spotsize in resonance with the plasma, it does not suffer from the effects of nonlinear pulse evolution. This mitigates the instability and irreproducibility associated with mismatched parameters, characteristic of prior wakefield accelerators. As a result, it is now possible to produce electron beams with energy up to 400 MeV in a stable and reliable manner. This technological advance permits the use of these electron accelerators for applications, such as the production of monoenergetic hard x-rays.

The use of 30 fs, high contrast laser pulses, long acceleration lengths, high peak laser power, and a plasma density that is resonant with the laser, leads to a regime where the electron beam charge is >100 pC, its brightness is 7.8×10^{7} electrons mrad^{-2}, and its fluctuation level is less than 1% in pointing and energy. A typical spectrum, in which the beam has energy of 320 MeV, an energy spread of 10% (limited by the spectrometer resolution), and an angular divergence of 6 mrad, is shown in Fig. 3. Here, the x-axis corresponds to the energy, and the y-axis to pointing and angular spread of the beam. Note the lack of any visible dark current at lower laser energies. Some of the important accelerator parameters are summarized in Table 2.

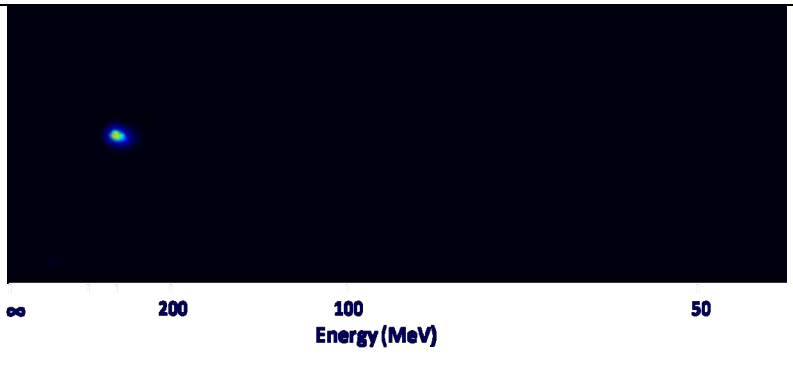

Figure 3: Monoenergetic, low-divergence beam, generated by 45 TW of laser power focused into a plasma with density of $7x10^{18}$ cm^{-3}. The energy is peaked around 320 MeV with a spread of 10%. The angular divergence of the beam (vertical axis) is 6 mrad.

Electron accelerator parameters	*Measured results*
Drive laser peak power	45 TW
Electron energy	320 MeV
ΔE/E	10%
Charge per bunch	100 pC
Electron beam divergence	6 mrad
Pointing and energy stability	1% over 30 shots

Table 2 Measured parameters of the UNL laser-driven wakefield accelerator.

The stability and reproducibility of the accelerator was also investigated in detail, and was found to sensitively depend on the laser contrast. Preliminary experiments in a low-laser–contrast mode, corresponding to a nanosecond pedestal of 3×10^{-7}, produced electron beams with large shot-to-shot angular variation of (10 mrad), and large energy fluctuation (approximately 20-30% shot-to-shot). When the contrast of the laser system was improved to 2×10^{-8}, the stability of the electron accelerator also improved, as summarized in Table 3.

Electron beam parameter	Angular position (mrad)	Divergence (mrad)	Energy (MeV)	Energy spread (MeV)
Mean	0	5.3	344	38.4
Standard deviation	1.1	1.7	35	4.8

Table 3: Stability of the UNL electron accelerator.

Current Activities and Future Plans

Proof-of-principle experiments are currently underway to use the electron beam and laser pulse discussed above to generate ultrashort pulses of 100-keV energy x-rays by means of Thomson scattering. As shown in Fig. 4, all optical elements have been aligned to focus the scattering laser pulse (in a counter-propagating direction) to overlap with the electron pulse, just as the latter exits the accelerator. Also, the requisite x-ray detectors and spectrometers have now been tested an integrated into the experiment.

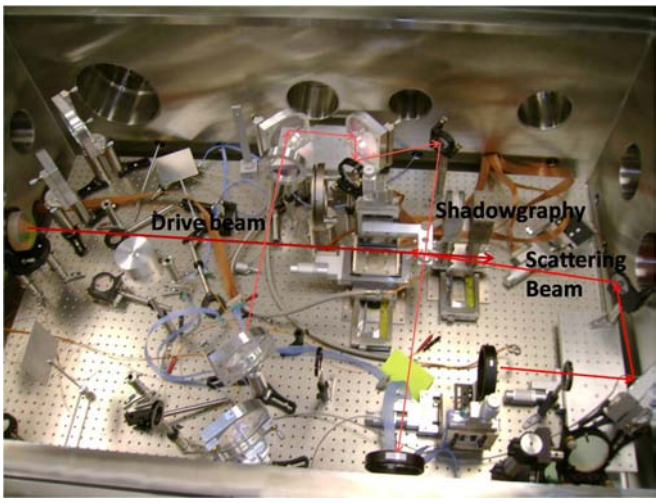

Figure 4: Photograph of the Thomson scattering experimental setup (taken with the lid of the vacuum chamber open). Red arrows indicate the directions and positions of the three laser beams: a drive beam to accelerate electrons, a scattering beam and a shadowgraphy beam to locate the optimal overlap position.

The Diocles laser system will soon be upgraded in peak power by an order of magnitude, to the PW level. To this end, an additional amplifier will be added, which will be pumped with four Nd:Glass pump lasers, each producing 25 J of pump power, to amplify the 800 nm beam from the current 5 J to 50 J per pulse. The amplified pulse will be compressed to 30 fs with output energy of ~30 J. When the PW amplifier is operated, the repetition rate of the system will be 0.1 Hz, the highest of any planned or existing PW laser in the U.S. An additional compressor chamber is currently being fabricated. The requisite larger diffraction gratings (60 cm x 50 cm) have already been manufactured and delivered to UNL. This power upgrade will allow the project to access to the highly relativistic Thomson scattering regime.

Acknowledgements

The P.I. gratefully acknowledges the significant contributions of the Diocles laboratory team, particularly Dr. Sudeep Banerjee. Besides DOE, partial financial support for the laser and experimental facilities used for this project was also provided by AFOSR, DARPA, and DHS.

DOE-Sponsored Publications (published within last three years)

1. Scott M. Sepke, Donald P. Umstadter, "Analytical solutions for the electromagnetic fields of flattened and annular Gaussian laser modes. I. Small F-number laser focusing," *JOSA B* **23**, 2157-2165 (2007).
2. D. Umstadter, S.Y. Chen, A. Maksimchuk, K. Flippo, V.Y. Bychenkov, Y. Sentoku, and K. Mima, "Short pulses of energetic electrons and ions produced by high-intensity lasers for laser fusion," Current Trends in International Fusion Research: Proceedings NRC Research Press, National Research Council of Canada, Ottawa, ON K1A OR6, Canada, Page 389 (2007).
3. S. Chen, M. Rever, P. Zhang, W. Theobald, and D. Umstadter, "Observation of relativistic cross-phase modulation in high-intensity laser-plasma interactions," *Phys. Rev. E* **74**, 046406 (2006).
4. Scott M. Sepke, Donald P. Umstadter, "Exact analytical solution for the vector electromagnetic field of Gaussian, flattened Gaussian, and annular Gaussian laser modes," *Optics Letters* **31**, 1447-1449 (2006).
5. Scott M. Sepke and Donald P. Umstadter, "Analytical solutions for the electromagnetic fields of tightly focused laser beams of arbitrary pulse length," *Optics Letters* **31**, 2589-2591 (2006).
6. D. Umstadter, S. Banerjee, S. Chen, S. Sepke, A. Maksimchuk, A., Valenzuela, A. Rousse, R. Shah, and K. Ta Phuoc, "Generation of ultrashort pulses of electrons, X-rays and optical pulses by relativistically strong light," AIP Conference Proceedings, SUPERSTRONG FIELDS IN PLASMAS: Third International Conference on Superstrong Fields in Plasmas, p. 86, vol. 827, (2006).
7. Scott M. Sepke, Donald P. Umstadter, "Analytical solutions for the electromagnetic fields of flattened and annular Gaussian laser modes. II. Large F-number laser focusing," *JOSA B* **23**, 2166-2173 (2006).
8. Scott M. Sepke, Donald P. Umstadter, "Analytical solutions for the electromagnetic fields of flattened and annular Gaussian laser modes. III. Arbitrary length pulses and spot sizes," *JOSA B* **23**, 2295-2302 (2006).
9. Sudeep Banerjee, Scott Sepke, Rahul Shah, Anthony Valenzuela, Anatoly Maksimchuk, and Donald Umstadter, "Optical Deflection and Temporal Characterization of an Ultrafast Laser-Produced Electron Beam," *Phys. Rev. Lett.* **95**, 035004 (2005).
10. Donald Umstadter, "Einstein's impact on optics at the frontier," *Phys. Letts. A* **347**, 121 (2005) [Einstein Special Issue - Edited by P. Holland].
11. Scott Sepke, Y. Y. Lau, James Paul Holloway, and Donald Umstadter, "Thomson scattering and ponderomotive intermodulation within standing laser beat waves in plasma," *Phys. Rev. E* **72**, 026501 (2005).

Cold and ultracold polar molecules

Jun Ye

JILA, National Institute of Standards and Technology and University of Colorado

Boulder, Colorado 80309-0440

Ye@jila.colorado.edu

Study of ultracold molecules promises important benefits such as novel control of chemical reactions and molecular collisions, precision measurement of fundamental physical properties, and new methods to study quantum phase transitions. We undertake two approaches to produce cold and ultracold polar molecular samples. In the first approach, we work directly with ground-state polar molecules such as hydroxyl radicals (OH) or formaldehyde molecules (H_2CO). After Stark deceleration through an inhomogeneously distributed electric field, OH molecules are prepared in a spatially confined packet with a density $>10^6$ cm^{-3} and temperature of ~70 mK. We then made the first experimental realization of ground state polar molecules confined in an external potential determined by combined electric and magnetic fields. The OH molecule possesses both electric and magnetic dipole moments and hence its dynamics under spatially inhomogeneous electric and magnetic fields are determined by a complex interplay between the strength of each interaction. Unlike in previous work where ground-state polar molecules are trapped inside an electric trap, our new trap configuration gives us the freedom to apply an external electric field to control dipole-dipole interactions while keeping the molecules trapped. This capability will be obviously important for the study of dipolar gas physics and cold dipolar collisions and reactions.

We then developed a more compact and efficient magnetic trap consisted of permanent magnets. Stark decelerated OH molecules are loaded into the trap by an application of large voltages to the magnets themselves. This creates a large stopping potential that is removed by turning off the electric field when molecules come to rest at the trap center. The simplicity and compactness of the trap make it ideal for the study of polar radicals. The open structure of this permanent magnetic trap has allowed us to perform the first experimental study of collisions between trapped molecules (OH) and external atomic (He) and molecular (D_2) beams. The D_2-OH collision cross sections are of interest to the wider astrophysics community in that a variety of interstellar masers, including those composed of OH, are predicted to be pumped by collisions with light molecules. Our ability to bring the heavier OH molecules to rest allows us to reach hitherto unexplored low-energy regimes in the center-of-mass frame. The use of trapped OH molecules also allows absolute cross sections to be determined at all collisions energies.

In the second approach, under active collaboration with D. Jin's group at JILA, we have produced ultracold polar molecules via association of ultracold dual gas mixtures near quantum degeneracy. Specifically, an interspecies magnetic Feshbach resonance between bosonic ^{87}Rb and fermionic ^{40}K permits efficient creations of heteronuclear Feshbach molecules. Subsequent optical spectroscopy reveals promising paths for efficient transfer of populations from the weakly bound to deeply bound molecular states. Using coherent adiabatic Raman transfer, we have created polar molecules at the rovibrational ground state of the triplet electronic ground potential, with a density of $10^{12}/cm^3$, 350 nK temperature, and a measured dipole moment of 0.05 D.

Author Index and List of Participants

Author Index

Author Index

Author Index

Author Index

Participants

Pierre Agostini
Ohio State University
Department of Physics
Columbus,OH 43210
Phone: (614) 247-4734
E-Mail: agostini@mps.ohio-state.edu

Ali Belkacem
Lawrence Berkeley National Laboratory
MS: 2R0100
Berkeley,CA 94720
Phone: (510)486-7778
E-Mail: abelkacem@lbl.gov

Itzik Ben-Itzhak
J.R. Macdonald Laboratory, Kansas State University
Department of Physics, Cardwell Hall
Manhattan,KS 66506
Phone: (785)539-2155
E-Mail: ibi@phys.ksu.edu

Nora Berrah
Western Michigan University
Physics Department
Kalmazoo,MI 49008
Phone: (269)387-4055
E-Mail: nora.berrah@wmich.edu

Michael Bogan
Stanford Linear Accelerator Center
2575 Sand Hill Road
Menlo Park,CA 94025
Phone: (650)926-2731
E-Mail: mbogan@slac.stanford.edu

John Bohn
JILA
UCB 440, University of Colorado
Boulder,CO 80305
Phone: (303)492-5426
E-Mail: bohn@murphy.colorado.edu

Philip Bucksbaum
Stanford/SLAC
2575 Sand Hill Road
Menlo Park,CA 94025
Phone: (650)926-5337
E-Mail: phb@slac.stanford.edu

Michael Casassa
US DOE, Basic Energy Sciences
SC22.1 DOE, 19901 Germantown Rd.
Germantown,MD 20874
Phone: (301)903-0448
E-Mail: michael.casassa@science.doe.gov

Zenghu Chang
Kansas State University
Physics Department, Cardwell Hall
Manhattan,KS 66503
Phone: (785)532-1621
E-Mail: chang@phys.ksu.edu

Shih-I Chu
University of Kansas
Department of Chemistry
Lawrence,KS 66045
Phone: (785)864-4094
E-Mail: sichu@ku.edu

C.L. Cocke
Kansas State University
Physics Department, Cardwell Hall
Manhattan,KS 66503
Phone: (785)532-1609
E-Mail: cocke@phys.ksu.edu

Robin Côté
University of Connecticut
2152 Hillside Road, U-3046
Storrs,CT 06269
Phone: (860)486-4912
E-Mail: rcote@phys.uconn.edu

Scott Crooker
Los Alamos National Laboratory
NHMFL-LANL
Los Alamos,NM 87545
Phone: (505)665-7595
E-Mail: crooker@lanl.gov

Steven Cundiff
JILA/NIST
440 UCB
Boulder,CO 80309
Phone: (303)492-7858
E-Mail: kalethl@jila.colorado.edu

Participants

Tatjana Curcic
AFOSR
875 N. Randolph St., Suite 325, Room 3112
Arlington,VA 22203
Phone: (703)696-6204
E-Mail: tatjana.curcic@afosr.af.mil

Alexander Dalgarno
Harvard University
CFA,60 Garden Street
Cambridge,Ma 02138
Phone: (617)495-4403
E-Mail: adalgarno@cfa.harvard.edu

David DeMille
Yale University
P.O. Box 208120
New Haven,CT 06520
Phone: (203)432-3833
E-Mail: david.demille@yale.edu

Louis DiMauro
The Ohio State University
191 W. Woodruff Avenue
Columbus,OH 43210
Phone: (614)688-5726
E-Mail: dimauro@mps.ohio-state.edu

Todd Ditmire
University of Texas at Austin
2511 Speedway RLM 12.204
Austin,TX 78712
Phone: (512)471-3296
E-Mail: tditmire@physics.utexas.edu

John Doyle
Harvard University
17 Oxford Street
Cambridge,MA 02138
Phone: (617)230-7880
E-Mail: doyle@physics.harvard.edu

Robert Dunford
Argonne National Laboratory
9700 S. Cass Ave.
Argonne,IL 60439
Phone: (630)252-4052
E-Mail: dunford@anl.gov

Joseph Eberly
University of Rochester
Department of Physics & Astronomy
Rochester,NY 14627-0171
Phone: (585)275-4576
E-Mail: eberly@pas.rochester.edu

Brett Esry
J.R. Macdonald Laboratory, Kansas State University
116 Cardwell Hall, Dept. of Physics
Manhattan,KS 66506
Phone: (785)532-1620
E-Mail: esry@phys.ksu.edu

Roger Falcone
Lawrence Berkeley National Laboratory
One Cyclotron Road, MS 80R0114
Berkeley,CA 94720
Phone: (510)486-6692
E-Mail: rwf@berkeley.edu

Jim Feagin
Cal State University Fullerton
800 N State College Ave
Fullerton,CA 92834
Phone: (714)278-3366
E-Mail: jfeagin@fullerton.edu

Kelly Gaffney
SLAC
2575 Sand Hill Rd.
Menlo Park,CA 94025
Phone: (650)926-2382
E-Mail: kgaffney@slac.stanford.edu

Thomas Gallagher
University of Virginia
Department of Physics
Charlottesville,VA 22904
Phone: (434)924-6817
E-Mail: tfg@virginia.edu

Oliver Gessner
Lawrence Berkeley National Laboratory
1 Cyclotron Rd
Berkeley,CA 94706
Phone: (510)486-6929
E-Mail: ogessner@lbl.gov

Participants

James Glownia
US DOE, Basic Energy Sciences
19901 Germantown Road
Germantown,MD 20874-1920
Phone: (301)903-2411
E-Mail: james.glownia@science.doe.gov

Phillip Gould
University of Connecticut
Physics Dept. U-3046, 2152 Hillside Rd..
Storrs, CT 06269
Phone: (860)486-2950
E-Mail: phillip.gould@uconn.edu

Chris Greene
JILA, University of Colorado
440 UCB
Boulder,CO 80309
Phone: (303)492-4770
E-Mail: chris.greene@colorado.edu

Murray Holland
JILA, University of Colorado
440 UCB
Boulder,CO 80309
Phone: (303)492-4172
E-Mail: murray.holland@colorado.edu

Robert Jones
University of Virginia
Physics Department, 382 McCormick Road,
P.O. Box 400714
Charlottesville,VA 22904
Phone: (434)924-3088
E-Mail: rrj3c@virginia.edu

Elliot Kanter
Argonne National Laboratory
9700 S. Cass Ave.
Argonne,IL 60439
Phone: (630)252-4050
E-Mail: kanter@anl.gov

Henry Kapteyn
JILA, University of Colorado
440 UCB
Boulder,CO 80303
Phone: (303)492-6763
E-Mail: kapteyn@jila.colorado.edu

Victor Klimov
Los Alamos National Laboratory
MS-J567
Los Alamos,NM 87545
Phone: (505)665-8284
E-Mail: klimov@lanl.gov

Bertold Krässig
Chemistry Division, Argonne National
Laboratory
9700 S Cass Ave
Argonne,IL 60439
Phone: 630-252-9230
E-Mail: kraessig@anl.gov

Jeffrey Krause
US DOE, Basic Energy Sciences
19901 Germantown Road
Germantown,MD 20874-1920
Phone: (301)903-5827
E-Mail: Jeff.Krause.science.doe.gov

Vinod Kumarappan
Kansas State University
116 Cardwell Hall, Dept. of Physics
Manhattan,KS 66506
Phone: (785) 532-1632
E-Mail: vinod@phys.ksu.edu

Allen Landers
Auburn University
206 Allison Laboratory
Auburn,AL 36849
Phone: (334)844-4048
E-Mail: landers@physics.auburn.edu

Chii-Dong Lin
Kansas State University
Department of Physics
Manhattan,KS 66506
Phone: (785)532-1617
E-Mail: cdlin@phys.ksu.edu

Igor Litvinyuk
Kansas State University
116 Cardwell Hall
Manhattan,KS 66506
Phone: (785)532-1615
E-Mail: ivl@phys.ksu.edu

Participants

Robert Lucchese
Texas A&M University
Department of Chemistry
College Station,TX 77843
Phone: (979)845-0187
E-Mail: lucchese@mail.chem.tamu.edu

Stephen Lundeen
Colorado State University
Dept. of Physics
Fort Collins,CO 80523
Phone: (970)491-6647
E-Mail: lundeen@lamar.colostate.edu

Joseph Macek
University of Tennessee
401 Nielsen Physics Bldg 1408 Circle Dr
Knoxville,TN 37996
Phone: (865)974-0770
E-Mail: jmacek@utk.edu

Steven Manson
Georgia State University
Dept of Physics & Astronomy
Atlanta,GA 30303
Phone: (404)413-6046
E-Mail: smanson@gsu.edu

Diane Marceau
US DOE, Basic Energy Sciences
19901 Germantown Road
Germantown,MD 20874
Phone: (301)903-0235
E-Mail: diane.marceau@science.doe.gov

Spiridoula Matsika
Temple University
Department of Chemistry
Philadelphia,PA 19122
Phone: (215)204-7703
E-Mail: smatsika@temple.edu

William McCurdy
U. C. Davis and LBNL
One Cyclotron Road, MS 50B-2245
Berkeley,CA 94720
Phone: (510)486-4283
E-Mail: cwmccurdy@ucdavis.edu

Vincent McKoy
California Institute of Technology
1200 E. California Blvd.
Pasadena,CA 91125
Phone: (626)395-6545
E-Mail: mckoy@caltech.edu

Alfred Z. Msezane
Clark Atlanta University
223 James P. Brawley Drive SW
Atlanta,GA 30314
Phone: (404)880-8663
E-Mail: amsezane@cau.edu

Shaul Mukamel
University of California, Irvine
1102 Natural Sciences II
Irvine,CA 92697
Phone: (949)824-7600
E-Mail: smukamel@uci.edu

Margaret Murnane
JILA, University of Colorado
440 UCB
Boulder,CO 80303
Phone: (303)492-6763
E-Mail: murnane@jila.colorado.edu

Keith Nelson
MIT
77 Massachusetts Avenue, Rm. 6-235
Cambridge,MA 02139
Phone: (617)253-1423
E-Mail: kanelson@mit.edu

Lukas Novotny
University of Rochester
The Institute of Optics
Rochester,NY 14627
Phone: (585)275-5767
E-Mail: novotny@optics.rochester.edu

Ann Orel
University of California, Davis
One Shields Ave. , Dept. of Applied Science
Davis,CA 95616
Phone: (530)752-6025
E-Mail: aeorel@ucdavis.edu

Participants

Thomas Orlando
Department of Chemistry & Biochemistry
Georgia Institute of Technology
901 State Street, MS&E Bldg., Room 2201B
Atlanta,GA 30332
Phone: (404)894-8222
E-Mail: thomas.orlando@chemistry.gatech.edu

Mark Pederson
US DOE, Basic Energy Sciences
19901 Germantown Road
Germantown,MD 20874-1920
Phone: (301)903-9956
E-Mail: Mark.Pederson@science.doe.gov

Ronald Phaneuf
University of Nevada, Reno
Department of Physics, MS-220
Reno,NV 89557
Phone: (775)784-6818
E-Mail: phaneuf@physics.unr.edu

Erwin Poliakoff
Louisiana State University
Chemistry Department
Baton Rouge,LA 70803
Phone: (225)578-2933
E-Mail: epoliak@lsu.edu

Herschel Rabitz
Princeton University
Frick Laboratory
Princeton,NJ 08544
Phone: (609)258-3917
E-Mail: hrabitz@princeton.edu

Georg Raithel
University of Michigan
450 Church Street
Ann Arbor,MI 48105
Phone: (734)647-9031
E-Mail: graithel@umich.edu

Chandra Raman
Georgia Tech
School of Physics, 837 State St.
Atlanta,GA 30332
Phone: (404)894-9062
E-Mail: craman@gatech.edu

Carlos Reinhold
Oak Ridge National Laboratory
Box 2008/Bldg 6000B
Oak Ridge,TN 37831
Phone: (865)574-4579
E-Mail: reinhold@ornl.gov

David Reis
University of Michigan
Department of Physics, 450 Church Street
Ann Arbor,MI 48109
Phone: (734)763-9649
E-Mail: dreis@umich.edu

Thomas Rescigno
LBNL
1 Cyclotron Rd. MS-2-100
Berkeley,CA 94720
Phone: (510)486-8652
E-Mail: tnrescigno@lbl.gov

Francis Robicheaux
Auburn University
206 Allison Lab
Auburn,AL 36849
Phone: (334)844-4366
E-Mail: robicfj@auburn.edu

Jorge Rocca
Colorado State University
1320 Campus Delivery ERC B329
Fort Collins,CO 80523
Phone: (970)491-8371
E-Mail: rocca@engr.colostate.edu

Christoph Rose-Petruck
Brown University
Dept. of Chemistry
Providence,RI 02912
Phone: (401)863-1533
E-Mail: Christoph_Rose-Petruck@brown.edu

Robin Santra
Argonne National Laboratory
9700 S. Cass Avenue
Argonne,IL 60439
Phone: (630)252-4994
E-Mail: rsantra@anl.gov

Participants

Richard Schaller
Los Alamos National Laboratory
MS-J585, C-PCS
Los Alamos,NM 87545
Phone: (505)664-0338
E-Mail: rdsx@lanl.gov

Robert Schoenlein
Lawrence Berkeley National Laboratory
1 Cyclotron Rd. MS: 2-300
Berkeley,CA 94720
Phone: (510)486-6557
E-Mail: rwschoenlein@lbl.gov

David Schultz
Oak Ridge National Laboratory
Physics Div., Bldg. 6010, P.O. Box 2008
Oak Ridge,TN 37831
Phone: (865)576-9461
E-Mail: schultzd@ornl.gov

Tamar Seideman
Northwestern University
2145 Sheridan Road
Evanston,IL 60208
Phone: (847)467-4979
E-Mail: t-seideman@northwestern.edu

Neil Shafer-Ray
University of Oklahoma
440 West Brooks Street
Norman,OK 73019
Phone: (405)325-2890x36123
E-Mail: shaferry@physics.ou.edu

Wade Sisk
DOE/BES
SC22.1 DOE, 19901 Germantown Rd.
Germantown,MD 20874
Phone: (301)903-5692
E-Mail: wade.sisk@science.doe.gov

Steve Southworth
Argonne National Laboratory
Bldg. 203, 9700 S. Cass Ave.
Argonne,IL 60439
Phone: (630)252-3894
E-Mail: southworth@anl.gov

Anthony F. Starace
University of Nebraska
Dept. of Physics & Astronomy, 116 Brace Lab
Lincoln,NE 68588
Phone: (402)472-2795
E-Mail: astarace1@unl.edu

Mark Stockman
Georgia State University
University Plaza
Atlanta,GA 30303
Phone: (678)457-4739
E-Mail: mstockman@gsu.edu

Vladimir Tarnovsky
Stevens Institute of Technology
Castle Point on Hudson
Hoboken,NJ 07410
Phone: (201)216-5099
E-Mail: vtarnovs@stevens-tech.edu

Uwe Thumm
Kansas State University
Physics Department, Cardwell Hall
Manhattan,KS 66503
Phone: (785) 532-1613
E-Mail: thumm@phys.ksu.edu

Donald Umstadter
University of Nebraska, Lincoln
212 Ferguson Hall
Lincoln,NE 68588
Phone: (402)472-8115
E-Mail: dpu@unlserve.unl.edu

C. Randy Vane
Oak Ridge National Laboratory
MS 6372, P.O. Box 2008
Oak Ridge,TN 37831
Phone: (865) 574-4497
E-Mail: vanecr@ornl.gov

Thorsten Weber
Lawrence Berkeley National Lab
One Cyclotron Road
Berkeley,CA 94720
Phone: (510)486-5588
E-Mail: TWeber@lbl.gov

Participants

Jun Ye
JILA, University of Colorado
UCB 440
Boulder,CO 80309
Phone: (303)735-3171
E-Mail: ye@jila.colorado.edu

Linda Young
Argonne National Laboratory
9700 S. Cass Ave.
Argonne,IL 60439
Phone: (630)252-8878
E-Mail: young@anl.gov